

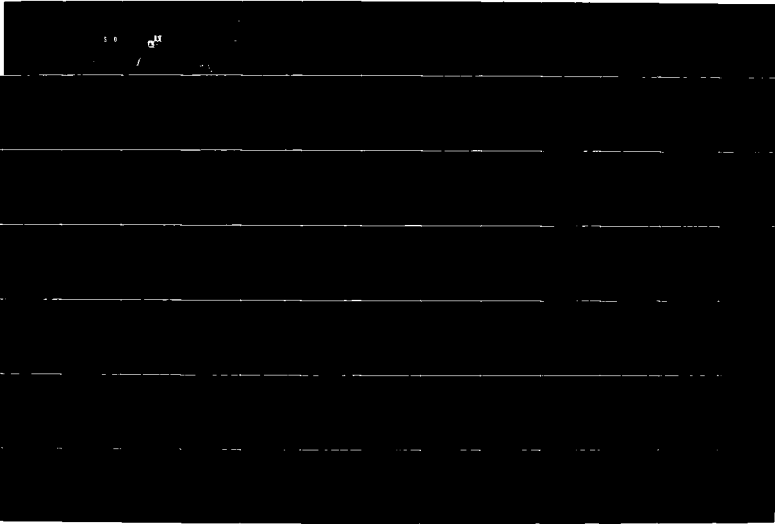
AD-A171 026

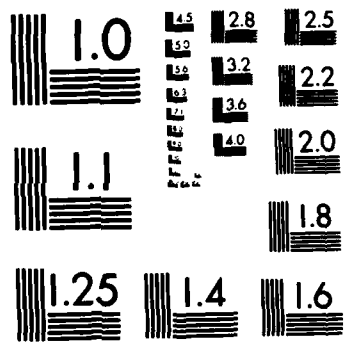
ABSTRACTS 21ST ANNUAL MEETING SOCIETY OF ENGINEERING  
SCIENCE INC OCTOBER 1-7 (U) VIRGINIA POLYTECHNIC INST  
BLACKSBURG D FREDERICK ET AL. 1984 ARO-21008 EG-CF  
DAGC29-84-M-0119 P/C 5/2

1/6

UNCLASSIFIED

ML





MICROCOPY RESOLUTION TEST CHART  
NATIONAL BUREAU OF STANDARDS-1963-A

PHOTOGRAPH THIS SHEET



INVENTORY

AD-A171 026

DTIC ACCESSION NUMBER

ABSTRACTS

LEVEL

SOCIETY OF ENGINEERING SCIENCE, INC.  
21 ANNUAL MEETING  
OCT. 15-17 1984

DOCUMENT IDENTIFICATION

DISTRIBUTION STATEMENT A

Approved for public release  
Distribution Unlimited

DISTRIBUTION STATEMENT

ACCESSION FOR

NTIS GRA&I

DTIC TAB

UNANNOUNCED

JUSTIFICATION



BY *letter on file*

DISTRIBUTION /

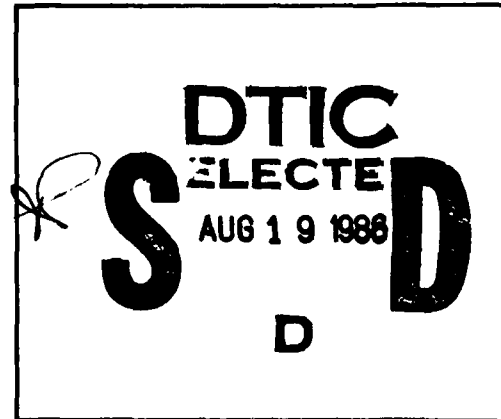
AVAILABILITY CODES

DIST

AVAIL AND/OR SPECIAL

A-1

DISTRIBUTION STAMP



DATE ACCESSIONED

DATE RETURNED

86 8 19 020

DATE RECEIVED IN DTIC

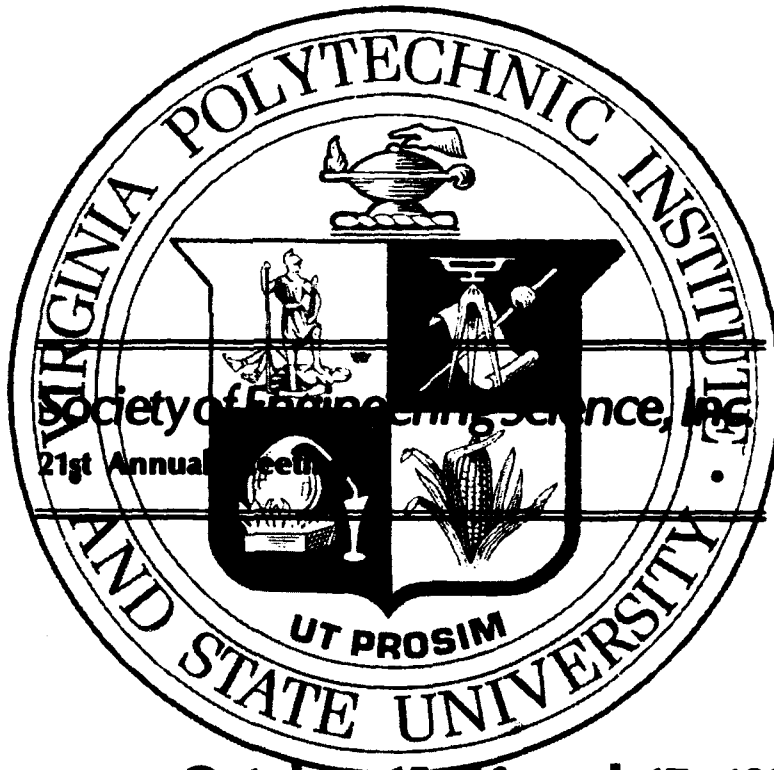
REGISTERED OR CERTIFIED NO.

PHOTOGRAPH THIS SHEET AND RETURN TO DTIC-DDAC

21008.1-EG-CF

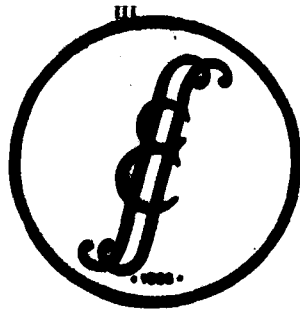
# Abstracts

AD-A171 026



October 15, 16, and 17, 1984

VIRGINIA POLYTECHNIC INSTITUTE  
AND STATE UNIVERSITY  
BLACKSBURG, VA, USA



UNCLASSIFIED  
 SECURITY CLASSIFICATION OF THIS PAGE (When Data Entered)

REPORT DOCUMENTATION PAGE		READ INSTRUCTIONS BEFORE COMPLETING FORM
1. REPORT NUMBER ARO 21008.1-EG-CF	2. GOVT ACCESSION NO. N/A	3. RECIPIENT'S CATALOG NUMBER N/A
4. TITLE (and Subtitle) Abstracts - 21st Annual Meeting Society of Engineering Science		5. TYPE OF REPORT & PERIOD COVERED 5 Jan. 1984 - 4 Jan 1985 Final Report
7. AUTHOR(s) Daniel Frederick and C. W. Smith Co-Chairman		6. PERFORMING ORG. REPORT NUMBER
9. PERFORMING ORGANIZATION NAME AND ADDRESS Virginia Polytechnic Institute and State University Blacksburg, VA.		8. CONTRACT OR GRANT NUMBER(s) DAAG29-84-M-0119
11. CONTROLLING OFFICE NAME AND ADDRESS U. S. Army Research Office Post Office Box 12211 Research Triangle Park, NC 27709		10. PROGRAM ELEMENT, PROJECT, TASK AREA & WORK UNIT NUMBERS
14. MONITORING AGENCY NAME & ADDRESS (if different from Controlling Office)		12. REPORT DATE
		13. NUMBER OF PAGES
		15. SECURITY CLASS. (of this report) Unclassified
		15a. DECLASSIFICATION/DOWNGRADING SCHEDULE
16. DISTRIBUTION STATEMENT (of this Report) Approved for public release; distribution unlimited.		
17. DISTRIBUTION STATEMENT (of the abstract entered in Block 20, if different from Report) NA		
18. SUPPLEMENTARY NOTES The view, opinions, and/or findings contained in this report are those of the author(s) and should not be construed as an official Department of the Army position, policy, or decision, unless so designated by other documentation.		
19. KEY WORDS (Continue on reverse side if necessary and identify by block number)		
20. ABSTRACT (Continue on reverse side if necessary and identify by block number)		

ABSTRACTS

21st ANNUAL MEETING  
SOCIETY OF ENGINEERING SCIENCE

OCTOBER 15, 16, 17, 1984

VIRGINIA POLYTECHNIC INSTITUTE  
AND STATE UNIVERSITY  
BLACKSBURG, VA, USA

### PREFACE

This publication contains all of the abstracts provided by authors participating in the 21st Annual Meeting of the Society of Engineering Science held on October 15-17, 1984 at the Donaldson Brown Conference Center on the campus of Virginia Polytechnic Institute and State University.

The following tables of contents and an authors' index at the back of the publication will assist the reader in locating abstracts and authors in specific disciplines. The abstracts included herein should give an idea of the current research in various fields of engineering science.

The local organizing committee wishes to thank the session organizers and the authors for their time and support of the meeting, and the U.S. Army Research Office, the Virginia Tech Foundation and the Department of Engineering Science and Mechanics at the Virginia Polytechnic Institute and State University for their generous financial support. It is also a pleasure to acknowledge the typing of many abstracts by Mrs. Marlene Taylor and Mrs. Norma Guynn, and general typing by Mrs. Vanessa McCoy.

J. N. Reddy  
Chairman, Proceedings

Daniel Frederick and C. W. Smith  
Co-Chairman

Blacksburg, Va.  
October, 1984

**21st ANNUAL MEETING OF SES**  
**ORGANIZING COMMITTEES**

**Program Planning**

R. A. Heller, Chm.  
J. E. Dunn  
D. J. Schneck

**Proceedings**

J. N. Reddy, Chm.  
M. P. Kamat  
D. J. Schneck

**Local Arrangements**

C. W. Smith, Chm.  
A. Pap (Transportation)  
G. W. Swift (Audio-Visual Equipment)  
Frances Frederick and Doris Smith (Spouses' Program)

**ORGANIZERS OF TECHNICAL SESSIONS**

H. F. Brinson (VPI & SU)	F. Kulacki (Delaware)
G. Sih (Lehigh)	J. N. Reddy (VPI & SU)
N. J. Salamon (W. Va.)	C. A. Babendreier (NSF)
W. S. Saric (VPI & SU)	A. C. Eringen (Princeton)
E. C. Aifantis (Michigan Tech.)	D. H. Morris (VPI & SU)
C. W. Bert (Oklahoma)	D. Post (VPI & SU)
D. J. Schneck (VPI & SU)	L. Y. Bahar (Drexel)
S. S. Wang (Illinois)	J. E. Dunn (Sandia National Labs)
C. W. Smith (VPI & SU)	R. T. Haftka (VPI & SU)
S. J. Spector (Southern Illinois)	R. Fosdick (Minnesota)
S. G. Lekoudis (Georgia Tech.)	T. G. Trucano (Sandia National Labs)
K. C. Valanis (Cincinnati)	S. L. Passman (Sandia National Labs)
M. Mehrabadi (Tulane)	W. Z. Sadeh (Colorado State)
K. L. Reifsnider (VPI & SU)	V. C. Li (MIT)
A. S. Krausz (Ottawa)	R. A. Heller (VPI & SU)
L. Meirovitch (VPI & SU)	M. P. Kamat (VPI & SU)
J. G. Simmonds (Virginia)	N. Kikuchi (Michigan)
J. L. S. Chen (Pittsburg)	A. Solomon (Oak Ridge National Lab)
L. S. Costin (Sandia National Labs)	
J. E. Fitzgerald (Georgia Tech.)	
R. C. Batra (Missouri - Rolla)	

**CONTENTS**  
**BY TECHNICAL AREAS**

	<u>Page</u>
 <u>COMPOSITES</u>	
Adhesion Science.....	1
Mechanics of Composite Materials.....	76
Composite Strength and Life Estimation.....	181
Heat Transfer in Composites and Heterogeneous Materials.....	280
Fracture of Composites.....	344
Analysis of Composite Material Structures.....	419
 <u>FRACTURE, DAMAGE</u>	
Fracture Mechanics I.....	7
Fracture Mechanics II.....	87
Time Dependent Fracture and Deformation.....	192
Damage Effects in Structural Materials.....	260
Photomechanics.....	351
 <u>DYNAMICS AND VIBRATIONS</u>	
Dynamics and Control of Structures I.....	201
Dynamics and Control of Structures II.....	266
Modern Trends in Dynamics I.....	360
Modern Trends in Dynamics II.....	431
Stability and Structural Dynamics.....	16
Vibrations.....	100
 <u>CONTINUUM MECHANICS</u>	
Numerical Solution of Contact Problems.....	29
Finite Elasticity.....	117
Some Recent Results in Endochronic Plasticity (Theory & Exp't). 140	
Continuum Mechanics I.....	273
Continuum Mechanics II.....	388
Constitutive Modelling.....	368
Thermal Stresses.....	444
 <u>STRUCTURES, COMPUTATIONAL METHODS</u>	
Mechanics of Shells.....	210
Computational Mechanics.....	290
Structural Optimization I.....	380
Structural Optimization II.....	451
Large Scale Computations in Mechanics.....	395
Adaptive Finite Element Methods for Large Scale Computations...	462
 <u>FLUIDS</u>	
Hydrodynamic Stability and Fluid Mechanics.....	38
Computational Fluid Mechanics.....	126

CONTENTS (continued)  
BY TECHNICAL AREAS

Non-Newtonian Flow and Heat Transfer.....	223
Fluid Mechanics.....	233
Non-Newtonian Flows.....	300
Turbulence in Fluids I.....	405
Turbulence in Fluids II.....	496

GEOMECHANICS

Mechanics of Microstructures I.....	49
Mechanics of Microstructures II.....	161
Mechanics of Microstructures III.....	255
Mechanics of Granular and Porous Media.....	151
Microcrack Damage and Acoustic Emission in Rock.....	246
Centrifuge Techniques in Geomechanics.....	311
Rapid Flow of Granular Materials.....	323
Mechanics of Earthquake Rupture I.....	412
Mechanics of Earthquake Rupture II.....	470

SPECIAL TOPICS

Mechanics of Wind Turbines and Solar Energy Generation.....	55
Biomedical Engineering.....	66
Electromagnetic Interaction with Materials.....	333
Mathematical Modelling of Alloy Solidification Processes.....	474
Special Topics I.....	168
Special Topics II.....	481

**TABLE OF CONTENTS**  
**TECHNICAL SESSIONS AS ORDERED**  
**IN THE PROGRAM\***

		<u>Page</u>
15AM1	ADHESION SCIENCE.....	1
15AM2	FRACTURE MECHANICS I.....	7
15AM3	STABILITY AND STRUCTURAL DYNAMICS.....	16
15AM4	NUMERICAL SOLUTION OF CONTACT PROBLEMS.....	29
15AM5	HYDRODYNAMIC STABILITY AND FLUID MECHANICS.....	38
15AM6	MECHANICS OF MICROSTRUCTURES I.....	49
15AM7	MECHANICS OF WIND TURBINES AND SOLAR ENERGY GENERATORS	55
15AM8	BIOMEDICAL ENGINEERING .....	66
15PM1	MECHANICS OF COMPOSITE MATERIALS.....	76
15PM2	FRACTURE MECHANICS II.....	87
15PM3	VIBRATIONS.....	100
15PM4	FINITE ELASTICITY.....	117
15PM5	COMPUTATIONAL FLUID MECHANICS.....	126
15PM6	SOME RECENT RESULTS IN ENDOCHRONIC PLASTICITY THEORY AND EXPERIMENT.....	140
15PM7	MECHANICS OF GRANULAR MATERIALS AND POROUS MEDIA.....	151
15PM8	MECHANICS OF MICROSTRUCTURES II.....	161
15PM9	SPECIAL TOPICS I.....	168
16AM1	COMPOSITE STRENGTH AND LIFE ESTIMATION.....	181
16AM2	TIME DEPENDENT FRACTURE AND DEFORMATION.....	192
16AM3	DYNAMICS AND CONTROL OF STRUCTURES I.....	201
16AM4	MECHANICS OF SHELLS.....	210
16AM5	NON-NEWTONIAN FLOW AND HEAT TRANSFER.....	223
16AM6	FLUID MECHANICS.....	233
16AM7	MICROCRACK DAMAGE AND ACOUSTIC EMISSION IN ROCK.....	246
16AM8	MECHANICS OF MICROSTRUCTURES III.....	255
16PM1	DAMAGE EFFECTS IN STRUCTURAL MATERIALS.....	260
16PM2	DYNAMICS AND CONTROL OF STRUCTURES II.....	266
16PM3	CONTINUUM MECHANICS I.....	273
16PM4	HEAT TRANSFER IN COMPOSITES AND HETEROGENEOUS MATERIALS.....	280
16PM5	COMPUTATIONAL MECHANICS.....	290
16PM6	NON-NEWTONIAN FLOWS.....	300
16PM7	CENTRIFUGE TECHNIQUES IN GEOMECHANICS.....	311
16PM8	RAPID FLOW OF GRANULAR MATERIALS.....	323
16PM9	ELECTROMAGNETIC INTERACTION WITH MATERIALS.....	333

**TABLE OF CONTENTS (continued)**  
**TECHNICAL SESSIONS AS ORDERED**  
**IN THE PROGRAM\***

17AM1	FRACTURE OF COMPOSITES.....	344
17AM2	PHOTOMECHANICS.....	351
17AM3	MODERN TRENDS IN DYNAMICS I.....	360
17AM4	CONSTITUTIVE MODELING.....	368
17AM5	STRUCTURAL OPTIMIZATION I.....	380
17AM6	CONTINUUM MECHANICS II.....	388
17AM7	LARGE SCALE COMPUTATION IN MECHANICS.....	395
17AM8	TURBULENCE IN FLUIDS I.....	405
17AM9	MECHANICS OF EARTHQUAKE RUPTURE I.....	412
17PM1	ANALYSIS OF COMPOSITE MATERIAL STRUCTURES.....	419
17PM2	MODERN TRENDS IN DYNAMICS II.....	431
17PM3	THERMAL STRESSES.....	444
17PM4	STRUCTURAL OPTIMIZATION II.....	451
17PM5	ADAPTIVE FINITE ELEMENT METHODS FOR LARGE SCALE COMPUTATIONS.....	462
17PM6	MECHANICS OF EARTHQUAKE RUPTURE II.....	470
17PM7	MATHEMATICAL MODELING OF ALLOY SOLIDIFICATION PROCESSES.....	474
17PM8	SPECIAL TOPICS II.....	481
17PM9	TURBULENCE IN FLUIDS II.....	496

\*The order in which abstracts appear in these Proceedings is based upon the program as of August 1, 1984. Changes subsequent to this date will appear in the final program distributed at the time of the meeting.

CHARACTERIZATION OF ADHESIVE/ADHEREND  
INTERFACES USING OPTICAL TECHNIQUES

by

F. J. Boerio  
Department of Materials Science  
and Metallurgical Engineering  
University of Cincinnati  
Cincinnati, Ohio 45221-0012

Characterization of adhesive/adherend interfaces is one of the most important problems associated with adhesive bonding of metals. In order to develop theories of adhesion it is essential to determine the nature of reactions occurring at interfaces between primers and substrates and between primers and adhesives. Moreover, it is essential to understand the nature of degradation reactions occurring at such interfaces in order to obtain durable bonds.

For some time we have been interested in the use of organofunctional silanes as primers for improving the hydrothermal stability of adhesive bonds to metals. The purpose of this paper is to describe results obtained using optical techniques such as infrared spectroscopy and ellipsometry to determine the nature of reactions occurring within silane primers and at the silane/oxide and silane/adhesive interfaces.

Results obtained from infrared spectroscopy indicate that  $\gamma$ -aminopropyltriethoxysilane ( $\gamma$ -APS) is adsorbed from aqueous solutions onto the oxidized surfaces of metals as hydrolyzed oligomers that polymerize during drying to form crosslinked siloxane polymers. These polymers usually absorb carbon dioxide from the atmosphere to form amine bicarbonate salts. In some cases (e.g., copper) the oxide is etched during adsorption of the silane, resulting in metal ions being complexed within the films. Heating the films causes the carbon dioxide to be desorbed and increases the crosslink density in the polymers, thereby increasing the ability of the films to inhibit hydration of the oxide and leading to improved durability of adhesive joints. However, excessive heating of the films can reduce the interaction between the silane primer and the adhesive, leading to low joint strengths.

Results obtained from infrared spectroscopy indicate that  $\gamma$ -methacryloxypropyltrimethoxysilane ( $\gamma$ -MPS) also forms hydrolyzed oligomers in aqueous solutions. There is some evidence indicating that these oligomers are adsorbed onto the oxidized surfaces of metals by hydrogen bonding with surface hydroxyls and then polymerize during drying. Results obtained from ellipsometry indicate that these polymers improve the wet strength of adhesive joints to aluminum by inhibiting hydration of the oxide during exposure to warm, moist environments.

## FINITE ELEMENT ANALYSIS OF TWO ADHESIVE SPECIMENS

by

Sheldon Mostovoy  
METM Department  
Illinois Institute of Technology  
Chicago, IL 60616

The study of adhesively bonded structures at the Illinois Institute of Technology is concerned with the modelling of structures with laboratory specimens using fracture mechanics methodology.

The modelling of bonded structures requires analysis of self-similar cracking in the presence of normal (Mode I) and shear loading (Modes II and III). Analysis of Mode I cracking has been accomplished for both monolithic and bonded specimens for both incremental and single-load cycle cracking using several crack-length-independent specimen geometries developed here. Assuming self-similar cracking is a worst case condition, the predominant shear loading of bonds requires the analysis of crack extension in both specimen and structure where loading is a mix of Modes I, II and III. A Mode II-Mode I specimen developed here (cracked lap shear, CLS) and used in a number of test programs does show self-similar crack extension, however, the ratio of Mode I to Mode II has not been solidly established. A newer crack length independent specimen, mostly Mode III, the Modified-Zero-K-Gradient (MZKG) specimen has also been tested and does exhibit self-similar cracking but analysis of this specimen for the ratio of Mode I to Mode III has not been uniquely defined.

Three dimensional finite element analysis has been run using SUPERSAP with the CLS specimen, using the 20 node, isoparametric, quarter point, singular element technique, that substantially shortens analysis time. Runs have been made using properties for metal adherends analysis time. Runs have been made using properties for metal adherends and dimensions specified by NASA-Langley in the "round-robin" finite element analysis program for this specimen. It should be noted that for short, thick adherends the specimen is no longer crack-length-independent.

Similar 3-D analysis using SUPERSAP has also been started with the MZKG specimens using dimensions for the aluminum adherend specimens described in the testing program.

Additional analysis on both specimen types is being carried out using ABAQUS. Preliminary runs have been made with the CLS and the MZKG specimen is scheduled for running later in the month. The advantage of ABAQUS is that the adhesive/adherend interaction can be modelled more closely than with SUPERSAP. It is expected that this technique will be used to analyze bonded structural elements that fail by self-similar-cracking in order to determine the effectiveness of the modelling study.

X-RAY PHOTOELECTRON SPECTROSCOPY (XPS) ANALYSIS OF FRACTURE  
SURFACES OF ADHESIVELY BONDED GRAPHITE FIBER  
REINFORCED POLYIMIDE COMPOSITES

by

J. P. Wightman, T. A. DeVilbiss, T. A. Furtsch, R. Lustig,  
D. L. Messick and D. J. Progar\*, K. A. Sanderson and P. R. Young\*  
Virginia Tech  
Center for Adhesion Science  
Department of Chemistry  
Blacksburg, VA 24061

\*NASA Langley Research Center  
Materials Division  
Hampton, VA 24065

Graphite fiber reinforced polyimide composites prior to adhesive bonding were pretreated in a number of different ways including mechanical, chemical and irradiation. SEM/XPS analysis of the pretreated composite surfaces was made prior to bonding. Significant differences were detected by XPS in the concentration of surface fluorine following the different pretreatments. The source of the fluorine is localized in the composite surface as deduced from depth profiling using Auger electron spectroscopy. Fluorine is presumably introduced onto the composite surface during the fabrication process. Critical surface tensions of the pretreated composites were determined from contact angle measurements using the Zisman method. A linear inverse correlation was noted between the fluorine concentration and the critical surface tension. XPS derivatization studies were made on surfaces of the delaminated composite. Surface functional oxy-groups were identified using this technique. Complementary reflectance FT-IR spectroscopy supported assignments based on the derivatization technique.

The composite panels were subsequently bonded with LARC-160 polyimide adhesive. Lap shear strengths were measured initially and after thermal aging up to 450°F for up to 1000 hrs. SEM/XPS analysis was made on each fracture surface. The initial lap shear strengths of the bonded composites were independent of surface pretreatment and hence independent of the surface fluorine concentration. Indeed, fluorine was not detected by XPS on the fracture surfaces of the unaged composites. Presumably, the fracture plane did not coincide with the original bonding plane.

SEM/XPS analysis was done on the thermally aged composites following lap shear fracture. The predominant failure mode was assigned based on SEM analysis. Fluorine was again detected on the fracture surfaces and significant differences were noted in the fluorine concentration. It is suggested that the fracture plane after thermal aging was close to the original bonding plane. The lap shear strength after thermal aging was dependent in part on the pretreatment. SEM/XPS results were also obtained for resin-rich composites.

## A MECHANICS MODEL FOR CRAZES

by

Yechiel Weitsman  
Texas A&M University,  
Department of Civil Engineering  
College Station, TX 77843

Crazes are thin, elongated defects that develop in many polymers. Although resembling cracks in their geometric configuration, namely length to thickness ratio of  $O(10^3)$ , crazes consist of interconnected voids that are transversed by thin fibrils which span the gap between opposite faces of the bulk polymer. These fibrils transmit substantial loads, thereby reducing the "craze opening displacement" to about one tenth of the opening displacement of a crack of equal length.

The present model represents the fibrils as a continuously distributed spring. The response of this spring may be linearly or non-linearly elastic, as well a viscoelastic. In addition the spring may have different responses during loading and unloading. All those possibilities were evaluated in accordance with available data. The surrounding bulk polymer was considered to be linearly elastic, or linearly viscoelastic.

The formulation of the boundary value problems for a single craze in an extended surrounding medium, subjected to uniformly distributed remote load, was cast in the form of a singular integral equation, akin to the case of a crack. The selected type of craze response determines the form of the boundary condition along the craze-region.

Solutions were obtained by reducing the Cauchy-type singular integral equation to a Fredholm integral equation with a logarithmic singularity. The latter equation was then solved numerically.

It was found that, for typical crazes, the stress intensity factor is substantially smaller than the stress intensity in an equivalent crack, namely  $K_{\text{craze}} \sim 1/5 - 1/4 K_{\text{crack}}$ . This value of  $K_{\text{craze}}$  does not vary noticeably even if the craze contains a central crack which extends over half of the craze's length. A possible criterion for craze growth is the existence of a stress intensity factor of critical magnitude. Such a criterion would explain the well known observations of crazes that grow in the absence of cracks, thus disassociating the analysis of craze behavior from fracture mechanics - to which it was artificially related in many previous investigations.

References:

Walton, J.R. and Weitsman, Y., "Deformation and Stress Intensities Due to a Craze in an Extended Elastic Material". Journal of Applied Mechanics, ASME (To appear Mar. 1984).

Weitsman, Y., "Viscoelastic Effects on Stresses and Stress Intensities in Crazes". In Recent Developments in Applied Mathematics, F.F. Ling and I.G. Tadjbakhsh, Editors, Rensselaer Press, 1983, pp. 220-234.

Weitsman, Y., "Non-Linear Analysis of Crazes". Forthcoming.

## GROWING CRACK IN A VISCOELASTIC ANISOTROPIC SOLID

by

M. Dahan

Laboratoire de Mecanique Appliquee, Faculte des Sciences  
F. 25030 - Besancon, France

The increasing utilization of polymers and the necessity to take into account the viscosity of the metals at high temperatures have led to the study of the fracture mechanics of viscoelastic materials. Most particular solutions concern a fixed crack, however the research of Atkinson and List (1972), Tsai (1980), has shown that, for a moving crack, the stress intensity factor is a function of the propagation speed and consequently of the material properties and the load. These applications of fracture problems have given rise to special studies in the whole range of isotropic viscoelasticity theory.

Today, with the increasing utilization of composite materials, a solution for an anisotropic medium must be found. We have shown (Dahan and Predeleanu, 1983) that two important classes of composites: the fiber-reinforced composite with fibres arranged hexagonally and the laminated medium are equivalent to homogeneous transversely isotropic solids exhibiting linear viscoelastic effects such that the instantaneous elastic response and Poisson ratios are time-invariable and the time-behavior in dilatation and shear deformation are similar. For this class of viscoelastic anisotropic materials the different compliances are written in the form  $C_{ij}(t) = c_{ij} g(t)$ .

This paper presents a closed form solution of the quasi-static propagation of a central crack when an arbitrary loading is applied on the crack surfaces. Using the techniques of Hankel transforms, the solutions are obtained and written down in terms of the sum and the difference of the characteristic roots, so that the results can easily be seen as real valued functions for both real and complex roots. In the case of a crack running at a constant speed under uniform pressure, the exact displacement distribution is given as the sum of the associated static solution and a dynamic term which depends on the viscoelastic model.

References

1. Atkinson, C., and List, R. D., "A Moving Crack Problem in a Viscoelastic Solid", Intl. J. Engng. Science, Vol. 10, 1972, pp. 309-322.
2. Dahan, M. and Predeleanu, M., "The Hertz Problem for an Axisymmetrical Indenter and a Viscoelastic Anisotropic Composite Material", Fibre Science & Technology, Vol. 18, 1983, pp. 301-315.
3. Tsai, Y. M., "Viscoelastic Effects in the Propagation of a Central Crack", Intl. J. Fracture, Vol. 16, 1980, pp. 385-395.

ANALYSIS OF PSEUDO-ELASTIC MATERIAL DAMAGE AND CRACK  
GROWTH USING STRAIN ENERGY DENSITY THEORY

by

Peter Matic  
General Dynamics Corporation  
Electric Boat Division  
Groton, CT 06340

and

George C. Sih  
Lehigh University  
Institute of Fracture and Solid Mechanics  
Bethlehem, PA 18015

Nonlinear structural response is the result of material yielding and/or fracture. Traditional methods of structural response address these two aspects of material behavior by separate failure criteria. In fact, yielding and fracture are intimately related by microstructural processes which dissipate energy and alter the load response of the material.

This investigation presents a failure criterion for which both yielding and fracture are based on the absorbed strain energy density  $(\Delta W/\Delta V)$ , of the material. The fundamental hypotheses of the criterion are used to generate a particular class of material behavior, in this case a pseudo-elastic behavior. The resulting model monitors the material damage and response from initial yield, at energy  $(\Delta W/\Delta V)_y$ , to final fracture, at energy  $(\Delta W/\Delta V)_c$ . Increasing levels of strain energy density beyond initial yield are associated with decreasing local stiffness, as obtained from the uniaxial stress-strain response of the material. The failure criterion is incorporated into finite element procedures which allow for yielding and crack growth at each specified load increment.

The criterion is used to numerically evaluate the influence of differing material toughness values,  $(\Delta W/\Delta V)_c$ , on two center cracked panel specimens which are otherwise identical. The nonlinear response, crack growth and failure loads of each panel are quantitatively evaluated by numerically suppressing, in turn, the yielding and fracture portions of the analysis. The high toughness panel sustains higher loads prior to final crack instability and failure. The global nonlinear load-displacement response of the panels are dominated by yielding, as apposed to fracture, in both panels for the material behavior considered. In the case of the high toughness panel, however, this is true to a greater degree because of the broader range of material nonlinearity between initial yield and fracture.

The failure criterion is then used to address the problem of scaling structural component behavior. Structural behavior is known to be influenced by material selection, geometry and size, and loading rate because energy dissipation rates are sensitive to these factors. Twenty-seven axisymmetric tensile specimens are numerically analyzed to parametrically examine three materials, three loading rates and three specimen sizes. Simple design procedures are obtained using the linear nature of the strain energy density factor (which characterizes the crack tip region) versus crack growth relation. Changes in specimen size are seen to produce translation of these lines parallel to one another, while material and loading rate influence the slopes and intersection points.

## A MESH ADAPTIVE METHOD FOR MODELING SLOW CRACK GROWTH

by

E. Thomas Moyer, Jr. and Harold Liebowitz  
School of Engineering and Applied Science  
The George Washington University  
Washington, D.C. 20052

The accurate modeling of slow crack growth requires the coalition of a careful stress analysis, a consistent crack growth criterion (or constitutive relation) and a numerical scheme which continually redefines the crack position and size. The numerical scheme employed must account for the local unloading and stress redistribution near the crack during the growth process.

Traditionally, the numerical schemes used to simulate crack growth either did not address the local unloading [1] (accurate for very low load levels only) or required a mesh density such that the crack tip element size corresponded exactly to one growth step (e.g., [2]). Other, more recent models employ springs at nodal points whose stiffness can be relaxed during the growth process (e.g., [3]). This approach has yielded extremely limited success and requires a nodal spacing consistent with the growth incrementation. The major drawback the methods employed to date is that the growth incrementation must be known a priori. Much of the work also couples the crack growth criterion and the mesh spacing into the same model making assessment of the validity of either impossible.

A new method is presented in this work which alleviates the drawbacks of the schemes described above. A standard elastic-plastic stress analysis is performed to the load at the initiation of crack growth. The load is then increased slightly. The amount of crack growth is then predicted corresponding to the current load level (the method will work with any fracture criterion). The near crack mesh is convected to the new location of the crack tip. The stress along the new section of crack is relaxed to zero and an update is made in the stress analysis. Finally, the new stress state is extrapolated to the current grid geometry. The process is repeated for each increment of crack growth.

An example problem in 2-dimensions is considered. A thin (.0625 inch) 2024 aluminum panel with a central crack is loaded uniaxially. The experimental Load vs Crack Growth curve is used to dictate the crack growth incrementation (this approach tests the validity of the numerical method independent of the fracture criterion). The load-displacement relation is predicted by the numerical method and compared to the experimental record. Three refinements of crack incrementation are employed to assure convergence. The

results show good agreement with the experimental load-displacement record.

By employing the technique described above, it is possible to test various fracture criteria for slow crack growth. These studies (to be reported subsequently) allow for a separation of numerical and mechanical growth modeling which is essential for delineating the validity of predicted results.

While the example presented in this work is 2-dimensional, the method will apply equally well in three-dimensions. Since larger, high order elements are employed, crack growth studies in 3-dimensions should be possible with current computer resources. The extension of nodal force release techniques to 3-dimensions requires far to many elements (for accurate modeling) to be solved with today's resources.

#### ACKNOWLEDGMENT

This work was sponsored by the Office of Naval Research under Contract #N00014-84-K-0027.

#### REFERENCES

- [1] Sih, G. C. and Moyer, Jr., E. T., "Path Dependent Nature of Fatigue Crack Growth", J. of Eng. Frac. Mech., Vol. 17, No. 3, 1983, pp. 269-280.
- [2] Lee, James D. and Liebowitz, Harold, "Considerations of Crack Growth and Plasticity in Finite Element Analysis", J. of Comp. and Struc., Vol. 8, No. 3/4, 1978, pp. 401-403.
- [3] Gifford, L. N. and Hilton, p. D., "Preliminary Documentation of PAPST - Nonlinear Fracture and Stress Analysis By Finite Elements", NDW-DTNSRDC 3960/43b, Feb. 1981.

A MICRO-MECHANICAL APPROACH TO THE ENVIRONMENTAL  
INFLUENCE ON FATIGUE CRACK PROPAGATION

by

K. S. Bae, P. K. Mazumdar and H. Conrad  
North Carolina State University  
Department of Materials Engineering  
Raleigh, North Carolina 27650

Fatigue crack propagation (FCP) is intimately related to localized plastic deformation, the prime effect of which is to form a cyclic plastic zone (CPZ) consisting of dislocation substructures (e.g. cell structures), which largely govern the material properties near the crack tip. Any degradation in the FCP behavior of a material due to the presence of an environment must therefore result from changes in the local material properties arising from a modification of the scale of the localized plastic deformation and thereby the extent of CPZ and the morphology of the dislocation substructures. Accordingly, a model for FCP rate ( $d\ell/dN$ ) has been developed giving

$$d\ell/dN = a(1/R_p)^m d \Delta K^n \quad (1)$$

$a$ ,  $m$  and  $n$  are constants which should be dependent upon the environment,  $R_p$  and  $d$  are the size of the CPZ and the dislocation cell size, both of which contribute to the near crack tip strengthening/weakening behavior. Equation 1 has the form of Paris' equation and has the advantage of being more fundamental for the purpose of analysis.

The FCP behavior in 316 stainless steel in naphthenic acid (an aggressive environment) and in silicone oil (an inert environment) are examined in the light of the above model. A decreased FCP rate in the silicone oil environment compared to the naphthenic acid environment was observed and found to be associated with (i) an increase in the near crack tip hardness (an indication of the strengthening effect), and (ii) an enlarged CPZ (an indication of the large amount of deformation). These observations are consistent with the above model. Studies on the morphology of the dislocation cell structures are underway. The importance of the size of the CPZ, dislocation cell size and local strengthening/weakening behavior will be discussed in interpreting the influence of environment on the FCP behavior of metals.

This research was supported by DOE Contract DE-FG22-80PC30236.

## AN ELASTIC-PLASTIC MODEL FOR MULTIAXIAL CYCLIC BEHAVIOR

by

Chin-chan Chu  
Metallurgy Dept., Ford Motor Comp.,  
P.O. Box 2053, Dearborn, MI 48121, USA

An elastic-plastic constitutive equation [1], derived from the generalized Mroz concept for anisotropic hardening, is utilized here to show its applicability in multiaxial fatigue behavior analysis. The model uses only classical plasticity theory assumptions which include the convexity of the yield surface and a universal stress-strain curve. It results in a simple incremental stress-strain relationship ( $d\epsilon = L: d\sigma$ ) similar to that of classical flow theory:

$$d\epsilon = d\epsilon^{el} + \frac{3}{2} \left( \frac{1}{E_t} - \frac{1}{E} \right) \frac{\xi: d\sigma}{k} \left[ 8 \left( \frac{\partial f}{\partial \xi} \right) \right]^{-1/2} \frac{\partial f}{\partial \xi},$$

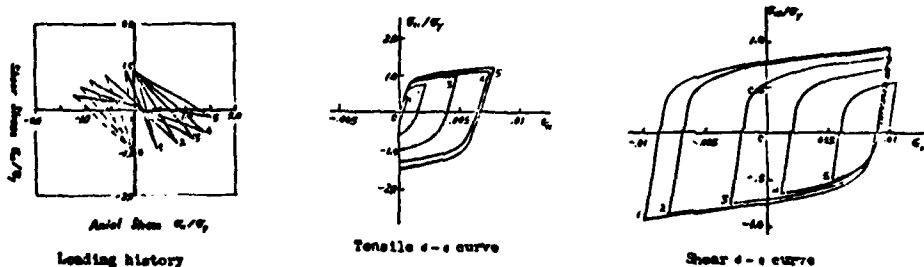
where  $k$  is the effective stress as well as a measure of the size of the yield surface. The latter in the deviatoric stress space is represented by

$$f(\xi) - k^2 = 0, \text{ with } \xi = s - \underline{q}.$$

Here  $f$  is the yield function,  $s$  is the deviatoric stress tensor and  $\underline{q}$  denotes the reference position such as the center of the yield surface. Corresponding to the yield function  $f$ ,  $g$  is found a function of  $d\epsilon^p$  defining the equivalent plastic strain increment. Also in equation (1),  $E_t$  and  $E$  are the tangent and Young's modulus respectively defined by the universal stress-strain curve. Equation (1) can thus be easily applied to complex geometric problems by means of the finite element method. The only extra effort required in such an application is to keep updated information on the active yield surfaces for each material element. Two complicated tension-torsion testing processes on cylindrical tubes [2] are simulated to evaluate the constitutive model. Comparisons between the theoretical prediction (as shown in the figures) and test results show very good agreement.

[1] C. Chu, J. Mech. Phys. Solid (1984) (in print).

[2] H. S. Lamba and O. M. Sidebottom, J. Eng. Mat. Tech. Trans. ASME 100, 96 (1978).



CUMULATIVE STRESS CONCENTRATION EFFECTS  
ON FATIGUE LIFE

by

Mohammad A. Hassibi

and

Bashir A. Sayar

Mechanical Engineering Department

South Dakota State University

Brookings, SD 57007

Fatigue failure of structures and machine components with stress raisers subjected to repeated loading represents one of the most unpredictable class of problems in engineering. The effects of various shapes and sizes of stress raisers under different types of static loads have been investigated in sufficient detail. Such studies show that stress concentration arising from the existence of multiple grooves is not always greater than that produced by a single groove. At times, it may be advantageous to form additional grooves close to an existing one in order to even the stress distribution at a particular section. At other times, it may be equally possible that presence of several grooves increase the stress concentration. What determines the cumulative stress concentration effect has been shown to be related to the relative location of the additional grooves (1).

Although various theoretical stress concentration factors  $K_t$ , are available for static loading, data on dynamic stress concentration factor  $K_f$ , is very limited. It is hoped that the results of this investigation shed further light on the subject and contribute to the better understanding of this phenomenon. The meager information available indicates that cumulative results of two stress concentration factors are ranged from 0.85 to 1.12 times the product of both factors (2).

This paper will present the result of investigation on fatigue loading of 100 SAE 1010, cold worked cantilever type specimen, with various combinations of 1/8 inch diameter holes and semi circular notches. The final results will determine if there are any possible relations among the  $K_f$ 's obtained from this study.

References:

1. Sors. L., "Fatigue Design of Machine Components", Pergamon Press, New York, NY, 1971.
2. Mowbray Jr., A. Q., "The Effects of Superposition of Stress Raisers on Members Under Static or Dynamic Loads". Proc. of the Society for Experimental Stress Analysis, Vol. No. 2, 1953.

## SOME RESULTS OF FATIGUE TESTS ON A BRITTLE POLYMER

by

Vernal H. Kenner

Department of Engineering Mechanics  
The Ohio State University  
Columbus, OH

Charles Y.-C. Lee

Air Force Materials Laboratory  
Wright-Patterson AFB, OH

Fatigue tests have been conducted on a brittle polymer frequently employed as a composite matrix material, EPON 828. The tests have utilized a miniature compact tension specimen, approximately 25-mm-square in plan dimensions, which has already been evaluated for the purpose of ascertaining fracture toughness in new polymers produced in very limited quantities. The servohydraulic loading system employed in the tests was controlled by a laboratory computer which was also used to collect and manipulate output data. Tests were conducted at 20 Hz and the ratio R of minimum to maximum load was nominally 0.1. The crack growth rate data for EPON 828 fit the well known Paris equation

$$da/dN = C(\Delta k)^n,$$

where  $da/dN$  is the crack advance per cycle,  $\Delta k$  is the cyclic change in stress intensity factor, C is a constant and n is an exponent associated with the material. In the case of EPON 828, n is quite high, in the neighborhood of 11.

For these tests the small specimen size required that the minimum value of the applied cyclic load be in the neighborhood of 4N. At such low loads apparently normal variations in test machine output cause the value of R to vary during the course of a test from the selected value, e.g.,  $0.11 < R < 0.26$  during one particular test. However, the continuous collection of test data by the computer permits the calculation of R,  $\Delta k$  and  $da/dN$  during each interval between crack length measurement and thus provides for correlation of crack growth rate with both  $\Delta k$  and R. Our data show that crack growth rate is significantly affected by relatively small changes in R. Preliminary results indicate that the R dependence of crack growth rate for EPON 828 can be reasonably fitted to a modified form of the Paris equation, namely,

$$da/dN = C(\Delta k)^n R^m.$$

Our data indicate that the exponent m is approximately equal to 5.

## DAMAGE TOLERANCE AND DURABILITY OF COMPOSITE AIRFRAME STRUCTURE

by

Lawrence W. Rehfield  
Center for Rotary Wing Aircraft Technology  
School of Aerospace Engineering  
Georgia Institute of Technology  
Atlanta, GA 30332

The next generation of military aircraft, particularly fighters and helicopters, will have large percentages of their structural weight in advanced composite materials. The new, expanded uses of composites will be in fuselage structures as current designs already exhibit largely composite lifting surfaces and rotor systems. The resistance of airframes to damage from manufacturing defects, service usage and weapons is of great, immediate concern, therefore.

The United States Air Force and Army are in the midst of damage tolerance and durability programs for composite structures for fighters, transports and helicopters. The rationale behind these programs will be described and the issues being addressed will be discussed. Particular emphasis will be given to interlaminar fracture or delamination and its prevention.

TWO-MODE BUCKLING OF VON KARMAN PLATES UNDER COMPRESSION:  
AN APPLICATION OF DOUBLE CUSP CATASTROPHE

David Hui  
The Ohio State University  
Department of Engineering Mechanics  
Columbus, OH 43210

This paper deals with the two-mode initial post-buckling behavior of isotropic homogeneous rectangular plates under axial compression. The plates are simply supported along all four edges and the two competing buckling modes are identified by  $m=n=1$  and  $m=2, n=1$  respectively, where  $m$  and  $n$  are the number of axial and transverse half sine-waves in the  $x$  and  $y$  directions. The aspect ratio at which the above two-mode buckling occurs simultaneously is found to  $L/B=(2)^{1/2}$ . Using Budiansky-Hutchinson's notation, the appropriate postbuckling coefficients are computed and the equilibrium equations of the two-mode buckling problem is found to be of the form of a Double-Cusp Catastrophe. The unfolding parameters include the amplitudes of the geometric imperfections in the form of each of these two modes and the applied load imperfections in the in-plane  $x$  and  $y$  directions. Other unfolding parameters in the form of small lateral loads are discussed.

The analysis is studied based on a solution of Von Karman equilibrium and compatibility equations for rectangular plates valid for moderately large deflections, written in terms of an out-of-plane displacement  $W$  and a stress function,  $F$ , in the form, respectively [1],

$$(D)(W_{,XXXX} + W_{,YYYY} + 2W_{,XXYY}) = F_{,YY}W_{,XX} + F_{,XX}W_{,YY} - 2F_{,XY}W_{,XY}$$

$$[1/(Eh)](F_{,XXXX} + F_{,YYYY} + 2F_{,XXYY}) = (W_{,XY})^2 - W_{,XX}W_{,YY}$$

Using a perturbation technique within the context of Koiter's theory of elastic stability, the two equilibrium equations valid for sufficiently small values of the imperfection amplitudes are [1],

$$b_1 \xi_1^3 + b_{12} \xi_1 \xi_2^2 + [1 - (\sigma/\sigma_1)] \xi_1 = (\sigma/\sigma_1) \bar{\xi}_1$$

$$b_2 \xi_2^3 + b_{21} \xi_1^2 \xi_2 + [1 - (\sigma/\sigma_2)] \xi_2 = (\sigma/\sigma_2) \bar{\xi}_2$$

After some lengthy computations, it is found that  $b_1 = b_2 = 5c^2/36$  where  $c = [3(1-\nu^2)]^{1/2}$  where  $\nu$  is Poisson's ratio. For  $\nu = 0.3$ , one obtains,  $b_1 = b_2 = 0.3791667$  which seems to be in disagreement with the result presented by Magnus and Poston [2]. Appropriate critical surfaces of the Double Cusp Catastrophe are plotted.

- [1] Hui, D., "Effects of Mode Interactions on Collapse of Short, Imperfect Columns", *J. of Appl. Mech.*, Vol. 51, Dec. 1984 (ASME Winter Annual Meeting, New Orleans, 1984).
- [2] Magnus, R. J. and Poston, T., "On the Full Unfolding of the Von Karman Equation at a Double Eigenvalue", Mathematics Report 109, Battelle, Geneva, 1977.

ARCHEMATICS AND UNFOLDINGS OF THOM'S THEOREM:  
SOME APPLICATIONS OF THE THEORY OF STRUCTURAL STABILITY

by

Giovanni Chiriatti, Fiorenzo Ferlaino, Manfredo Montagnana  
Giacinto Plescia, Alessandro Porcu  
Department of Mathematics  
Politecnico of Torino  
10129 Torino, Italy

Thom's theory of elementary catastrophes forms a system of topological morphogenesis (1,2,3) which has already been used in various applications. But the semantics encountered in previous works has required more pregnant logos shapes. We could have got over the lack of generalizations of Thom's classification theorem, by considering infinitesimal morphogenetic changes (4,5,6). However, this would have broken the isology with the semantics, as it happens for combinatorial logics in informatics.

Hence we suggest a theory that connects the catastrophic system of structural stability with the catastrophic 'syntagma' defined in (9,10), by means of transversal manifolds. The elementary classification form shall be

s	F(oid)	F'	F''	systems of Thom,
y	C(usp)	C'	C''	Arnol'd, Petitot,
n	S(wallowtail)	S'	S''	Aleksandrov, etc.
t	B(utterfly)	B'	B''	
a	H(yperbolic umbilic)	H'	H''	
g	E(lypticumbilic)	E'	E''	
m	P(arabolic umbilic)	P'	P''	
a				

The only syntagma yet formalized is the catastrophic spiral, obtained by connecting syntagmatic units, paradigms of a system. The result was gained by exploring possible connections among the elementary catastrophic manifolds; these connections suggest transversal manifolds, such as spirals, helicoids, bifurcations, new polyhedral manifolds, which are isologic to the semantic archetypes.

The manifolds may be crossed by a spatial chiasmus which regulates their equilibria. The 'changing lemma' models the variance archetype, that moves across syntagmatic units or paradigmatic manifolds developed into different systems. The theory is still at a topological stage, but it could be the outset of a catastrophic syntagmatic logic useful in reaching consistency in many scientific applications: unification of forces in physics; moving genes in biology, overcoming the classical DNA helicoidal model; qualitative dynamics of biochips; microcellular catabolias; biological space models relative to creativity and imagination.

The authors have already partially used the syntagmatic theory of elementary catastrophes while modelling the effects of technological innovations on post-industrial space (7,8,9,10,11). Further work is proceeding on problems concerning: spatial desirability in productive and reproductive units; housematic

design, paradoxes in natural and artificial perception; aesthetical morphologies in science and art.

Thom's project of turning his theory on structural stability from one among many formal models into a qualitative "language" for all sciences, may be about to reach the stage of achievement.

#### References

1. Thom, R., Structural Stability and Morphogenesis, London, 1975.
2. Thom, R., Modeles Mathematiques de la Morphogenese, Paris, 1974.
3. Thom, R., "Topological Models in Biology", Towards a Theoretical Biology, II, 1, Drafts, 1968.
4. Arnol'd V.I., Singularity Theory, London, 1981.
5. Aleksandrov, A. G., "Normal Forms of One-Dimensional Quasihomogeneous Complete Intersections", Moscow, 1983.
6. Petitot Cocorda, J., Identite et Katastrophe, Paris, 1977.
7. Chiriatti, G., Plescia, G., Porcu, A., "Allosteresi Industriale e Sinecismo Morfogenico", Notiziario UMI, No. 5, 1980.
8. Chiriatti, G., Montagnana, M., Plescia, G., Porcu, A., "Analysis of Post-Industrial Spatial Archemorphisms", AMSE, Nice, 1983.
9. Chiriatti, G., Montagnana, M., Plescia, G., Porcu, A., "Analysis of Post-Industrial Spatial Archemorphisms", AMSE, Nice, 1983.
10. Chiriatti, G., Dotta Rosso, M., Ferlaino, F., Montagnana, M., Plescia, G., Porcu, A., "Syntagmatic Archemorphisms for Post-Industrial Space", RSA Intl. Conf., Milano, 1984.
11. Chianese, L., Chiriatti, G., Dotta Rosso, M., JFerlaino, F., Montagnana, M., Plescia, G., Porcu, A., "Archetipi, Software, Modelli Tipologico-Strutturali della Progettualita nuova", P.F. C.N.R. P.E., Roma, 1984.

SIMPLE ALGORITHM TO SOLVE FOR DYNAMIC OPTIMIZATION  
OF STRUCTURES

by

Rusk Masih  
University of Hartford  
College of Engineering  
Hartford, CT 06033

INTRODUCTION AND STATE OF ART

Quite a number of algorithms have been developed to optimize a structure subjected to frequency constraint. None of them seem to be simple enough for application by industry or general enough to be applied for every case, specifically framed structures.

1. All the published research so far has failed to recognize the fact that a structure can be dynamically optimized for one mode of vibration at a time. This research recognizes this fact. Each mode would require an optimization shape different from other modes.

2. This algorithm is extremely simple, practical and powerful.

3. All the published research is for structures carrying their own structural mass, or very simple and limited cases of structures carrying non-structural mass. This research is valid for structures carrying their own structural mass as well as non-structural mass at random.

STATEMENT OF THE PROBLEM

A rectangular cross-sectional member with a variable width and depth, its structural mass is given by the integral

$$\bar{M} = \int_0^l m(x) dx = \int_0^l \rho b(x)y(x) dx \quad (1)$$

This mass is subject to dynamic constraint which is the maximum kinetic energy of the conservative system equals its maximum potential energy.

$$\int_0^l \{ \omega^2 m(x) [W(x)]^2 - EI(x) [W''(x)]^2 \} dx = 0 \quad (2)$$

Equations (1) and (2) form

$$\phi = \int \{ \rho by + \lambda [KbyW^2 - by^3(W'')^2] \} dx \quad (3)$$

where

$\lambda$  is the Lagrange multiplier

$W$  is the deflection of the member

$$\dot{W} \text{ is } \frac{\partial W}{\partial t}, \quad W'' \text{ is } \frac{\partial^2 W}{\partial x^2}$$

$I$  is the moment of inertia of the member, a function of  $x$

$E$  is the modulus of elasticity of the material

$\omega$  is the frequency of vibration.

$m$  is the mass per unit length of the member, a function of  $x$

$K$  is  $12\omega^2\rho/E$

varying  $W$ ,  $b$ ,  $y$  throughout the interval 0 to  $l$  in eq. (3) gives

$$\begin{aligned} \delta\phi = \int_0^l \{ & \rho b \delta y + \rho y \delta b + \lambda [KbW^2 \delta y + KyW^2 \delta b \\ & + 2KbyW\delta W - y^3 (W'')^2 \delta b - 3by^2 (W'')^2 \delta y \\ & - 2by^3 W'' \delta W'' ] \} dx \end{aligned} \quad (4)$$

Eq. (4), after integration by parts, yields the differential equations and boundary conditions

$$\rho b + \lambda KbW^2 - 3by^2 \lambda (W'')^2 = 0 \quad (5)$$

$$\rho y + \lambda KyW^2 - \lambda y^3 (W'')^2 = 0 \quad (6)$$

$$KbyW - (by^3 W'')'' = 0 \quad (7)$$

$$\lambda by^3 W'' \delta W' \Big|_0^l = 0 \quad (8)$$

$$\lambda (by^3 W'')' \delta W \Big|_0^l = 0 \quad (9)$$

Further integration and modifications yield the following algorithm

$$y^2 = \frac{12}{Eb} \frac{M(x)}{\left(\frac{16U}{E}\right)} = C M(x) \quad (10)$$

This result is significant; it states that optimization takes place when the depth of the member  $y(x)$  is made proportionate to the bending moment diagram values when the member is positioned at its max strain energy due to the vibration in a specific mode.

This result is valid for any boundary conditions because it was derived from the general equation of vibration without imposing any boundary conditions, and it should be valid for continuous structures as well as beams. Several examples showed convergency and considerable material saving.

## DESIGN FOR BUCKLING OF CORRUGATED STEEL GIRDER

by

M.S. Troitsky, Z.A. Zielinski and M.S. Pimprikar  
 Department of Civil Engineering  
 Concordia University  
 Montreal, H3G 1M8

In the design of plate girders, usually the web is reinforced by stiffeners to improve the buckling strength. By employing corrugation parallel to the height of the girder it is possible to eliminate stiffeners and reduce thickness of web. The available information is inadequate to provide a simplified method of design and analysis of corrugated plate girders.

This paper gives an approximate method of analysis to develop expressions defining critical force and buckling behavior. The paper is treating two cases. In the first case, analysis of a corrugated girder under influence of local concentrated load is considered. As a basis for analysis, a beam on elastic support<sup>1</sup>, with simply supported edge is considered. In the second case state of stresses of such girders under uniformly distributed load is analyzed. Fourier trigonometric series<sup>2</sup> is used to analyze the plane orthotropic plate with geometric properties characteristics of corrugated webs, subjected to uniform distributed load  $q$ .

## 1. STABILITY OF CORRUGATED WEBS UNDER CONCENTRATED LOAD:

The girder consists of three elements - two flanges and a corrugated web and loaded in a general case by concentrated load  $P$  and moment  $M$ . Considering a vertical cut along height of the girder  $h$ , such a beam is supported on an elastic foundation with the origin of coordinates at the point of application of load. The differential equation for elastic deflection of the beam is

$$\frac{d^4 y}{dx^4} + \frac{P}{D} \frac{d^2 y}{dx^2} + \frac{k}{D} y = \frac{f(m)}{D} \quad \dots (1)$$

where

$$D = \frac{E\delta^3}{12(1 - \nu^2)}; \quad \delta - \text{thickness of web}; \quad \nu - \text{Poisson's ratio};$$

$E$  = Young's modulus;  $k$  - coefficient of elasticity;  
 $f(m)$  = indicates influence of moment  $M$ .

$$\text{where } f(m) = \sum_{n=1}^{\infty} B_n \sin \frac{n\pi x}{h} \quad \text{and} \quad B_n = \frac{2n\pi}{h^2} M. \quad \dots (2)$$

Using a Fourier trigonometric series and boundary conditions under consideration, expressions for deflection  $y$  and critical force  $P_{cr}$  is obtained as,

$$y = \frac{2h^2 M}{\pi^3 D} \sum_{n=1}^{\infty} \frac{n}{C_n} \sin \frac{n\pi x}{h} \quad \dots (3)$$

and 
$$P_{cr} = \frac{E\delta^2}{R} \sqrt{\frac{1}{3(1-\nu^2)}} \quad \dots (4)$$

where  $R$  = Radius of curvature of half wave.  
 $C_n$  - non-dimensional value and  $n$  is an integer

## 2. UNDER UNIFORMLY DISTRIBUTED LOAD:

Considering a plane orthotropic plate, with directions of axes  $x$  and  $y$  superimposed on the principal directions of elasticity, elastic constants  $E_1$ ,  $E_2$ ,  $\nu_1$ ,  $G_1$  are determined by equivalence of stiffness for tension and shear of plane orthotropic plate and corrugated plate. Further, for the uniformly distributed loading condition, the stress distribution was obtained using a Fourier series. The differential equation for the stress function  $F(x,y)$  is,

$$\frac{1}{E_2} \frac{\partial^4 F}{\partial x^4} + \left( \frac{1}{G_1} - \frac{2\nu_1}{E_1} \right) \frac{\partial^4 F}{\partial x^2 \partial y^2} + \frac{1}{E_1} \frac{\partial^4 F}{\partial y^4} = 0 \quad \dots (5)$$

Solution for the differential equation (5) was obtained by determining a stress function

$$F(x,y) = \sum_{n=1}^{\infty} f_n(y) \sin \alpha x, \quad \dots (6)$$

which satisfies the differential equation and the boundary conditions.

i.e. 
$$F(x,y) = \left[ \left( U_n \cosh \frac{s n \pi y}{\ell} + V_n \sinh \frac{s n \pi y}{\ell} \right) \cos \frac{t n \pi y}{\ell} + \left( W_n \cosh \frac{s n \pi y}{\ell} + C_n \sinh \frac{s n \pi y}{\ell} \right) \sin \frac{t n \pi y}{\ell} \right] \sin \frac{n \pi x}{\ell} \quad \dots (7)$$

where  $U_n$ ,  $V_n$ ,  $W_n$ ,  $C_n$  are coefficients of the series;  $s$  and  $t$  - roots of the characteristic equation,  $\ell$ -span of girder. Solution of equation (7) was obtained in terms of function  $\phi_1$ ,  $\phi_2$ ,  $\phi_3$ . Thus knowing constants of loading series and functions  $\phi_1$ ,  $\phi_2$ ,  $\phi_3$ , normal and tangential stresses at the top and bottom flanges and web junction are calculated using basic equations of elasticity.

## 3. CONCLUSIONS:

A simplified method for analysing a corrugated steel girder subjected to local concentrated loads and uniform loadings is presented. Equations (3) and (4) provide deflection and critical force for a corrugated girder under local concentrated load. Stresses in web and flanges of the girder under uniform loading are determined using stress function given by equation (7).

## REFERENCES:

1. Timoshenko, S.P., Strength of Materials Part II Advanced Theory and Problems, D. Van Nostrand Co. Inc. New York, 1956, pp. 1-15.
2. Pilon, L.N.G, Solution for stresses by means of trigonometric series, Transactions of Royal Society (London), Series A, Vol. 201, 1903, p. 63.

APPLICATION OF THE RAYLEIGH-SCHMIDT METHOD TO PROBLEMS  
OF NONUNIFORM-COLUMN BUCKLING AND PLATE  
BENDING, BUCKLING, AND VIBRATION

by

Charles W. Bert  
The University of Oklahoma  
School of Aerospace, Mechanical and Nuclear Engineering  
Norman, OK 73019

Recently, Schmidt introduced a new version of the well-known Rayleigh method<sup>1</sup>. He applied the method to a variety of problems including elastic torsion, buckling, and vibration<sup>1-4</sup>.

Here, the efficiency of this method for obtaining improved upper-bound estimates of buckling loads and natural frequencies is demonstrated. The method is considerably more accurate than the familiar Rayleigh method, with only a small amount of additional computation. Also, the method requires much less computation than collocation, finite difference, boundary integral, and finite element methods. It is demonstrated here for the first time that this new method can be especially accurate when applied to the complementary energy approach (Timoshenko bound) rather than the more widely used potential energy method (Rayleigh quotient).

Problems which are solved very efficiently and accurately in this paper include:

1. Stepped columns
2. Smoothly tapered columns
3. Deflection of a point-loaded circular plate resting on an elastic foundation
4. Buckling of a circular plate resting on an elastic foundation
5. Free vibration of a circular plate of varying thickness

In each problem, the results are compared with those obtained previously by exact or approximate methods or experimentally.

References

1. Schmidt, R., "A Variant of the Rayleigh-Ritz Method," Industrial Mathematics, Vol. 31, 1981, pp. 37-46.
2. Schmidt, R., "A Method for Estimating Torsional Rigidity of Prismatic Bars," Industrial Mathematics, Vol. 32, 1982, pp. 133-136.
3. Schmidt, R., "Estimation of Buckling Loads and Other Eigenvalues via a Modification of the Rayleigh-Ritz Method," ASME Journal of Applied Mechanics, Vol. 49, 1982, pp. 639-640.
4. Schmidt, R., "Technique for Estimating Natural Frequencies," Journal of the Engineering Mechanics Division, Proc. ASCE, Vol. 109, 1983, pp. 654-657.

STABILITY CHARACTERISTICS OF UNIFORMLY LOADED FLEXIBLE BARS  
OF BI-LINEAR MATERIALS BEHAVIOR

by

Gilbert Lewis<sup>+</sup>, and Frank Monasa\*  
Michigan Technological University  
Houghton, Michigan

Flexible bars having a small flexural rigidity, form a curve with large deflections and slopes when subjected to loads. Therefore, geometrical nonlinearity arises and the solution of the problem must be formulated according to the nonlinear theory of bending. Applications of the nonlinear bending theory to flexible struts have been confined to linear elastic materials only (1). The objective of this paper is to present the solution for the finite deflections, slopes, and the stability and post-buckling behavior of vertical cantilever struts of bilinear materials behavior and subjected to uniformly distributed loads. Figure 1 shows a vertical strut of rectangular cross-section and of length  $L$ . A point  $(x,y)$  on the deflected central axis of the strut can be identified by the  $x$  and  $y$  coordinates, or the arc length  $s$  and the angle of rotation  $\theta$ .

The solution of this problem is formulated according to the nonlinear theory of bending, and the exact expression of the curvature of the central axis of the strut must be used in the moment-curvature relationship. The resulting nonlinear differential equations are solved numerically using a fourth-order Runge-Kutta technique. The validity of the numerical solution will be examined by comparing the deflections and slopes of flexible struts of linear materials, obtained by using the numerical solution developed in this paper, with previously published results. Vertical and horizontal deflections as well as the rotations of the central axis of struts of bi-linear materials behavior will be tabulated or represented graphically. Also, the stability and post-buckling characteristics of these struts will be examined.

- (1) Frisch-Fay, R., Flexible Bars, Butterworth & Co., Ltd., London, 1962.

---

+ Associate Professor, Department of Mathematical and Computer Sciences

\* Professor, Department of Civil Engineering.

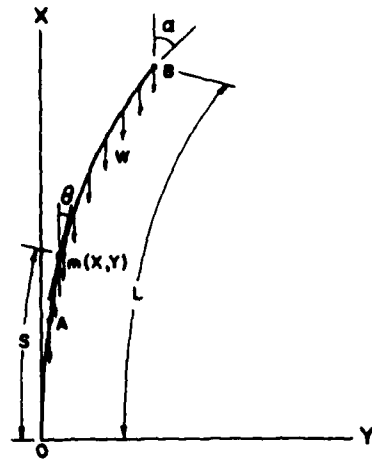


Figure 1 - Deflected shape of a slender strut

## CIRCULAR ARCH BUCKLING DUE TO RADIAL AND SHEAR LOAD

by

Victor Maderspach  
Associate Professor  
Department of Engineering Science & Mechanics  
Virginia Polytechnic Institute & State University  
Blacksburg, VA 24061

In this paper we present solutions for the problem of instability of circular rings subjected to different, but symmetrical radial and shear loads. The problem arises in connection with the design of wind stiffening girders of large cylindrical tanks. The designers of such tanks want to have an answer to the following question: will the ring buckle due to the wind load acting on the shell before the bending stresses developed in the stiffening ring exceed the maximum allowable limit? It is decided on the basis of measurements made on the shell that the problem could be narrowed to the study of a circular arch with frictionless pin supports at both ends, and acted upon by symmetrically distributed radial and shear loads. A governing differential equation with variable coefficients is set up, but no analytical solution is attempted due to the complexity of the functions involved. A finite difference approach is used for specific loading and boundary conditions. The results are compared with the results obtained by other investigators, and the discrepancies are explained by the different fundamental assumptions used in the different investigations. It is found in all cases that failure due to bending would occur in the stiffening ring before it would become unstable. The critical buckling load with different loads and supports is shown in Table 1.

## CRITICAL BUCKLING LOAD WITH DIFFERENT LOADS AND SUPPORTS

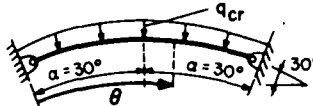
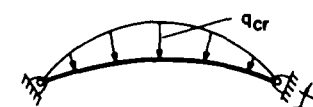
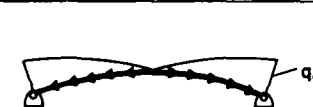
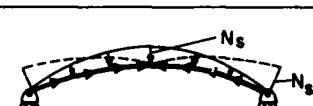
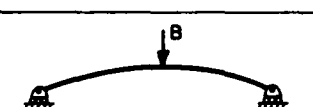
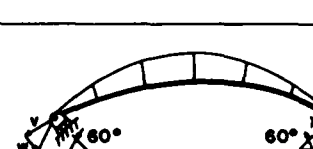
ITEM	FOR ALL CASES: $E = 30(10)^6 \text{ psi}$ $R = 1680 \text{ in.}$ $I = 10 \text{ in}^4$ $\alpha = 30^\circ$	
1		UNIFORMLY COMPRESSED CIRCULAR ARCH $q_{cr} = \frac{EI}{R^3} \left( \frac{\pi^2}{\alpha^2} - 1 \right) = 2.21 \text{ lb/in.}$
2		RADIAL LOAD ONLY $q_{cr} = 3.425 \sin \frac{\pi}{2\alpha} \theta$
3		RADIAL LOAD ONLY, DIFFERENT SUPPORT $q_{cr} = 6.42 \sin \frac{\pi}{2\alpha} \theta$
4		SHEAR LOAD ONLY $q_{cr} = 10.63 \cos \frac{\pi}{2\alpha} \theta$
5		RADIAL AND SHEAR LOAD $N_s = B \sin \frac{\pi}{2\alpha} \theta$ $\lambda = 1$ $B_{cr} = 9.63$ $N_{s\theta} = \lambda B \cos \frac{\pi}{2\alpha} \theta$ $\lambda = 1.5$ $B_{cr} = 12.84$ $N_{s\theta} = \lambda B \cos \frac{\pi}{2\alpha} \theta$ $\lambda = 2.9$ $B_{cr} > 100$
6		CONCENTRATED FORCE ONLY $B_{cr} = 10.614 \text{ lb}$
7		RADIAL LOAD WITH THE MOST REALISTIC SUPPORT CONDITIONS $ v  > 2 w $ No buckling!

TABLE 1

A MODEL FOR THE BUCKLING AND THE  
STABILITY OF THIN ELASTOPLASTIC PLATES

by

T. Hadhri  
Centre de Mathematiques Appliquees  
Ecole Polytechnique  
Cedex France

In this paper we present two mathematical models which yield some mechanical aspects of thin elastoplastic plates bending.

The first model proves insufficient if we keep up the classical Sobolev spaces framework.

With the second model, an existence result for the transverse displacement problem formulation is obtained when the load does not exceed a critical value defined below.

The study of the stability problem leads us to differentiate a projector on a closed convex set which is a difficult question; nevertheless, we introduce an hypothesis of regularity of the solution of some plasticity problem, and we show the existence of a critical load under which we have stability, in some sense.

REFERENCES

- Hadhri, T., Etude des modeles de plaques elasto-plastiques, These de Docteur-Ingenieur, Univ. P. & M. Curie, Paris, 1981.
- Lions, J.L. & Magenes, E., "Non homogeneous boundary value problems and applications," Springer Verlag, 1972.
- Massonet, Ch., "Elasto-plastic membranes plates," Engineering Plasticity, Cambridge, 1968, pp. 456-459.
- Schwartz, L., "Analyse Hilbertienne," Hermann, Paris, 1979.
- Suquet, P., "Existence et regularite des solutions des equations de la plasticite parfaite," These de 3eme cycle, Univ. Paris VI, 1978 and C.R.A.S., t. 286, Serie D, 1978, pp. 1201-1204.
- Timoshenko, S., & Woinowsky-Krieger, S., "Theorie des plaques et des coques," Librairie Polytechnique, Ch. Beranger, 1961.
- Zarantonello, E.H., "Contributions to nonlinear functional analysis," Academic Press, 1971, pp. 237-341.

NUMERICAL SOLUTIONS TO CONTACT AND FRICTION  
PROBLEMS WITH APPLICATIONS

Billy Fredriksson

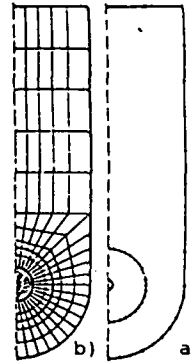
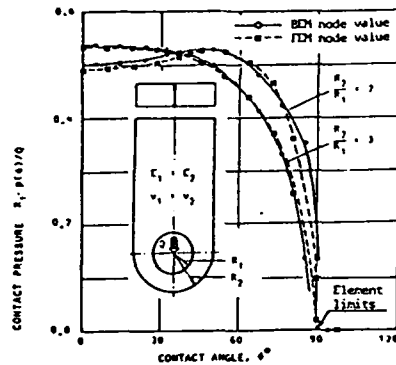
SAAB-SCANIA AB, Aircraft Division  
S-591 88 Linköping, Sweden

Contact and friction problems have attracted a lot of attention during recent years from both engineers and mathematicians. This is also justified by the prime importance of contact and friction problems in engineering structures. Structural joints with high contact stresses and frictional forces together with relative motions are the most fatigue critical areas where cracks initiates and developes.

Contact and friction problems are mathematically very difficult problems where existence and uniqueness of solutions have not yet been proved. Interesting references are Duvaut and Lions (1), Panagiotopoulos (2) and Oden and Kikuchi (3) and for friction laws also Michalowski and Mroz (4) Excellent overview papers on variational formulations are given by Kalker (5) and more recently by Klarbring (6).

The present paper dicusses both continuum and discrete formulations using both the finite element and boundary element methods as analysis tools for the numerical solution (7-12). Different numerical methods for solving both elastic and elastic plastic contact and friction problems will be discussed. The methods are restricted to small displacements and strains. Discrete formulations resulting in linear complementarity problems as formulated and solved by Klarbring (7) seems promising. The method will be briefly discussed.

The different algorithms have been implemented in the general purpose program ASKA and a series of practical applications will be presented. Examples of applications are contact problems in attachment lugs, combined contact and crack problems in wing rudder attachment lugs, contact and friction problems in joints and elastic and elasticplastic contact problems in bearing applications. As an example the figure shows a finite element and a boundary element model of a twodimensional lug together with contact pressure curves.



Contact pressure curves between bolt and lug as a function of the ear thickness

BEM model (a) and FEM model (b) of a linkage assemblage. The lug thickness is equal to the radius of the bolt.

#### REFERENCES

- (1) Duvaut G. Lions J.L. Inequalities in Mechanics and Physics. Springer Verlag, Berlin 1976.
- (2) Panagiotopoulos P.D., Nonlinear Programming Approach to the Unilateral Contact and Friction Boundary Value Problem in the Theory of Elasticity Ing. Arch. Vol 44 1975 pp 421-432.
- (3) Oden J.T., Kikuchi N., Finite Element Methods for Constrained Problems in Elasticity Int J. Num. Meth. in Eng. Vol 18, 1982, pp 701-725.
- (4) Michalowski R., Mroz Z., Associated and Nonassociated Sliding Rules in Contact Friction Problems. Archives of Mechanics 1978 pp 259-276.
- (5) Kalker J.J. Variational Principles of Contact Elastostatics. J. Inst Maths Appl Vol 20 1977 pp 199-219.
- (6) Klarbring A., Variational Principles of Contact Mechanics, A Survey on Formulations of Interest for Numerical Treatments. Report LiTH-IKP-R-263 Linköping University 1982.
- (7) Klarbring A., Contact Problems with Friction - Using a Finite Dimensional Description and the Theory of Linear Complementarity. Linköping University. Report LIU-TEK-LIC-1984:3 1984.
- (8) Torstenfelt B., Contact Problems in General Purpose Finite Element Computer Programs. Computers & Structures Vol 16, 1-4 pp 407-493, 1983.
- (9) Torstenfelt B., Fredriksson B., Pressure Distribution in Crowned Roller Contacts. Engineering Analysis. 1984, Vol 1 No 1
- (10) Endahl U., Finite Element Analysis of Elastoplastic Contact Problems without Friction Proc. 7th Int. Conf. on Struct. Mech. in Reactor Techn. Chicago Ill. 1983.
- (11) Andersson T., Fredriksson B., Persson B.G.A., The Boundary Element Method Applied to Two-dimensional Contact Problems Proc. Second Int. Seminar on Recent Advances in Boundary Element Methods. Southampton, England, 1980.

## NUMERICAL SOLUTION OF CONTACT PROBLEMS

by

M. J. Hartnett  
 The Torrington Company  
 59 Field Street  
 Torrington, CT 06790

The accurate estimation of interface pressures which result from the contact of mechanical components has long been an endeavor of critical importance to the design of reliable systems. This problem was first addressed in rigorous form by H. Hertz [1], [2], and published over a century ago. Hertz showed that when the assumption of a half-space was invoked the linear elastic field equations could be solved using potential functions theory (3) and that the normal stress distribution at the interface computed if the shapes of the contacting bodies were restricted to ellipsoids in the immediate neighborhood of contact. Hertz's contribution although significant, left the more general and practical problem of contacting elastic bodies of arbitrary shapes unsolved.

In modern times time numerous researchers (see [3-7], among many others) sought to develop solutions that can be applied to a wide family of problems. Because of the need to solve contact problems for more generalized conditions, numerical methods were naturally employed. In this work a numerical method of solution for a very wide range of three-dimensional counterformal elastic body contact problems is discussed.

By using nomenclature of Timoshenko [8] the following relationships for the contact of two elastic bodies is derived:

$$w_1 + w_2 + z_1 + z_2 = \alpha \quad (1)$$

(inside the contact region)

In addition to the above displacement requirement we can impose two restrictions on force:

$$\int_A p(x', y') dx' dy' = F \quad (2)$$

$$p(x', y') \geq 0 \quad (3)$$

where  $p(x', y')$  is the contact stress distribution,  $F$  is the applied load, and  $A$  is the contact area.

Next, introduce the force-displacement relationship for a half-space derived by Boussinesq [9] and derive the following Fredholm integral equation:

$$k \int_A \frac{p(x', y') dx' dy'}{[(x-x')^2 + (y-y')^2]^{1/2}} + z_1 + z_2 = \alpha \quad (4)$$

The discretization of the expected contact region into rectangular regions, and the introduction of the assumption that pressure is

constant over a rectangular region, permits the development of the following system of ill-conditioned linear algebraic equations.

$$\sum_{j=1}^r P_j f_{ij} = D_i \quad i = 1, 2, \dots, r \quad (5)$$

Where  $P_j$  is the pressure on region  $j$ ,  $f_{ij}$  is a term representing the influence of region  $i$  on  $j$ , and

$$D_i = \alpha - z_{1i} - z_{2i} \quad (6)$$

A stable method for the solution of (5) for the unknown pressures can be found in reference [10].

#### References

- [1] Hertz, H., "Miscellaneous Papers - On the Contact of Elastic Solids," translation by Jones, D. E., Macmillan and Col., Ltd., London 1896.
- [2] Hertz, H., "Miscellaneous Papers = On the Contact of Elastic Solids and on Hardness," translation by Jones, D. E., Macmillan and Co., Ltd., London, 1896.
- [3] Conry, T. F. and Seireg, A., "A Mathematical Programming Method for Design of Elastic Bodies in Contact," Journal of Applied Mechanics, Trans. A.S.M.E. 1981, pp. 387-392.
- [4] Singh, K. P., and Paul, B., "Numerical Solution of Non-Hertzian Elastic Contact Problems," Journal of Applied Mechanics, Trans. A.S.M.E., Vol. 41, No. 2, June 1974.
- [5] Oh, K. P., Trachman, E. G., "A Numerical Procedure for Designing Profiled Rolling Elements," Journal of Lubrication Technology, Trans. A.S.M.E., October 1976.
- [6] Fessler, H. and Ollerton, E., "Contact Stresses in Toroids Under Radial Loads," Brit. Journal Apl. Phys., 8: 10, 1957, pp. 387-393.
- [7] Goodman, L. E., and Keer, L.M., "The Contact Stress Problem for an Elastic Spheres Indenting an Elastic Cavity," International Journal of Solids and Structures, 1965, Vol. 1, pp 407-415.
- [8] Timoshenko, S., and Goodier, J. N., "Theory of Elasticity," McGraw-Hill Book Company, 3rd edition, 1970.
- [9] Filonenko-Borodich, Theory of Elasticity, Dover Publications, NY 1965.
- [10] Hartnett, M., "A General Numerical Solution for Elastic Body Contact Problems," in Solid Contact and Lubrication, edited by Cheng and Keer, ASME publication number AMD-39, 1980, pp. 51-66.

FINITE ELEMENT INCREMENTAL CONTACT ANALYSIS AND APPLICATION  
TO SOME CONTACT PROBLEMS IN ENGINEERING

by

Noriaki Okamoto and Masaru Nakazawa

Mechanical Engineering Research Laboratory, Hitachi Ltd., JAPAN

Contacting components such as gear teeth in mesh, shrinkfitted shafts and bosses, flange connections of pressure vessels and dovetails of turbine blades are widely used in machines and structures. Analysis of stress and displacement of two or more arbitrary shaped elastic bodies in contact with each other has long been a problem in engineering.

Non-linearities often occur in contact problems and are due to changing contact regions and frictional effects. Contact problems are classified into three kinds; linear, reversible non-linear and irreversible problems.

In this paper a summary of our work on the development of an efficient numerical method of solution to contact problems and its application are presented. This method is based on the finite element method and load incremental theory. The geometrical and static boundary conditions on contact surfaces are treated as additional conditions independent of stiffness equations. As a result, the algorithm is simplified and it is then necessary to solve only simultaneous equations for parts related to the contact surfaces instead of the overall stiffness equations at each load step. Through this method a substantial amount of computer time can be saved [1].

This method has been applied to many engineering problems. The two problems described below were chosen to show how the method can be applied to cases of nonlinearity due to changes of contact regions and irreversibility resulting from friction.

(1) Micro-Hertzian Stresses in Hydraulic Motors

Hydraulic motors are widely used in machines such as hydraulic excavators and cranes. Contact stress occurs due to pressure acting on a small area of a ball in contact with a cam-ring. This contact stress is responsible for the eventual metal fatigue of the ball surface. The effect of surface roughness of the cam-ring on contact stress below the surface of the ball is analyzed using various kinds of two dimensional finite element models. One result of such analyses is shown in Fig. 1. It can be seen that high shear stress gradients exist below the surface of the ball due to the asperity ridges of the cam-ring, and the micro-Hertzian stress fields are combined with the macro-contact stress field as suggested by Leibensperger [2].

## (2) Torsional Problems of Polygon Drive Connections

Polygonally shaped shafts and bores have many application advantages in fixed or sliding drive connections. However, designers usually have to take fretting fatigue into consideration. Contact stress and relative slip amplitude between the two surfaces of a shaft and bore are two of the most important factors influencing fretting fatigue strength. The torque carrying mechanism of polygon drive connections is discussed with the results of finite element analysis and experiment. The present method seems to make available a means for analyzing irreversible contact problems as shown in Fig. 2.

## References

1. Okamoto, N. and Nakazawa, M., " Finite Element Incremental Contact Analysis with Various Frictional Conditions ", Int. J. Mech. Sci. Vol. 14, pp 337-357 (1979)
2. Leibensperger, R. L. and Brittain, T. M., " Shear stresses Below Asperities in Hertzian Contact as Measured by Photoelasticity ", Journal of Lubrication Technology, Trans. ASME, Series F, Vol. 95-3, pp 277-286 (1973)

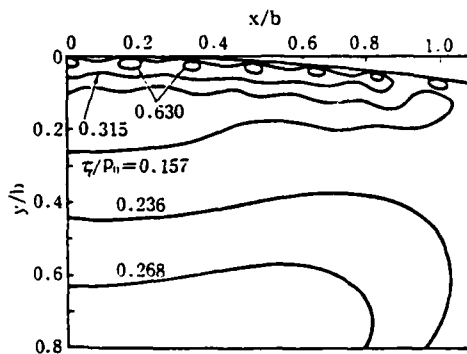


Fig. 1 Shear Stress Field of a Metal Ball.

$\tau_1$  : maximum shear stress  
 $P_0$  : maximum preessure of Hertz solution  
 $b$  : contact width of Hertz solution

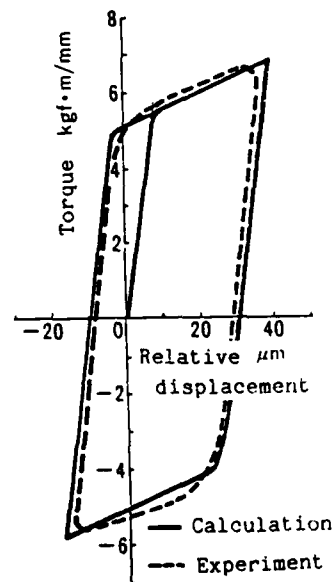


Fig. 2 Comparison of Calculated and Experimental Results

FRICIONAL VIBRATIONS OF METALLIC BODIES  
USING THE FINITE ELEMENT METHOD

by

J. Martins and J. T. Oden  
TICOM, University of Texas at Austin  
Austin, Texas 78712

In this paper, finite element methods are used to study the dynamic behavior of metallic bodies which come into contact with rough dry foundations. The metallic bodies are assumed to be deformable with a linearly elastic behavior (no bulk plastic deformations). For the range of normal loads considered, characteristic of engineering sliding interfaces, the normal deformation of these rough interfaces is assumed to satisfy an empirical constitutive equation of the form: normal pressure  $\propto$  (penetrating approach)<sup>m</sup> where the power m ranges from 2.0 to 3.33. The friction stresses are assumed to satisfy a regularized form of Coulomb's law.

In this model, the kinetic coefficient of friction is not assumed to be a decreasing function of the sliding velocity as it is often done by authors who have studied stick-slip oscillations. To the contrary, in this work we are especially interested in simulating numerically the (experimentally observed) strict synchronism between tangential and normal jumps of the sliding bodies during stick-slip oscillations, even when the kinetic coefficient of friction is independent of the sliding velocity.

The extreme sensitiveness of the friction stresses to small changes in the normal penetrating approach between the contacting bodies and the coupling between the tangential and normal degrees of freedom of the deformable sliding body are shown to be responsible for the stick-slip oscillations. In addition, it is demonstrated how certain "experimental" relations between coefficients of friction and sliding velocity obtained during stick-slip experiments are actually the result of the variation of the normal contact force and that this variation is often not taken into account correctly in interpreting or designing these experiments.

THE INFLUENCE OF PLASTIC BEHAVIOR ON CONTACTING  
BODIES - A FINITE ELEMENT SIMULATION

Steve H. Chang and N.J. Salamon  
Department of Mechanical and Aerospace Engineering  
West Virginia University  
Morgantown, West Virginia 26506

A direct incremental finite element method for elastoplastic bodies with isotropic and/or kinematic hardening is developed and used to study the influence of material plasticity on contact behavior. The method subdivides the problem into a series of events, each of which occurs over an increment in load. The sequence of events is decided by scaling the residual load so that either the contact region changes or the yielded region grows and choosing that event requiring minimum load. A cross product technique is used to detect contact and the von Mises criterion yielding. Interpenetrations are prevented by a set of constraint equations which release tangential deformations of contacting surfaces, but slave normal deformations to neighboring master nodes. After each event, boundary conditions and material properties are updated to be consistent with the deformation and stress state.

Some interesting phenomena are discovered for an old problem - the two-dimensional Hertz problem. In plane strain, yielding initiates about 70% of the half contact length above the contact plane, but in plane stress, yielding initiates at the contact plane. Hence a wide roller will tend to envelop a track of equal width. Moreover contact between elastoplastic bodies with hardening requires a larger load to develop the same area of contact as elastic bodies.

Experience has shown that numerical solutions using discrete models for elastoplastic bodies is very sensitive to the mesh size. Despite good agreement with the elastic Hertz solutions for the extent of contact and contact pressure, the accurate calculation of equivalent stress in determining yielding is difficult. This is caused by subtle differences in stress components and is aggravated by the use of simplex triangles which in turn are used because they render plastic stiffness corrections easy. Hence a very fine mesh is necessary not only in the region of potential contact, but also in that of potential yielding.

by

N. Chakrapani  
Department of Computer Science  
Wichita State University  
Wichita, KS 67208

Understanding the source code of a program in a programming language is enhanced when the source listing of the program is presented in an elegant manner making its control flow organization more apparent. Towards this end, programs coded in structured languages like Pascal are keyed in so that control structures like 'if then else', 'while do' etc., are indented so that the enclosed code in those structures is clearly delineated. This indentation capability is not available as a normal feature in many Pascal compilers. In this paper, we present the design and implementation details of an indentation preprocessor developed by the author at the Wichita State University.

The programming language Pascal has many control structures that enable the generation of well-structured programs. The preprocessor scans the source program for various control structures and produces a source listing file where the body of code of a given control structure is indented with respect to the reserved words of that structure. The nesting of control structures also is truly reflected in the listing file. In addition to this indenting of source code, the listing file provides information as to the level of nesting of each control structure by means of an index number in the left margin.

The preprocessor package is coded in a high level language and is easily portable. It has thirteen procedures and needs approximately 16K bytes of storage on IBM 370.

**WAVE INTERACTIONS IN SWEEP-WING FLOWS**

Helen L. Reed  
Assistant Professor  
Department of Mechanical Engineering  
Stanford University  
Stanford, California 94305 USA

Modern transports are being designed with swept wings. Because of wing sweep, the flow over the wing is three-dimensional. The profile of the crossflow velocity component contains an inflection point, a situation known to be dynamically unstable. Streamwise vortices that all rotate in the same sense are created. These dominate disturbance growth in the leading-edge region. On the other hand, the mid-chord region is dominated by the classical Tollmien-Schlichting instability (T-S waves).

One major unanswered question concerns the interaction of crossflow vortices and T-S waves. It is well known that streamwise vortices in a boundary layer strongly influence the behavior of other disturbances. Nayfeh (1981) shows that Görtler vortices produce a double-exponential growth of T-S waves. That is, the amplification rate increases exponentially in this case. Herbert and Morkovin (1980) show that the presence of T-S waves also produces a double-exponential growth of Görtler vortices, while Floryan and Saric (1980) show a similar behavior for streamwise vortices interacting with Görtler vortices.

Amplification of the cross-flow vortices near the leading edge produces a residual spanwise nonuniformity in the mid-chord regions where T-S waves are strongly amplified. Should the T-S wave undergo double-exponential growth because of this, the usual transition prediction methods would fail. Thus it is important to study interactions of this sort and to develop more realistic criteria for transition prediction.

In this work, the crossflow/Tollmien-Schlichting wave interactions that are characteristic of flows over swept wings are modeled analytically as a nonlinear instability after the work of Herbert (1984). The spatial stability of the basic state (comprised of a three-dimensional incompressible boundary-layer flow over an infinitely swept convex or flat surface with a superposed flow corresponding to steady streamwise vortices rotating in the same sense) is examined. This mean flow is typical of the upper surface of a swept wing. Crossflow vortex instability is expected to be important in the leading-edge negative pressure-gradient region. These vortices may linger to the almost zero pressure-gradient mid-chord region and affect stability there.

Using the method of multiple scales, we superpose onto this basic state two oblique traveling harmonic Tollmien-Schlichting waves in a secondary-instability analysis. Resonance conditions are established which could lead to magnified growth of the T-S waves beyond that predicted by straight linear theory.

Under these resonance conditions, we follow the T-S waves to ascertain their stability characteristics. Since the flow is complicated by the presence of streamwise vortices, marching along the characteristics defined by the group velocity ratio may not be the only applicable criterion. We find analytical expressions for the growth rates of the T-S waves which are then integrated numerically to find amplitude ratio. These results will be correlated with experimental data to establish more meaningful transition-prediction criteria.

#### References

- Floryan, J. M., and Saric, W. S. (1980), "Wavelength Selection and Growth of Görtler Vortices," AIAA Paper No. 80-1376.
- Herbert, Th. (1984), "Analysis of the Subharmonic Route to Transition in Boundary Layers," AIAA Paper No. 84-0009.
- Herbert, Th., and Morkovin, M. V. (1980), "Dialogue on Bridging Some Gaps in Stability and Transition Research," in Laminar-Turbulent Transition, R. Eppler and H. Fasel (eds.), TUTAM Symposium, Stuttgart, Germany, Sept. 16-22, 1979, Springer-Verlag, New York, p. 37.
- Nayfeh, A. H. (1981), "Effect of Streamwise Vortices on Tollmien-Schlichting Waves," Journal of Fluid Mechanics, Vol. 107, p. 441.

INSTABILITIES OF THE TAYLOR TYPE AND POLYMERIC  
DRAG REDUCTION IN ROTATING CHANNEL FLOW

by

Charles G. Speziale  
Stevens Institute of Technology  
Mechanical Engineering Department  
Hoboken, N.J. 07030

When a laminar pressure-driven channel flow is subjected to a steady spanwise rotation, an instability of the Taylor type occurs at intermediate rotation rates. This instability, which occurs in Newtonian and non-Newtonian fluids, is characterized by the development of a secondary flow in the form of longitudinal roll cells. At more rapid rotation rates, the instability disappears as a direct consequence of a generalization of the Taylor-Proudman theorem which states that slow steady flows in a rotating framework are approximately two-dimensional sufficiently far from solid boundaries (1).

In this paper, it will be demonstrated numerically that the introduction of a minute amount of a high molecular weight polymer to a Newtonian liquid can have a stabilizing effect on rotating channel flow and, furthermore, give rise to secondary flows with a substantially reduced frictional drag. This will be accomplished by the modification of the numerical procedure used in Speziale and Thangam (2) for the corresponding Newtonian case. The dilute viscoelastic fluid behavior is characterized by two distinct models (i.e., the Maxwell fluid and Rivlin-Ericksen fluid of the second grade) which, for this case, yield the same approximate equations of motion. Specific computer calculations will be presented for the stability boundaries, the secondary flow cell spacing, and the secondary flow frictional drag as a function of the Weissenberg number. Comparisons will be made with the qualitatively similar results obtained for the Couette flow of dilute polymer solutions (3).

REFERENCES

1. Speziale, C.G., Developments in Theoretical and Applied Mechanics 12, (in press).
2. Speziale, C.G. and Thangam, S., J. Fluid Mech. 130, 377 (1983).
3. Denn, M.M. and Roisman, J.J., AIChE J. 15, 454 (1969).

LAMINAR NATURAL CONVECTION ABOUT VERTICAL CYLINDERS -  
WITH VARIABLE FLUID PROPERTIES

by

Michael L.C. Papple

J.D. Tarasuk

The University of Western Ontario  
Faculty of Engineering Science  
London, Ontario, Canada N6A 5B9

The steady, laminar natural convective temperature field outside heated vertical cylinders was studied. The effects of transverse curvature and variable fluid properties on the cylinder temperature profiles were examined. The ambient fluid was taken to be air.

Both experimental and numerical studies are reported. An interferometric technique was used to obtain the temperature field in the boundary layer. These results were then compared with numerical solutions of the boundary layer equations.

For vertical cylinders it was necessary to consider the effect of the transverse curvature of the surface. When the thermal boundary layer was significant compared to the cylinder radius, the transverse curvature affected the heat transfer, temperature and velocity profiles.

A second factor which influences these results is the variation of the ambient fluid properties with temperature. When the temperature difference between the cylinder surface and the ambient fluid is large, the fluid viscosity and conductivity can vary significantly over this temperature range as shown in Figure 1.

In the numerical approach the boundary layer equations were solved using a method termed "the method of lines". First a similarity transformation was used. The temperature and velocity profiles were described in terms of two variables  $\xi = (2^{3/2}x)/(aG_{rx}^{1/4})$  and  $\eta = (r^2 - a^2)/2ax(G_{rx}/4)^{1/4}$  rather than the two spacial variables  $x$  and  $r$ . The variable  $\xi$  is a measure of the transverse curvature.

The derivatives with respect to  $\xi$ , the axial variable, were replaced by finite differences while the derivatives with respect to  $\eta$  were retained. The resulting equations were solved using ordinary differential equation methods.

The gas dynamic viscosity and thermal conductivity were assumed proportional to  $T^{0.75}$ , where  $T$  is the absolute temperature. The Prandtl number and specific heat were taken to be constant. Prandtl numbers of 0.68 and 0.72 were examined, which are typical for air and the monatomic and diatomic gases.

Results were obtained for curvature parameters  $\xi$  up to 4.0, which corresponds to vertical wires. Temperature ratios  $T_s/T_\infty$  varying from 0.25 to 4.0 were considered. The local heat transfer and temperature profiles were found to be strong functions of

curvature and the temperature ratio. In addition, both the curvature and the variable property effects must be considered simultaneously. To the best of our knowledge, no other information is available in literature for this problem, other than the thesis (1) from which this paper was taken. The results for vertical plates with variable properties as calculated by Sparrow (2) are not applicable for cylinders.

In the experimental approach the refractive index fields, and hence the temperature fields about two heated vertical cylinders in air were measured using a Twyman-Green interferometer. Cylinders of radii 0.04953 and 0.03813 m were heated to 600 and 525 K while the ambient air was maintained at 300 K. Interferograms were photographed and the resulting interference fringes were measured. Values of curvature parameters up to 0.15 were possible.

For axisymmetric refraction fields the difference between the local and ambient refraction indices was calculated from the fringe shift field using the Able inversion (1)

$$\Delta n(r) = -\frac{\lambda}{\pi} \int_r^{\infty} \epsilon'(R)(R^2 - r^2)^{-1/2} dR \quad (1)$$

In this equation, the derivative of the fringe shift field  $\epsilon'(R)$  must be measured accurately to evaluate the refraction field. The accuracy depends on the available number of fringes.

For the two cylinders considered, 11 to 14 fringes were available. The measured local heat transfer and temperature profiles were found to be in good agreement with those predicted from boundary layer theory.

#### References

1. Papple, M.L.C., "Laminar Natural Convection About Vertical Cylinders - With Variable Fluid Properties", M.E.Sc. Thesis, to be published, The University of Western Ontario, London, Ontario, Canada.
2. Sparrow, E.M., "Free Convection With Variable Properties and Variable Wall Temperature", Ph.D. Thesis, Harvard University, Cambridge, Massachusetts, May 1956.

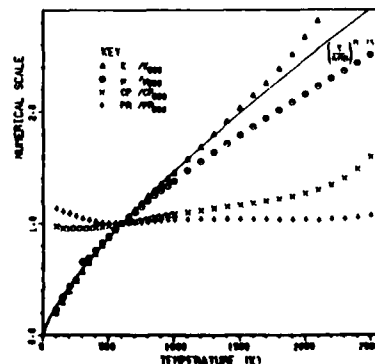


Fig. 1. Non-dimensional properties of air vs. temperature

by

K. Muralidhar and F. A. Kulacki  
University of Delaware  
Newark, Delaware 19716

A mixing-layer arises from two parallel streams of a fluid with a different mean speeds  $U_2$  and  $U_1$ , coming in temperatures, the velocity distribution in the mixing-layer is buoyancy affected. Here we consider the case of a horizontal, laminar mixing-layer and the influence of buoyancy relative to the velocity ratio  $U_2/U_1$  calculated at the first point-of-contact. We assume that buoyancy can be introduced in the governing equations in the framework of a Boussinesq approximation. For a two-dimensional steady-flow system, the forced convection problem affords a similarity solution with  $\eta = y/\sqrt{x}$  as a similarity variable. For small temperature differences, it is possible to isolate the buoyancy effects to a first-order problem ( $f_1$ ), the zeroth order ( $f_0$ ) being the forced-flow situation. With this approach the buoyancy parameter defined as  $\epsilon = g\beta\Delta T(x\nu)^{1/2}/U_1^{5/2}$ , must be less than unity. The combined solution ( $f$ ) is approximately expressible in the form:

$$f = f_0 + \epsilon f_1$$

In this way we are led to solve a three-point boundary-value-problem for ordinary differential equations written for a dimensionless stream-function and temperature, in terms of the similarity variable as the independent coordinate. The integration of these equations is accomplished by a fourth-order Runge-Kutta scheme, starting at the interface and going above and below it, to the edge of the mixing-layer. Initial values at the interface are obtained by the Nachtsheim-Swigert (NS) scheme, for a variety of velocity ratios.

The advantage of solving a laminar problem is that it presents a mathematically closed problem requiring no empirical information. This must be contrasted with the case when the flow is turbulent. The numerical scheme adopted here is general enough to hold for any set of values of the velocity ratio and Prandtl number. The integration scheme is iterative in nature and required both the convergence to an updated initial value and its size-convergence with respect to the mixing-layer thickness. For extreme values of  $Pr$ , and velocity ratio, we have observed that size convergence could be significantly delayed, especially for the first order problem. In a physical situation, this condition might represent a turbulent flow field, even for a slow moving fluid. Figure 1 is valid for  $Pr = 0.72$  with the hotter stream below the colder one.

We have made the following observations:

- (a) Buoyancy effects become significant away from the first point of contact.
- (b) Buoyancy effects are present for both the thermally stable and unstable configurations.

- (c) Buoyancy is more important when the faster moving stream is at a higher temperature, than when it is the colder stream. Thus for an unstable stratification of density, buoyancy effects significantly reduce as velocity ratio  $U_2/U_1$  is increased.
- (d) It is generally true that as  $Pr$  becomes smaller than unity, the regime of mixed convection become predominant, though this aspect remains to be investigated in detail.
- (e) The influence of buoyancy on the velocity profile is through momentum transport, as seen by the presence of kinematic viscosity in the definition of  $\eta$ . This is however not true for the turbulent case, where molecular effects might be conveniently ignored for  $Pr$  above unity.
- (f) The influence of buoyancy on temperature profile is uniformly small for the Prandtl number considered here.

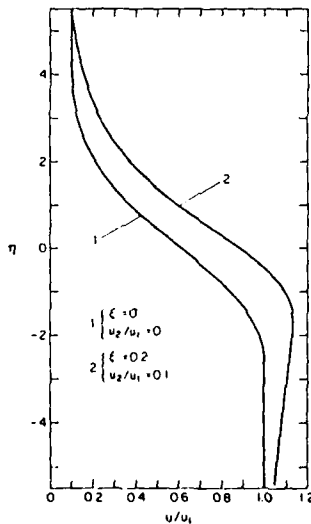


Fig. 1. Velocity profile in the mixing-layer.

#### References

- 1) Potter, O.E., "Laminar boundary layers at the interface of co-current parallel streams" Quart J. Mech. Appl. Math. Vol. 10, pp. 302-311, 1957.
- 2) Mori, Y., "Buoyancy effects in a forced laminar convection flows over a horizontal flat plate". ASME J. Heat Transfer, Vol. 82, pp. 479-482, 1961
- 3) Nachtsheim, P.R., and Swigert, P., "Satisfaction of asymptotic boundary conditions in numerical solution of systems of non-linear equations of the boundary-layer type", NASA TN D3004, October 1965.

## TURBULENCE SCALES IN THE ENTRAINMENT ZONE

by

Ranganathan Kumar  
 Department of Mechanical Engineering  
 Clemson University, Clemson, SC 29631

In a buoyancy-driven penetrative convection experiment, a narrow region develops between the turbulent convective region and the nonturbulent stable region atop. This thin region is called the entrainment zone or the interface. From laser Doppler measurements, the entrainment zone was seen to be characterized by both its thickness and temperature discontinuity. Some of the scatter in the experimental data may be attributed to experimental error. But, a definite trend in the scatter for various stable temperature gradients reveal the presence of different length and temperature scales in the entrainment zone. Analyzing the heat flux profile which becomes negative at the interface, it seems reasonable to assume that the turbulence time scale in the entrainment zone is proportional to the Brunt-Vaisala period. This assumption, combined with the integration of a simple force balance across the entrainment zone gives a new length scale and a temperature scale as follows:

$$\ell = w_* / \sqrt{\beta g \Gamma} \quad \text{and} \quad \theta = \Gamma \ell$$

where  $\Gamma$  is the temperature gradient in the stable region. Although the new scales are concocted from a non-mixing parcel of constant temperature in a process where there is dissipation, they appear to collapse the data well.

Conditional averaging techniques and probability density distributions have been employed to infer the properties of fluid elements in the entrainment zone. The flow was visualized using a vertical sheet of laser beam and entrainment was observed deep in the middle of the convective layer. But such entrainment was also seen to be infrequent. With the help of the abovementioned tools and third order turbulent moments collapsed with the new scales, a simple but adequate physical model has been developed to explain the process of penetrative convection in the entrainment zone.

Reference :

- [1] Kumar, R. and Adrian, R.J., "Higher Order Moments in Unsteady Turbulent Penetrative Thermal Convection," 22nd ASME/ASChE National Heat Transfer Conference, Niagara Falls, 1984.

## HYDRODYNAMIC WAVE INSTABILITIES IN ACOUSTIC MEDIUM

T.J. Chung and J.L. Sohn  
Department of Mechanical Engineering  
The University of Alabama in Huntsville

## ABSTRACT

Hydrodynamic wave instabilities are usually determined by means of the Orr-Sommerfeld equation. However, in the presence of acoustic waves such as in solid propellant rocket motors, the two distinctly different waves, hydrodynamic and acoustic, are combined, interacting with each other, and thus requiring a special method of solution. Toward this end, governing equations for all variables are constructed, and stability integrals are derived via Green's function, including the mean flow field and acoustic oscillatory velocities and vortices. From the growth constants for acoustic and hydrodynamic contributions, stability boundaries are determined in terms of Reynolds numbers. The numerical results via finite elements indicate that an overall instability phenomenon results from certain combinations of acoustic and vortical frequencies. It is also found that stability boundaries for acoustics-coupled hydrodynamic oscillations are somewhat similar to the classical hydrodynamic stability boundaries, but they occur in the form of multiple islands. The turbulent flow field appears to contribute toward instability, and this trend increases with larger transition angles of the rocket motor cross-section.

## WAKE MODEL FOR LOW SPEED FLOWS PAST THIN AIRFOILS WITH SPOILERS

by

Piero Bassanini  
 Università di Roma "La Sapienza"  
 Dipartimento di Matematica  
 00185 Roma, Italy

Spoilers and split flaps are widely used in aircraft design as roll control devices, speed brakes and lift dumpers; but, in spite of this, very little theoretical information exists, even for two-dimensional flows at low speed [1]. A simple model for steady flows based on Helmholtz free streamline theory for incompressible inviscid fluids has recently been proposed by Elcrat and Wentz [2,3]. In Elcrat's model the free streamlines are convex and the underpressure coefficient  $\sigma$  is zero. Both these restrictions can be removed by adopting a suitable finite wake model.

The simple nonlinear model adopted here is the one proposed by Wu with a few minor modifications (cf. [4]). The wake comprises two parts a near-wake or dead-air region and a far-wake or turbulent region. The technique of solution is based on Riemann-Hilbert methods and a numerical "shooting" procedure, following an idea of Street (cf. [4]).

Figure 1 shows the physical flow plane for  $\alpha > 0$  (spoiler case); for  $\alpha < 0$  one has the split flap case. The near-wake is the region ABCC', while the far-wake extends from CC' to infinity E.

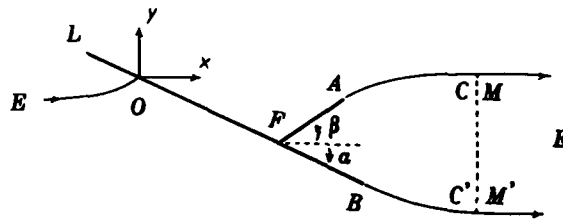


Figure 1

Figure 2 reports values of the drag coefficient vs. the spoiler deflection  $\delta = \alpha + \beta$ , for  $\sigma = 0, 0.2$  and  $\alpha$  between  $5^\circ$  and  $10^\circ$ . As expected, the predicted values are too low, due to neglect of viscosity, but the results improve as  $\sigma$  increases.

Figure 3 shows results for the incremental lift  $\Delta C_L = C_L - 2\pi \sin \alpha$  vs.  $\delta$  for  $\alpha = 5^\circ, 10^\circ$  and  $\sigma = 0.2$ , when the average wake length is of order  $0.3|LB|$ . In both Figures 2 and 3 the dashed lines represent experimental values from [3], and  $|LF| = 0.775|LB|$ ,  $|AF| = 0.1|LB|$ .

An interesting result of our analysis is the prediction of wakes with zero drag and wakes with overpressure ( $-1 < \sigma < 0$ ) in the split flap case ( $\alpha < 0$ ). Then the free streamlines have one inflection point, which recedes to the point C or C' when  $C_D = 0$  [4].-

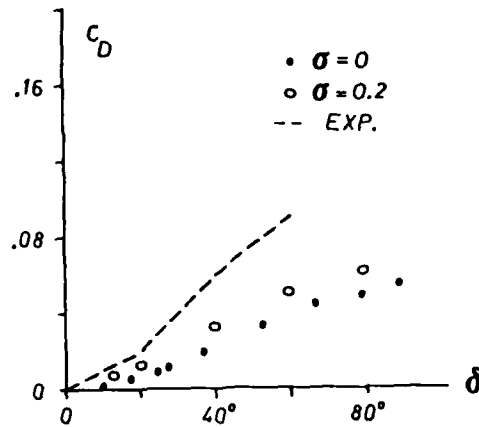


Figure 2

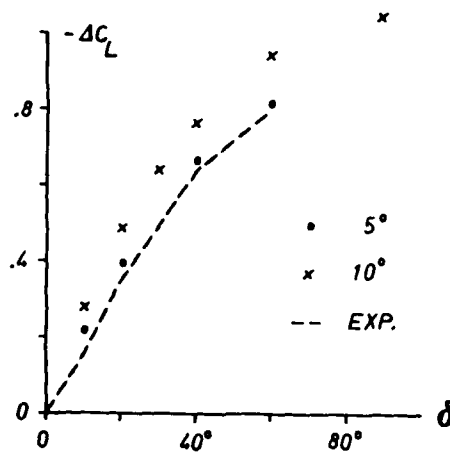


Figure 3

## References

- [1] Pfeiffer, N.J., and Zumwalt, G.W., "Computational Model for Low Speed Flows Past Airfoils with Spoilers", AIAA J., Vol. 20, 1982, pp. 376-382
- [2] Elcrat, A.R., "Separated Flow Past a Plate with Spoiler", SIAM J. Math. Anal., Vol. 13, 1982, pp. 632-639
- [3] Elcrat, A.R., and Wentz, W.H.Jr., "Forces on a Split Plate (Airfoil with Spoiler) Obtained by Conformal Mapping of the Hodograph", submitted to the J. of Fluid Mech. (October 1983)
- [4] Bassanini, P., "Wake Flow Past a Plate with Spoiler", submitted to J. Appl. Math. Phys. (ZAMP) (October 1983).

## EFFECTIVE ACOUSTOELASTIC RESPONSE OF ROLLED PLATES

by

George C. Johnson  
Department of Mechanical Engineering  
University of California  
Berkeley, CA 94720

Acoustoelasticity is a nondestructive technique proposed for the evaluation of active and residual stresses within structural components. It is based on the fact that in most materials, including aluminum and steel alloys, the speeds at which waves propagate through a body depend on the state of stress or deformation to which that body is subjected. While the majority of the work in this field has used the assumption of isotropy, most structural materials are polycrystalline aggregates whose forming (rolling, drawing, forging, etc.) leaves them with a macroscopic response which is anisotropic. The purpose of this paper is to consider the effective aggregate response in terms of the response of the constituent crystals and the orientation distribution of those crystals.

In order to model the observed behavior of velocity as a function of deformation, the constitutive relation between stress and strain has been taken to be nonlinear. This is usually accomplished by allowing the strain energy to be a cubic function of the strain, with the coefficients of the quadratic and cubic terms called the second-order and third-order elastic constants, respectively. A method is given for the estimation of the effective second- and third-order elastic constants of an aggregate exhibiting rolling texture (orthorhombic symmetry) made up of crystals in the cubic classes with highest symmetry ( $43m$ ,  $43m$ ,  $43m$ ). In modelling the texture, the orientation distribution function for the crystallites, which gives the probability that a grain will be oriented in a particular way, is taken to be given as an infinite series of generalized spherical harmonics in the Euler angles. The effective constants are evaluated using both Voigt- and Reuss-type assumptions in which the stiffness and compliance tensors, respectively, are averaged, weighted by the orientation distribution function. It is shown that only a finite number of terms of the orientation distribution function (seven) are required to give the exact representation of the aggregate response in terms of the crystal response.

An aluminum aggregate has been examined both crystallographically and ultrasonically to obtain the orientation distribution function and aggregate response characteristics. Taking published data for the single crystal constants, the method outlined here is used to compute estimates of the effective aggregate properties for both the Voigt and Reuss assumptions. These estimated constants are then compared with the constants obtained from the ultrasonic examination of the material. Given the rather severe assumptions made in the Voigt and Reuss procedures, the comparison results are reasonable.

## ELASTIC EFFECTS ON TWO PHASE MICROSTRUCTURES

William C. Johnson  
Carnegie-Mellon University  
Department of Metallurgical Engineering  
and Materials Science  
Pittsburgh, PA 15213

Two effects of elastic misfit strains and applied stress on material microstructure will be discussed. The first concerns elastically induced shape bifurcations of inclusions. Shape change transitions of elastically misfitting inclusions are predicted to occur when the inclusions are softer than the matrix. Below the size where the transition occurs, the shape is dictated by minimizing interfacial energy without regard to the elastic contribution. The transition is to lower symmetry shape that is influenced by the elastic contribution. Transitions analogous to a second-order phase transition are predicted for an isotropic two-dimensional or plane-strain case, while transitions analogous to first-order phase transitions are predicted for an isotropic three-dimensional case. The effects of applied stress will also be discussed.

The effects of misfit strains on the stability against coarsening of second phase particles will also be addressed. Regions are delineated where small particles can grow at the expense of larger particles. The appropriate boundary conditions for such a problem will be discussed.

SOME ASPECTS OF MICRO-MACRO TRANSITION IN  
THE INELASTIC DEFORMATION OF METALS

by

G. J. Weng  
Department of Mechanics and Materials Science  
Rutgers University  
New Brunswick, N.J. 08903

The inelastic behavior of polycrystalline metals are known to be intimately related to those of their constituent grains, and whose behavior are in turn controlled by their dislocation activities and the associated structural changes. At relatively low temperatures inelastic deformation of metals is primarily caused by dislocation glide, but at high temperature dislocation climb could be equally active. In this paper we take into account the nature of these deformation mechanisms and the stress heterogeneity in a polycrystalline aggregate to examine how the inelastic properties on the micro-scale are transformed to the macroscale at different temperature levels. Both time-independent plastic and time-dependent creep behavior are considered.

Based on metallurgical observations, a temperature-dependent constitutive equation capable of describing both active and latent hardening is introduced for the slip system. This equation, together with the self-consistent relation for grain-matrix interactions, are used to determine the local plastic deformation of each constituent grain. Then by means of an averaging procedure the global plastic behavior of the aggregate at various temperatures are evaluated. Next, a time-dependent micro constitutive equation and a self-consistent relation suitable for time-dependent deformation are subsequently used to determine the creep properties of metals. In this context the difference between the self-consistent relations for plastic and creep deformation is also discussed. Finally, it is shown that the mechanism of crystallographic slip alone is not sufficient for the prediction of high temperature creep, and that the introduction of the additional dislocation climb is essential in the determination of such behavior. The micromechanics of dislocation climb under a combined stress and the associated flow rate are first established, and then an appropriate constitutive equation for lattice diffusion is used to evaluate this additional contribution to the creep deformation of metals. The summation of both glide and climb strains is taken to calculate the creep strains of the constituent grains, and then of the aggregate.

In all cases considered, the theoretical predictions are seen to be in a reasonable accord with experimental data.

ON THE COMPARISON BETWEEN MICROSCOPIC AND MACROSCOPIC  
INSTABILITY MECHANISMS IN A CLASS OF FIBER REINFORCED COMPOSITES

by

N. Triantafyllidis and B. N. Maker  
Aerospace Engineering Dept.  
The University of Michigan  
Ann Arbor, MI 48109-2140

One of the most important problems for composite materials is the prediction of their failure mechanism under a given set of loads. Customarily a composite medium is idealized by a homogeneous anisotropic continuum whose properties have been obtained by using an appropriate averaging technique (e.g., self-consistent method, homogenization method) which takes into account the solid's microstructure. The question of the composite's stability is usually addressed by investigating the (homogeneous) macroscopic properties of the material and not by going back for a look at the microstructural level. Very few attempts have been made to correlate the stability predictions of the continuum model with the corresponding exact microstructural failure mechanism for a given composite.

One of the first studies in this direction for the case of finitely strained solids was made by V. Tvergaard [1] for the localization of deformation in porous metals. There in view of the complexity of the microstructural instability problem only numerical solutions would be obtained which were compared with localization results obtained from a semiempirical macroscopic model.

To consistently study the relation between the macro and micro instability phenomena one would desire to work on a case where both instability problems have an exact analytical solution. As such a case we have decided to investigate a fiber reinforced composite (made of alternating layers of two different materials) under plane strain conditions and stretched (stretch ratio  $\lambda$ ) along  $x_1$ , the direction of the reinforcement. The microstructural instability is attributed to a bifurcation (i.e., loss of uniqueness) of the uniform (i.e., independent of  $x_1$ ) solution in the form of a wavy pattern. In spite of the problem's complexity the bifurcation results can be obtained in a nice closed form solution. No separation of layers is considered assuming a perfect bonding between them. We also note here that a special case of this buckling problem has been studied by Biot [2] using a different approach. The microscopical incremental moduli of the composite are obtained analytically, using homogenization theory. The loss of ellipticity (i.e., onset of shear localization) of the homogenized moduli is the corresponding macroscopic instability mechanism. For a given geometry and a set of material properties we compare the micro and macro critical values of the stretch ratio  $\lambda$  as well as the corresponding instability patterns. The investigation is done for a class of a power law type elastic-plastic materials as well as for a class of rubber elastomers. For the elastic-plastic case the biggest discrepancies (about 40%) between the micro and macro instability predictions

are found for the case of tensile loading ( $\lambda > 1$ ). For the Mooney-Rivlin elastic material the discrepancies were much higher even to the point of non-existence of macroscopic instabilities in a certain range of geometry and material properties. Some interesting asymptotic (with respect to wavelength of the buckling pattern in the  $x_1$  direction) results are also discussed.

#### REFERENCES

- [1] Tvergaard, V., Danish Center Appl. Math. Mech. Report 159, Technical University of Denmark (1979).
- [2] Biot, M., Mechanics of Incremental Deformation (New York: Wiley, 1965).

RECENT RESULTS IN THE MODELING OF  
ENVIRONMENTAL CRACK PHENOMENA

by

David J. Unger  
Department of Engineering Mechanics  
The Ohio State University  
Columbus, OH 43210

An overview of a theory of steady-state [1]-[3] and non-steady [4] environmental crack growth is presented. Two empirical relationships that have been used in the modeling of hydrogen embrittlement and stress corrosion cracking are rationally derived. Various rate-limiting mechanisms of crack propagation are examined within the context of this theory. Applications to many different materials and aggressive environments are discussed.

- [1] Unger, D. J., Aifantis, E. C., "On the Theory of Stress-Assisted Diffusion with Implications for Environmental Cracking Phenomena", Presented at the Ninth U.S. National Congress of Applied Mechanics at Cornell University, 1982, pp. 489-490, ASME.
- [2] Unger, D. J., Gerberich, W. W., Aifantis, E. C. "Further Remarks on the Implications of Steady-State Stress-Assisted Diffusion on Environmental Cracking", Scripta Metallurgica, Vol. 16, 1982, pp. 1059-1064.
- [3] Unger, D. J. and Aifantis, E. C., "On the Theory of Stress-Assisted Diffusion", II, Acta Mechanica, Vol. 47, 1983, pp. 117-151.
- [4] Chung, H., Unger, D. J., Macdonald, D. D. and Aifantis, E. C., "Steady and Non-Steady Crack Growth Under Environmental Conditions", Presented at the Sixteenth ASTM National Symposium on Fracture Mechanics, Battelle Memorial Laboratories, Columbus, OH, 1983.

SPECIAL TOPICS IN THE AERODYNAMICS  
OF WIND TURBINES

by

Andrew H. P. Swift  
Assistant Professor, Department of Mechanical Engineering  
University of Texas at El Paso, Texas

David A. Peters  
Chairman, Department of Mechanical Engineering  
Washington University, St. Louis, Missouri

The PROP Code is an aerodynamic rotor performance algorithm proposed by Wilson and Lissaman some ten years ago (1), which combines annular strip theory, blade element theory and momentum theory to calculate unknown local induced rotor velocities and then overall rotor performance as a function of blade geometry, pitch angle, airfoil lift and drag characteristics and operating tip speed ratio. Although useful for estimating rotor performance, the model provides only a steady state performance estimate and ignores unsteady effects which can have a significant impact on wind turbine rotor performance in an atmospheric environment. This paper addresses two of these unsteady aerodynamic performance effects, in addition to a third aerodynamic effect unrelated to performance estimation.

The first unsteady effect involves the increase in rotor performance that is obtained when measured performance of full size wind turbines is compared with values predicted by the PROP code using conventional two-dimensional wind tunnel airfoil data. (See Fig. 1). Viterna and Corrigan of the NASA-Lewis Research Center have published a mostly empirical method to correct the airfoil data, (2), which provides reasonable correlations of output power. Their corrections, however, do not take into account unsteady, three-dimensional boundary layer effects on rotating airfoils which may lead to erroneous conclusions as to the significance of inboard airfoil performance characteristics. These effects can be quite powerful as illustrated in Fig. 2, from Himmelskamp (3).

A second unsteady factor affecting performance is the effect of atmospheric turbulence on predicting the energy output for various turbine-generator configurations. Most wind turbines presently utilize either a grid connected constant speed induction (or synchronous) generator or a variable speed alternator with static inverter. The rotor and alternator are usually matched so that in steady state operation a constant tip speed ratio at the maximum performance coefficient is obtained. Since the correctly matched variable speed alternator theoretically operates at the optimum power coefficient, while the induction or synchronous generator operates at variable power coefficient, dependent on the wind speed, the variable speed design is generally expected to deliver more energy, other factors being equal. In steady

state operation this is indeed the case.

However, analytically supported test results (4) indicate a possible degradation in optimum aerodynamic performance when a variable speed rotor is operated in a turbulent atmosphere, thus possibly negating the purported performance advantage of the variable speed rotor. Preliminary results indicate that primarily rotor inertial effects, and to lesser extent dynamic in flow effects, degrade the expected performance of variable speed rotors in a turbulent atmosphere.

The third specific topic in wind turbine aerodynamics addressed in this paper, involves aerodynamic forces developed in articulated rotors that affect the yaw control system of the hinged, horizontal axis wind turbine rotor. The current trend in medium and large wind turbine rotor design appears to be toward two-bladed hinged rotor designs, often upwind of the tower. Although the hinged, or teetered, rotor alleviates the oscillating gyroscopic loads present during yaw of a rigid-two-bladed rotor, the yawing of hinged rotors produce rotor aerodynamic moments about the yaw axis that result in negative yaw damping and can cause yaw control problems. A spring restraint system for the hinged rotor is under investigation which both alleviates the unacceptable shaft loads of a rigid-two-bladed rotor in yaw, and yet lessens the undesirable, yaw induced aerodynamic moments that can adversely affect the yaw control characteristics of this type rotor. A brief discussion of this problem and the hinge spring concept is presented within.

#### REFERENCES

1. Wilson, R. E. and Lissman, P. B. S., "Applied Aerodynamics of Wind Power Machines," Oregon State University, May 1974.
2. Viterna, L. A. and Corrigan, R. D., "Fixed Pitch Rotor Performance of Large Horizontal Axis Wind Turbines," Proceedings of the "Large Horizontal Axis Wind Turbines" Conference, July 28-30, 1981, Cleveland, Ohio, DOE Pub. Conf - 810752.
3. Schlichting, H., Boundary Layer Theory, McGraw Hill.
4. Swift, A., "Extension to the Wilson-Lissaman Prop Code For Steady and Dynamic Rotor Performance Prediction," ASME Wind Symposium II, January 30 - February 3, 1983, Houston, Texas.

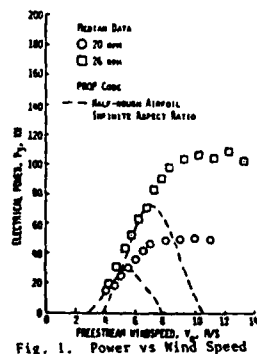


Fig. 1. Power vs Wind Speed

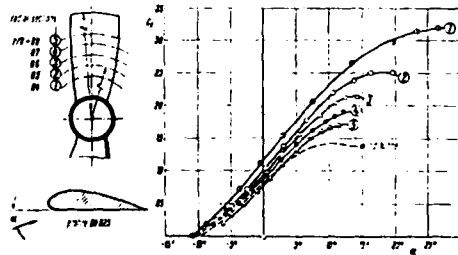


Fig. 2.  $C_L$  vs Angle of Attack

## DYNAMIC RESPONSE OF A FLEXIBLE WINDMILL ROTOR BLADE

by

Kenneth G. Craig  
The University of Oklahoma  
School of Aerospace, Mechanical and Nuclear Engineering  
Norman, OK 73019

A high-speed windmill rotor system was developed which combines a high-efficiency airfoil section with automatic pitch change as rotor speed varies. The pitch control mechanism utilizes no moving parts or mechanical linkages, but it does require a rotor blade with low torsional stiffness. The airfoil section developed for the rotor has a thin cross section which results in low stiffness not only in torsion but also in bending. Pitch varies with rotor speed due to the action of a "pitch control weight" attached near the tip of the rotor blade.

Efficiency of a test rotor was lower than had been calculated by computer modeling. In order to explain this lower efficiency, the effect of blade coning on the pitch control mechanism was investigated. High-speed photographs of blade tips during rotor operation showed that pitch change was less than had been calculated by a mathematical analysis which neglects coning. A new mathematical model, including effects due to coning, was proposed. Attempts to correlate this model with blade photographs were hampered by the dynamics of the interaction between blade twist, rotor thrust, and coning. An "average" blade twist versus rpm was calculated, and computer analysis using this value agreed well with observed performance.

EXPERIMENTAL INVESTIGATION OF THE MECHANICAL BEHAVIOR OF  
FLEXIBLE, CAMBERED COMPOSITE WIND TURBINE BLADES

by

Pierre M. Veragen  
The University of Oklahoma  
School of Aerospace, Mechanical and Nuclear Engineering  
Norman, OK 73019

As an initial effort in studying the deformations and stresses of an horizontal-axis windmill blade, an experimental investigation was conducted to determine the unusual mechanical behavior of a cambered flexible blade (see Figure 1). The material used was composite: unidirectional glass fibers and vinyl ester resin.

Experiments and field data showed that a complete study of the blade mechanical behavior had to include two nonlinear phenomena:

- (1) Since there is initial transverse curvature (camber), the airfoil experiences large transverse deformations due to the anticlastic curvature phenomenon<sup>1,2</sup>. To the present investigator's knowledge, there is no existing analysis including end effects in which such transverse deformation of the cross section is constrained at a given section (the root section) but free over the remaining length.
- (2) Large deflections also must be considered. A tip deflection of 10% to 20% of the blade length has been observed in normal operation.

These experiments are to be used to develop a new approach to anticlastic curvature and large deflection. Furthermore, this study is a first step in assessing the new technology of "soft rotors". The latter uses centrifugal stiffening to provide the necessary blade rigidity.

The author acknowledges the encouragement of his adviser, Professor Charles W. Bert.

References

1. Ashwell, D.G., "The Anticlastic Curvature of Rectangular Beams and Plates", Journal of the Royal Aeronautical Society, Vol. 54, 1950, pp. 708-715.
2. Banks, P.J., "Anticlastic Curvature in Anisotropic Beams", Aeronautical Journal, Vol. 78, 1974, pp. 525-528.

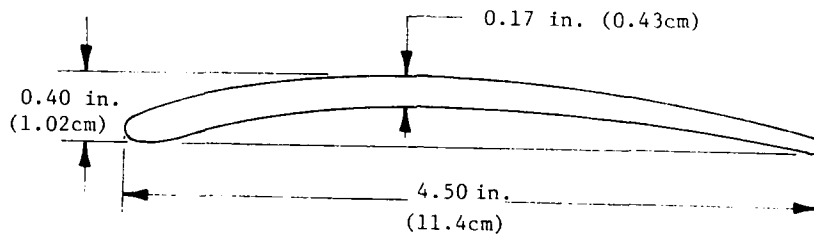


Figure 1. Airfoil Cross Section

A TECHNIQUE FOR MODELLING SITE WIND CHARACTERISTICS AND  
ENERGY OUTPUT OF SMALL WIND ENERGY CONVERSION SYSTEMS

by

James L. Heller and Dharam Pal  
Naval Civil Engineering Laboratory  
Port Hueneme, CA 93043

This paper discusses the use of a microprocessor-based data logger to develop models of the wind characteristics at a remote wind energy conversion site. The models are then applied to predict the power and energy output of small wind energy conversion systems (SWECS) with rotor diameters of 50 feet or smaller.

Presently, much of the wind data collected for siting SWECS is oriented toward recording a time history of wind speed and direction. Data retrieved in this form requires a tedious reduction process, and the detail that this information provides is often unnecessary. The United States Navy has adopted the use of a microprocessor-based data logger capable of operating unattended for a period of six months. The microprocessor performs a statistical analysis on the data and stores it on a memory chip. The data are retrieved in the form of wind speed and direction distributions, diurnal variation of wind speed, directional variability of the wind, and peak gust and longest lull of the wind speed.

In this form, the average wind speed and available energy and power in the wind are easily extracted. The information retrieved is further used to quantify the turbulent intensity of the wind and identify the effects that the surrounding terrain has on the wind speed and direction.

Finally, an estimate is made of the power and energy that a SWECS could produce in the modelled wind regime. The estimate is compared with the power and energy output from a Navy SWECS installation in order to verify the accuracy of the analysis technique.

A CONTRIBUTION FOR THE DESIGN OPTIMIZATION  
OF A SOLAR HEATED HOUSE

by

Dr. Eng. A. Arafa  
University of Northern Iowa  
Department of Industrial Technology  
Cedar Falls, Iowa 50614

A transient simulation model for an integrated solar heating system in a building has been developed. This model is used to investigate the influence of different parameters of the building on its heating load with the objective of minimizing this load and using it in optimizing the solar heating system.

The model considers a three-dimensional thermal analysis in the flat plate collector, the stratification in the storage tank and the effect of wall capacity of the building. Two different methods have been used in the numerical solution of the non-linear coupled differential equations resulting from the model.

One uses the Runge-Kutta method and the other uses a self-devised method. The self-devised method gives very small deviations in the results compared to the Runge-Kutta method and reduces the computing time drastically. The comparison between results measured and predicted of various solar collector types operating under different weather conditions, shows good agreement.

In addition, qualitative comparisons between data and predictions are presented for a domestic solar heating system installed in two different houses in the northern and southern parts of West Germany.

DEVELOPMENT OF A TEST FACILITY FOR RESIDENTIAL  
AIR-TO-AIR HEAT EXCHANGERS

J.W. Reid

J.D. Tarasuk

The University of Western Ontario  
Faculty of Engineering Science  
London, Ontario, Canada N6A 5B9

Air-to-air heat exchangers are becoming increasingly important in the design of energy efficient dwellings and working spaces. Energy from exhaust air is reclaimed by incoming fresh air with the result that space air quality is maintained at minimal expense. The proper function of the air-to-air heat exchanger depends on such variables as indoor and outdoor temperatures, relative humidities, air flow rates and the response to pressure differentials between the space and the outdoors.

A test facility was constructed as shown in Figure 1 with provisions for:

- 1) Simulation of the following winter conditions:  
Fresh air:  $-40^{\circ}\text{C}$  to  $+15^{\circ}\text{C}$  at RH = 0%  
Stale air:  $20^{\circ}\text{C}$  to  $30^{\circ}\text{C}$  at RH = 10% - 90%;
- 2) Varying the flowrates of the supply and exhaust streams between 100 and 300 CFM;
- 3) Varying the static pressure of the supply and exhaust air streams; and
- 4) Injection and measurements of a tracer gas to estimate cross contamination.

In dealing with the cold side of the test facility; the air was supplied to the heat exchanger at a temperature as low as  $-40^{\circ}\text{C}$  for the duration of the test. To achieve this an evaporator coil using refrigerant 502 was used. To alleviate the problems associated with moisture in the cold air stream the air was dehumidified before any testing was done by allowing the evaporator coil to cover in frost. The ice was thawed and then drained out of the system by means of a quick coil defrost. The cold side of the facility was a closed sealed system, thus once the cold air was dehumidified, the evaporator coil operated for the duration of the test without frost build-up. To obtain temperature readings of the air streams at the inlets and outlets of the heat exchanger, thermocouple grids were employed. In the warm stream, the wet bulb temperature was obtained by means of thermocouples. One of the difficulties encountered in designing the test facility was an accurate method of measuring the flowrates over the required test range (100 to 300 CFM). To measure such low flowrates, the method used was a thermister grid calibrated by a positive displacement apparatus. The positive displacement apparatus measured the time to fill a predetermined volume. Pressure variation was obtained by varying the fan capacity and with variable constrictions in the duct sections. To vary the humidity of the warm air, a vapac

steam humidifier was used. The humidifier responded to an electrical sensor with a linear steam output up to 10 kg/hr.

To control the parameters involved in the testing of an air-to-air heat exchanger (temperatures, humidity, flowrates) for the duration of a test, it was required that an automatic system be devised. A micro computer using analogue to digital hardware to interpret the signals from the measuring devices (thermocouples, thermistors, pressure transducers), and digital to analogue hardware to output signals to the heaters, humidifier, and blowers was used. Use of this system enabled complete control during the testing of the energy recovery system. A set of typical results is given in Figure 2.

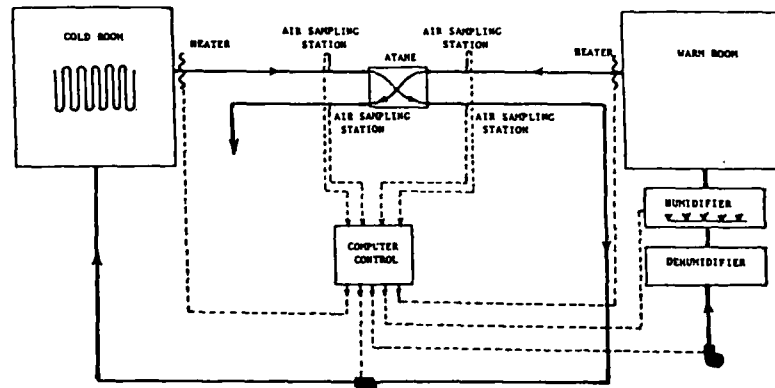


Figure 1. Schematic of Test Facility

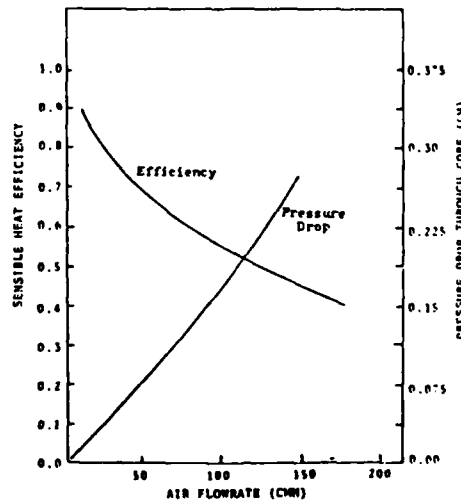


Figure 2. Typical Set of Test Results

AN EXPERIMENTAL STUDY OF THE THERMAL STABILITY  
OF AN ATRIUM

W.A. Farr

J.D. Tarasuk

Faculty of Engineering Science  
The University of Western Ontario  
London, Ontario, Canada, N6A 5B9

The development and description of a three dimensional plume has important applications both in meteorology and engineering. One such engineering application is in the design of high rise atriums where instability may result due to the existence of a cold air mass on top of a warm air mass. As an example, the Hong Kong Bank has a conditioned atrium 40 meters high above an open warm walk-way. Figure #1 illustrates the atrium currently under construction [1,2].

To predict the instability of the cold air mass above the warm air, a water model was constructed to simulate the flow patterns. For ease of study, an inverted system was designed as shown in Figure #2.

This study appears to be the first of its kind therefore, directly related material is almost non-existent. However, references [3-5] are excellent for obtaining a general knowledge of the behaviour of the thermal plumes.

In geometries such as an atrium, the parameters that affect the initiation of unstable flow include:

- 1) The temperature potential.
- 2) The height of each cavity.
- 3) The dimensions of the atrium cross-section.
- 4) The dimensions and geometry of the opening joining the atrium and the adjacent cavity.
- 5) The influence of the positive supply ventilation to the atrium chamber.
- 6) The effects of a basic state horizontal laminar flow in the upper cavity.

The flow patterns were studied by injecting neutrally buoyant dyes and particles. Shadowgraph methods, using the expanded beam of a helium-neon laser, were also used and information was recorded on video cassettes.

Results are presented showing the influence of the initial plume cross-section, the criterion for stabilizing the two thermally stratified fluids by pressurizing the atrium, and the development of the three dimensional plume as a function of time.

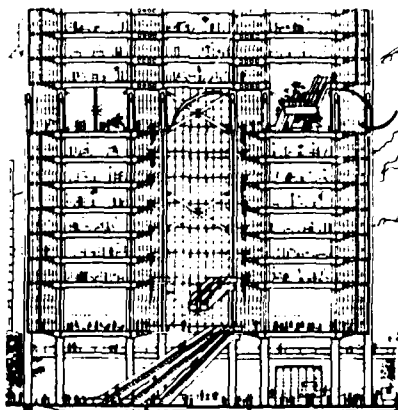


Figure #1 Bank of Hong Kong  
Atrium and Lobby

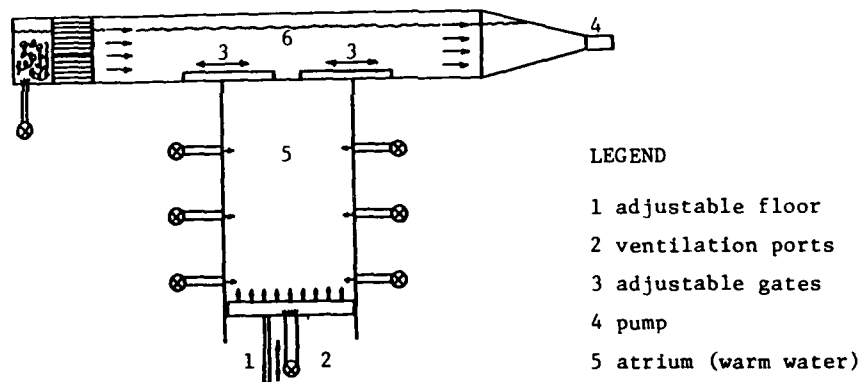


Figure #2 Schematic Diagram of the  
Bank of Hong Kong Water  
Model

LEGEND

- 1 adjustable floor
- 2 ventilation ports
- 3 adjustable gates
- 4 pump
- 5 atrium (warm water)
- 6 lobby (cold water)

References

1. Glancey, J., "Hong Kong Bank", *Architectural Review*, Vol. 69, May 1981, pp. 268-272.
2. Buchanan, P., "Foster, Rodgers: High-Tech: Classical Gothic", *Architectural Review*, Vol. 162, May 1981, pp. 265-268.
3. Turner, J.S., "Buoyancy Effects In Fluids", Cambridge at The University Press, 1973, pp. 165-194.
4. Sblien, D.J., Boxman, R.L., "Laminar Starting Plume Temperature Field Measurement", *Int. J. Heat Mass Transfer*, Vol. 24, No. 5, 1981, pp. 919-931.
5. Higgins, J.M., Gebhart, B., "Measurements of Instability and Disturbance Growth in Vertical Buoyancy Induced Flows In Cold Water", *Int. J. Heat Mass Transfer*, Vol. 25, No. 9, 1982, pp. 1397-1409.

ANALYSIS OF COUPLED THERMAL AND OSMOTIC PHENOMENA  
IN THE CRYOPRESERVATION OF LIVING TISSUE

by

Kenneth R. Diller and Klaus D. Kulbe  
Fraunhofer Institut für Grenzflächen- und Bioverfahrenstechnik  
7000 Stuttgart 80, Federal Republic of Germany

The frozen banking of living tissue holds great potential for ameliorating the problem of limited availability of histo-compatible donor tissue for transplantation. Successful procedures have been developed and implemented for the long term storage by freezing of numerous tissues including erythrocytes, lymphocytes, bone, and various gametes. These techniques are based on prefreezing chemical alteration of the material by addition of a cryoprotective agent in conjunction with directed manipulation of the thermal history at subzero temperatures. However, acceptable cryopreservation protocols are yet to be identified for many of the human tissues which would be of great clinical benefit such as granulocytes, heart, kidney, pancreas, and liver. We believe that an effective program of investigation to solve these problems must be based on a rigorous analysis of fundamental phenomena governing the freezing of living tissue, which is the focus of the present work.

A biological cell is subjected to coupled thermal and osmotic stresses during the freeze-thaw process. When ice forms in the extracellular medium, solutes are concentrated in the remaining liquid phase, imposing an osmotic stress on adjacent cells. The cell membrane acts to regulate both the efflux of water in response to this stress and the propagation of ice to the intracellular medium. Injury to cells occurs as a consequence of the magnitude of manifestation of either of these processes. The modulation of cellular volume during freezing and thawing may be described by a simple transport model (1,2).

$$\frac{dV_w^i}{dT} = \frac{L_{pg} ART}{Bv_w} \exp \left[ \frac{\Delta E_{lp}}{R} \left( \frac{1}{T_g} - \frac{1}{T} \right) + \Delta E_{os} \left( \frac{1}{\pi} - \frac{1}{\pi_g} \right) \right] \ln \frac{X_w^i}{X_w^o} \quad (1)$$

The nomenclature is defined in the original publications. Application of this model is predicted on the availability of accurate experimental data for the membrane permeability ( $L_{pg}$ ) and its thermal ( $\Delta E_{lp}$ ) and osmotic ( $\Delta E_{os}$ ) coefficients for the cell type of interest at subfreezing temperatures. Although such data is predictably scarce we have recently made the necessary experimental measurements using a combined cryomicroscopic (3) and computer image analysis (4) technique for granulocytes (2), skin (5), and yeast (6). The results show very good agreement between model and experiment in the domain of freezing and thawing governed by osmotic effects.

The foregoing analysis applies to individual cells subjected to a specific localized thermal protocol within a freezing system. In practical applications systems of finite dimensions are frozen, resulting in a temperature field which may vary significantly in three dimensional and with time. Thus, whereas the osmotic response

to freezing occurs on a microscopic scale, the driving thermal process is macroscopic and requires modeling in a completely different framework. The general solution of the temperature field determines, in conjunction with the proper thermodynamic equation of state for the system, the local osmotic stress on individual cells. The local thermal state also governs the membrane transport as indicated in Eq. (1). The freezing process involves a phase change within the tissue and may be described by

$$\frac{\partial}{\partial t} (\rho c T + \rho L) = \nabla k \nabla T \quad (2)$$

which has the internal moving boundary constraint at the solid-liquid interface as

$$k_1 \nabla T_1 + \rho L S = k_s \nabla T_s \quad (3)$$

Since biological tissue is heterogeneous and usually has a complicated geometry, we solved the thermal problem by the finite element technique (7), enabling local thermal histories to be obtained (8) by which the osmotic response of individual cells can be predicted from Eq. (1). This combination of macroscopic and microscopic modeling techniques for describing the thermal and osmotic behavior of a freezing tissue affords us the capability for rigorously simulating the cryopreservation process in evaluating effects of various protocol design parameters.

This work was sponsored in part by a Research Fellowship from the Alexander von Humboldt Foundation of the Federal Republic of Germany.

#### References

1. Knox, J. M., Schwartz, G. J. and Diller, K. R., "Volumetric Changes in Cells During Freezing and Thawing", J. Biomech. Engr., Trans. ASME, Vol. 102, 1980, pp. 91-97.
2. Schwartz, G. J. and Diller, K. R., "Analysis of the Water Permeability of Human Granulocytes at Subzero Temperatures in the Presence of Extracellular Ice", J. Biomech. Engr., Trans. ASME, Vol. 105, 1983, pp. 360-366.
3. Diller, K. R., "Quantitative Low Temperature Optical Microscopy of Biological Systems", J. Microscopy, Vol. 126, 1982, pp. 9-28.
4. Dietz, T. E., Diller, K. R. and Aggarwal, J. K., "Automated Computer Evaluation of Time-Varying Cryomicroscopical Images", Cryobiology, Vol. 21, 1984, pp. 200-208.
5. Aggarwal, S. J., Diller, K. R. and Baxter, C. R., "Membrane Water Permeability of Isolated Skin Cells at Subzero Temperatures", Cryo-Letters, Vol. 5, 1984, pp. 17-26.
6. Schwartz, G. J. and Diller, K. R., "Osmotic Response of Individual Cells During Freezing. II. Membrane Permeability Analysis", Cryobiology, Vol. 20, 1983, pp. 542-552.
7. Hayes, L. J. and Diller, K. R., "Implementation of Phase Change in Numerical Models of Heat Transfer", J. Energy Resources Technology, Trans. ASME, Vol. 105, 1983, pp. 431-435.
8. Hayes, L. J., Diller, K. R., Lee, H. S. and Baxter, C. R., "On the Definition of an Average Cooling Rate During Freezing", Cryo-Letters, Vol. 5, 1984, pp. 85-98.

A BIOMECHANICAL ANALOG OF CURVE PROGRESSION AND  
STABILIZATION OF IDIOPATHIC SCOLIOSIS

Avinash G. Patwardhan, Ph.D.

and

Wilton H. Bunch, M.D., Ph.D.

Department of Orthopedics and Rehabilitation  
Loyola University Medical Center, Maywood, Illinois

Kevin P. Meade, Ph.D.

Department of Mechanical Engineering  
Illinois Institute of Technology, Chicago, Illinois

Ray Vanderby, Jr., Ph.D.

Department of Orthopedic Surgery  
Northwestern University Medical Center, Chicago, Illinois

Gary Knight, M.S.

Rehabilitation Research and Development Center  
Hines VA Hospital, Hines, Illinois

Scoliosis is a lateral deformity of the spine. Mild-to-moderate scoliosis is most often treated conservatively with an orthosis. The role of an orthosis is to reduce the curve as much as possible and then hold it until the curve is stable. Orthoses for scoliosis have been used for over 200 years, but empiricism has marked their use. With experience, clinicians have developed expectations as to general results. This empirical approach results in bracing of a high percentage of non-progressive curves. A reliable biomechanical model that better predicts the results of bracing has clearly been lacking.

This paper presents a mathematical analog whose purpose it is to describe, in a general sense, the biomechanics of curve progression and stabilization in idiopathic scoliosis. This analysis is based upon the rationale that the progression of a scoliotic curve can be described by the progressive deformation of an initially curved beam-column. Furthermore, the ratio of load bearing capacity of a scoliotic spine to that of a normal spine can be characterized by the ratio of the critical load of a curved beam-column to that of a straight beam-column. This ratio is defined as the critical load ratio ( $P_c$ ). This dimensionless quantity appears in the exact solution of the governing differential equation and boundary conditions. Hence, it provides a convenient means for conducting parametric studies. Thus, this analysis examines the stability of an unsupported (without an orthosis) scoliotic spine as a function of: the magnitude of the curvature; and the curve pattern such as single, double major, or primary and compensatory curves. Furthermore, it evaluates the stability of an orthotically supported scoliotic spine as a function of: the magnitude of the

curvature, the end support conditions indicating the extent of motion constraint imposed by an orthosis on the ends of the curve, and the magnitude and type of the stabilizing transverse load exerted by an orthosis on the curve.

This study provides a biomechanical explanation as to why larger curves are more progressive than smaller curves, and why a brace is only effective in small and moderate degrees of curvature. Furthermore, this study shows that a double major curve has a greater load-carrying capacity and, therefore, is more stable than a comparable single curve with a compensatory curvature. These results are in general agreement with the clinical findings based upon retrospective studies of patients undergoing orthotic management for scoliosis.

ULTRASONIC VELOCITY AND DENSITY RELATING TO BONE AS A BIPHASIC  
COMPOSITE MATERIAL

By

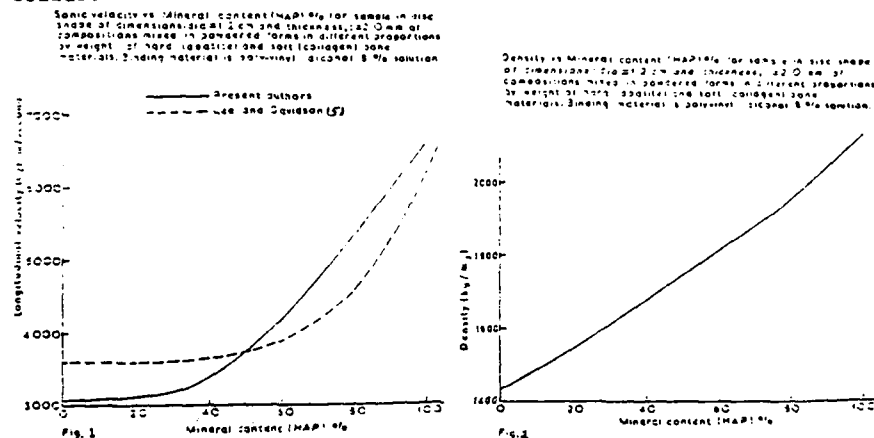
Singh, S.  
Department of Orthopaedic Surgery  
Louisiana State University Medical Center  
Shreveport, LA- 71130

Bone, as a material, has been studied in details in the recent past. From the standpoint of material study, the current investigation of bone which consists of collagen fibers and hydroxyapatite (HAP) crystal is expected to offer an explanation for mineralization alongwith suggestion to design new composite materials (1). In the present study, ultrasonic velocity and density were measured for differnt bone compositions.

Collagen and apatite as obtained from the full bone by standard technique (2), were crushed in the powdered form. Thus obtained powder was subjected to grinding with the help of dry ball-milling. Grinding was being done to obtain particle size between 150-200 mesh for attainment of chemical equilibrium. Collagen and apatite were taken in different proportions (by weight from 0% apatite to 100% apatite) in the powdered form. These ingredients were homogenized by ball-milling in the dry polythene jar. The above mentioned bone compositions were dissolved in a common solvent (5% Formic acid and Ethyldiamine in equal volumes). The solution was subjected to magnetic stirring for proper mixing. Thus treated solution was evaporated and solute was dried in an electric oven at temperature 100-120°C. The dried material were mixed with 8% solution of polyvinyl alcohol in a ratio of 2-3% by weight of the material and after that it was compressed into disc shape at a pressure of 11.04 tons/cm<sup>2</sup>. The disc were of the typical dimensions: diameter= 12mm and thickness= 2.0 mm.

The measurements of ultrasonic propagation velocity in test pieces of bone compositions was carried out using pulse-echo technique. The apparatus used in the measurement to generate ultrasound waves was Ultrasonic Material Tester (Type UCT-2). The frequency of the ultrasound was 800 Khz. The transducer was coupled directly to the sample with the help of coupling medium Glycerin. The same transducer was used as transmitter as well as receiver. The time-delay in traversing the to and fro journey through the sample was directly displaced between the first and second reflected pulse on the soniscope. The velocity of ultrasound was calculated by taking the ratio of the thickness of the specimen to the half of the time-delay. The same experiment was repeated of other samples of differnt bone compositions. Density was measured using direct as well as displacement method as reported earlier by the author (3).

The results of ultrasonic velocity and density for different bone materials are shown in Fig. 1 and 2 respectively. These data show that both ultrasonic velocity and density had a definite trend of variation with increase in the proportion of apatite. From Fig. 1, it is clear that the variation of ultrasonic velocity with apatite was linear for the all proportions greater than 50% of apatite; however, this is not true for proportions less than 50% of apatite. Fig. 2 shows that density increased linearly with the increase in the proportions of apatite. These findings are consistent with the reported results of others (4,5,6,7). These results further indicate that bone as a composite material may probably belong to Reuss solids.



#### REFERENCE

1. Maeda, M., Tsuda, K. and Fukada, E., "The Dependence of Temperature and Hydration of Piezoelectric, Dielectric and Elastic Constants of Bone", Japanese J. Appl. Phys., Vol. 15, No. 12, 1976, pp. 2333-2336.
2. Becker, R.O. and Brown, F.M., "Photoelectric Effects in Human Bone", Nature, Vol. 206, 1965, pp. 1325-1326.
3. Singh, S., "Ultrasound Generation and Propagation in Hard Tissues", Ph. D. Thesis, JNU, India, 1982.
4. Singh, S., "Ultrasonic Velocity Dispersion in Bone Materials", 36th ACEMB, 1983, pp.149.
5. Lees, S. and Davidson, C.L., "A Theory Relating Sonic Velocity to Mineral Content in Bone", Ultrasonic Tissue Characterization, Vol. 525, 1979, pp.179-187.
6. Lees, S. and Davidson, C.L., "The Role of Collagen in the Elastic Properties of Calcified Tissues", J. Biomech., Vol.10, 1977, pp.475-486.
7. Katz, J.L., "Hard Tissues as a Composite Material—I Bounds on the Elastic Behavior", J. Biomech., Vol.4, 1971, pp.455-473.

A NUMERICAL MODEL FOR THE DYNAMIC RESPONSE  
OF THE HUMAN OTOLITH ORGANS

by

William A. Best

and

Wallace Grant

Engineering Science and Mechanics Department  
Virginia Polytechnic Institute and State University  
Blacksburg, Virginia 24061

The Otolith organs are the linear motion sensors of the Mammalian system. Their importance to normal activity is critical. As part of the Vestibular System, these small organs are located in the inner ear in close proximity to the body's angular motion sensors, the Semicircular Canals. Mathematically modelled they consist of an overdamped second-order system with an inertially active mass. The governing equations of motion which describe the relative displacement of the inertial mass with respect to the skull have already been developed. When these equations are nondimensionalized they yield two non-dimensional parameters which characterize the dynamic response of the system.

A finite difference solution to the non dimensional set of three, coupled, partial-integral differential equations indicates that the mass displacement is proportional to linear velocity of the skull over the range of normal physiologic motion. The system frequency response from this analysis has a much higher upper brake point frequency than that measured by many experimental determinations. Since the experimental measurements all involve other parts of the human system to measure output instead of just the transducer itself these elements must be slower than the otolith.

A THEORETICAL MODEL OF THE CORNEA AS A THIN SHELL  
OF VARIABLE THICKNESS IN RELATION TO RADIAL KERATOTOMY

by

Sharon Lee Williams

and

Wallace Grant

Engineering Science and Mechanics Department  
Virginia Polytechnic Institute and State University  
Blacksburg, Virginia 24061

A theoretical study of the deformation fields of the cornea under internal pressure is presented. The general elasticity equations describing a thin shell of variable thickness are solved using finite difference techniques. To gain insight into the natural corneal structure, the constant thickness case is compared to one of normal thickness. The bending stresses are found to influence the cornea's natural curvature. In the third case, the normal thickness is increased 10% to model the edematous state resulting from the incisions made during radial keratotomy. A comparison of the third case reveals the increased thickness in the peripheral cornea makes a minor contribution to the displacement; but moreover, the curvature change is opposite to that desired from radial keratotomy. The incisions are necessary to weaken the lateral support of the shell allowing the displacement and change in curvature which corrects myopia.

## COMPUTER SIMULATION BASED ON NETWORK THERMODYNAMICS

by

Donald C. Mikulecky  
Department of Physiology and Biophysics  
MCV/VCU - Box 551 MCV Station  
Richmond, VA 23298-0001

Network thermodynamics is the next logical step in the development of thermodynamic reasoning. It is now obvious that classical (equilibrium) thermodynamics is the generalized study of multiport capacitors and that Onsager's nonequilibrium thermodynamics is the generalized study of multiport resistors. Furthermore, the classical results of Onsager concerning reciprocity have been shown, in recent unpublished work of Peusner, to result more rigorously from topological and differential geometrical considerations through Tellegen's theorem rather than from molecular statistics. Network thermodynamics unifies these ideas, incorporates kinetics in a natural manner, and provides a metric structure for thermodynamics [see Callen, H., "A Symmetry Interpretation of Thermodynamics" in *Foundations of Continuum Thermodynamics* (J.J.D. Domingos, M.R. Nina, and J.H. Whitelaw, eds.) Wiley, N.Y. (1973) pp. 61-80].

It has been over ten years since network thermodynamics was first offered as a paradigm for the analysis of complicated interacting biological systems [Peusner, L., "The Principles of Network Thermodynamics, Theory and Biophysical Application" (1970), Ph.D. thesis, Harvard, Cambridge, MA; Oster, G., A. Perelson, and A. Katchalsky, *Network Thermodynamics*, *Nature* 234:393-399 (1971)]. Since then, a multitude of different problems have been simulated using network thermodynamic principles particularly using the version of network thermodynamics first offered by Peusner in his Ph.D. thesis. (For a comprehensive review, see Mikulecky, D.C., "Network thermodynamics: a candidate for a common language for theoretical and experimental biology," *Am. J. Physiol.* 245, 1983, R1-R9.) Network thermodynamics provides a framework for simulation because it is a simple, accurate way for the average biologist to simulate his own experiments without the need of a computer expert to do it for him. By translating the biological problem into its representation as a dynamic system in electrical network symbolism (Peusner, 1970) it can be readily simulated using circuit simulation packages such as NET-2, SPICE-2, ASTEC and many others. This paradigm rests on the thermodynamic analogy between all the dissipative components of a system and electrical resistance, certain forms of energy storage and electrical capacitance, and in some cases, inertial energy storage and inductance. By appropriately manipulating sources, either independent or dependent, more sophisticated effects such as nonlinearity and coupling in multiports can be modeled. Thus, in the same way that circuit analysts build transistor models, membrane elements or reaction steps can be simulated. Since the conservation laws

used when mass or charge balance equations are written are naturally incorporated in circuit simulation programs through Kirchhoff's laws, most of the difficulty of solving the problem has been relegated to the program. It sets up the differential equations and applies the conservation laws in harmony with a network topology chosen to be consistent with the biological system's structure. In this way, structure-function-relationships are modeled in a natural way and a minimum of explicit mathematical manipulation is required. This is often comforting to the biologists and enables experimentalists to achieve results previously only accessible to those with far more mathematical training.

The success of the paradigm to date suggests that a new generation simulation-programs may be needed and justified. The process of translating the biological network into an electrical one is forced by the nature of the existing network simulation programs. It would be convenient for programs to be designed for direct application to biological networks written in language familiar to the biologist and circumventing the conceptual leap necessitated by the circuit simulation programs. In the process of making this next step, the link between the thermodynamic fundamentals and the role of topology will become clearer and the fact that the network simulation paradigm has its roots in some very fundamental concepts should re-emerge. Oster, *et al.*, were quick to point this out, but, since they used a more difficult diagrammatic representation, namely bond-graphs [see Mikulecky, D.C. and S. R. Thomas, "Some Network Thermodynamic Models of Coupled, Dynamic Physiological Systems," *J. Franklin Inst.* 308:309-326 (1979)] they failed to stimulate any large scale response on the part of biologists.

A large part of future work in network simulation should focus on problems of parameter estimation and optimization. Some interesting results have been obtained from the existing models and will be mentioned in an effort to stimulate interest in these problems.

MECHANICS OF COMPOSITE MATERIALS:  
PAST, PRESENT, FUTURE

by

C.C. Chamis  
NASA Lewis Research Center  
Cleveland, Ohio 44135

Composite mechanics has evolved to encompass a wide range of "continuum" mechanics methods used to study and predict fiber composite behavior. The composite behavior is studied or predicted at various inherent scales ranging from the microstructural characteristics (inter-constituents) to composite structural response. The corresponding composite mechanics disciplines associated with these scales include: micromechanics, macromechanics, laminate theory, singularity mechanics, life/durability theories and structural mechanics (used herein in the broadest context). The level of sophistication has also evolved from simple strength of materials concepts to intricate asymptotic methods, finite element methods and other approximate and numerical methods. Many of these methods are applicable to several scales while others are applicable to only one. The level of composite mechanics sophistication used in a specific study and scale centers mainly on three equally important considerations: (1) capturing the inherent physics at the different scale levels; (2) the degree of local detail desired; and (3) the technical interest of the individual investigator. These equally important considerations have led to numerous significant contributions at the various scales of composite behavior.

In the present paper, we discuss composite mechanics at its various levels of sophistication and attendant scales of application. Correlation with experimental data is used as the prime discriminator between alternative methods and level of sophistication. Major emphasis is placed on: (1) where composite mechanics has been; (2) what has it accomplished; (3) where it is headed, based on present research activities; and (4) at the risk of being presumptuous, where it should be headed.

The discussion is developed using selected but typical examples of each composite mechanics discipline, identifying degree of success and problems remaining. The discussion is centered about fiber/resin composite. However, problem areas for high temperature composites are also identified. Hybrid composites, composites made from fabric or cloth, and environmental effects are included. Finally, problem areas of current interest such as: impact resistance, compression fatigue, delamination, durability and composite quality assurance are addressed. This is done in order to stimulate technical discussion and thinking on composite mechanics focused research in an attempt to resolve some of the present concerns in the composites community in a timely manner.

## ANALYSIS OF PROGRESSIVE MATRIX CRACKING IN COMPOSITE LAMINATES

by

George J. Dvorak  
Dept. of Civil Engineering,  
University of Utah,  
Salt Lake City, UT 84112

and

Norman Laws  
Dept. of Mech. Engineering  
University of Pittsburgh  
Pittsburgh, PA 15260

In many fibrous composite systems the failure strain of the matrix is much smaller than that of the fiber. Under load, the difference leads to progressive matrix cracking which gradually reduces the elastic moduli of a composite ply. In laminated plates, and in other composite structures, matrix cracking may affect each ply in a different way and thus cause changes both in local stress and strain fields and in the overall thermoelastic properties of the structure. This paper describes: (i) development of constitutive equations for cracked fibrous composites, (ii) fracture mechanics of progressive cracking in a composite ply, and (iii) analysis of growth of internal crack systems in laminated plates, and their effect on average local fields and overall instantaneous thermoelastic properties.

In the first part of the paper we discuss stiffness changes in unidirectional composites caused by crack systems. Aligned slit cracks on parallel planes in the fiber direction, as well as slit and penny-shaped cracks in the transverse plane are considered. Closed form estimates of elastic stiffnesses and compliances and thermal stress vectors of fibrous composites containing one of these crack systems are obtained with the self-consistent method. Two models of the cracked composite are used: a three-phase model with interactions between fiber, matrix and cracks, and a two-phase model in which fibers are regarded as small compared to cracks and thus are combined with the matrix into a single phase which then contains interacting cracks.

In the second part of the work, the thermoelastic properties and average local fields of the cracked composite are applied to fibrous composite plies, and combined with fracture criteria for growth of cracks in a ply. This makes it possible to formulate an incremental procedure for evaluation of instantaneous crack density, average local fields, and overall thermoelastic properties of a ply subjected to an arbitrary strain history which may be combined with uniform thermal changes.

The third part of the study extends the above results to laminated plates. Lamination plate theory is modified for use with cracked plates and used to derive another incremental procedure for evaluation of instantaneous crack densities and average local fields in individual cracking layers, and of overall instantaneous stiffnesses, compliances, and thermal stress and strain vectors of the laminated changes. Applications to bent plates are also discussed. The results are illustrated by sample calculations for several angle-plyed graphite-epoxy plates. Comparisons with experimental results show good agreement with the theory.

Many additional aspects of the theory are discussed. These include, for example, interaction between cracks in a ply and adjacent plies, selection of preferential crack systems (axial or transverse, in matrix or fibers), and the effect of slit cracks in one ply on initiation of matrix and fiber cracks in adjacent plies. However, the principal emphasis of the paper is on overall behavior of cracking composite structures, on techniques for their analysis, and on the analogies which one can draw between the opposing effects of reinforcement and cracking in composite materials.

Some of the results in the first part have appeared in N. Laws, G. J. Dvorak, and M. Hejazi, Mechanics of Materials, 2, 123-137, 1983. An example of an application of the theory is shown in Fig. 1.

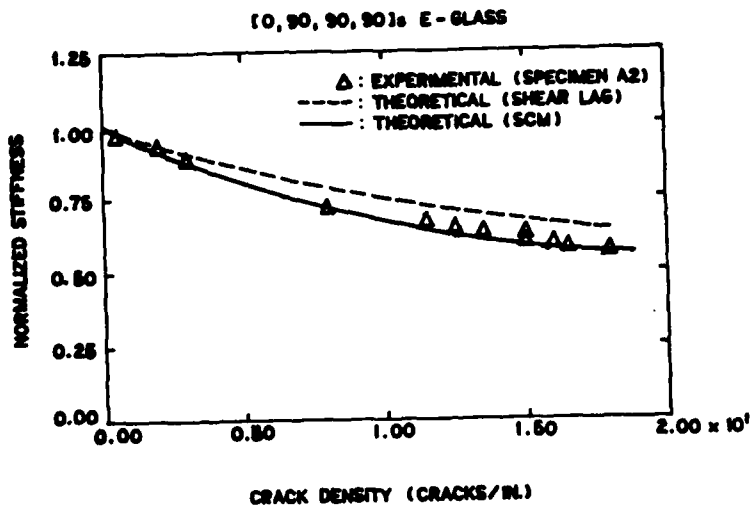


Figure 1. Comparison with theoretical predictions of experimentally observed stiffness changes and crack densities. The (SCM) curve was calculated from the self-consistent estimate of stiffness in 90° plies. Experimental data and shear lag analysis are taken from Highsmith and Reifsnider (1982).

A LINEAR ELASTIC MODEL FOR PREDICTING THE DIRECTION  
OF CRACK EXTENSION IN COMPOSITES

by

Carl T. Herakovich  
Michael A. Gregory  
Department of Engineering Science & Mechanics  
Virginia Polytechnic Institute & State University  
Blacksburg, VA 24061

Matthew B. Buczek  
Atlantic Research Corporation  
Alexandria, VA 22314

A new theory for predicting the direction of crack extension in composite materials [1] is reviewed and compared to results obtained using other theories. Following upon the known results for isotropic materials, the new theory assumes that the direction of crack extension is a function of the normal stress  $\sigma_{\phi\phi}$  acting on planes emanating from the crack tip. The theory differs from that for isotropic materials in that the direction of crack growth is also assumed to be a function of the tensile strength  $T_{\phi\phi}$  on these planes (Fig. 1). The tensile strength varies with the angle  $\phi$  due to the anisotropy of the material. The preferred direction of crack extension is then assumed to be in the direction of the maximum ratio

$$R(r_o, \phi) = \frac{\sigma_{\phi\phi}}{T_{\phi\phi}}$$

measured at some small distance  $r_o$  from the crack tip. The strength  $T_{\phi\phi}$  is assumed to have the form (Fig. 1)

$$T_{\phi\phi} = X_T \sin^2 \beta + Y_T \cos^2 \beta$$

This definition of  $T$  satisfies the three limiting cases: isotropic material, strength in the fiber direction, and strength transverse to the fibers. The theory has been incorporated into a finite element code and results for the direction of crack extension in unidirectional off-axis coupons under tensile load were compared with other theories and experiment. Results are presented for a variety of fiber orientations and initial crack directions in graphite-epoxy. It is shown that the new theory provides the best correlation with experiment. As an example, the new theory successfully predicts that a crack will grow parallel to the loading (and fiber) direction for a  $0^\circ$  unidirectional coupon with a center slot perpendicular to the loading direction.

Results are also presented showing that the theory successfully predicts that a transverse crack can change direction into a delamination at a  $0/90$  interface in a cross-ply laminate under axial load.

## REFERENCES

1. Buczek, M. B., and Herakovich, C. T., "Direction of Crack Growth in Fibrous Composite," Mechanics of Composite Materials, (G. J. Dvorak, ed.), ASME AMD - Vol. 58, Am. Soc. Mechanical Engineers, 1983, pp. 75-82.

## ACKNOWLEDGEMENT

This work was supported by the NASA Virginia Tech Composites Program, NASA Grant NAG 1-343, and Hercules Incorporated.

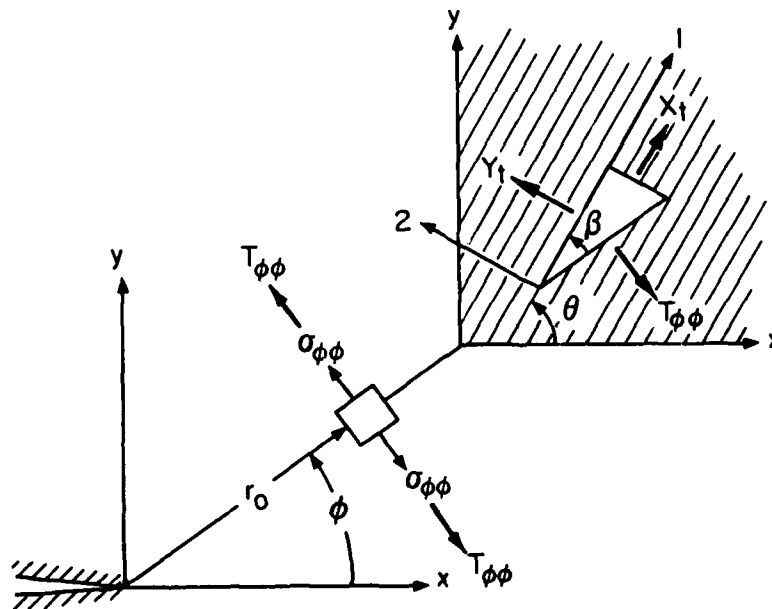


Fig.1 Normal Stress Ratio Parameters

ON THE GEOMETRY AND ELASTIC RESPONSE OF INVOLUTE BODIES  
OF REVOLUTION

by

N. J. Pagano  
Air Force Wright Aeronautical Laboratories  
Wright-Patterson AFB, Ohio 45433

Involute construction is an approach used in contemporary rocket motor technology for the fabrication of exit cones and other bodies of revolution and consists of laminating identical composite sheets of uniform thickness along curved trajectories, called involute surfaces. In this presentation, we shall review the theoretical and practical considerations governing the nature of the involute surface as well as its image, or plv pattern, in the as-delivered flat composite sheet material. Included in this description will be the prediction of the material distortion that takes place when incorrect plv pattern designs are employed in the fabrication process.

The development of a recent theory to define the axisymmetric elastic response of involute bodies shall also be discussed. The model is based upon the application of Reissner's variational principle and an assumed stress field to given sub-regions of the body and approaches the theory of elasticity in the limit of vanishing sub-region thickness. The new model incorporates the influence of pore pressure, free expansion strains, body forces, and temperature-dependent elastic properties.

Example problem solutions will be given to demonstrate the unique response characteristics of involute bodies to loading and environmental conditions.

ACCELERATION WAVES IN INEXTENSIBLE FIBER  
REINFORCED THERMOELASTIC SOLIDS

by

S. Dost, The University of Calgary  
Dept. of Mechanical Engineering  
Calgary, Alberta, Canada T2N 1N4

H. Balci, Ege University  
Department of Mechanical Engineering  
Izmir, Turkey

The propagation of acceleration waves of arbitrary form propagating into a deformed inextensible fiber reinforced thermoelastic solid is investigated. An acceleration wave is defined as a second order propagating surface of discontinuity on which the position vector and absolute temperature, and their first order derivatives with respect to time and space coordinates are continuous while the second derivatives of these quantities may suffer jumps but are continuous everywhere else. By computing the jumps of the balance equations on the singular surface, implicit equations for wave speeds corresponding to non-zero amplitudes of acceleration wave are obtained.

The same equations from wave speeds are also derived for isotropic materials. In the case of principle waves, assuming the medium is in thermal equilibrium and at rest ahead of the wave front, the speeds for longitudinal and transverse waves are obtained in explicit forms, and the conditions of existence of real wave speeds are investigated. Furthermore, the restrictions imposed by inextensible fibers on the propagation of principal waves are discussed in detail for some special waves.

INFLUENCE OF MIX PROPORTIONING IN THE DESIGN AND APPLICATION  
OF A FIBRE REINFORCED CONCRETE

by

G. Corradini, L.A. Pajewski, G. Scoccia, R. Volpe  
Istituto di Chimica Applicata e Industriale  
Facoltà di Ingegneria, Università dell'Aquila  
Italy

This paper presents the result obtained by a series of tests performed on the basis of a factorial experiment, whose aim is the statistical evaluation of the main characteristics of a steel-fibre reinforced concrete, in order to determine the necessary parameters for design calculation.

The following factors were chosen as influencing the mechanical properties: fibre content, cement content and water/cement ratio.

Steel fibres (1.50 mm and  $\varnothing$  0.50 mm) were used.

All the concrete mixes contained a superplasticizer.

These factors were considered as follows:

- fibre content (4 levels): 0, 0.5, 1.0 and 1.5% in volume;
- cement content (2 levels): 400 and 475 kg/m<sup>3</sup>;
- water/cement ratio (3 levels): 0.4, 0.5 and 0.6 in weight.

The tests were iterated three times.

On the samples taken from each concrete mix, the following properties were measured:

- flexural, compressive and tensile (Brazilian test) strength;
- secant modulus of elasticity.

By means of the flexural test the 1<sup>st</sup> crack moment and the corresponding strains ( $\epsilon_c$  and  $\epsilon_t$ ), the number, width and depth of the cracks, the deflection and the respective moments up to breakage were determined.

Test results reliability was evaluated by means of variance analysis and F-tests at determined significance levels.

The main effects and the interactions among the various experimented factors are given for each property.

The results aimed at determining the parameters necessary for the construction of a forecasting model for steel-fibre reinforced concrete behaviour, in order to evaluate its main and characteristic design data.

INTEGRATED MODEL ANALYSIS AND  
CHARACTERIZATION OF THREE-DIMENSIONAL  
WOVEN FIBER COMPOSITES

by

Chang Long Ma  
Department of Mechanical Engineering  
Fushun Institute of Petroleum Technology  
Fushun City, Liaoning Province  
The People's Republic of China

Woven fiber materials are gaining increasing technological importance as reinforcements for polymeric and metal matrix composites. In the case of two-dimensional woven fabric composites, a significant effort has been made by Chou and Co-Workers (1-6) to investigate the relation between fabric structure and properties. They identified the various types of weaves by the material and geometrical patterns of repeats as well as the size of yarns. They also have established analytical models for analyzing the thermo-mechanical properties including the nonlinear stress-strain behavior.

The purpose of this paper is to present a new method of integrated model analysis of the stiffness and strength properties of three-dimensional woven fiber composites. The model of unit cell is idealized as an assemblage of some intersecting laminae and pieces of matrix. The methodology of the analysis applies to 3-D woven structures in general. However, for the convenience of comparison with experiments, we consider Magnaweave composites in particular. Figure 1 depicts the general configuration of unit cell with the interlocking of fibers at point d. The essence of the analysis involves the consideration of the contributions to the total strain energy of the composite due to the yarn axial tension, bending and compression by jamming forces. The magnitudes of the jamming forces are then determined from the application of an energy principle. Comparisons of analytical results with experiments have indicated good predictability of the present theory. The analysis and characterization work are being extended to Magnaweave composites based upon metal matrices.

References

1. Ishikawa, T., and Chou, T. W., "Elastic Behavior of Woven Hybrid Composites", Journal of Composite Materials, Vol. 16, Jan. 1982, pp. 2-19.
2. Ishikawa, T., and Chou, T. W., "One-Dimensional Micro-Mechanical Analysis of Woven Fabric Composites", AIAA Journal, in press.
3. Ishikawa, T., and Chou, T. W., "Stiffness and Strength Behavior of Woven Fabric Composites", Journal of Materials Science, 17, 3211 (1982).

4. Ishikawa, T., and Chou, T. W., "In-Plane Thermal Expansion and Thermal Bending Coefficients of Fabric Composites", Journal of Composite Materials, 17, 92, (1983).
5. Ishikawa, T., and Chou, T. W., "Thermo-Elastic Analysis of Hybrid Fabric Composites", Journal of Materials Science, in press.
6. Ishikawa, T., and Chou, T. W., "Non-Linear Behavior of Woven Fabric Composites", Journal of Composites, in press.

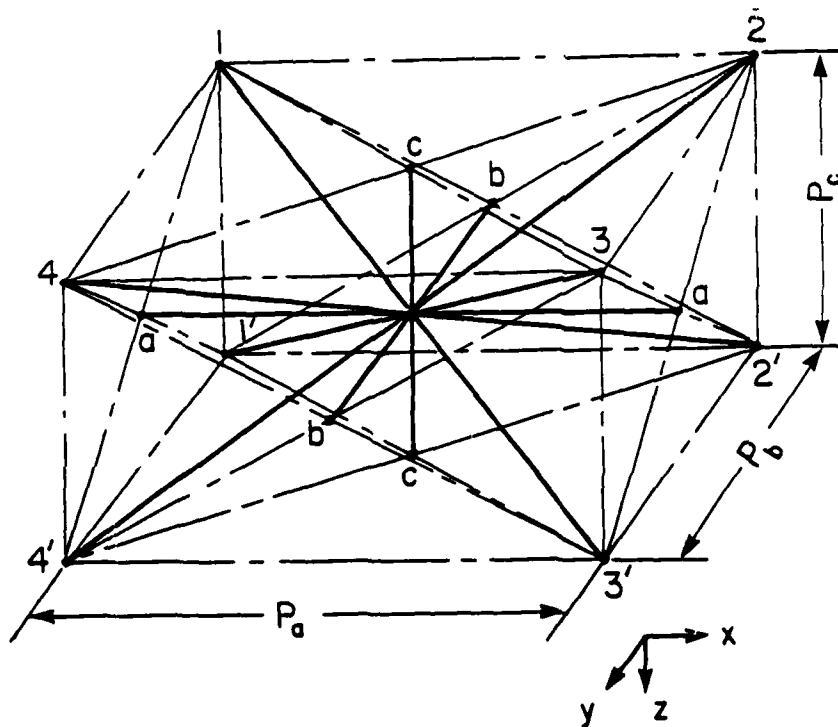


Fig. 1. A "unit cell" structure for modelling 3-D woven fiber composites.

NONLINEAR MATERIAL MODELS FOR COMPOSITE PLATES AND SHELLS<sup>†</sup>

by

K. Chandrashekhara and J. N. Reddy

Department of Engineering Science and Mechanics  
Virginia Polytechnic Institute and State University  
Blacksburg, Virginia 24061 USA

Composite materials are known to exhibit significant nonlinearity in stress-strain behavior even at low strains. The nonlinearity is not isotropic but varies with direction, as do the elastic properties. Models for such elastic-plastic behavior of orthotropic and anisotropic materials are not well developed.

In the present study material models are developed for composite plates and shells, and numerical results for bending are presented using the finite element method as exact solutions are not tractable for elastic-plastic problems involving complex geometries and/or strain hardening materials. The following material models are used in the present study.

1. Modified Ramberg-Osgood Model. The basic Ramberg-Osgood relation is based on the deformation theory of plasticity in which we fit a curve to the stress-strain data before the stress analysis problem is attacked. But this approach is valid for unidirectional stress-strain data and has to be modified for multiaxial stress state. The modified model can be used to approximate experimental curves exhibiting strain softening.

2. Hill's Anisotropic Yield Criteria (Elastic-Perfectly Plastic Material). Hill's yield criteria is based on the incremental theory and when applied to isotropic material it reduces to the familiar Von-Mises (distortion) theory. The Hill's theory is based on the assumptions of the incompressibility of plastic strains and no yielding due to hydrostatic (spherical) stress states. Although these assumptions are not valid in general, Hill's criteria is widely used.

3. Modified Hill's Criteria (with Hardening). Hill's anisotropic yield criteria can be modified to include hardening effect like isotropic hardening for monotonic loading, kinematic hardening to predict the Bauschinger effect during cyclic loading and/or combination of isotropic-kinematic hardening.

---

<sup>†</sup>This research was conducted during an investigation supported by the Structural Mechanics Section of NASA Lewis Research Center. The authors are grateful to Dr. C. C. Chamis for the support.

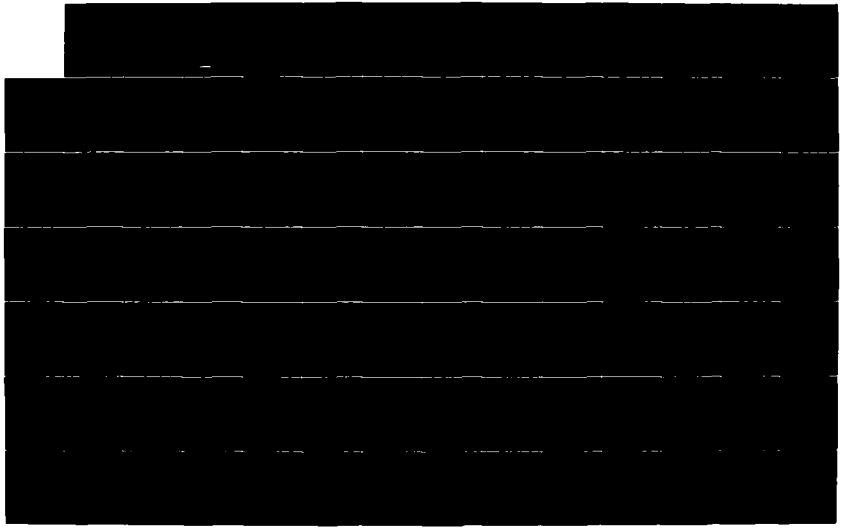
AD-A171 026

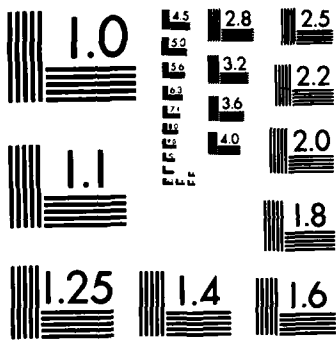
ABSTRACTS 21ST ANNUAL MEETING SOCIETY OF ENGINEERING  
SCIENCE INC OCTOBER 1 (U) VIRGINIA POLYTECHNIC INST  
BLACKSBURG & FREDERICK ET AL. 1984 ARO-21888 EC-CF  
DAG29-84-M-0119 1/6 5/2

2/6

UNCLASSIFIED

NL





MICROCOPY RESOLUTION TEST CHART  
NATIONAL BUREAU OF STANDARDS-1963-A

USE OF THE KOLSKY BAR IN DYNAMIC  
FRACTURE INITIATION

by  
J. Duffy  
Brown University  
Division of Engineering  
Providence, Rhode Island 01912

A description is presented of an experimental technique used to determine the value of the stress intensity factor at fracture initiation under dynamic conditions [1]. The value of  $K_I$  achieved by this means is  $2 \times 10^6 \text{ MPa} \sqrt{\text{ms}}^{-1}$ , which is about the same or slightly higher than obtained by using the Charpy test. However, the present technique has the advantage over Charpy in that it provides a direct measure of the load at the fracture site as well as of crack opening displacement, both as functions of time. The accuracy of the technique is discussed in light of a finite element analysis provided by Nakamura et. al. [2].

The specimen used in this experiment consists of a precracked notched round bar produced by machining circumferentially to a uniform depth and then growing a uniform fatigue crack by bending the bar as a rotating beam, Figure 1. The load is provided by a tensile pulse initiated at one end of the bar by the detonation of an explosive charge. Strain gages mounted on the bar record the tensile pulse incident on, reflected from and transmitted through the crack section. Following Kolsky [3], the last of these records gives a measure of the load and hence of average stress at the fracture site as a function of time. Notch opening displacement as a function of time is measured optically by an adaptation of the Moire technique. Eliminating time between these two measurements provides a load-displacement curve from which the fracture initiation parameters can be calculated. For a nominally brittle material  $K_{Ic}$  is found by using

$$K_I = (P/\pi R^2) \sqrt{\pi R} F(2R/D) \quad (1)$$

where  $R$  is the radius of the unfractured ligament,  $P$  is the load at the fracture site as calculated from the load-displacement curve,  $D$  is the diameter of the bar and  $F(2R/D)$  is a size function [4]. When testing more ductile materials the value of  $J$  can be calculated from a modified expression for the load-displacement curve

$$J = \frac{1}{2\pi R^2} \left( 3 \int_0^\delta P d\delta - P\delta \right) \quad (2)$$

where  $\delta$  is the notch-opening displacement.

A critique of the above technique was presented by Nakamura et. al. [2], based on a finite element analysis of the circumferentially notched round bar during the passage of a tensile pulse. In their analysis the bar is taken as elastic-plastic and the uniaxial stress-strain curve is taken from results of dynamic tests with an AISI 1020 hot-rolled steel. In the analysis a uniform rate of loading is applied at one end of the bar to generate a long loading pulse, Figure 2. The finite element analysis clarifies the applicability of the load-point displacement formula, Equation (2),

employed in the analysis of test results, for the determination of dynamic fracture toughness. It shows that this formula is accurate if the circumferential precrack is sufficiently deep. For a precrack of 75% the error in  $J$  is about 15% for elastic behavior decreasing to about 5% for fully plastic section. The error in an equivalent  $K$  is about half as great. The finite element analysis also shows that the location of the strain gages on the bar at a distance of one diameter from the crack provides an accurate measure of the transmitted load. Furthermore, the analysis reveals that the formula for the  $J$ -integral, Equation (2), must be based on the load transmitted across the ligament and the notch opening displacement. This was indeed the equation employed in [1]. In summary then, the finite element analysis shows that this fracture initiation experiment can provide an accurate value of  $J_I$  (or  $K_I$ ) during dynamic fracture initiation, if the notch in the bar is made deep enough.

#### References

1. Costin, L.S., Duffy, J. and Freund, L.B., "Fracture initiation in Metals under Stress Wave Loading Conditions", Fast Fracture and Crack Arrest, Am. Soc. Testing Mat., STP 627, 1977, pp 302-318.
2. Nakamura, T., Shih, C.F., and Freund, L.B., "Elastic-Plastic Analysis of a Dynamically Loaded Circumferentially Notched Round Bar", Brown University Report, NSF Contract No. DMR-8216726/152, 1984. Submitted for publication in Engineering Fracture Mechanics
3. Kolsky, H., "An Investigation of the Mechanical Properties of Materials at Very High Rates of Loading", Proc. Phys. Soc., London, v 62-R, 1949 pp 676-700.
4. Tada, H., The Stress Analysis of Cracks Handbook, Del Research Corporation, 1973, Hellertown, Pennsylvania.

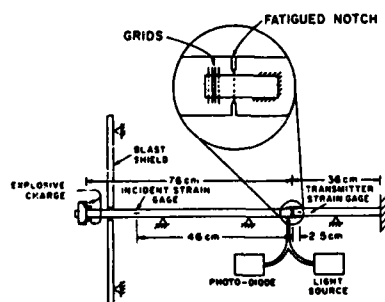


Figure 1

DIRECTION OF  
PULSE PROPAGATION



Figure 2

by

C. W. Smith, J. S. Epstein and O. Olaosebikan  
Department of Engineering Science & Mechanics  
Virginia Polytechnic Institute & State University  
Blacksburg, VA 24061

Linear elastic fracture theory was conceived [1]-[3] within a two dimensional analytical framework, and when it was extended to three dimensional problems [4],[5], the bodies so examined were infinite. In 1970, Sih [6] conjectured that linear elastic fracture mechanics (LEFM) breaks down when a crack approaches a free boundary. Subsequently, Folias [7] has studied the problem and, recently Benthem [8],[9] has obtained an accurate solution for the lowest eigenvalue of the local stress and displacement fields at the free surface of a half space when intersected by a quarter infinite crack at right angles to the surface. This solution confirms Sih's conjecture.

The first author and his associates have developed an integrated-interactive optical method for studying three dimensional cracked body problems using frozen stress photoelasticity and high density Moire interferometry [10]. In this paper, recent [11],[12] and new results for the use of this method near free boundaries are presented and compared with analytical results.

#### References

- [1] Griffith, A. A., "The Phenomena of Flow and Rupture in Solids", Philosophical Transactions of the Royal Society of London, Vol. A-221, 1921, pp. 163-197.
- [2] Westergaard, H. M., "Bearing Pressures on Cracks", Journal of Applied Mechanics, Vol. 6, 1939, pp. 49-53.
- [3] Paris, P. C. and Sih, G. C., "Stress Analysis of Cracks", Fracture Toughness Testing and Its Applications, ASTM-STP 381, 1965, pp. 49-53.
- [4] Sneddon, I. N., "The Distribution of Stress in the Neighborhood of a Crack in an Elastic Solid", Proceedings of the Royal Society of London, Vol. A-187, pp. 229-260.
- [5] Kassir, M. and Sih, G. C., "Three Dimensional Stress Distribution Around an Elliptical Crack Under Arbitrary Loadings", Journal of Applied Mechanics, Vol. 33, No. 3, 1966, pp. 601-611.
- [6] Sih, G. C., "Review of the Three Dimensional Stress Problem for a Cracked Plate", International Journal of Fracture Mechanics, Vol. 7, No. 1, March 1971, pp. 39-62.
- [7] Folias, E. S., "On the Three Dimensional Theory of Cracked Plates", Journal of Applied Mechanics, Sept. 1975, pp. 663-672.

- [8] Benthem, J. P., "On an Inversion Theorem for Conical Regions in Elasticity Theory", Journal of Elasticity, Vol. 9, No. 2, 1979, pp. 159-169.
- [9] Benthem, J. P., "The Quarter Infinite Crack in a Half Space; Alternative and Additional Solutions", International Journal of Solids and Structures, Vol. 16, 1980, pp. 119-130.
- [10] Smith, C. W., "Use of Optical Methods in the Stress Analysis of Three Dimensional Cracked Body Problems", Journal of Optical Engineering, Vol. 21, No. 4, 1982, pp. 696-703.
- [11] Smith, C. W. and Epstein, J. S., "Measurement of Three Dimensional Effects in Cracked Bodies" (In Press), Proceedings of the Fifth International Congress on Experimental Mechanics, June 1984.
- [12] Smith, C. W., Epstein, J. S. and Olaosebikan, O., "A Proposed Rationale for Accounting for Boundary Layer Effects in Designing Against Fracture in Three Dimensional Problems" (In Press), Proceedings of Eleventh Canadian Fracture Conference, June 1984.

## ON THE GEOMETRY DEPENDENCE OF R-CURVES

Mitchell I. Jolles, Michael A. Schroedl and Thomas J. Watson

Naval Research Laboratory  
Washington, DC 20375

The development of an elastic-plastic fracture predictive methodology requires the selection of a suitable fracture characterizing parameter and fracture criterion. The most common approach to ductile fracture analysis has been to combine the J-integral with the concept of the crack growth resistance curve (R-curve). Such a J-R curve, requiring the determination of J as a function of stable flaw growth for a material of interest, is regarded as a material property. Thus, in order to successfully relate crack behavior in test specimen and structure, the measured J-R curve must be independent of geometry. However, recent work indicates that different R-curves are obtained from tests on two standard specimen (compact tension and single edge notched bend) geometries.

Experiments and three-dimensional finite element analyses of compact tension and single edge notched bend specimens are performed in order to assess the geometry dependence of the R-curves. A computer assisted experimental technique has been developed which provides R-curves of high accuracy and reproducibility. The procedures and methods of data analysis are detailed and results presented for several materials exhibiting a range of behavior. Finite element analyses are described including flow theory solution techniques and determination of generalized energy release rates and the J-integral.

A geometry dependence of the R-curves is observed. This is explained in terms of factors such as the test method and data analysis procedures utilized, shear lip formation along the fracture surface and constraint in the remaining ligament. The implications of the results on techniques for elastic-plastic fracture predictive methodology are discussed.

## ANALYSIS OF DYNAMIC FRACTURE PROPAGATION USING THE SAMCR CODE

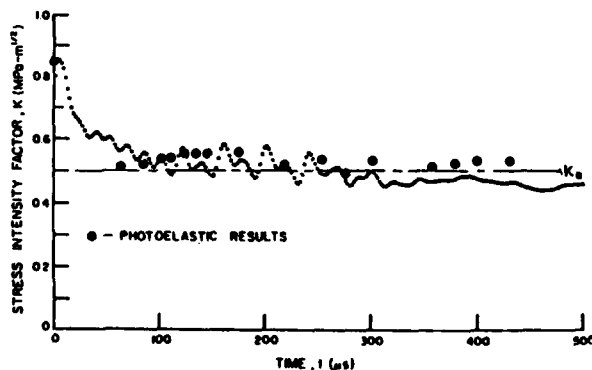
by

C. W. Schwartz, R. Chona, W. L. Fourney and G. R. Irwin  
University of Maryland  
College Park, Maryland 20742

SAMCR (Stress Analysis of Moving CRacks) is a general purpose finite element code for the analysis of rapid fracture propagation and arrest under Mode I conditions. SAMCR is based on linear elastic fracture mechanics theory and operates in a predictive fracture "application" mode: the increment of crack extension at each time step is automatically computed based on the calculated stress intensity factor ( $K$ ) at the crack tip and the specified crack tip velocity ( $a$ ) vs.  $K$  fracture propagation criterion for the material. Major noteworthy features of SAMCR include: (a) efficient formulation based on four-node isoparametric elements and explicit time integration; (b) crack advance simulation based on a crack tip restraining force model; (c) a moving contour J-integral formulation for calculation of  $K$ , and (d) incorporation of thermal effects, both for strains and for the  $a$  vs.  $K$  fracture propagation criterion.

The accuracy of the SAMCR code has been evaluated through an extensive series of verification studies including comparisons with simple analytical solutions reported in the literature, comparisons with photoelastic experimental studies of fracture propagation in modified compact tension (MCT) Homalite 100 specimens, and comparisons with results from the Thermal Shock Experiments (TSE) on A508 steel cylinders conducted by the Oak Ridge National Laboratory. Figure 1 shows a typical comparison between the calculated and photoelastically-determined  $K$  vs. time response for a Homalite 100 MCT specimen. For the three MCT experiments analyzed, the computed crack jumps differed by less than 1% from the experimental values. For the four TSE crack jump events analyzed, the maximum difference between the predicted and measured crack jump was 19%. This larger discrepancy is due in part to a limited knowledge of the correct  $a$  vs.  $K$  fracture propagation criterion for A508 steel.

Figure 1. Predicted and Experimental Values of  $K$  vs. Time for Homalite 100 MCT Specimen (Test P9)



STRESS INTENSITY DISTRIBUTIONS FOR CORNER CRACKS EMANATING  
FROM OPEN HOLES IN PLATES OF FINITE WIDTH

by

Gianni Nicoletto  
Istituto di Meccanica Applicata alle Macchine  
Universita di Bologna  
Viale Risorgimento, 2  
Bologna, Italy

A series of frozen stress photoelastic experiments on the corner crack at a open hole problem are presented. Due to its technological geometries on which the effort of numerical researchers, particularly of the Finite Element Alternating Method developers, has been directed [1]. In the present paper experimental SIF distributions are compared to FEAM distributions for approximating flaw shapes. Furthermore natural corner cracks obtained fatiguing PMMA specimens have  $\nu = .37$  [2], are correlated to monotonic flaw shapes observed in photoelastic specimens whose  $\nu = .5$ . Natural flaws appear to propagate under nearly constant SIF except for a localized SIF increase when approaching the free surfaces.

References

- [1] Kullgren, T. E., Smith, F. W., Ganong, G., Journal Engineering Materials & Technology, Vol. 100, 1979.
- [2] Grandt, A. F., Macha, I. E., Engineering Fracture Mechanics, Vol. 17, 1983, pp. 63-73.

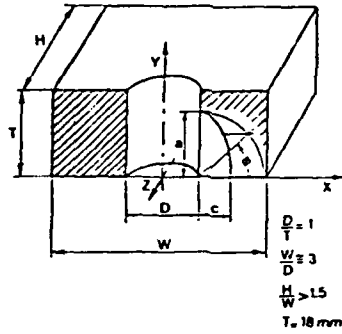


Fig. 1 Corner crack problem and specimen geometry.

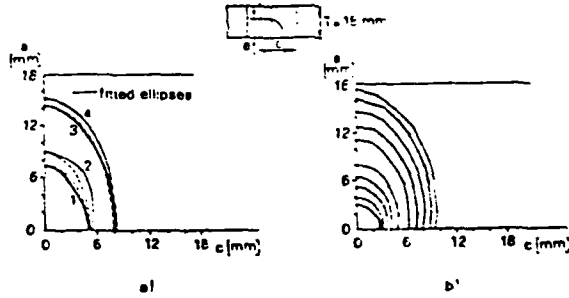


Fig. 2 Experimental flaw shapes a) monotonic in photoelastic material ( $\nu = .5$ ); b) fatigue flaws in PMMA, [2].

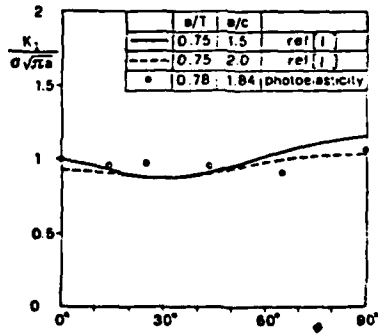


Fig. 3 Numerical and experimental SIF distributions.

ON CRACK PATHS AND CRACK GROWTH STABILITY  
IN PLANE PROBLEMS OF BRITTLE FRACTURE

by

Lekan Olaosebikan  
Virginia Polytechnic Institute & State University  
Department of Engineering Science & Mechanics  
Blacksburg, VA 24061

A variational principle is used to predict crack trajectories in two dimensional (2D) brittle fracture problems. The principle rests on the postulate that amongst all continuous and piecewise smooth paths, subject to specified end constraints, the actual crack path is the one that renders the net energy loss an absolute minimum. The end constraints for the admissible crack paths include conditions such as specified crack initiation point at one end and intersection with a free boundary at the other end. The variational principle is first applied to purely mechanical fracture problems in a manner proposed by Fridman and Morozov [1] and is then extended to thermomechanical cases in which heat exchange is significant. The same principle is used to predict the rate of crack advance in self-similar flaw growth and for cases where the crack path can be specified a priori.

Energy considerations are further applied to investigate conditions which are necessary and sufficient for the stability of certain plane (2D) problems of crack growth. Following an outline given by Nemat-Nasser [2], we consider the total energy  $\pi$ , available for crack growth in the form

$$\pi = E + S$$

where E is the strain energy and S is the total surface energy, such that the vanishing of the first variation  $\delta\pi$ , of  $\pi$ , yields the equilibrium conditions from which critical values of the energy release rate  $G_c$ , can be determined. Thereafter, subject to some conditions specified in terms of  $G_c$ , the second variation  $\delta^2\pi$ , of  $\pi$ , leads to stability conditions derivable from the criteria that

$$> 0 \text{ for stable growth}$$

$$\delta^2\pi = 0 \text{ for critical state}$$

$$< 0 \text{ for unstable growth}$$

The various conditions obtained for crack path prediction and crack growth stability are applied to specific examples of 2D cracked body problems and agreement with known experimental results (e.g., Smith's [3]) and other theoretical results (e.g. Cotterell and Rice's [4]) are inferred. Finally, some means of extending the analysis to three-dimensional problems are outlined.

## References

1. Fridman, Ya. B. and Morozov, E. M., "Application of the Hamilton-Ostrogradskii Principle in the Study of the Regularity of the Breakdown of Solid Bodies", Soviet Physics-Doklady, Vol. 7, No. 5, 1962, pp. 442-444.
2. Nemat-Nasser, S., "Variational Methods for Analysis of Stability of Interacting Cracks", Proc. IUTAM Symp. on Variational Methods in the Mechanics of Solids, Ed. S. Nemat-Nasser, 1978, pp. 249-253.
3. Smith, C. W., "Stress Intensity and Flaw-Shape Variations in Surface Flaws", Experimental Mechanics, Vol. 20, No. 4, 1980, pp. 126-133.
4. Cotterell, B. and Rice, J. R., "Slightly Curved or Kinked Cracks", Intl. J. of Fracture, Vol. 16, No. 2, 1980, pp. 155-169.

ON CRACK TIP STRESS STATE: AN EXPERIMENTAL EVALUATION  
OF THREE DIMENSIONAL EFFECTS

by

A. J. Rosakis  
Graduate Aeronautical Laboratories  
California Institute of Technology  
Pasadena, CA 91125

and

K. Ravi-Chandar  
Department of Mechanical Engineering  
University of Houston  
Houston, TX 77004

The extent of the region of three dimensionality of the crack tip stress field is investigated using reflected and transmitted caustics. The range of the applicability of two dimensional crack tip solution is thus established experimentally.

Experiments are performed using plexiglas and high strength steel compact tension specimens. A wide spectrum of specimen thicknesses is investigated. At each thickness, measurements are performed at various distance  $r$  from the crack tip ranging from  $r/h \sim 0.1$  to  $r/h \sim 2$ , where  $h$  is the specimen thickness. The results indicate that plane-stress conditions prevail at distances from the crack tip greater than half the specimen thickness while no significant plane strain region is detected.

The experimental results are compared with the recent analytical work of Yang and Freund [1]. The agreement is excellent in all aspects considered in the experimental work.

Reference

1. W. Yang and L. B. Freund, "Transverse Shear Effects for Through-Cracks in an Elastic Plate", Brown University Technical Report, November 1983.

## SURFACE MICRO-CRACKING INDUCED BY TWO APPROACHING RAYLEIGH WAVES

by

J. V. Horan, J. F. Cardenas-Garcia and D. C. Holloway  
Department of Mechanical Engineering  
University of Maryland  
College Park, MD 20742

Previous work [1,2] has shown the experimental and theoretical Rayleigh wave (R-wave) extension of surface micro-cracks. In addition, experimental work has been done with regard to the superposition of two approaching R-waves. Dally [3] has analyzed this occurrence without the extension of a surface micro-crack and Rossmannith and Fournery [4] have shown that superposition causes such extension, but no detailed theoretical analysis was performed.

This paper is concerned with the experimental and theoretical study of micro-crack extension resulting from two approaching R-waves. Experimentally, using dynamic photoelasticity, it is possible to photograph the propagation of two approaching R-waves and the resulting extension of a surface micro-crack which results from their interaction. Theoretically, using the Lamb solution based full-field results of the R-wave by Thau and Dally [5] and by the application of the Griffith-Irwin energy release rate fracture criterion [6,7], it is possible not only to model the experimental isochromatic patterns quite accurately, but also to predict crack growth. The experimental and theoretical results can then be compared.

#### References

1. Swain, M. V. and Hagan, J. T., "Some Observations of Overlapping Interacting Cracks", Engineering Fracture Mechanics, Vol. 10, 1978, pp. 299-304.
2. Cardenas-Garcia, J. F., "On Rayleigh Waves and Rayleigh Wave Extension of Surface Micro-Cracks", Doctoral Dissertation submitted to the University of Maryland, at College Park, Maryland, December 1983.
3. Dally, J. W., "A Dynamic Photoelastic Study of a Doubly Loaded Half-Plane", Developments in Mechanics, Vol. 4, 1968, pp. 649-664.
4. Rossmannith, H. P. and Fournery, W. L., "The Reciprocal Character of Rayleigh-Waves and Cracks", Rock Mechanics, Vol. 14, 1981, pp. 37-42.
5. Thau, S. A. and Dally, J. W., "Subsurface Characteristics of the Rayleigh Wave", Intl. J. Eng. Sci., Vol. 7, 1969, pp. 37-52.
6. Griffith, A. A., "The Phenomenon of Rupture and Flow in Solids", Philosophical Transactions of the Royal Society of London, Vol. A221, 1920, pp. 163-198.
7. Irwin, G. R., "Fracture Dynamics", Fracturing of Metals, American Society for Metals, 1948, p. 152.

## A SIMPLE MODEL FOR USE IN DETECTING CRACKS IN ELASTIC BEAMS

by

H.-Y. Chang and H. J. Petroski  
Department of Civil & Environmental Engineering  
Duke University  
Durham, North Carolina 27706

A simple model has been developed for the vibration response of an elastic beam containing a stable crack. Fourier series representations incorporating the crack size and location, as well as the location of an exciting force, enable one to obtain analytical expressions for a cracked beam's response to an input such as a hammer tap. These expressions may be employed to explore various strategies for inferring from the vibration signal the size and location of a crack and thus provide an analytical foundation for non-destructive testing. Elementary rational approaches to optimal testing strategies are possible by means of the analytical model, and the salient features of the vibration of a cracked beam are captured in analytical expressions that are readily interpreted.

THREE-DIMENSIONAL RADIATION AND SCATTERING OF  
ELASTIC WAVES

by

F. J. Rizzo  
D. J. Shippy  
M. Rezayat  
University of Kentucky  
Department of Engineering Mechanics  
Lexington, KY 40506

This presentation is concerned with the propagation of elastic waves in a homogeneous, isotropic, unbounded medium exterior to a finite region bounded by a closed surface  $S$ . The finite region may be a scatterer of incident waves or the source of radiation into the exterior medium through specification of boundary data on  $S$ . Emphasis is on time-harmonic problems; however, this work forms the basis for transient analysis through Fourier synthesis and Laplace-transform inversion, both done numerically.

The method used here for the mentioned problems involves a Boundary Integral Equation (BIE) in vector form defined on  $S$  only. Thus, in effect, a problem originally defined in three spatial dimensions is reduced to a two-dimensional problem on  $S$ . Solving the BIE numerically, by means of a system of algebraic equations which approximates the BIE, makes use of a discretization of  $S$  reminiscent of finite-element procedures. However, here, all discretization being confined to  $S$ , the problem of "where to stop elements" in the unbounded medium does not arise.

Two important features of the specific BIE formulation used here are the following. First, surface traction and surface displacement, rather than wave potentials, are explicit variables, such that well known difficulties with boundary conditions using wave potentials are avoided. Second, the BIE's usually written for elasticity problems, both static and dynamic, are not only singular but contain integrals which exist only in the sense of the Cauchy Principal Value (CPV). In this work, all CPV integrals are transformed to nonsingular ones, and all numerical work thus may be based on stable, well-conditioned ordinary Gaussian-quadrature schemes.

The presentation includes an outline of the BIE formulation, including the transformation to nonsingular integrals, an indication of the approximating numerical solution procedures, and several numerical examples. Included in the latter are problems of scattering of several types of waves from a spherical surface and radiation from a cube. Finally, extending the range of applicability of the formulation, the more difficult problem of scattering from a hemispherical indentation in an elastic half-space is considered.

Acknowledgement This work is motivated by a class of elastic wave problems of interest in geotechnical engineering, and it is supported by the National Science Foundation under Grant No. CEE-8013461.

FINITE ELEMENT ANALYSIS OF FLOW INDUCED OSCILLATIONS  
OF TUBES CONVEYING FLUIDS

by

D. Allaei, C. M. Krousgrill  
School of Mechanical Engineering  
Purdue University  
W. Lafayette, IN 47907

Much work has appeared in the literature on the investigation of oscillations developed in flexible tubes transporting fluids. These studies have focused on the effects of the interaction of nonconservative follower forces with conservative gyroscopic forces on the critical flow rates for the onset of flutter. In particular, the work in reference [1] investigates the effect of a terminal, inclined nozzle on the dynamics of the tube. The static effect of such a nozzle is to produce a pronounced deformation in the mathematical model of the tube, emulating the curvature naturally existing in physical tubes as a result of manufacturing processes. The analysis of the above mentioned work deals with nonplanar motion of a cantilevered tube about its statically deformed configuration. Through a perturbation approach to the eigenvalue problem and its corresponding adjoint problem, it was found that the static solution can become unstable in the plane of the statically deformed tube or in the direction perpendicular to this plane, depending on the size of the fluid/tube mass ratio. With the perturbation parameter in this analysis being the nozzle angle, it is understood that this approach is restricted to relatively small nozzle angles.

The intent of this investigation has been to determine through a finite element approach the quantitative and qualitative effects of larger nozzle angle on the critical flow velocities; in particular, to ascertain whether the transfer of instability between in-plane and out-of-plane motions is adequately predicted by the small angle perturbation analysis. The in-plane and out-of-plane motion about the static deformation are represented by a set of uncoupled, integral-differential equations. The finite element formulation of these equations has been developed using a set of hermite-cubic shape functions and yields the usual mass, gyroscopic and stiffness matrices. Due to the nonconservative nature of the follower-type forces on the tube, the stiffness matrix appears in a nonsymmetrical form. This, coupled with the presence of velocity dependent forces, produces eigenvalues off the imaginary axis. As the flow rate parameter,  $\rho$ , is increased, the static solution becomes unstable by a pair of complex conjugate eigenvalues crossing the imaginary axis into the positive, real half of the complex plane.

Shown in Figures 1 and 2 are the nondimensional, critical flow rates  $\rho_{cr}$  (i.e. the flow rate corresponding to the first crossing of the imaginary axis) as a function of the nozzle angle,  $\theta_j$ , for 3 values of the fluid/tube mass ratio,  $\beta$ . As expected,<sup>1</sup> the finite element and perturbation analyses predict nearly the same critical flow rates for small nozzle angles while for larger nozzle angles, the results differ both quantitatively and qualitatively. For larger  $\beta$  values the finite element analysis show abrupt drops in  $\rho_{cr}$  with increasing  $\theta_j$ . These abrupt changes in  $\rho_{cr}$  result from multiple crossings of the imaginary axis as the flow rate is increased. With the exception the mass ratio of  $\beta = 0.3$  in the in-plane direction, the small angle expansion solution overestimates the critical flow rates for larger nozzle angles. In the results shown for in-plane motion with a large nozzle angle, the critical flow rate appears to be independent of  $\beta$ .

#### Reference

1. Lundgren, T.S., P.R. Sethna and A.K. Bajaj, "Stability Boundaries for Flow Induced Motions of Tubes with an Inclined Terminal Nozzle", Journal of Sound and Vibration, 64, (1979), pp. 553-571

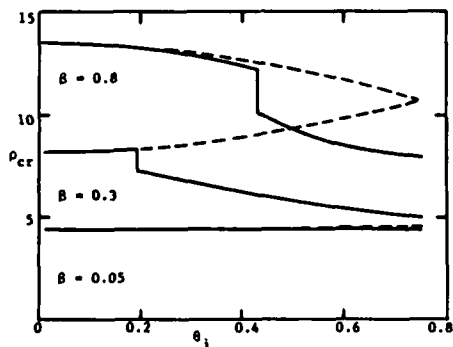


Figure 1 Out-of-plane motion  
— finite element, - - - perturbation

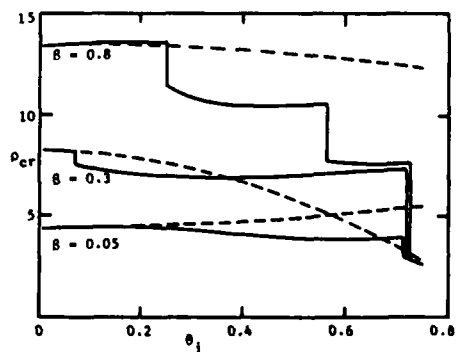


Figure 2 In-plane motion — finite element,  
- - - perturbation

LONGITUDINAL WAVES WITH RADIAL MOTION IN A  
LONG ROD OF ELASTIC-PLASTIC MATERIAL

by

Peter C.T. Chen and Joseph E. Flaherty\*  
USA AMCCOM, Armament Research and Development Center,  
Benet Weapons Laboratory  
Watervliet, N.Y. 12189

Motivated by recent interest in long rod penetrators, we have obtained a formulation for the study of longitudinal waves with radial motion in a long rod of elastic-plastic material. We have included the effect of lateral inertia and shear in a manner similar to [1-3]. This formulation allows us to consider perfect plasticity and nonlinear hardening effect in a unified approach. The material is assumed to obey the von Mises yield condition, the Prandtl-Reuss flow theory and the isotropic hardening rule. We have obtained all the characteristic equations and the differential equations satisfied along the characteristic curves. Explicit expressions for the characteristic wave speeds have been found. The elastic wave speeds are obtained as a special case. The initial-boundary value problem for the system of hyperbolic equations is solved by an adaptive finite element method [4]. The method automatically adapts the computational mesh as the solution progresses in time and is, thus, able to follow and resolve relative sharp transitions at wave fronts. This permits an accurate solution to be calculated with fewer mesh points than permits an accurate solution to be calculated with fewer mesh points than would be necessary with a uniform mesh. We hope to compare our computational results with experiments involving normal impact of cylindrical rods.

References

- [1] Mindlin, R.D. and Herrmann, G., Proc. 1st U.S. Nat. Cong. Appl. Mech., 1950, pp. 187-191.
- [2] Plass Jr., H.J., Plasticity, Proc. 2nd Symp. on Naval Structural Mechanics, 1960, pp. 453-474.
- [3] Wright, T.W., Proc. IUTAM Symp. on Finite Elasticity, Nijhoff Publisher, 1980. Also ARBRL-TR-02324, Ballistic RES. Lab., APD, MD.
- [4] Davis, S.F. and Flaherty, J.E., SIAM J. Sci.. Stat. Comput., Vol. 3, No. 1, 1982, pp. 6-27.

\*Also Department of Mathematical Sciences, Rensselaer Polytechnic Institute, Troy, N.Y. 12181

NARROW BAND INHOMOGENEOUS  
THIN FILM (FILTER) DESIGN

by

E. Berkcan and G.H. Cohen  
University of Rochester  
Department of Electrical Engineering  
Rochester, NY 14627

A new CAD technique based on the direct method of the calculus of variations is developed for the design of narrow band inhomogeneous thin films. The method, a generalization of the technique in Ref. (1), obtains an optimum profile for the index of refraction for given desired characteristics and arbitrary inequality constraints on the refractive indices and thicknesses. This includes (but is not restricted to) optimization and sensitivity analysis with respect to spectral and angular bandwidth.

The exact solvability of the associated state (Riccati) and costate equations (2) is also shown.

The method is in addition applicable to the computer aided design of non-uniform transmission lines and wave guide filters.

A brief review of the existing (major) design techniques (3) and a discussion of their (dis)advantages will be given.

The Fourier Transform method, (4) for example, is one of the most powerful techniques of design. It cannot however be used for filters which require a particular response at several angles of incidence (3) and the control of the refractive index is difficult. Moreover, the success of the method depends upon a "good" guess of an unknown even function of the desired transmittance.

We use the first order gradient technique; to treat the case of narrow band filters, we discretize the wavelength scale and compute the contributions from each wavelength to  $\delta\eta(\cdot)$ ,  $\delta d$ , the variations in the index of refraction and thickness respectively. This allows us to impose rigid spectral constraints at specific frequencies; we thus achieve better than 99.99% reflection efficiency over  $\pm 30^\circ$  angle of incidence and bandwidths of less than  $5\lambda_0$  for a peak at wavelength  $\lambda_0$ ,

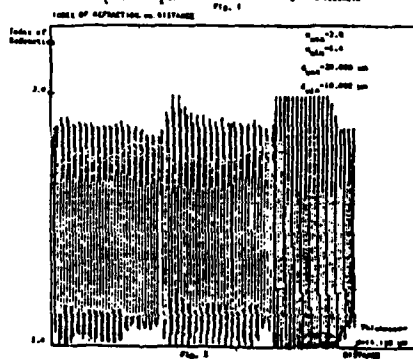
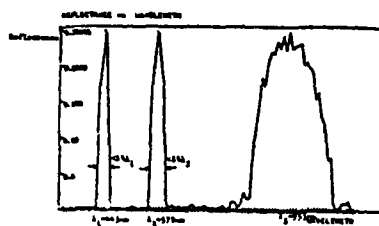
A typical result (with two narrow peaks and a low-pass edge) and the refractive index profile are given in Figs. 1 and 2 below.

More details and complete derivation/proof of our results will be presented (during the talk).

REFERENCES

1. Cohen, G.G., unpublished.
2. Berkcan, E., to be published.

3. See, for example, Liddell, H.M., CAD Techniques for the Design of Multilayer Filters, Adam Hilger Ltd., Bristol.
  4. Sossi, L., Easi NSV Tead. Akad. Toim. Fuus. Mat., 23, 229(1974); ibid 25, 171(1976).
- Dobrowolski, F.A., and D. Lowe, Appl. Opt. 17, 3039, 1978.



## A SIMPLE DESIGN PROCEDURE TO DETERMINE VIBROIMPACT STRESSES

by

A. Fathi and N. Popplewell  
 Department of Mechanical Engineering  
 University of Manitoba, Winnipeg, Canada, R3T 2N2

Elastic stops are often used to deliberately produce collisions to attenuate excessive deflections of a moving structure [1-3]. However, collisions usually create large transient stresses which may lead to detrimentally high noise levels and fretting wear of the colliding components. Hence, it is crucial to design the stops such that the attenuation is achieved with a minimum stress penalty.

A structure's velocity is discontinuous at an impact so that the principle of superposition does not hold generally. Consequently, unlike linear systems, a straightforward extrapolation from a specific vibroimpact case seems impossible. Therefore, vibro-impact designs are based normally upon "brute-force" numerical procedures where a complete computer run is required for every case. Numerical computations may typically require fifteen minutes of execution time on an Amdahl 470/V7 main frame computer even for the simplest vibroimpact problem.

A much more computationally economical approach has been developed for predicting the practically important impact stresses. The main novelty lies in the effective use of non-dimensional vibroimpact parameters. The parameters can be employed to quickly and straightforwardly generalize the results of any given but invariant structural - stop configuration. The viability of this new approach is assessed by considering a simple vibroimpacting beam with the properties shown in the accompanying figure. The dimensionless group for this example is,†

$$\frac{k[h - y(b,0)]}{N}, \frac{k\ell^3}{EI}, \frac{h - y(b,0)}{y(b,0)}, \frac{\dot{y}(b,0)}{\omega y(b,0)} \text{ and } \frac{\sigma}{\sigma_0}.$$

These parameters have been used to predict impact stresses for different combinations of parameters by extrapolating parameter relationships determined in a single case. Specifically,  $\sigma/\sigma_0$  may

be evaluated from alterations in  $\frac{k[h - y(b,0)]}{N}$  due solely to changes in  $\frac{k\ell^3}{EI}$ . Accuracy was found reasonable and, better yet, the

required computations were at least four orders faster than conventional calculations. Furthermore, the approach needs very little computer storage so that a programmable pocket calculator can be employed.

† See figure for nomenclature.

AN ANALYTICAL SOLUTION FOR THE FREE VIBRATION ANALYSIS  
OF SIMPLY SUPPORTED THIN TRIANGULAR PLATES

by

D. J. Gorman  
University of Ottawa  
Department of Mechanical Engineering  
770 King Edward Avenue  
Ottawa, Ontario K1N 6N5

It is well known that the achieving of accurate analytical solutions for a triangular plate's free vibration is something that has eluded researchers over the years. This is a result of the difficulty encountered in trying to simultaneously satisfy the governing differential equation and prescribed boundary conditions.

In a recent publication [1] the author has presented highly accurate solutions for the simply supported right triangular plate. This was accomplished by means of the superposition method. A judicious choice of rectangular plate forced vibration problems, for which exact solutions are known, were superimposed. The driven edges of these plates enclosed a right triangular shape and by properly constraining driving coefficients appearing in their solutions, a free vibration solution was obtained for simply supported right triangular plates.

In the paper described here the above superposition technique was extended to handle the general case of simply supported triangular plates of any geometry. It will be appreciated that any triangle may be considered as a combination of two right triangles with one common edge. Accordingly solutions for these two triangles were obtained and conditions of continuity across their common boundary were enforced. The solution thus obtained satisfies exactly the governing differential equation and boundary conditions are satisfied to any desired degree of accuracy. Convergence is found to be quite rapid.

Computed eigenvalues and mode shape information are presented for the general simply supported triangular plate. It is shown how the solution agrees exactly with certain reference values which can be extracted from simply supported rectangular plate theory. To the author's knowledge, this represents the first accurate analytical solution to this important industrial problem.

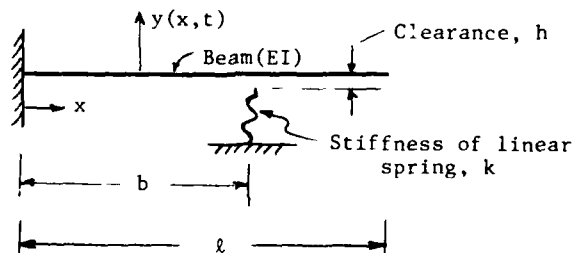
References

- [1] Gorman, D.J., "A Highly Accurate Analytical Solution for Free Vibration Analysis of Simply Supported Right Triangular Plates", Journal of Sound and Vibration, 89(1), 1983, pp. 107-118.

Although relatively simple, the example used provides insight into more realistic systems like hydraulic piping with several stops. Then collisions are likely more numerous so that computational savings should be correspondingly greater especially if an "optimum design is required.

#### References

- [1] Lo, C.C., "A Cantilever Beam Chattering Against a Stop", Journal of Sound and Vibration, 69, 1980, pp. 245-255.
- [2] Rogers, R.J. and Pick, R.J., "On the Dynamic Response of a Heat Exchanger Tube With Intermittent Baffle Contacts", Nuclear Engineering and Design, 36, 1976, pp. 81-90.
- [3] Fathi, A., Young, D.R. and Popplewell, N., "Computer Aided-Design of Vibroimpact Stops", Modelling and Simulation in Engineering, Volume III of the IMACS Transactions on Scientific Computations, 1982.



$\sigma, \sigma_0$  Stresses with and without impact  
 $\omega$  Circular frequency  
 $N$  Impact force

by

Bulent A. Ovunc  
 University of Southwestern Louisiana  
 USL 40172, Lafayette, LA 70504

The forced bending vibration of plates is determined by means of numerical integration. The acceleration along the transversal direction is considered as linearly varying. At a time station  $s$ , the acceleration and the velocity in the transversal direction can be written as

$$\ddot{W}_s = \frac{1}{\beta_0 \Delta t^2} (W_s + \sum b_k W_{s-k})$$

and

$$\dot{W}_s = \frac{1}{\beta_0 \Delta t} (c_0 W_s + \sum c_k W_{s-k})$$

where the coefficients  $b_k, c_k$  are expressed in terms of two known parameters  $\beta_0, \gamma_0$ .

The equation of motion at a time station  $s$ , for an infinitesimal element of the plate can be written as:

$$\Delta \Delta W_s + \beta^4 W_s = \beta^4 \sum b_k W_{s-k}$$

or in complex domain,

$$\frac{\partial^4 W_s}{\partial z^2 \partial \bar{z}^2} - \frac{\beta^4}{16} W_s = \frac{\beta^4}{16} \sum b_k W_{s-k}$$

where

$$\beta = \frac{\rho}{D \Delta t^2 \beta_0}$$

The right side of the above equation is a known function in terms of the dynamic deflection functions  $W_{s-k}$ , of the previous time stations. The general solution for the homogeneous part of the above Helmholtz differential equation is:

$$W_{sh} = \text{Re} \{ p_n(z, \bar{z}) \}^T \{ a_n \}$$

where,

$$\{ p_n(z, \bar{z}) \}^T = (L_n(z, \bar{z}) \quad M_n(z, \bar{z}) \quad P_n(z, \bar{z}) \quad R_n(z, \bar{z}))$$

and  $L(z, \bar{z}), M(z, \bar{z})$  are the first kind and  $P(z, \bar{z}), R(z, \bar{z})$  are the second kind newly defined Bessel functions, and  $\{ a_n \}$  is the vector of integration constants.

The total dynamic deflection function is  $W_s = W_{sh} + W_{sp}$ .

15PM3

The particular solution  $W_{sp}$  is determined from the deflection functions of previous time stations. Once the dynamic deflection function is obtained the bending moments, torsion, shearing forces can be evaluated from their expression in complex variable. The above procedure is applied to circular plates. 110

LOGARITHMIC DECREMENT OF DAMPING FOR FREE  
VIBRATION OF A NEARLY TUNED COUPLED SYSTEM

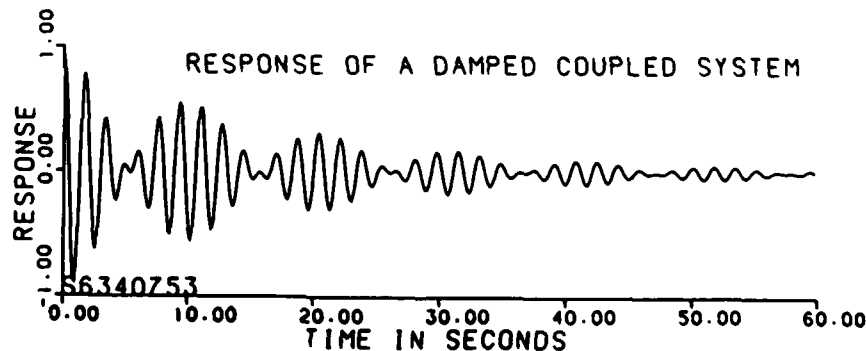
by

Bashir A. Sayar  
South Dakota State University  
Mechanical Engineering Department  
Brookings, SD 57007

The concept of logarithmic decrement is well understood and its application to the response of a damped second order system is well explained in vibration books. At the same time, beat phenomenon, which results from the coupling of two second order systems in the vicinities of their tuned frequencies is also explained for undamped systems.

When a nearly tuned coupled system is damped, the beats are contained in a decaying envelope which is not identical to either one of the envelopes of the uncoupled sub-systems. Therefore, one begins to wonder how to measure the damping of coupled systems from their complex measured response. If the complexity of such responses as shown below is studied, one will not be even sure if the logarithmic decrement approach will be applicable anymore. Literature on the subject is shy in providing detailed explanation of the mechanism of measuring damping under such conditions. Therefore, the little work done on this subject may prove useful if and when such combination of circumstances are met in the course of future scientific work.

A simplified mathematical expression for logarithmic decrement is derived from the coupled response equations and is expressed in terms of the damping constants and frequencies of the uncoupled sub-systems. The validity of this expression is checked against experimental results and it has been noticed that the agreement is excellent.



TORSIONAL OSCILLATIONS OF A SEMI-CYLINDER OF  
A SIMPLE FLUID ON A BED OF MERCURY

by

Aydeniz Siginer  
Department of Mechanical Engineering  
Auburn University  
Auburn, Alabama 36849, USA

The determination of the free surface shape on a non-Newtonian liquid forms the basis for the free surface viscometry. The combination of an analytical expression for the free surface with experimental measurements yields values for the constitutive constants embedded in the constitutive structure of that particular liquid which constants are enough to predict the motion of the same liquid in that particular class of motions for which the constitutive structure has been determined.

This paper presents the results of an analytical investigation to determine the shape of the free surface on an incompressible simple fluid resting on a bed of mercury. The fluid is set in motion by a vertical cylinder undergoing torsional oscillations of amplitude  $\Lambda$  and frequency  $\omega$ . The mercury bed has been motivated by two things. First, Peter and Noetzel [1] remarked that in a geometry similar to the one treated in this paper they did not observe the expected Weissenberg phenomena and secondly, almost frictionless conditions may be assumed in any experiment at the interface of the layer of a non-Newtonian fluid and the mercury bed.

The field equations and the boundary conditions satisfied by the mathematical problem are

$$\begin{aligned} \rho \frac{Dy}{Dt} &= -\nabla\phi + \nabla \cdot \mathcal{S}, \quad \phi = p + \rho gz, \quad \nabla \cdot y = 0 \quad \text{in } R \\ R &= \{r, \vartheta, z \mid -\infty < r < r_0, 0 < \vartheta < 2\pi, -L < z < h(r; \Lambda)\} \\ y(r_0, z, t) &= e_\theta \Lambda r_0 \sin \omega t \\ S_{rz} = S_{z\theta} &= 0 \quad \text{at } z = -L \\ S_{n\theta} = X_{z\theta} - h_{,r} S_{r\theta} &= 0 \quad \text{at } z = 0 \\ S_{nt} = h_{,r} (S_{zz} - S_{rr}) + (1 - h^2)_{,r} S_{rz} &= 0 \quad \text{at } z = 0 \\ w = y \cdot e_z = h_{,t} + (y \cdot e_r) h_{,r} &= 0 \quad \text{at } z = 0 \\ \mathfrak{g} \cdot [-p \mathbf{1} + \mathcal{S}] \cdot \mathfrak{g} &= \sigma J \quad \text{at } z = 0 \end{aligned}$$

where  $\mathfrak{g}$ ,  $\mathfrak{t}$ , and  $h$  represent the outward directed unit normal, the unit tangent vector to the free surface and the free surface height respectively. The last condition represents the balance of the jump of the normal stress across the free surface by the surface tension  $\sigma$  times the mean curvature  $J$  of the surface. The origin of the coordinate system is on the vertical axis of symmetry and on the free surface of the rest state which prevails when  $\Lambda = 0$ .

The volume of fluid under the free surface must be conserved 113

$$\int_0^{r_0} r h(r, t; \Lambda) dr = 0$$

This condition determines the constant in the representation of the pressure field. The extra-stress is assumed to be given by the constitutive structure of a fluid of integral type of order N

$$\underline{S} = \int_0^{\infty} \zeta(s) \underline{G}(s; \Lambda) ds + \int_0^{\infty} \int_0^{\infty} \{ \beta(s_1, s_2) \underline{G}(s_1, \Lambda) \underline{G}(s_2, \Lambda) + \alpha(s_1, s_2) [\text{tr} \underline{G}(s_1, \Lambda)] \underline{G}(s_2, \Lambda) \} ds_1 ds_2$$

where  $\zeta$ ,  $\beta$ ,  $\alpha$  are temperature dependent material functions and  $\underline{G}(s)$  represents the history of the motion.

A domain perturbation method, perturbing simultaneously the flow domain and the non-linear field equations, is used. The coefficients of the perturbation series in terms of the perturbation parameter  $\Lambda$ , the amplitude of the oscillation, are the partial derivatives of the field variables with respect to  $\Lambda$  evaluated at the rest state, i.e. when  $\Lambda = 0$ .

At first order the contribution to the pressure field and the deformation of the free surface is zero. The velocity field assumes the form

$$\underline{v}^{(1)}(r, t) = e_{\theta} \left[ \frac{r_0}{2i} \frac{I_1(\lambda r)}{I_1(\lambda r_0)} e^{i\omega t} - \frac{r_0}{2i} \frac{I_1(\bar{\lambda} r)}{I_1(\bar{\lambda} r_0)} e^{-i\omega t} \right]$$

$$\langle n \rangle = \frac{\partial^n \langle \cdot \rangle}{\partial \Lambda^n} \Big|_{\Lambda=0}, \quad \lambda^2 = \frac{i\omega\rho}{\eta}, \quad \eta \int_0^{\infty} G(s) e^{-i\omega s} ds$$

where  $I_1$  and  $G(s)$  are the modified Bessel function of the first kind and the shear relaxation modulus respectively. At 2nd order the velocity field is axially symmetrical  $\underline{v}^{(2)} = e_r u + e_z w$  and the field variables together with the free surface deformation are decomposed into a mean part, time averaged over a cycle of period  $2\pi/\omega$ , and a component which oscillates with frequency  $2\omega$ .

$$\psi^{(2)} = \psi_m + \psi_1 e^{2i\omega t} + \bar{\psi}_1 e^{-2i\omega t}$$

$$\phi^{(2)} = \phi_m + \phi_1 e^{2i\omega t} + \bar{\phi}_1 e^{-2i\omega t}$$

$$h^{(2)} = h_m + h_1 e^{2i\omega t} + \bar{h}_1 e^{-2i\omega t}$$

It is found that the mean flow is zero and the mean pressure field is determined together with the mean free surface deformation through

$$\frac{\sigma}{r} (r h_{m,r})_{,r} - \rho g h_m = -\phi_m, \quad h_{m,r}(r_0) = h_{m,r}(0) = 0$$

#### Reference

- [1] Über einige Experimente zur Frage der Existenz des Weissenberg - Effectes, Ann. Physik. Chem., 21, 422-431, 1959.

by

M. Swaminadham  
University of Hartford  
College of Engineering  
200 Bloomfield Avenue  
West Hartford, CT 06117

Results of a finite-element numerical study to determine the natural vibration characteristics of a radial impeller blade are presented in this paper. A representative impeller blade, integral with its backplate and hub is modeled as a sectorplate and its resonant frequencies and mode shapes are determined using thin and thick plate elements. Analytical results discuss the emergence and nature of several mode shapes as in relation to changes in variables like thickness of plate and ratio of inner to outer radii. Analytical results, where possible, are compared with the experimental values.

## NUMERICAL ANALYSIS OF VIBRATIONS BY CONTINUOUS TRANSFER MATRICES

by

Maurice I. Young  
Professor of Mechanical and Aerospace Engineering  
University of Delaware  
Newark, Delaware 19716  
U.S.A.

A numerical method of free and forced vibration analysis by continuous transfer matrices is presented. This extends the methods of Holzer, Mykelstad, Prohl, Bishop et al,<sup>2,3</sup> to cases where the inertia and rigidity properties are more properly and effectively represented by continuous rather than discrete, lumped parameter models.

The method is illustrated for the case of the torsional vibrations of a propeller-rotor type system, where its mass polar moment of inertia and torsional rigidity distributions vary widely but continuously over the span. The appropriate continuous transfer matrices for bending and coupled bending-torsion are also presented.

<sup>1</sup>R.E.D. Bishop, G.M.L. Gladwell and S. Michaelson, "The Matrix Analysis of Vibration", Cambridge University Press, London, 1965, p. 212.

<sup>2</sup>N.O. Mykelstad "A New Method of Calculating Natural Modes" Journal of Aeronautical Sciences, April 1944., pp. 153-162.

<sup>3</sup>M.A. Prohl, "A General Method for Calculating Critical Speeds of Flexible Rotors", Transaction ASME, Vol. 166, 1945, p. A-142.

PARADOXES AND MISCONCEPTIONS OF CLASSICAL THEORIES  
OF BEAM VIBRATIONS

by

Edwin T. Kruszewski  
Consultant, Dynamics and Structural Mechanics  
Newport News, VA 23606

The development of the Space Shuttle has in turn triggered the development of new large space systems. Many of these systems, such as receiving and transmitting antennas and solar power systems, require the maintenance of very accurate surfaces and precise pointing ability. The design of such systems depend on accurate prediction of transient response, to static and dynamic loads.

Current procedures for predicting transient or wave motion utilize one of three basic classical governing equations: The Bernoulli Euler equation that is based on plane sections remaining plane and normal to the neutral axis. The Rayleigh equation which adds the influence of rotary inertia to the Bernoulli equation. Finally, the Timoshenko equation which adds shear deformation to the Rayleigh equation.

The results using these classical governing equations are not very satisfactory. The Bernoulli Euler equation results in infinite speeds of propagation thus implying that the effect of a concentrated load is felt instantaneously at every point on the beam. A very unrealistic conclusion. The Rayleigh equation does give a finite speed of propagation if the displacement of the beam,  $w$ , is assumed to be

$$w = a \sin \frac{2\pi}{\lambda} (\pi - ct)$$

where  $c$  is a phase velocity and  $\lambda$  a wave length. The wave velocity using this method, however, deviates from the three dimensional results of  $c = \sqrt{E/\rho}$ . The Timoshenko equation, using the same displacement assumption, results in a more accurate approximation. However it does so only in the first mode (i.e., large  $\lambda$ ). When modal approaches were used to try to predict displacements due to a point load, 50 to 60 modes were required for convergence. When finite difference methods were used to solve the same problem divergence difficulties made it necessary to use more than two hours on NASA large computer complex to follow the distortion less than one beam length. Obviously a new prospective on transient dynamics of solids is needed.

This paper will deal with three topics:

- (1) The paradoxes that come about through the use of the three classical dynamic equations.
- (2) The misinterpretation of the static beam relationships and the basic dynamic principals in deriving the equations.
- (3) The derivation of relationships that result in more realistic prediction of energy transportation and velocities that agree with the exact three dimensional wave speeds.

by

Rohan Abeyaratne  
Michigan State University  
College of Engineering  
East Lansing, MI 48824

Two separate problems, both concerning the effect of voids on a finitely deformed elastic material, are considered.

The first problem [1] concerns the plane strain response of a rectangular block of a Mooney-Rivlin-like incompressible material having a very fine periodic distribution of identical cylindrical voids. In an overall sense, the resulting porous body behaves in a homogeneous and compressible manner. The effective constitutive behavior of this material is determined using homogenization theory. It is found that, in particular, the homogenized model loses ellipticity at sufficiently severe strain levels (despite the fact that the matrix material itself remains elliptic at all deformations). This is reminiscent of the behavior of the Blatz-Ko material, a foamed polyurethane rubber which exhibits a similar phenomenon.

In the second problem [2] we consider a hollow circular cylinder of (compressible) Blatz-Ko material. The outer boundary is subjected to a prescribed radial stretch  $\lambda$  while the cavity surface remains free of traction. A closed-form solution to this problem is obtained. Attention is focused on the growth of the cavity in the particular case in which its undeformed radius is small. It is found that first, the cavity radius increases slowly as the applied stretch is increased until it reaches a certain value  $\lambda_{CF}$ . Rapid growth suddenly takes place beyond this point. The limiting case of an infinitesimally small cavity is also examined.

#### References

1. Abeyaratne, R. and Triantafyllidis, N., "An Investigation of Localization in a Porous Elastic Material Using Homogenization Theory", J. of Appl. Mech., in press.
2. Horgan, C. O. and Abeyaratne, R., "Growth of a Small Cavity in a Compressible Nonlinearly Elastic Medium", to appear.

\* This work was supported by the U.S. National Science Foundation (Grant CME 81-06581) and the U.S. Army Research Office (Grant DAAG29-83-K-0145).

MINIMIZATION IN NONLINER ELASTICITY WITH  
THE CONSTRAINT OF INCOMPRESSIBILITY

by

R. L. Fosdick  
Aerospace Engineering  
and Mechanics  
University of Minnesota  
Minneapolis, MN 55455

G. P. MacSithigh  
Engineering Mechanics  
University of Missouri-Rolla  
Rolla, MO 65401

I shall discuss necessary conditions for the existence of minimizers within a class of deformations that allows for the possibility of strain discontinuities. This possibility is manifested in materials with non-convex stored energy functions.

## STRAIN ENERGIES FOR SOLIDS THAT CHANGE PHASE

by

R. D. James  
Division of Engineering  
Brown University  
Providence, RI 02912

The need for constitutive equations which describe solid materials undergoing first order phase transformations arises in a variety of applications in materials science and geophysics. Constitutive equations presently in use treat the phases essentially as fluids, or treat the deformations as infinitesimal or one-dimensional. Consequently, the applications are often limited to special states of stress. As an alternative, we consider a free energy function which accounts for large changes of shape as a model for diffusionless transformations. Properties of this free energy reflect the underlying symmetry of the parent and product phases as well as an exchange of stability from parent to product at the transformation temperature  $T_0$ . We concentrate upon two questions: (i) How can loads be applied so as to cause the body to transform at temperatures above  $T_0$ ? (ii) Can the parent phase be recovered by applying some system of loads below  $T_0$ ? We contrast the results with predictions on the effect of an hydrostatic pressure.

LARGE DEFLECTION BEHAVIOR OF RECTANGULAR PLATES OF ELASTIC  
ISOTROPY AND PLASTIC ANISOTROPY

by

M. Gorji  
Department of Civil Engineering  
Portland State University  
Portland, OR 97207

The elastic-plastic large deflection behavior of a rectangular plate with preferred orientations of crystal planes is considered. The material under investigation is isotropic in the elastic range. However, due to the development of preferred orientations of crystal planes beyond the elastic limit or the presence of a residual stress field due to cold work it behaves orthotropically. The concept of the equivalent load (1) is used to treat the inelastic components of strain as well as the nonlinear terms of displacements as an additional set of loads acting on the plate. A modified version of Hill's plasticity theory for anisotropic metals is used in obtaining solution for a rectangular, simply supported plate made of 2024-T341 aluminum.

References

1. Lin, T. H., "Theory of Inelastic Structures", Wiley, New York, 1968.

## VARIATIONAL PRINCIPLES IN FINITE ELASTICITY

by

E. Reissner

University of California

San Diego, CA

The principle of minimum potential energy, as a variational principle for displacements admits a ready formulation in finite elasticity [2], with appropriate specialization for the equations of infinitesimal elasticity. Given that the basic boundary value problems are problems with prescribed surface displacements, or with prescribed surface stress, it was of interest, early on, to also have a variational principle for stresses, with this leading to the formulation of the principle of minimum complementary energy in infinitesimal elasticity. An analogous formulation for finite elasticity, as proposed by Hellinger [1], was eventually recognized to be faulty and is now generally considered to be unobtainable. In the process of his attempted formulation Hellinger encountered, in essence without recognizing its independent significance, a result which is most simply designated as variational principle for stresses and displacements. Hellinger's version of this principle suffers from the same defects as his formulation for stresses alone. The basic cause of these defects is just that element of his analysis which allowed the formal establishment of the complementary energy principle for finite elasticity, namely the use of components of stress associated with the names of Lagrange and Piola [5].

Nearly forty years subsequent to the considerations of Hellinger, the writer, independently and motivated by a probable significance on connection with direct methods procedures, reopened the question of a variational principle for stresses and displacements in finite elasticity. The outcome of this was a non-faulty formulation, through use of components of stress associated with the names of Kirchhoff and Trefftz [3].

The manifest impossibility of using the above result for the derivation of a finite-elasticity variational principle for stresses alone led Frayes de Veubeke about twenty years later to a formulation involving stresses, translational displacements and rotational displacements. He then showed that this result made possible one of the previously unrealized aims, the formulation of a complementary principle not involving components of translational displacement [4].

The present discussion has as its main aim the further clarification of this complex of questions [6].

References

1. E. Hellinger, Die allgemeinen Ansätze der Mechanik der Kontinua, Enzyklopadie der Mathematischen Wissenschaften, Vol. IV, 4, Art. 30, pp. 654-655, 1914.
2. E. Trefftz, Mathematische Elastizitätstheorie, Handbuch der Physik, Vol. 6, Chapter 2; p. 140, 1927.

3. E. Reissner, "On a Variational Theorem for Finite Elastic Deformations", J. Math. & Phys., 32, pp. 129-135, 1953.
4. B. Frayes de Veubeke, "A New Variational Principle for Finite Elastic Deformations", Intern. J. Engng. Sci., 10, pp. 745-763, 1972.
5. E. Reissner, "Variational Principles in Elasticity", Handbook of Finite Element Methods, McGraw Hill Book Co. (to appear).
6. E. Reissner, "On the Formulation of Variational Theorems in Geometrically Nonlinear Elasticity", ASCE J. Eng. Mech. (to appear).

## REMARKS ABOUT ST. VENANT SOLUTIONS IN FINITE ELASTICITY

by

David Kinderlehrer  
School of Mathematics  
University of Minnesota  
Minneapolis, MN 55455

The semi-inverse solutions introduced by J. Ericksen are one possible generalization of the St. Venant solutions to finite elasticity. The motivations for considering them, their relationship to the original St. Venant functions, and the question of their existence are discussed.

by

Kenneth Sawyers  
Center for the Application of Mathematics  
Department of Mechanical Engineering & Mechanics  
Lehigh University  
Bethlehem, PA 18015

A primary theoretical problem within the study of finite elastic deformations is the deduction of constraints that must be satisfied by a particular constitutive assumption to ensure that it may represent "physically realistic" behavior of the material it is intended to describe. This subject, somewhat loosely called "material stability", might also find practical application within the context of the numerical analysis of boundary value problems, particularly if solutions are sought for ranges of variables that exceed those determined by experiment.

Progress in this subject, notably for isotropic materials, has recently been both rapid and definitive. It is my intention here to give an account of these developments.

ON BIFURCATION IN FINITE ELASTICITY:  
BUCKLING OF A RECTANGULAR ROD

by

Henry C. Simpson  
Department of Mathematics  
University of Tennessee  
Knoxville, TN 37996

Scott J. Spector  
Department of Mathematics  
Southern Illinois University  
Carbondale, IL 62901

We treat the problem of plane strain compression of a rectangular slab composed of elastic material. The top of the slab is vertically displaced keeping the bottom and two side faces fixed against frictionless walls. The other faces are left free. We denote the ratio of final to initial heights by  $\lambda$  and suppose, after compression, that  $\lambda$  is less than one.

Experiments on certain rubbers (Beatty and Dadras) reveal that the resulting configuration remains rectangular if  $\lambda$  is not too far below 1, but that at a lower critical value,  $\Lambda$ , this shape loses its stability. These experiments show that when  $\lambda$  is decreased past  $\Lambda$  the body either buckles to one side or else it bulges symmetrically.

We consider the problem from the mathematical point of view as a nonlinear boundary-value problem in two dimensions treating  $\lambda$  as a variable parameter. We first seek conditions for the loss of linearization stability (infinitesimal stability) of the trivial solution at some  $\Lambda$ .

The loss of linearization stability then leads us to the problem of continuous bifurcation from the value  $\Lambda$ . Our line of attack is to verify the hypotheses of a theorem of Crandall and Rabinowitz concerning bifurcation at a simple eigenvalue. We reformulate the problem equivalently as a map between appropriate function spaces and seek zeros of this map near the bifurcation point. Thus, assuming the linearized map has a one-dimensional null space and that the corresponding zero eigenvalue crosses zero transversely as  $\lambda$  is varied through  $\Lambda$ , a bifurcation is rigorously established.

Finally, we consider various physical aspects of the two solution branches. In particular we show that the buckled branch is infinitesimally stable if and only if the bifurcation is supercritical and that this bifurcation is always Pitchfork (to one side of the bifurcation point). These results provide rigorous confirmation to previous investigations of Koiter.

Beatty, M. and P. Dadras, "Some Experiments on the Elastic Stability of Highly Elastic Bodies", *Int. J. Eng. Sci.*, Vol. 14, 1976, pp. 233-238.

Crandall, M. and P. Rabinowitz, "Bifurcation from Simple Eigenvalues", *J. Func. Anal.*, Vol. 8, 1971, pp. 321-340.

by

Saad A. Ragab  
Lockheed-Georgia Company  
Marietta, GA 30063.

Viscid-inviscid interaction techniques for vortex separation from a smooth surface require the development of methods for solving the Euler and boundary layer equations. In this abstract we present solutions to the three-dimensional Euler and boundary-layer equations for flows over an ellipsoid of revolution at high angle of attack. The unsteady Euler equations are solved by using a finite-volume method and an explicit Runge-Kutta time marching scheme. Details of the method can be found in Reference 1. The boundary layer equations are solved by using a finite-difference method with provision to approach an open separation line. Matching conditions are given by the potential flow theory, and the transition line is inferred from the experiments of Reference 2.

The pressure distribution over an ellipsoid inclined at 30 degrees to the free-stream is depicted in Figure 1 along with the exact analytic values for irrotational flow at zero Mach number. From the excellent agreement between the two solutions we conclude that, for subcritical flow conditions the Euler solution is irrotational and no vorticity is being shed from the ellipsoid surface.

Comparison between experimental and computed friction coefficient distributions is shown in Figure 2. The experiments of Reference 2 showed that a small region of laminar separation exists near the tip of the ellipsoid. In the calculations, however, laminar separation in that region was avoided by modifying the transition line so that transition to turbulent flow takes place whenever laminar separation is approached. That explains the sudden increase in the friction shown in figure 2 at  $X/L=0.05$  and  $\Theta=120$  degrees. Further downstream, separation is turbulent, and at  $X/L=0.48$  the computed separation occurs at  $\Theta=140$  deg. while the observed separation was at  $\Theta=130$  deg. The difference is basically due to the influence of separation on the inviscid pressure distribution which is not accounted for in the present calculations.

#### REFERENCES

1. Jameson, A., Schmidt, W., and Turkel, E., "Numerical Solutions of the Euler Equations by Finite-Volume Methods Using Runge-Kutta Time-Stepping Schemes", AIAA Paper No. 81-1259, June 1981.
2. Meier, H. U., and Kreplin, H. -P., "Experimental Investigation of the Transition and Separation Phenomena on a Body of Revolution", Z. Flugwiss. Weltraumforsch. 4, Heft 2, 1980, pp. 65-71.

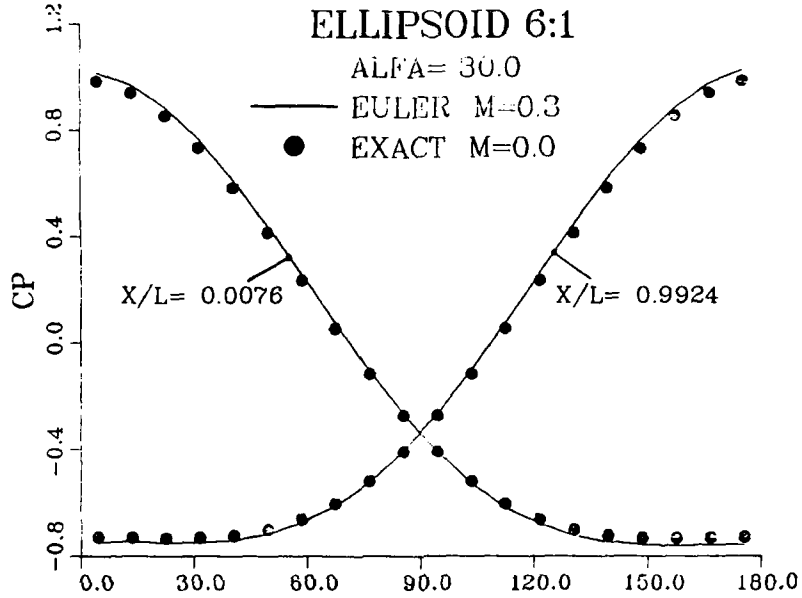


FIGURE 1. PRESSURE COEFFICIENT DISTRIBUTION

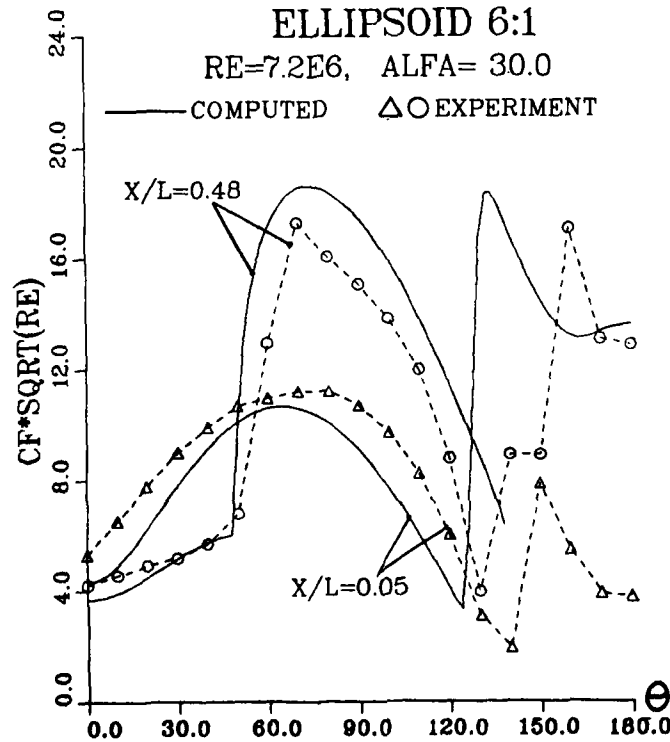


FIGURE 2. FRICTION COEFFICIENT DISTRIBUTION

## NUMERICAL SOLUTION OF UNSTEADY TRANSONIC FLOWS

by

N. L. Sankar  
School of Aerospace Engineering  
Georgia Institute of Technology  
Atlanta, Georgia 30332

and

J. B. Malone  
Department 72/74  
Lockheed-Georgia Company  
Marietta, Georgia 30063

Some recent applications of a strongly implicit approximate factorization procedure are described. This procedure solves the two- and three-dimensional, steady and unsteady transonic potential flows in a body-fitted coordinate system. When used as a steady flow solver, the convergence characteristics of this procedure are enhanced by coupling it with the multigrid procedure. Weak viscous effects are accounted for by solving a steady or unsteady integral boundary layer equation. In supersonic regions, an artificial compressibility method is used to stabilize the calculations.

Numerical results are presented and compared with published results for the following cases:

- a. Unsteady viscous flow over a NACA 64A010 airfoil at  $M_\infty = 0.796$ , undergoing periodic plunging motion
- b. Steady viscous flow over the RAE 2822 airfoil at  $M_\infty = 0.73$  and  $\alpha = 2.7^\circ$
- c. Unsteady transonic potential flow over a F-5 Fighter Wing at several Mach numbers and angles of attack

by

Thomas Wicks  
Institute of Applied Mathematics  
University of Missouri-Rolla, Rolla, MO 65401

Augmented Lagrangian techniques, when used with the finite element method, generate an uncoupled system of equations for problems with constraints. A critical decision which determines the efficiency and convergence of the method is one concerning the choice of trial and test functions for the velocity and pressure fields. A tempting choice is the  $Q_1$  (velocity)  $\times$   $\mathbb{P}_0$  (pressure) element since this allows one to solve for the pressure explicitly over each element. However this element is unstable and necessitates "post-processing" to produce convergent pressure fields. Alternatives which are stable are elements such as the  $\mathbb{P}_{4/3} \times \mathbb{P}_1$  element (Ruas), the  $Q_1 \times \mathbb{P}_0$  macroelement (LeTallec) and the  $\mathbb{P}_{4/3} \times \mathbb{P}_0$  macroelement (Ruas).

We are interested in an algorithm where different interpolation functions are used for the trial and test spaces for pressure. We show that by using continuous trial functions for the pressure, along with a particular set of discontinuous test functions, an explicit system results. The construction of these functions is local over each element and involves a "small" additional effort in computation. Stability and convergence of the scheme is proven for several important elements, such as the  $Q_2 \times Q_1$  and  $Q_2 \times \mathbb{P}_1$  elements, and some numerical results are presented.

A FINITE VOLUME-LAX-WENDROFF SOLUTION  
OF THE FLOW FIELD RESULTING AT THE OPEN END OF A SHOCK TUBE

by

M.B. Khalil and E.G. Plett  
Department of Mechanical and Aeronautical Engineering  
Carleton University, Ottawa, Ontario Canada K1S 5B6  
and  
D.H. Gladstone  
DND, Valcartier, Quebec

In this paper, a numerical analysis of the flow of gases from the open end of a shock tube into the atmosphere is described and the results presented. The computations begin in the shock tube following the breaking of the diaphragm separating the driver and driven section of the shock tube. When the shock front emerges from the open end, changes to conditions in the surrounding flow field are computed.

The computations inside the shock tube are carried out with the assumption of a one-dimensional, non-viscous flow and the shock tube walls are assumed to be adiabatic. The computations in the field outside the shock tube at its open end are carried out utilizing the two dimensional  $(r,z)$  conservation equations. Allowance for the viscosity of the flow is included in this region. The numerical technique applied to cast the conservation equations into finite difference form is a modified Lax-Wendroff 2-step technique using a finite volume approach.

The numerical computations are carried out simultaneously in the shock tube and in the field using a common time step to follow the development of the flow. The time step is obtained through the application of the Courant, Friedrichs and Levy (CFL) stability criterion to the flow in the shock tube as well as to the flow outside the tube. The smallest time step is chosen to advance the time of computations. Artificial viscosity was incorporated into both flows to avoid excessive over and under-shooting at the discontinuity of the flow properties resulting from shock waves.

Several numerical experiments were carried out on a DEC LSI 11/23 microcomputer. The effect of cell dimensions, grid size, artificial viscosity and pressure ratio across the diaphragm on the stability of the numerical solution were investigated.

It was found that choosing very small cell dimensions, with a limited total number of cells possible because of computer limitations resulted in distortions and instability on a large scale. This was attributed to the fact that small cell dimensions result in large gradients of properties thereby straining the stability of the solution. In addition, having a somewhat limited computation field results in reflections at the computation field boundary which acts as a disturbance that travels upstream and disturbs and distorts the flow. Artificial viscosity was necessary for a stable solution with the cases examined.

A range of pressure ratios across the shock tube diaphragm was used for computations. It was concluded that high pressure ratios (greater than 15) require a large grid and small time step to obtain a stable solution. Then, however, the overall computation time becomes prohibitively high on a microcomputer of the type used. Therefore, 5 cm grid sizes were used more successfully than smaller sizes.

For a shock tube diaphragm pressure ratio of 3, with a 42 by 42 grid field and cell dimensions of 5 cm by 5 cm, the results agreed very well with experimental measurements. Plots of pressure and density contours and velocity vectors throughout the field indicated that there are vortices that form and develop as the flow progresses with time. These vortices interact with the shock waves and also with any reflection at the boundaries thereby producing a very complicated flow field. As the flow from the shock tube subsides, the disturbance in the field is observed to continue moving downstream for a while before it dissipates as well.

A FINITE ELEMENT ANALYSIS OF HYPERSONIC LAMINAR  
BOUNDARY LAYER FLOWS

by

R.J. Matus and S.W. Kim  
Department of Aerospace Engineering  
University of Texas at Arlington  
Arlington, Texas 76019

In hypersonic boundary layer flows over blunt bodies, the stagnation temperature reaches several thousand degrees Kelvin, and the gas dissociates and ionizes. Also, due to its high temperature, gas properties such as molecular viscosity and heat diffusivity change by several factors inside the extremely thin boundary layer. To predict wall heat transfer rates more accurately, one needs to use accurate gas property equations as well as accurate numerical methods.

Due to lack of powerful numerical techniques in the past, hypersonic boundary layer flows have usually been solved using some similarity assumptions, with sacrifice of accuracy. Even the finite difference solution by Smith and Clutter (2), which is considered the most accurate until now, employs a stream function formulation in which several material properties are merged into a single parameter; the stream function.

In the present study, it is shown that a previously developed numerical technique (1) can be extended quite easily to hypersonic boundary layer flows. The same coordinate transformation is used for the conservation of momentum and conservation of energy; the pressure gradient term, instead of the inviscid velocity term, enters into the momentum equation directly. Some of the important features of the previous method solves the boundary layer equations using the primitive variables, so that more accurate material property data (3) can be used in the numerical analysis. The computational results are compared with experiments and solutions by other numerical methods.

References

- [1] Kim, S.W. and Payne, F.R., "Finite Element Analysis of Incompressible Laminar Boundary Layer Flows," Proceedings of the 5th International Symposium on Finite Elements and Flow Problems, U.T. Austin, Int. J. Num. Meth. Fluids.
- [2] Smith, A.M.O., and Clutter, D.W., "Machine Calculation of Compressible Laminar Boundary Layers," J. AIAA, Vol. 3, 1965, pp. 639-647.
- [3] Hansen, C.F., "Approximations for the Thermodynamic and Transport Properties of High-Temperature Air," NACA TN-4150.

AN INCREMENTAL LINE GAUSS-SEIDEL METHOD  
FOR THE NAVIER-STOKES EQUATIONS

by

M. Napolitano, Istituto di Macchine, Bari - Italy

Robert W. Walters, North Carolina State University, Raleigh, NC

This paper provides an incremental line Gauss-Seidel method for the incompressible and compressible Navier-Stokes equations in two dimensions. For the case of incompressible flows, the vorticity-stream function equations are considered in a general curvilinear coordinate system; a relaxation-like time derivative is added to the stream function equation to parabolize it and the two equations are discretized in time by an implicit Euler scheme and linearized - neglecting terms of order  $\Delta t^2$ , by means of the incremental (delta) approach of Beam and Warming (1). The incremental terms are discretized in space using central differences for the viscous terms and upwind differences are used for all of the nonincremental terms. In this way, artificial viscosity is introduced during the pseudo-transient, to stabilize it, but at convergence the solution is free of numerical viscosity and second order accurate. Also, the resulting linear system to be solved at every time level has a strong diagonal dominance which guarantees the line Gauss-Seidel solution method to converge. The method is full implicit in the crossflow direction (i.e., across the viscous layer) and marches downstream in the streamwise direction, so that the time iteration process needs only to account for the nonlinearities and for the weak up-stream influence due to separation. For the case of compressible flows, starting from the Navier-Stokes equations in conservation-law form, the numerical procedure proceeds in a similar way. The incremental viscous terms are discretized using first-order upwind differences based on the continuously differentiable flux vector splitting method of Van Leer (2) and again only block-tridiagonal systems need to be solved along each column of the computational grid. With respect to the similar block-ADI methods of Napolitano (3) and Beam and Warming (1), the present LGS methods require less computer time per iteration, converge in fewer iterations and, most importantly, converge for high Reynolds number separated flow cases, in which the ADI methods fail. Results have been obtained for the incompressible separated flow in a channel of complex geometry proposed by Roache (4), for values of the Reynolds number as high as  $10^6$ , at an extremely low computer cost (1 CPU minute on a HP 9000/9020 mini-computer); this is a very remarkable result considering that the ADI method of Ref. 3 fails to converge for  $Re > 10^3$ . The results, which are in very good agreement with those by Roache (4), will be given in the final paper. The complex compressible flow problem proposed by Kumar (5) has also been considered and the results are presented in figures 1 and 2. The present results have been obtained in about half of the computer time required by the standard ADI method of Ref. 1, using the same spatial discretization. Further results and comparisons will be given in the final paper.

## REFERENCES

1. Beam, R.M. and Warming, R.J., AIAA J., Vol. 16, no. 4, 1978, pp. 393-402.
2. Van Leer, B. "Flux vector splitting for the Euler equations," ICASE report 82-30.
3. Napolitano, M., "Efficient ADI and spline ADI methods for the Navier-Stokes equations," Int. J. Num. Methods in Fluids, to appear.
4. Roache, P.J., "Scaling of High Reynolds number weakly separated channel flows," Symp on Num. and Phys. aspects of Aerodynamic flows. Cal. State Un. Long Beach, CA, January 19-21, 1981.
5. Kumar, A., "Some observations on a new num. meth. for the N.S. equations" NASA TP 1934.

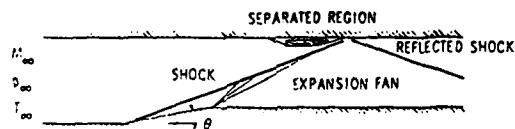


Figure 1.- Sketch of the supersonic inlet problem.

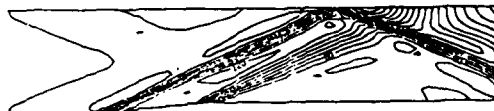


Figure 2 - Pressure contours for a 5° wedge angle with an entrance Mach number of 3.

STOKES FLOW IN A TWO-DIMENSIONAL CAVITY  
WITH MOVING END WALLS

by

Leroy D. Sturges  
Iowa State University  
Department of Engineering Science and Mechanics  
Ames, IA 50011

Fluid in a two-dimensional, rectangular cavity is driven by moving end walls. The resulting flow consists of a pattern of one or more eddies depending on the aspect ratio (ratio of width to depth) of the cavity. Of interest in this paper is the way in which the eddy patterns change from one to another and the stress distributions which cause them to change.

For aspect ratios less than one, the flow pattern consists of a single eddy which fills the entire cavity. As the aspect ratio increases, this eddy pinches off in the center forming two eddies. As the aspect ratio increases further, small eddies form at the center of the side walls, grow toward the center, and finally coalesce into a central, counter-rotating eddy. The process is then repeated as the central eddy elongates and pinches off to form a pair of eddies.

by

S.W. Kim and D.R. Wilson  
Department of Aerospace Engineering  
University of Texas at Arlington  
Arlington, Texas 76019

The channel flow of a magnetohydrodynamic (MHD) power generator can be effectively analyzed numerically by solving the core flow and the boundary layer flow interactively. In the present study, a finite element analysis of the MHD boundary layer flows and of the heat transfer rate through the channel walls is discussed.

Due to the difficult flow field, i.e., Mach No. of approximately 0.8 to 1.2 and operating temperature of about 2400-2800 degrees Kelvin, and the severe interaction between the flow field and the electromagnetic field, usual boundary layer solution techniques cannot yield reasonably accurate results to be used for design. The finite element method developed previously [3] is extended to solve the boundary layer flows of the electric wall and the magnetic wall for the MHD channel flow. To predict the heat transfer rate and the difficult flow field accurately, it is necessary to use accurate gas properties [1] and an appropriate turbulence model. Then the heat transfer rate is obtained using the converged solution of the conservation of energy equation. Discussion will include: computational results obtained by using the Cebeci and Smith's [4] eddy viscosity and eddy diffusivity model and other turbulence models; further development of the present study to solve the three dimensional MHD corner flows; extension of the existing Navier-Stokes equation solver (NSFEM-FORTRAN CODE) to solve the Maxwell's equation; and application of the moving finite elements [2] to solve the inviscid core flows.

#### References

- [1] Gordon, S. and McBride, B.J., "Computer Program for Calculation of Complex Chemical Equilibrium Compositions, Rocket Performance, Incident and Reflected Shocks, and Chapman-Jouquet Detonations," NASA SP-273, 1971.
- [2] Mueller, A. and Casey, G.F., "Stefan Problems Using Moving Elements," Proceedings of the 5th Int. Symp. on Finite Elements and Flow Problems, U.T. Austin, 1984.
- [3] Kim, S.W. and Payne, F.R., "Finite Element Analysis of Incompressible Laminar Boundary Layer Flow," Proceedings of the 5th Int. Symp. on finite Elements and Flow problems, U.T. Austin, 1984. Also will appear in the Int. J. Num. Meth. Fluids.
- [4] Cebeci T. and Smith, A.M.O., Analysis of Turbulent Boundary Layers, Academic Press, 1974.

NUMERICAL SIMULATION OF SHOCK/BOUNDARY-LAYER  
INTERACTION USING A FINITE-VOLUME  
RUNGE-KUTTA TIME-STEPPING SCHEME\*

by

Ramesh K. Agarwal  
McDonnell Douglas Research Laboratories  
St. Louis, MO 63166

An efficient numerical algorithm is presented for solving the unsteady compressible Navier-Stokes equations. The solution procedure is based on a finite-volume method and employs a fourth-order Runge-Kutta time-stepping scheme which is stable for Courant numbers  $\leq 2\sqrt{2}$ . The spatial terms are central-differenced and a combination of second- and fourth-order artificial dissipation is added to stabilize the algorithm. The algorithm also employs enthalpy damping and variable time steps to speed convergence to steady state.

The algorithm is used to calculate the flowfield due to the oblique impingement of a shock-wave on a laminar boundary-layer on a flat plate. This flow has been used as a standard test case to check the accuracy and efficiency of a variety of Navier-Stokes algorithms. Numerical results are compared with the calculations of other investigators, the triple-deck theory (asymptotic large Reynolds number theory), and the experimental data. The numerical experiments indicate that the solution procedure is accurate, robust, and efficient.

\*This work was supported by the McDonnell Douglas Independent Research and Development program.

THE SOLUTION OF PARABOLIZED NAVIER-STOKES EQUATIONS  
BY THE SPLITTING UP METHOD

by

V.M. Kovenya and S.G. Cherny  
USSR Academy of Sciences  
Institute of Theoretical and Applied Mechanics  
Novosibirsk 630090, USSR

The application of simplified, parabolized Navier-Stokes equations of a compressible gas for solving the stationary problems of supersonic flow-past enables one to decrease the dimension of problems and to find efficiently their numerical solution. In the paper, it is suggested an efficient numerical algorithm for solving the parabolized Navier-Stokes equations based on the method of splitting up in terms of the physical processes and the spatial directions (1,2). The use of the splitting up leads to a system of difference equations the solution of which can be obtained by scalar sweeps. The accuracy of the method and its convergence are studied. The techniques for computation of the local subsonic zones where an initial problem is incorrect are suggested. A system of coordinates adaptive to the flow is introduced that allows to expand a class of problems under consideration. Computations of supersonic flow around the bodies of a spatial configuration at different angles of attack by the flow of a viscous heat-conducting gas have been carried out. The algorithm for computation of pointed and blunt bodies is presented. There is obtained a pattern of the flow near the streamlined bodies incorporating the vortex and separation zones. The results of computations are discussed.

REFERENCES

1. Kovenya, V.M., N.N. Yanenko, "The Method of Splitting Up in Problems of Gas Dynamics," Novosibirsk, Nauka, 1981.
2. Kovenya, V.M., S.G. Cherny, "The Marching Method of Solving Stationary Simplified Navier-Stokes Equations," Journal of Comp. Math. and Math. Phys., Vol. 23, No. 5, 1983.

THE INVARIANT FINITE-DIMENSIONAL APPROXIMATION  
OF THE EVOLUTIONAL EQUATIONS

by

B.Yu. Scobelev

Institute of Theoretical and Applied Mechanics  
USSR Academy of Sciences, Novosibirsk 630090, USSR

The effective way of studying the evolutional equations trajectories is replacing the initial system of equations by the smaller dimensionality system on integral manifold. Firstly integral manifolds are considered by A.M. Lyapunov [1]. At the last time the notion of local invariant manifold have received extension in the bifurcation theory [2].

In this paper there are studying the attractive finite-dimensional invariant manifolds of nonlinear evolutional equations with unbounded operators. There are received the existence conditions of analytical invariant manifolds for broad class of equations containing Navier-Stokes equations. There is suggested the method of finding the projection of a evolutional equation on a finite-dimensional invariant manifold that enables one, for example, to reduce the initial-boundary value problem for the partial differential equations to a finite system of the ordinary differential equations with analytical right parts. The numerical computation and the stability analysis of auto-oscillating regimes bifurcating from Poiseuille flow are carried out with the help of the four-dimensional invariant approximation of Navier-Stokes equations.

1. Lyapunov A.M. *Obshchaya zadacha ob ustojchivosti dvizhenij*, L.M.: ONTI, 1935, 386 pp.
2. Marsden J., McCracken M. *The Hopf bifurcation and its applications*. *Appl. Math. Sci.*, Vol. 19, Springer-Verlag, N.-Y., 1976, 408 pp.

by

K. C. Valanis  
University of Cincinnati

Endochronic constitutive theory deals directly with the concept of memory paths and their role in the formulation of equations of evolution of thermodynamic states. The basis of the theory is the principle that the memory of a system of its previous states, is with respect to an intrinsic time  $\zeta$ , which is a material property of the system.

In plastic materials with initially elastic unloading,  $\zeta$  is the length of the path in the plastic strain space. In the context of linear irreversible thermodynamics the stress is a linear function of the history of plastic strain with respect to a time scale  $z$  such that  $dz = d\zeta/f(\zeta)$ , where  $f(\zeta)$  is the hardening function.

Numerous solutions for the stress response are discussed with comparison with experiment, in a number of (effectively) one-dimensional and two-dimensional homogeneous strain histories. Also the numerical solution of the problem of stress and strain fields in a plate with two edge cracks, symmetrically placed, is discussed when the plate is subjected to cyclic axial loading in a direction normal to the plane of the cracks.

In all cases analysis agrees exceedingly well with experiment.

by

H. E. Read  
Systems Science and Software  
La Jolla, California

The basic inelastic deviatoric response characteristics of the new endochronic theory with singular kernel are explored by examining the behavior of the theory for several different non-proportional stress and strain paths. In one case, a non-proportional stress path involving an abrupt change in the loading direction is considered; for this, an analytical solution is obtained in the neighborhood of the abrupt change as a function of the angle between the original and new loading directions. In the other cases, numerical methods are used to investigate the inelastic features along the entire lengths of several non-proportional stress and strain paths; for these cases, comparisons are given between predicted and measured inelastic response features for soil and concrete. In general, the basic inelastic response features of the new theory are found to differ very significantly from those of classical plasticity.

by

Han C. Wu  
Department of Civil Engineering  
The University of Iowa  
Iowa City, Iowa 52242

A combined theoretical-experimental investigation of the stress response to complex, non-proportional strain-paths in the axial-torsional strain space is reported in this paper. Type 304 stainless steel tubular specimens have been tested at a constant strain rate of  $5 \times 10^{-4}$  per second. Several strain-paths have been investigated including paths with cyclic straining.

The endochronic theory with a plastic strain defined intrinsic time has been shown to predict the experimental results satisfactorily.

FINITE ELEMENT ANALYSIS OF ANISOTROPIC FINITE  
PLASTIC DEFORMATIONS

A.G.Groehs, G.J.Creus  
Department of Civil Engineering  
Universidade Federal do Rio Grande do Sul  
90000 - Porto Alegre, RS - Brasil

This paper describes the theoretical foundations and implementation of a finite element code for the analysis of anisotropic finite plastic deformations.

The deformation processes studied are isothermal and quasi-static and the material is inviscid. The elastic stress-strain relations for the stress-free element are isotropic and independent of past events (including previous plastic deformations). A yield function is assumed, whose arguments are the Cauchy stresses and some internal variables that, jointly, define the state and orientation of the material element. The yield function depends on the previous deformation through these internal variables; in general, it becomes anisotropic during the deformation process. The yield function acts as a potential for the plastic deformation rates, which are volume preserving. The theory, based on ideas of E.T.Onat [1], may be found fully developed in [2].

The numerical analysis is performed incrementally, with an updated Lagrangian approach. In order to avoid errors due to the incompressibility of plastic flow, the modified functional proposed in [3] as well as reduced integration options are available in the program.

As an example, the finite (up to  $\Delta H/H = 0.5$ ) plastic deformations of a hollow cylinder in axial compression are determined and the results are compared with the values obtained experimentally in [4]. Fig. 1 - a indicates the geometry of the axisymmetric problem. Eighteen axisymmetric isoparametric linear elements we use to model half the tube. Fig. 1-b indicates the stress-strain curve for the material and the approximation used in the analysis. Fig. 1-c shows the numerical results, that accompany fairly well the experimental curve.

REFERENCES

1. Onat, E.T., "Representation of inelastic behavior in the presence of anisotropy and finite deformations", Ch.5 of Recent Advances in Creep and Fracture of Engineering Materials and Structures, Pineridge Press, 1982.
2. Groehs, A.G., "ESFINGE, Uma linguagem orientada para cálculo elastoplástico de estruturas", Ph.D. Theses, UFRJ/RJ, 1983.

3. Nagtegaal, J.C. et al, "On numerically accurate finite element solutions in the fully plastic range", Comp. Meth. Appl. Mech. and Engng, 1(2):153-77, Sept. 1974.
4. Herbertz, R., "Zur Brauchbarkeit eines starr-viscoplastischen Materialgesetzes bei der Lösung umformtechnischer Probleme mit Hilfe der Finite Elemente Methode", Ph.D. Theses, Technischen Hochschule Aachen, 1982.

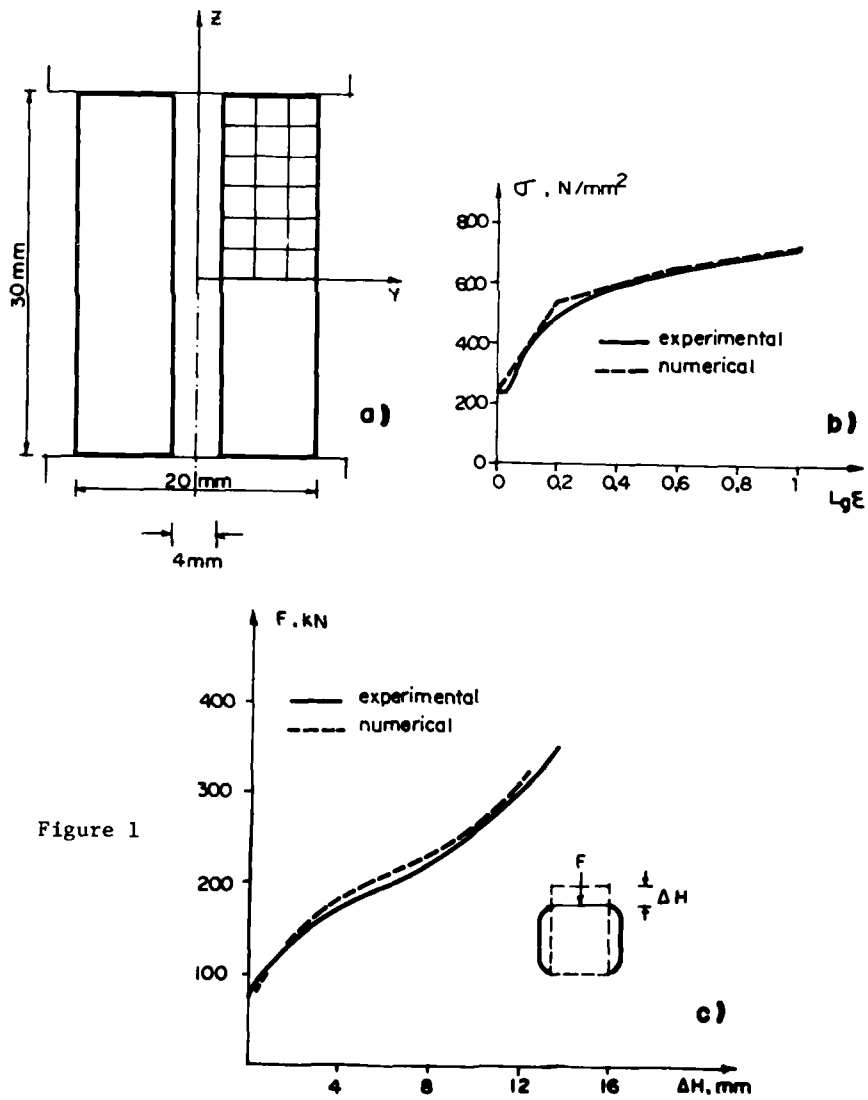


Figure 1

by

Marek-Jerzy Pindera  
CertainTeed Corporation  
Levecque Technical Center  
Blue Bell, PA 19422

The nonlinear response of oriented composites is a complex phenomenon having roots in a variety of mechanisms operating at the microscale and consequently it is not easily amenable to rigorous and comprehensive analytical description in the traditional micro-mechanics sense.

The generality of the model to accurately predict the following types of material response observed in the graphite-polyimide system is illustrated:

- i) linear or nonlinear elastic response along fiber direction
- ii) dissipation in shear and transverse tension characterized by permanent strain accumulation, nonlinear unloading and reloading, resulting in generation of hysteresis loops
- iii) dissimilar "strain-hardening" in shear and transverse tension characterized by markedly different exponents in commonly employed power-law approximations
- iv) influence of transverse as well as longitudinal stress on the nonlinear shear strain and vice versa: an often observed phenomenon commonly referred to as stress-interaction
- v) often highly nonlinear response along a particular material direction (e.g., shearing parallel to fibers) characterized by absence of readily noticeable transition point between reversible and dissipative response and yet exhibiting relatively small strains at failure.

The theory is developed with stresses as one of the sets of independent variables and consequently strains are related to stresses through path-dependent integrals which are functionally dependent on the so-called intrinsic time measure assumed to be a material property. The concept of an intrinsic time measure governing the nonlinear response of a medium is a natural one for modelling the stress-interaction phenomena often observed in composite materials, as is demonstrated on the basis of available empirical and analytical evidence. Furthermore, a methodology of evaluating certain intrinsic time measure parameters with the aid of micro-mechanical analysis is also discussed along with the introduction of the concept of multiple time scales for predicting cyclic response of the above material system.

## SOME COMMENTS ON REQUIREMENTS FOR PLASTICITY MODELS FOR SOILS

by

John F. Peters

Civil Engineer, Soil Mechanics Division

Geotechnical Laboratory

U.S. Army Engineer Waterways Experiment Station

Vicksburg, MS 39180

An ongoing problem in the development of constitutive equations for soils based on the theory of plastic materials is the difficulty in resolving the requirement for material stability, as postulated by D. C. Drucker, with real soil behavior. It is generally accepted that frictional systems in general, and soils in particular, do not obey the stability requirement. Also, there is general agreement that stability is not a thermodynamic requirement for a material and valid constitutive relationships have been formulated that violate the stability requirement. Nevertheless, analysts routinely adopt plasticity models that satisfy Drucker's stability postulate to avoid possible computational difficulties. Comparative numerical analyses, using associated versus nonassociated flow laws, are often cited as a justification for artificially imposing stability on material models. What is often over looked in such studies is that the examples chosen to demonstrate the acceptability of associated flow laws for soils do not involve loading conditions for which the most serious ramifications of violating stability can be observed. Several examples of soil behavior are presented to demonstrate how imposing normality in the constitutive relationships can preclude the occurrence of important phenomenon. For example, liquefaction of saturated sands cannot be captured by any model that obeys stability. Therefore, the choice of restrictions to be imposed on a material model is not solely a tradeoff between algorithmic reliability and precision. In some cases such restrictions inhibit the very behavior the analysis is intended to model.

SHEAR BAND FORMATION IN SIMPLE SHEAR  
OF THERMAL VISCO-PLASTIC MATERIALS\*

by

T. G. Shawki, R. J. Clifton, G. Majda\*\*  
Division of Engineering  
Brown University  
Providence, RI 02912

Simple shearing deformations are analyzed as a means of investigating the effects of strain hardening, thermal softening, and strain-rate sensitivity on the formation of shear bands. The phenomenology of shear band formation is illustrated by an exact solution for a special case of a non-Newtonian fluid. Finite difference solutions are obtained for the fully nonlinear system of partial differential equations that govern dynamic, simple shear of a thermal visco-plastic material with heat conduction and elasticity. Boundary conditions of prescribed velocities and no heat flow are assumed. A groove is included as a geometrical imperfection. Computational efficiency is enhanced by using alternative (parabolic or hyperbolic) difference methods for the mechanical variables depending on whether the deformation is dominated by dissipation or wave propagation, respectively. Main features of plastic response for the class of problems considered are illustrated by numerical solutions for a hot-rolled steel and a cold-rolled steel, each modeled as having a thermal visco-plastic response that is described by a power law. For the cold-rolled steel, CRS-1018, the development of a shear band begins after the slope of the stress-strain trajectory becomes zero due to strain hardening being offset by thermal softening. This condition is satisfied first in the thinned region at the groove. Initially the ratio of the strain rate in the thinned region to the strain rate at points outside this region increases slowly. This localization tends to accelerate and to lead to failure by the formation of a narrow shear band that accounts for all further deformation. The additional strain required for full localization to occur depends strongly on the strain-rate sensitivity with less strain being required for materials with low strain-rate sensitivity.

From these difference solutions, the effects of elasticity and heat conduction are shown to be negligible in the analysis of shear band formation for the geometries and the strain rates of  $10^3 \text{ s}^{-1}$  and  $10^4 \text{ s}^{-1}$  in torsional Kolsky bar experiments. Neglect of these two effects greatly simplifies the analysis and allows explicit results to be obtained for a linear perturbation analysis. These explicit results illustrate the role of strain-rate sensitivity and the slope of the stress-strain curve in the post-peak regime in determining the rate at which localization is completed.

\* This research was supported by the U.S. Army Research Office under Grant DAAG29-81-K-0121 to Brown University.

\*\* Division of Applied Mathematics, Brown University.

References

1. T. G. Shawki, R. J. Clifton, and G. Majda, "Analysis of Shear Strain Localization in Thermal Visco-Plastic Materials", Brown University Technical Report No. AROIDAAG29-81-K-0121/3, October 1983.
2. R. J. Clifton, J. Duffy, K. Hartley, and T. G. Shawki, "On Critical Conditions for Shear Band Formation at High Strain Rates", to appear in Scripta Met, 1984.

APPLICATION OF THERMAL ACTIVATION THEORY  
TO HIGH STRAIN RATE PLASTICITY

by

C. S. Ting  
Senior Consulting Scientist  
AVCO Systems Division  
Wilmington, Massachusetts 01887

Radiographic images of a polycrystalline metal liner deforming plastically at strain rates of  $10^5\text{s}^{-1}$  were recorded in the testing of a Self-Forging Fragment device. The plastic deformation of the metal liner is a result of the uneven velocity distribution caused by the explosive impulse loading in the first 30  $\mu\text{s}$  after initiation of the explosive charge. Very large plastic deformation with equivalent strain of about 300% is achieved in the subsequent several hundred microseconds while the hydrostatic pressures are at insignificant levels. Experimental data includes polycrystalline aluminum, OFHC copper, Armco iron and pure tantalum.

The experiments were simulated on the HEMP computer program implemented with a temperature and strain rate dependent strain hardening constitutive model. An adiabatic process was assumed to compute the temperature rise in the deformed liner from the initial shock loading and subsequent dissipative plastic work. Formulation of temperature and strain rate dependent flow stress is based on the thermal activation theory, in which a single rate controlling deformation mechanism was assumed. Material constants in this model for each material were determined through dynamic test data to  $10^3\text{s}^{-1}$  available in the literature. Using this constitutive model, the deforming liner shapes predicted by HEMP code computation show a very reasonable agreement with the shapes obtained in radiographic records. Generality of this constitutive model is also verified by successfully modeling Taylor anvil cylinder impact test data which covered a wide range of initial temperature and impact velocities. Strain rates in the deforming cylinder during impact are on the order of  $10^4$  to  $10^5\text{s}^{-1}$  depending on initial conditions.

Experimental data and computer simulation results presented in this paper strongly suggest that combined-stress plastic deformation in polycrystalline pure aluminum, copper, iron and tantalum is controlled by thermally-activated mechanisms up to strain rates of  $10^5\text{s}^{-1}$ . This is contrary to conclusions made in a number of publications which state that transition to a viscous flow mechanism occurred at plastic strain rates of  $10^3\text{s}^{-1}$  based on test data from Split Hopkinson pressure bars and plate impact tests. Further attention to this fundamental theory in high strain rate metal plasticity is required to resolve this issue.

## FINITE ELEMENT ANALYSIS OF SUPERPLASTIC BLOWFORMING

R. Varahamurti and T.D. Burton  
 Department of Mechanical Engineering  
 Washington State University  
 Pullman, WA 99164-2920

Superplastic behavior of certain alloy systems (e.g., Ti and Al) occurs at temperatures of about half the melting point and at low strain rates ( $\sim 10^{-4}$ - $10^{-3}$ /sec). Under these conditions the material deforms much like an incompressible, highly viscous non-Newtonian fluid, obeying (approximately) the uniaxial constitutive relation  $\sigma = k\dot{\epsilon}^m$ , where  $\sigma$  = stress,  $\dot{\epsilon}$  = strain rate,  $k$  = material constant, and the index  $m = m(T, \dot{\epsilon}) < 1$ . The low working loads and large neck free deformations possible make the process suitable for forming light, complex parts which would otherwise be difficult to manufacture.

We present a finite element analysis of superplastic blowforming of a thin sheet into a hat section (Fig. 1). We model the process as a non-Newtonian Stokes flow and use the von Mises theory to extend the aforementioned uniaxial constitutive model to the multi-dimensional case. Our finite element formulation differs from previous ones in the way in which the incompressibility condition is handled. The analysis was verified through comparison with experimental forming results obtained by Ghosh and Hamilton (preprint SC-PP-79-164, AIME Mat. & Proc. Cong., 1979). A sample sheet thickness distribution in the formed part is shown in Fig. 2. We present additional results showing how the quality of the formed part is influenced by die geometry, die/sheet friction, material nonlinearity, and forming pressure history.

flange length

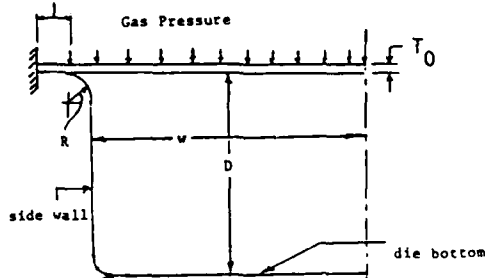
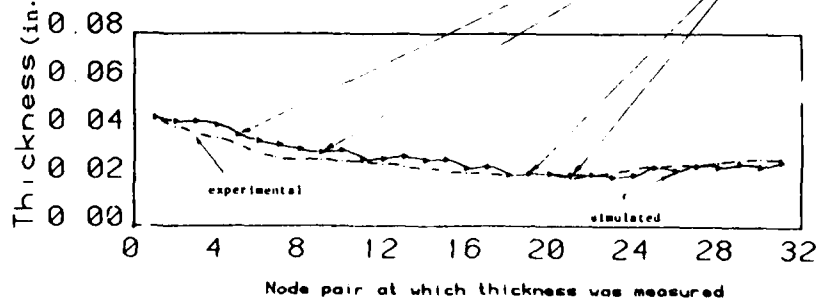


Figure 1 (left): Geometry

Figure 2 (below): Thickness variation in formed part  
 (Temp. = 1700F,  $T_0 = 0.045$  in.,  
 Time = 1209 sec.,  $w=D=1.0$  in)



THE EFFECT OF MATERIAL CONSOLIDATION  
ON STATIC BIN PRESSURES

by

Stephen C. Cowin  
Tulane University  
Department of Biomedical Engineering  
New Orleans, LA 70118

The formulas of Janssen give the static stresses exerted on bin walls by the weight of bulk material contained within. Cowin [1] gave a less restrictive derivation of Janssen's formulas which are referred to here as the improved formulas of Janssen. The improved formulas prescribe lower bounds on  $V$  and  $H$ , where  $V$  is the vertical compressive stress in the granular material averaged over the cross-sectional area of the bin and  $H$  is the horizontal compressive stress in the granular material averaged over the perimeter of the cross-section of the bin. It is assumed that these two average stresses are related by a constant  $K_0$ :  $H = K_0 V$ .  $K_0$  is called the pressure ratio but, more precisely, it is the ratio of the horizontal stress averaged over the perimeter to the vertical stress averaged over the cross-sectional area. The improved Janssen formulas are

$$V \geq \gamma_0 \ell_0 + (P - \gamma_0 \ell_0) e^{-z/\ell_0}, \quad (1)$$

and

$$H \geq \gamma_0 \ell_0 K_0 + (PK_0 - \gamma_0 \ell_0 K_0) e^{-z/\ell_0}, \quad (2)$$

where  $\ell_0 = A(\mu L K_0)^{-1}$ , and where  $\gamma_0$  is the weight density of the material,  $A$  is the cross-sectional area of the bin,  $L$  is the length of the perimeter of the cross-section,  $\mu$  is the coefficient of friction between the material and the bin wall,  $P$  is the vertical surcharge stress applied at the free surface of the granular material, and  $z$  is a coordinate measured positive downward from the free surface of the material.

In the improved Janssen formulas it is assumed that the weight density of the stored granular material is a constant throughout the bin. This assumption is not consistent with observations, experience and experiment for many bulk materials. Cowin [2] extended the improved formulas to cover the effect of material consolidation. Rather than assuming that  $\gamma_0$  and  $K_0$  were constants as they are in equations (1) and (2),  $\gamma_0$  was replaced by  $\gamma$  and  $K_0$  by  $K$  where  $K$  and  $\gamma$  are assumed to depend upon the average vertical consolidation pressure  $V$ . Cowin assumed that  $K(V)$  and  $\gamma(V)$  satisfied the inequalities

$$K = K(V) \leq K_0(1 + mV), \quad (3)$$

$$\gamma = \gamma(V) \geq \gamma_0(1 - nV), \quad (4)$$

where  $\gamma_0$  is now the weight density of the unstressed bulk material,  $K_0$  is now the pressure ratio of the unstressed bulk material, and  $m(m > 0)$  is the pressure ratio consoli-

dation factor and  $n(n>0)$  is the weight density consolidation factor. Both  $n$  and  $m$  have the same dimensions, the inverse of stress. The interpretation of the assumptions (3) and (4) is two fold; either  $K(V)$  and  $\gamma(V)$  are given exactly by the right hand sides of (3) and (4) with the inequalities replaced by equalities, or  $K(V)$  and  $\gamma(V)$  are given by functions which are bounded as indicated by the linear functions of  $V$ . Corrections to the improved Janssen formula (1) for  $V$  and  $H$  as a consequence of the more general assumptions (3) and (4) for  $K$  and  $\gamma$ , respectively, are

$$V = V_1 G(z) - V_2, \quad H = K(V)V \quad (5)$$

where

$$G(z) = \frac{1 - J e^{-z/\ell}}{1 + J e^{-z/\ell}}, \quad J = \frac{V_1 - V_2 - P}{V_1 + V_2 + P}, \quad -1 \leq J \leq \frac{V_1 - V_2}{V_1 + V_2} \leq 1, \quad (6)$$

$$V_1 = \frac{\lambda_0}{2m\ell}, \quad V_2 = \frac{1}{2m}(1 - n\gamma_0 \ell_0), \quad \frac{1}{\ell} = \frac{1}{\ell_0} \sqrt{(1 - n\gamma_0 \ell_0)^2 + 4\gamma_0 \ell_0 m}. \quad (7)$$

These results show that, while the material consolidation increases the weight density of the material, it also increases the pressure ratio  $K$ , and these two effects thus tend to compensate for one another and reduce the overall effect of material consolidation on the formulas of Janssen. In fact, it is shown that if  $n$  is exactly equal to  $m$ , the asymptotic value of the vertical stress is exactly that predicted by Janssen's formulas. This work also reports an experimental study in which  $n$  and  $m$  were measured for wheat silage, haylage, corn silage, whole shelled corn, cracked shelled corn, ground ear corn, barley and coal. The predictions of the stresses exerted on bin walls are found to change substantially when the actual numerical corrections are made for material consolidation of these materials.

#### REFERENCES

- [1] Cowin, S. C., "The Theory of Static Loads in Bins," J. Appl. Mech., Vol. 44, 1977, p. 409-412.
- [2] Cowin, S. C., "The Pressure Ratio in the Theory of Bin Pressures," J. Appl. Mech., Vol. 46, 1979, pp. 524-528.

## SHOCK-WAVE PROPAGATION IN SATURATED POROUS MEDIA

Jean H. Prevost  
Princeton University  
Department of Civil Engineering  
Princeton, NJ 08544

In this paper, the transient response of fluid-saturated porous media is analyzed. The saturated medium is modeled as a two-phase system consisting of a solid and fluid phase. The coupled field equations based on mixture theories are presented, and solved numerically by the use of the finite element method. The solid skeleton is modeled as nonlinear elastic-plastic, and the fluid as linear and compressible. Numerical results on the propagation of compressional waves are presented. The results illustrate the effects of the water compressibility, of the coupling between the two phases, and of the skeleton nonlinear behavior.

DETERMINATION OF THE FREQUENCY DISTRIBUTIONS OF COORDINATION NUMBER  
AND CONTACT FORCE INTENSITY IN A RANDOMLY PACKED BED OF  
EQUAL SPHERES BY A TITRATION TECHNIQUE

by

Mohsen Shahinpoor  
Department of Mechanical and Industrial Engineering  
Clarkson University  
Potsdam, N.Y. 13676

A novel acid-base titration technique is utilized here to determine the frequency distributions of contacts among neighboring spheres (coordination number) and contact force intensity in random packing of equal spheres. The acid-base titration technique utilizes a pH tuning scheme in which short duration pulses of gaseous HCl is injected into a steam flow and the mixture is then blown through a randomly packed bed of equal spheres. The spheres being soft and elastic ( $E \approx 500$  psi) are coated with a thin layer of an indicator such as bromphenol blue acting as a pH calibrator. The mixture flow decreases the surface pH of spheres enough to induce a sharp color change from blue to yellow. The areas of contacts do not react enough with the HCl to change color and remain blue. The reason is that the diffusion regime within the areas of contact is basically molecular and governed by the Knudsen's law of free molecular flow. It is shown that the penetration of  $H_2O + HCl$  mixture between the contacting areas is negligible both theoretically and experimentally. Because the spheres are soft and elastic, there results a distribution of blue contact areas within the granular assembly. The assembly, having undergone the complete color change, is carefully dismantled and the number of blue contact areas per sphere is counted, and the corresponding diameter of each circular blue area is measured and recorded. The frequency histogram for the coordination number is then constructed by counting the number of spheres with the same number of blue areas of contacts. The diameters of circular contact areas is correlated with the intensity of the contact force between the spheres. A calibration technique is used for this purpose using the Instron Model 1331 Servohydraulic Testing Machine. The experimental setup is such that it can be loaded for a practical range of confining pressure to test the effect of overburden pressure on the frequency distribution of contact force in 3-D random packing of equal spheres. The experimental setup consists of randomly packed soft elastic balls of equal diameter. These elastic balls are either latex balls ( $E=470$  psi), elastic rubber balls ( $E=500$  psi), or elastic balloons ( $E=600$  psi). The softness is reflected here in the rather small values of the modulus of elasticity  $E$  compared to that of steel ( $E=30 \times 10^6$  psi). The idea is to create circular contact areas of finite diameter and easily discernible upon inspection. The randomly packed assembly is produced by random pouring of these balls in a cylindrical container of about 20 inches in diameter and 24 inches long. The balls are surface coated in a dusty box of an indicator after being uniformly coated by spray adhesives. As mentioned above, for the contact areas where the surface concentration of bromphenol blue is twice as large as other noncontact surfaces, due to decreased diffusivity (Knudsen No.)

15PM7

the rate of  $[H^+]$  ions available for the modification of surface pH is not enough to cause any color change during the titration. 155

The results obtained so far indicates a biased Maxwellian trend towards the population of denser "Voronoi Cells" [1] with increasing overburden pressure for both distributions. The two frequency distributions are important in the statistical description of the mechanics of granular materials because they are intimately connected with other important granular internal distributions such as the distribution of voids, potential failure surfaces, and stochastic transport variables.

Acknowledgments: This research is supported by NSF-Geotechnical Engineering grant NSF-8310632.

References

Shahinpoor, M., "Some Recent Results on the Behavior of Granular Materials" Adv. Mech. Flow. Granular Mats. Vol. 1 (1983) pp. 297-330.

A MODEL FOR PLANE DEFORMATIONS  
OF IDEAL GRANULAR MATERIALS

by

Lallit Anand  
Department of Mechanical Engineering  
Massachusetts Institute of Technology  
Cambridge, MA 02139

The flow rule based on a double shearing model developed by Spencer [1], and Mehrabadi and Cowin [2] is intended for use in analyzing fully developed plane flows of rate-independent, isotropic, rigid perfectly plastic frictional and dilatant (dry) granular materials. With the view of extending the range of applicability of this physically based flow rule to the prepeak (prelocalization) regime, we systematically introduce elasticity and isotropic hardening. The final constitutive equations are expressed in a new revealing form which should aid in the implementation of these equations in finite element computer codes for the solution of plane boundary value problems.

A "shear-band" bifurcation analysis using these constitutive equations is performed and a comparison is made between experimentally measured (Arthur et al [3]) and theoretically predicted shear-band orientations. The agreement is found to be excellent. It is noted that at localization, the orientation of the velocity characteristics --- "shear bands" --- does not coincide with that of the stress characteristics in the pre-localization regime.

REFERENCES

1. Spencer, A.J.M., "Deformation of Ideal Granular Materials," Mechanics of Solids, The Rodney Hill 60th Anniversary Volume (edited by H.J. Hopkins and M.J. Sewell), p. 607. Pergamon Press, Oxford, 1982.
2. Mehrabadi, M.M. and Cowin, S.C., "Initial Planar Deformation of Dilatant Granular Materials," J. Mech. Phys. Solids, Vol. 26, 1978, pp. 269-284.
3. Arthur, J.R.F., Dunstan, T., Al-Ani, Q.A.J.L., and Assani, A., "Plastic Deformation and Failure in Granular Media," Geotechnique, Vol. 27, 1977, pp. 53-74.

A LINEAR THEORY FOR THE MECHANICAL RESPONSE  
OF FLUID-FILLED POROELASTIC SOLIDS

by

Noriko Katsube  
Ohio State University  
Department of Engineering Mechanics  
Columbus, Ohio 43210

The problem of fluid flow through porous media can be approached from different points of view. On the one hand, there is the phenomenological theory of Biot which has been applied with considerable success. On the other hand, the continuum theory of mixtures provides a more fundamental description of the interaction of the fluid and the solid constituents. In this theory, each point of space is assumed to be occupied by a fluid particle and a solid particle, and the systems of equations were developed to describe the mechanical response of each constituent and also their interactions.

In applying mixture theory to problems of flow through porous geological materials, one encounters some conceptual difficulties due to the fact that porosity does not appear as a kinematic variable. In the present work we avoid this difficulty by treating fluid-filled porous material as a mixture whose constituents are a porous solid and a porous fluid. The mechanical behavior of these individual constituents is based on averaging procedures applied to the representative volume element and their interaction is described by the conventional mixture theory. The resulting theory is compared with Biot's phenomenological theory and in fact it reduces to Biot's theory when the effects of the fluid velocity gradients are ignored.

Two steady state boundary value problems were solved as examples. The velocity profiles were found to depend on the ratio of a characteristic length of the microstructure to a characteristic length defined by the boundary conditions. Also the existence of a non-Darcy flow closer to the boundary was shown. For most practical purposes, however, the phenomenological theory is a good approximate theory when one is not interested in wall effects. The propagation of plane waves in an infinite porous material filled with ideal fluid was also investigated, and the existence of two dilatational waves and one shear wave was established.

NUMERICAL METHOD FOR CALCULATING  
PARTICLE-PARTICLE INTERACTION PRESSURE

William Rogers and Atul Padhye  
Mechanical and Aerospace Engineering  
West Virginia University  
Morgantown, West Virginia 26506

The influence of particle interactions, via collisions, on the movement of particles in gas-fluidized beds of solid particles is significant at high particle loadings. These interactions produce transport property contributions from the solid phase such as solid pressure, and solid viscosity. Quantitative descriptions of these solid transport properties are necessary for accurate numerical modeling of fluidized bed systems. The need for accurate quantitative descriptions and the lack of available data for application to numerical modeling routines for a fluidized bed coal gasifiers has led to the work described here.

This work is an attempt to numerically obtain the value of solid pressure in gas-solid particle systems. This value is calculated from the phase space trajectories of individual particles as computed in a "scaled-up" molecular dynamics program.

Molecular dynamics routines have been used by physical scientists to model the movement of microscopic point particles, i.e. atoms and molecules, through phase space. Use of these phase space co-ordinates is made to determine thermodynamic and transport properties of fluid. Atoms and molecules are allowed to interact through either "hard particle" impacts or continuous potentials that are a function of interparticle distance. Using the forces resulting from these interparticle potentials, Newton's equations of motion are integrated to follow the movement of each particle.

Scaling-up the molecular dynamics concept to finite sized particles involves the inclusion of the influences of gravity and the interstitial fluid along with the particle interactions when describing forces acting on the particles. In this work the continuous interparticle potential is used to model a finite particle. This produces a particle with a "soft" surface, such as that of a hot coal particle. The scaled up version is then used to calculate solid pressure in a densely loaded systems where particles are falling through ambient air influenced by gravity and particle interactions only. The numerical results have been compared with the experimental measurements.

## ENTROPY ANALYSIS OF LIQUEFACTION PREDICTION ACCURACY

by

Kingsley Harrop-Williams and Samuel Uche Ejezie  
Department of Civil Engineering  
Carnegie-Mellon University  
Pittsburgh, PA 15213

Entropy is a general measure of uncertainty. Like the variance it can be used to measure the variability of quantitative random variables. Unlike the variance, however, it can also measure the variability of qualitative random variables. Common uses of entropy can be found in thermodynamics, where it is employed to quantify the randomness in systems; and in information theory, where it serves as a measure of information. In this paper entropy is used to evaluate the accuracies of the different models formulated for the prediction of soil liquefaction resulting from seismic and dynamic forces.

Dynamic loading on a saturated sand under undrained conditions, such as during an earthquake, results in a progressive increase in pore water pressure. Liquefaction occurs when the pore pressure becomes equal to the confining pressure. In this case the effective stress reduces to zero and the sand has lost its strength. Many random factors such as earthquake magnitude, location of liquefiable deposits, stress transmission through the soil and heterogeneity of the soil make it virtually impossible to develop a deterministic model that correctly predicts liquefaction. The catastrophic nature of the phenomenon has however forced researchers to develop approximate models. Many such models exist but none can claim to be reliable or even superior to the other.

If a model predicts that a site will liquefy with a probability,  $P$ , one will be more surprised if it liquefies when  $P = 0.01$  than if it liquefies when  $P = 0.99$ . Also it would be less surprising to hear later that liquefaction did indeed occur if liquefaction was predicted than if no prediction was made. It follows then that a liquefaction predicting model, depending on its accuracy, will reduce the surprise associated with liquefaction. This reduction of surprise is quantified as the entropy between prediction and observation. Using an extensive and updated list of earthquake case histories, where liquefaction did and did not occur, the entropy in the prediction of nine of the most common models are evaluated. The models are then ranked as to their entropy (reduction in surprise). The entropy also gives a measure of the total randomness of each model as it is compared with the maximum possible entropy (when all the predictions are correct). Finally, correction factors are found for these models that maximize the entropy of each model prediction subject to the constraints imposed by the model formulation and the case histories.

EFFECTS OF MOISTURE ABSORPTION ON MECHANICAL AND  
PHYSICAL PROPERTIES OF THE DYKERSBURG SHALE

by

Yoginder P. Chugh  
Southern Illinois University  
Department of Mining Engineering  
Carbondale, IL 62901

The physical and mechanical properties of shales significantly change on moisture absorption and effect the stability of underground excavations (tunnels, mine openings, underground chambers). The results for Dykersburg shale overlying Harrisburg coal seam in Illinois form the content of this paper.

Moisture gain, swelling strain and strength and deformation properties of the shale in compression, and flexural loading conditions were studied at 90, 95, and 100 percent constant relative humidity (R.H.) levels and under immersed water conditions. Cylindrical samples 2.5 cm in diameter and 5.0 cm long and beams 3.7 cm x 3.7 cm x 15 cm were utilized in these studies. For cylindrical samples, moisture absorption mostly occurred along the bedding planes of shale. For beam samples, moisture absorption was permitted to occur parallel to bedding planes by coating five (5) sides of a beam with latex. Similar studies were also conducted under cyclic humidity conditions where a shale sample was subjected to a 100% R.H. level for a certain period of time (200-1000 hrs.) and then subjected to a 70% R.H. level for a similar period of time. After attaining equilibrium conditions at a particular relative humidity, the samples were studied for changes in strength and deformation properties of the shale. The depth of moisture penetration in a sample was estimated by measuring the changes in rock hardness using the Vickers microhardness measurements. Using the basic mass transfer concepts, effective diffusion coefficients along and across the bedding planes were computed for the shale.

The results showed: 1) strength and elastic modulus decreased exponentially with increasing moisture content in the shale and a maximum decrease of 75%-95% was observed in compression and flexural loading conditions, 2) Poisson's ratio increased from 0.11 at natural moisture content to 0.46 at 100% R.H., 3) moisture absorption and desorption occurred 5-8 mm at 95% R.H. and 8-11 mm at 100% R.H., 4) the effective diffusion coefficients varied from  $2.5 \times 10^{-10}$  m<sup>2</sup>/s at 90% R.H. to  $40.59 \times 10^{-10}$  m<sup>2</sup>/s for immersed water conditions, 5) under cyclic humidity conditions, the slope of the moisture content - swelling strain seems to decrease with successive wetting and drying cycles indicating changes in the structure of the shale, 6) all cracks in the samples were transverse and formed within 72 hours after being placed in a drying chamber, and 7) maximum tensile stresses occur in the beam samples immediately after the samples are placed in a particular humid environment and they decrease as the depth of moisture penetration in the beam increases.

## FINITE ELEMENT ANALYSIS OF FLUID FLOW THROUGH DEFORMABLE POROUS MEDIA

by

Ranbir S. Sandhu  
Department of Civil Engineering  
The Ohio State University  
Columbus, OH 43210

Since the first application of the finite element method to the coupled problem of flow and deformation, considerable progress has been made in the theoretical formulation as well as the computational procedures. Recent advances include variational formulation of the coupled problem allowing for limited smoothness of the finite element bases, experimentation with several different spatial interpolation schemes and investigation of various temporal approximation methods. The finite element method has been applied to soils exhibiting secondary compression, nonlinear soil behavior and finite deformation. Response to dynamic loads and to wave propagation has also been analyzed by this method. Developments in solution procedures include use of integral transforms and boundary integral equation formulations in conjunction with finite element concepts. It had been difficult to reproduce accurately the pore fluid pressure distribution near loaded free-draining boundaries immediately after application of the load. Special elements capable of modeling line singularities have been proposed to overcome this difficulty.

Herein we review the development and the state of the art of use of finite element methods for solution of the coupled problem of fluid flow in deformable porous media under static as well as dynamic loading. Comparative studies of numerical performance of various schemes will be presented. Solution of static as well as dynamic problems will be discussed.

PROBABILISTIC KINETICS OF TIME  
DEPENDENT PLASTIC DEFORMATION AND  
FRACTURE: APPLICATIONS TO METALS AND ROCKS

by

K. Krausz and A.S. Krausz\*  
\*Department of Engineering Management  
University of Ottawa  
Ottawa, Ont. K1N 6N5

The fundamental process of both plastic flow and fracture is the sequence of atomic bond breaking and establishment. In plastic flow each breaking is followed by the establishment of another bond between two atoms not connected previously; crack propagation occurs when the breaking rate is greater than the healing rate. Each step is described rigorously by the rate equation

$$k \propto \exp \left( - \frac{\Delta G}{kT} \right)$$

where  $k$  is the average number of activations,  $k$  is the Boltzmann constant and  $T$  is the temperature. The apparent free energy  $\Delta G$  is the thermal energy of the solid: it is the function of the average atomic vibrational amplitude. Consequently, atomic bond breaking and establishment are controlled by probabilistic processes: plastic constitutive equations and fracture processes must be considered as probabilistic physical phenomena.

It is shown that the rate controlling mechanisms and the microstructure determines  $\Delta G$  defined as

$$\Delta G = \Delta G^\dagger \pm W(\sigma, \text{specimen geometry}),$$

where  $\Delta G^\dagger$  is the atomic bond energy,  $W$  is the mechanical work and its sign is associated with bond breaking and healing respectively. Both  $\Delta G^\dagger$  and  $W$  are functions of the mechanism, the microstructure, and the composition of the material.

The probabilistic physical concepts of flow and fracture are applied to metals and rocks. In doing so the kinetics of the process has to be established: the behavior in one dimensional loading is discussed for selected metals and minerals and the consequences of the probabilistic behavior is emphasized.

ANISOTROPIC FEATURES REQUIRED FOR A MODEL  
TO REPRESENT SHEAR BANDING

by

L. Seaman, Ove Dullum, and Thomas Cooper  
Stanford Research Institute

Shear banding occurs in explosively expanded cylinders, in projectile penetrations, in Taylor tests, and in high-rate machining. We have attempted to simulate the first three types of experiments using constitutive models of varying complexity. Based on the correspondence between the computed results and the experimental observations, we have derived criteria for a suitable constitutive model.

The constitutive models we used were (1) a standard Mises model with isotropic plastic flow, (2) an anisotropic plastic model using the concept of yield on a number of specific planes (like the model of Batdorf and Budiansky [1]), (3) the anisotropic model with thermal softening, and (4) the anisotropic model with shear band processes and damage.

Simulations of exploding cylinders were conducted with models 1, 2, and 3 to determine the orientations and levels of plastic strain throughout the cylinders. For the Mises model, the plastic strain on specific orientations was determined from the equivalent plastic strain using the Reuss relations and the known stresses on any plane. The results showed essentially the same strains throughout the cylinders from all three models.

Two calculations for 4340 steel projectiles penetrating rolled homogeneous armor targets were computed using model 4. The first was an impact at about twice the ballistic limit. After a penetration of about one-third of the target, the computations showed that the front of the projectile was shear banded and that a strip of material in the target adjacent to the penetrator had shear banded. This production of a large plastic region ahead of the projectile is typical of results obtained with a simple Mises model also. In the second computation the projectile was fired at the ballistic limit. With model 4 the projectile was damaged as before, but the shear banding in the target was very different. Here a line of computational cells shear banded directly through the plate, forming a plug. A few other cells in a single layer along the impact face were also shear banded. This computed result matches well the observations. Yet for this case a Mises model would still provide the general yielding behavior noted in the higher velocity impact.

The third type of experiment that we simulated was a Taylor test. In a Taylor test a projectile is fired against a very hard target for the purpose of determining the yield strength of the projectile material. But if the velocity is too high, the projectile can produce shear bands and fragments: in this case it is representative of the behavior of projectiles penetrating

hard targets. Two orientations of shear banding damage are observed:

- \* cone-forming bands that proceed from the outer edge of the plane of impact to the axis, leaving a small cone-shaped pyramid adjacent to the target, and
- \* self-sharpening bands that act to remove outer rings of material and thereby to produce a projectile with a sharp nose.

Simulations were performed with models 2 and 3 to obtain distributions of plastic strains in the projectile near the impact plane. From model 2 the distributions showed the maximum plastic strains near the impact and along the axis. But with thermal softening (model 3) the maximum plastic strains occurred at the outer radius at the impact plane and showed the development of a plane of high distortion along a cone. Thus the thermal softening provided the correct (observed) locations and types of damage and model 2 did not. Thus it appears that the level of capability of the model required for treating shear banding depends on the experiment to be simulated. Any plastic model should be adequate for expanding cylinders and for projectile-target interactions at velocities well above the ballistic limit. Near the ballistic limit, the target must be represented by a model that at least shows an active shear banding process on specific planes. For treatment of the projectile for impacts that will just cause incipient banding, the model must also provide for thermal softening.

- [1] S. B. Batdorf and B. Budiansky, A Mathematical Theory of Plasticity Based on the Concept of Slip, Tech Note No. 1871 of National Advisory Committee for Aeronautics, Washington, April 1949.

## ON RATE DEPENDENT PLASTICITY MODELS\*

by

D. J. Bammann  
Sandia National Laboratories  
Livermore, CA

A rate dependent plasticity theory is developed based upon concepts in classical rate independent plasticity and a simplified model of dislocation motion during plastic deformation. The theory establishes a relationship between the yield surface in stress space and the balance of momentum for dislocations as proposed by Bammann and Aifantis (1). In using the momentum balance for dislocations it is assumed that the motion of a dislocation is controlled by a local internal stress field which determines the acceleration of that dislocation. The effect of the applied stress field on a particular dislocation is determined by the resolved shear stress acting on the glide plane of that dislocation. Motion of the dislocation occurs when this resolved shear stress reaches some critical value determined by the local internal stress field surrounding the dislocation. This local stress field is due to obstacles surrounding the dislocation such as point defects, other dislocations, and grain boundaries when the dislocation begins to be a function of the dislocation velocity. These resultant forces determine the acceleration of the dislocation which in turn manifests itself as macroscopic plastic strain in the body.

Classical rate independent plasticity accounts for hardening through the introduction of internal variables, which control the size and shape of the yield surface. A simple model of combined kinematic and isotropic hardening would include, for example, a scalar variable which defines the size of the yield surface and a tensor variable which defines its location in stress space. The isotropic variable is analogous to the mechanical threshold since no plastic deformation occurs if the applied stress is less than this variable, while the kinematic variable represents the stress field due to dislocations in subgrains or cell walls. The effect of the viscous force on the dislocation is modelled by assuming that the yield surface depends on the plastic part of the velocity gradient since this quantity is proportional to the dislocation velocity. Instead of specifying a constitutive equation for the plastic stretching (symmetric part of the plastic velocity gradient), it is determined through consistency condition which assures that stress state does not lie outside the yield surface. This is equivalent to assuming that the momentum balance of the dislocation is not violated at the microscopic level. The consistency condition yields a non-linear differential equation in the magnitude of the plastic stretching which can be solved under conditions of constant total stretching. Examples are given of the behavior of this model under various loading conditions such as uniaxial tension, creep, and stress relaxation. These results are compared with predictions obtained using the model in which the yield surface depends on the total stretching (2).

\*Work supported by the U.S. Department of Energy under Contract DE-AC04-76DP00789.

References

1. D. J. Bammann and E. C. Alfantis, *Acta Mechanica*, 45, pp. 91-121 (1982).
2. D. J. Bammann and G. C. Johnson, *Proceedings 5th ASCE-EMD Conference, Laramie, WY (1984)*.

## TOWARDS A MECHANICS OF MICROSTRUCTURES

by

Elias C. Aifantis

Dept. of Mechanical Engineering & Engineering Mechanics  
Michigan Technological University  
Houghton, MI 49931

A unifying program for a mechanics of microstructures is outlined. The new physical concept of distinguishing among "normal" and "excited" material states is discussed. Phenomenological models of inelasticity can be generated within this framework and predictive models for the localization of microstructures can be derived. The effect of microstructural patterning on the macroscopic response is evaluated.

by

Dmitry Altshuller  
 Department of Mathematics  
 University of Missouri  
 Columbia, MO 65211

It is customary in engineering calculations to assume that all functions involved in differential equations are Lipschitz continuous. Such an assumption allows us to take for granted that the model equations always have solution, and furthermore, that this solution is unique and continuous. All of the existing numerical methods require that the latter statement be true for them to work.

It has, however, been shown by Viswanathan and Aris (1) that certain chemical reactors are described by a differential equation that fails to satisfy Lipschitz property at some points. An attempt to generalize their results led to the following equation (2):

$$\frac{dv}{dx} = \frac{-F(v)}{f'(v) - \gamma} \quad (1)$$

Here the function  $F(v)$  describes the rate of chemical reaction. We may assume to be continuous and monotonically increasing. The function  $f(v)$  is known as adsorption isotherm. The topological structure of the solutions to the Eq. 1 depends on the properties of this function such as convexity and monotonicity.

If the function  $f(v)$  is monotonically increasing and concave then there can be at most one point where  $f'(v) = \gamma$  and hence at most one point where the equation fails to be Lipschitz. The results of Viswanathan and Aris apply with almost no change. If the function is monotone but not always concave, there may be up to  $n+1$  singular points where  $n$  is a number of the points of inflection (usually one). A detailed analysis of this case is given in (3).

If the function  $f(v)$  is monotone, it is possible to prove that there is at most one continuous solution and that a solution (possibly discontinuous at some points) always exists provided that an additional boundary condition is specified. We can also develop the criteria for existence of continuous solution. The right-hand side of the Eq. 1 being Lipschitz on the interval under consideration is a necessary but not sufficient condition for the latter.

If the function  $f(v)$  is not monotone then we will show that even imposition of the additional boundary condition will not rectify the situation: the equation can still have more than one solution. More importantly, the multiplicity occurs even for the conventional fixed-bed reactor ( $\gamma = 0$ ). We will examine the structure and possibly the stability of these solutions.

It is also important to mention that  $f(v)$  is not monotone, the equation remains singular even when diffusion is present in the reactor. The equation then takes the form

$$\frac{d^2 v}{dx^2} + \frac{kf''(v) - f'(v) - \gamma}{kf'(v)} \frac{dv}{dx} - \frac{\mu}{kf'(v)} F(v) = 0 \quad (2)$$

The eq. 2 fails to meet Lipschitz condition whenever  $f'(v) = 0$ . If  $f(v)$  is monotone, this never happens. The behavior of the eq. 2 can be understood using the phase plane. This will allow us to establish criteria for existence, uniqueness and continuity of the solutions for this equation.

These examples indicate that singular differential equations actually occur in applications thus showing how indispensable theoretical analysis is and how important the development of new methods is even now when computers are penetrating very deeply in all areas of engineering science.

#### REFERENCES

- [1] Viswanathan, S. and Aris, R., "An Analysis of the Counter-Current Moving Bed Reactor", SIAM-AMS Proceedings, Vol. 8, 1974, pp. 99-124.
- [2] Altshuller, D., "Design Equations and Transient Behavior of the Counter-Current Moving Bed Chromatographic Reactor", Chem. Eng. Commun., Vol. 19, 1983, pp. 363-375.
- [3] Altshuller, D., "Problems in the Design of the Countercurrent Moving Bed Catalytic Reactor: A Geometric Approach", in Chemical and Catalytic Reactor Modeling, M. P. Dudukovic and P. L. Mills, eds., ACS Symposium Series, 1984.

ELECTRIC POLARIZABILITIES OF NOBLE GAS ATOMS AND e-NOBLE-GAS-ATOM  
SCATTERING LENGTHS BY ELECTRON CYCLOTRON RESONANCE SPECTROSCOPY

by

A. P. Kabilan  
Department of Physics  
College of Engineering  
Anna University  
Madras 600 025, India

The ECR-spectroscopy technique consists in computer simulation of experimental electron cyclotron resonance (ECR) absorption spectrum on the basis of the well known integrals of the kinetic theory for ECR-absorption intensity and electron energy distribution function  $f(\epsilon)$ . The energy dependence of momentum-transfer cross section  $\sigma_M(\epsilon)$  in these integrals was expressed by the low-energy partial-wave expansion, and the phaseshifts in this expansion were represented by the modified effective range theory (MERT) expressions.

$$\eta_0/q = -A - 0.2839 \alpha \epsilon^{1/2} - 0.0490 A \alpha \epsilon \ln \epsilon + B \epsilon \quad (1)$$

$$\eta_1/q = 0.05679 \alpha \epsilon^{1/2} - 0.07353 C \epsilon \quad (2)$$

$$\eta_L/q = 0.8517 \alpha \epsilon^{1/2} / [(2L+3)(2L+1)(2L-1)] \quad (3)$$

for  $L = 2, 3, 4$

where  $q = (2m\epsilon)^{1/2}/\hbar$  is the de Broglie wave number of electron in units of  $a_0^{-1}$ ;  $a_0$  is the Bohr radius;  $m$  is the electronic mass. The scattering length  $A$  is expressed in units of  $a_0$ , the polarizability and the parameters  $B$  and  $C$  in units of  $a_0^3$ . The electron energy  $\epsilon$  is given in eV.

The continuous ECR spectra in the five noble gases were obtained by employing a slow magnetic scanning and simultaneously integrating the detected X-band microwave pulses of 1  $\mu$ s duration that interacted with the afterglow at a selected time after the discharge pulse end. The experimental conditions were chosen so that the electrons in the transient afterglow had relaxed to the neutral temperature (300°K) before interaction with the sensing microwave and their energy distribution was predominantly within 0.1 eV during the resonance heating by microwaves. For energies less than 0.1 eV, as follows from Eqs. (1) and (2), the S- and P-wave phaseshifts are not very sensitive to parameters  $B$  and  $C$  respectively. Hence the values for these parameters were adopted from previous experiments of cross section measurements. Thus the simulation procedure reduced to two-parameter ( $\alpha$  and  $A$ ) fitting of the MERT formulas (1)-(3) so that the corresponding  $\sigma_M(\epsilon)$  and  $f(\epsilon)$  ensured the agreement between the experimental and simulative ECR spectra with the required precision. The optimum values for the parameters  $\alpha$  and  $A$  that yielded the best suitable simulative ECR spectra for the five rare gases are given below.

Atom		He	Ne	Ar	Kr	Xe
Parameter						
Electric Polarizability	$\alpha [a_0^3]$	1.41	2.73	11.2	17.0	27.5
Scattering Length	$A [a_0]$	1.17	0.205	-1.56	-3.40	-6.30

## CORROSION DUE TO ACID RAIN

by

S. A. Blair and R. D. Sisson, Jr.  
Materials Engineering Laboratories  
Mechanical Engineering Department  
Worcester Polytechnic Institute  
Worcester, Massachusetts 01609

A study of the effects of acid precipitation on electrical connector alloys has been conducted. Accelerated laboratory corrosion tests employing elevated temperatures and selectively modified solution chemistries have been used. Standard corrosion testing procedures using corrosion coupons, galvanic couples and anodic polarization measurements were conducted.

The results of this investigation are reported with special emphases on the effects of the chemistry of acid rain on corrosion phenomena and the accelerated corrosion rates due to acid rain.

PROPAGATION OF DISCONTINUITIES IN A HOT RELATIVISTIC  
PLASMA IN INTENSE MAGNETIC FIELDS

by

H. N. Singh  
Department of Mathematics  
U.N. Post Graduate School  
Padrauna, Deoria (U.P.), India

The relativistic theory of nonlinear wave propagation has been developed to meet the needs of modern scientists due to recent advances in space technology and astrophysics. The growth of discontinuities in a very hot relativistic plasma at temperatures of 10K or above in intense magnetic fields has been studied. The effects of radiation pressure and radiation energy density have been taken into account, while the profiles structured by the radiant heat transfer are assumed to be embedded in the discontinuities. The modes of propagation of weak MHD waves have been determined. The fundamental growth equation governing the growth and decay of weak wave fronts propagating into a hot relativistic plasma in presence of transverse magnetic fields has been obtained and solved. The relativistic results are found to be in full agreement with the earlier results of classical magnetohydrodynamics in the Newtonian limit. The curvature effects on the global behavior of wave amplitude have been investigated and a finite time is determined for the formation of caustics due to focusing. The problem of the breakdown of weak waves and the consequent formation of shock waves has also been completely solved and a finite critical time  $t_c$  is determined when a weak wave will terminate into a shock wave due to nonlinear steepening. The critical amplitude of the initial wave has been determined such that any compressive wave with an initial amplitude greater than the critical one always develops into a shock wave, while an initial amplitude less than the critical one results in a decay of the wave. The relativistic, magnetic and radiation effects on the global behavior of weak discontinuities have also been investigated and illustrated graphically. Special cases have been discussed and it has been found that the relativistic and magnetic effects delay the shock formation whereas the radiation effect accelerates it.

ON THE BEHAVIOR AND STABILITY OF SOLUTIONS TO A  
MODEL OF NUCLEAR FLUID

by

Salvatore Rionero  
Dipartimento di Matematica e Applicazioni  
"R. Caccioppoli", Mezzocannone, 8  
80134 Napoli, Italy

As is well known, the study of the absorption of  $\gamma$ -rays by nuclei has shown that the photoabsorption cross section is characterized by a strong peak or giant dipole resonance (G.D.R.) that is a common feature in all but the lightest nuclei [1,2,3,4].

The discovery of the G.D.R. in nuclei has led to the understanding that nuclei exhibit prominent collective motion and that the G.D.R. is an excellent example of such motion. In order to describe the G.D.R., models are to be proposed in which the nucleus is considered as being composed of two kinds of fluids, a proton fluid and a neutron fluid and - in the linear case - estimates of the G.D.R. energies as function of mass number have been found [5,6,7].

In this paper the behavior and stability of solutions to some models of nuclear fluid are studied and - both in the linear and nonlinear case - estimates of the G.D.R. energies are found.

REFERENCES

- [1] Levinger, J. S., Nuclear Photodisintegration, Oxford University Press, London, 1960.
- [2] Fuller, E. G., Haywood, E., "Nuclear Reactions", Vol. 2, North Holland, 1962.
- [3] Danos, M., Fuller, G., Annual Review of Nuclear Science, Vol. 15, 1965.
- [4] Spicer, B. M., "The Giant Dipole Resonance", Advances in Nuclear Physics, Plenum Press, Vol. 2, 1969.
- [5] Steinwedel, H., Jensen, J. H., Naturforsch, Z., 5a, 1950, p. 413.
- [6] Wiczorek, R., Hasse, R. W., Sussman, G., "Third Symposium of the Physics and Chemistry of Fission", Rochester, NY, 1973.
- [7] Auerbach, N., Yevrechyahu, A., "Nuclear Viscosity and Widths of Giant Resonance", Annals of Physics 95, 1975, pp. 35-52.

STATISTICAL EVALUATION OF SUPERPLASTICIZED CONCRETE BEHAVIOUR  
BY MEANS OF A MICROCOMPUTER

by

G. Corradini, G. Scoccia, R. Volpe  
Istituto di Chimica Applicata e Industriale  
Facoltà di Ingegneria, Università dell'Aquila  
Italy

The statistical approach is an interesting methodology both for the evaluation of superplasticized concrete behaviour and for the construction of mathematical models which describe it. In fact statistically the minimum number of tests required to obtain significant results at the desired levels of reliability may be rationally programmed. One may also determine whether a given factor influences or not a given property, whether interactions among the various factors exist, and finally one may determine the best mathematical model to describe a given behaviour.

A description of the methodology used and the results obtained in the evaluation of the rheological-mechanical behaviour of a superplasticized concrete is reported.

Research was conducted according to the following phases:

- i - choice of factors which influence the main properties of the concrete and definition of number of experimental tests to be carried out.
- ii - Evaluation of the effects of the factors and confidence analysis of the estimate.
- iii - Construction of concrete behaviour mathematical models and choice of the best model.

In particular, the models of the rheological-mechanical behaviour of a superplasticized concrete were found.

The obtained models are extremely simple and can be easily introduced in more complex mathematical models for the technical-economic optimization of the "placed concrete" productive system.

REACTOR ANALYSIS AND OPTIMIZATION  
USING NON LINEAR PROGRAMMING

by

Pablo A. Longoria Treviño  
Simulation Systems Manager  
Research & Development Division  
HYL Steel Technology  
Monterrey, N.L.  
México

and

Kenneth A. Van Wormer  
Professor  
Chemical Engineering Dept.  
Tufts University  
Boston, Mass.  
U.S.A.

This paper shows the application of the Wilson-Han-Powell NLP Optimization Technique to the Modeling and Analysis of Reacting Systems. The reactor design and optimization problem is formulated as one of non linear programming with constraints. The differential equation representing the material and energy balance of the system constitute the set of constraints.

Using an appropriate numerical technique, the constraints are transformed into a system of algebraic equations which constitutes the NLP problem to be solved by The Powell Algorithm. The results obtained using the present approach to simulate the system A B C show that this new way to formulate the design and optimization of chemical reactors has great potential in the solution of problems involving :

- Split boundary conditions
- Estimation of kinetic parameters
- Fitting model parameters to experimental data

References:

Han S. P., "Superlinearly Convergent Variable Metric Algorithm for General Nonlinear Programming Problems", Mathematical programming 11, p. 263-282 North-Holland Publishing Co. (1976).

Han S. P., "A Globally Convergent Method for Nonlinear Programming", Journal of Optimization Theory and Applications Vol. 22, No. 3 p. 297, July (1977).

Powell M. J. D. "Algorithm for Nonlinear Constraints That Use Lagrangian Functions", Ninth International Symposium on Mathematical Programming, Budapest, (1976).

Powell M. J. D., "A Fast Algorithm for Nonlinearly Constrained Optimization Calculations", 1977 Dundee Conference on Numerical Analysis, (1977).

Powell M. J. D., "The Convergence of Variable Metric Methods for Nonlinearly Constrained Optimization Calculations", Nonlinear Programming 3, edited by: Mangasarian, Meyer y Robinson, Medison Winsconsin, (1978).

Wilson R. B., "A Simplicial Algorithm for Concave Programming", Doctoral Thesis, Harvard University, Cambridge Mass., (1963).

## STRENGTH AND DEFORMATION BEHAVIOR OF T-SHAPED RC SHORT COLUMNS

by

Cheng-tzu Thomas Hsu and Tony Nader  
Department of Civil and Environmental Eng.  
New Jersey Institute of Technology  
Newark, New Jersey

The elastic and inelastic strength and deformation behavior of T-shaped Reinforced concrete columns has been a constant concern for a structural engineer to design a safe and economic structure in modern buildings. The research studies herein will report both analytical and experimental investigations of T-shaped reinforced concrete short columns under combined biaxial bending and axial compression. The analysis and experimental results of the present study can be found useful for the limit analysis and design of reinforced concrete structures.

A numerical and computer analysis was developed to calculate the strain, strength, and curvature for any arbitrary structural concrete cross-sections under axial load combined with biaxial flexure. Based on this analysis, a complete biaxial moment-curvature curve and a complete load-deflection curve can be obtained from zero load up to the maximum moment capacity of the section. To compare with the above analysis results, nine one quarter scale direct models of the short, tied columns with T-shaped cross-section were constructed for the present study. All the specimens were tested and loaded by a combination of biaxial bending and axial compression. Their end conditions were assumed to be pinned-ended. The columns were tested in the horizontal position and were loaded using Enerpac 100-ton capacity hydraulic cylinder ram. From the pressure readings the loads can be calculated. The measurements of strains and curvatures were done by the demec gage method. The demec points were placed on the concrete surface around the mid-span of the column, about 6-in. apart for each pair. A minimum of four pairs of demec points were used in x- or y-direction. The strain was calculated from measured deformation, between a pair of demec points, divided by the distance between these two points. The curvature can then be calculated from the strain distribution across the cross section in x- or y-direction. The resulting experimental moment-curvature and load-deflection curves were compared with the above computer analysis, a satisfactory agreement was found through all load stages from zero load up to the maximum moment capacity of the column cross-section.

The present study concludes that an analytical model developed can simulate the moment-curvature behavior of T-shaped reinforced concrete columns subject to axial compression and biaxial flexure; this information can also be used to calculate the load-deflection curves and study the ductility behavior of concrete structures.

by

Peter Nwoye O. Mbaeyi  
Division of Theoretical Chemistry  
University of Tuebingen  
D-7400 Tuebingen 1  
Federal Republic of Germany

This contribution introduces, amongst others, the concept of diffusional force in the classical context of theoretical mechanics. In many problems of practical importance - crystal nucleations, reactors (bio)membrane filtration processes, solid state chemistry, (material) phase transitions, etc. - the process designated diffusion is usually one of the key influence factors, and assumes largely the role of dissipative distributor agent. In biological processes, this same process is not only an agent of distribution, but also one of accumulation, e.g. chemical energy conservation (especially through (bio)membrane energy transduction processes), memory processes on molecular chemical bases. Therefore, in employing the classical definition of diffusion (see Shewmon, *Diffusion in Solids*, 1963), it has become necessary to introduce the concept of negative diffusion, e.g. for crystallization problems (Murray, Tuebingen seminar lecture 1978, Div. of Theor. Chemistry); this procedure is not without controversies.

For purposes of quantized field models of energy-matter aggregations, it is crucial to re-investigate the problem of motions of ensembles from new perspectives; this development leads to a definition of diffusional force. Imbedded in this result is the fact that the classical definition of diffusion is a special case, and that the classical diffusion coefficient is a function of some vectorial quantities. Therefore, in this wider concept, orientation reversal is a natural consequence, and does away with the need for the extra artifact of negative diffusion. Other results include characterizations of types of diffusional distributions, a conjecture on the onset of nucleus formation for crystallization processes. Besides showing how these relate to classical diffusion concept, a sketch is given of the special conditions for transitions to Einstein-Smoluchowski-Uhlenbeck diffusions (derivations of diffusion coefficients in terms of mechanical molecular properties). All developments are constructive and use only elementary infinitesimal calculus.

NOVAL PRESSURE SENSOR FROM ANACARDIUM  
OSCIDENTYLE LATEX

by

K.S. Sivanandan  
Regional Engineering College, Calicut  
Electrical Engineering  
Calicut - Kerala - South India - India

This paper deals with a noval method for the development of a capacitive pressure transducer using the latex of anacardium - oscidentyle - a plant which is growing abundantly in various parts of the world. When boiled with a high elastic material at high temperature conditions, this natural polymer has behaved as a dielectric material which can be used as a high sensitive capacitive pressure sensor. The capacitance change has been dependent on the simultaneous variation of two transduction quantities viz: the thickness of the material and the dielectric constant E. The paper deals with the following characteristic performance studies.

1. Pressure  $V_s$  Output Voltage
2. Pressure  $V_s$  thickness
3. Pressure  $V_s$  dielectric constant E

A proto type model of the sensor has been developed and tested for various pressure changes.

The method is simple, precise and very sensitive to input variations ranging from low to high values of pressure.

PROMISING ELECTRICAL PROPERTIES OF ANACARDIUM - OSCIDENTYLE  
LATEX - NEOPRINE MIXTURE FOR CAPACITIVE SENSORS

by

K.S. Sivanandan  
Regional Engineering College, Calicut  
Electrical Engineering  
Calicut - Kerala - South India - India

This paper deals with the electrical properties of a new dielectric material prepared by heating Anacardium Oscidentyle Latex to a high temperature and pouring this to a foamy synthetic polymer and allowing the material to cool at natural conditions to room temperature.

Under the influence of an alternating-electric field it is found that the dielectric material is sensitive to pressure variations, i.e., the dielectric properties (namely dielectric constant  $E$ ) vary substantially with respect to pressure the amplitude and frequency of the applied electric field has a direct influence over the dielectric property ( $E$ ).

At high frequencies, i.e., in the order of megahertz the dielectric properties have been very sensitive to pressure changes and this makes it an effective capacitive pressure sensor in instrumentation field.

The variation of ( $E$ ) based on frequency variation was very marked, (above kilo-Hertz frequency region under the application of a constant pressure and field voltage) and therefore, it may find application as frequency sensing device.

Anacardium Oscidentyle is a commonly seen plant in almost all parts of the world, and its availability may not be a serious problem at all.

## A DAMAGE MODEL FOR CONTINUOUS FIBER COMPOSITES

by

D.H. Allen  
S.E. Groves  
Aerospace Engineering Department

and

R.A. Schapery  
Civil Engineering Department  
Texas A&M University  
College Station, TX 77843

It is now well known that ultimate failure of continuous fiber composite components is preceded by a sequence of microstructural events such as microvoid growth, transverse cracking, fiber-matrix debonding, interlaminar cracking, edge delamination, and fiber fracture which are all loosely termed damage. The significance of this damage lies in the fact that numerous global material properties such as stiffness and residual strength may be substantially altered during the life of the component.

A continuum mechanics approach is utilized herein to develop a model for predicting the thermomechanical constitution of continuous fiber composites subjected to both monotonic and cyclic fatigue loading. In this method damage is hypothesized to be characterized by a set of vector valued internal state variables representing locally averaged measures of matrix microvoids, transverse cracks, interlaminar delaminations, and fiber-matrix debonds. Utilization of the thermodynamics with internal state variables leads to constraints on the allowable form of constitutive relations. It is shown in the process that if the medium is initially elastic, the J-integral may be utilized to construct a quasi free energy which leads to stress-strain relations with damage. These relations are then simplified utilizing an irreducible integrity basis for transversely isotropic media.

The resulting local constitutive relations are utilized in a laminate stiffness formulation in order to construct equations useful for experimental comparison. It is shown in this process that numerous experimentally determined parameters are required in order to characterize the model.

Finally, internal state variable growth laws are proposed for microvoids and transverse cracks and the model is compared to results obtained for a  $[0/90]_s$  laminate with transverse cracks.

It is concluded that although the model requires further development and extensive experimental verification, it may be a useful tool in characterizing the constitutive behavior of continuous fiber composites with damage.

A SIMPLIFIED ANALYSIS OF PLY CRACKING  
IN COMPOSITE LAMINATES

by

H. Thomas Hahn  
Washington University  
Department of Mechanical Engineering  
and Materials Research Laboratory  
St. Louis, MO 63130

Ply cracking is one of the most frequently observed subcritical failure modes in composite laminates. Although much work has been done in this area, no solutions are available which can be readily used. The purpose of this paper is to provide a simple solution in closed form at the sacrifice of rigor. Yet the solution is shown to be in good agreement with experimental data.

The approach is based on the existence of an inherent crack in plies and an improved shear lag analysis. As an example,  $[0_n/90_n]_s$  laminates are treated. The inherent crack is in the  $90^\circ$  plies partially through the width. The energy release rate associated with the growth of this crack is then independent of the crack length and is simply equal to the energy difference between the initial and the final fully crack state [1]. The problem thus becomes amenable to the two-dimensional analysis, and a kinematically admissible displacement field can be judiciously chosen to provide a solution for the energy release rate. Once the first cracking is done, the subsequent cracking can be predicted similarly and the accompanying stiffness change estimated.

A good correlation is shown between the analytical results and experimental data on glass/epoxy and graphite/epoxy composites. The effect of residual stresses is also discussed.

- [1] Hahn, H. T. and Johannesson, T., "Fracture of Unidirectional Composites: Theory and Applications," AMD Vol. 58, G. J. Dvorak, Ed., ASME, 1983, pp. 135-142.

AD-A171 026

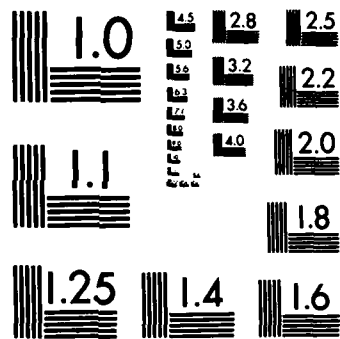
ABSTRACTS 21ST ANNUAL MEETING SOCIETY OF ENGINEERING  
SCIENCE INC OCTOBER 1-7 (U) VIRGINIA POLYTECHNIC INST  
BLACKSBURG D FREDERICK ET AL. 1984 ARO-21008 EG-CF  
DAGC29-84-M-0119 F/C 5/2

3/6

UNCLASSIFIED

ML

\*\*\*



MICROCOPY RESOLUTION TEST CHART  
NATIONAL BUREAU OF STANDARDS-1963-A

DAMAGE DEVELOPMENT IN COMPOSITE MATERIALS  
UNDER LONG-TERM LOADING

by

W. W. Stinchcomb  
Materials Response Group  
Engineering Science and Mechanics Department  
Virginia Polytechnic Institute and State University  
Blacksburg, VA 24061-4899

During the life of composite structures, numerous micro-damage events occur and interact to progressively change the strength, stiffness, and life of the structures. The unique and distinctive features of damage in composite materials, as compared to metals for example, require that special concepts, based on an understanding of the progressive damage development process, be introduced into damage accumulation philosophies and models if damage assessment is to provide the basis for reliable predictions of residual strength and remaining life.

Cumulative damage affects the response of a composite structure in a way dependent on the loading history. Predictions of long-term behavior of composites are particularly important to insure reliable performance of a structure throughout its service life. In most cases, design for a ten year service life must be based on representative data collected over a much shorter time period and must account for damage induced by cyclic loads (fatigue damage), sustained loads (creep damage), and environmental conditions (thermal, moisture, radiation damage). Over the past ten years, a number of attempts have been made to develop accelerated test methods to study long-term behavior. Although these attempts have met with limited success in some cases, they have one common, major weakness -- they fail to account for the effect of the accelerated parameter on damage growth rates and failure modes. If stress is the accelerating parameter, the amount and distribution of damage which accumulates in composite laminates is a function of the cyclic stress level and the number of stress cycles. The fracture modes of

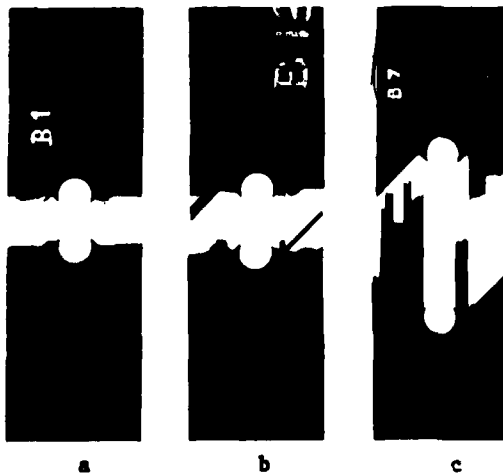


Fig. 1. Failure modes in notched laminates:  
(a) monotonic tension;  
(b) residual tensile failure after  $2 \times 10^5$  cycles,  $\sigma_{\max} = 0.8 \sigma_{\text{frac}}$ ,  $\sigma_{\text{res}} = 1.4 \sigma_{\text{frac}}$ ;  
(c) fatigue failure,  $2.2 \times 10^5$  cycles,  $\sigma_{\max} = 0.8 \sigma_{\text{frac}}$ .

these laminates with short and long fatigue lives are notably different (Fig. 1).

Center notched, [+45,90,-45,0]<sub>g</sub> graphite epoxy laminates failed due to monotonically increasing tensile loads at a mean applied stress of 36.4 ksi. The hole related damage followed a sequence of matrix cracks in off-axis plies (initiating at an applied stress of 50 percent of the mean tensile strength) and delamination of the 45/90 and 90/-45 interfaces (initiating over the stress range between 60 and 80 percent of the mean tensile strength). The fracture surfaces were predominantly perpendicular to the load direction and extended along the horizontal axis of the hole. The influence of the pre-fracture matrix cracking and delamination can be seen in Fig. 1(a) as an irregular fracture surface near the hole.

Specimens subjected to cyclic loading at  $\sigma_{\max} = 0.7 \sigma_{\text{frac}}$  (R=0.1) survived  $10^6$  cycles. The amount and extent of early matrix cracking and delamination after 100 cycles were comparable to the damage in monotonically loaded specimens at  $0.7 \sigma_{\text{frac}}$ . As cyclic loading continued, the matrix cracks in all plies extended away from the hole and the delaminations grew. By  $10^6$  cycles, the matrix cracks in the 45 degree plies extended to the edge of the specimen, cracks in the zero degree plies were two hole diameters long, and delaminations appeared on all ply interfaces. The residual tensile strength measured after  $10^6$  cycles was 135 percent of the initial tensile strength.

Cyclic loading at a higher stress level ( $\sigma_{\max} = 0.95 \sigma_{\text{frac}}$ , R = 0.1) introduced the same damage modes (matrix cracking and delamination) which appeared at the lower stress level. However, the damage appeared earlier in the cyclic lifetime and accumulated at a faster rate. After 10 cycles at the higher stress level, the amount and extent of matrix cracking were similar to that in specimens cycled at the lower stress level after  $10^4$  cycles, although the delaminations were much less developed after 10 cycles at the 95 percent stress level. The damage pattern, including matrix cracks and delaminations, after  $10^4$  cycles at the high stress level resembled the damage pattern after  $10^6$  cycles at the low stress level. Interestingly, an additional  $10^4$  cycles at the high stress level ( $2 \times 10^4$  total cycles) reduced the strength of the laminate and caused failure, a characteristic of the accelerated damage rates at the higher stress levels.

The results discussed in this paper indicate that there is some correlation between high stress-short life behavior and low stress-long life behavior. However, careful consideration must be given to the damage modes, the damage states, the rates of damage development, and the attendant response if predictions of long-term behavior are to be reliable.

## STUDY OF DAMAGE MECHANISMS IN TRANSPARENT FIBROUS COMPOSITES

by

I. M. Daniel

Department of Mechanical and Aerospace Engineering  
Illinois Institute of Technology  
Chicago, IL 60616

H. C. Soo

China Steel Corporation  
Kaohsiung, Taiwan

Damage mechanisms and damage accumulation in composites have been studied by a variety of methods, including edge replication techniques, ultrasonic scanning, and X-radiography. Each method is best suited for detecting certain types of flaws and results from one method often complement those from another method.

In recent years transparent birefringent fibrous composites have been produced as realistic models of prototype composites for use in anisotropic photoelastic stress analysis [1,2]. These materials are glass-fiber reinforced plastics with the matrix and the fibers having the same index of refraction. They can be made in any desired layup to simulate the inhomogeneity and anisotropy of opaque composites such as graphite/epoxy. The property of transparency makes them ideal for observing failure mechanisms such as matrix cracking and delamination without the need of any special setup or instrumentation. Furthermore, the ability to detect and characterize flaws optically can serve to set standards for calibration of conventional nondestructive evaluation instrumentation such as ultrasonics.

The material investigated was an E-glass/epoxy incorporating type 1062 glass roving impregnated with Maraset 658/558 epoxy resin. The following unidirectional and multidirectional laminates were studied under quasi-static and cyclic loading conditions:  $[0_8]$ ,  $[90_8]$ ,  $[0/90]_{2s}$ ,  $[90/0]_{2s}$ ,  $[\pm 45]_{2s}$ ,  $[0/\pm 45/90]$ , and  $[90/\pm 45/0]$ . Stress-strain curves to failure were obtained for quasi-static loading and visible failure mechanisms were photographed at various loads. Cyclic tensile tests were also conducted and S-N curves obtained. Visible failure mechanisms were photographed at various numbers of cycles up to failure.

Under static loading the unidirectional specimens did not show any visible damage until very near failure. The  $[0/90]_{2s}$  laminate shows gradually increasing transverse cracking up to failure, corresponding to the measured stiffness reductions. At failure there is evidence of longitudinal cracking localized along some fiber bundles. The  $[90/0]_{2s}$  laminate behaves similarly, except that at failure longitudinal cracking is distributed over a small area near the failure section. The  $[0/\pm 45/90]$  laminate shows gradually increasing transverse cracking with more short cracks near the edges. Cracking increases in a somewhat discontinuous fashion. Many cracks are not continuous across the width of the specimen. At high loads small areas of edge delamination appear. At failure there is extensive and distributed longitudinal cracking and delamination in the

failed region. The behavior is similar in the  $[90/\pm 45/0]$  laminate with no evidence of edge delamination until failure. Longitudinal cracking at failure is more limited.

Under cyclic loading the  $[90]_8$  specimen shows no visible cracking before failure. The  $[0/90]_8$  shows increasing transverse cracking preceding and accompanying failure. The  $[\pm 45]_2$  laminate shows extensive but localized cracking along the fibers<sub>2</sub> with necking prior to failure. The  $[0/\pm 45/90]_8$  laminate shows gradually increasing transverse cracking starting from the edges towards the interior. Edge delaminations also grow and propagate towards the interior until they encompass the entire width of the specimen prior to failure. Cracking along the  $\pm 45$ -deg fibers appears in the later stages of fatigue life. The  $[90/\pm 45/0]_8$  laminate shows similar behavior with delamination encompassing the entire specimen prior to failure.

The damage mechanisms above were compared with those detected in similar graphite/epoxy laminates by means of X-radiography.

#### References

1. Daniel, I. M., Niro, T., and Koller, G. M., "Development of Orthotropic Birefringent Materials for Photoelastic Stress Analysis," NASA CR-165709, May 1981.
2. Daniel, I. M., Koller, G. M., and Niro, T., "Development and Characterization of Orthotropic Birefringent Materials," to be published in Experimental Mechanics, 1984.

A DAMAGE TOLERANT DESIGN PARAMETER  
FOR GRAPHITE/EPOXY LAMINATED COMPOSITES

by

C. E. Harris\* and D. H. Morris  
Department of Engineering Science and Mechanics  
Virginia Polytechnic Institute and State University  
Blacksburg, Virginia 24061

The results of an extensive experimental investigation of the fracture behavior of notched graphite/epoxy T300/5208 laminates are presented. Twenty seven laminates with different stacking sequences and thicknesses have been studied. The data suggest that a damage tolerant design parameter exists which is relatively independent of ply stacking sequence and thickness.

The mean value of the design parameter (fracture toughness) computed from 113 tests was  $28.52 \text{ Ksi}\sqrt{\text{in}}$ . All data were within a  $3\sigma$  deviation of the mean value. The design parameter was the value of fracture toughness defined as the linear elastic fracture mechanics stress intensity factor at the load where the 5% offset from the initial load-crack opening displacement slope intercepted the load-COD record. This design parameter was interpreted to be the fracture toughness at the onset of significant notch-tip damage.

---

\* Current Address: Department of Aerospace Engineering, Texas  
A&M University, College Station, TX 77843

EFFECT OF FRICTION AND GAPS ON THE STRENGTH OF  
MECHANICAL JOINTS IN COMPOSITES

by

E. Nweke, N. Kikuchi, R. A. Scott  
Department of Mechanical Engineering and Applied Mechanics  
University of Michigan  
Ann Arbor, Michigan 48109

Recently Chang, Scott and Springer [see (1)], addressed analytically and experimentally the failure strength and mode of mechanically fastened laminated composites. In the analysis, classical plate lamination theory was used together with a finite element simulation. An exhaustive series of tests were performed on a T300/1034-C graphite-epoxy composite and on the whole, reasonable accuracy (to within, at worst, 40%) was found. However, some important issues still need to be addressed. In their work on a row of holes in series, the bolt-hole radial stress distribution was taken to follow a cosine distribution and the contact zone was assumed known in advance. For this case, and the case of a series of holes in parallel, friction was ignored. Moreover the possibility of gaps was not considered. These effects are explored in the present work.

Here stresses are evaluated using classical plate-lamination theory and finite element modelling. The Yamada-Sun failure criterion is adopted, which states that failure occurs when the stresses satisfy

$$\left(\frac{\sigma_{x'}}{X_c}\right)^2 + \left(\frac{\tau_{x'y'}}{S_c}\right)^2 = e^2 \quad \begin{array}{l} e \geq 1 \rightarrow \text{failure} \\ e < 1 \rightarrow \text{no failure} \end{array}$$

where:  $x', y'$  are coordinates along and perpendicular to the ply, respectively (see Fig. 1).  $\sigma_{x'}$  is longitudinal stress,  $\tau_{x'y'}$  is shear stress,  $X_c$  is the longitudinal strength of a lamina,  $S_c$  is the shear strength of a cross-ply laminate of the same thickness. An issue is where the stresses used in the failure criterion are calculated. Chang et al. introduced a so-called characteristic curve given by (see Fig. 1).

$$r_c = D/2 + R_{ot} + (R_{oc} - R_{ot}) \cos \theta, \quad -\pi/2 \leq \theta \leq \pi/2$$

where:  $D$  is the diameter of the hole,  $R_{ot}$  is the characteristic length in tension,  $R_{oc}$  is the characteristic length in compression.

The stresses are calculated at selected points on the characteristic curve and  $P$  is increased until  $e = 1$ . The failure mode is given by:  $|\theta| < 15^\circ \rightarrow$  bearing mode failure;  $30^\circ < |\theta| < 60^\circ \rightarrow$  shear out mode failure;  $75^\circ < |\theta| < 90^\circ \rightarrow$  tension mode failure.

If  $\psi(x, y)$  and  $\phi(x, y)$  are the surface functions for the pin and the hole respectively, the inward normal to the pin surface is given by:

$$N = N_\alpha \vec{i}_\alpha = \frac{1}{|\nabla_\alpha \psi|} \left( \frac{\partial \psi}{\partial x} \vec{i} + \frac{\partial \psi}{\partial y} \vec{j} \right)$$

Then a gap function is specified

$$\vec{g} = \frac{\phi - \psi}{|\nabla \alpha \psi|} \left( \frac{\partial \psi}{\partial x} \vec{i} + \frac{\partial \psi}{\partial y} \vec{j} \right)$$

Then the contact boundary conditions are:

$$U_n - g_n \leq 0 \text{ (contact)}, \sigma_n \leq 0, \sigma_n (U_n - g_n) = 0$$

$$|\vec{\sigma}_t| < -\mu \sigma_n \text{ then } \Delta \vec{U}_t = 0 \text{ (no sliding)}$$

$$|\vec{\sigma}_t| = -\mu \sigma_n \text{ then for some } \lambda \geq 0 \Delta \vec{U}_t = -\lambda \vec{\sigma}_t \text{ (sliding)}$$

In the weak form of the equilibrium equations the normal and tangential stresses are modeled by a penalty method.

$$\sigma_n = \begin{cases} -\frac{1}{\varepsilon} (U_n - g_n) & \text{if } (U_n - g_n) > 0 \\ 0 & \text{if } (U_n - g_n) \leq 0 \end{cases} \quad \sigma_t = \begin{cases} \mu \sigma_n \left( \frac{\Delta \vec{U}_t}{|\Delta \vec{U}_t|} \right) & \text{if } |\Delta \vec{U}_t| > \varepsilon_1 \\ \mu \sigma_n \left( \frac{\Delta \vec{U}_t}{\varepsilon_1} \right) & \text{if } |\Delta \vec{U}_t| \leq \varepsilon_1 \end{cases}$$

Where  $1/\varepsilon$  is a spring constant, and  $\varepsilon_1$  is a displacement parameter that depends on the relative shear moduli of the laminate and the pin.

#### NUMERICAL PROCEDURE

1) The load is set at the force boundary and the stiffness matrix and load vector is constructed and stored, and recalled in subsequent iterations. 2) The stiffness matrix and load vector are modified by the contact boundary conditions. 3) The equation is solved for the displacement vector, and resolved until the displacement vector reaches a stable value. 4) The failure criterion is applied. 5) If the failure parameter has not attained value unity, the applied load is increased by a factor of the reciprocal of the parameter, and steps 1-4 are repeated.

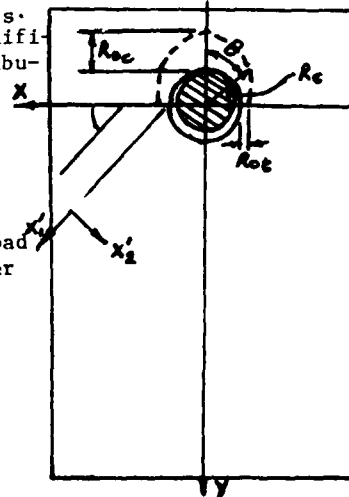
#### CONCLUSIONS

Preliminary results obtained tend to suggest the following for the lay up investigation  $[(90_2/\pm 60/\pm 30)_2]$  and  $[(0/\pm 30/\pm 60)_2]_S$ .

1. The normal stress distribution is significantly different from a cosine load distribution assumed previously even for the frictionless case.
2. Inclusion of friction tends to yield higher failure loads, in particular  $\mu = 0.1$  increases failure load by about 3% for  $[(90_2/\pm 60/\pm 30)_2]_S$ .
3. Gaps tended to increase the failure load for instance gaps of about 10% of diameter increase failure load about 20%.

1. Chang, F. K., Scott, R. A. Springer, G. S., "Design of Composite Laminates Containing Pin Loaded Holes," J. of Composite Materials, May, 1984.

Fig. 1



ONE-DIMENSIONAL AND AXISYMMETRIC BUCKLING  
OF A DELAMINATED PLATE

by

Wan-Lee Yin and Zhizhong Fei  
School of Engineering Science and Mechanics  
Georgia Institute of Technology, Atlanta, Georgia 30332

Delamination of a composite laminate reduces the over-all stiffness and thereby lowers the buckling load of the plate. Along the boundary of delamination, the singular stress distributions associated with elastic postbuckling solutions may initiate delamination growth when the stress intensity factors or the energy-release rates become sufficiently large. Various analyses of the buckling and postbuckling behavior and the growth phenomena of a one-dimensional delamination model have appeared in several recent studies. These were followed by more recent studies of the postbuckling and growth behavior of a circular delamination in an axisymmetrically thrust or bent plate. A crucial result is that, by using the path-independent  $J$ -integral or  $M$ -integral, a simple expression of the energy-release rate can be obtained in terms of the bending moments and the membrane forces acting across the various cross-sections adjacent to the boundary of the delamination.

An analysis of the critical buckling load of a general one-dimensional delamination model was presented in a recent paper [3]. In the present work, we determine the critical buckling loads of a circular plate containing a parallel concentric circular delamination for the cases of clamped and simply-supported edge conditions. Let  $\alpha$  and  $\tau$  denote, respectively, the ratio of the radius and the ratio of the thickness of the delamination vs. the plate, and let  $\kappa^2$  stand for the ratio of critical in-plane compressive load to the bending stiffness of the intact portion of the plate. Then the characteristic equations governing the buckling of the delaminated plate are

$$\frac{Y_1(\kappa/\alpha)}{J_1(\kappa/\alpha)} = \frac{\kappa Y_0(\kappa) - Y_1(\kappa) F(\kappa, \tau)}{\kappa J_0(\kappa) - J_1(\kappa) F(\kappa, \tau)}$$

for the clamped edge condition and

$$\frac{(\kappa/\alpha) Y_0(\kappa/\alpha) - (1 - \nu) Y_1(\kappa/\alpha)}{(\kappa/\alpha) J_0(\kappa/\alpha) - (1 - \nu) J_1(\kappa/\alpha)} = \frac{\kappa Y_0(\kappa) - Y_1(\kappa) F(\kappa, \tau)}{\kappa J_0(\kappa) - J_1(\kappa) F(\kappa, \tau)}$$

for the simply-supported edge condition, where  $\nu$  is the Poisson's ratio,  $J_0$ ,  $J_1$ ,  $Y_0$  and  $Y_1$  are Bessel functions and

$$F(\kappa, \tau) \equiv 6\tau(1-\tau) + \tau^3 \frac{(\kappa/\tau) J_0(\kappa/\tau)}{J_1(\kappa/\tau)} + (1-\tau)^3 \frac{\frac{\kappa}{1-\tau} J_0\left(\frac{\kappa}{1-\tau}\right)}{J_1\left(\frac{\kappa}{1-\tau}\right)}$$

When the critical buckling loads are normalized with respect to the corresponding critical loads of a perfect plate without delamination, the results depend on the normalized radius and thickness ( $\alpha$  and  $\tau$ ) in a way extremely close to the corresponding results of a one-dimensional delamination.

The present authors showed in another paper that if a circular plate containing a thin concentric delamination is subjected to both in-plane compression and bending, then the phenomenon of snap-through replaces the phenomenon of bifurcation from membrane states [4]. In the present work, we study the same phenomenon in a one-dimensional delamination model, and determine the snap-through load for a symmetric one-dimensional delamination of arbitrary thickness.

#### References

- [1] Yin, W.-L. and Wang, J.T.S., "Postbuckling growth of a one-dimensional delamination. Part I: Evaluation of the energy-release rate," Submitted to J. Appl. Mech., 1983.
- [2] Yin, W.-L., "Axisymmetric buckling and growth of a circular delamination in a compressed laminate," Submitted to Int. J. Solids Structures, 1983.
- [3] Simitses, G. J., S. Sallam and Yin, W.-L., "Effect of delamination on axially-loaded laminated plates," Proceedings of AIAA/ASME/ASCE/AHS 25th SDM Conference, Paper 84-0964. Palm Springs, CA., May 1984.
- [4] Fei, Z. and Yin, W.-L., "Postbuckling growth of a circular delamination in a plate under compression and bending," Proceedings of the Southeastern Conference on Theoretical and Applied Mechanics (SECTAM XII), Callaway Gardens, GA., May 1984.

## COMPUTER SIMULATION OF POLYMERIC SYSTEMS\*

by

J. H. Weiner  
Brown University  
Division of Engineering  
Providence, RI 02912

Polymeric solids above the glass-transition temperature are characterized by high atomic mobility. This large-amplitude thermal motion is primarily responsible for the particular characteristics of the thermo-mechanical behavior of these systems. The *computer simulation* of atomistic models provides physical insight into this behavior.

Techniques for the computer simulation of these systems will be described and the results of the simulation for several models will be presented. For some cases, the computer results may be compared with theoretical solutions based on entropic considerations. Good agreement is found for the overall results. In addition, it is found that the computer simulation provides additional dynamic results which are not obtained by the entropic approach.

\*Research supported by the Gas Research Institute and by Brown University's Materials Research Laboratory funded by the National Science Foundation.

## TIME DEPENDENT FAILURE OF CERAMICS

by

Sheldon M. Wiederhorn  
Center for Materials Science  
Inorganic Materials Division  
Washington, DC 20234

Modern structural ceramics are used in applications in which mechanical thermal loading can degrade the strength of these materials as a function of time, resulting in a potential time delay to failure in many applications. Although materials scientists and engineers are aware of the long term susceptibility of ceramic materials to strength degradation, the engineering techniques for addressing the problem are limited. The usual approaches used to improve lifetime include empirically derived safety factors, and fracture mechanics based crack growth theory. The first technique requires extensive practical familiarity with both the design concept and the material used for the design. Although the use of safety factors is an effective method of design, the method usually entails an extensive trial-and-error process to select a satisfactory design for a given material. The application of fracture mechanics based crack growth theory for material design is more efficient than the safety factor method because the theory is deterministic in nature, permitting predictions of lifetime to be made from relatively simple laboratory measurements. For this reason, the fracture mechanics method has been used successfully to design electronic substrates, spacecraft windows, grinding wheels, optical fibers and electronic capacitors. Whereas both the safety factor and the fracture mechanics techniques are useful for predicting structural reliability at ambient temperatures, experience in high temperature applications suggest the need for more effective lifetime prediction techniques at the elevated temperatures. In this paper, we review current techniques of assuring structural reliability, and demonstrate the problems that are encountered with these material at elevated temperatures. An alternate approach to design is suggested. Although probabilistic in nature, the approach also includes the science of fracture mechanics within its framework. Application of the method to structural materials is discussed with regard to high temperature, non-oxide materials currently intended for heat exchangers and heat engine applications.

## FRACTURE KINETICS OF CORROSION FATIGUE

by

K. Krausz and A. S. Krausz  
Faculty of Science & Engineering  
University of Ottawa  
Ottawa, Ontario K1N 6N5  
Canada

Corrosion fatigue results from a complex combination of cyclic loading and corrosion assisted crack growth. It is shown that corrosion cracking under cyclic loading is a thermally activated process that consists of parallel and consecutive combination of transportation, chemical reaction and crack propagation steps. A detailed analysis of the processes by the application of rate theory and fracture kinetics demonstrates the temperature and frequency dependence of corrosion assisted fatigue, in good agreement with experimental results. The full description includes the rebonding effect as well, and the corresponding kinetics is reviewed in the light of tests results published in the literature.

## ON ENVIRONMENTAL FRACTURE

by

Elias C. Aifantis  
Department of Mechanical Engineering & Engineering Mechanics  
Michigan Technological University  
Houghton, MI 49931

A theoretical framework for environmental fracture is given. Emphasis is put on modelling the effects of microstructure and its interaction with the crack tip. Relations for threshold stress intensity factors, crack velocities, and features of the process zone are derived, and comparisons with experiments are made.

A CONUNDRUM APROPOS OF THE STRESS- AND TEMPERATURE-DEPENDENCIES  
OF THE SUBCRITICAL CRACK VELOCITY

by

S. D. Brown  
University of Illinois at Urbana-Champaign  
Department of Ceramic Engineering  
Urbana, IL 61801

and  
M. K. Ferber  
Oak Ridge National Laboratory  
Metals and Ceramics Division  
Oak Ridge, TN 37831

Subcritical cracking in a wide variety of materials is known to involve at least one time-, temperature-, and stress-dependent process. Usually, several different processes act sequentially and/or competitively to propagate a crack. In some cases, sequential processes may assume a cyclic character. Some processes may act competitively to retard crack propagation. And, competitive sets of processes may proceed simultaneously by different mechanisms to propagate separate cracks in the same specimen of material. This paper reviews the multibarrier kinetics of subcritical crack growth, and points out an interesting conundrum apropos of the stress- and temperature-dependencies of the crack velocity in certain widely diverse systems.

The general equation for the subcritical crack velocity (e.g., Refs. 1-7) can be truncated to the following form for simple Region I crack growth:

$$v = C_0(RT/Nh)e^{-\frac{(U_e^\ddagger - b)}{RT}} \left[ 1 - e^{-\frac{\Lambda(K - K^*)}{RT}} \right] \quad (1)$$

Here,  $v$  represents the crack velocity, m/s;  $R$ , the gas constant;  $T$ , the absolute temperature;  $N$ , Avogadro's number;  $h$ , Planck's constant;  $U_e^\ddagger$ , the stress-independent experimental activation energy;  $K$ , the stress intensity factor; and  $K^*$ , the threshold value of  $K$ .  $C_0$ ,  $b$  and  $\Lambda$  are theoretically defined, lumped constants of appropriate dimensions. Ordinarily, the reverse reaction is neglected, reducing Eq. (1) further to

$$v = v_0 e^{-\frac{(U_e^\ddagger - bK)}{RT}}, \quad (2)$$

where  $v_0 = C_0(RT/Nh)$ .

The conundrum arises from experimental data (e.g., Refs. 5,8-11) that seem to imply a substantial stress dependence in the pre-exponential factor,  $v_0$ . Theoretically, there should be none. Possible explanations are discussed.

References:

1. Hillig, W. B. and Charles, R. J., "Surfaces, Stress-Dependent Surface Reactions, and Strength," in High-Strength Materials. Edited by Zackay, V. F., Wiley & Sons, New York, 1965, pp. 682-705.
2. Wachtman, J. B., Jr., "Highlights of Progress in the Science of Fracture of Ceramics and Glass," J. Am. Ceram. Soc., Vol. 57, No. 12, 1974, pp. 509-519.
3. Brown, S. D., "The Charles-Hillig Subcritical Crack Velocity Reconsidered," J. Am. Ceram. Soc., Vol. 61, No. 7-8, 1978, pp. 367-368.
4. Brown, S. D., "Multibarrier Kinetics of Brittle Fracture: I, Stress Dependence of the Subcritical Crack Velocity," J. Am. Ceram. Soc., Vol. 62, No. 9-10, 1979, pp. 515-524.
5. Brown, S. D., "A Multibarrier Rate Process Approach to Subcritical Crack Growth," in Fracture Mechanics of Ceramics, Vol. 4. Edited by Bradt, R. C., Hasselman, D. P. H., and Lange, F. F., Plenum, New York, 1978, pp. 597-621.
6. Krausz, A. S., "The Theory of Thermally Activated Processes in Brittle Stress Corrosion Cracking," J. Eng. Fracture Mech., Vol. 11, No. 1, 1979, pp. 33-42.
7. Krausz, A. S. and Mshana, J., "The Steady-State Fracture Kinetics of Crack Front Spreading," Int'l. J. of Fracture, Vol. 19, No. 4, 1982, pp. 277-293.
8. Williams, D. P. and Nelson, H. G., "Gaseous Hydrogen-Induced Cracking of Ti-5Al-2.55Sn," Metall. Trans. A, Vol. 3, No. 8, 1972, pp. 2107-2113.
9. Avigdor, D. and Brown, S. D., "Delayed Failure of a Porous Alumina," J. Am. Ceram. Soc., Vol. 61, No. 3-4, 1978, pp. 97-99.
10. Ferber, M. K. and Brown, S. D., "Delayed Failure of Plasma-Sprayed Al<sub>2</sub>O<sub>3</sub> Applied to Metallic Substrates," J. Am. Ceram. Soc., Vol. 64, No. 12, 1981, pp. 737-743.
11. Gerberich, W. W. and Stout, M., "Discussion of Thermally Activated Approaches to Glass Fracture," J. Am. Ceram. Soc., Vol. 59, No. 5-6, 1976, pp. 222-225.

## KINETIC THEORY APPLIED TO A SHIELDED CRACK TIP

by

S. J. Burns

Materials Science Program

Dept. of Mechanical Engineering

University of Rochester

Rochester, NY 14627

Rate-activation analysis has been successfully applied in solids, the thermally activated deformation produced by a uniform stress. Fracture and slow crack growth show all the characteristics of rate-activated processes - however even the crack driving force and its conjugate state variable in the fracture case are in dispute.

It will be shown that atomic process near a sharp crack are shielded from the applied stress intensity factor by near crack tip deformation. Thus, except for materials that are ideally brittle the reaction coordinate driving forces are modified from the applied driving forces. Several examples of crack tip shielding effects will be presented. The effects on general reaction kinetics will be explored.

## TERTIARY CREEP AND CREEP FRACTURE

Alan J. Levy

Department of Mechanical and Aerospace Engineering  
Syracuse University, Syracuse, N.Y. 13210

## Abstract

It is well known that metals, when stretched at constant forces and appreciable temperatures, undergo an accelerated strain rate prior to failure. This aspect of behavior, known as tertiary creep, represents a departure from steady state conditions and may be caused by a number of contributing factors. These factors may be microstructural in nature, i.e., the nucleation and growth of voids on grain boundaries in the material or, they may be nonlinear effects arising from large changes in geometry (for example the decrease in area of a tension specimen at increasing longitudinal strain). In addition, factors such as local fluctuations in geometry, material properties, and temperature causing non-uniform and localized straining, may also contribute to tertiary creep. By understanding the factors giving rise to tertiary creep a clear picture of creep fracture may be obtained.

As a starting point for an investigation of this phenomenon uniaxial and multiaxial forms of a constitutive equation characterizing the creep-damaging behavior of metals, at small strains, are developed based on Dyson's constrained cavity growth mechanism. The model employs a single scalar internal variable which can be identified with the area fraction of cavitated boundaries. This variable, together with the power law creep model is capable of exhibiting the basic behavior common to polycrystalline metals under creep conditions i.e., steady creep, tertiary creep and dilatation arising from the nucleation and growth of grain boundary voids. Elastic effects are accounted for in the usual manner by assuming the total strain rate to be the sum of a creep component, and an elastic component which is related to the stresses via Hooke's Law. A generalization of the equations to large strains is then postulated and the problem of a bar, characterized by this constitutive model, is solved for the case of constant load and constant stress. The solutions indicate the relative contributions of the mechanisms of cavitation and geometrical effect to tertiary creep and fracture.

## CREEP BUCKLING OF PANELS

by

Hamdy A. Ashour\* and Magdi Adib Shaker\*\*

\* Associate Professor, Dept. of Mechanical Engineering, Qatar University, Doha, Qatar.

\*\* Graduate Student, Cairo University, Cairo, Egypt.

This work presents an analysis for the creep buckling problem of geometrically imperfect isotropic circular cylindrical panels under axial compression with simple support boundary conditions. The analysis is based on a non-dimensional form of Donnell-type equations for a slightly imperfect circular cylindrical panel. The elastic constitutive equations for a thin panel are employed. The basic elastic equilibrium equations in the middle surface displacement components are derived through the employment of the principle of virtual displacements. For creep deformation, Odqvist's constitutive equations for steady creep are employed.

Based on the present analysis, a computer program called CBIP (Creep Buckling of Imperfect Panels) has been developed for the creep buckling of circular cylindrical panels. The panel ends are assumed to be simply supported. The applied loading is assumed to be a constant uniform axial compression.

Numerical results are presented for flat rectangular plates as well as circular cylindrical panels. For imperfect isotropic plates, the results of the present analysis compare favorably with previous finite element solutions. A parametric study has been carried out to investigate the effect of several factors such as the panel curvature, level of the applied load, direction, mode shape, and amplitude of the initial imperfection. The present results suggest that each of these factors has an apparent effect on the creep buckling time of geometrically imperfect simply supported cylindrical panels under axial compression. According to the present results, the frequently implemented intuitive process of considering initial imperfections with the same shape as the classical buckling mode of the structural element, does not seem to be justified in some panel cases. In addition, the present results for curved panels indicates that outward (away from the center of curvature) initial imperfections result in substantially higher creep buckling times. Consequently, it seems desirable to intentionally incorporate small outward initial imperfections (e.g. in the form of a small outward out-of-roundness) in cylindrical panels subjected to in-plane compression. It is believed that a slight inward (towards the center of curvature) eccentricity of the applied load can generate the same effect and substantially increase the creep buckling time of a panel. Such factors have to be taken into consideration when an optimum design for such panels is sought.

FAILURE ACCOMMODATION IN CONTROL SYSTEMS  
THAT DEAL WITH APPRECIABLE  
STRUCTURAL DYNAMICS

by

Raymond C. Montgomery  
NASA Langley Research Center  
Hampton, VA

This paper presents a design method for the management of redundancy to deal with control system component failures. Emphasis is placed on systems that must handle structural vibrations. The method involves two phases: One is the pre-operation or off-line design phase which involves component selection and placement strategies. The other is the on-line phase which involves failure detection and control system reconfiguration and recovery during system operation. The design process is illustrated in an application to the grid experimental apparatus at the Langley Research Center. Simulations of the grid are used to study the tolerance of the system to failures and its recovery potential during operation.

**DISCRETE SUBSTRUCTURE SYNTHESIS**

by

L. Meirovitch and R. D. Quinn  
Department of Engineering Science and Mechanics  
Virginia Polytechnic Institute and State University  
Blacksburg, Virginia 24061

This paper presents a method for the dynamic synthesis of large flexible structures consisting of discrete substructures. The substructures are discretized using the finite element method and their order is reduced by means of discretized admissible functions called admissible vectors.

This paper demonstrates that structures can be synthesized by connecting the substructures and reducing their order with admissible vectors simultaneously. The process involves multiplication by a pseudo-inverse matrix, with the matrix that must be inverted being diagonal and positive definite, where the matrix multiplications for the pseudo-inverse are trivial. Thus, continuity is maintained at all substructure connections, although the admissible vectors are applied to the substructures only in a least-squares sense.

This method does not fail computationally regardless of the chosen admissible vectors. Of course, the accuracy of the eigensolution depends on this choice. This is clearly advantageous when only certain degrees of freedom need be included. The iterative procedure entails choosing a simple set of admissible vectors, checking the eigensolution to determine which substructures require more degrees of freedom and then adding admissible vectors to these substructures to yield a more accurate eigensolution. As a numerical example, the eigenvalue problem of a three-dimensional space structure is solved.

**References**

Meirovitch, L., Computational Methods in Structural Dynamics, Sijthoff-Noordhoff International Publishers, The Netherlands, 1980.

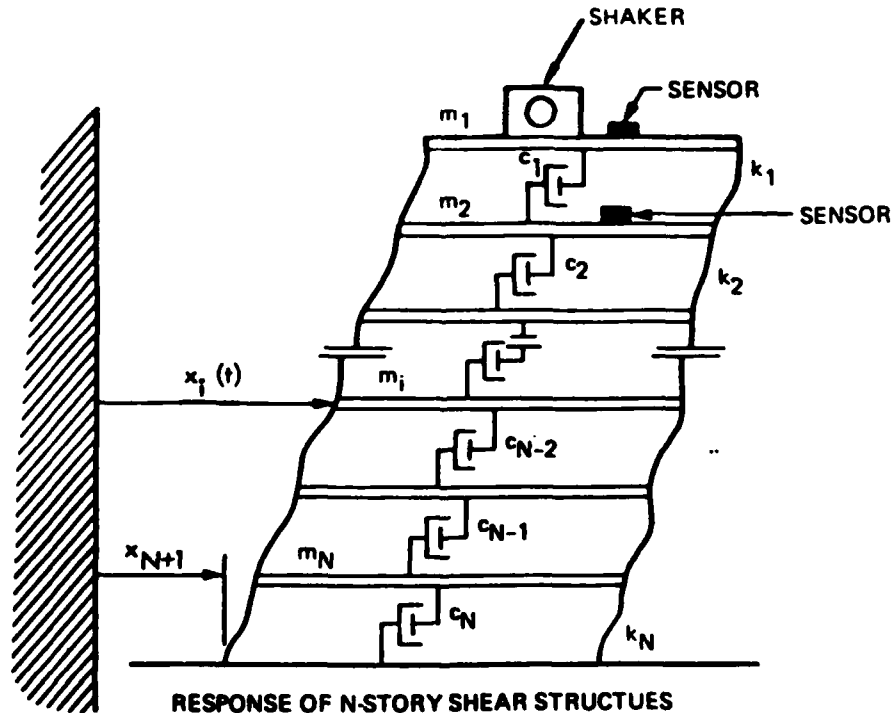
Meirovitch, L., and Hale, A. L., "A General Dynamics Synthesis for Structures with Discrete Substructures," Journal of Sound and Vibration, Vol. 85, 1982, pp. 445-457.

UNIQUENESS IN THE IDENTIFICATION OF BUILDING  
STRUCTURES FROM FORCED VIBRATION TESTS

by

F. E. Udwadia  
University of Southern California  
Department of Civil Engineering  
Los Angeles, California 90089

The need for accurate predictions of the dynamic responses of structural systems has led to the widespread use of forced vibration testing for obtaining knowledge of the dynamic properties of the systems under consideration. This paper is concerned with the uniqueness of the results in the identification of such properties. More specifically, the damping and stiffness distributions which are of importance in the linear range of response, have been investigated. An  $N$  storied structure is modeled as an  $N$ -degree of freedom lumped mass system consisting of masses, springs and dampers. Assuming that the mass distribution is known, the conditions under which unique identification of the stiffness and damping distributions can be obtained, are established. Several useful results on the ability to identify uniquely some, but not all, of the properties of the system have also been obtained.



by

O. Chang  
Department of Electronic Engineering  
Chug Cheng Institute of Technology  
Ta-Shi, Taoyuan  
Taiwan 325  
Republic of China

A switchable algorithm with integrated alpha-beta filter, and kalman filter to execute an optimal adaptive tracking scheme is developed in this paper.

The decision making of selecting alpha-beta filter, or kalman filter is based upon the switching condition which is calculated by considering the measurement of actual residual condition and its weighting factor. Kalman filter will be utilized only as the larger residual is calculated and serious target maneuver is sensed. For the sake of real time consideration, alpha-beta filter is operated in the earlier phase of engagement and only a slight target maneuver is sensed. Since the switching algorithm will decide the best characteristics to be managed in different environments, the most advantageous performances of these two filters are utilized.

These two filters and switching algorithm are developed and simulated with a large computer. But for real time purpose and practical application, it would be most desirable to implement them by a microprocessor. Finally, the adaptive filter merged in proportional navigation guidance system is developed and its good performance in the guidance system is also presented.

## ANALYSIS OF A CONTROL CONFIGURED COMPOSITE STRUCTURE

by

Hayrani Oz\* and Susan L. McCleary\*\*  
The Ohio State University  
Department of Aeronautical and Astronautical Engineering  
2036 Neil Avenue  
Columbus, Ohio 43210

When a structure is designed, it is normally designed with specific loading and size requirements in mind. If some particular type of motion of the structure (bending vibration for example) requires control, it becomes the task of the control system designer to design a control device which will damp the motion. For isotropic structures this may become a particularly tedious and costly process. If, for example, a steel beam (designed for a specific size and loading scheme) vibrates at such a rate that current control devices cannot damp the undesired vibration within required performance criteria, a new control system may be designed or the existing design must be modified. In some cases, no control system will be able to economically satisfy the performance criteria with available hardware and the structure itself must be redesigned, thus possibly creating additional problems from a structural point of view.

Working within given time and frequency domain requirements this paper investigates the extent to which the bending motion of a composite (graphite/epoxy) plate may be controlled by varying the orientation of its layers. The motion of the plate itself may be mathematically described in terms of the modal natural frequencies, and the modal damping coefficients. Both of these variables are functions of the structural material and the geometry. While the geometry will remain fixed, material is variable by virtue of the variety of layer orientation schemes available.

In essence the composite structure can be configured from inside, leaving its shape and size untouched, to meet closed-loop control system requirements not normally met in a previous design process. The primary objective of this investigation is to develop an efficient method of approaching the problem and to identify areas of significant improvement in the performance of the control system in the time and frequency domains. Optimum layer orientations will be sought to achieve the desired degree of controllability. By doing so it may be possible to use a cheaper or less sophisticated control system to elicit the desired response.

\*Assistant Professor, Member AIAA  
\*\*Undergraduate Student, Honor Program

## ON THE STABILITY GENERAL LINEAR DYNAMIC SYSTEMS

Mehdi Ahmadian  
Daniel J. Inman  
Mechanical and Aerospace Engineering Department  
State University of New York at Buffalo  
Buffalo, New York 14260

This work analyzes the stability of linear lumped-parameter elastic systems which can be described by the second order vector differential equation

$$M\ddot{x} + C\dot{x} + Kx = 0$$

Where the  $n \times n$  real asymmetric matrices  $M, C$ , and  $K$  are referred to as mass, damping, and stiffness matrices. Liapunov's direct method is employed for this purpose. Different functions are suggested and are used to provide conditions on the stability, asymptotic stability, and instability of the equilibrium in the aforementioned systems.

It is clearly demonstrated that the results presented here can be used in design and to estimate the effect of qualitative and quantitative changes of the coefficient matrices in the stability of the system.

The present work is compared with previously published works [1-3]. The advantage of the proposed results over the solution of the Liapunov equation are illustrated. Furthermore, it is shown that the results presented here maybe preferred over the results in [1-3].

## References

1. Walker, J.A., "On the Stability of Linear Discrete Dynamic Systems," ASME Journal of Applied Mechanics, Vol. 37, pp. 271-275.
2. Walker, J.A., "On the Application of Liapunov's Direct Method to Linear Lumped Parameter Elastic Systems," ASME Journal of Applied Mechanics, Vol. 41, pp. 278-284.
3. Mingari, D.L., "A Stability Theorem for Mechanical Systems with Constraint Damping," ASME Journal of Applied Mechanics, Vol. 37, pp. 253-258.

ON THE APPLICATION OF TIME STEPPING ALGORITHMS  
IN STRUCTURAL DYNAMICS

by

Dimitris Karamanlidis  
Civil & Environmental Engineering  
University of Rhode Island  
Kingston, RI 02881

In recent years, the development of so-called direct time integration or time stepping algorithms for the numerical treatment of initial value problems in structural dynamics has attracted an increasing number of investigators. This is merely due to ((i) increasing practical importance of dynamic analyses in various areas of engineering (for example, design and analysis of earthquake resistant structures, crashworthiness of vehicles, safety design of structural components in nuclear power plants, etc.) and (ii) limited applicability of classical methods of mechanics (normal mode superposition method, Laplace transformation, etc.) to general structural dynamic problems including large deformations and/or material nonlinearities. In most studies attention has been concentrated on the development of new methods, and on the formulation and verification of general performance-evaluation criteria. These studies have established stability and accuracy as the most important attributes of a time stepping algorithm, and there is an emerging consensus on the use of evaluation criteria appropriate to the treatment of initial value problems in structural dynamics.

The purpose of this paper is twofold: (i) to show how time stepping algorithms can be developed and analyzed systematically; (ii) to summarize merits and drawbacks of several well-established algorithms when applied to the numerical integration of the equations of motion of structural dynamic and continuous systems. Implementation aspects (required storage, computational effort, programming implications, etc.) are also discussed in detail. The performance of these algorithms is evaluated on the basis of a series of numerical experiments with multi-d.o.f. systems, both with and without damping, with emphasis on the characteristics of these time integration algorithms with regards to stability, artificial damping and period elongation.

## OPTIMIZATION AND CONTROL OF DYNAMIC VIBRATION ABSORBERS

by

Maurice I. Young  
Professor of Mechanical and Aerospace Engineering  
University of Delaware  
Newark, Delaware 19716  
U.S.A.

The optimization and control of system dynamic response in a vibration environment is examined by employing modern control theory<sup>1</sup> applied to a tuned, damped dynamic absorber<sup>2,3</sup>. It is shown that the classical optimum response of a tuned, damped, dynamic vibration absorber<sup>4</sup> is only one of a broad class of optimized responses which can be obtained via quadratic minimization techniques. Effects of environmental vibration excitations are considered in the light of differing performance criteria. It is seen that modern control theory provides a direct approach to obtaining optimal designs which are extended to include cyclic stress, cost, weight and other significant system design factors.

<sup>1</sup>K. Ogata, "Modern Control Engineering", Prentice-Hall, Inc., Englewood Cliffs, N.J., 1970, pp. 750-753, 778-779.

<sup>2</sup>J.P. Den Hartog, "Mechanical Vibrations", 4th Edition, McGraw-Hill Book Co., New York, 1956, pp. 93-102.

<sup>3</sup>F.S. Tse, I.E. Morse, R.T. Hinkle, "Mechanical Vibrations, 2nd Edition, Allyn and Bacon, Inc., Boston, 1978, pp. 170-174.

<sup>4</sup>J. Ormandroyd and J.P. Den Hartog, "The Damped Vibration Absorber", Trans. ASME, V. 50, No. 7, p. 9, 1928.

A PSEUDO-COMPLEMENTARY FINITE ELEMENT APPROACH  
FOR THE VIBRATION ANALYSIS OF THIN PLATES IN BENDING\*

by

D. Karamanlidis  
Department of Civil and Environmental Engineering  
University of Rhode Island  
Kingston, Rhode Island

The present paper is concerned with the numerical analysis of the steady-state and transient response of thin elastic plates. Based on a modification of the variational principle due to Hamilton wherein in contrast to the classical formulation not only displacements but also stress resultants represent independent (primary) variables, a new mixed hybrid finite element model is proposed. Introducing separate approximations for the displacement and stress field, the stiffness and consistent mass matrix of a triangular plate element with 3 kinematic degrees of freedom per nodal point are obtained. The performance of the new element scheme is evaluated on the basis of several test examples representing a broad range of circumstances encountered in linear elastokinetic thin plate analysis. The numerical results obtained demonstrate that in terms of efficiency, reliability and accuracy the new element scheme competes most favorably with a series of well-established plate elements.

\*Work supported partially by the Deutsche Forschungsgemeinschaft

## THE INTRINSIC NONLINEAR DYNAMICAL THEORY OF SHELLS

by

Avinoam Libai

Technion, Israel Institute of Technology, Haifa, Israel 32000

and

University of Virginia

Department of Applied Mathematics and Computer Science

Charlottesville, VA 22901

Attention is directed to those formulations of the nonlinear shell equations which avoid the use of the position (or displacements) of the reference surface in the field equations. The name "intrinsic formulations" has found wide usage. In shell statical theories, the well known "strain-curvature approach" is the best example.

Corresponding formulations for the nonlinear dynamical theory of shell range from the semi-intrinsic forms which retain the velocities (either linear or angular) to the more complete intrinsic form which utilizes the metric and curvature tensors (plus an additional potential function) and their time derivatives as the only field variables.

The "complete" intrinsic form will be presented in more detail. The kinematics, equations of motion, constitutive relations and initial and boundary conditions will be discussed. Some advantages and disadvantages of this approach will be pointed out.

The presentation will be concluded by (a) Discussion of a possible scheme for integrating the equations numerically in a rate form, and (b) Specialization to the case of axisymmetric deformations of shells of revolution where the equations are expressed in terms of the two components of the metric tensor (including their space and time derivatives) as field variables.

SOLUTION OF THE FINITE ELEMENT EQUATIONS FOR THE NONLINEAR  
DYNAMIC ANALYSIS OF SHELLS

by

Lois Mansfield  
University of Virginia  
Department of Applied Math and Computer Science  
Charlottesville, VA 22901

We consider the large displacement, small strain, dynamic analysis of elastic shells. For the static analysis, in [1], it was shown that a mixed finite element method derived from a modified form of the Hellinger-Reissner stationary principle where the stresses and bending moments appear as dependent variables in addition to the displacements is much more efficient than the conventional minimum potential energy method. This greater efficiency is due to the fact that the mixed method is quadratic in its unknowns while the potential energy method is cubic in its unknowns. A mixed method for the time dependent problem was introduced in [2]. In addition, an unconditionally stable integration procedure was introduced. This is in contrast to the Newmark  $\beta$  method which is known not to be unconditionally stable for nonlinear problems. Here we present efficient methods to solve the nonlinear systems of equations which must be solved at each time step. These methods use Newton's method along with the conjugate gradient method.

- [1] Mansfield, L., "On the Solution of the Finite Element Equations for Nonlinear Shell Analysis," SIAM J. Sci. Stat. Comput., 3 (1982), 447-459.
- [2] Mansfield, L., "Analysis of Finite Element Methods for the Nonlinear Dynamic Analysis of Shells," Numer. Math. 42 (1983), 213-235.

"APPROXIMATING CURVED SHELLS WITH FLAT ELEMENTS"

By Gerald Wempner  
Georgia Institute of Technology  
Department of Engineering Science and Mechanics  
Atlanta, Georgia 30332

The notion of approximating curved shells by flat elements seems incongruous at first glance. However, such elements are inherently simple and, consequently they have been employed with considerable success for two decades. Certain difficulties are also inherent; foremost is the excessive stiffness which has been termed "shear locking".

This presentation explores fundamental questions about such elemental approximations, difficulties, advantages and limitations. Alternative procedures for the formulations are considered as well as the peculiar difficulties which arise with elements of irregular form, triangles and arbitrary quadrilaterals, as opposed to the regular rectangular or trapezoidal elements which are generated by orthogonal nets.

The basic problems and some solutions are illustrated by examples.

## BOUNDARY CONDITIONS FOR PLATES AND SHELLS\*

by

Frederic Y. M. Wan  
Applied Mathematics, FS-20  
University of Washington  
Seattle, WA 98195

The classical Germain-Kirchhoff theory of thin elastic plates [1,2,3] is known to be the leading term of the outer (asymptotic expansion or interior) solution in a small thickness parameter for the linear elastostatics of thin, flat, isotropic bodies [4,5,6,7]. This leading term (or the actual) outer solution alone cannot fit arbitrarily prescribed data along the edge of the plate. On the other hand, the complementary inner (asymptotic expansion or edge zone) solution is usually intractable. For stress edge-data, Saint-Venant's principle has frequently been invoked (e.g., [3], [8], [9]) to generate a set of stress boundary conditions for classical plate theory and for higher order terms in the interior solution (giving various thick plate theories), without any reference to the complementary edge zone solution. Previous attempts to derive the corresponding boundary conditions for displacements and other types of edge-data for general shape plates have not been successful (e.g., [9]; see also discussion and other references in [10]).

By a novel application of the Betti-Rayleigh reciprocal theorem, a method for deducing a correct set of boundary conditions for the classical and higher order plate theories for any admissible set of edge-data were obtained for the first time in [10,11]. The special case of a semi-infinite plate in a state of plane strain, induced by edgewise uniform data, is first analyzed [10]. In this case, the stress and displacement fields generated by our boundary conditions differed from the corresponding exact solutions by only exponentially small terms away from the plate edge. For stress edge-data, the boundary conditions obtained rigorously justify the application of Saint-Venant's principle for this particular class of problems. Our method of solution also shows that the only previous general results [9] for displacement edge data are incorrect.

Similar results for more general edge-data and plate geometries will then be presented. The results for axi-symmetric bending of a circular plate show that the indiscriminate use of Saint-Venant's principle for plates (see [3] and [8] for examples) may lead to quantitatively and qualitatively incorrect solutions for the plate behavior even in the interior of the plate. In particular, the estimated level of stress and displacement may be low by several orders of magnitude. The results obtained here in fact delimit the range of applicability of Saint-Venant's principle for axi-symmetric bending. Extension of the method to shell structures will also be discussed.

\* The research is partly supported by a U.S.-NSF Grant No. MCS-8306592 and a Canadian NSERC Operating Grant No. A 9259. The author is on leave from the University of British Columbia.

References

1. Germain, S., Recherches sur la theorie des surfaces elastiques, Mme. V. Courcier, Paris, 1821.
2. Kirchhoff, G., "Über das Gleichewicht und die Bewegung einer elastischen Scheibe", J. Reine Ange. Math. (Crelle), Vol. 40, 1850, p. 51.
3. Love, A. E. H., A Treatise on the Mathematical Theory of Elasticity, 4th Ed., Dover, New York, 1944 (see p. 132 & p. 459).
4. Friedrichs, K. O. and Dressler, R. F., "A Boundary Layer Theory for Elastic Bending of Plates", Comm. Pure Appl. Math., Vol. 14, 1961, pp. 1-33.
5. Reiss, E. L., "Symmetric Bending of Thick Circular Pltes", J. of S.I.A.M., Vol. 10, 1962, pp. 596-609.
6. Gol'denveiser, A. L., "Derivation of an Approximate Theory of Bending of a Plate by the Method of Asymptotic Integration of the Equations of the Theory of Elasticity", P.M.M., Vol. 26, No. 4, 1962, pp. 668-686.
7. Gol'denveiser, A. L. and Kolos, A. V., "On the Derivation of Two-Dimensional Equations in the Theory of Thin Elastic Plates", P.M.M., Vol. 29, No. 1, 1965, pp. 141-155.
8. Timoshenko, S. and Goodier, N., Theory of Elasticity, 2nd Ed., 1951, McGraw-Hill, New York (see p. 33 & pp. 351-351).
9. Kolos, A. V., "Methods of Refining the Classical Theory of Bending and Extension of Plates", P.M.M., Vol. 29, No. 4, 1965, pp. 771-781.
10. Gregory, R. D. and Wan, F. Y. M., "Decaying States of Plane Strain in a Semi-infinite Strip and Boundary Conditions for Plate Theory", J. of Elasticity, Vol. 14, 1984, to appear.
11. Wan, F. Y. M., "On Plate Theories and Saint Venant's Principle", to appear in International J. Solids & Structures, 1984.

EFFECTS OF GEOMETRIC IMPERFECTIONS, AXIAL CONSTRAINTS & MODE  
INTERACTION ON THE FUNDAMENTAL FREQUENCIES OF CLAMPED CYLINDRICAL  
SHELLS

by

David Hut  
Department of Engineering Mechanics  
The Ohio State University  
Columbus, Ohio 43210

This paper deals with the effects of geometric imperfections and in-plane axial boundary conditions on the linear fundamental frequencies of simply supported and clamped cylindrical shells. Both asymmetric and axisymmetric geometric imperfections are considered along with the three-term vibration mode which involves the drive mode, the companion mode and the axisymmetric mode. It is found that the presence of small geometric imperfections may significantly raise or lower the linear fundamental frequencies. Further, the vibration behavior depends on the sign of the axisymmetric imperfections. Interaction between the asymmetric and axisymmetric modes results in a significant reduction of the vibration frequencies. The effects of the shell length and radius to thickness ratio are examined via the Batdorf parameter.

The Donnell-type nonlinear dynamic equilibrium and compatibility equations for cylindrical shells written in terms of an out-of-plane displacement  $w$  and a stress function  $F$ , incorporating the possibility of geometric imperfection are employed [1]. The vibration mode and the forcing function, valid for simply supported and clamped boundary conditions, can be written in the separable form [2] involving the driven mode, the companion mode and the axisymmetric mode, respectively ( $w(x) = \sin(mx)$  for sinusoidal and  $w(x) = [1/(1+k)] \cdot [\cos(mx) + k \cosh(mx)]$  for clamped),

$$w(x,y,t) = w(x) [A(t) \cos(ny) + B(t) \sin(ny) + C(t)]$$

$$q(x,y,t) = w(t) [q_A(x) \cos(ny) + q_B(t) \sin(ny) + q_C(t)]$$

The geometric imperfection is assumed to be of the form,

$$w_0(x,y) = w_0(x) [\mu_A \cos(ny) + \mu_C]$$

Substituting the vibration mode and the geometric imperfection into the linearized compatibility equation, the stress function which satisfies this equation exactly is sought. The Galerkin procedure is used to satisfy the linearized dynamic equilibrium equation approximately. The in-plane boundary conditions are satisfied on the average at the two edges of the cylindrical shell. The single valuedness of the circumferential displacement is enforced. The fundamental mode corresponds to one axial half wave and the fundamental frequency is obtained by minimizing the computed frequency with respect to all possible discrete circumferential wave numbers.

- [1] Hui, D., "Influence of Geometric Imperfections and In-Plane Constraints on Nonlinear Vibrations of Simply Supported Cylindrical Panels", ASME J. of Applied Mechanics, Vol. 51, No. 2, 1984 (ASME Paper 84-APM-14).
- [2] Dowell, E. H. and Ventres, C. S., "Modal Equations for the Non-linear Flexural Vibrations of a Cylindrical Shell", Intl. J. of Solids & Structures, Vol. 4, 1968, pp. 975-991.

## ANALYSIS OF AXISYMMETRIC SHELLS WITH CUBIC SPLINES

Jaan Kiusalaas and Abhijit Gupta  
Dept. of Engineering Science & Mechanics  
The Pennsylvania State University  
University Park, PA 16802

The paper presents a method of analyzing thin, axisymmetric shells with the aid of cubic B-splines. The spline approximations are employed in virtually all aspects of modelling: describing the geometry of the middle surface, specifying the variation of the wall thickness along the meridian, and interpolation of the displacement field and the distributed surface loads.

In the interior of the shell, the degrees of freedom are the displacements of the knots (nodes). At the edges, the rotation of the meridian, as well as the displacements, are used. Since these edge degrees of freedom are also present in most (finite) bending elements, the spline model of the shell is compatible with the finite element method of analysis. In other words, the shell can be incorporated in any finite element computer program in the form of a "super element" or substructure.

The use of cubic splines offers the following advantages over conventional finite element models:

- (1) The spline interpolation produces more accurate results than attainable from a finite element model with the same number of degrees of freedom. Much of this superiority is due to the following two items.
  - (2) Smoothness, in the form of continuity of the meridional curvature before and after deformation, is automatically assured by the cubic spline interpolation. This desirable feature cannot be enforced in a simple manner with finite elements.
  - (3) Use of splines also satisfies automatically the requirement that the displacement field of the model must admit rigid-body displacements and rotations. This condition causes considerable difficulty in finite element modelling of shells and is, therefore, frequently satisfied only in an approximate manner.
- (4) B-splines greatly facilitate the mathematical representation of free-form meridional shapes and thickness variations. Hence their use is ideally suited to design of shells by trial-and-error, or in structural optimization algorithms.

The paper is illustrated with several numerical examples that compare the results of the spline interpolation with the finite element method.

ADVANCES IN NONLINEAR THEORIES FOR THIN ELASTIC SHELLS  
UNDERGOING SMALL OR FINITE STRAINS

by

Rudiger Schmidt  
Ruhr-Universitat Bochum, Institut fur Mechanik  
D-4630 Bochum 1, Federal Republic of Germany

In recent years a novel approach to shell theory has been given in the works of Pietraszkiewicz. He applied the polar decomposition theorem to shell theory in a way which makes it possible to derive appropriate constrained theories for restricted strains and rotations. In the present paper we first review the recent progress achieved for the formulation of first-approximation theories for shells undergoing small strains and either moderate, large or unrestricted rotations. Furthermore, we shall give an extension of these results to problems in which the strains no longer can be assumed small. In recent literature, Libai and Simmonds and Chernykh, deal with large strain bending shell theory, taking into account the change of shell thickness as a major effect. We shall derive a fully consistent nonlinear shell theory for the above problem using the Mooney-Rivlin material law. The main advantages of the present formulation are: (i) all shell equations are given in an entirely Lagrangian approach, (ii) all geometric and static boundary conditions are properly given, (iii) the equilibrium equations and static boundary conditions are obtainable as Euler-Lagrange equations from an appropriate variational principle.

LARGE-DEFORMATION AND STABILITY BEHAVIOUR OF  
UNDERGROUND ALUMINUM PIPING\*

W. Szyszkowski and P.G. Glockner  
Department of Mechanical Engineering  
The University of Calgary  
Calgary, Alberta, Canada T2N 1N4

In designing thick-walled underground tubing, a linearized analysis is usually satisfactory for predicting stresses and deformations in such pipes [1,2]†. For thin-walled flexible tubing, linearization and associated approximations are not admissible since relatively large deflections can occur which may significantly affect the pipe-soil interaction and lead to undesirable load redistributions, a reduction in the pipe's load carrying capacity and to its collapse.

This paper presents an approximate geometrically and materially non-linear analysis of the large deformation and stability behaviour of buried flexible tubing. The tube material was assumed to have a typical bilinear elastic-strain hardening curve with material constants taken from commercial aluminum tube specifications. The soil was assumed to exert a vertical, active pressure,  $q_v$ , on the pipe which is a function of the depth of overburden. Lateral resistance or passive pressure, proportional to the horizontal deflection of the tube, with a soil resistance coefficient  $k$ , was also assumed. The deflected shape was taken to be symmetrical and elliptical in form, arrived at from the originally circular shape by isometric deformations, leading to flattening of the pipe.

Typical results are given in Fig. 1 where  $q_v$  is plotted against the tube flattening,  $w_A$ , for different values of  $k$ . The present non-linear solution clearly differs significantly from the linear one, both in magnitude and characteristics. It shows that for given soil conditions there is a maximum value of  $q_v$ , referred to as the critical pressure,  $q_v^{cr}$ , beyond which dynamic collapse of the tube will occur. The decrease in tube stiffness, exhibited by the descending unstable branches of the curves are due to the so-called 'wedge effect' resulting from increasing flattening of the tube and a corresponding increasing concentration of lateral force on the decreasing soil contact area. The terminal increase in tube stiffness occurs at very large deformations and is due to strain hardening effects.

The influence of initial imperfections on the overall pipe behaviour is given in Fig. 2 where  $q_v^{cr}$  is plotted against  $k$ , for various initial 'out-of-roundness'. These results show that  $q_v^{cr}$  is significantly affected by initial 'flattening' of the tube which for thin-walled pipes can result from 'stacking' during long-term storage. Details of the analysis and its use in designing safer underground piping are given in [3].

\* The results presented here were obtained in the course of research sponsored by the Natural Sciences and Engineering Research Council of Canada, Grant No. A-2736.

† Numbers in square brackets refer to publications listed under References.

References

1. Rubin, C., "Buried Pipe Deflections Using Elasticity Theory", J. Structural Division, ASCE, Vol. 101, No. ST 12, December 1975.
2. Spangler, M.G., Handy, R.L., Soil Engineering - 4th Edition, Harper and Row Publishers, New York, N.Y., 1982.
3. Szyszkowski, W., Glockner, P.G., "Design and Analysis of Flexible Underground Aluminum Tubing", Report No. 289, Dept. of Mech. Engg., The University of Calgary, Calgary, Alberta, 1984.

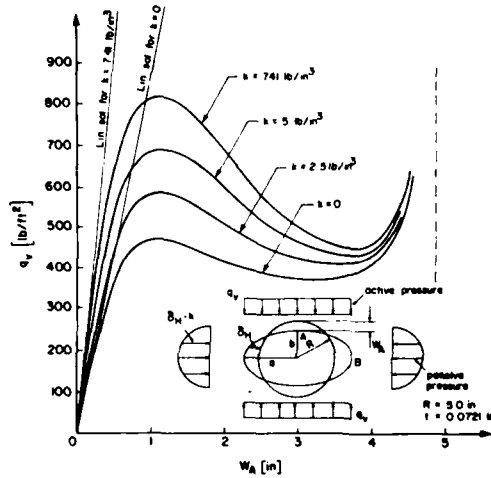


FIG 1 LOAD-DEFLECTION CURVE FOR FLEXIBLE BURIED TUBING

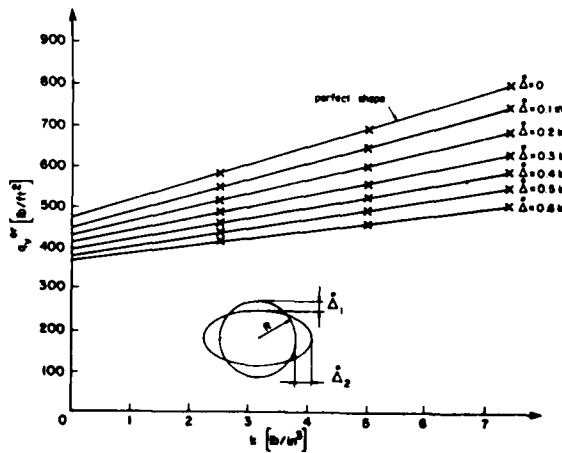


FIG 2 VARIATION OF CRITICAL PRESSURE WITH SOIL RESISTANCE AND INITIAL FLATTENING

FINITE BENDING OF A SELF REINFORCED CIRCULAR  
PLATE INTO A SPHERICAL SHELL

by

P.D.S. Vera

Regional Engineering College  
Kurukshetra 132119  
India

Using the finite strain components in the linear constitutive law of Belfield, Rogers and Spencer [1983] for a locally transversely isotropic self reinforced material, we show that a circular plate of radius,  $d$ , can be bent into a spherical shell by forces and couples applied to the edges only, the inner and outer surfaces of the shell being free from traction. The self reinforcement director has components  $(0,1,0)$  everywhere. Radius of the plate,  $d$ , is taken to be small as compared with  $a$  and  $b$ , the inner and outer radii of the shell, so that  $(d/a^2)$  and its higher powers can be neglected. The particular case, in which Poisson's ratio is equal to  $1/3$  has been considered in detail. The percentage of the decrease in the thickness of the plate and the change in the edge radii have been calculated. Reinforcement is found to increase the applied couple, needed for bending the plate, by about 30 percent. Interestingly in this paper we are able (i) to find the exact solution to the nonlinear equations involved and (ii) to establish the utility of Spencer's idea of introducing the continuous distribution of self reinforcing fibres all over the material instead of putting the reinforcing rods in a composite in some particular arrangement. We are justified in using the finite strain components in linear law as here we are dealing with only geometrically nonlinear deformation.

Belfield, A. J., Rogers, T. G., and Spencer, A. J. M., "Stress in Elastic Plates Reinforced by Fibres Lying in Concentric Circles", J. Mech. Phys, Solids, Vol. 31, No. 1, 1983, pp. 25-54.

A REFINED SHEAR DEFORMATION THEORY FOR LAMINATED SHELLS<sup>†</sup>

by

C. F. Liu and J. N. Reddy

Department of Engineering Science and Mechanics  
Virginia Polytechnic Institute and State University  
Blacksburg, Virginia USA

The Love's first approximation shell theories are expected to yield sufficiently accurate results when (i) the lateral dimension to thickness ratio is large, (ii) the dynamic excitations are within the low frequency range, and (iii) the material anisotropy is not severe. However the application of such theories to laminated shells could lead to as much as 30% or more errors in deflections, stresses and frequencies. This is due to the neglect of the transverse shear strains in the classical shell theories.

The paper presents a refined shear deformation theory that is an extension of the theory of Hildebrand, Reissner and Thomas [1]. The present theory is based on a cubic expansion of the surface displacements in terms of the thickness coordinate, and the transverse deflection is assumed to be independent of the thickness coordinate. The additional displacement functions introduced in the expansion (nine in all) are reduced to five by requiring that the transverse shear stresses be zero on the bounding surfaces of the laminate. The resulting shear stresses vary parabolically through the laminate thickness and hence no shear correction coefficients are required. The principle of virtual work is used to derive the associated differential equations of equilibrium and boundary conditions [2]. Exact solutions are presented for cylindrical and spherical shells with simply supported boundary conditions and cross-ply lamination scheme.

REFERENCES

- [1] Hildebrand, F. B., Reissner, E. and Thomas, G. B., "Note on the Foundations of the theory of small displacements of orthotropic shells," NACA Technical Note No. 1833, March 1947.
- [2] Reddy, J. N., ENERGY AND VARIATIONAL METHODS IN APPLIED MECHANICS, John Wiley, New York, 1984.

---

<sup>†</sup> This research is sponsored by NASA Langley Research Center. The authors express their sincere thanks to Dr. Norman Knight, Jr. (NASA) for his encouragement and support of the work.

## VISCOELASTIC FLUIDS IN TURBULENT CIRCULAR PIPE FLOW

by

E.Y. Kwack and J.P. Hartnett  
Energy Resources Center  
University of Illinois at Chicago  
Box 4348, Chicago, IL 60680

Viscoelastic fluids in turbulent channel flow exhibit more complex friction factor and heat transfer behavior than Newtonian fluids. In particular, the turbulent pressure drop and heat transfer of aqueous solutions of high molecular weight polymers are influenced by a number of factors including solute and solvent chemistry, polymer concentration and mechanical degradation. In general, the friction factor and heat transfer decrease with increasing polymer concentration until a minimum asymptote is reached. Degradation is associated with an increase in both friction factor and heat transfer. The effects of the solvent and the solute chemistry are more complicated than the effects of either polymer concentration or polymer degradation. However, it was found that for fully developed conditions all of these factors may be successfully accounted for by introducing two dimensionless quantities, the Reynolds number and the Weissenberg number. The Reynolds number arises in the study of Newtonian fluids, whereas the Weissenberg number is an additional parameter which accounts for the fluid elasticity. Experiments conducted with aqueous solutions of polyacrylamide reveal that the friction factor and dimensionless heat transfer coefficient are functions only of the Reynolds number and the Weissenberg number for fully developed hydrodynamic and thermal conditions in turbulent pipe flow.

Another important finding is that critical Weissenberg numbers exist for friction and heat transfer. The critical Weissenberg number for friction is of the order of 5-10 and that for heat transfer is of the order of 100 where the Weissenberg number is based on the characteristic time evaluated by the Powell-Eyring model. Above the corresponding critical Weissenberg numbers, the friction factor and the dimensionless heat transfer coefficient are at their minimum asymptotic values and are functions only of the Reynolds number for fully developed conditions.

Viscoelastic fluids in turbulent pipe flow exhibit entrance lengths which are considerably longer than those encountered with a Newtonian or a purely viscous fluid. The entrance lengths increase with increasing Weissenberg number. The hydrodynamic entrance length corresponding to the minimum drag asymptote is about 100 pipe diameters, while the thermal entrance length corresponding to the minimum heat transfer asymptote may be as long as 400 to 500 pipe diameters. These values are in sharp contrast to the entrance lengths found in most Newtonian fluids which are of the order of 10-15 pipe diameters for turbulent pipe flow.

The available experimental data have been used in conjunction with relatively simple turbulent flow models to obtain insight into the momentum and thermal eddy diffusivity behavior of viscoelastic fluids in turbulent pipe flow.

HEAT TRANSFER IN FLOWING MOLTEN OR  
THERMALLY SOFTENED POLYMER SYSTEMS

by

Richard G. Griskey, P.E.  
School of Engineering  
University of Alabama in Huntsville  
Huntsville, Alabama 35899

Heat transfer to and from flowing molten or thermally softened polymer systems represent an important but highly complex process. Important, in that all polymer processing operations (extrusion, injection molding, blow molding, etc.) require such heat transfer; and highly complex, since such systems are non-Newtonian, incompressible, sometimes viscoelastic and subject to a high degree of viscous heating.

Conventional heat transfer correlations and solutions are not applicable to the case for flowing molten or thermally softened polymer systems. In fact, if such approaches are taken, errors of several hundred percent are possible.

This paper will review the status of experimental and theoretical research in the area. Also, all work will be evaluated as to relative merit in handling this important processing question. New unpublished research will also be presented. Finally, a set of recommended procedures will be given that represent the most efficacious approach to heat transfer in molten or thermally softened polymer systems.

For example, this paper will discuss the best available experimental methods of measuring temperature profiles in these systems. Attention will be directed toward reproducibility, reduction of experimental error, and increased precision. Additionally, data from such measurements will be used to focus on the effects of the aforementioned parameters such as viscous heating, thermal expansion effects, fluid properties, as well as the development of temperature profiles with axial length.

Nusselt-Graetz correlations for these systems that incorporate Brinkman number behavior for both heating and cooling will be presented. Actual process computations will be used to show the application of the foregoing.

The paper also deals with the questions of free convection, effect of viscoelasticity and polymer property parameters.

## STABILITY AND FLOW PROPERTIES OF ALTERNATE MIXTURE FUELS - A REVIEW

by

James M. Ekmann  
United States Department of Energy  
Pittsburgh Energy Technology Center  
Pittsburgh, Pennsylvania 15236

Although a large body of data exists on alternate fuel mixtures, no completely satisfactory understanding of either the viscometric properties or the stability has resulted for any of the fuels in this category. Engineering data is available to develop acceptable fuels from selected solid and liquid constituents (a particular coal and water for example) but generalized models or correlations have not been developed.

The last decade has seen extensive research into the use of solid-liquid suspensions as a direct feed to a range of combustion, gasification, and liquefaction equipment. Coal-oil mixtures (COM) were studied as a retrofit fuel for boiler and furnace applications. Coal-water mixtures (CWM) are being examined for use in conventional boilers, fluidized bed combustors, furnaces, gas turbines, gasifiers, and liquefaction processes. Other alternate mixtures, such as coal-alcohol mixtures, have also been proposed for a number of energy-related technologies.

The wide variety of materials proposed for the fuel constituents and the broad range of applications result in a group of fuels with diverse characteristics. For example, the required particle size distribution in a CWM for use in fluidized bed combustion is much coarser than that proposed for a gas turbine.

Proposed application may place restrictions on the compositional parameters, such as a prohibition against alkali metals which are often present in dispersing and stabilizing additives.

The potential application of an alternate fuel mixture to a process requires extensive characterization of the fuel flow and storage properties as a function of the process requirements. Numerous studies of the stability characteristics and viscometric properties of these suspension fuels have been conducted using a diverse group of techniques and experimental equipment. As these fuels are generally pseudo-homogeneous suspensions which behave in a manner similar to non-Newtonian fluids, the choice of the measurement techniques is an important consideration.

This paper will review a number of proposed alternate fuel mixtures and their applications. Compositional parameters, like ash content and particle size distribution, will be discussed when appropriate. Studies conducted on these fuels to date will be reviewed with emphasis on the nature of the measuring techniques employed. Models for stability on flow properties which have been applied to these fuels will be discussed. As the Pittsburgh Energy Technology Center has been involved in research activities for a number of alternate slurry fuels, a detailed discussion of the results from these activities will be included.

FLOW OF A NON-NEWTONIAN FLUID BETWEEN  
HEATED PARALLEL PLATES

by

K. R. Rajagopal and A. Z. Szeri  
Department of Mechanical Engineering  
University of Pittsburgh  
Pittsburgh, PA 15261

The flow of a thermodynamically compatible incompressible homogeneous fluid of grade 3 between heated parallel plates is studied, in the presence of an external pressure gradient along the plates. The stress  $\underline{T}$  in such a fluid is given by (cf. Fosdick and Rajagopal [1])

$$\underline{T} = -p\underline{1} + \mu(\theta)\underline{A}_1 + \alpha_1(\theta)\underline{A}_2 + \alpha_2(\theta)\underline{A}_1^2 + \beta_3(\theta) (\text{tr}\underline{A}_1^2)\underline{A}_1,$$

where  $p$  is the pressure,  $\mu(\theta)$  is the coefficient of viscosity,  $\alpha_1(\theta)$  and  $\alpha_2(\theta)$  are material moduli referred to as normal stress coefficients, and  $\underline{A}_1, \underline{A}_2$  are the first two Rivlin-Ericksen tensors (cf. Rivlin and Ericksen [2])

In the case of constant heat flux at the walls, a similarity transformation reduces the appropriate partial differential equation into an ordinary differential. We calculate the Nusselt number as a function of the parameter  $\Gamma = \frac{\mu V^2}{k(\theta_b - \theta_w)}$  which determines

the viscous dissipation, and the parameter  $\Lambda = \frac{\beta_3 V^2}{\mu h^2}$  which is a

measure of the non-Newtonian nature of the fluid.  $V$  is a characteristic velocity given by  $V = \frac{-h^2}{2\mu} \frac{dp}{dx}$ ,  $h$  is the distance between the plates,  $k$  is the thermal conductivity,  $\theta_b(x)$  represents the bulk fluid temperature and  $\theta_w(x)$  the wall temperature. It is found that when  $\Gamma$  is large, even a small departure from Newtonian behavior is sufficient to cause a significant decrease in the Nusselt number (cf. Figure 1)

In the case of the constant wall temperature we analyse two temperature dependent viscosity models, the non-Newtonian coefficients being assumed to be constant. It is found that the temperature dependence of viscosity is not very important. This is marked contrast to the behavior of a purely linearly viscous fluid. If the fluid is even slightly non-Newtonian (in terms of the parameter  $\Gamma \neq 0$ ), variable viscosity solutions are not too distant from constant viscosity solutions.

- [1] Fosdick, R. L., and Rajagopal, K. R., "Thermodynamics and Stability of Fluids of Third Grade", Proc. Roy. Soc. London., Ser A, Vol. 339, 1980, pp. 351-377.
- [2] Rivlin, R. S., and Ericksen, J. L. "Stress Deformation Relation for Isotropic Materials", J. Ration. Mech. An., Vol. 4, 1955, pp. 323-425

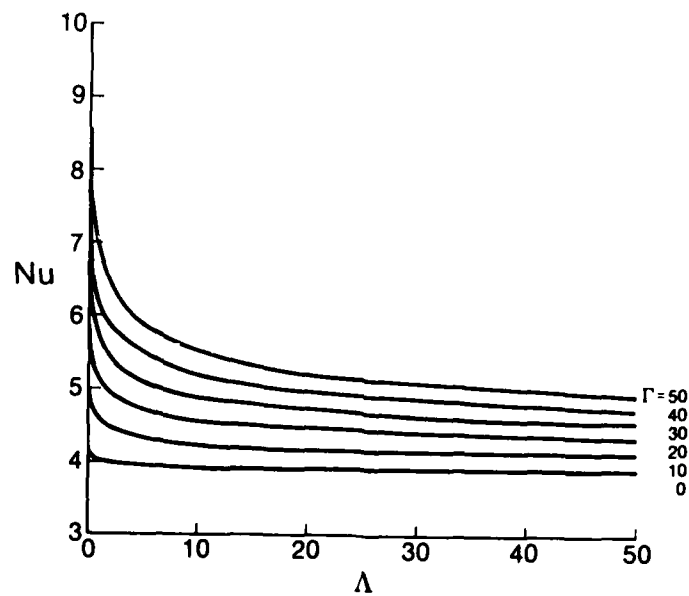


Figure 1

RHEOLOGY OF DIRECT COAL LIQUEFACTION SLURRIES DURING  
COAL DISSOLUTION\*

by

Richard N. Chapman  
Sandia National Laboratories  
P.O. Box 5800  
Albuquerque, NM 87185

In direct liquefaction, coal is dissolved in a process-derived solvent at pressures and temperatures up to 2000 psig and 450°C. As the coal dissolves, the slurry passes through a gel phase during which the viscosity increases by as much as three orders of magnitude. In order to measure viscosities during gelling, it is necessary to continuously monitor data from 10 to 10,000 cp at shear rates from 100 to 1000 sec<sup>-1</sup> (because the slurries are non-Newtonian); maintain homogeneity; and withstand the erosive/corrosive slurries at process conditions. As a result of these rather stringent requirements, little gelling data have been generated to date. The need for this data motivated the development of a novel rheometer that is both easy to operate and ideal for gelling studies. This device, called the Helical Screw Rheometer (HSR), is an extension of extruder technology in that shear stresses are determined from the differential pressure generated by rotating a close tolerance helical screw in a high pressure and high temperature vessel. Shear rates are determined from the rotation rate. A prototype of the HSR has been constructed and used to generate viscosity data during gelling as a function of temperature, pressure, shear rate, coal concentration and solvent quality. Models which predict slurry viscosities were developed to enhance the design of coal dissolution reactors.

---

\*This work supported by the U.S. Department of Energy at Sandia National Laboratories under contract DE-AC04-76DP00789.

SINGLE-PHASE FLOW AND TWO-PHASE SLUG FLOW HEAT TRANSFER WITH  
NON-NEWTONIAN LIQUIDS IN LARGE DIAMETER PIPES

by

Richard G. Sam; Creare R&D Inc., Box 71, Hanover, NH 03755  
Graham B. Wallis; Dartmouth College, Hanover, NH 03755  
Bharatan R. Patel; Creare R&D Inc., Box 71, Hanover, NH 03755  
Dhiren C. Mehta; Int. Coal Refining Co., Box 2752,  
Allentown, PA 18001

This paper presents experimental and analytical results for non-Newtonian single-phase flow and transient two-phase slug flow heat transfer in horizontal pipes. The test loop replicates 1 1/2 full-size coils of a rectangular coal slurry/hydrogen gas fired heater designed for operation in a solvent refined coal production plant. The rectangular coil is constructed of 6.75 in. inner diameter Lexan pipe with overall dimensions of 40 ft. and 10 ft. The heat transfer test section is installed in the last leg of the loop and consists of a 6 ft. long steel pipe jacketed with aluminum block resistance heaters (constant heat flux or power input).

The single-phase flow experiments were performed with two non-Newtonian water/polymer (sodium carboxymethyl cellulose) solutions to simulate the coal slurry rheology. A range of liquid flow rates corresponding to average liquid velocities in the pipe between 2 and 6 ft/sec were tested. The two-phase slug flow experiments were performed using the water/polymer solutions as the liquid phase and Freon-12 as the gas phase. The experiments were performed at a pressure of 80 psia to simulate the density of hydrogen at the prototypical operating conditions. The range of average gas velocities tested was 4 to 12 ft/sec.

Measurements of the axial and circumferential variation of the convective heat transfer coefficient along the test section are reported. The single-phase flow data are presented as steady-state heat transfer coefficients. The two-phase slug flow data are presented as transient heat transfer coefficients (derived from fast-response thermocouple data) which vary significantly depending on whether a liquid slug or gas bubble is in contact with the measurement location. An analysis of the single-phase flow data is developed and shown to predict the observed trends. The analysis is extended to the case of slug flow using a homogeneous flow theory approach. The modified theory is shown to be in agreement with much of the slug flow data.

NON-NEWTONIAN SLUG FLOW CHARACTERISTICS IN LARGE DIAMETER  
HORIZONTAL AND INCLINED PIPES

by

Richard G. Sam; Creare R&D Inc., Box 71, Hanover, NH 03755  
Bharatan R. Patel; Creare R&D Inc., Box 71, Hanover, NH 03755  
Dhiren C. Mehta; Int. Coal Refining Co., Box 2752,  
Allentown, PA 18001

This paper presents experimental and analytical results for non-Newtonian slug flow characteristics in large diameter horizontal and inclined pipes. The test loop replicates 1 1/2 full-size coils of a rectangular coal slurry/hydrogen gas fired heater designed for operation in a solvent refined coal production plant. The rectangular coil is constructed of 6.75 in. inner diameter Lexan pipe with overall dimensions of 40 ft. and 10 ft. Flow regime characteristics are reported for a horizontal pipe configuration as well as for 1° upward and 1° downward pipe inclinations.

The experiments were performed with two non-Newtonian water/polymer (sodium carboxymethyl cellulose) solutions to simulate the coal slurry rheology and Freon 12 to simulate the hydrogen gas density. A range of liquid and gas flow rates corresponding to superficial liquid velocities of 2, 4, and 6 ft/sec and superficial gas velocities of 4, 8, and 12 ft/sec were tested. Measurements of flow regime characteristics such as slug length, velocity, and frequency, pressure drop across various sections of the test loop, as well as the superficial liquid velocities defining the transition between slug flow and stratified flow are reported. Flow regimes were observed directly in the transparent Lexan piping.

The flow regime transition data are compared with the Taitel-Dukler flow regime map and analytical transition criteria. The slug velocity (holdup) data are compared with the Hughmark correlation and the Zuber-Findlay drift flux model. Finally, the pressure drop data are compared with correlations and models developed by Shu, Vermeulen and Ryan, Lockhart and Martinelli, and our own extension of the Dukler and Hubbard model.

VISCOUS HEAT DISSIPATION WITH PRESCRIBED WALL HEAT FLUX  
FOR POWER-LAW FLUID

by

P. R. Comrie, J. Curtis, A. R. Rizzo, B. Shapiro and C. Laohakul  
The Cooper Union School of Engineering  
The Cooper Union for the Advancement of Science and Art  
Cooper Square, New York, NY 10003

A problem of viscous heat dissipation with a prescribed wall heat flux is analysed for laminar flow of power-law fluid in slit and tube. Analytical expressions for the temperature distribution, bulk temperature and local Nusselt number are derived. Numerical results of various power-law index are presented. For large distance downstream, thermally fully-developed temperature distribution, bulk temperature and local Nusselt number are obtained in closed forms. It is further shown that the bulk temperature obtained from the thermally fully-developed solution is also the exact solution regardless of the axial distance downstream. Finally, a simple expression is given for the case in which there will be no rise in bulk temperature.

A SCALAR (MASS/HEAT) TRANSFER CORRELATION FOR FLOW AROUND  
A SUBMERGED SPHERE OF ARBITRARY COMPOSITION

by

P. O. Brunn  
Columbia University  
New York, NY 10027

Scalar (mass or heat) transfer from a sphere is important in many fields of science and technology. If the sphere is small enough the Reynolds number will be small and Lamb's general solution to the equations of creeping motion may be utilized to describe the local flow field. No matter what type of sphere is considered (rigid sphere, sphere with slip, droplet, or droplets encapsulated by a liquid or elastic membrane) Stokes solution depends upon one parameter,  $F_0$ . Physically this is the dimensionless drag force and can vary in magnitude only between the limits  $2/3$  (e.g. gas bubbles) and  $1$  (rigid sphere). Utilizing numerical results Clift obtained two simple formulas for the Nusselt number  $Nu$ , valid over the whole range of Peclet numbers  $Pe$  for these two limiting cases ( $F_0 = 2/3$  and  $F_0 = 1$ , respectively).

In order to obtain the average Nusselt number  $Nu$  as a function of  $Pe$  for arbitrary  $F_0$  we concentrate on the high Peclet number range ( $Pe > 10^3$ ) where the Friedlander approximation might be employed. Carefully studying the  $Nu$ -behavior in that Peclet number range and considering the Clift correlation for bubbles as the  $F_0 = 2/3$  limit of a general  $Nu = Nu(P, F_0)$  correlation allows us to obtain an explicit expression for that correlation for arbitrary  $F_0$  ( $2/3 \leq F_0 \leq 1$ ) and arbitrary Peclet numbers ( $0 \leq Pe < \infty$ ). The error involved in our formula is estimated to be less than 6 percent.

Being simple in form yet highly accurate the correlation should thus prove practically useful.

## CERTAIN FLUID DYNAMICAL ASPECTS OF CRYSTAL GROWTH TECHNOLOGY

by

J.M. Floryan  
 The University of Western Ontario  
 Faculty of Engineering Science  
 London, Ontario, Canada, N6A 5B9

Single crystals are obtained in a carefully controlled change of phase process. The possible methods involving hydrodynamics are solidification of a melt, growth from a super-saturated solution, condensation of a vapour or growth by chemical reactions of gases. The associated presence of spatial gradients of composition and temperature gives rise to solutal and thermally-driven convective motions which impinge on the chemical homogeneity of crystals, a factor of major significance for electronic device fabrication [1].

In this paper we concentrate on the floating zone process (Fig. 1). A rod made of a material to be processed is locally melted and resolidified by means of a ring heater. The liquid phase is held in place by surface tension forming a bridge. Since the melt does not come into contact with other materials, this technique is particularly attractive when manufacturing materials of controllable purity such as silicon, that are highly corrosive in the molten state.

Quite large temperature gradients exist along the surface of the molten zone which give rise to a strong thermo-capillary convective flow. This flow is gravity independent and can give rise to time-dependent behaviour under some conditions [2,3]. The unsteady flow in the liquid phase causes the quality of the growing crystal to deteriorate considerably [2] and should be avoided.

Our investigation is focused on the analysis of thermo-capillary convection in liquid bridges. For simplicity we consider the fluid to be Newtonian, incompressible and of constant properties, with the exception of surface tension which decreases with temperature. Numerical simulation of the dynamics of the bridge involves simultaneous determination of the velocity and temperature fields together with the shape of the interface (moving boundary problem). We have selected primitive-variables formulation, artificial compressibility method, compact fourth-order differencing based on the Hermitian polynomials and the ADI pseudo-unsteady solution procedure. We limit our investigation to the axisymmetric bridges and we select the aspect ratios and volumes of the bridge so as to assure its static stability. We will report results for a wide range of aspect ratios and volumes of the liquid in the bridge.

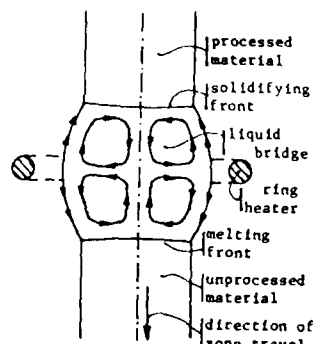


Fig. 1 Schematic Representation of Floating-Zone Process

REFERENCES

- [1] Hurle, D.T.J., "Current Growth Techniques in Crystal Growth: a Tutorial Approach", (edited by Bardsley, W., Hurle, D.T.J., and Mullin J.B.), North Holland, Amsterdam, 1979, pp. 91-138.
- [2] Schwabe, D., "Marangoni Effects in Crystal Growth Melts", *Physico-Chemical Hydrodynamics*, Vol. 2, 1981, pp. 263-280.
- [3] Preisser, F., Schwabe, D., and Scharmann, A., "Steady and Oscillatory Thermocapillary Convection in Liquid Columns with Free Cylindrical Surface", *J. Fluid Mech.*, Vol. 126, 1983, pp. 545-567.

EFFECTS OF WALL AND INTERFACE CURVATURE ON  
THE STOKES RESISTANCE OF A SPHERE

by

A. Falade  
University of Lagos  
Department of Mechanical Engineering  
Lagos, Nigeria

It is demonstrated that the hydrodynamic resistance of a particle moving in close proximity to an arbitrary curved boundary which may be a solid surface or an interface between two immiscible fluids, can be decomposed into two components. One of the components - termed here as the 'distance effect' - is the resistance the particle would experience when moving near a plane boundary provided the distance of such plane boundary from the particle is the same as the distance of the normal from a point  $O$  affixed to the particle to the curved boundary. The plane boundary is to be oriented perpendicular to this normal. For the sphere exact determination of the distance effect can be made using the results of Jefferey (1), Stimson and Jefferey (2), Brenner (3), and Lee and Leal (4). For non-spherical particles, the method of Hirschfeld et al (5) can be used (after extension to two-phase flow) provided  $\beta$  and  $k$ , which are respectively the ratios of the characteristic particle size, on the one hand, to its distance from the plane boundary and to the radius of curvature of the boundary, on the other, are both much smaller than unity.

The other component of the resistance - termed the curvature effect - is that due to the curvature of the boundary. This paper describes how the latter component may be determined to any desired order in  $k$  (for  $k \ll 1$ ) by employing a regular perturbation technique. For particles such as the sphere for which exact solutions for the particle - plane - boundary problems are known, the results would be valid in all of the range  $0 < \beta < 1$ . For other particles the results would be valid to second order in  $\beta$  provided  $(1 - \beta)/\beta \gg 1$ . The procedure for calculating the curvature effect involves solving a sequence of plane-boundary-value problems. To illustrate the procedure the problems of spherical particle in the vicinity of the paraboloidal surface of a rotating fluid are solved. The relative magnitudes of distance and curvature effects are compared.

REFERENCES

1. Jeffery, H.B., Proc. Roy. Soc. A 87, 109, 1912.
2. Stimson, M. and Jeffery, G.B., *ibid* A 117, 110, 1926.
3. Brenner, H. Chem. Eng. Sc. 16, 242, 1961.
4. Lee, S.H. and Leal, L.G., J. Fluid Mech. 98, 193, 1980.
5. Hirschfeld, B.E., Brenner H. and Falade, A., Physico Chemical Hydn. in press 1984.

ON THE STEADY FLOW PRODUCED IN FLUID-PARTICLE SUSPENSION  
BY AN INFINITE ROTATING DISC WITH SURFACE SUCTION

by

L. V. K. V. Sarma and S. K. Kumar  
*Department of Mathematics*  
Indian Institute of Technology  
Madras, India

A numerical solution is given for the steady flow of a fluid-particle suspension over an infinite rotating disc with suction using least square finite element method. In the investigation a suction parameter  $A$  is introduced and some typical results for both fluid and particle phases and density distributions of particles are presented graphically for  $A = 3.0$  in order to illustrate some interesting features of the solution. It is observed that the radial velocity of the particle phase attains its maximum on the surface of the disc and the particle slips in the tangential direction on the disc. The magnitudes of the radial velocity components of both the fluid and particle phase are found to decrease rapidly as suction increases. It is observed that the velocity of the fluid reduces due to the presence of particles. The boundary layer thicknesses for both phases are found to be approximately equal. The accuracy of the numerical technique is depicted by comparing with another method.

by

Aydeniz Siginer  
 Department of Mechanical Engineering  
 Auburn University  
 Auburn, AL 36849

It is well known that few exact solutions of the Navier-Stokes equations exist. An exact solution can be given to Stokes' second problem where the flow geometry consists of the fluid filled half space above the  $x$  axis which coincides with an infinitely long plate oscillating in time with amplitude  $U$  and frequency  $n$ . This paper presents the results of a study of the same problem for an incompressible simple fluid of the memory type.

The mathematical problem satisfies the following field equations and boundary conditions.

$$\rho \frac{Dy}{Dt} = -\nabla\phi + \nabla \cdot \underline{\underline{S}}, \quad \phi = p - \rho gz, \quad \nabla \cdot \underline{y} = 0 \text{ in } R$$

$$y(x, 0, t) = e_x U \sin nt$$

$$y(x, y, t) \text{ is finite as } y \rightarrow +\infty$$

$$R = \{x, y \mid -\infty < x < +\infty, 0 \leq y < +\infty\}$$

The constitutive structure of the fluid given by the extra-stress response functional may be uniformly approximated by integral polynomials when the domain of the response functional is a suitable function space. The extra-stress can be expressed by a series of multiple integrals of tensor polynomials in the histories of the motion. The polynomial forms involving at most an  $N$  tuple integral are called stress tensors for fluids of integral type of order  $N$ .

$$\underline{\underline{S}} = \int_0^\infty \zeta(s) \underline{\underline{G}}(s) ds + \int_0^\infty \int_0^\infty \{ \beta(s_1, s_2) \underline{\underline{G}}(s_1) \underline{\underline{G}}(s_2) + \alpha(s, s) [\text{tr} \underline{\underline{G}}(s)] \underline{\underline{G}}(s) \} ds_1 ds_2 + \int_0^\infty \int_0^\infty \int_0^\infty \dots$$

where  $\zeta, \beta, \alpha$  are temperature dependent material functions and  $\underline{\underline{G}}$  represents the history of the motion.

It can be shown that for incompressible materials and for small strains the coefficient of the material function  $\alpha(s_1, s_2)$  is of third order in any perturbation analysis. Expressing the history  $\underline{\underline{G}}(s)$  by a series

$$\underline{\underline{G}}(s; U) = U \underline{\underline{G}}_1(s) + U^2 \underline{\underline{G}}_2(s) + O(U^3)$$

a new representation for the extra-stress may be obtained

$$\begin{aligned} \xi = & U \int_0^{\infty} \zeta(s) G_1(s) ds + U^2 \int_0^{\infty} \zeta(s) G_2(s) ds \\ & + U^2 \int_0^{\infty} \int_0^{\infty} \beta(s_1, s_2) G_1(s_1) G_1(s_2) ds_1 ds_2 + O(U^3) \end{aligned}$$

Field variables are expanded into perturbation series in terms of the amplitude  $U$  of the oscillation of the plate. At first order we find that there is no contribution to the pressure field and the velocity field is given by

$$\underline{v}^{<1>}(y, t) = \underline{e}_x (e^{-\lambda y + i n t} + e^{-\bar{\lambda} y - i n t}), \quad \lambda^2 = \frac{i \rho n}{\eta}, \quad \eta = \int_0^{\infty} G(s) e^{-i n s} ds$$

The symbol  $\langle \cdot \rangle$  denotes the partial derivative with respect to  $U$  evaluated at  $t = 0$ . To calculate second order variables the history of the first order motion must be computed. At second order a null velocity field is found and the pressure field is decomposed into a mean part, time averaged over a cycle of period  $2\pi/n$ , and a component which oscillates in time with frequency  $2n$ .

$$\phi^{<2>} = \phi_m + \phi_1 e^{2i n t} + \bar{\phi}_1 e^{-2i n t}$$

The shear relaxation and quadratic shear relaxation moduli  $G(s)$  and  $\Upsilon(s_1, s_2) = \Upsilon(s_2, s_1)$  derived from the material functions  $\zeta(s)$  and  $\beta(s_1, s_2)$  respectively are approximated by a Maxwell model of one degree of freedom  $k$ .

$$G(s) = -\frac{\mu}{\alpha_1} e^{-\frac{\mu}{\alpha_1} s}, \quad \Upsilon(s_1, s_2) = \alpha_2 k e^{-k(s_1 + s_2)}.$$

Then the pressure field at second order is represented by

$$\begin{aligned} \phi = & \rho n e^{-\sqrt{2} v y} \{ F_1(\mu, k, n, \alpha_1, \alpha_2) + F(\mu, k, n, \alpha_1, \alpha_2) \sin(2nt - \sqrt{2} v y) \\ & + F_3(\mu, k, n, \alpha_1, \alpha_2) \cos(2nt - \sqrt{2} v y) \} U^2 + O(U^3) \end{aligned}$$

$F_1, F_2, F_3$  are functions of the viscosity  $\mu$ , material constant  $k$ , frequency of the oscillation  $n$ , and the Rivlin-Ericksen constants  $\alpha_1, \alpha_2$ :

$$\begin{aligned} v = & \frac{\rho n \sqrt{\mu^2 + n^2 \alpha_1^2}}{\mu^2} \\ F_1(\mu, k, n, \alpha_1, \alpha_2) = & \frac{\sqrt{\mu^2 + n^2 \alpha_1^2}}{\mu^2} \left\{ \frac{2\mu^2}{\alpha_1 [1 + (\frac{\mu}{n\alpha_1})^2]} + \frac{\alpha_2 k}{n^2 [1 + (\frac{k}{n})^2]} \right\} \\ F_2(\mu, k, n, \alpha_1, \alpha_2) = & \frac{\alpha_2 k}{\mu^2 (k^2 + n^2)^2} (\mu n^2 + 2k\alpha_1 n^2 - k^2 \mu) - \frac{2\mu\alpha_1}{\mu^2 + 4n^2 \alpha_1^2} \\ F_3(\mu, k, n, \alpha_1, \alpha_2) = & \frac{\alpha_2 k n}{\mu^2 (k^2 + n^2)^2} (k^2 \alpha_1 + 2\mu k - \alpha_1 n^2) - \frac{4n\alpha_1^2}{\mu^2 + 4n^2 \alpha_1^2} \end{aligned}$$

## A SINGLE PARTICLE APPROACH FOR ANALYZING FLOW SYSTEM

by

Uzi Mann and Michael Rubinovitch  
 Department of Chemical Engineering  
 Texas Tech University  
 Lubbock, Texas 79409

Abstract

A methodology is presented for characterizing and analyzing general continuous flow system with special emphasis on particulate processes. The methodology is based on describing the history of individual particles (or fluid elements) in the process. The movements of particles are expressed in terms of the flow regions they visit using a Markov chain presentation. Explicit expressions as well as computational methods are derived for various process characteristics of interest. These include the distributions, means and variances of: the number of visits to any specified flow region; the total number of regions visited, and the number of visits to any specified set of regions. This methodology yields information on bulk properties as well as on individual particle behavior and deviations among particles.

Further, relationships between the local particle flow rate, number of visits to a flow region, and net flow rate through the system are derived. Specifically, it is shown that

$$\left( \begin{array}{c} \text{Flow rate} \\ \text{through a} \\ \text{region} \end{array} \right) = \left( \begin{array}{c} \text{net flow} \\ \text{rate through} \\ \text{the system} \end{array} \right) \times \left( \begin{array}{c} \text{mean number of} \\ \text{visits to the region} \\ \text{by a fluid element} \end{array} \right)$$

This relation is valid for any general flow system and any general region in the system. It holds true irrespective of the number of inlets and outlets to the region or of the nature of the internal mixing in the region. It is further shown how this relation leads to an experimental method for measuring local flow rates.

by

D. A. Nelson and E. J. Shaughnessy  
Duke University  
Department of Mechanical Engineering & Material Science  
Durham, NC 27706

Prevailing theories of interactions between electric fields and fluids often incorporate an assumption of constant fluid properties in the development of couplings between the equations of motion and Maxwell's equations of electrodynamics. This is a severe limitation in that two of the three electric body forces acting on the fluid arise from gradients in fluid properties (mass density and electric permittivity). These effects are included in the present theory by describing property variations by Taylor series expansions about a datum value. The first-order theory incorporates a number of additional terms beyond those described by Flippen's (1982) zeroth-order theory. Some of these terms can be neglected on the basis of physical estimates, leading to an electrohydrodynamic analog to the Boussinesq approximation of classical fluid mechanics. The interactions described by the theory include natural convection due to joule heating in the fluid, Coulombic and electrostrictive body forces, and interfacial tractions associated with permittivity gradients. The significance of each effect is then discussed using examples illustrating real situations in liquids and gases.

- [1] Flippen, L. D., "Electrohydrodynamics", Ph.D. dissertation, Duke University, 1982.

## FLUID DYNAMICS OF FOIL BEARINGS

by

Dr. Rama Subba Reddy Gorla  
Professor of Mechanical Engineering  
Cleveland State University  
Cleveland, OH 44115

A foil bearing consists of two surfaces, one sensibly rigid and the other relatively thin and flexible, separated by a fluid film induced by the motion of either one or both surfaces.

The theory of foil bearing was first investigated by Blok and Van Rossum [1]. Wildman and Wright [2] included the effect of external pressure on foil bearings. Further investigations are carried out by Eshel and Elrod [3], Ma [4], Barlow [5], and Eshel [6]. All these authors assumed that the lubricant fluid is incompressible with constant properties.

In the present work, the theory of fluid lubrication with a flexible boundary is studied. The effects of compressibility and variable viscosity are taken into consideration and the governing differential equations for the film thickness and the film pressure are derived. The general expressions for the load carrying capacity and the friction force of the bearing are shown. A numerical solution is presented for the nonlinear boundary problem and several examples are studied.

References

- [1] Blok, H. and Van Rossum, J. J., *Lubrication Engineering*, 9, 1976, pp. 310-320.
- [2] Wildman, M. and Wright, A., *Trans. ASME, J. Basic Engineering*, 87, 1965, pp. 631-640.
- [3] Eshel, A. and Elrod, M. G., *Trans. ASME, J. Basic Engineering*, 87, 1965, pp. 831-836.
- [4] Ma, J. T. S., *Trns. ASME, J. Basic Engineering*, 87, 1965, pp. 837-846.
- [5] Barlow, E. J., *Trans. ASME, J. Basic Engineering*, 87, 1965, pp. 986-990.
- [6] Eshel, A., *Trans. ASME, J. Lubrication Tech.*, 96, 1974, pp. 432-436.

ON MODELLING, INFORMATION CONSTRUCTION AND OPTIMIZATION FOR  
DISTRIBUTED PARAMETER CONTROL OF MULTICOMPONENT CHEMICAL PROCESSES

by

Dr. Eng. Waclaw Niemiec  
Silesian Technical University, Ul. Barska 33,  
PL-33-300 Nowy Sacz, Poland

Based on the reciprocity principle for isotropic and anisotropic nonhomogeneous media with space and time memories, a system of partial differential constitutive state equations describing multicomponent chemical processes in fluid- and gasphase are derived.

The system of partial differential constitutive state equations fulfills all conditions of mathematical model, as information for physical-chemical phenomenal distributed parameter control of multicomponent chemical processes in fluid- and gasphase.

The system of partial differential constitutive state equations for multicomponent chemical processes in fluid- and gasphase has been solved analytically. Obtained in this way: dynamical working space-time characteristics, statistical working space characteristics, dynamical phenomenal Green functions, as working space-time transfer functions, statical phenomenal Green functions, as space transfer functions are complete information for phenomenal distributed parameter control of multicomponent chemical processes in fluid- and gasphase. In these considerations important are properties of phenomenal Green functions, and superposition principle of potential fields to rotational fields.

EVOLUTION OF COMPRESSIBLE TURBULENT SEPARATED FLOWS  
IN THE NEIGHBORHOOD OF COMPRESSION/EXPANSION CORNER COMBINATIONS

by

A.A. Zheltovodov, E.H. Schilein, and V.N. Yackovlev  
USSR Academy of Sciences  
Institute of Theoretical and Applied Mechanics  
Novosibirsk 630090, USSR

The results of systematic experimental studies of the peculiarities of the turbulent boundary layer - shock waves and rarefaction fans mixed interaction in the neighborhood of corner configurations are considered. An asymptotic behavior of the large-scale separated zone with increasing an angle of deviation of the compression surface from  $0^\circ$  up to  $90^\circ$  is examined. The comparisons of the jet and separated flows specifying their similarity are carried out.

The feasible main factors determining the relaxation of the disturbed boundary layer at conditions of different flow prehistory are discussed. In particular, there is considered the influence of the turbulence intensity and scales as well as of the onset of regulated longitudinal vortices at some conditions and of the process of forming a new boundary layer after the mixing layer reattachment at separated flow conditions.

It is shown that the boundary layer - shock interaction and its separation prevent from the flow relaminarization in the negative pressure gradient regions. The physical phenomena explaining these peculiarities are considered. A systematic comparison with known experimental and computational studies is carried out.

NEW METHOD OF CALCULATION OF HIGH-SPEED  
GAS LUBRICATED BEARINGS

by

Vsevolod P. Shidlovsky  
Computing Center, Academy of Science of USSR  
Moscow 117333, USSR

and

Iraida I. Shidlovskaja  
Moscow Institute for Automotive and Highway Engineering  
Moscow, USSR

The majority of engineering methods for calculation of gas lubricated bearings is connected (sometimes implicitly) with neglect of the following parameters:

$$Re^* = Uh^2 / (LV_0), \quad \alpha = (\chi - 1) Pr M^2 \equiv (\chi - 1) Pr U^2 / (\chi p_0 \rho_0^{-1}), \quad \chi - 1 = (T_1 - T_0) / T_0.$$

where  $h$  is characteristic thickness of a lubrication layer,  $L$  - characteristic outer dimension of a bearing, while subscript "0" refers to characteristic values of some flow parameters, except of temperature for which might exist two characteristic values. Linearization approaches aimed at the enhancing of the ranges of variation of the parameters mentioned are not always correct and might lead to wrong conclusions.

Taking into account a statistics on working characteristics of gaseous bearings exploited in modern machinery one is led to conclusion that the only justifiable assumption in corresponding theory is that of a smallness of the parameter  $\lambda = h/L$ . As it was noted by Tuck & Bentwich (1983), under this assumption Navier-Stokes equations reduce to those of the boundary layer, but the main distinction of resulting theory from that of Prandtl consists in pressure gradient being not prescribed but serving as one of the unknown quantities. Moreover, the pressure distribution stays usually as a principal goal in solution of the problem.

Within the frame of 2D problem, boundary-layer type of presentation of the momentum and energy equations permits to reformulate these in form of integral relations. After using the approximate trigonometric representations for velocity and inverse temperature one is able to obtain a governing equation for the pressure variation in the lubrication layer. The equation obtained is not more difficult to solve than that of an ordinary gas lubrication theory [see, for example, Tipei (1962)], though its solution depends on three additional parameters:  $Re^*$ ,  $\alpha$  and  $\chi$ .

The method proposed is free of the limitations connected with classical theory and might be considered as universal, within the degree of accuracy determined by approximate representations of velocity and temperature

variations. The extension of a present approach to the 3D case remains to be a subject for future investigation.

#### References

- Tuck, E. O. and Bentwich M., "Sliding Sheets: Lubrication with Comparable Viscous and Inertia Forces", J. of Fl. Mech., Vol. 135, October 1983, pp. 51-69.
- Tipei, N., Theory of Lubrication, Stanf. Univ. Press, Stanford 1962

## ACOUSTIC EMISSIONS AND THE MICRODEFORMATION OF ROCKS

by

Ted A. Koelsch  
Exxon Production Research Co.  
Houston, Texas 77001

Acoustic emission detection and analysis has proven to be very useful in the experimental study of the micromechanics of rock deformation. Investigations using both brittle and ductile rocks indicate that detectible emissions are generated by non-fracturing twinning processes as well as microfracturing.

Analysis of the acoustic signals generated during the ductile deformation of triaxially deformed marble revealed two major types of signals. These signals were distinguishable by their main frequency content and waveform. From the comparison of these signals with simultaneous dilatancy, load-displacement, and velocity change measurements, a specific correlation of these signals to microscopic twinning and microfracturing processes could be made. These correlations were then used to study the effect of confining pressure and grain size.

The results from this study demonstrated: 1) the importance of twinning as an effective mechanism for microfracture nucleation, and that 2) the increase in ductility observed as a function of confining pressure and grain size was due to increases in both the degree of intracrystalline twinning and the stability of microfracture propagation.

THE OBSERVATION OF LOCALIZED DILATANCY  
BY ULTRASONIC COMPUTER TOMOGRAPHY

by

Takashi Yanagidani  
Department of Mineral Science and Technology  
Faculty of Engineering Kyoto University  
Kyoto, 606 Japan

To observe how dilatancy localizes before faulting under uniaxial compression, ultrasonic computer tomography is applied. This is to reconstruct the profile of a P-wave velocity inhomogeneity within a certain sliced plane using many scanned travel time data. And that is analogous to the technique used in Computer Assisted Tomography (CAT or CT) in radiology except that ultrasonics are used as radiation instead of X-rays. The transmission of seismic waves carries the information along the propagated path. The spatial distribution of propagation velocity is calculated from line integrals along rays in the scanned plane by assuming straight ray path. Algebraic reconstruction technique (SIRT) is used, because that works for asymmetric objects and imperfections in the data set. Here we present the preliminary result of reconstruction made on the sample that was recovered intact at the post-peak region. The velocity field within the plane parallel to the loading axis is reconstructed (Figure 1). It is clear that the microcracks localize into the central portions of the sample. The relatively high velocity cells form the hourglass-like structure. Furthermore the reconstructed velocity profile is in good agreement with the densities of dye-impregnation after the travel time measurements. The effects of velocity anisotropy and ray bending on the reconstruction are also discussed.

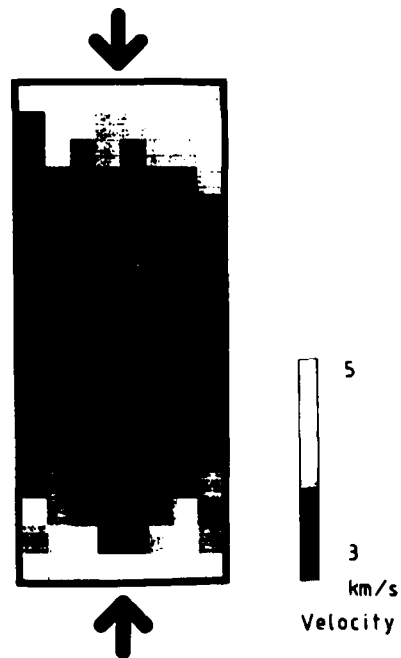


Figure 1. Velocity inhomogeneity of Ohshima granite that is recovered intact beyond the peak stress.

## A MEGAHERTZ SEISMOMETER FOR NONDESTRUCTIVE TESTING

by

H. Spetzler<sup>+</sup>, F. Boler<sup>+</sup> and I. C. Getting<sup>o</sup>

<sup>+</sup>Department of Geological Sciences and Cooperative Institute  
for Research in Environmental Sciences, Box 449,  
University of Colorado/NOAA Boulder, CO 80309

<sup>o</sup>Cooperative Institute for Research in Environmental Sciences,  
Box 449, University of Colorado/NOAA, Boulder, CO 80309

A useful seismometer for earthquake studies measures surface displacements, has a known sensitivity, a known frequency response and has a sensor that has dimensions that are a small fraction of a wavelength. Conventional transducers that are used for the detection of acoustic emissions (AE) during nondestructive testing, do not fit the above description of a seismometer. In general, their size is on the order of several wavelengths and they have various resonance modes in the frequency range of interest. These characteristics make them useful for measuring first arrivals for the location of AE, possibly for determining first motion for obtaining initial slip direction and for obtaining the rate at which AE occur. Beyond that, little information that is not contained in the first arrival can be milked from the AE signal.

We have built a seismometer that has a flat frequency response from 50kHz to 6MHz. It has a sensing area that is a small fraction of one mm<sup>2</sup> and a sensitivity of 2mV/nm with a displacement resolution of  $\sim 10^{-11}$  m, approaching that of conventional piezoelectric transducers. At this time our seismometer measures only one component of motion, that perpendicular to the surface. We are however developing a three component seismometer.

The seismometer incorporates the technology that RCA (Radio Corporation of America) developed for their Video Disc system. The sensing element is a capacitor ( $10^{-5}$  pF) that is formed between the flame polished end of a 100 $\mu$ m diameter platinum wire and the conducting surface of the specimen. This capacitance probe is part of a 910MHz resonance circuit. Changes in distance between the probe and the specimen surface change the resonance frequency which after demodulation constitutes the desired signal. The average distance between the probe and the specimen surface is maintained at approximately 100nm. This is accomplished by advancing or retracting the platinum probe which is attached to the diaphragm of a small commercial loudspeaker. A feedback circuit with a response time of  $\sim 0.3$ sec controls the current to the loudspeaker coil and maintains a constant resonance frequency.

The seismometer is presently used in studying acoustic signals from conventional fracture mechanics tests and in the calibration of piezoelectric transducers.

FRACTURE CLOSURE IN ROCKS UNDER STRESS:  
THE EFFECT ON FLUID AND ELECTRICAL TRANSPORT

by

Michael L. Batzle  
ARCO Oil and Gas Company  
Exploration and Production Research Center  
P. O. Box 2819  
Dallas, Texas 75221

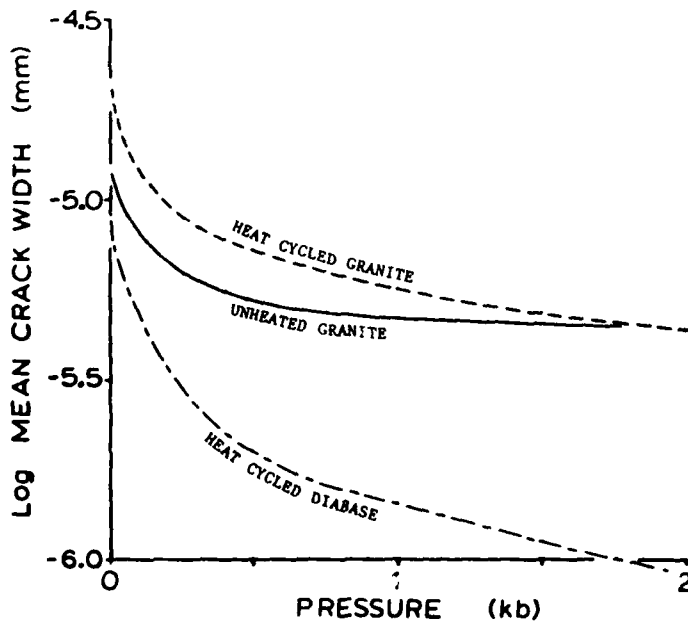
In tight rocks, fractures may provide the only paths for fluid and electrical transport. Confining pressure forces the fractures to close, progressively reducing or eliminating flow paths. The specific pressure behavior is dependent on the surface topography of the fractures and the closure mechanism. Strain, water permeability, and electrical conductivity were measured on samples of Westerly (RI) granite and Frederick (Md) diabase as functions of pressure. The measurements were made on both unheated samples and samples heat cycled at room pressure to as much as 700°C. Thus, we could examine the effects of both natural and artificial, thermally induced microcracks as these cracks closed under increasing stress.

The new population of cracks produced by heat cycling increased the flow properties of the rocks by orders of magnitude. In the granite, this population is superimposed on a pre-existing set of fractures. Permeability and conductivity in the unheated granite drop rapidly at low pressure, but reach approximately constant values at higher pressure. The initial increases in flow properties and fracture porosity in the heat cycled granite are decreased rapidly with pressure. By two kilobars confining pressure, the new fractures have all been effectively closed and the flow values have been reduced to those of the unheated granite at the same pressure. The unheated diabase has no measurable fracture porosity and as a result the permeability and conductivity are too low to measure. Heat cycling produces sufficient fracture paths to give the diabase permeabilities and conductivities similar to those of the granite. The decrease in these transport properties with pressure is initially slower in the heated diabase than in the granite. However, at higher pressures, the values for the heated diabase continue to decline since there is no initial population to limit the decrease. These behaviors can be seen in the calculated mean crack width shown in the figure. Assuming that all flow is through a single planar fracture, the permeability and conductivity can be used to calculate the width. The new cracks in the diabase continue to close with pressure, in contrast to the granite at high pressure.

These same unheated and heat cycled rocks were observed in the scanning electron microscope (SEM) under uniaxial stress. Good qualitative agreement was found between the fracture behavior indicated by the flow properties and the behavior observed in

SEM. The natural fractures in the unheated granite have irregular mismatched walls. This is a result of in situ mineral solution or deposition on the walls. As a result, the crack is propped open and closure is slow and inefficient. The new cracks in the heat cycled granite, however, have opposing walls that are well matched. Closure is rapid and efficient at low stress. The heat cycled diabase also has fractures with well matched walls. Closure also tends to be complete, but it is much slower. This may be due to the observed increase in slippage along the fracture, rather than just closure normal to the walls.

The cracks can be modelled as opposing surfaces covered with bumps or asperities. By using suitable spatial and height distributions of these asperities, stress-deformation relationships can be developed to describe fracture closure, permeability, and conductivity. Crack closure with pressure is impeded as asperities come into contact across the crack. Natural fractures, being rough and irregular, can be modelled with densely spaced asperities with a wide distribution of lengths. Inducing new fractures superimposes new distributions. Asperities are longer but sparser in the artificial cracks. Hence, although the transport properties are initially greater, these new cracks close more rapidly since they have fewer asperities acting as proppants.



MICROMECHANICS OF THERMAL CRACKING AND SHEAR LOCALIZATION  
IN CRUSTAL ROCKS

by

Teng-fong Wong  
State University of New York  
Department of Earth & Space Sciences  
Stony Brook, New York 11794

Scanning electron microscopy has been performed on several crustal rocks (Westerly granite, San Marcos gabbro, Frederick diabase) which were either heated to temperatures up to 800°C or mechanically deformed through the pre- and post-failure stages.

Thermoelastic mismatch and thermal expansion anisotropy induced microcracks to initiate at triple junctions and propagate along grain boundaries at relatively low temperatures. Further heating results in intragranular cracking in a radial direction, and no appreciable crack coalescence is observed except at very high temperatures. Stereological techniques were used to characterize the crack orientation distribution and no significant thermally-induced anisotropy was observed. The micromechanics of thermal cracking can be modelled with linear elastic fracture mechanics in a relatively simple manner.

On the other hand, samples which have undergone different stages of deformation under conventional triaxial loading show significant stress-induced anisotropy. Extensive microcrack interaction and coalescence are observed in samples deformed to near the peak stress and through the post-failure region, culminating in shear localization. The micromechanics of faulting is influenced by mineralogy, grain orientation and grain scale inhomogeneity including pre-existing cracks, pores, elastic anisotropy and cleavage planes.

## ANISOTROPIC DAMAGE SURFACES FROM ACOUSTIC EMISSIONS\*

by

David J. Holcomb and Larry S. Costin  
Sandia National Laboratories  
Geomechanics Division, 1542  
Albuquerque, NM 87185

Under compressive stresses, brittle polycrystalline materials fail as the result of the accumulation of multiple microfailures. Constitutive laws for such materials must incorporate the effects of the microfailures, in particular, the inelastic strain and reductions in elastic moduli. Attempts have been made to model the accumulating damage using plasticity theory, but little success has been achieved. Dilatancy (increase in volume under compressive loading) and changing moduli are not readily compatible with the usual formulations of plasticity. A straightforward approach, attempting to calculate individual microfailures, is not useful because of the myriad of failures involved. An alternative method of incorporating accumulating failures into a continuum model is to replace the details of crack density, size, orientation, and development with a state variable, damage. For damage to be a useful concept, a method must be found for measuring the relationship between  $D$  and  $\sigma_{ij}$  or  $\epsilon_{ij}$ .

We are developing techniques for measuring damage in brittle materials. An analogy with the more familiar field of plasticity may be helpful in indicating the direction of our research. In developing constitutive equations for elastic-plastic materials, an essential element is the yield surface which is the boundary between states where the material is elastic and states where plastic strain is generated. Various simple analytical expressions, such as the yield criteria of von Mises or Tresca, are used to represent the yield surface. These expressions are a compromise between convenience for the theorist and the realities of material behavior. Usually the forms chosen are isotropic, but anisotropy can also be accommodated. Experimentally, the yield surface is defined by the locus of points on various paths in stress space beyond which plastic strain is observed. Damage, in the sense used here, is analogous to plastic strain in an anisotropically hardening material.

Our method for detecting damage is based on a generalization of the Kaiser effect for acoustic emissions, originally discovered in tensile testing of metals by Kaiser. Since acoustic emissions (AE) are assumed to be the elastic energy released from local failure, it seems plausible that AE could be used as an indicator of stress states that produce damage. Then surfaces of constant damage could be mapped by approaching the surface along different stress paths, using the onset of acoustic emission activity as an indicator that the surface had been reached. The simplest example of this method of defining and locating damage surfaces is the Kaiser effect, which can be viewed as a means of detecting, at one point in stress space, a previously generated damage surface.

\*This work was supported by the U.S. Department of Energy.

Our work to date, using granite, has shown that an anisotropic damage surface can indeed be induced and then detected using the onset of acoustic emissions. Having determined the initial damage surface, which was spherical, by uniaxial testing of variously oriented core from the as-received sample, the next step was to modify the damage. To do this, a large sample was stressed until the preexisting damage surface was reached, as indicated by acoustic emissions, and then exceeded. Initial sample size was sufficiently large that subcores could be taken at various orientations. This required an initial sample size to be about 20 cm by 40 cm in length. The newly induced damage surface was determined by taking subcores at various orientations relative to the load axis and conducting triaxial tests on each subcore, while monitoring for acoustic emissions. When the stresses at which acoustic emissions had begun in the subcore were plotted as a function of subcore angle from the initial loading axis, an ellipsoidal damage surface was revealed. Along the initial loading axis, the damage surface had elongated to the stress reached in initial loading. At  $90^\circ$  to the initial loading axis, the damage surface was reached at the same stress as in the unstressed sample. At intermediate angles, intermediate stresses were required to induce acoustic emissions.

## MODELS FOR ROCK BOLTING STRATEGIES IN UNDERGROUND OPENINGS

by

Adrian M. Crawford and K.C. Lau  
University of Toronto  
Department of Civil Engineering  
Toronto, Ontario Canada M5S 1A4

For most mining and civil engineering structures situated in rock, the presence of a discontinuous media is inevitable and unavoidable. As a consequence, the engineer must design an opening or slope taking account of the presence of such discontinuities. This paper addresses the problem of predicting the support requirements for underground excavations in jointed rock masses.

A numerical, mechanistic model is developed, the basis of which is the generation of discontinuity patterns in two-dimensions using Monte-Carlo simulation techniques. Input parameters include the statistical distributions of joint lengths and joint spacings. From such an analysis, the sizes and distributions of isolated wedges of rock may be determined. Combined with a knowledge of the in-situ stress conditions, the physical properties of the rock discontinuities and opening dimension the stability of such wedges may be evaluated. If the wedges are non self-supporting, a strategy has been developed to determine the optimum size, spacing, length and hence the cost of the required rock bolt support system.

From a consideration of these cases, it is deduced that the average joint spacing and average joint length have an influence not only on the bolt length and bolt spacing but also on the bolting strategy for underground openings. For openings in closely spaced joint systems it is more reasonable to use pattern bolting, while for wider space joints spot bolting is more economical. Nevertheless, for each case it is possible to estimate the numbers of bolts required. The effect of decreasing the mean joint length is to decrease the required length of rock bolt.

The work presented in this paper provides a mechanistic basis for an understanding of the behavior of underground openings in jointed rock masses. It gives insight into the physical phenomena and is relatively uncomplicated and simple to implement. The proposed method is compared with currently used practical techniques which are based on interaction analyses or rock mass classification systems.

PLASTICITY THEORY FOR FRICTIONAL  
COHESIONLESS SOILS

Jean H. Prevost  
Princeton University  
Department of Civil Engineering  
Princeton, NJ 08544

A general analytical model which describes the nonlinear, anisotropic, path-dependent stress-strain-strength properties of cohesionless soils is presented. The model is based on kinematic plasticity theory and uses the concept of multiple yield surfaces. In order to reflect the strong frictional dependence of cohesionless soils on their behavior, the yield surfaces are taken as conical. The multi-dimensional constitutive equations are presented. It is shown that the model parameters required to characterize the behavior of any given soil can be derived entirely from the results of conventional triaxial soil tests. The model's accuracy and versatility are illustrated by a number of examples. Implementation of the model in a general finite element program is discussed.

**SOIL ELASTOVISCOPLASTICITY**  
**A Macroscopic Answer and a Microscopic Challenge**

Yannis F. Dafalias, Victor Kaliakin, and Kandiah Arulanandan  
Department of Civil Engineering  
University of California Davis  
Davis, CA 95616

**ABSTRACT**

Soils exhibit deformation characteristics which can be described macroscopically within the framework of combined elastoplasticity-viscoplasticity. Such characteristics are rate independent, rate dependent and time dependent irreversible responses. Focusing on the last two, the rate dependent response is more difficult to measure experimentally in a way that guarantees the stress/strain homogeneity of the macroscopic sample. On the other hand, the time dependent response is a well-established behavior in soil mechanics commonly called secondary consolidation, for drained conditions, or deviatoric creep strain and pore water pressure increase with time under undrained conditions. A consistent constitutive model should be capable of predicting all these aspects of soil deformation, and such a model is presented using the macroscopic concepts of overstress and bounding surface elastoviscoplasticity.

This macroscopic approach yields successful simulation of experimental data on triaxially loaded specimens of clays. In constructing the model, different constants are introduced. It is clear what kind of effect these constants have on the modeling of the soil response and, therefore, this is the key for their macroscopic calibration, often by trial and error. But it is not clear how these constants can be related to the microscopic soil structural characteristics such as formation of domains connected by weak chains of particles, cluster formation with intra and intercluster voids (double porosity), viscous properties of double-layer formations, mineral and pore fluid composition, etc. This constitutes a formidable challenge indeed to a microscopic approach. It even poses a question utilitarian in nature: to what extent a micro to macroscopic connection can provide useful information for the latter? This point is discussed briefly from the point of view of difficulties associated with the macroscopic calibration of the constitutive model, and the characterization of the microstructure by nondestructive techniques. An example of the latter is ongoing research under the direction of the third author to obtain information on the inter and intracluster voids by electrical measurements of conductivity and dielectric constants of a soil sample, and their relation to macroscopic parameters entering the constitutive model.

MODELING OF INELASTIC, FRICTIONAL, CONTACT FORCES IN  
FLOWING GRANULAR ASSEMBLIES\*

by

Otis K. Walton, Julius Brandeis, John M. Cooper  
Lawrence Livermore National Laboratory  
Livermore, CA 94550

A partially latching normal spring coupled with incrementally slipping tangential friction is used to model the contact forces between inelastic frictional spheres. This model eliminates force discontinuities present in previous visco-elastic models. It also produces force deflection curves that closely resemble the actual forces existing between elastic-plastic spheres with friction. The approximate Hertzian theory for normal contact forces acting between elastic bodies and Mindlin's description of the tangential friction forces acting in such contacts served as guides in developing this model. Dynamic and quasistatic finite element calculations of normal forces acting between elastic and elastic-plastic spheres indicate that a nearly linear force-deflection relation can replace Hertz's three-halves power relation when elastic-plastic spheres interact. A linear unloading at a steeper slope closely resembles the finite element unloading curve and also produces the desired inelastic collision behavior. The slope selected for unloading depends on the maximum loading achieved so that the variation of the coefficient of restitution with impact velocity agrees with measured behavior.

The model is implemented in a computationally efficient algorithm that avoids calls to any square-root or trigonometric functions and is coupled with a simple "leap-frog" integration of the differential equations-of-motion of each granule in a molecular-dynamics like simulation of granular flow. This model is being used in a calculational study of the shearing behavior of flowing granular solids.

\*Work performed under the auspices of the U.S. Department of Energy by the Lawrence Livermore National Laboratory under contract number W-7405-ENG-48.

## DISCRETE ELEMENT MODELS FOR ROCK

by

Michael E. Plesha  
University of Wisconsin  
Department of Engineering Mechanics  
Madison, WI 53706

Many types of rock are characterized by nonlinear mechanical behavior. These nonlinearities arise primarily from the interaction of intact pieces of rock along frictional boundaries and from the formation and nucleation of microcracks and fractures within the rock itself. Discrete element, or rigid block computer modeling techniques have been shown to be very useful for the qualitative and quantitative analysis of the mechanical response of such a medium.

This presentation will feature an overview of the discrete element method in which a two-dimensional aggregate medium is idealized as a system of rigid bodies which interact along common straight boundaries. Emphasis will be placed on the development of constitutive laws which characterize how the pieces of the aggregate interact; since the intact pieces of rock are assumed to be rigid, this permits attention to be focused on the effects of the aggregate interface constitutive relations alone.

Examples will be considered involving the static and dynamic behavior of tunnels and caverns sited in densely jointed rock. In these examples, the joint constitutive equations are obtained using a Coulomb friction law and a zero joint tension constraint. The primary source of nonlinearity is due to joint slip and separation. Also to be considered is the mechanical response of a cemented aggregate material in which the aggregate interfaces have finite tensile and shear strengths. The primary source of nonlinearity is due to the formation and nucleation of microcracks.

## THE MICROPHYSICAL APPROACH TO CONSTITUTIVE MODELING

by

L.G. Margolin  
Earth and Space Sciences Division  
Los Alamos National Laboratory  
Los Alamos, N.M. 87545

The inelastic response of solids can often be associated with changes in the microstructure of the solid material. For example, fracture can be described in terms of the growth, interaction, and coalescence of microcracks that are present in brittle materials. Thus, one might expect that a constitutive model for brittle materials would be based on crack mechanics. However, most constitutive models of inelastic behavior, including fracture, are macroscopic -- are based on plasticity theory -- and ignore the microstructure.

Constitutive models that contain a detailed description of microstructure are called microphysical models. The microphysical approach is a relatively recent and attractive alternative for representing inelasticity. The key element of the microphysical approach is the use of effective elastic moduli to relate the microscopic detail to macroscopic material properties. The effective moduli allow us to write the constitutive law in the form of an equation of state. That is, stress is uniquely determined as a function of strain plus certain internal variables that arise naturally from the theory.

The rate equations derived from a constitutive law based on effective moduli have the form of a Maxwell (viscoelastic) solid with variable relaxation times. In this form, we can explicitly identify the inelasticity with the evolution of the microstructure. One advantage of the microphysical approach is the identification of model parameters with physically measurable quantities. It is important to emphasize that the microphysical models are not equivalent to plasticity theory. Plasticity does not contain any fundamental scales of length nor time. The microphysical models do contain embedded scales of length and time which enable their use over a wide range of physical phenomena. That is, the microphysical models are capable of scaling without varying the parameters of the model.

by

Wolf Elber  
NASA Langley Research Center  
Hampton, Virginia 23665

The development of new high-performance composite materials is largely driven by the aerospace industry. They require a damage tolerant composite for both tension and compression loading for which the manufacturing costs can be foreseen to remain competitive with the metallic materials they replace. In the search for impact toughness, resin energy absorption has been singled out as the prime material parameter requiring improvement. But many of the resulting new thermoset matrix materials fail to meet requirements of long-term or hot/wet compression stability. While several promising thermoplastics can meet these criteria, it is difficult to envision how they can be used at competitive cost levels. The research community must realize that composite materials may be at a critical point in their development. Major jumps in resin technology or producibility are needed rather than exhaustive refined descriptions of material behavior. New opportunities for application of composite materials to primary aircraft structure may appear within the next decade. If suitable materials are not available, manufacturers may well elect to accept the incremental improvements that can be achieved with improved aluminums and a "window of opportunity" may be missed.

## THE PHYSICAL AND MATHEMATICAL DESCRIPTION OF CREEP DAMAGE

by

F. A. Leckie

Department of Mechanical Engineering and  
Theoretical and Applied Mechanics  
University of Illinois Urbana-Champaign  
Urbana, IL 61801

When metals are subjected to stress at temperatures in excess of  $0.3T_m$  where  $T_m$  is the melting temperature of the material, it is observed that the metal suffers time-dependent deformation. It is also observed that the deformation rate increases with time until the metal ruptures. For low stress levels and long rupture times the rupture strains can be very small and specimen thinning does not take place. Metallurgical investigation often reveals that the material has suffered damage in the form of voids which have nucleated and grown on the grain boundaries. The presence of damage causes an increase in the deformation rate, and it is the coupling between the damage and deformation rate equations which is responsible for the tertiary portion of the creep curve. The results of multiaxial stress loading experiments indicate that the damaged state is frequently anisotropic, and that rupture times are dependent on the triaxial nature of stress as well as on its level.

In the presentation some of the damage growth mechanisms will be discussed. A tensorial description of damage will then be presented and it will be shown how this description is related to the actual physical damage by means of a tensor series. The results of non-proportional stress paths on the behavior of different metals will be described and it will be shown how suitable constitutive equations which describe the growth of both the growth of damage and strain can be developed.

## A STUDY OF WEAR AND FATIGUE IN A HSLA STEEL

by

Nabil A. Ibrahim  
Department of Manufacturing & Mechanical Engineering  
Bradley University  
Peoria, IL 61625

and

George M. Romack  
TC-A Vehicle Performance & Dynamics  
Caterpillar Tractor Co.  
Peoria, IL 61629

A high strength low alloy (HSLA) steel has been heat treated in order to produce two different microstructures. The first microstructure consisted of ferrite plus pearlite ( $\alpha+P$ ) while the second microstructure consisted of ferrite plus martensite ( $\alpha+M$ ). Abrasive wear and fatigue tests were systematically performed on each microstructure. The wear resistance was quantified in terms of wear factor while fatigue resistance was quantified in terms of a fatigue strength parameter. Tensile data were generated in order to determine the work hardening characteristics of each microstructure. The ( $\alpha+P$ ) microstructure was characterized by high ductility, moderate strength but relatively low work hardening capacity. The ( $\alpha+M$ ) microstructure was characterized by high ductility, moderate strength but relatively low work hardening capacity.

The ( $\alpha+M$ ) microstructure showed superior wear resistance associated with higher fatigue strength compared with the ( $\alpha+P$ ) microstructure. A model based on the concept of a localized critical strain energy has been developed to rationalize data. The model emphasizes the importance of work hardening and fracture toughness in current attempts to optimize wear and fatigue resistance of high strength steels.

CIRCULAR DUCTILE CRACK IN A TRANSVERSELY  
ISOTROPIC PLATE OF FINITE THICKNESS

by

Y.M. Tsai  
Iowa State University  
Department of Engineering Science and Mechanics  
Ames, Iowa 50011

Many fiber-reinforced composite materials and platelet systems are characterized as transversely isotropic media which have five elastic constants (1). Metallic substances which have hexagonal aeolotropic crystals are also characterized as being transversely isotropic. The techniques of two harmonic functions were used to investigate the three-dimensional stress distributions in transversely isotropic media (2).

In the present work, the Dugdale model has been extended to the problem of an internal penny-shaped crack in a transversely isotropic plate of arbitrary thickness. The problem is solved using the techniques of Hankel transform. An exact expression for the finite stress condition at the crack tip is obtained and written as a non-dimensional function of the ratios of material constants. The expression is used to determine the width of the inelastic annulus zone surrounding the crack. After the finite stress condition is satisfied, the normal stress at the outer tip of the inelastic zone is shown to be continuous at the value of the material yield stress.

Exact expressions for the crack shape function and the crack opening displacement are also obtained and written as the product of dimensional quantities and a non-dimensional function. The values of the non-dimensional functions were calculated numerically for five different materials. E glass-epoxy and graphite-epoxy composites and magnesium were used as example materials, and all gave real characteristic roots. An isotropic material and zinc which gave complex roots were also used as example materials.

The effects that the material anisotropy has on the inelastic zone size, the crack shape, and the crack opening displacement are clearly revealed in the numerical results obtained. The effects of material anisotropy for the composites are compared to those for the metallic substances.

ACKNOWLEDGMENT

This research was supported by the Engineering Research Institute of Iowa State University.

REFERENCES

1. Christensen, R.M., Mechanics of Composite Materials, John Wiley & Sons (1979), P. 75 and 140.
2. Elliott, H.A., "Three-Dimensional Stress Distributions in Hexagonal Aeolotropic Crystals," Proc. Cambridge Philos. Soc., Vol. 44 (1948), pp. 522-533.

## A DISLOCATION APPROACH TO STEADY CRACK GROWTH

by

Mitsunori Denda  
Rutgers University  
Department of Mechanics and Materials Science  
New Brunswick, NJ 08903

A numerical study is made of steady-state crack growth under the assumption of small scale yielding. A mode I plane strain crack in an elastic-ideally plastic solid with Poisson's ratio  $\nu = 0.5$  is investigated. The formulation is based on dislocation theory.

A dislocation dipole which represents a slip over an infinitesimal slip line is defined. The problem is discretized by introducing a mesh. In this mesh, the plastic slip in each of the active or yielded elements and its trailing wake is represented by a continuous planar distribution of dislocation dipoles. The Green's function for each slip element is obtained using the analytic function method of a complex variable. The total stress is expressed, through superposition, in terms of the unknown quantities associated with the plastic slip rate in each of the active elements and the applied stress intensity factor. A yield condition is applied to each active element to determine these unknown quantities.

The numerical results verify nearly all the near crack tip features discovered earlier by others in analyses focusing on the asymptotic behavior near the advancing crack tip. The exception is the angular extent of the elastic unloading sector behind the tip. In addition, a basic parameter which cannot be obtained in the asymptotic analysis is determined from the numerical results.

To produce competitive results, in terms of accuracy, the proposed numerical approach requires significantly fewer elements than in the finite element method approach to the same problem. On the other hand, the method used for solving the simultaneous equations was more laborious than corresponding techniques which have been used to obtain finite element solutions.

ELASTIC BUCKLING OF A CRACKED COLUMN BY  
SUBTANGENTIAL FORCE

by

A.K. Azad, N. Al-Shayea and M.H. Baluch  
University of Petroleum & Minerals  
Department of Civil Engineering  
UPM Box No. 1469, Dhahran, Saudi Arabia

In recent years, advances in fracture mechanics have led to the study of the influence of flaws or cracks on the structural stability of frame type members. Refs. (1) and (2) have attempted to objectively determine the effect of a single crack on the stability of columns by adopting a structural model in which a nonpropagating Mode I type crack is modelled as a rotational spring of known compliance.

In this paper, the elastic stability of a cracked cantilever column subjected to a nonconservative force has been reexamined to generate the stability boundaries for various crack compliances and prescribed line of action of the applied force. The latter varies from the case of a pure axial load (Euler column) to that of a tangential load (Beck's column). The mathematical model used is essentially similar to that proposed in Refs. (1) and (2) but incorporates a correction to an erroneous boundary condition stipulated in (2) that led to controversial conclusions.

The results presented demonstrate the influence of single or two multiple cracks of known compliances on the divergence and flutter stability of a cantilever column subject to a follower force by comparing the results with those of a perfect column (3).

REFERENCES

1. Okamura, H., Liv, H.W., Chu, C.S. and Liebowitz, H., "A Cracked Column Under Compression," Engg. Fracture Mech., Vol. 1, 1969.
2. Antifantis, N. and Dimaroganas, A., "Stability of Columns with a Single Crack Subjected to Follower and Vertical Loads," Int.

## DYNAMICS OF A BODY SUPPORTED BY SHEAR SPRINGS\*

by

Millard F. Beatty  
Department of Engineering Mechanics  
University of Kentucky  
Lexington, KY 40506

The exact solution of the problem of the undamped, finite amplitude oscillations of a mass supported symmetrically by simple shear mounts, and perhaps also by a smooth plane surface or by roller bearings, is derived for the class of isotropic hyperelastic materials for which the strain energy is a quadratic function of the first and second principal invariants and an arbitrary function of the third [1]. The Mooney-Rivlin and Hadamard material models are special members for which the finite motion of the load is simple harmonic and the free fall dynamic deflection always is twice the static deflection. Otherwise, the solution is described by an elliptic integral which may be inverted to obtain the motion in terms of Jacobi elliptic functions. In this case, the frequency is amplitude dependent; and the dynamic deflection in the free fall motion from the natural state always is less than twice the static deflection. Some results for small amplitude vibrations superimposed on a finitely deformed equilibrium state of simple shear also are presented. Practical difficulties in execution of the simple shear, and the effects of additional small ending deformation are discussed [2]. Instability induced by inertial effects acting on a vehicle which is supported by shear springs is described [3].

References

1. Beatty, M. F., "Finite Amplitude Vibrations of a Body Supported by Simple Shear Springs", J. Appl. Mech., 1984 (In Press).
2. Rivlin, R. S., and Saunders, D. W., "Cylindrical Shear Mountings", Trans. Inst. Rubber Ind., Vol. 24, 1949, pp. 296-306.
3. Beatty, M. F., and Bhattacharyya, R., "Motion of a Vehicle Supported by Shear Springs", (In Preparation).

---

\* This work was supported by a grant from the National Science Foundation.

EXPONENTIALLY STABILIZING FINITE-DIMENSIONAL CONTROLLERS  
FOR LINEAR DISTRIBUTED PARAMETER SYSTEMS

by

Mark J. Balas, Associate Professor  
Electrical, Computer & Systems Engineering Department  
Rensselaer Polytechnic Institute  
Troy, NY 12181

The Galerkin method is presented as a way to develop finite-dimensional controllers for linear distributed parameter systems (DPS). The direct approach approximates the open-loop DPS and then generates the controller from this approximation; the indirect approach approximates the infinite-dimensional stabilizing controller. The indirect approach is shown to converge to the stable closed-loop system consisting of DPS and infinite-dimensional controller; conditions are presented on the behavior of the Galerkin method for the open loop DPS which guarantee closed-loop stability for large enough finite-dimensional approximations.

## FREE AND FORCED RESPONSE OF A COMBINED STRING-OSCILLATOR SYSTEM

by

Lawrence A. Bergman and James W. Nicholson  
 Department of Theoretical & Applied Mechanics  
 University of Illinois at Urbana-Champaign  
 Urbana, IL 61801

A new result, recently reported by the authors, for the determination of the exact natural frequencies, mode shapes, and the orthogonality relation for combined linear undamped dynamical systems is discussed in the context of a uniform taut string coupled to a multiplicity of linear oscillators (see Figure 1). The problem is solved by the method of separation of variables, and the solution is given in terms of the Green's function of the vibrating string, which is readily found. The method encompasses distributed structures, such as strings, membranes, beams, plates, etc., coupled at discrete points to masses, linear oscillators and spring supports, as well as to other distributed structures.

The forced response to arbitrary loading of the string and/or one or more oscillators is obtained by expansion in terms of the undamped modes of vibration and subsequent modal analysis. The criterion to be satisfied for a proportionally damped system is identified, and the exact closed form solution for the response is given as an infinite series. When the criterion is not satisfied, the system is nonproportionally damped. The modal expansion is truncated at a finite number of terms,  $N$ , and a discrete eigenproblem of dimension  $2N$  is solved for the "damped modes" of vibration. An approximate closed form solution for the system response is given as a weighted sum of these "modal" solutions.

Two pertinent examples are discussed. In the first, the string-oscillator system is subjected to an inertial load, modeled by a unit step acceleration at the supports. In the second, a unit impulse is applied to an oscillator. For both, response are computed at various locations along the string and at the oscillators.

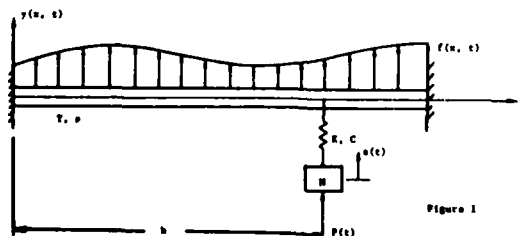


Figure 1

A CONTROLLER/STRUCTURE DESIGN OPTIMIZATION  
APPROACH FOR MANY DEGREE OF FREEDOM SYSTEMS

John L. Junkins  
Department of Engineering Science and Mechanics  
Virginia Polytechnic Institute and State University  
Blacksburg, Virginia 24061

We consider the problem of simultaneously optimizing a set of dynamical model and control system parameters imbedded a discrete linear dynamical system (e.g., a linear elastic structure) with input from a linear, constant gain, output feedback control system. The present developments are designed to begin where traditional methods end; namely we assume a nominal structural design and a nominal control system design are available as the starting point. The nominal control system design would probably, but not necessarily, be the result of an optimal regulator design for a fixed nominal specification of the structural parameters. We submit that both the structure and the control system parameters should be considered as subjects for further optimization. However, it is apparent that the high dimensionality of such optimization problems is a serious obstacle to achieving practical results.

We define optimality and constraint criteria in the eigenspace of the closed loop system. We introduce homotopy and continuation algorithms for modifying simultaneously chosen finite subsets of structural parameters (e.g., cross section areas, mass parameters for discrete elements, etc.) and control system parameters (e.g., control gains, actuator locations, sensor locations, etc.) to move toward a more favorable design, vis-a-vis the eigenspace optimality and constraint criteria. Implicit in the algorithm is the decision to seek minimum changes (to the present parameter vector) to achieve incremental improvement in the performance measure and the worst violated constraints. The selection of the finite parameter subsets for optimization cannot be done in a globally rigorous fashion, but we introduce heuristic concepts which do yield a practical scheme. As a consequence of these heuristic schemes, the resulting designs remain sub-optimal. The resulting algorithm can be viewed as a generalized eigenvalue placement/optimization algorithm but is shown to be more general than existing methods in three ways: (i) we have not found it necessary to introduce restrictive assumptions which constrain the admissible form of the feedback in physically undesirable ways (as is typical in the pole placement literature), (ii) we seek to move closed loop eigenvalues into acceptable regions of the complex plane, as opposed to constraining (or attempting to constrain) a large number of eigenvalues to lie at (ad hoc) specified points, and (iii) we have been successful in numerical implementations involving an order of magnitude increase in the number of parameters in the optimization process.

The results presented represent significant progress, and can provide a practical strategy for optimizing moderate dimensional systems; we have successfully optimized systems with up to fifty parameters.

**CONTROLLABILITY AND OBSERVABILITY OF FLEXIBLE GYROSCOPIC SYSTEMS**

Mehdi Ahmadian

Daniel J. Inman

Department of Mechanical and Aerospace Engineering  
State University of New York at Buffalo  
Buffalo, New York 14260

This work provides easily verified controllability and observability conditions on pseudo conservative systems under the influence of gyroscopic forces. These systems have received increased attention in recent years with advent and use of large flexible structures both in the field of space structures and in the control and design of flexible link robots.

The problems addressed here are those resulting from systems which can be modeled successfully by second order linear vector differential equations with constant matrices, i.e.,

$$M\ddot{x} + G\dot{x} + Kx = f$$

Where the  $n \times n$  matrices  $M = M^T > 0$ ,  $G = -G^T$ , and  $K$  are referred to as mass, gyroscopic, and stiffness matrices. The  $n_c \times 1$  and  $n \times 1$   $f$  and  $x$  vectors represent the force input and displacement vectors, respectively. For the case when  $K$  is symmetric, in [1-3] easily verified conditions on the controllability of (1) when

$$f = BU,$$

Where  $U$  is an  $n_c \times 1$  control vector, and on the observability of  $q$  and  $\dot{q}$  when the  $n_o \times 1$  output vector is defined by

$$Y = Pq + R\dot{q}$$

are presented.

The present work is an extension of these results to the pseudo-conservative case (i.e., the case when  $K$  is asymmetric but symmetrizable). Easily verified controllability and observability conditions are developed. It is shown that these results can be used to determine the minimum actuator and sensor requirements for active control of a general flexible gyroscopic system.

**References**

1. Hughes, P.C. and Skelton, R.E., "Controllability and Observability of Linear Matrix-Second-Order Systems," JAM, Vol. 47, pp. 415-420.
2. Juang, J.N., and Balas, M.J., "Dynamics and Control of Large Spinning Spacecraft," The Journal of Astronautical Sciences, Vol. 28, pp. 31-48.
3. Inman, D.J., Hsieh, C.I., "Controllability and Observability of Non-Self-Adjoint Flexible Systems, ASME paper #83-WA/DSC-16, Nov. 1983.

MULTI-LEVEL SUBSTRUCTURING OF LARGE EIGENPROBLEMS  
USING QUADRATIC SUBSPACE ITERATION

by

Roengdeja Rajatabhothi and  
Chulalongkorn University  
Department of Civil Engineering  
Bangkok 10500, Thailand.

C. Philip Johnson  
The University of Texas  
Department of Civil Engineering  
Austin, Texas 78712-1080.

The eigenproblem encountered in mode superposition and stability analyses of a multi-degree-of-freedom (DOF) structural system can be stated as

$$K\delta = \lambda M\delta \quad (1)$$

For a structure with a large number of DOF, an approximate eigen-solution can be obtained by use of a substructuring technique known as "quadratic reduction" (1,2). In this procedure, the coordinates  $\delta$  are systematically reduced from the structure to leave a relatively small number of coordinates selected by partitioning the structure into an assemblage of substructures. Essentially a Ritz approximation, the reduction of coordinates leads to a quadratic eigenproblem of the form

$$\bar{K}_{jj} \bar{\delta}_j = \bar{\lambda} \bar{M}_{jj} \bar{\delta}_j + \bar{\lambda}^2 \bar{N}_{jj} \bar{\delta}_j \quad (2)$$

where  $\bar{K}_{jj}$  is the reduced stiffness,  $\bar{M}_{jj}$  the reduced mass and  $\bar{N}_{jj}$  the corrective mass which accounts for inertia effects associated with the eliminated DOF.

The reduction of the large eigenproblem of Eq.(1) to the smaller eigenproblem of Eq.(2) constitutes a major computational effort in the analysis. The frontal method can effectively be employed in conjunction with multi-level substructuring to minimize computational effort and core storage requirements. An adopted procedure is to select a multi-level substructuring pattern that will allow the substructure system in the final level to be analyzed in core by inverse iteration with shifting (2). However, the size of the original structure and the desired number of accurate modes may sometimes be so large that the resulting quadratic eigenproblem exceeds the core capacity of the computer. The solution therefore requires the use of an out-of-core solution technique such as subspace iteration. The technique can be extended to handle a quadratic eigenproblem (3) and implemented as a frontal solver in a finite element program with multi-level substructuring capability.

The quadratic eigenproblem, Eq.(2), can be rewritten in general form as

$$K_r X_q \Lambda = M_r X_q \Lambda + N_r X_q \Lambda^2 \quad (3)$$

where  $\Lambda_q$  is the diagonal matrix of eigenvalues and  $X_q$  the modal matrix of the  $n \times n$  reduced system. Suppose it is desired to compute the first  $p$  eigenpairs, where  $p < n$ . The solution is performed in two phases. First, a starting solution is obtained by employing subspace iteration to solve the linear eigenproblem

$$K_r X_g \Lambda = M_r X_g \Lambda \quad (4)$$

Multi-level substructuring is applied to the system of substructures to reduce out the frontal coefficients of  $K_r$  before iteration begins. During iteration, the reduced coefficients are retrieved from disk storage and utilized in the forward and backward substitution to update the matrix  $\bar{X}_g$  that contains  $p$  Ritz basis vectors. At the end of the iteration process, we have the linear eigensolution  $(\Lambda_g, X_g)$  and the matrix  $\bar{X}_g$  as approximations to  $(\Lambda_q, X_q)$  and  $\bar{X}_q$  for the quadratic eigenproblem.

The second phase is to perform subspace iteration on Eq.(3). The equation is linearized by postmultiplying both sides by  $\Lambda_q^{-1}$ , giving

$$K_r \bar{X}_q = M_r X_q + N_r X_q \Lambda_q \quad (5)$$

This equation is used to compute an improved approximation to  $\bar{X}_q$ . The matrix  $\bar{X}_q$  is then used in the Ritz transformations of  $K_r$ ,  $M_r$  and  $N_r$  to result in the  $p$ -order eigenproblem

$$K^* Q = M^* Q \Lambda + N^* Q \Lambda^2 \quad (6)$$

The eigensolution  $(\Lambda, Q)$  of the transformed problem is obtained in core by employing inverse iteration with shifting, and is used to update the iteration vectors in the next cycle.

Plate bending examples with up to 4356 DOF were used to test the developed method. It was shown that very accurate eigensolutions can be obtained after only a few cycles of quadratic subspace iteration. In addition, the use of multi-level substructuring leads to substantial savings in storage and computation, particularly the effort in eliminating the frontal coefficients.

#### References

1. Johnson, C.P., Craig, R., Rajatabhothi, R., and Yargicoglu, A., "Quadratic Reduction for the Eigenproblem", Int. J. of Num. Meth. in Engrg., Vol. 15, No. 6, 1980, pp. 911-923.
2. Johnson, C.P., "Computational Aspects of a Quadratic Eigenproblem", Proc., 7th Conf. on Electronic Computation, George Washington U., 1979, pp. 418-431.
3. Rajatabhothi, R., and Johnson, C.P., "Subspace Iteration for the Quadratic Eigenproblem", Proc., 3rd EMD/ASCE Specialty Conf., U. of Texas, Austin, 1979, pp. 373-376.

## A NEW FORMULATION OF MIXTURE THEORY\*

by

Stephen L. Passman  
Division 1533  
Sandia National Laboratories  
Albuquerque, NM 87185

A careful look at the origins of the classical theory of mixtures shows that it is based on an attempt of J. Clerk Maxwell to construct a kinetic model for the behavior of mixtures of monatomic gases. For that application it is extremely good. The mathematical elegance of the theory is so great that it is reasonable to try to use it beyond its intended range of application. It became clear very early that the theory is not entirely appropriate, even for such relatively simple systems as liquid solutions. Nonetheless, theories of the classical type have been used for applications which have been successively farther and farther from the range made plausible by the original molecular motivation. Often, those who formulated such theories allowed for their intended range of applicability by adding new physical variables with appropriate balance principles and constitutive equations while attempting to maintain the elegant symmetry of the original formulation. It is entirely clear, however, that such attempts for systems which need consideration for application to current technology, are seriously handicapped because they lack an underlying metatheory which can motivate the axioms of the theory in a systematic fashion. Such systems include porous solids, "multiphase" liquids, and other mixtures which are in a rather widely accepted terminology, phase separated. Good candidates for metatheories for phase separated materials are the so-called "averaging" theories, which assume conventional continuum theories hold on the scale of a sub-body, which corresponds to a body in the conventional sense, except that it is an open set. They then let a body of the mixture be the union of a large finite number of such sub-bodies with their boundaries, where these boundaries, which are called interfaces, may have mechanical properties of their own. Characteristically, such theories have very strong physical motivation, but yield questionable answers because the mathematics used to formulate the theories is not sufficiently general to describe such theories adequately. I give a basis for showing that rather ordinary modern mathematics suffices to formulate such theories, and makes precise some of the terminology which is currently used in an imprecise fashion.

\* This work was supported by Grant DE-AC04-DP00789 from the United States Department of Energy to Sandia National Laboratories.

## ON EMBEDDING THEORIES WITHIN THEORIES

by

Robert G. Muncaster  
University of Illinois at Urbana-Champaign  
Department of Mathematics  
Urbana, IL 61801

There are numerous examples in continuum mechanics of multiple-theory descriptions of material behavior for a single class of physical problems: several theories are all capable of predicting behavior for this class, each with its own degree of sophistication of description. It is natural in such situations to require consistency of the several theories in the sense that their separate predictions agree, in some sense, for the class of problems in question. A Principle of Consistency capturing this idea has not yet been introduced into the general structure of continuum mechanics.

This lecture addresses the notion of consistency for a special type of multiple-theory occurrence. One theory, called the fine theory, gives a very detailed description of the phenomenon in question, more detailed than is practically desired, while a second one, the coarse theory, provides detail about the problem that exactly suits a certain application. For the analysis of gas flows near equilibrium the kinetic theory of gases is an example of a fine theory when contrasted with a conventional continuum theory of gas dynamics as the coarse theory. Three-dimensional elasticity theory (a fine theory) could be used in the study of elastic rod shaped bodies, but more often a separate Cosserat theory is proposed (the coarse theory) which gives a description sufficiently detailed for most applications. I will present a process by which a coarse theory may be viewed as embedded within an associated fine theory such that there is consistency of predictions in a precise sense. Equivalently, there is a natural way in which a coarse theory can be completely derived from a given fine theory.

Reference

1. Muncaster, R. G., "Invariant Manifolds in Mechanics I: The General Construction of Coarse Theories from Fine Theories", Archive for Rational Mechanics and Analysis, Vol. 84, No. 4, 1984, pp. 353-373.

## DERIVATIVES OF TENSOR-VALUED FUNCTIONS

by

Donald E. Carlson  
 Department of Theoretical and Applied Mechanics  
 University of Illinois at Urbana-Champaign  
 Urbana, IL 61801

Given a real-valued function  $f$  of a real variable, it has been customary in continuum mechanics to construct the associated symmetric tensor-valued function  $\underline{\underline{F}}$  of a symmetric tensor variable by

$$\underline{\underline{F}}(\underline{\underline{A}}) = \sum f(a_i) \underline{\underline{e}}_i \otimes \underline{\underline{e}}_i,$$

where  $(a_i, \underline{\underline{e}}_i)$  denotes an eigenpair of  $\underline{\underline{A}}$  and  $\{\underline{\underline{e}}_i\}$  is an orthonormal basis for the underlying vector space. Important examples include the square root (right and left stretch tensors) and the logarithm (Hencky strain tensor). Often the time rates of change of these tensors are needed, and the nonuniqueness of the eigenvectors in the above definition makes their calculation difficult.

Here, we use the equivalent definition

$$\underline{\underline{F}}(\underline{\underline{A}}) = \sum f(a_i) \underline{\underline{E}}_i,$$

where the summation is over only the distinct eigenvalues of  $\underline{\underline{A}}$  and

$$\underline{\underline{E}}_i = \prod_{i \neq j} \frac{(\underline{\underline{A}} - a_j \underline{\underline{1}})}{(a_i - a_j)}$$

is the perpendicular projection on the null space of  $\underline{\underline{A}} - a_i \underline{\underline{1}}$ . This allows us to determine the derivative of  $\underline{\underline{F}}$ , and then we can get the time rate of change of  $\underline{\underline{F}}(\underline{\underline{A}})$  via the chain rule. Particular attention is paid to the Hencky strain tensor.

by

K. R. Rajagopal  
Department of Mechanical Engineering  
University of Pittsburgh  
Pittsburgh, PA 15261

and

A. S. Wineman  
Department of Mechanical Engineering and Applied Mechanics  
University of Michigan  
Ann Arbor, MI 68109

Exact solutions are established for some boundary value problems in the non-linear theory of elasticity. A remarkable feature in all the problems that are dealt with is the possibility of multiplicity of solutions. The stability of these multiple solutions remains an open problem.

In the case of elastic materials with non-convex stored energy functions, several interesting phenomena, like solutions with discontinuous deformation gradients, are possible.

## ACCELERATION WAVES IN ELASTIC FLUIDS

Mike Scheidler  
Ballistic Research Laboratory  
Aberdeen Proving Ground, MD 21005

Restricting attention to elastic fluids, we investigate acceleration waves of arbitrary initial shape propagating into a region of fluid undergoing a generally nonuniform motion. The existing literature is limited to the case of waves propagating into equilibrium regions. In this case the wave fronts form a family of parallel surfaces, the normal speed of the wave is nonzero, and the rays and normal trajectories coincide and are straight lines. None of these conditions will hold in general, however, when no restrictions are placed on the motion of the fluid ahead of the wave. For this general case we derive the equations governing the wave front geometry and equation for the wave amplitude. The growth or decay of the amplitude is determined by competition between the mean curvature of the wave front and terms arising from the motion ahead of the wave. Critical amplitudes and the formation of caustics are discussed for some special motions ahead of the wave.

ON THE RESIDUAL STRESS  
POSSIBLE IN AN ELASTIC  
BODY WITH MATERIAL SYMMETRY

by

Anne Hoger  
Department of Theoretical and Applied Mechanics  
University of Illinois at Urbana-Champaign  
Urbana, IL 61801

Residual stress is defined here to be the stress present in a body in an unloaded reference configuration. So, the residual stress field is in equilibrium with the body force and surface traction both zero. An elastic body with a particular material symmetry can admit only those residual stress fields that commute with the elements of the symmetry group of the material. Using this condition, Coleman and Noll† obtained the forms for residual stress fields appropriate to specific material symmetries. Here, the additional restrictions imposed by equilibrium and zero traction are explored. For example, in the isotropic case the commutation requirement implies that the residual stress is a pressure; by equilibrium the pressure must be uniform, and then the zero traction condition forces the pressure to vanish. Other symmetries are approached in the same way. Additional results can be found in the context of particular body geometries. As an example, the states of residual stress possible in a transversely isotropic right circular cylinder are discussed.

†B. D. Coleman and W. Noll, "Material Symmetry and Thermodynamic Inequalities in Finite Elastic Deformations," Arch. Rational Mech. Anal., Vol. 15, No. 4, 1964, pp. 87-111.

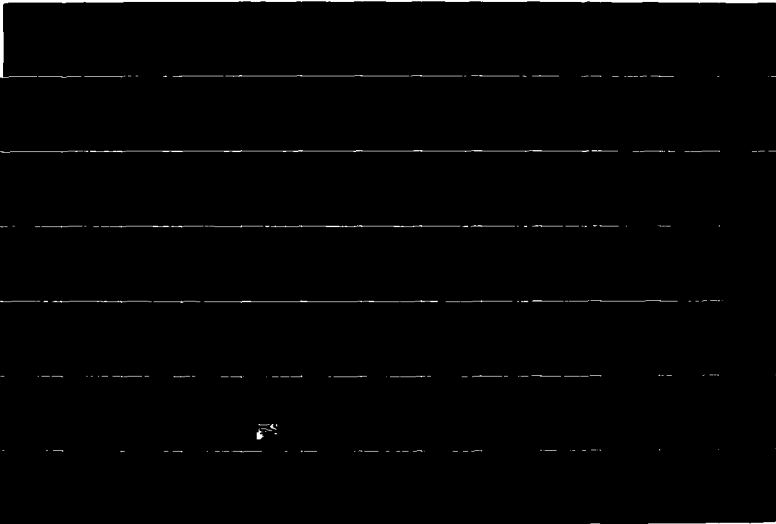
AD-A171 026

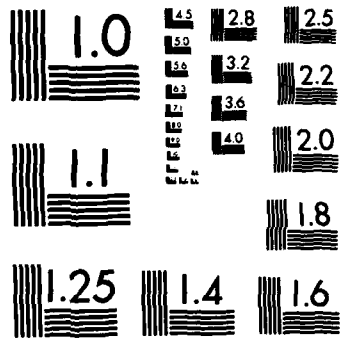
ABSTRACTS 21ST ANNUAL MEETING SOCIETY OF ENGINEERING  
SCIENCE INC OCTOBER 1-7 (VI) VIRGINIA POLYTECHNIC INST  
BLACKSBURG & FREDERICK ET AL. 1984 ARO-21000 EC-CF  
DAAG29-84-M-0119 P/G 5/2

4/6

UNCLASSIFIED

ML





MICROCOPY RESOLUTION TEST CHART  
NATIONAL BUREAU OF STANDARDS-1963-A

MODELING OF BLAST RESPONSE OF A DISCONTINUOUS HEMISPHERE SUBJECTED  
TO EXTREMUM BOUNDARIES

by

Aaron DasGupta, Mechanical Engineer  
Henry J. Wisniewski, Mathematician  
U.S. Army Ballistic Research Laboratory  
U.S. Army Armament, Munitions & Chemical Command  
Aberdeen Proving Ground, MD 21005

The influence of various edge boundary conditions along the edges of a large cutout for equipment access on the structural response of a hemispherical containment structure due to an internal explosive blast has been determined. The model employs a finite-difference shell response code i.e., PETROS 3.5 developed at M.I.T. for the U.S. Army Ballistic Research Laboratory (BRL).

Although the cutout is closed by a heavy steel door clamped to the enclosure wall during a test, the edges can move to a small extent. The ideally clamped approximation in the numerical modeling may not be achieved under field operating conditions. It is therefore desired to bracket the response under two extreme edge boundary conditions to assure structural integrity of the enclosure.

The comparison of responses due to fixed and hinged boundary conditions indicates small transverse oscillation in addition to predominantly radially outward vibration at the pole in both cases. Although strains, in general, appeared to be somewhat lower at critical locations for the hinged door enclosure, the displacements were very nearly the same for both cases. Lower strains were probably due to lack of bending wave propagation from the restrained edges towards the pole. However, both stresses and displacements were small enough to be in the linear elastic regime which satisfied the design requirements.

STATISTICAL APPROACH TO TRANSIENT HEAT CONDUCTION  
IN COMPOSITE MATERIALS

by

Seichi Nomura  
Department of Mechanical Engineering  
University of Texas at Arlington  
Arlington, Texas 76019

Tsu-Wei Chou  
Department of Mechanical and Aerospace Engineering  
University of Delaware  
Newark, Delaware 19716

This paper provides a new method to analyze transient heat conduction in composite materials. Although mathematical techniques for solving transient heat conduction in solids are well developed, works on heat conduction for inclusion and matrix type composites are few. We present a new mathematical technique to obtain the temperature distribution that takes the shape of inclusions and their distribution in a matrix phase into account for given boundary and initial conditions. Based upon a statistical approach, the equilibrium equation of temperature field is expressed by a term due to reference properties and a term due to fluctuating fields. By introducing the Green's function of heat conduction for the reference medium, the equilibrium differential equation is converted into an integro-differential equation. This integro-differential equation can be solved by a Neumann type series with arbitrary initial and boundary conditions. It is shown that statistical information on correlation functions is needed to evaluate each term of the series. This approach is applicable to a wide range of phase geometries and reduces to the static case by eliminating the time factor.

## EXPERIMENTAL THERMOPHYSICAL PROPERTIES OF COMPOSITE MATERIALS—

## A STATE OF THE ART ASSESSMENT

Daniel M. Maguire and F. A. Kulacki  
Department of Mechanical and Aerospace Engineering  
University of Delaware  
Newark, Delaware 19716

Extensive research has been performed in the area of mechanical properties of composite materials, but much less has been conducted in the area of thermophysical properties. The purpose of this presentation is to collect and analyze as much of the existing literature as possible concerning thermophysical properties, concentrating on thermal conductivity, specific heat, and coefficient of thermal expansion. The material systems considered include long and short fiber systems, as well as particulate systems, and properties are studied along the fiber axis as well as transverse to it. Data on graphite/epoxy, boron/epoxy, and glass fiber/epoxy materials are most numerous and obtainable.

Our summary of the literature and comparative analysis will attempt to determine how well the experimental literature has been developed concerning these properties, how the experimental results tabulated so far compare with the theoretical predictions, and what new needs are evident for future research. Our results show that certain material systems have been well-researched while others have been virtually ignored. Carbon-based systems have been particularly well researched, while metal matrix, particulates, and other organic matrix composites have not been as well researched. Scatter in the data seems to be a recurring problem for all material systems, though there is good agreement in the graphite/epoxy systems studied by different researchers, when variables such as fiber volume fraction and packing geometry are similar.

Most of the research conducted so far in the area of thermophysical properties is focused on the graphite/epoxy or carbon/carbon material systems, as evidenced by the work done by Han and Boyce [1] and Taylor [2]. An extensive compilation of thermophysical properties of graphite/epoxy, boron/epoxy, and glass fiber/epoxy has been made by Touloukian and Ho [3]. Zimmerman [4] presents a review of theoretical predictions and modelling of transverse thermal conductivity, but no experimental data. In addition, Askins [5] has made an extensive study of various carbon and SiC-based commercially available composites. However, very little literature exists on the thermophysical properties of metal matrix or resin matrix composites.

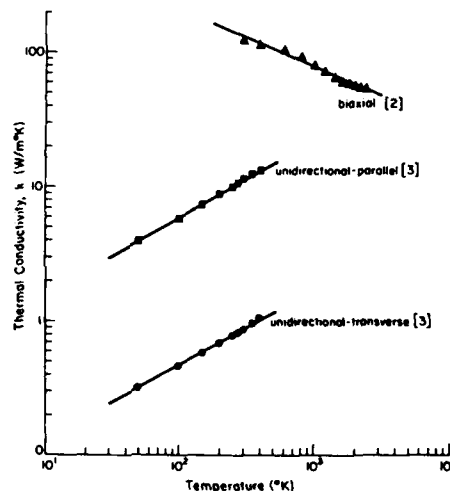
Opportunities for further research and development in this area would seem to center around metal-matrix composites and on attempting to eliminate some of the scatter found in the data of the other material systems. Measurement techniques could be

improved upon, and the inverse heat conduction problem should be studied to determine the feasibility of experimentally verifying the theory.

Typical results of our summary are shown in Figure 1. Figure 1 shows thermal conductivity as a function of temperature for carbon based material systems based on results obtained by Taylor [2] on biaxial carbon/carbon and data compiled by Touloukian and Ho [3] on unidirectional graphite/epoxy.

FIGURE 1

## TEMPERATURE DEPENDENCE OF THERMAL CONDUCTIVITY



## REFERENCES

1. Han, L. S. and Boyce, W. F., "Thermal Conductivities and Diffusivities of Graphite-Epoxy Composites", AFWAL-TR-83-3002, Feb. 1983.
2. Taylor, R. E., Groot, H., and Shoemaker, R. L., "Thermophysical Properties of Fine-Weave Carbon-Carbon Composites", Spacecraft Radiative Transfer and Temperature Control, Horton, T.E., ed, Progress in Astronautics and Aeronautics Series, Vol. 83, AIAA, New York, 1981, pp. 96-108.
3. Touloukian, Y. S. and Ho, C. Y., eds., Thermophysical Properties of Selected Aerospace Materials, Part II, CINDAS, West Lafayette, IN, 1977, pp. 111-216.
4. Zimmerman, R. H., "Predicting the Transverse Conductivity of Unidirectional and Bidirectional Filamentary Composites", AFOSR 78-3640, Ohio State University Research Foundation, Columbus, Ohio, 1980.
5. Askins, D. R., "Development of Engineering Data on Advanced Composite Materials", AFWAL-TR-81-4172, Feb. 1982.

TRANSIENT TEMPERATURE AND THERMAL STRESS FIELDS  
OF A THERMALLY AND ELASTICALLY ORTHOTROPIC SLAB

by

Hong-Sheng Wang, Tsu-Wei Chou, Francis A. Kulacki  
Mechanical and Aerospace Engineering Department  
University of Delaware, Newark, Delaware 19716

Considerable attention has been given in recent years to the study of the thermo-mechanical behavior of anisotropic elastic materials. Fiber composites are certainly well known examples of such materials. The thermal response of composites is an important consideration not only in fabrication and processing but also for material durability and long term performance. However, owing to the mathematical complexity in dealing with the thermal elastic problem of anisotropic media, only a very limited number of solutions are available. The thermal stress problem of anisotropic material is most well studied for the case of transverse isotropy. Both steady state and transient thermal stress problems have been investigated for transversely isotropic materials in the shapes of circular cylinder and thick plate. In the category of thermally and elastically orthotropic materials, to the authors' knowledge, only solutions of steady state temperature and thermal stress fields have been investigated.

The purpose of this paper is to examine the transient temperature and thermal stress fields of a thermally and elastically orthotropic rectangular slab. The slab initially held at a constant temperature, is suddenly subjected to an arbitrary temperature variation on one of its edges. The temperature distribution in the rectangular region is assumed to satisfy the transient heat conduction equation with constant orthotropic conductivities and thermal diffusion coefficients. The temperature field has been obtained in closed form by using the principle of superposition and the method of Fourier series expansion. The transient thermal stress analysis for the rectangular slab is performed based upon the displacement-potential approach [1,2]. It is found that thermal orthotropy has very significant influence on the thermal stress distributions. Numerical results for the case simulating unidirectional fiber composites have been obtained. The effect of length to width ratio of the rectangular slab on the temperature and stress distributions also have been examined. The present work points out the important implications of transient thermal effects in problems concerning, for instance, boundary layer stress concentrations and interfacial damages in composite laminates.

References

- (1) Sharma, B., "Thermal Stresses in Transversely Isotropic Semi-Infinite Elastic Solid," Journal of Applied Mechanics, 1958, 25, 86-88.
- (2) Aköz, A. Y. and Tauchert, T. R., "Thermoelastic Analysis of a Finite Orthotropic Slab," J. Mech. Eng. Sci., Vol. 20, 65-71, 1978.

A NEW METHOD FOR SOLVING TRANSIENT  
HEAT CONDUCTION THROUGH COMPOSITE MEDIA

by

M. Necati Özisik  
Mechanical and Aerospace Engineering Department  
North Carolina State University  
Raleigh, N. C. 27695-7910

The transient temperature distribution and heat flow through a composite medium consisting of several layers, each having different physical properties has been the subject of numerous investigations. Formal analytic solutions are available for such problems; but to implement the formal solution for practical purposes, one needs the eigenvalues, eigenfunctions and the normalization integral associated with the problem. This leads to the necessity of solving the corresponding eigenvalue problem, which is not of the conventional type because of discontinuity of the coefficient functions. Fast, accurate computation of the eigenfunctions without missing any one of them and the corresponding eigenfunctions is a tricky piece of work.

Recently, there has been a significant development in the method of computation of the eigenvalues of the Sturm-Liouville problem with discontinuous coefficients. The basic idea originally applied [1,2] for the computation of the natural frequencies and buckling loads in linear elastic skeletal structures, has been adopted [3,4] for the determination of the number of eigenvalues of the Sturm-Liouville problem, lying between zero and some prescribed value of the eigenvalue parameter. Such an information establishes the basis for the implementation of the solution of the eigenvalue problem for practical purposes. That is, an efficient algorithm can be prepared for the fast and accurate determination of as many eigenvalues as needed, without missing any one of them.

In the classical approach, the eigenvalues are determined by solving infinite number of real roots of the transcendental equation obtained from the eigenvalue problem and expressed symbolically in the form

$$\det [K(\mu)] = 0$$

In the new Sign-Count method, instead of solving such a transcendental equation, we seek the number of positive eigenvalues  $N(\bar{\mu})$ , lying between zero and some prescribed value of  $\mu = \bar{\mu}$ , from the relation

$$N(\bar{\mu}) = N_0(\bar{\mu}) + S\{[K(\mu)]\}$$

where  $N_0(\bar{\mu})$  = number of positive eigenvalues not exceeding  $\bar{\mu}$ , when all components of the coefficient vector corresponding to  $[K(\bar{\mu})]$  are zero, (i.e., decoupled system).  
 $S\{[K(\mu)]\}$  = the sign-count of  $[K(\bar{\mu})]$ .

It is shown in references [3,4] that, for the particular system considered here  $N_0(\bar{\mu})$  is given by

$$N_0(\bar{\mu}) = \sum_{k=1}^n \text{int} \left( \frac{\bar{\mu}_k l_k}{\pi} \right)$$

where the symbol "int (z)" denotes the largest integer not exceeding the value of the argument z of the function and  $l_k$  is the thickness of the k-th layer.

The sign-count,  $S\{[K(\bar{\mu})]\}$  is shown [2] to be equal to the number of negative elements along the main diagonal of the matrix  $[K^{\Delta}(\bar{\mu})]$ , which is the triangulated form of the matrix  $[K(\bar{\mu})]$ .

With the information thus available for the number of positive eigenvalues  $N(\bar{\mu})$  lying between zero and some prescribed value of  $\mu = \bar{\mu}$ , and efficient, simple algorithm can readily be written to compute as many eigenvalues as desired automatically, without missing any one of them, with high degree of accuracy and with very little computer time. Once the eigenvalues are available, the eigenfunctions and the normalization integrals are readily determined. Knowing the eigenfunctions, eigenvalues and the normalization integral, the transient temperature and the heat flow rate through a composite wall containing any number of layers, and for any values of thermal conductivity are readily calculated from the formal expressions given in references [4,5].

The method is also applicable for the solution of eigenvalue problems involving variable property, by treating the problem as that of a composite medium consisting of layers in contact; or to other more involved eigenvalue problems which can be recast as a problem of layers in contact [6].

#### REFERENCES

1. Wittrick, W. H., and F. W. Williams, "A General Algorithm for Computing Natural Frequencies of Elastic Structures", Quart. J. Mech. Appl. Math., 24, 263-284 (1971).
2. Wittrick, W. H., and F. W. Williams, "Buckling and Vibrations of Anisotropic or Isotropic Plate Under Combined Loading", Int. J. Mech. Sci., 16, 209-239 (1974).
3. Mikhailov, M. D., M. N. Özişik, and N. L. Vulchanov, "Diffusion in Composite Layers with Automatic Solution of the Eigenvalue Problem", Int. J. Heat Mass Transfer, 26, 1131-1141, (1983).
4. Mikhailov, M. D., and M. N. Özişik, United Analysis and Solutions of Heat and Mass Diffusion, John Wiley, New York, (1984).
5. Özişik, M. N., Heat Conduction, John Wiley, New York, (1980).
6. Özişik, M. N., M. A. Boles, and R. M. Cotta, "Eigenvalues Basic to Diffusion in the Part of a Sphere Cut Out by a Cone", J. Heat Transfer (In press).

EFFECT OF MICROSTRUCTURAL AND COMPOSITIONAL VARIABLES  
ON THE CONDUCTION OF HEAT IN STRUCTURAL MATERIALS FOR  
HIGH-TEMPERATURE USE

by

D. P. H. Hasselman  
Department of Materials Engineering  
Virginia Polytechnic Institute and State University  
Blacksburg, VA 24061 USA

The basic mechanisms of electron, phonon and photon transport for the conduction of heat in solids are controlled by variables at the atomic level. Critical for engineering purposes is that the heat conduction behavior of solids also is controlled by microstructural and compositional effects. An overview is presented of such effects in the conduction of heat in single-phase and composite materials for applications such as turbine engines, aerospace, and other purposes which involve extreme temperatures. The experimental data were obtained by the laser-flash diffusivity method.

Silicon nitride, a candidate material for the highly efficient "ceramic" turbine engine, exhibited a thermal diffusivity which depended on the manufacturing time, amount and degree of crystallinity of the grain boundary phase, the direction with respect to the pressing direction, and the extent of solid-solution alloying. Silicon nitride and silicon carbide with a dispersed phase of boron nitride exhibit considerable anisotropy in their ability to conduct heat.

Heavily micro-cracked materials, for potentially severe thermal shock applications, exhibited a thermal diffusivity which was a function of grain size, thermal history, and amount of second phase inclusions.

A glass-ceramic material developed for aerospace applications was found to exhibit a thermal diffusivity strongly dependent on the degree of crystallization achieved during fabrication.

A glass-ceramic, dispersion-toughened by means of a crystalline alumina second phase exhibited a thermal conductivity and diffusivity strongly dependent on the volume fraction of the dispersed phase.

A composite of silicon carbide fiber - toughened lithium aluminosilicate (LAS) glass-ceramic showed excellent thermal insulating ability, due to the low thermal conductivity of both the amorphous silicon carbide fibers and the LAS matrix. The positive temperature dependence of the thermal conductivity of the silicon carbide is evidence for a large contribution to the heat conduction by photon transport.

A graphite-fiber reinforced noncrystallized lithium aluminosilicate glass exhibited an irreversible increase in thermal diffusivity on heating and cooling due to the combined effects of

TRANSIENT HEAT CONDUCTION IN A PARTIAL COMPOSITE CYLINDER  
SUBJECTED TO CYCLIC TEMPERATURE CHANGE<sup>\*</sup>

by

Jin Kim, Hideki Seine<sup>\*\*</sup> and Minoru Taya  
Department of Mechanical and Aerospace Engineering  
University of Delaware  
Newark, Delaware 19716

Metal matrix composites are often to be used under various temperature excursions, including thermal cycling. To obtain a better understanding of the thermo-mechanical behavior of the composite subjected to such a thermal environment, we have focused on the transient heat conduction problem of a partial composite cylinder subjected to cyclic temperature change. The composite consists of two concentric cylinders, the inner cylinder made of composite, thus being transverse isotropic and the outer cylinder made of monolithic metal with isotropic properties.

The closed form solutions are obtained in series form after formal procedure, separation of variables, Laplace transform and inverse Laplace transform. Some numerical results are given as a demonstration.

---

\* This work was supported partially by a grant from the Honda R&D Company.

\*\* Present address: Department of Engineering Science, Tohoku University, Sendai, Japan.

AN EXPERIMENTAL STUDY OF NATURAL CONVECTIVE HEAT  
TRANSFER IN ECCENTRIC HORIZONTAL ANNULI

by

D. Naylor  
Graduate Student

J.D. Tarasuk  
Associate Professor

The University of Western Ontario  
Faculty of Engineering Science  
London, Ontario, N6A 5B9

Natural convection in concentric horizontal annuli has wide engineering applications and has been extensively studied over the past 50 years. The present investigation examines the influence of eccentricity and Rayleigh number on natural convective heat transfer through air between horizontal isothermal cylinders (see Figure 1). By judicious design the eccentricity effect could be utilized to reduce or increase heat transfer across the fluid-filled gap.

A recent numerical solution by Badr [1] for vertical eccentricities over the range of  $Ra$  from 0 to  $10^4$  ( $Pr = 0.70$ ) indicates a pronounced effect of eccentricity on both local and overall heat transfer coefficients. Projahn et al [2] have also obtained a numerical solution for vertical eccentricities and have extended their techniques to horizontal eccentricities ( $10^2 < Ra < 10^5$ ,  $Pr = 0.70$ ). To our knowledge heat transfer measurements for non-vertical eccentricities have not been made for  $Ra < 3 \times 10^4$ , and while some overall heat transfer data exists for vertical eccentricities the correlation is not yet well defined.

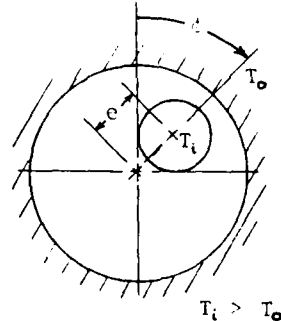


FIGURE 1. SCHEMATIC DIAGRAM OF THE ANNULUS

A 40 cm long test section has been constructed for use in a Mach-Zehnder interferometer (see Figure 2). The inner cylinder is copper with an outside diameter of 9.66 mm. Power was supplied to this inner rod by passing direct current through a nichrome wire

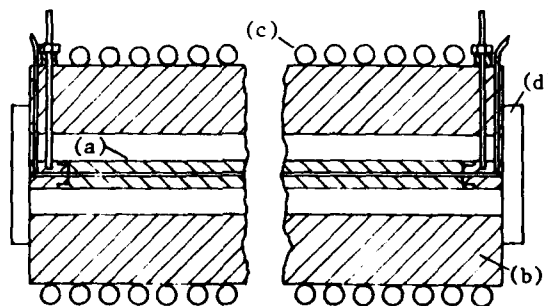


FIGURE 2. SCHEMATIC DIAGRAM OF EXPERIMENTAL APPARATUS  
(a) INNER CYLINDER (b) OUTER CYLINDER  
(c) COOLING WATER TUBES (d) OPTICAL WINDOW

located along its center line. The cooled outer cylinder, machined from solid aluminum has an inside diameter of 2.510 cm resulting in a diameter ratio of 2.60, compatible with the numerical studies.

Graphical correlations are presented delineating the effect of  $e/L$  and  $\phi$  on the temperature field, local heat transfer and overall heat transfer for  $Ra$  from  $9 \times 10^2$  to  $2 \times 10^3$ . Comparisons are made with numerical predications.

#### Nomenclature

$e$  = eccentricity  
 $L$  = average gap width ( $R_o - R_i$ )  
 $Pr$  = Prandtl number  
 $Ra$  = Rayleigh number based on  $L$   
 $\phi$  = angle of eccentricity

#### References

- [1] Badr, H.M. "Study of Laminar Free Convection Between Two Eccentric Horizontal Tubes", to be published in the ASME Journal of Heat Transfer.
- [2] Projahn, U., H. Rieger, H. Beer, "Numerical Analysis of Laminar Natural Convection Between Concentric and Eccentric Cylinders", Numerical Heat Transfer, Vol. 4, 1981, pp. 121-146.

VARIATIONAL INEQUALITIES AND PENALTY METHODS FOR A  
CLASS OF PROBLEMS IN ELASTO-PLASTICITY

by

B.D. Reddy  
University of Cape Town  
Depts. of Applied Mathematics & Civil Engineering  
Rondebosch, Cape, South Africa 7700

In a series of recent papers (1), (2), (3) it has been shown how the classical rate problem in plasticity may be approached by minimizing a Gateaux-differentiable functional  $J$  of displacement rates  $v$  and plastic multipliers  $\lambda$ . The differentiability of  $J$  makes the use of this functional an attractive alternative to approaches based on the classical minimum principle, in which the corresponding functional  $K(v)$  is non-differentiable. Minimization of  $J(u, \lambda)$  is required in a subset  $\Lambda = \{\lambda \in L_2(\Omega) \mid \lambda \geq 0 \text{ a.e. in } \Omega\}$ ; in the corresponding discrete problem a simple algorithm is used to carry out the minimization.

The present contribution is aimed at a re-examination of the rate problem, in the light of the above experiences. It is shown that the solution to this problem satisfies a variational inequality involving displacement rates and plastic multipliers, and that the corresponding minimization problem amounts to finding  $(u, \lambda) \in H \times \Lambda$  satisfying

$$J(u, \lambda) \leq J(v, \mu) \quad \forall (v, \mu) \in H \times \Lambda$$

where  $J$  is the functional derived in (1) and mentioned above. From the point of view of variational boundary-value problems, then, it would seem that the approach based on the use of  $J(v, \mu)$  forms a more natural setting for the rate problem than that based on the classical minimum principle.

Questions of existence of a solution are discussed, and it is shown how the problem may be tackled by using penalty-finite element approximations. The relationship of the penalized problem to the original problem is discussed; in particular, criteria for convergence of the penalized solution to the exact solution are given. Examples using the penalty method are described.

REFERENCES

1. J.B. Martin, "On the Kinematic Minimum Principle in Classical Plasticity," J. Mech. Phys. Solids 23 (1975), 123.
2. J.B. Martin and B.D. Reddy, "A Programming Approach to the Solution of the Rate Problem for Elastic, Plastic Solids," in: R.N. Dubey and N.C. Lind, (eds.), Mechanics in Engineering, (Univ. of Waterloo Press, Waterloo, Ontario, 1977).
3. B.D. Reddy and G.P. Mitchell, "The Analysis of Elastic-Plastic Plates: A Quadratic Programming Problem and Its Solution by Finite Elements," Comp. Meth. Appl. Mech. Eng., 41 (1983) 237-248.

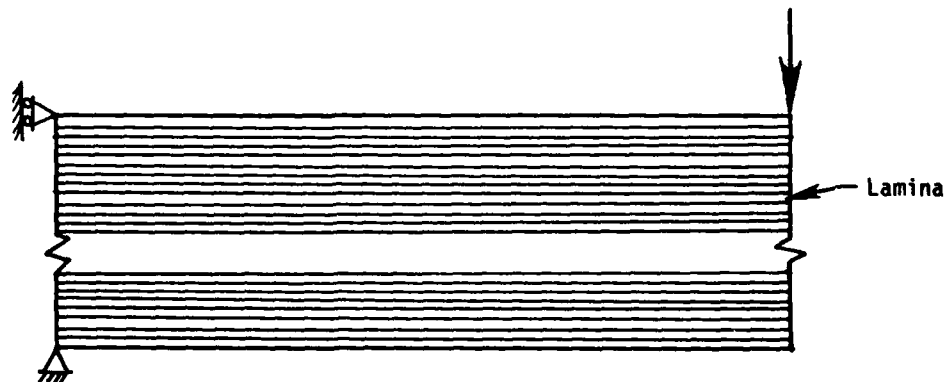
A SIMPLE RECTANGULAR ELEMENT FOR  
ANALYSIS OF LAMINATED COMPOSITES

by

John D. Whitcomb  
NASA Langley Research Center  
Hampton, VA 23665

The development of an appropriate finite-element mesh is a key step in successful finite-element analysis. For homogeneous materials the mesh refinement is dictated by geometrical considerations. The shape of a structure should be faithfully modeled. Also, extra mesh refinement is required in regions with strong strain gradients caused by holes, cracks, or boundary conditions. For laminated materials the analyst must also account for the different material properties of the various laminae. These ideas are illustrated by the laminated composite beam shown in the figure below. Geometrical considerations require very few elements except close to the point where the load is applied, where strain gradients are large. But if standard finite elements are used, the elements must not span across lamina boundaries. Hence, because of the laminated character of the material, the mesh must be highly refined even where the strain gradients are small.

The objective of this paper is to introduce a simple rectangular element which eliminates the need to add elements to a model simply to account for the material properties of various laminae. Explicit integration of the element stiffness matrix in terms of generalized displacements minimizes the algebraic effort required to account for various laminae. Explicit integration of the element stiffness matrix in terms of generalized displacements minimizes the algebraic effort required to account for the various laminae within a single element. A substitute shape function technique is used to improve the performance of the element in modeling bending type deformation. After describing the theoretical aspects of the element, results from analysis of several simple configurations are discussed.



Beam with many lamina  
(not all lamina shown)

AN ALGORITHM FOR RECEDING/ADVANCING UNILATERAL  
CONTACTS WITH INDEPENDENT CONSTRAINTS

by

N.J. Salamon and T.P. Pawlak  
West Virginia University  
Department of Mechanical and Aerospace Engineering  
Morgantown, WV 26506

F.F. Mahmoud  
Zagazig University  
Department of Mechanical Engineering  
Zagazig, Egypt

The phenomenon of receding/advancing contact between elastic bodies is an important one because it is a characteristic of the behavior of structural elements on foundations. The general problem is complicated by friction as well as the interdependence of continua. However, many practical problems lend themselves to simplification, for instance use of the classical Winkler approximation provides good agreement with experiment. In this case, the individual foundation elements are independent of relative tangential motion (and friction) and of each other. We take advantage of these simplifications in formulating what is ostensibly the simplest numerical algorithm for the solution of unilateral contact problems.

The algorithm subdivides the problem into a series of linear events, each of which occurs over an increment in load. The sequence of events, either contact or separation, are determined by scaling the residual load and choosing the event corresponding to the minimum scale factor. It is proven that scale factors for events of interest lie in the closed interval  $(0,1)$ . In cases where several scale factors are equal, the event associated with a maximum interpenetration is chosen as the tie-breaker. The algorithm ends when no further events are detected under the prescribed applied load. The key to its efficiency is that the detection process is purely kinematic.

The algorithm will progress to the final contact configuration whether the initial boundary prescription under or over constrains the problem. If the curvature of the response along a constraint direction contains no inflection point, the solution sequence is direct, otherwise some iteration is necessary. This is particularly acute in solving plate problems.

A number of plate and beam problems are solved. Good accuracy is shown by comparison with known solutions. Certain results for previously unsolved problems will be offered and a videotape on the simulation of receding/advancing contact of beams on foundations will be shown.

BEM AND FEM ANALYSIS OF STATIONARY AND MOVING  
CRACKS IN CREEPING SOLIDS

by

Subrata Mukherjee and Vinod Banthia  
Cornell University  
Department of Theoretical and Applied Mechanics  
Ithaca, NY 14853

The behavior of existing flaws in a metallic structure, loaded at an elevated temperature, is of concern in this paper. Depending on various factors such as geometry, material, load level and temperature, an existing crack in a structure might remain stable, grow slowly and allow continued use of the structure, or grow at a rapid rate and cause catastrophic failure.

A study of this important problem can be divided into two main components. The first is the mechanics boundary value problem of determining the stresses and deformations in a loaded structure with flaws present in it. Inelastic deformation of the structure including creep must be taken into account in this analysis. The second is the determination of a suitable crack growth law, i.e., if the crack is predicted to grow, one must determine the crack velocity as a function of the stresses and deformations around the crack tip and possibly other important quantities. These two pieces of the puzzle must fit together in order to get a complete solution of the problem.

A crack growth law under creeping conditions, it appears, must be determined by proper correlation of mathematical modelling and experiments. Several different regimes, such as crack growth under small scale or extensive creep conditions, or under steady or time-dependent (especially cyclic) loading are of interest. Different theories have been proposed and many experiments are in progress, although little experimental data is, as yet, available for transient crack growth under small scale creeping conditions. In summary, in the judgement of the present authors, no single reliable theory for crack growth under creeping conditions is, as yet, available and further experimental, theoretical and numerical research is necessary.

Turning now to the second important piece of the puzzle, namely the solution of boundary value problems for the determination of stresses and deformations in a flawed structure, analytical and numerical methods are in order. Significant analytical research in this subject area has recently been carried out by Riedel, Rice and Hui (e.g. [1]). While this research is of great value in providing a better understanding of the stress fields around cracks in creeping solids, the range of applicability of the asymptotic analytical solutions is rather limited. It appears difficult, for example, to obtain analytical solutions to problems under transient creep conditions, under general time-varying loading situations or if a relatively complicated constitutive model is used to describe creep of the material.

In order to obtain a complete solution of the creep-fracture boundary value problem, therefore, it appears essential to develop efficient and accurate numerical techniques. The finite element method (FEM) has been applied to study creep relaxation around a stationary crack tip by Bassani and McClintock [2]. Mukherjee and his group have been very successful in obtaining accurate results for stresses around stationary crack tips in creeping solids, under transient, small scale creeping conditions, by the boundary element method (BEM) [3]. This special application of the BEM is based on a formulation that includes the effect of a traction-free crack directly in the kernels of the integral equations. This formulation thus obviates the necessity of having unknowns on the crack boundary and is able to model the changing stress distribution near a crack tip, with time, very accurately. A particular advantage of the BEM is that one is not locked in, a priori, to a special stress singularity near the crack tip as typical FEM applications with special elements (eg. [2]), usually are.

The BEM and FEM applications described previously have recently been extended by Banthia and Mukherjee to the case of moving cracks in creeping solids [4]. In the absence of a reliable crack growth law under creeping conditions, the crack velocity  $\dot{a}$  is taken to be a prescribed constant in these simulations. This assumption, however, can be easily relaxed. The formulations further assume that the geometrical effect of crack extension, which causes an increase in the crack tip stress, and stress relaxation at the crack tip due to creep, can be additively superimposed. Numerical results have been obtained by integrating appropriate rate equations, for the case of the BEM, and incremental quantities, for the FEM, by marching forward with discrete time steps and suitable updating of the geometry [4].

The primary conclusion regarding the two methods, drawn from this work, is that while both methods are very useful, each appears best suited for the study of a different regime of inelastic deformation. The BEM appears better suited for transient stress analysis near a crack tip under small scale creeping conditions, while the FEM appears best suited for analysis of problems in a cracked body undergoing extensive creep deformation throughout most of the structure. The two methods, in this sense, complement each other.

#### References

1. Hui, C. Y. and Riedel, H., "The Asymptotic Stress and Strain Field Near the Tip of a Growing Crack Under Creep Conditions," Int. J. Fracture, Vol. 17, No. 4, 1981, pp. 409-425.
2. Bassani, J. L. and McClintock, F. A., "Creep Relaxation of Stress Around a Crack Tip," Int. J. Solids Structures, Vol. 17, No. 5, 1981, pp. 479-492.
3. Mukherjee, S., "Boundary Element Methods in Creep and Fracture," Applied Science Publishers, London, 1982.
4. Banthia, V. and Mukherjee, S., "BEM and FEM Analysis of Planar Moving Cracks in Creeping Solids," submitted for publication.

## FREE CONVECTION HEAT TRANSFER IN SHALLOW ANNULAR CYLINDRICAL SECTORS USING PENALTY FINITE ELEMENTS

by

V. Dakshina Murty  
Multnomah School of Engineering  
University of Portland  
Portland, OR 97203

This paper is concerned with the application of the finite element method to a class of convection heat transfer problems, namely natural convection. Such problems arise very frequently in individual settings. The flow regime is considered laminar, and the fluid is considered to be incompressible within the Boussinesq approximation. The fluid motion is then described completely by the conservation of mass, linear momentum and energy equations. With the use of Galerkin's method, this set of continuum equations is transformed into a set of discretized equations involving only the nodal point velocity, temperature and pressure. This set of nonlinear equations is solved using Picard's method.

The continuity equation can be modelled using one of the two methods; Lagrange multipliers and penalty method. In the former pressure appears explicitly as an interpolation variable. In the latter, however, the continuity equation is treated as a constraint which is imposed by means of a penalty parameter  $\epsilon$ . The accuracy and the rate of convergence of the numerical solution are strongly dependent on the value of  $\epsilon$ . In the penalty method the only interpolation variables are the velocity and temperature. In this study this method is used to study free convection heat transfer in shallow horizontal cylindrical sectors. In all the cases studied, the aspect ratio (difference in radii to mean arc length) is held a constant at 0.1. The vertical sides are held at constant temperature while the top and bottom sides are insulated. For low values of the Rayleigh number, the heat transfer is dominated by conduction. This is evidenced by nearly straight isotherms. As the Rayleigh number is increased, convection effects become apparent. Also the flow seems to develop a small vortex at each end of the channel. As the included angle is increased, the symmetry of the flow gets destroyed. However, at moderate included angles the flow pattern and isotherms are similar to the straight channel. For the angles studied, the only numerical difficulty encountered was the increased number of iterations required for convergence.

THE INFLUENCE OF CONSTRAINTS, BODY SIZE, AND LOAD AND  
FRICTION LEVELS IN STICK-SLIP CONTACTS USING FINITE ELEMENTS

by

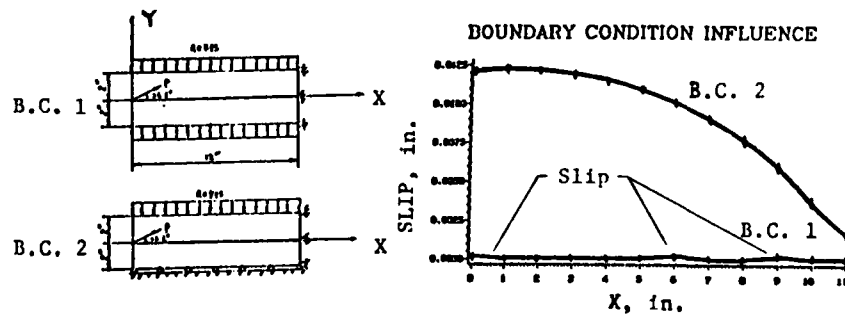
T.X. Xu and N.J. Salamon  
Dept. of Mechanical and Aerospace Engineering  
West Virginia University  
Morgantown, WV 26506

A direct incremental finite element method based upon the model proposed by Okamoto and Nadazawa (1) is used to study the influence of prescribed parameters on stick-slip contact between elastic bodies. The deformations are assumed small and the conventional Coulomb law for dry friction is used. The method subdivides the problem into a series of linear events, each of which occurs over an increment in load. The sequence of events is determined by scaling the residual load to those values necessary to cause impending action (contact or separation, stick or slip) and choosing that event requiring the minimum load. After each event, boundary conditions are updated to be consistent with the deformation state.

With the works by Dundurs and Comninou (2) used as a backdrop, we investigate the influence of boundary conditions (kinematic vs. kinetic), body size, load level and friction coefficient magnitude on the distribution of stick-slip zones along the contacting interface. All play a major role, but the prescription of boundary conditions is the most dramatic.

REFERENCES

1. Okamoto, N. and Nadazawa, M., "Finite Element Incremental Contact Analysis with Various Frictional Conditions," Int. J. for Num. Methods in Eng., Vol. 14 (1979), pp. 337-357.
2. Dundurs, J. and Comninou, M., "An Educational Elasticity Problem," Parts I and II, J. Appl. Mechanics, Vol. 48 (1981), pp. 841-845 and Vol. 49 (1982), pp. 47-51.



## A BOUNDARY ELEMENT ANALYSIS OF METAL FORMING PROCESSES

by

Abhijit Chandra  
Mathematics Department  
General Motors Research Laboratories  
Warren, MI 48090-9055

Metal forming processes such as extrusion, rolling, sheet metal forming, etc. generally subject the workpiece to finite strains and displacements. The components of elastic strains, in these examples are generally limited to about  $10^{-3}$  since the elastic moduli of metals are typically about three orders of magnitude larger than the yield stress. Thus, the nonelastic strain components, which can be of the order of unity, greatly dominate the elastic strains.

A considerable body of literature [1-5] exists where the finite element method (FEM) has been used to analyze metal forming problems using various time independent and time dependent material models.

The boundary element method (BEM -- also called the boundary integral equation method) is another powerful general purpose method. Recently a BEM formulation capable of incorporating both material and geometric nonlinearities has been obtained by Chandra and Mukherjee [6-8]. This BEM formulation is extended here to analyze metal forming problems. The BEM formulation is capable of using any of a class of combined creep-plasticity constitutive models with state variables for the description of material behavior. The particular material model used is that originally proposed by Hart [9] and later modified to include large strains [4,5,9,10].

The specific problems considered are in plane stretching of ASTM-E8 tensile specimen and plane strain bulging of sheet metal. Results obtained by BEM are compared to those obtained by FEM with regard to accuracy and efficiency.

## REFERENCES

1. Li, G. J., and Kobayashi, S., "Rigid-plastic finite element analysis of plane strain rolling", ASME 81-WA/Prod-13, Winter Annual Meeting (1981).
2. Lee, E. H., Mallett, R. L., and Yang, W. H., "Stress and deformation analysis of the metal extrusion process," *Comp. Meth. Appl. Mech. Engg.*, 10, 339-353 (1977).
3. Onate, E., and Zienkiewicz, O. C., "A viscous shell formulation for the analysis of thin sheet metal forming," *Int. J. Mech. Sci.*, 25, 305-335 (1983).
4. Chandra, A., and Mukherjee, S., "A finite element analysis of metal forming problems with an elastic-viscoplastic material model", *Int. J. Num. Meth. Eng.* (in press).
5. Chandra, A., and Mukherjee, S., "A finite element analysis of metal forming processes with thermomechanical coupling," *Int. J. Mech. Sci.* (submitted for publication).
6. Chandra, A., and Mukherjee, S., "Boundary element formulations for large strain large deformation problems of viscoplasticity," *Int. J. Sol. Struct.* (in press).
7. Chandra, A., and Mukherjee, S., "Applications of the boundary element method to large strain large deformation problems of viscoplasticity," *J. Strain Analysis*, 18, 4, 261-270 (1983).
8. Chandra, A., and Mukherjee, S., "A boundary element formulation for large strain problems of compressible plasticity," ASCE Winter Annual Meeting, Atlanta, GA (1984).
9. Hart, E. W., "Constitutive relations for the non-elastic deformation of metals," *ASME, J. Eng. Mat. Tech.*, 98, 193-202 (1976).
10. Hart, E. W., "The effects of material rotations in tension-torsion testing," *Int. J. Sol. Struct.*, 18, 1031-1042 (1982).

SYMBOLIC MANIPULATION LANGUAGE FOR THE ANALYSIS OF  
FLOW THROUGH CASCADE

by

F.F. Mahmoud and A.F. Abdel-Azim  
Zagazig University  
Mechanical Engineering Department  
Zagazig, Egypt

The present paper introduces a special purpose computer language aimed primarily at the analysis of aerodynamic flow through cascade using the finite element method. The finite element has become one of the most useful computer-oriented tool for solving partial differential equations of boundary value problems in engineering. So far, the evaluation of the finite element software covers dimensions of package implemented for analysis and design for special types of applications, automatic geometry and load generations by using optimizers of storage and precision, symbolic generation of finite element matrices, or interactive computer graphic system to display the input data and output results.

The objectives of the present paper is to introduce a proposed software for an automatic finite element procedure investing all capabilities of previous dimensions to give the aerodynamist the facility of formulating and solving the problem of the flow through cascade as an elliptic differential boundary value problem. The communication between the aerodynamist and the computer machine will be via an interactive symbolic manipulation language. To address this facility a symbolic manipulation processor has been implemented. However the system is limited to two dimensional flow through cascade, it could be enhanced easily to handle the three dimensional case.

## SWIRLING FLOW OF NEWTONIAN AND NON-NEWTONIAN FLUIDS

by

K.R. Rajagopal  
Department of Mechanical Engineering  
University of Pittsburgh  
Pittsburgh, PA 15261

The flow of the linearly viscous fluid between two infinite parallel plates rotating with constant (but different) angular velocities about a common axis has been studied in great detail. The assumptions which have been employed to study this problem have always led to axi-symmetric solutions. It is shown that the axi-symmetric flow is imbedded in a one-parameter family of solutions of the Navier-Stokes equation and thus within the class of all solutions of the Navier-Stokes equation to this problem, the special axi-symmetric solutions are never isolated solutions.

Existence of a one-parameter family of solutions to the flow of the linearly viscous fluid between two plates rotating at different angular velocities about non-coincident axes is also discussed. The flow has relevance to the flow occurring in an orthogonal rheometer. When the angular velocities of the plates are the same, the form assumed for motion is one of constant stretch history and this simplifies the equations of motion in the case of a general simple fluid to the same order as the Navier-Stokes equation, though in general much more non-linear. The problems associated with non-linear viscoelastic fluids of the Integral type are discussed.

HOLE PRESSURES AND NORMAL FORCES  
IN NON-NEWTONIAN FLUIDS

by

D. G. Baird  
Virginia Polytechnic and State University  
Blacksburg, VA 24061

Yann-Rin Ju  
Illinois Institute of Technology  
Chicago, IL 60616

and

David S. Malkus  
Mathematics Research Center  
University of Wisconsin  
Madison, WI 53705

This paper concerns the measurement of the first normal stress difference in non-Newtonian fluids by observation of the difference between the pressures at the top and bottom of a transverse slot, over which a fluid moves in a shearing motion. The paper also concerns attempts to verify the basic measurement relation between first normal stress difference and pressure difference in such flows using numerical simulation. It has been proposed that, under certain assumptions, pressure differences over the slot,  $P_e$ , the wall shear stress in undisturbed flow,  $\sigma$ , and the first normal stress difference,  $N_1$ , are related by an integral expression [1,2]. The validity of this relation is explored in this paper from an experimental and numerical point of view.

The stress-birefringence measurements of ref. 3 using Dow STYRON 678 show that the assumptions underlying the derivation of the integral expression relating  $N_1$ ,  $\sigma$  and  $P_e$  are significantly violated in the observed flows. Nevertheless, the directly measured values of  $P_e$  are found to be in good agreement with the integral relation whose derivation is suspect.

The numerical simulation involves the techniques of refs. 4 and 5, using the constitutive equation of Curtiss and Bird [6]. The same violations of the assumptions relating  $P_e$ ,  $N_1$ , and  $\sigma$  are found. The qualitative agreement between numerical and experimental results documenting the violations of the assumptions is quite good. But the numerical model also predicts that the deviation between simulated  $P_e$  and the prediction of the integral relation differ significantly in the same range of shear rates in which the experiments show good agreement. The numerical model predicts that the simulated  $P_e$  is significantly lower than the prediction of the integral relation using  $N_1$  and  $\sigma$  from the numerical simulation.

It is observed that the Curtiss-Bird constitutive equation does not fit the viscometric data of STYRON 678 very accurately and, most important for the integral relation, the shape of the curve  $N_1/\sigma$  plotted against  $\sigma$  is quite different for the Curtis-Bird fluid than the experimental fluid. This paper will discuss the robustness of the numerical results with respect to choice of constitutive equation and report on recent progress in attempts to find constitutive equations more suited to modelling flows of STYRON 678 over transverse slots.

Acknowledgements: The first author acknowledges the support of the Petroleum Research Fund, Grant No. 14158-AC7-C. The third author is supported by NSF Grant MCS-83-01433 and at the Mathematics Research Center, is sponsored by the United States Army under Contract No. DAAG29-80-C-0041.

- [1] Higashitani, K. and W. G. Pritchard, "A kinematic calculation of intrinsic errors in pressure measurements made with holes", Trans. Soc. Rheology, Vol. 16, 1972, pp. 687-696.
- [2] Lodge, A. S. and L. de Vargas, "Positive hole pressures and negative exit pressures generated by molten low-density polyethylene flowing through a slit die", Rheologica Acta, Vol. 22, 1983, p. 151.
- [3] Pike, R. D. and D. G. Baird, "Evaluation of the Higashitani and Pritchard analysis of the hole pressure using flow birefringence", J. Non-Newtonian Fluid Mechs., to appear.
- [4] Malkus, D. S. and B. Bernstein, "Flow of a Curtiss-Bird fluid over a transverse slot using the finite element drift function method", J. Non-Newtonian Fluid Mechs., to appear.
- [5] Ju, Marie Y.-B., M.S. Thesis, Illinois Institute of Technology, Chicago, 1984.
- [6] Curtiss, C. F. and R. B. Bird, "Kinetic theory for polymer melts", Parts I and II, J. Chem. Phys., Vol. 74, 1981, pp. 2016-2033.

## ON NON-NEWTONIAN FLOW THROUGH CONSTRICTIONS

by

Mogens Henriksen and Harry A. Hogan  
Mechanical Engineering Department  
College of Engineering  
Texas A&M University  
College Station, Texas 77843

The constitutive behavior of blood has been reported as Newtonian, micropolar and as that of a Bingham fluid. This presentation reports on development of computational techniques for the two non-Newtonian flow models cited. Because of possible clinical significance, special emphasis is placed on determination of accurate wall shear stresses and recirculation near a stenosis in the small arteries. A review of currently available constitutive data is included. The presentation covers work currently in progress.

PRESSURE PULSE PROPAGATION IN NON-NEWTONIAN  
FLUIDS CONTAINING SMALL GAS BUBBLES

by

Hans J. Rath and Peter Desch  
University of Bremen  
Dept. of Mechanics and Fluid Mechanics  
D-2800 Bremen, FRG

In this paper a theoretical model is developed, to describe the influence of polymer additives on the pressure pulse velocity and on the damping effect of the propagation of pressure waves in two-phase mixtures, where the carrier fluid is assumed to be a Non-Newtonian liquid in which are distributed small gas bubbles of variable radius. In connection with studies on cavitation it is desirable to have mathematical expressions for the phase velocity and the damping parameter of the system.

The increasing interest in drag reduction by polymer additives have stimulated some publications in cavitation and bubble dynamics. For our analytical calculation we consider the compressibility of the gas inside of the bubbles, rheological constants of the carrier fluid, the momentary volume fraction of the gas phase, surface tension and inertia effects due to the bubble oscillations. We neglect changes in temperature. For the gas bubbles we consider an isothermal gas law and constant mass. As a plane acoustic wave is passed through the liquid-gas mixture, the gas bubbles pulsate radially and oscillate in the translational direction. If the radius of the bubbles is small compared with the incident wavelength, then for the radial oscillations of the bubbles the fluid can be assumed to be incompressible.

In many flows of practical interest the volumetric concentration of the gas bubbles is small, so it is suitable to assume that the value of the void fraction of the mixture is small compared with unity. By means of some analytical calculations we obtain for the propagation of pressure waves of high frequency a wave equation of fourth order.

The results show that the phase velocity as well as the damping of the pressure waves depend on the rheological constants, on the momentary value of the void fraction, on the frequency of the ultrasonic field and on the elasticity of the pipe wall material.

FINITE DIFFERENCE SOLUTIONS FOR LOW REYNOLDS  
NUMBERS NON-NEWTONIAN FLOWS THROUGH PIPE  
EXPANSIONS

by

R.S.S. Adusumilli and G.A. Hill  
Department of Chemical Engineering  
University of Saskatchewan  
SASKATOON, Saskatchewan  
Canada S7N 0W0

Engineers, principally in the disciplines of Mechanical and/or Chemical Engineering, are aware of the problem of frictional eddy losses due to flow through pipe expansions. These eddies occur due to the abrupt change in diameter of the pipe and the relative relationship between inertial and viscous forces. Up to now, only macroscopic equations which use dubious assumptions have been available.

A mathematical model has been developed to solve the continuity and generalized momentum equations in two-dimensional form. The technique uses the Marker-and-Cell<sup>(1)</sup> (MAC) finite difference method but incorporates the viscous terms using the second invariant of strain and any desired relationship between stress and strain (viscometric model).

Results will be shown for the laminar flow of Newtonian, power law and truncated power law fluids as they traverse a pipe expansion for Reynolds numbers from 15 to 100. The pressure profiles calculated by the model are shown to agree with the experimental data and macroscopic predictions where available. Complete velocity profiles will be used to demonstrate both the steady state and transient growth of secondary flows.

(1) Harlow, F.H. and J.E. Welch, "Numerical Calculation of Time-Dependent Viscous Incompressible Flow", Phys. Fluids, 8, 1965, p. 2181.

## STABILITY OF THERMALLY STRATIFIED HARTMANN FLOW

by

R. K. Rathy  
 Meerut University  
 Meerut, U.P., India  
 and  
 Raj Pal Singh  
 L. R. College  
 Sahibabad, U.P., India

The stability of thermally stratified Hartmann flow between two parallel horizontal plates is investigated using asymptotic approximation method followed by Gage and Reid. The Hartmann flow gives normalized basic velocity distribution as  $U(y) = (\cosh My - \cosh My) / (\cosh M - 1)$ , where  $M$  is the Hartmann number. The viscous dissipation and the joule's heating are taken to be negligible which give constant temperature gradient in the basic flow. The fluid may be heated from above, giving positive temperature gradient, or heated from below, giving negative temperature gradient. The perturbations are taken to be two-dimensional and the normal component of perturbation velocity is taken to be an even function.

Neutral curves have been obtained for different values of Richardson number  $\eta$  and Hartmann number  $M$ , and their asymptotic behaviors have been analyzed. It is found that the lower and upper branches of the neutral curves behave differently when the Hartmann number is less than or greater than a certain value which depends on  $\eta$ . Kinks appear in the upper branches of neutral curves.

When the fluid is heated from above, statically stable configuration, we find that in the inviscid limit of Reynolds number  $R \rightarrow \infty$ , the phase velocity  $c \rightarrow 0$ , while the wave number  $\alpha \rightarrow \alpha_s \neq 0$ . This establishes the existence of standing waves in the neutral state. Moreover,  $\alpha_s$  increases with  $M$ . In  $(\alpha, c)$ -plane the neutral curves form close loops. When the fluid is heated from below, statically unstable configuration, we find that as  $R \rightarrow \infty$ ,  $c \rightarrow c_s \neq 0$  and  $\alpha \rightarrow \alpha_s \neq 0$ , along the upper branch, while  $c \rightarrow c_s \neq 0$ ,  $\alpha \rightarrow 0$ , along the lower branches, indicating the existence of neutral waves with finite or zero wave number. It also establishes a band of unstable modes in the limiting case of inviscid fluid.

The critical values of Reynolds number for different values of Hartmann number  $M$  and the Richardson number  $\eta$  have been obtained and it is shown that the magnetic field has a strong stabilizing effect. It is also found that the critical wave number decreases with increase in  $M$ .

## MOMENTUM TRANSPORT IN A WALL-JET OF POWER LAW FLUIDS

by

S. Bhaduri, Associate Professor  
and  
A. F. Amiri, Formerly Graduate Student  
Mechanical & Industrial Engineering Department  
The University of Texas at El Paso  
El Paso, TX 79968-0521

The similarity solutions for the longitudinal velocity distribution in laminar wall jets of power law fluids have been obtained by using a boundary layer type of analysis. The governing equations were normalized by specially developed similarity parameters. The approximate computer solutions have been obtained by using Runge-Kutta and Keller's numerical methods. The normalized velocity distributions for a few pseudoplastic ( $n < 1$ ) and dilatant fluids ( $n > 1$ ) are presented graphically. The  $n$  values used for the computer simulations are 0.7, 0.748, 0.763, 0.80, 0.873, 0.891, 0.9, 1.00, 1.20, and 1.30. It is observed that for the pseudoplastic fluids, the lateral variation of longitudinal velocity is less than that for the Newtonian fluid and the lateral variation of longitudinal velocity for the dilatant fluids is more than that for the Newtonian fluids. In addition, the decay of the dimensionless maximum velocity, the growths of the inner and outer layer thicknesses and the shear stress at the jet wall have been computed and presented graphically.

The results of the present study for Newtonian fluids compare favorably with those obtained by Glauert. Since the present study yields almost identical results for the Newtonian case, it is reasonable to expect that the results for the pseudoplastic and dilatant fluid cases are reasonably accurate.

The characteristic decay rate of the maximum longitudinal velocity in wall jet shows that, for the pseudoplastic fluid jet, it is faster than that of Newtonian fluid jet. For large values of the downstream distance, the decay rates approach asymptotic values.

The growth rate of the inner and outer layer of the wall jet shows that pseudoplastic wall jet is thicker than the Newtonian wall jet and the dilatant jet is thinner than the Newtonian wall jet. The variation of the dimensionless shear stress at the wall in the downstream direction shows that for pseudo-plastic fluid, it decreases more than that for the Newtonian fluid. For the dilatant fluid jet, the decrease in shear stress at the wall is less than that for the Newtonian fluid jet.

## LAMINAR JETS OF POWER - LAW FLUIDS

S. Bhaduri

Associate Professor

Mechanical and Industrial Engineering Department

The University of Texas at El Paso

El Paso, Texas

and

J. Van Reet

Engineer, El Paso Natural Gas Co.

El Paso, Texas

The similarity solutions for the longitudinal velocity distributions in laminar plane jets and circular jets of non-Newtonian power-law fluids, so-called pseudo-plastics and dilatants, have been obtained by using boundary layer type of analysis. The plane jet is assumed to emerge from a two-dimensional narrow opening and carries with it some of the surrounding fluid which is originally at rest, because of the viscous friction developed at the jet periphery. The axisymmetric circular jet emerges from a circular opening and carries some of the surrounding fluid with it. The basic governing equations of both jets are written in dimensionless forms by using similarity parameters.

The basic features of the jets are that (a) they spread outwards in the downstream direction, (b) the longitudinal velocity in the center decreases in the downstream direction and (c) the constant ambient pressure is imposed on the jets. The total longitudinal momentum remains constant and is independent of the downstream distance from the origin.

The normalized governing equations with appropriate boundary conditions, were solved numerically by using fourth-order Runge-Kutte method. Computer programs were used for the computations. The normalized velocity as function of normalized lateral distance is graphically presented for the power-law exponent values of  $n = 0.50, 0.75, 1.00, 1.25$  and  $1.50$  for both the plane and circular jets.

The results of the present solutions for Newtonian fluid jets ( $n = 1.0$ ), are compared with those for the plane jet and circular jet given by White and Schlichling respectively and are found to be in good agreement.

It is observed that for pseudoplastic fluid ( $n < 1$ ) jets are wider than that of Newtonian fluid jets and that the dilatant fluid ( $n > 1$ ) jets are narrower than the Newtonian jets.

## SOLUTION TO STOKES' PROBLEM IN A VISCOELASTIC MEDIUM

by

David H. Jen, William Squire, and Severino L. Koh\*  
Department of Mechanical and Aerospace Engineering  
West Virginia University  
Morgantown, West Virginia 26506

The problem of a concentrated, time-dependent force acting in a viscoelastic medium of the Kelvin-Voigt type is considered. The force is taken to be a unidirectional, exponential function. The Theorem of Correspondence of Linear Viscoelasticity is applied to obtain the solution from that of a corresponding problem involving an elastic medium, with the displacements readily obtained in the Laplace transform domain.

Five methods of numerical inversion of the transform solution were tested. These included the use of a Fourier series expansion, a Laguerre polynomial expansion, Gaussian quadrature, and two new methods: one developed by Hosono (1) and the other by Gaver (2) and Stehfest (3). An error analysis of the five methods of inversion was made, comparing the results from each of the methods with the elastic solution.

A time-varying plot of the displaced configuration of an initial unit circle centered at the point of application of the force demonstrated the distortion of the unit circle. Reflecting the form of the exponential forcing function, a dimple developed in the rear of the "circle" (180 deg opposed to the direction of the force). The axial and radial components of the displacement field were obtained for different materials.

(1) Hosono, T., "Numerical Inversion of Laplace Transform and Some Applications to Wave Optics", Radio Science, Vol. 16, No. 6, 1981, pp. 1015-1019.

(2) Gaver, D.P., "Observing Stochastic Processes and Approximate Transform Inversion", Operations Research, Vol. 14, No. 3, 1966, pp. 444-459.

(3) Stehfest, H., "Numerical Inversion of Laplace Transforms", Communications of the ACM, Vol. 13, No. 1, 1970, pp. 47-49.

\*DHJ is currently with the Department of Mechanical Engineering, Stanford University, and SLK is on leave from WVU, currently with the Office of Basic Energy Sciences, U.S. Department of Energy, Washington, D.C. 20545.

A NUMERICAL SOLUTION OF THE FLOW OF VISCOPLASTIC  
FLUIDS IN 180° CHANNELS

by

V. Dakshina Murty  
Multnomah School of Engineering  
University of Portland  
Portland, OR 97203

Some of the most important industrial fluids like greases, slurries, dough, pastes, etc. cannot be described by the usual Newtonian (power-law) fluid models. These fluids have the common property that they behave like solids when the shear stress is less than the yield stress and flow like a fluid when the shear stress exceeds the yield stress. Such fluids can be adequately described by the Bingham plastic model. In the present investigation a numerical scheme based on the finite element method is developed to analyze steady flow of Bingham plastics.

As mentioned above, the simplest constitutive equation which can exhibit the phenomenon of yield stress is the Bingham plastic model. The shear stress tensor for such a fluid is given as follows:

$$\tau_{ij} = \kappa + \eta D_{ij} \quad \text{when } \frac{1}{2} \tau_{ij} \tau_{ji} \geq \kappa^2 \quad (1)$$

$$D_{ij} = 0 \quad \text{when } \frac{1}{2} \tau_{ij} \tau_{ji} < \kappa^2 \quad (2)$$

where  $\kappa$  is the yield stress of the fluid and  $D_{ij}$  is the symmetric part of the velocity gradient. From a computational standpoint, it is very hard to impose the condition of no deformation before yield. In the present investigation, (1) and (2) are replaced by the following:

$$\tau_{ij} = \begin{cases} \kappa(1 - \frac{\eta}{\eta_r}) + \eta D_{ij} & \text{when } \dot{\gamma} \geq \dot{\gamma}_y \\ \eta_r D_{ij} & \text{when } \dot{\gamma} < \dot{\gamma}_y \end{cases} \quad (3)$$

where  $\dot{\gamma}$  and  $\dot{\gamma}_y$  are the strain rate and yield strain rate, and  $\eta_r$  is the pre-yield viscosity such that  $\eta/\eta_r \ll 1$ . In the present work  $\eta/\eta_r = 0.001$ . The remaining formulation follows the usual finite element scheme wherein, the continuity and linear momentum equations together with (3) are discretized and a set of equations involving nodal point unknowns is obtained. This numerical scheme is applied to the problem of flow through a 180° channel. The fluid is driven by means of a pressure gradient. The effect of the curvature and yield stress on the flow pattern and the convergence of the scheme will be demonstrated.

## THE NATIONAL GEOTECHNICAL CENTRIFUGE FACILITY

by

James A. Cheney  
University of California, Davis  
Center for Geotechnical Modeling  
Davis, CA 95616

A large centrifuge formerly utilized in the Apollo space program at NASA Ames Research Center in Mountain View, California, has been modified and rededicated for the use of the geotechnical engineering community. This centrifuge is designed for upgrading to a capacity of 2 million g-tons, carrying 40,000 lbs. at 100 g. Initially, at the present, the capacity is limited to 6,000 lbs. at approximately 100 g. This limitation is due to the torque limits on the gear train driving the arm and can be overcome by several architectural changes in the centrifuge rotunda which will reduce aerodynamic drag on the arm.

The arm radius to the floor of the swing platform is 30 feet. The platform is 6 feet in the direction of spin and 7 feet lateral, having a very stiff floor. A clear height of 5 feet above the floor is normally available for experiment packages. This limit can be modified for lower g applications with a modification to the pivot brace.

Over 100 electrical slip rings are available for transmission of instrumentation signals. Signal conditioning packages for strain gages, accelerometers, LVDTs, and pore pressure gages are available at the hub prior to transmission through the slip rings to permit a higher signal-to-noise ratio. In the control room a DEC LSI 11/23 mini-computer is available for data acquisition and reduction. Room and on-board TV cameras, and on-board 35 mm photographic camera, are available for visual observation and recording.

Access to the facility offers no problems for American citizens, permanent residents, or citizens of Western block countries. Researchers from the Eastern block will require approvals through the Department of State, and other special arrangements. The Ames Research Center is reached by traveling south from San Francisco 60 miles along the Bay Shore Freeway or north from San Jose about 20 miles.

Research on the NGC planned so far includes: Vibration of Machine Foundations, Explosive Cratering in Alluvium, Near Surface Explosions in Water, Cratering in Ice, Containment of Explosives Near Rubble Chimneys, Plane Strain Modeling of Clay Foundations, Stability of Tall Towers in Clay.

by

Keith A. Holsapple  
University of Washington FS-10  
Seattle, WA 98195

An analysis of the similarity transformations that leave invariant the fundamental field equations of continuum mechanics in their general form is given. Additional invariance requirements arising from the constitutive equations are considered. Two classes of problems are identified. In the first class are those constitutive equations that are both size- and rate-independent, but include arbitrary hysteretic and non-linear behavior, such as general non-linear plasticity and/or fracture. In this case, subscale simulations are possible directly in the material of interest, require elevated gravity in inverse proportion to the model scale if gravity-dependent, and no further specific knowledge or assumptions about the constitutive behavior are necessary.

In the second class of problems there are material parameters governing either rate- or size-dependent properties. In this case, elevated gravity testing is still possible, but must be based upon specific knowledge of, and certain simplicity of, the form of the constitutive equations, and requires matching the specific dimensionless groups that arise from the constitutive equations and govern the process. The assumption of linear viscosity and the resulting Reynolds number in fluid dynamics is a foremost example of this class of problems. Extension of the range of testing in these cases can in principle be made with substitute materials, but this approach is risky in geomechanics.

Examples of interest utilizing a centrifuge in geomechanics problems will be presented. These include dynamic processes in dry and saturated soils, with potential liquefaction effects that are size and possibly rate dependent. Also to be discussed are problems in rate-dependent materials such as ice and viscous fluids, gravity wave generation and propagation and bubble growth.

## TWO MODELING EFFECTS IN A GEOTECHNICAL CENTRIFUGE

by

Chiang C. Mei  
Massachusetts Institute of Technology  
Department of Civil Engineering  
Cambridge, MA 02139

Since their introduction in the 1930's in the Soviet Union, several centrifuge laboratories have been established in the West, the latest being the U. S. National Geotechnical Centrifuge at the University of California, Davis. Their applications have ranged from soil consolidation to dynamical problems involving cyclic loadings.

As in all laboratory experiments it is important to assess those additional effects which result from the model and are absent in the prototype. The obvious effects are: 1) the limited size of the soil container when modeling a large region, 2) variation of gravity with depth, and 3) Coriolis force. The first is also of common concern in laboratory experiments in a stationary environment. The second is the result of finite length of the rotating arm and can be neglected only if the model depth is sufficiently small compared to R. Coriolis force, if important, brings in physical effects which are less familiar in soil mechanics. It has been regarded as being inconsequential in earlier days of the centrifuge when the rotational speeds were rather low (Schofield, 1976).

As the centrifuge has already been used in an increasing number of static and dynamical problems in soil mechanics, and its potential is likely going to expand to other technical fields, it is worthwhile to examine quantitatively these modeling effects so as to facilitate proper interpretation of experimental results. In this paper we focus our attention on only two aspects: 1) Coriolis force in seepage problems, 2) the variation of gravity with depth on the consolidation of a thin soil layer under its own weight. We shall begin by an order-of-magnitude analysis in order to sort out the circumstances in which these effects are not negligible, and then work out the theoretical solutions to some problems in order to compare with their nonrotating counterparts. These problems are simple enough to be experimentally checked in a centrifuge.

Schofield, A.N., "General Principles of Centrifuge Model Testing and a Review of Some Testing Facilities," p. 328-339; "The Role of Centrifuge Modeling," p. 342-350, in Offshore Soil Mechanics. Ed. by P. George and D. Wood. Cambridge University and Lloyd's register of Shipping.

CENTRIFUGE CRATERING EXPERIMENTS:  
IMPORTANT NEW IMPACT AND EXPLOSION SCALING RESULTS

by

Robert M. Schmidt  
Weapon Effects and Shock Physics  
Boeing Aerospace Co. M/S 13-20  
P.O. Box 3999, Seattle, WA 98124

Very large full scale impact or explosion cratering events are physically, economically and politically impossible to perform. How then, do we study the behavior for these large events that play a significant role in the understanding of planetary evolution and nuclear weapon effects?

To investigate the cratering phenomenon, an experimental technique employing a centrifuge to properly scale size for dynamic soil mechanics has been developed. With the variation of gravity alone, using small explosives, or impacts from a hypervelocity projectile gun, scaling rules for ultra-large cratering events can be determined. The dependence of the crater volume upon gravity alone has been found to provide the key to the complete determination of the dynamic and kinematic behavior of crater formation as well as ejecta phenomena. In addition to scaling results, details of test techniques will be presented. These will include discussion of various rotor-mounted hardware: a 2-stage light-gas gun, rotating-prism movie camera, and stereo cameras. Some discussion will be devoted to data acquisition for dynamic response measurements on a time scale of 10's of microseconds.

This cratering investigation provides an important example of the utility and suitability of a centrifuge to provide data in a regime otherwise unobtainable. Furthermore, validation of the centrifuge technique for this class of dynamic problems has been demonstrated by numerous favorable comparisons between subscale simulations of field prototypes at scales of 300 or 400 to 1. To the best of the authors knowledge, this work is the first direct comparison between subscale centrifuge tests with full-scale prototypes for dynamic phenomena.

## APPLICATION OF CENTRIFUGE FOR FLUID MECHANICAL PROBLEMS

by

Tokuo Yamamoto

Division of Ocean Engineering

Rosenstiel School of Marine and Atmospheric Science

University of Miami

Miami, Florida 33149

Gravity water waves of various kinds interact with soils and present many important engineering mechanical problems. Some problems may not be solved theoretically but may require experimental methods because of the very complicated physical processes involved. Some such problems are discussed in this paper relative to possible applications of geotechnical centrifuges.

The first problem is the generation of water waves by impulse sources such as a large nuclear explosion on the continental shelf and a large body of earth sliding into a bay or a lake. If the initial free surface disturbance is known or predictable, the subsequent wave propagation problem can be solved mathematically as an initial value problem known as the Cauchy-Poisson problem. However, no theory is available for predicting the initial free surface disturbances by these impulsive sources. They have to be determined by properly scaled model tests. The basis for centrifuge testing of this problem has been shown by Holsapple and Schmidt (1) and is also presented by them at this conference.

The second problem is the flow slide development in the earth structures and slopes by various kinds of water waves. Numerous failures of seawalls and embankments have been caused by the "suck-out" induced by severe wind waves (2). The "suck-out" is a phenomenon of soils flowing out from behind a seawall when the water surface draws down by the waves. The sea level fluctuates considerably, on the order of + 5 m, at high altitudes such as Norway. Many massive flow slides of submarine slopes in the Fjords have been reported (3). The submarine land slides occur almost always at low tides. Undoubtedly the large sea level draw-downs by tides are responsible for the initiation of submarine slope slides. Similar submarine slope slides are caused by tsunamis (3).

The above observations suggest the same failure mechanism of earth structures and submarine slopes by wind waves, tides and tsunamis; the cyclic loading associated with a large water surface drawn-down. Just like other flow slide problems, this problem must be tested under the prototype stress state. Experimental procedures required for centrifuge test will be presented. The scaling effects for time, seepage flow and stress associated with centrifuge experiments will be discussed.

## References:

1. K. A. Holsapple and R. M. Schmidt, "On the scaling of crater dimensions 2; impact processes," *J. Geophys. Res.*, 87, 1849-1870, 1980.
2. Osamu Toyoshima, Coastal Engineering for Field Engineers, Vols. 1 and 2, Morikita Publisher, Tokyo, Japan, 1976. (in Japanese).
3. Svend Saxov and J. K. Nieuwenhuis (Ed.) Marine Slides and Other Mass Movements, Plenum Press, New York, 1982.

DYNAMIC STRESS WAVE REFLECTION/ATTENUATION  
AND EARTHQUAKE SIMULATION  
IN CENTRIFUGE SOIL MODELS

by

Jean H. Prevost and Robert H. Scanlan  
Department of Civil Engineering  
Princeton University  
Princeton, NJ 08544

Standing wave reflections during dynamic centrifuge soil experiments are studied. The experimental evidences presented clearly show the presence and prominence of standing waves excited by various dynamic inputs in a sand deposit contained in a centrifuge bucket. It is shown that the potentially negative influence of wave reflections in forced vibration-type experiments may be circumvented through an appropriate sizing of the bucket. However, the strong detrimental effects of wave reflections for earthquake simulation can only be cured through the design of absorptive boundaries. A modest degree of success toward producing a model earthquake is reported via two devices: a certain kind of physically tuned internal excitor and an effective absorbent material at the walls.

CENTRIFUGE MODELLING OF TECTONIC PROCESSES:  
RHEOLOGIC PROPERTIES OF SOME ANALOG MATERIALS  
AND COMPARISON TO NATURAL PROTOTYPES

by

John M. Dixon  
Dept. of Geological Sciences  
Queen's University  
Kingston, Ontario, K7L 3N6

The Experimental Tectonics Laboratory at Queen's University is equipped with a large-capacity centrifuge that is capable of subjecting tectonic models measuring 127 x 76 mm in plan and up to 51 mm in depth to accelerations as high as 20,000 x g. This high capacity greatly extends the range of potential analog materials and permits the use of relatively stiff and/or brittle substances.

A number of new techniques of model construction have been devised, that permit internal and surface strain patterns and kinematic evolution to be monitored in detail. One particularly useful technique allows the preparation of highly uniform anisotropic multilayers composed of alternating layers of Plasticine and Silicone Putty, with individual layers thicknesses as low as 20 microns and with controllable ratio of thickness between the relatively competent and incompetent units.

The commonly used model material, silicone putty, has been subjected to a series of rheological tests. The tests indicate that at strain rates in the range  $10^{-6}$  to  $10^{-3}$  s<sup>-1</sup> (applicable to the centrifuge experiments) the silicone putty exhibits power-law rheology with  $n = 7 \pm 2$ . It has an effective yield strength of about 300 Pa at a strain rate of  $10^{-6}$  s<sup>-1</sup>. At strain rates faster than  $10^{-2}$  s<sup>-1</sup> the material appears to tend towards linear behavior.

Evaluation of published data on the rheologic properties of plasticine in the light of our own experience suggests that this material exhibits power-law flow with  $n = 6-9$  over a wide range of strain-rate ( $10^{-6}$  to  $10^{-1}$ ), and an effective yield strength of 15-150 kPa (at a strain rate of  $10^{-6}$  s<sup>-1</sup>).

Dimensional analysis using available rheological data, standard scaling laws and appropriate model ratios (model ratio of length =  $10^{-5}$  to  $10^{-6}$ , model ratio of specific gravity = 0.6, and model ratio of time =  $10^{-10}$ , for typical experiments run at 2000 to 7500 x g) suggests that the microlaminated plasticine-silicone putty multilayer is a suitable analog, in centrifuged experiments, for interbedded sequences of indurate limestone and incompetent shale. The excellent degree of dynamic similitude attained is confirmed by the realistic forms of fold and fault structures developed in models constructed of this material.

Model studies in progress and recently completed have simulated a range of tectonic processes such as folding and faulting due to lateral compression of horizontally stratified rocks in a foreland setting, faulting of stratified sedimentary cover over salt diapirs, subsidence of synclinal troughs between mantled gneiss domes, and magmatic intrusion of laccoliths into stratified country rocks.

## MODELING OF PILE FOUNDATIONS

by

Hon-Yim Ko  
University of Colorado  
Department of Civil Engineering  
Boulder, CO 80309

Centrifuge modeling of geotechnical phenomena and structures has received increasing acceptance recently. However, the validity of the method has to be eventually confirmed with performance of the prototype being modeled. It is rare that such prototype data are available for ascertaining the accuracy of the centrifuge test results, due to the immense costs of conducting such experiments and the difficulties in carrying some of them to failure.

Such an opportunity arose when two full scale load tests of pile foundations produced a wealth of information on the behavior of two different pile types on two different soils. A laboratory test program was conducted on the 10 g-ton geotechnical centrifuge at the University of Colorado to model these field tests. The centrifuge can apply an acceleration of 100 g on a 200 lb. soil model, and through the two hydraulic rotary joints loading mechanisms can be operated to transmit forces to piles being tested. Electric signals from transducers are transmitted through the 56 electric slip rings.

In the first modeling testing series, tapered timber in sand at the Locks and Dam 26 site near St. Louis were modeled. It was found to be necessary to install the model piles while the centrifuge is in flight in order to model correctly the embedment, and therefore, the load resistance of piles in granular soils. Single piles at 50, 70 and 100th model scales were tested at the corresponding gravity levels for their behavior and capacity under axial loading. The results of these modeling of model tests were found to be self consistent and to correlate well with the prototype measurements.

The single piles were also tested in lateral loading at 70 g. In addition, the 2 by 4 pile group in the prototype was also modeled. In all testing, the main factor to be simulated in the prototype foundation is the friction angle of the foundation sand. It was estimated that the prototype soil has a friction angle of 40 degrees and a dry unit weight of 100 lb./cu.ft. Considerable effort was spent in duplicating these conditions.

In the second modeling testing series, hollow pipe piles tested in the Beaumont clay on the Houston area were modeled in the centrifuge test program. Hollow aluminum tubes were used as the model piles. Strain gages were attached to the inside of these tubes to measure the stress generated in the piles during loading. Thus, it is possible to measure the load transfer characteristics during axial loading and the bending moment distribution under

The undrained shear strength in the prototype foundation was estimated to be 2.4 ksf, with a slight increase over the 40 ft. length of the pile. Kaolin was used to model the Beaumont clay, while the strength profile was reproduced by a combination of surcharge loading outside the centrifuge followed by centrifugation. It was not possible to always duplicate the desired profile. However, in each test, the inflight strength was determined by vane shear testing on the centrifuge. From the results obtained over several model scales of 50, 70 and 100, the capacities of the model piles show very consistent correlation to the undrained shear strength. When these model results are extrapolated to the full scale, the prototype measurements also fall in the same trend.

The 3 by 3 pile group in the prototype was also modeled in the centrifuge test program. In both the single pile tests and the pile group tests, the loading transfer in individual piles showed that these piles act as friction piles and the skin friction measured in the models confirmed the value determined in the prototype tests.

The work in this project demonstrated that it is possible to carry modeling of pile foundations in the centrifuge. However, it is necessary to pay special attention to the condition in the prototype foundation material. Since it is often impossible to refine the foundation information, centrifuge testing makes it possible to carry out parametric studies on the influence of various parameters on the performance of the pile foundation without incurring excessive costs.

## GEOTECHNICAL CENTRIFUGE MODELLING

by

Deborah J. Goodings  
Department of Civil Engineering  
University of Maryland  
College Park MD 20742

Geotechnical engineering, the study of the role of soil and rock in civil engineering projects, is an important and relatively new discipline which has become more a science than an art since Karl Terzaghi's contributions in the 1920's. It has become a subject of prolonged research for two reasons: the engineer usually has no choice but to deal with the soil and rock as it exists at his site, and the behavior of that soil and rock is non-linear and may change over time according to loading and environment conditions. With the rapid growth of computer technology, the emphasis of American research in geotechnical engineering took the direction of numerical analysis, however, important gaps in the understanding of the mechanics of soil and rock limited such techniques in certain instances. This caused the research community to consider physical models.

Large scale physical models have the advantage that they require no scaling compromises, but they may be difficult to control, expensive dangerous, and in certain instances, may involve loading conditions which are impossible to produce, as in the case of earthquakes and floods. Nonetheless, it is important for correct modeling in soils and rocks that the full scale stress gradient, with zero stress at the soil surface increasing in value according to depth, be replicated in any model. Herein lie the major attributes of the reduced scale centrifuge model: it is constructed of real soil or rock to whatever configuration exists in situ, a wide range of loadings may be applied to it and the responses monitored, and that crucial full scale stress gradient is correctly replicated by increasing the self weight of the model by the same multiple as the model dimensions have been reduced, by means of centrifugal acceleration.

This technique was conceived for application in geotechnical engineering over fifty years ago, independently, but simultaneously, by three researchers: one American and two Soviets, but only the Soviet researchers went on to apply it to their especially difficult geotechnical problems. Over the past fifteen years the technique has attracted new attention in the West, becoming more commonly accepted in the United States only since 1977. The range of problems examined over the years has included: slope stability, foundation design, off-shore gravity drilling platforms, embankment dams, trench stability, tunnel collapse, and earthquake modelling, among others.

This paper will examine the principles of geotechnical centrifuge modelling, the limitations, and some examples of successful applications.

PARTICLE ROTATION AND STRESSES IN  
A SIMPLE SHEAR FLOW OF UNIFORM DISCS

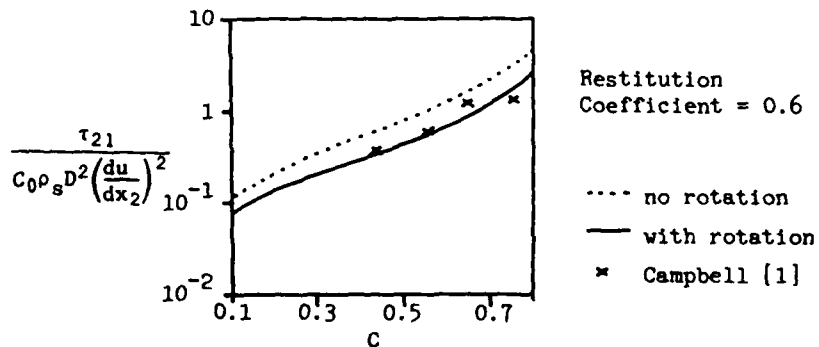
by

Mark A. Hopkins and Hayley H. Shen  
Department of Civil and Environmental Engineering  
Clarkson University, Potsdam, N.Y. 13767

Stresses generated in a shearing flow of granular solids have been quantified as the rate of momentum transfer due to binary collisions among the granular solids [2, 3, 4, 5]. The concentration and the material properties of the granular solids determine the rate at which these collisions occur and the amount of momentum transfer during these collisions. In all the existing theories that explicitly formulate the stresses, the rotational motion of solids is neglected. Not only is this inconsistent with the frictional impact, which the existing theories consider in detail, but also this contradicts the observations of real or computer simulated granular flows.

In this study, the stresses generated in a simple shear flow of uniform discs is analyzed. The rotational motion of individual disc induced by frictional impacts are incorporated in the formulation. It is found that the mean rotation is a function of the mean shear rate. The fluctuation of rotation is determined as a function of the mean shear rate, the material properties and the concentration of the discs. In general, the stresses is lower as the rotational motion is included.

The result is compared with data obtained in a computer simulated simple shear flow [1]. This comparison is shown in the figure below.



References:

1. Campbell, C.S., Ph.D. Thesis, Cal. Institute of Technology, 1982.
2. Jenkins, J.T. and Savage S.B., J. Fluid Mech., V. 130, p. 187, 1983.
3. Ogawa, S., Omemura, A. and Oshima, N., ZAMP, V. 31, p. 483, 1980.
4. Shen, H.H. and Ackermann, N.L., ASCE/EM5, p. 748, 1982.
5. Shen, H.H. and Ackermann, N.L., J. Engrg. Sci., to appear.

## KINETIC THEORIES FOR RAPID GRANULAR FLOWS

by

C. K. K. Lun and S. B. Savage  
Department of Civil Engineering & Applied Mechanics  
McGill University  
Montreal, Canada

Statistical methods analogous to those used in the kinetic theory of dense gases are applied to derive conservation equations and constitutive equations for the rapid flow of granular materials such as sand, mineral concentrate, grains, fertilizers, pills and powder snow. The granular material is idealized as a mass of uniform, rough, inelastic spherical particles. The present theory differs from the classical kinetic theory of dense gases because of the need to incorporate the effects of energy dissipation resulting from collisions between rough, inelastic particles. A constant coefficient of restitution  $e$  is used to characterize the inelasticity of the particles and a roughness coefficient is adopted to characterize the inelasticity of the particles and a roughness coefficient is adopted to characterize the effects of surface friction in collisions between grains.

The first part of the study considers the case of perfectly smooth but slightly inelastic particles using an approach analogous to the approximation scheme developed in the Chapman-Enskog theory. The singlet and pair velocity distribution functions are evaluated using the moment equations derived from the Maxwell transport equation. The constitutive equations for stress, energy flux and rate of energy dissipation, which incorporate both the kinetic and collisional contributions, can be applied to the computation of general flow fields. The specific case of Couette flow is analysed and compared with experimental data. The predicted stresses are found to agree fairly well with the experimental measurements.

The second part considers the case of rough, slightly inelastic particles. Simple forms for the singlet and pair velocity distribution functions are employed to study the effects of rotary inertia due to surface friction of the particles. The collisional stress tensor is found to be asymmetric during general deformations, however for the special case of Couette flow it remains symmetric. The partition of fluctuation kinetic energy between the translational and rotational modes is examined; equipartition is achieved only for the case of perfectly rough particles. In agreement with previous investigations, the stresses are found to increase with increasing  $e$ . The effects of rotary inertia due to roughness generally reduce the stresses except for the case of almost perfectly rough particles. The normal stresses are reduced more than the shear stresses. As a result the predicted ratio of shear to normal stress, i.e. the dynamic friction angle, is higher for rough particles than for smooth ones and agrees more closely with experimental measurements.

## A TURBULENT MODEL FOR THE RAPID FLOW OF GRANULAR MATERIALS

by

Mohsen Shahinpoor  
 Department of Mechanical and Industrial Engineering  
 Clarkson University  
 Potsdam, NY 13676

As is well known, the rapid flow of granular materials is generally maintained by particle collision and transfer of momenta in an inertia setting such that the granules in such rapid motions end up having highly irregular paths due to high rate of collision—a situation reminiscent of turbulent flow in the presence of local velocity fluctuations. Here the techniques of dealing with hydrodynamic turbulence is applied to the analysis of rapid flow of granular materials to see if any meaningful result may emerge out of the analysis. It turns out that results remarkably close to experimentally observed data on rapid granular flow can be deduced from the turbulent modeling [1]. Here, from the global equations of balance for particulate media and by means of a special ensemble averaging technique, the local equations governing the mean motion and the random fluctuations in a rapid flow of granular materials are derived. The resulting equations resemble those of a compressible turbulent flow. Approximate expressions for the components of the fluctuation stress tensor are obtained which are computable and rather new. Simplified for a plane rapid shear granular flow they read

$$\tau_{xy} = \eta \rho_0 d^2 v^{1/3} (v_m - v)^{-2} \left| \frac{\partial \bar{v}_x}{\partial y} \right| \frac{\partial \bar{v}_x}{\partial y}, \quad (1)$$

$$\sigma_{xx} = -\gamma_1 \rho_0 d^2 v^{1/3} (v_m - v)^{-2} \left( \frac{\partial \bar{v}_x}{\partial y} \right)^2, \quad (2)$$

$$\sigma_{yy} = -\gamma_2 \rho_0 d^2 v^{1/3} (v_m - v)^{-2} \left( \frac{\partial \bar{v}_x}{\partial y} \right)^2, \quad (3)$$

where  $\eta$ ,  $\gamma_1$ ,  $\gamma_2$ , are constants,  $\rho_0$  is the grain density,  $d$  is the grain diameter,  $v$  is the solid volume fraction,  $v_m = \max v$ ,  $\bar{v}_x$  is the component of the velocity in the  $x$ -direction as a function of  $y$ ,  $(x, y)$  forming a rectangular system of coordinates. The shear stress, obtained thus, has been plotted (Fig. 1) against the experimental data of Bagnold [2] and McTigue [3]. As can be seen remarkable agreement is obtained.

#### References

- Ahmadi, G. and Shahinpoor, M., "Towards a Turbulent Modeling of Rapid Flow of Granular Materials," Powder Tech. vol. 35 (1983), pp. 241-248.
- Bagnold, R.A., "Experiments on a Gravity-Free Dispersion of Large Spheres in Newtonian Fluid Under Shear," Proc. Roy. Soc. London, vol. A.225 (1954), pp. 49-63.

McTigue, D.F., "A Nonlinear Constitutive Model for Granular Materials: Application to Gravity Flow," Trans. ASME J. App. Mech. Vol. 49 (1982), pp. 291-298.

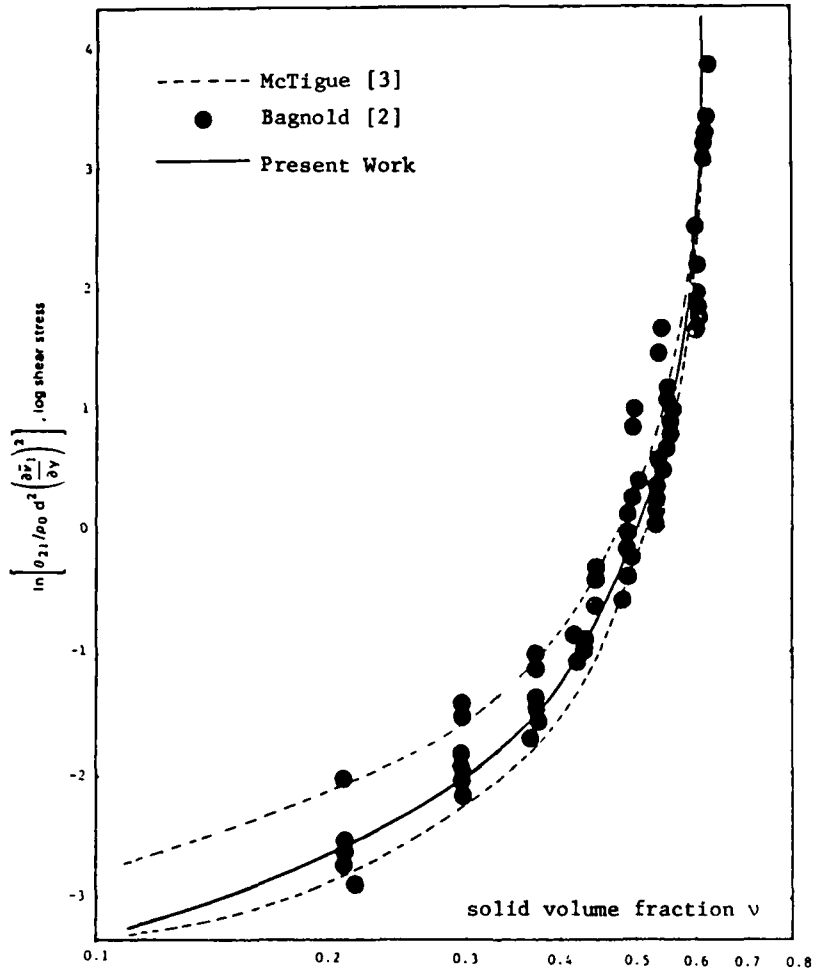


Fig. 1 - Dimensionless natural log of shear stress versus the variations of solid volume fraction of solids; Bagnold [2], McTigue [3].

ESTIMATION OF STRENGTH PROPERTIES OF GEOLOGICAL  
MATERIALS FROM SHOCK HUGONIOT CHARACTERISTICS

by

Aaron Das Gupta  
Mechanical Engineer  
US Army Ballistic Research Laboratory  
US Army Armament Research and Development Command  
Aberdeen Proving Ground, Maryland 21005.

Characterization of constitutive behavior of three geological materials e.g., unsaturated and saturated tuffs and a oil shale has been obtained from shock compression behavior of such materials and their Hugoniot characteristics. Although the equations-of-state in the form of pressure-density relationships for shock propagation in such mediums can be markedly nonlinear, the characterization technique in this investigation is currently restricted to materials with linear Hugoniot characteristics at all pressure ranges.

Under the assumptions of unidimensional shock propagation and conservation law of mass, momentum and energy, the equations - of - state could be transformed to bulk moduli versus volume strain relationships using the methodology described in this paper. The transformed characterization is compatible with the tension cut-off curve description material model in the ADINA nonlinear finite element analysis program.

The method could be readily extended to partially saturated soil and sand with nonlinear characteristics through multilinear approximation during the loading and unloading phase. The resulting constitutive relationships will allow explicit modeling of the surrounding medium around shallow buried structures and realistic simulation of soil-structure interaction which can significantly alter the dynamic response behavior of such structures due to shock wave attenuation.

EFFECT OF HEATED WALL BOUNDARY CONDITION ON FREE CONVECTION  
IN VERTICAL ANNULI FILLED WITH SATURATED POROUS MEDIA

by

V. Prasad  
Department of Mechanical Engineering  
Clemson University, Clemson, SC 29631

and

F. A. Kulacki  
Department of Aerospace and Mechanical Engineering  
University of Delaware, Newark, DE 19716

Natural convection in vertical annuli filled with saturated porous media has been numerically investigated for both constant temperature (CT) and uniform heat flux (UHF) boundary conditions on the inner wall. The outer wall is assumed to be isothermally cooled whereas the top and bottom are insulated. The effects of curvature and heated wall boundary condition on the temperature and flow fields, and heat transfer rates have been studied for wide range of parameters  $1 < \kappa < 26$ ,  $0.3 < A < 20$  and  $Ra^*$  up to  $10^4$ , where  $\kappa$ ,  $A$ , and  $Ra^*$  are radius ratio (outer/inner radii), aspect ratio (height-to-gap) and modified Rayleigh number, respectively.

The isotherm and streamlines show that the introduction of curvature effects ( $\kappa > 1$ ) completely disturbs [1,2] the centro-symmetric behavior of the temperature and flow fields observed in the case of isothermally heated cavity ( $\kappa = 1$ ) [3]. The change in boundary condition from constant temperature (CT) to uniform heat flux (UHF) further adds to this asymmetric behavior. For shallow annuli ( $A < 1$ ), an increase in radius ratio beyond unity has a stabilizing effect on the multi-cellular flow behavior of shallow cavity [4]. Higher the radius ratio, lower is the aspect ratio required for the multi-cellular flow to exist for a fixed  $Ra^*$  [2]. The change in boundary condition from CT to UHF has a similar effect on the flow structure.

The aforementioned asymmetry in the temperature field results in the lower effective sink temperature for the boundary layer on heated wall, which in turn, enhances the heat transfer rate. The Nusselt number on inner wall,  $Nu_1$ , thus increases with an increase in radius ratio [1,2] and/or for a change in boundary condition from CT to UHF. The slope of  $\ln(Nu_1)$ -versus- $\ln(\kappa)$  curve is not a constant, and is observed to decrease with an increase in  $\kappa$ ; the slope being maximum at  $\kappa = 1$ . This brings the annulus results close to

the heat transfer rates for a heated cylinder embedded in an infinite porous medium maintained at the cold wall temperature, and is true for any type of boundary condition on the heated wall.

Though a change in boundary condition from CT to UHF enhances the heat transfer rates for both cavities [5] and annuli, the difference in two Nusselt numbers is a strong function of  $Ra^*$ ,  $A$  and  $\kappa$ . Higher the Rayleigh number, larger is this difference for given values of  $A$  and  $\kappa$ . Similarly, an increase in aspect ratio results in higher heat transfer coefficient for the uniform heat flux case as compared to the constant temperature boundary condition, whereas the effect of radius ratio is reverse. Any increase in curvature effect is observed to reduce the difference between two heat transfer rates. Since the difference between two values of  $Nu_1$  diminishes fast as  $A$  is reduced below unity, a change in boundary condition from CT to UHF does not produce any appreciable effect on the heat transfer rate for a shallow annuli ( $A < 1$ ); the critical radius ratio being a function of Rayleigh number and aspect ratio.

#### REFERENCES

1. Prasad, V., and Kulacki, F.A., "Natural Convection in a Vertical Porous Annulus," International Journal of Heat and Mass Transfer, Vol. 27, pp. 207-219, 1984.
2. Prasad, V., and Kulacki, F.A., "Natural Convection in Porous Media Bounded by Short Concentric Vertical Cylinders," Journal of Heat Transfer (submitted).
3. Weber, J. E., "The Boundary Layer Regime for Convection in a Vertical Porous Layer," International Journal of Heat and Mass Transfer, Vol. 18, pp. 589-593, 1975.
4. Prasad, V., and Kulacki, F. A., "Convective Heat Transfer in a rectangular Porous Cavity - Effect of Aspect Ratio on Flow Structure and Heat Transfer," Journal of Heat Transfer, Vol. 106, pp. 158-165, 1984.
5. Prasad, V., and Kulacki, F.A., "Natural Convection in a Rectangular Porous Cavity with Constant Heat Flux on One Vertical Wall," Journal of Heat Transfer, Vol. 106, pp. 152-157, 1984.

INTERACTION OF SCIENCE AND ENGINEERING IN DESIGNING  
OPTIMUM DRILLING FLUIDS FOR OIL AND GAS WELLS

by

A. Ghalambor, A. Hayatdavoudi and J. M. Griffin  
Department of Petroleum Engineering  
University of Southwestern Louisiana  
Lafayette, Louisiana 70504

This paper will examine the present capabilities and limitations of several drilling fluid systems for oil and gas drilling. The current and future needs of the industry are also reviewed in their applications and tolerance. They are water base muds, saturated salt solutions, low solids muds, inhibited muds and oil base muds.

Water based muds behave according to the Bingham plastic model. Due to the visco-elastic behavior of clay species for this type fluid, a thorough understanding of yield point in static and dynamic conditions is needed. The fatigue characteristics or time-flow responses of these clays are not well documented. The effect of particle size and rheology must also be investigated.

The filtration properties of saturated salt solutions do not provide adequate wall cake. Their tolerance for solids content is low, and at certain pressures and temperatures, they will crystallize and produce an undesirable precipitate. Additionally, supersaturated salt solutions provide less or equal density than a near-saturated solution. The rapidly expanding utility of heavy brines for well completions has necessitated the pressure and temperature effects which are significant in changing the brine density being evaluated. Proven mathematical models and experimental data are needed to predicting compressibilities, pH and densities of the various brine fluids used for oil well completions and workovers.

The advantage of low solids muds is limited and has been overshadowed by their low weight and viscosity. As drilling and workovers get deeper, applications for low solids muds will soon require an increase in their weight with adequate viscosity (approximately 300 cp maximum) and a temperature tolerance of nearly 500°F. Adjustments in rheological properties with respect of minimum filtration time and particle size will be needed. The involvement of polymers creates other problems, such as the high adsorption rate in high clay systems, and sieving out the high viscosity-high molecular weight portions at high temperatures.

Most inhibited muds can produce an adequately circular borehole, but they may not be feasible due to toxicity (chromium, zinc, bromine, etc.), and the temperature tolerance is too low. At high temperatures, they become highly viscous and form a cushion under the drill bit, which retards penetration rate. Mathematical models of the crossflows against the cushion in the visco-elastic medium are nonexistent and must be developed to achieve optimized drilling.

Oil base muds have created environmental, social and technological responses in the industry. Substitute materials are needed, and should be of the type that will not retard the bit tooth penetration of the rock. The separation of the solid cuttings from the oil muds remains a solids control challenge.

Suggestions and possible avenues of solutions to some of these problems are given; however, the main objective of the paper will be the identification and exposition of the problems and needs of the industry as regards drilling fluids research. It is important that a solution to these problems be found, because the energy crisis and continued increase in the cost of oil and gas production makes them a vital area of concern for the industry, and challenging problems for scientists and engineers to solve.

**MODELING AVALANCHES**

by

J.T. Jenkins  
Cornell University  
Department of Theoretical and Applied Mechanics  
Ithaca, New York 14853

and

Hayley Shen  
Clarkson College  
Department of Civil Engineering  
Potsdam, New York 13676

We derive a relatively simple system of nonlinear partial differential equations governing the evolution of an avalanche profile and the mean energy of the particle velocity fluctuations. These equations are obtained by depth averaging the balance laws for mean momentum and fluctuation energy obtained using kinetic theory. Numerical solutions of the system are presented that show how avalanche profiles and energies depend, for example, upon the coefficient of restitution and the diameter of the particles.

## SOLITONS IN ELECTROMAGNETIC ELASTIC SOLIDS

by

Gérard A. Maugin  
 Université Pierre-et-Marie-Curie,  
 Laboratoire de Mécanique Théorique associé au C.N.R.S.,  
 Tour 66, 4 Place Jussieu  
 75230 Paris Cedex 05, France.

Nonlinear wave propagation is a subject matter of great interest, from the point of view both of experiments and basic physics, in electromagnetic deformable solids. As examples in the first framework we note shock waves as a means for measuring high-order (e.g., fourth) elastic properties, the phenomenon of harmonic generation and anisochronism in piezoelectric resonators and SAW systems and the phenomenon of (electric) polarization of a ceramic specimen by a mixed electro-mechanical shock wave. Here, however, we are more specifically interested in more basic physical processes where competition between nonlinearities and dispersion allows for the existence of solitary waves which, in certain circumstances, are indeed solitons, i.e., they belong in a class of nonlinear waves which, like particles, recover their individuality after interaction (E.g., collision with another wave of the same type). Such solitons may be shown to exist in rigid ferromagnets and ferroelectrics and, more generally, in electromagnetically ordered structures (then they are solitons in a variable which has a pure electromagnetic interpretation). In the present talk the whole picture is complicated by the existence of electro-magneto-mechanical couplings. This complication which results in an increased mathematical complexity in the analysis of solutions, is nonetheless rewarding since it provides a rather satisfactory physical description of sophisticated phenomena.

To illustrate our talk we have selected the nonlinear electro-mechanical problem involving the structure in domains and walls in elastic ferroelectrics for which sodium nitrite  $\text{NaNO}_2$  provides a prototype. The question then is to know the structure and both electrical and mechanical state induced by the domains and walls. To that purpose a rather simple microscopic model is devised for ferroelectric crystals with a molecular group. A fully phenomenological nonlinear continuum approach could be used as well [1]. Discarding high optical branches, the crystal is schematized by a one-dimensional monoatomic chain equipped with microscopic electric dipoles associated with molecular groups. Three degrees of freedom can be distinguished in this picture: longitudinal and transverse displacements and rigid-body rotational motion of electric dipoles (rotational motion of molecular groups). The displacements are supposed to remain relatively small but the rotation of dipoles may have large amplitudes. This naturally leads to the description of the electric-dipole switching. Continuum nonlinear equations are then deduced from the set of discrete equations. In fact, a nonlinear micropolar elastic continuum emerges thus, so that the problem could also be attacked through this notion [2]. In addition, electromechanical interactions play a predominant role in the study. The full nonlinear coupled system consists of (i) wave equations for elastic displacements and (ii) a sine-Gordon equation governing the rotational motion of the molecular groups, these equations being nonlinearly coupled through electromechanical couplings.

The solution of this involved problem can be described in terms of solitons.

The first case examined is the one of a single soliton which, mathematically, can be reduced to a double sine-Gordon equation. The solution can be interpreted as the motion, coupled to elastic phenomena, of a Néel wall separating two ferroelectric domains. In addition, the states of stress and strain generated by the ferroelectric soliton through electromechanical couplings are also determined since the strain-compatibility conditions are satisfied in this case. Insofar as multiple-soliton solutions are concerned, one has to develop both analytical and numerical schemes to solve the nonlinear problem which can be solved but only approximately since a perturbation scheme (singular perturbations) must be envisaged [3]. In this case the electromechanical coupling is considered as a perturbation which alters the zeroth-order solution which is already nonlinear. The perturbation scheme devised amounts to determining corrective terms of the first order in the small parameter. In the process the nonlinear coupled solution is sought in the form of an asymptotic expansion which satisfies a secular condition for the first-order terms. The latter, or radiations, can be reached by means of a Green's function. This function is built with the help of the inverse-scattering method and Bäcklund transformations. The radiations in elastic displacement and orientation angle of molecular groups are obtained and the asymptotic behaviors of the solution at the first order for large values of the spatial variable are established. With an appropriate numerical scheme for nonlinear hyperbolic equations, numerical illustrations of the involved phenomena for a typical soliton-antisoliton are given. Finally, the influence of an applied electric field upon a moving wall (deceleration or acceleration) is outlined in the framework of the above perturbation scheme and numerical graphs are also reported in this case. To conclude, the case of a starting motion of a ferroelectric wall, hence the process of polarization of a specimen, under the influence of a bias field, is evoked. Many of the methods and results obtained here, which bring a deep understanding in the theory of domains and walls in ordered electromagnetic structures, can be applied or translated to the case of elastic ferromagnets with the appropriate modifications [4].

- [1] Maugin G.A. and Pouget J., "Electroacoustic Equations in One-Domain Elastic Ferroelectrics", J. Acoust. Soc. Amer., Vol. 68, 1980, pp.575-587.
- [2] Maugin G.A. and Miled A., "Solitary Waves in Elastic Continua with Microstructure" (work in progress).
- [3] Pouget J. and Maugin G.A., "Solitons and Electroacoustic Interactions in Ferroelectric Crystals", Physical Review B, submitted for publication, 1984.
- [4] Motogi S. and Maugin G.A., "Solitons and Magnetoacoustic Interactions in Elastic Ferromagnets" (work in progress).

The collaboration of Joel Pouget in many of the studies reported is gratefully acknowledged.

PULSE PROPAGATION IN ABSORBING MEDIA:  
REGIONS WHERE THE GROUP VELOCITY BECOMES INFINITE

by

Steve Chu  
AT&T Bell Laboratories  
Holmdel, NJ 07733

It is well known that the group velocity  $v_g = \frac{d\omega}{dk} = \frac{c}{n(\omega) + \omega(dn/d\omega)}$  describes the propagation of an electromagnetic pulse in a linear dispersive but nonabsorbing medium. However, in regions of strong anomalous dispersion,  $\omega(\frac{dn}{d\omega}) \gg n(\omega)$ , and the group velocity can exceed  $c = 3 \times 10^{10}$  cm/sec or even become negative. The common belief is that the meaning of group velocity breaks down, and the behavior of the pulse becomes much more complicated. Indeed, the well-known work of Sommerfeld and Brillouin<sup>1</sup> shows that for a pulse that turns on abruptly at some given instant, and then follows a sinusoidal modulation, the original pulse becomes distorted as it travels through the medium, and although there are precursors of the pulse that travel at  $c$ , the main part of the pulse arrives at a "signal velocity" slower than  $c$ . If, however, the pulse envelope is gaussian instead of a step function, Garrett and McCumber<sup>2</sup> have shown that under certain easily satisfied approximations that the pulse propagates with a pulse velocity  $v_p$  equal to the group velocity even when  $v_g > c$ ,  $v_g = \pm\infty$ , or  $v_g < 0$ .

The work reported here<sup>3</sup> verifies their predictions in the region where  $v_g$  passes through  $\infty$  and becomes negative. The pulse velocity  $v_p$  is measured in a thin crystal of GaP:N as a pulsed laser is turned around a narrow exciton absorption line. Using a picosecond time-of-flight technique, the pulse propagation was measured and compared to  $v_g$ . The group velocity was determined by measuring the absorption coefficient  $\alpha(\omega)$  with a transmission measurement of  $I_t = I_0 e^{-\alpha(\omega)\Delta l}$ . The Kramers-Kronig relations are numerically applied to  $\alpha(\omega)$  to obtain the real part of the index of refraction  $n(\omega)$ . Once  $n(\omega)$  is known,  $k_r = \omega \frac{n(\omega)}{c}$  and  $\frac{1}{v_g} = \frac{dk_r}{d\omega}$  is also obtained. In this way the pulse velocity  $v_p$  can be unambiguously compared to  $v_g$ .

These counter intuitive results do not violate special relativity, information transfer, or causality, and a brief discussion will also be given to assuage the listener's wounded intuition.

1. L. Brillouin, Wave Propagation and Group Velocity,  
(Academic Press, New York, 1960).
2. C.G.B. Garrett and D.E. McCumber, Phys. Rev. A1,  
305 1970.
3. S. Chu and S. Wong, Phys. Rev. Lett. 48, 738, (1982)  
S. Chu and S. Wong, Phys. Rev. Lett. 49, 1292, (1982).

## SOME NONLOCAL EFFECT IN OPTICS AND ELECTROMAGNETIC-ELASTIC SOLIDS

by

A. Cemal Eringen  
Princeton University  
Princeton, NJ 08544

There exist a variety of observed physical phenomena which cannot be explained by means of classical electromagnetic field theories. To cite a few, we have the infrared dispersion and lattice vibrations, natural optical activity, anomalous skin effect, dispersion of high frequency optical waves, Debye screening of electrons, magnetic spin waves, and superconductivity, which take their origins from the microscopic and atomic considerations. Yet, the outcome is macroscopic. Recently I developed a nonlocal continuum theory of electromagnetic elastic solids which appear to extend the domain of applicability of Maxwell electromagnetism to the physical phenomena in the microscopic and atomic scales. Results of my calculations based on this theory are in excellent agreement with those known from the theory of electrons and lattice dynamics. Yet the theory has applications on more complicated engineering materials and the nonlinear phenomena. Here I present a brief account on the theory and apply it to a few physical phenomena that fall outside of the domain of classical field theories.

1. A. Cemal Eringen, "Theory of Nonlocal Piezoelectricity", Journal of Math. Physics, Vol. 25, 1984, pp. 717-727.

A GENERALIZATION OF THE NEWTONIAN-OHM EQUATION OF  
ELECTRIC CONDUCTION FOR MAGNETIZABLE CONTINUA

by

Yasar Ersoy  
Planetenlaan 1  
5632 DG Eindhoven, The Netherlands

In this work, the consequences of the residual entropy inequality is examined in detail to obtain a nonlinear constitutive equation for the nonstationary electric current. It is shown that the Newtonian-Ohm equation of electric conduction can be deduced from the constitutive assumptions, which were set forth recently by the author, and generalized for magnetizable continua.

It is worthwhile to mention that the residual entropy inequality for the electric conduction employed in the present paper is significantly different from that in classical continuum mechanics because of the supplementary term and the constitutive variables. The term involves the product of the partial derivative of the thermodynamic potential-the modified internal energy-with respect to the electric current vector and the response function describing the temporal evolution of the electric current vector.

Concerning a new electrical equilibrium state we set up the most general  $n$ th-order expansion of the response functions. To describe galvanomagnetic and electrical conducting effects for the nonstationary fields, the expansion is then truncated at certain terms and reexpressed for isotropic materials. Thus, a fourth-order theory for isotropic solids is, in particular, studied to exhibit results of the new methodology.

Furthermore, some restrictions on the material moduli, which are employed in describing the generalized Newtonian-Ohm equation of electric conduction, are sought out theoretically. Such restrictions may allow us to determine some material moduli easily since they fulfill certain relations. Finally, some special cases of the constitutive equation is discussed.

## ULTRASONIC MEASUREMENT OF THE NONLINEAR PROPERTIES OF SOLIDS

by

M. A. Breazeale  
The University of Tennessee  
Department of Physics  
Knoxville, TN 37996-1200

For a number of years it has been apparent that an understanding of the basic properties of solids could not be obtained on the basis of a linear (or harmonic) theory. Such properties as the pressure and temperature dependence of the elastic constants, thermal expansion, phonon interaction, the difference between adiabatic and isothermal elastic constants, and the temperature dependence of the lattice specific heat can only be described by a nonlinear (or anharmonic) theory. Thus, the ability to measure the nonlinear coefficients is becoming increasingly important.

Over the past several years we have developed a technique for measuring the nonlinear properties of solids by measuring the nonlinear distortion of an initially sinusoidal ultrasonic wave. The results of the measurements lead to values of the third-order elastic (TOE) constants. Measured values of TOE constants between room temperature and 3°K are presented for single crystals of copper, germanium, silicon and a number of other solids and are discussed in relation to modern theories of the solid state. (Research sponsored by the Office of Naval Research.)

## SHOCKS AND SIMPLE WAVES IN PERFECT MAGNETOELASTIC MEDIA

by

J. Bazer  
Courant Institute of Mathematical Sciences  
New York, NY 10012

Shock and simple wave motion in a perfect magnetoelastic medium (an infinitely conducting, electrically neutral, nonmagnetizable, elastically perfect, compressible solid) are studied. All state variables are assumed to depend upon one space variable and time; however, no restriction is placed on the orientation of the velocity, magnetic and strain fields. To simplify the exposition, this talk will deal chiefly (but not exclusively) with the special case where the stress-strain relation is linear (Hookean) so that the nonlinearity of the governing equations derive essentially from the interaction of the magnetic field with itself, the velocity and strain fields and with the scalar entropy field. In this case, despite the complexity of the equations (magnetogasdynamic is a marginal special case corresponding to a scalar pressure), we obtain almost completely explicit simple-wave and shock-wave solutions. As in magnetogasdynamics, there are slow, intermediate and fast simple-wave and shock-wave solutions which together with constant states, may be pieced together on nonoverlapping space-time to obtain solutions of one-dimensional propagation problems having sufficiently simple initial and/or boundary conditions. A solution of one such problem is described in some detail both to illustrate the theory and to adduce a mechanism for generating intense magnetic fields by purely mechanical means.

## WAVES IN SATURATED DIELECTRICS\*

Sadik Dost and Marcelo Epstein

Department of Mechanical Engineering, The University of Calgary,  
Calgary, Alberta, Canada

In the study of wave propagation in dielectrics [1] it has been customary to adopt as the field equations, in addition to the mechanical balance laws, the laws of conservation of charge and the electrical balance in which no inertia is associated with the polarization. This results in the impossibility of obtaining a purely electrical wave as would be the case in a rigid dielectric. Some recent publications [2-5], based mainly on lattice dynamics considerations, have accommodated such an inertia term and even attributed to it a numerical value. In this paper we propose to study the effect of such an inertia in providing a finite speed of propagation for the purely electrical wave. Thus, we confine our attention to rigid dielectrics. In addition, the important case of saturated polarization and its effects on wave speeds and amplitudes is discussed.

We adopt the singular surface approach to derive, first, the propagation condition and, then, the decay-induction equation governing the variation of the amplitude of the wave at the wave front. Attention is then focused to principle waves, which are appropriately defined by analogy with their elastic counterparts. Under conditions of saturation the amplitude vector must be orthogonal to the polarization vector thereby reducing the possible wave speeds to two. For the case of plane and spherical waves explicit decay expressions for the wave amplitude are provided and the possibility of shock formation is investigated.

References:

1. Dost, S., M. Epstein and S. Gozde: "Propagation of Acceleration Waves in Generalized Thermoelastic Dielectrics", in The Mechanical Behaviour of Electromagnetic Solid Continua (Ed. G.A. Maugin), Elsevier Science Publishers B.V. (North-Holland), IUTAM-IUPAP, 211-216, 1984.
2. Maugin, G.A.: "Deformable Dielectrics. I. Field Equations for a Dielectric Made of Several Molecular Species", Arch. Mech., 28, 679-692, 1976.
3. Maugin, G.A.: "Deformable Dielectrics. II. Voigt's Intramolecular Force Balance in Elastic Dielectrics", Arch. Mech., 29, 1, 143-151, 1977.
4. Maugin, G.A. and J. Pouget: "Electroacoustic Equations for One-domain Ferroelastic Bodies", J. Acoust. Soc. Am., 68(2), 575-587.
5. Aşkar, A., J. Pouget and G.A. Maugin: "Lattice Model for Elastic Ferroelectrics and Related Continuum Theories" in The Mechanical Behaviour of Electromagnetic Solid Continua (Ed. G.A. Maugin), Elsevier Science Publishers B.V. (North-Holland), IUTAM-IUPAP, 151-156, 1984.

\* The results presented here were obtained in the course of research sponsored by the Natural Science and Engineering Research Council of Canada, Grants No. A-1628 and A-4662.

SUBWAY - A COMPUTER CODE FOR THE CALCULATION OF  
DYNAMIC COUPLED ELECTROMECHANICAL RESPONSE OF DIELECTRICS.  
PART I: FUNDAMENTALS\*

by

Patrick F. Chavez, Stephen T. Montgomery and Peter J. Chen  
Sandia National Laboratories  
Albuquerque, NM 87185

Understanding the transient responses of electromechanically coupled dielectrics, such as piezoelectric crystals and ferroelectric ceramics, due to shock wave loading is important for the analysis of transducers and power supplies [1,2]. SUBWAY is a fully coupled two-dimensional hybrid computer code developed for the calculation of the electromechanical responses of dielectrics. The code utilizes both finite difference and finite element techniques to solve for the material response. In particular, SUBWAY uses standard finite difference methods [3] to calculate the mechanical motion resulting from applied forces or stresses generated by applied potentials. Electric fields that occur in dielectrics and regions of vacuum are calculated with a finite element technique. The wide variety of circuits associated with transducers and power supplies can be accommodated by SUBWAY. Part I considers the fundamentals; problem formulation, code implementation and verification.

References

1. P. J. Chen, L. Davison and M. F. McCarthy, "Electrical Responses of Nonlinear Piezoelectric Materials to Plane Waves of Uniaxial Strain", *Journal of Applied Physics*, Vol. 47, 1976, pp. 4759-4764.
2. J. E. Besancon, J. David and J. Videl, "Ferroelectric Transducers", Proceedings of the Conference on Megagauss Magnetic Field Generation by Explosives and Related Experiments, Frascati, Italy, Sept. 21-23, 1965, Euratom, Brussels, 1966.
3. J. W. Swegle, "TOODY IV - A Computer Program for Two-Dimensional Wave Propagation", SAND-78-0552, Sandia National Laboratories, Albuquerque, NM, Sept. 1978.

\* This work was supported by the U.S. Department of Energy under contract DE-AC04-76DP00789.

SUBWAY - A COMPUTER CODE FOR THE CALCULATION OF  
DYNAMIC COUPLED ELECTROMECHANICAL RESPONSE OF DIELECTRICS  
PART II: APPLICATIONS<sup>†</sup>

by

Stephen T. Montgomery, Patrick F. Chavez, and Peter J. Chen  
Sandia National Laboratories  
Albuquerque, NM 87185

Understanding the transient responses of electromechanically coupled dielectrics, such as piezoelectric crystals and ferroelectric ceramics, due to shock wave loading is important for the analysis of transducers and power supplies [1,2]. SUBWAY is a fully coupled two-dimensional hybrid computer code developed for the calculation of the electromechanical response of dielectrics. Application of the code to two problems is described here. The response of a linear piezoelectric disc is considered first. The disc is assumed to be connected across a resistive load. The output voltage is compared for the cases of a one-dimensional motion resulting from a constant applied pressure and a two-dimensional motion resulting when relief from the lateral surface occurs. The next problem describes results when the disc is assumed to be composed of a ferroelectric ceramic which undergoes reorientation of its ferroelectric domains under mechanical loading [3]. The voltage obtained in this case is compared to the results obtained for the linear piezoelectric disc.

References

1. P. J. Chen, L. Davison, and M. F. McCarthy, "Electrical Responses of Nonlinear Piezoelectric Materials to Plane Waves of Uniaxial Strain", *Journal of Applied Physics*, Vol. 47, pp. 4759-4764 (1976).
2. J. E. Besancon, J. David and J. Videl, "Ferroelectric Transducers", Proceedings of the Conf. on Megagauss Magnetic Field Generation by Explosives and Related Experiments, Frascati, Italy, Sept. 21-23, 1965, Euratom, Brussels (1966).
3. P. J. Chen, "Three Dimensional Constitutive Relations for Ferroelectric Materials in the Presence of Quasi-Static Domain Switching", *Acta Mechanica*, Vol. 48, pp. 31-42 (1983).

<sup>†</sup> This work was supported by the U.S. Department of Energy under contract DE-AC04-76DP00789.

## FRACTURE OF ANISOTROPIC AND COMPOSITE MATERIALS

R. E. Rowlands  
Department of Engineering Mechanics  
University of Wisconsin  
Madison, WI 53706

A broad look is taken of fracture and the presence of cracks or flaws in composite and anisotropic materials. Analytical, numerical and experimental information are utilized. Highly directional fiber-reinforced plastics, laminated composites, wood, synthetic-fiber reinforced wood and paperboard are considered. Wood and paper tend to be less heterogeneous than synthetic-reinforced composites. Wood is extremely anisotropic while paper is much less so. Specific aspects addressed include the enhanced engineering toughness achieved in wood through fiber reinforcement, static and running cracks, effect of material orientation on COD, crack growth from holes of bolted joints, stress-singularity, influence of material properties on fracture, self-similar and non-self-similar crack growth, and orientation of crack growth relative to that of principal material directions. While crack propagation in highly directional fiber-reinforced plastics normally parallels the fibers, crack growth in paperboard often occurs transverse to the fibers.

A CRITICAL REVIEW OF  
ORTHOTROPIC FRACTURE MECHANICS

by

L. W. Zachary  
Associate Professor  
Engineering Science & Mechanics and  
Engineering Research Institute  
Iowa State University  
Ames, IA 50011

Linear elastic fracture mechanics (LEFM) has obviously become an important discipline in the area of metal fatigue and fracture. The classical methods have been extended by taking into account the plastic zone, crack closure, short cracks, three-dimensional effects and environmental conditions. Can the LEFM method be extended to composites or other orthotropic materials? The works of Sih, Paris and Irwin along with Wu and Renter are reviewed. The characterization of the crack tip stress field in orthotropic materials was developed by these researchers, and stress intensity factors were found to exist in these materials as well. The basic assumptions in the development and their consequences are discussed.

There has been a very limited number of experiments performed in this area. These few are discussed, and a new method of using orthotropic photoelasticity to determine orthotropic stress intensity factors is reviewed. Finally, the application of LEFM to orthotropic materials in specific cases and the possible direction of further research are addressed.

LONGITUDINAL SPLITTING IN UNIDIRECTIONAL  
COMPOSITES, "ANALYSIS AND EXPERIMENTS".

Jeffrey M. Wolla  
Naval Research Laboratory  
4555 Overlook Avenue, S.W.  
Washington, DC 20375

and

James G. Goree, Professor  
Department of Mechanical Engineering  
Clemson University  
Clemson, SC 29631

An experimental study is conducted to determine the fracture behavior of center notched, unidirectional graphite/epoxy laminates when subjected to tensile loading. The actual behavior is compared to the behavior predicted by a mathematical model based on classical shear-lag assumptions. The model allows for damage to occur in the form of longitudinal matrix yielding and splitting with the matrix assumed to fail in pure shear. Acoustic emission monitoring techniques are used to detect the initiation of matrix splitting, while radiographic and brittle lacquer coating techniques are used to determine the amount of matrix damage as a function of remote stress.

Results indicate that the model is capable of predicting split initiation stress levels accurately, but does not describe the subsequent split growth adequately. The model predicts rapid split growth following split initiation due to shear failure, while the actual behavior involves a slow split growth region prior to the rapid growth region. It is suggested that transverse matrix normal stresses are responsible for split initiation and the early, slow split growth. The model predicts the actual initiation stress levels reliably, and also appears to be able to predict the point at which the shear failure mode begins to dominate. The shear failure mode does eventually dominate, but at a slower rate than predicted. The nonuniform structure of the graphite/epoxy laminates is thought to be responsible for decreasing the split growth rate due to shear failure.

It is suggested that the mathematical model be modified to evaluate the transverse matrix normal stresses properly and include them in the failure criteria. In addition, the interaction between the failure modes during the transition from slow to rapid split growth needs to be better understood. Further experimental studies should use laminates with high uniformity in structure such as boron/epoxy.

3-D STRESS FIELDS NEAR SEVERAL INTERACTING  
MATRIX CRACKS IN COMPOSITE LAMINATES

A.S.D. Wang, N.N. Kishore and C.A. Li  
Drexel University  
Philadelphia, PA. 19104

Structural composite laminates made of unidirectional plies frequently suffer intralaminar and interlaminar cracks in the matrix or in the matrix-fiber interface well before the final rupture of the laminate [1]. An example is the cross-ply  $(0/90)_s$  type laminates under uniaxial tension. In this case, matrix cracks in the 90 plies transverse to the loading direction can be induced at the applied tensile strain as low as 0.2%, depending on the thickness of the 90 plies [2,3]. As the applied tension increases, more transverse cracks are formed in the 90 plies [4]. This happens when the load is both monotonically and/or cyclically applied. During the late-stage loading but still before the breaking of fibers in the 0 plies, several other matrix cracking modes may emerge. One such mode is the longitudinal splitting of the 0 plies over the 90 transverse cracks [5-7]. Interaction between a longitudinal split in the 0 plies and a transverse crack in the 90 plies can cause excessive stress concentration near their intersection point. The stress field near this point is highly three dimensional; the stress components acting on the 0/90 interface can, in turn, induce localized delamination emanating from the intersection point [5-7]. Coalescence of these localized delamination cracks eventuates a rapid disintegration of the lamination structure [6,7].

Matrix cracking in laminates of more complicated lamination geometry experiences similar crack-modes interactions before massive laminate rupture [6,7]. Experiments have established that the entire matrix cracking process, including the crack state that exists just prior to final laminate rupture, is essentially generic to the laminate type and the nature of the applied loading. But, an analytical description on how that crack state come about and a physical understanding on why that crack state is critical to the laminate's final failure remain scarcely explored.

The purpose of this paper is to examine the behavior of several major types of crack-modes interaction by actually calculating the fully three dimensional stress field associated with each type of the crack modes interactions. Specifically, a finite element routine [8] is employed to calculate the stresses near three types of crack-modes interaction regions: (1) the intersection of a longitudinal split in the 0 plies and a transverse crack in the 90 plies of a family of laminates in the form  $(0_2/90_n)_s$ ,  $n=1,2$  and  $4$ ; (2) the intersection of a transverse crack in the 90 plies with the free edge boundary of the same laminate family as in (1); and (3) the crack-front of a pre-planted internal delamination in the mid-plane of a  $(0/90/\pm 45)_s$  laminate subjected to axial compression. In all cases, both thermally (curing) induced stress field and the mechanical load induced stress field are calculated. The individual stress components are displayed graphically by three dimensional isometric representations.

A discussion on the particular finite element technique used and the numerical results obtained will be presented. But, emphasis is placed on analyzing the major factors that influence the various stress field behaviors. The analysis represents the necessary first step toward understanding why and how a particular crack-modes interaction precipitates the ensuing crack events because of its effects.

## REFERENCE

- [1] Wang, A.S.D., "Fracture Mechanics of Sublaminar Cracks in Composite Laminates," in Characterization, Analysis and Significance of Defects in Composite Materials, NATO Pub. No. 355, London, 1983. p. 15-1. Also to appear in Comp. Tech. Rev. Vol. 6, No. 2, 1984.
- [2] Harrison, R.P. and Bader, M.G., "Damage Development of CFRP Laminates Under Monotonic and Cyclic Stressing," Fibre Sci. Tech., Vol. 18, 1983. pp. 163-180.
- [3] Flagg, D.L. and Kural, M.H., "Experimental Determination of the In-situ Transverse Lamina Strength in Graphite Epoxy Laminates," J. Comp. Matls., Vol. 16, 1982. pp. 103-116.
- [4] Wang, A.S.D., Chou, P.C. and Lei, S.C., "A Stochastic Model for the Growth of Matrix Cracks in Composite Laminates," in Advances in Aerospace Structures, Materials and Dynamics, ASME Pub. AD-06, New York, 1983. pp. 7-16.
- [5] Wang, A.S.D., Chou, P.C., Lei, S.C. and Bucinell, R.B., "Cumulative Damage Model for Advanced Composite Materials," AFWAL Contract Report for F33615-80-C-5039, Sep., 1983.
- [6] Jamison, R.D. and Reifsnider, K.L., "Advanced Fatigue Damage Development in Graphite Epoxy Laminates," AFWAL-TR-82-3103, Dec., 1982.
- [7] Ryder, J.T. and Crossman, F.W., "A Study of Stiffness, Residual Strength and Fatigue Life Relationships for Composite Laminates," NASA-CR-172211, Oct., 1983.
- [8] Wang, A.S.D., Kishore, N.N. and Li, C.A., "A Three Dimensional Finite Element Analysis of Delamination Growth in Composite Laminates," NADC-84018-60, Nov., 1983.

DELAMINATION FAILURE OF LAYERED COMPOSITE PLATES LOADED IN  
COMPRESSION

L. Ascione (\*), D. Bruno (\*), A. Grimaldi (\*\*), F. Maceri (\*\*)  
(\*)Dipartimento di Strutture, Università della Calabria, Italia.  
(\*\*)Dipartimento di Ingegneria Civile, II Università di Roma, Italia.

Plates laminated in orthotropic layers are increasingly used in aerospace, civil and mechanical engineering structures. If the edges of laminates are not secured properly, delamination can occur either due to the presence of normal tensile stress or due to the imperfect bonding between layers. In the latter case the delamination can propagate especially if loads transverse to the laminate, or normal compression loads are applied. Delamination induced by buckling of the single layers can highly influence the failure characteristics of compressively-loaded laminated plates (1,2).

In this paper an unilateral contact approach, developed in a previous study (3), is used to model the propagation of delamination of two layer plates under uniform axial compression.

The adhesion strength between layers is modeled by springs with finite tensile strength. The flexural behaviour of the plate is modeled by means of the Hencky-Mindlin type shear deformation theory. A finite element model of the formulation is developed and applied to investigate some examples of buckling delamination of two layer plates with specified initial bonding defect.

For the case of one-dimensional delamination the present approach is validated by comparing finite element-results with analytical solutions. The relationship between the brittle fracture mechanics approach and the present approach is also discussed.

## REFERENCES

1. Sternes, J.H.-Williams, Jr. and J.G., "Failure characteristics of graphite-epoxy structural components loaded in compression", Proc. of the IUTAM Symposium on Mechanics of Composite Materials, VPI Blacksburg-USA August 16-19, 1982, Pergamon Press, 1983, pp.283-306.
2. Early, J.W., "Compression induced delamination in a unidirectional graphite/epoxy composite", Report MM-372 A-81-14, Texas A-M University, College Station, Texas, December 1981.
3. Grimaldi, A.-Reddy, J.N., "On Delamination in Plates: A Unilateral-Contact Approach", Report No. VPI-E-82.23, Department of Engineering Science and Mechanics, Virginia Polytechnic Institute and State University, Blacksburg, Virginia, August 1982.

MOMENT INTENSITY FACTOR FOR A CRACKED  
ORTHOTROPIC PLATE SUBJECTED TO DYNAMIC LOADING

by

A. M. Sadegh and M. Kassir  
The City College of The City University of New York  
New York, NY

The problem of an orthotropic plate containing a through crack and subjected to a suddenly applied bending moment is considered. Laplace and Fourier transformations are employed to reduce the transient dynamic problem to the solution of dual integral equations in the Laplace transformation plane. The dual integral equations yield a Fredholm integral equation of the second kind whose solution can be accomplished numerically. A numerical Laplace inversion technique is used to compute the values of the dynamic moment intensity factor for several orthotropic materials. In particular, attention is focused on finding out the degree of influence of material orthotropy on the overshoot in the moment intensity factors and the time needed to reach the peak value in each case.

## FIBER OPTIC STRAIN SENSORS

by

J.S. Sirkis and C.E. Taylor  
University of Florida  
Department of Engineering Science  
Gainesville, FL 32611

The use of optical fibers as strain sensors is explored. Single mode fibers may be bonded to a surface in a manner similar to that commonly employed for bonding electric resistance strain gages or they may be embedded within a composite material without greatly altering the mechanical properties of the composite. Fiber optic strain sensors are less influenced by electromagnetic effects than are conventional electric strain gages.

By using a reference fiber of suitable geometry, temperature effects may be suppressed. The relative change between reference fiber optical path length and sensing fiber optical path length is directly proportional to the strain. Laser light emerging from the reference and sensing fibers produces Young's fringes, the change in which is shown to be related to the change in strain. Theoretical and experimental results are in good agreement.

## MOIRE INTERFEROMETRY FOR DEFORMATION STUDIES IN SOLID MECHANICS

Daniel Post  
 Virginia Polytechnic Institute and State University  
 Engineering Science and Mechanics Department  
 Blacksburg, VA 24061

Recent developments in moire interferometry have enhanced the sensitivity of traditional moire methods by nearly two orders of magnitude. The potential of moire has fascinated engineers for many years. It is unique inasmuch as it can give whole-field information for linear and nonlinear elastic problems, plastic, viscoelastic, isotropic, orthotropic and anisotropic problems in solid mechanics. It provides contour maps of in-plane deformation fields -- precisely the experimental counterpart to the primary output of theoretical studies by the modern finite element method and related computer analysis methods. The sensitivity of traditional moire, however, has been inadequate for most engineering applications in which stiff structural materials are employed. Now, moire interferometry provides the needed sensitivity and promises to be an extraordinary useful method of experimental solid mechanics.

Moire interferometry is an optical technique that uses coherent laser light and produces two-beam optical interference patterns of high contrast. The presentation will review the basic method and describe recent advances. Numerous applications will illustrate its capabilities.

A comprehensive description appears in the reference: D. Post, "Moire Interferometry at VPI & SU", *Experimental Mechanics*, 23(2), pp. 203-210 (June 1983). Sponsorships by the National Science Foundation and NASA Langley Research Center are gratefully acknowledged.



x-displacement field near the corner of an adhesive joint between two graphite-epoxy composite plates subjected to bending. Sensitivity corresponds to moire with 2400  $\lambda$ /mm (60,960  $\lambda$ /in.).

APPLICATION OF PHOTOELASTIC COATING IN DYNAMIC STRESS ANALYSIS  
OF A CLOTHES DRYER FAN

by

Prof. N. A. Rubayi

Dept. of Engineering Mechanics & Materials

Southern Illinois University, Carbondale, IL 62901

The primary objective of this investigation was to utilize the method of photoelastic coating to determine the magnitude and locations of the dynamic stress concentration in a pre-designed clothes dryer fan under operating dynamic loading at a maximum speed of 1550 rpm. Furthermore, it was intended to obtain the residual stresses locked in the material of the fan during the forming and pressing processes. Also, by using photoelastic coating technique, bolt stresses which are developed while bolting the fan into the mounting hub were also determined.

Eight identical fans of the same material and design were utilized in this investigation. The fans were manufactured from steel sheets known as Cold Rolled Draw Quality Aluminum Killed Steel of an average thickness of 0.031 inch. Several plastic sheets of PL-8 were cast from liquid form for contouring to the complex shape of the fan. Each plastic sheet was calibrated accurately for determining the material constants.

The locations of high and low stress areas were determined at the maximum operating speed of 1550 rpm by using the stroboscopic light and the reflection polariscope. The fan was tested in the variable speed dynamometer and the magnitude of the dynamic stresses were also obtained at various operating speeds. Initial fringe orders were measured first at various locations on the fan at zero speed. All fans were initially balanced statically and dynamically before testing. Correction factors for both reinforcement and bending were used in the calculations of the stresses.

Residual stresses were obtained by introducing small cuts in the coated areas at the critical locations of the stress concentration. Cuts were made with a small and fine saw blade and air was used as a coolant during cutting. Static fringe orders were measured before and after the cuts were made to determine the residual stresses locked into the material of the fan.

Strains at the bolts were also obtained by cementing contoured plastic sheets on the center portion of the fan and the method of extrapolation was used to obtain the strains at the edge of the bolts when they were torqued to the manufacturer's specifications of 70 in-lb.

The present investigation revealed that an average residual stress of 5,880 psi was present in the material of the fan due to manufacturing processes. Also, the values of the stresses at the critical locations of stress concentration areas were within the yielding region of the material of the fan. In addition, stresses at the edges of the bolts were also found to be at the high range of the yielding zone. Several design criteria and modifications were recommended to the manufacturer to safeguard the failure of the fan when it is operating dynamically at its maximum speed of 1550 rpm.

THE APPLICATION OF FLOW BIREFRINGENCE TO THE FLOW  
OF VISCOELASTIC FLUIDS

by

D. G. Baird and M. R. Read  
Department of Chemical Engineering  
Virginia Polytechnic Institute and State University  
Blacksburg, VA 24061-6496

The method of flow birefringence appears to be extremely useful for analyzing the flow of viscoelastic polymeric fluids. The procedures, including the use of a linear stress-optic law, are similar to those used in solid mechanics. We illustrate the use of the technique by analyzing two flows. In the first case we study pressure driven cavity flow while in the second case we look at the flow of a polymeric melt at the exit of a slit-die. Each of these flows is of practical significance because of the possibility of obtaining the primary normal stress difference ( $N_1$ ), which is associated with fluid elasticity, from pressures generated in these flows.

In the case of pressure driven cavity flow, the difference between the pressure measured at the base of the fluid-filled cavity and that which would be measured if the cavity was not present is referred to as the hole pressure ( $P_H$ ). According to the analysis of Higashitani and Pritchard,  $P_H$  is related to  $N_1$ , the shear stress ( $\sigma$ ), and the wall shear stress ( $\sigma_w$ ) by the following integral evaluated along the centerline of the slot from the bottom of the slot to the opposite die wall:

$$P_H = \int_0^{\sigma_w} \frac{N_1}{2\sigma} d\sigma. \quad (1)$$

Flow birefringence has been used to determine  $N_1$ , and  $\sigma$ , along the center of the slot. Values of  $P_H$  obtained from flow birefringence data and eqn. (1) agree well with values obtained by direct pressure measurements. Furthermore, from the equation of motion one can obtain the following expression for  $P_H$  which is independent of any assumptions.

$$P_H = \int_{y_b}^{y_w} \frac{\partial \sigma}{\partial x} dy \quad (2)$$

Here  $P_H$  is obtained by integrating the derivative of  $\sigma$ , which is obtained from flow birefringence data, with respect to  $x$  over the region of the slot and then integrating from the bottom of the slot to the opposite wall. These values agree fairly well with those obtained by means of eqn. (1). The effect of slot dimensions and rounding of the corners on  $P_H$  has also been determined.

In the second case, flow at the exit of a die has been analyzed to

determine what contribution  $N_1$  makes to the residual stress in the extrudate. This residual stress, which is referred to as the exit pressure ( $P_{ex}$ ), has also been considered as a method for measuring fluid elasticity. Again values of  $N_1$  and  $\sigma$  obtained in the region of the die exit can be used to determine the contribution of  $N_1$  to the residual stress at the die exit.

The measurements also provide a detailed view of the stress field for two flows which have been of concern lately by those carrying out numerical simulation of the flow of viscoelastic fluids. In particular the stress at points in the flow region which have lead to numerical convergence problems can be analyzed in detail.

A REFLECTION POLARISCOPE FOR HALF FRINGE PHOTOELASTIC ANALYSIS OF  
ADHESIVE JOINTS IN FIBER REINFORCED COMPOSITES

by

C. Burger\*, D. Mallik\*\*, A. Voloshin\* and S. Mahadevan\*

\*Department of Engineering Science & Mechanics  
and Engineering Research Institute  
Iowa State University  
Ames, Iowa 50011

\*\*Intel Corp., Santa Clara, CA 95051

The traditional arrangement of the optical elements in a reflection polariscope for normal incidence introduces errors because it ignores the polarization that occurs in the partial mirror that is used to deflect the incident beam through  $90^\circ$  onto the photoelastic coating. Half-fringe photoelasticity (HFP) is a newly developed on-line digital procedure for photoelastic stress analysis. It's resolution in optical analysis is about two orders of magnitude better than in traditional reflection photoelasticity. As a consequence, new techniques that utilize thin low modulus coatings have become feasible. These coatings can be used effectively on relatively thin composite plates with different lay-ups and composition. Problems associated with failure development and resistance to defects in such materials can now be studied with photoelasticity directly on prototypes.

The fringe orders are likely to be significantly less than 1, which makes the inherent errors of the normal incidence reflection polariscope set-up unacceptable.

This paper describes a new design for a normal incidence polariscope which is free of the troublesome errors. It proceeds to demonstrate the effectiveness of this new optical arrangement and applies it to the analysis of a coating on an adhesive joint between a composite and an isotropic sheet.

This new procedure opens up a large body of problems in fiber reinforced composites and ceramics to experimental investigation in a mode which does not require special optical tables and vibration isolation. It is potentially suitable for use in an industrial environment.

AN INTERFEROMETRIC STUDY OF MIXED CONVECTIVE  
HEAT TRANSFER FROM AN ISOTHERMAL HORIZONTAL  
CYLINDER TO A CROSSFLOW OF AIR

by

J.R. Krause  
Graduate Student

J.D. Tarasuk  
Associate Professor

The University of Western Ontario  
Faculty of Engineering Science  
London, Ontario, N6A 5B9

Convective heat transfer from horizontal cylinders has numerous engineering applications. Both pure natural, and pure forced convective heat transfer have been studied extensively, but convective heat transfer by mixed natural and forced convection has received far less attention. The present study investigates mixed convective heat transfer from a horizontal isothermal cylinder with a Mach-Zehnder interferometer.

Previous experimental studies for an isothermal cylinder in air [1, 2, 3], and water [4, 5], have been limited to energy balance techniques. These only allow the study of overall heat transfer coefficients, and have resulted in varied heat transfer correlations that are a function of angle,  $Re$ , and  $Gr$ . To the best of our knowledge no local heat transfer results or temperature fields are available for the isothermal cylinder. Most analytical, and numerical studies have dealt with the case where the forced flow is upward. Badr [6, 7] has published numerical studies for horizontal, upward, and downward forced flows. His published results cover the range  $5 < Re < 40$  but his technique can be extended up to  $Re = 200$ .

Experiments were performed in an open circuit wind tunnel integrated with a Mach-Zehnder interferometer, as shown in Figure 1. The test section of the wind tunnel was rotated to allow the study of various attack angles of forced flow. Air was drawn into the test section to minimize free stream turbulence, and the heated cylinder was located near the entrance of the wind tunnel where the velocity distribution was uniform across the heated portion.

The cylinder models (Figure 2) were designed to be isothermal, and to generate a two dimensional temperature field. The models consist of a heated central portion with insulating end pieces. An isothermal surface was established by constructing the heated section of the models from pure copper. They were heated electrically with a high resistance wire located axially in the centre of the cylinder. The insulating end pieces help to approximate a two dimensional temperature field and also locate the heated portion of the cylinder outside the boundary layer formed on the wind tunnel side walls.

Results are presented for the following range of variables:  $150 < Re < 700$ ,  $9000 < Gr < 300,000$ ,  $0^\circ < \theta < 180^\circ$ . Local heat transfer coefficient distribution, and temperature fields are shown. The overall heat transfer coefficients are compared to existing correlations and data.

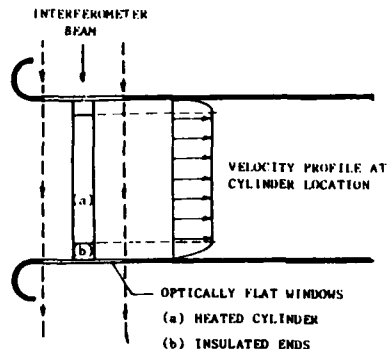


FIGURE 1—SCHEMATIC OF WIND TUNNEL AND INTERFEROMETER

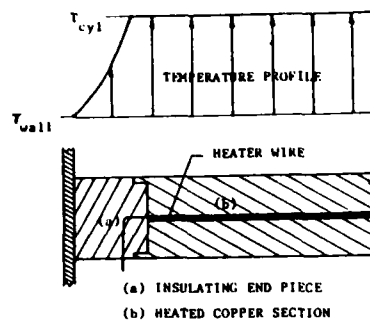


FIGURE 2—SCHEMATIC OF ISOTHERMAL CYLINDER

#### NOMENCLATURE

Re = Reynolds number based on diameter  
 Gr = Grashof number based on diameter  
 $\theta$  = Attack angle of forced flow

#### REFERENCES

1. Hatton, A.P., James, D.D., Swire, H.W., "Combined Forced and Natural Convection with Low-speed Air Flow over Horizontal Cylinders", J. Fluid Mech., Vol. 42, Part 1, 1970, pp. 17-31.
2. Sharma, G.K., Sukhatme, S.P., "Combined Free and Forced Convection Heat Transfer From a Heated Tube to a Transverse Air Stream", J. Heat Transfer, Vol. 91, August 1969, pp. 457-459.
3. Oosthuizen, P.H. Madan, S., "The Effect of Flow Direction on Combined Convective Heat Transfer From Cylinders to Air", J. Heat Transfer, Vol 93, May 1971, pp. 240-242.
4. Gand, R.M., Keswani, K.K., "Combined Natural and Forced Convection Heat Transfer From Horizontal Cylinders to Water", Int. J. Heat Mass Transfer, Vol. 16, 1973, pp. 1176-1191.
5. Bennon, W.D., Incropera, F.P., "Mixed Convection Heat Transfer from Horizontal Cylinders in the Crossflow of a Finite Water Layer", J. Heat Transfer, Vol. 103, August 1981, pp. 540-545.
6. Badr, H.M., "A Theoretical Study of Laminar Mixed Convection From a Horizontal Cylinder in a Cross Stream", Int. J. Heat Mass Transfer, Vol. 26, No 5, 1983, pp. 639-653.
7. Badr, H.M., "Laminar Combined Convection From a Horizontal Cylinder-Parallel and Contra Flow Regimes", Int. J. Heat Mass Transfer, Vol. 27, No. 1, 1984, pp. 15-27.

HYBRID ANALYTICAL-NUMERICAL PROCESSING OF PHOTOMECHANICAL  
DISPLACEMENT DATA

by

M. Hamdi AbdelMohsen and R. E. Rowlands  
Applied Superconductivity Center  
University of Wisconsin  
Madison, WI 53706

Experimental methods such as moire are advantageous because displacements are recorded. The latter, being the basis of continuum mechanics, makes moire suitable irrespective of geometry or constitutive response. The most challenging aspects of moire involve having sufficient sensitivity and differentiating measured displacements to obtain strains. An expedient method is presented for processing moire fringe data into strains for isotropic elastostatics. Like finite-elements, the  $u$ - and  $v$ -displacements are represented throughout sub-regions by polynomials involving coordinates and coefficients which are determined here from measured displacements. Imposing  $\nabla^2 u_1 = \nabla^2 J_1 = \nabla^2 w_2 = 0$  and equilibrium significantly reduces the number of independent coefficients to be determined. If  $u$  and  $v$  are each represented by complete sixth-order polynomials, the imposed side conditions reduce the original 98 coefficients to 14 independent coefficients. These are evaluated from moire measured displacements. Smoothing is introduced through regression analysis and excess experimental data. The technique is demonstrated by application. Accuracy, limited amount of experimental data needed and relatively large elements employable are illustrated.

## ON NONLINEAR DYNAMICAL SYSTEMS

by

P. R. Sethna  
Department of Aerospace Engineering  
and Mechanics  
University of Minnesota  
Minneapolis, Minn. 55455

Dynamical systems modeled by nonlinear ordinary or partial differential systems will be the subject of the lecture. This discussion will emphasize the approach of the geometrical theory and how it relates to well established ideas and methods in the field.

Among the topics to be discussed will be bifurcation theory in co-dimension one as well as co-dimension two problems and the relevance of these approaches to the formulation and study of physical problems. Chaotic motions, the circumstances under which they seem to occur and the several approaches to their study will be discussed.

Motion of tubes conveying a fluid and free surface motions of a fluid in a container will be among the examples used to demonstrate the more mathematical ideas of the lecture.

## DECAY RATES FOR LINEAR DYNAMICAL SYSTEMS\*

by

Daniel J. Inman  
 Kwang H. Yae  
 University at Buffalo  
 State University of New York  
 Department of Mechanical and Aerospace Engineering  
 Buffalo, New York 14260

This work examines the transient response of linear non conservative dynamic systems that can be successfully modeled by a set of ordinary differential equations of the form

$$M\ddot{x} + C\dot{x} + Kx = 0 \quad (1)$$

where  $M$ ,  $C$  and  $K$  are real symmetric  $n \times n$  positive definite matrices,  $x = x(t)$  is a  $n$ -vector of displacements and the overdots denote total derivatives with respect to the time  $t$ . A decay rate is defined for the transient response of (1) to arbitrary, but known initial conditions.

For single degree of freedom systems, the concept of a decay rate is easily defined in terms of the logarithmic decrement. However, for multiple degree of freedom systems such as (1), the situation is not as clear. Obviously, many simple numerical techniques are available to solve for  $x(t)$ . Then, the decay rate can easily be obtained by plotting the response norm. This is not the approach taken here. Rather, decay rates are defined and calculated using as little information about the solution as possible. Results are presented based upon assuming that (1) is underdamped [1] and symmetric.

Results for two separate cases are presented. The first case assumes that (1) possesses classical normal modes. Under this assumption, an estimate of the decay rate of (1) is developed in terms of the largest and smallest eigenvalues of the damping and stiffness matrices. Both per mode decay rates and global decay rates are derived. The global decay rate derived here is shown to yield a better bound on the response of (1) than those obtained by using a standard Lyapunov approach [2] based on a state space description of equation (1).

The remainder of the work reviews previous work on the related problem of calculating response bounds and discusses the problem of formulating a global decay rate for the more general non-normal mode

\*Research sponsored by AFOSR, Air Force Systems Command, USAF, under grant No. AFOSR 820242. The U. S. Government is authorized to reproduce and distribute reprints for government purposes not withstanding any copyright notation hereon.

case. In particular, the symmetry of the second order formulation is exploited to define decay rates which yield more precise bounds than those obtained by standard state space methods.

- [1] Inman, D. J. and Andry, A. N., Jr., "Some Results on the Nature of Eigenvalues of Discrete Damped Linear Systems", ASME J. of Applied Mech., Vol. 47, 1980, pp. 927-930.
- [2] Hahn, W., Theory and Application of Liapunov's Direct Method, Prentice-Hall, Inc., Englewood Cliffs, N.J., 1963, pp. 56-57.

## A SIMPLIFIED DERIVATION OF THE LEWIS INVARIANT

by

Leon Y. Bahar and Harry G. Kwatny  
Department of Mechanical Engineering and Mechanics  
Drexel University  
Philadelphia, PA 19104

Conservation laws for dynamical systems with time-varying coefficients are considerably more difficult to derive than invariants corresponding to systems with constant coefficients. The most typical time-varying problem which has been investigated in the literature from this viewpoint is that of a harmonic oscillator with time-dependent frequency. The illustrative example commonly used for this purpose is a simple pendulum of variable length.

In [1] Lewis derived an invariant for the time-dependent harmonic oscillator by showing that the adiabatic invariant derived earlier by Kruskal [2] was in fact an exact invariant. Since that time, many investigators have been concerned with various generalizations of the Lewis invariant to classical as well as quantum mechanics. The majority of these derivations are based on group-theoretical methods, particularly Noether's theorem [3]. While this method is very general, the level of mathematical sophistication involved does not make it sufficiently attractive to most engineers to enable them to use it as a practical tool of analysis. In addition, the results obtained in this manner do not always lend themselves to direct physical interpretation.

In the present paper, two different approaches to the derivation of the Lewis invariant are given. The first is an extension of the direct approach developed in [4]. The second method is based on augmenting the system with an auxiliary oscillator of the same frequency vibrating in a direction perpendicular to the original one. The initial problem then becomes embedded in a two-dimensional plane, which allows the use of conservation of angular momentum associated with resulting central force problem. By extending this idea originally introduced in [5], it is not only possible to derive the Lewis invariant which is a quadratic one, but also linear first integrals. Finally, the results are generalized to viscously damped harmonic oscillators by using a method recently developed by the authors [6].

REFERENCES

1. Lewis, H. R., "Class of Exact Invariants for Classical and Quantum Time-dependent Harmonic Oscillators", J. Math. Phys., Vol. 9, No. 11, 1968, pp. 1976-1986.
2. Kruskal, M., "Asymptotic Theory of Hamiltonian and Other Systems with All Solutions Nearly Periodic", J. Math. Phys., Vol 3, No. 4, 1962, pp. 806-828.
3. Lutzky, M., "Noether's Theorem and the Time-dependent Harmonic Oscillator", Phys. Letters, Vol. 68A, No. 1, pp. 3-4.
4. Sarlet, W. and Bahar, L. Y., "A Direct Construction of First Integrals for Certain Non-Linear Dynamical Systems", Int. J. Non-Linear Mech., Vol. 15, No.2, 1980, pp. 133-146.
5. Eliezer, C. J., and Gray, A., "A Note on the Time-dependent Harmonic Oscillator", SIAM J. Appl. Math., Vol. 30, No. 3, 1976, pp. 463-468.
6. Bahar, L. Y., and Kwatny, H. G., "Generalized Lagrangian and Conservation Law for the Damped Harmonic Oscillator", Amer. J. of Phys., Vol. 49, No. 11, 1981, pp. 1062-1065.

DERIVATION OF STATIONARITY CONDITIONS FOR A  
CLASS OF NON-LOCAL ACTION FUNCTIONALS BY THE  
METHOD OF LAGRANGIAN MULTIPLIERS

Vuk M. Fatić

Department of Electrical and Computer Engineering  
Tri-State University, Angola, IN 46703 U.S.A.

The class of variational principles considered here:

$$\delta \int_{t_0}^{t_1} L(t, \underline{q}, \underline{\dot{q}}, \underline{\ddot{q}}) dt = 0 \quad (1)$$

has a Lagrangian  $L$ , which is a function of time ( $t$ ),  $n$  generalized coordinates ( $\underline{q}$ ) and  $n$  velocities ( $\underline{\dot{q}}$ ), and  $m$  integrals

$$\underline{\dot{q}} \triangleq \int_{t_0}^t \underline{f}(\tau, \underline{q}, \underline{\dot{q}}, \underline{\ddot{q}}) d\tau, \quad t_0 \leq t \leq t_1 \quad (2)$$

with specified  $\underline{f}(\cdot)$  and a free upper limit. Since  $\underline{q}$  are path-dependent in general, Lagrangian which depend on  $\underline{q}$  is actually a functional.

Stationarity conditions for the functional (1) are differential-integral equations:

$$\begin{aligned} \frac{d}{dt} \frac{\partial L}{\partial \underline{\dot{q}}} - \frac{\partial L}{\partial \underline{q}} + \left( \frac{d}{dt} \frac{\partial \underline{f}}{\partial \underline{\dot{q}}} - \frac{\partial \underline{f}}{\partial \underline{q}} \right) \frac{\partial L}{\partial \underline{q}} + \frac{d}{dt} \left( \frac{\partial \underline{f}}{\partial \underline{\ddot{q}}} \right) \frac{\partial L}{\partial \underline{q}} - \\ - \left( \frac{d^2}{dt^2} \frac{\partial \underline{f}}{\partial \underline{\ddot{q}}} - \frac{d}{dt} \frac{\partial \underline{f}}{\partial \underline{\dot{q}}} + \frac{\partial \underline{f}}{\partial \underline{q}} \right) \int_{t_0}^t \frac{\partial L}{\partial \underline{q}} d\tau = 0 \end{aligned} \quad (3)$$

derived in [1] by direct application of classical variational procedure.

Much simpler derivation is given here, based on the application of Lagrangian multipliers. Components of  $\underline{q}$  are considered as a second set of independent variables  $\underline{u} \equiv \underline{q}$ , which is permissible provided we add the condition

$$\underline{\dot{u}} - \underline{f}(t, \underline{q}, \underline{\dot{q}}, \underline{\ddot{q}}) = 0 \quad (4)$$

as the constraint to the problem. The condition (4) is accounted for by modifying the Lagrangian

$$\tilde{L} \triangleq L(t, \underline{q}, \underline{\dot{q}}, \underline{u}) + \lambda^T(t) [\underline{\dot{u}} - \underline{f}(t, \underline{q}, \underline{\dot{q}}, \underline{\ddot{q}})] \quad (5)$$

Lagrangian equations

$$\frac{d^2}{dt^2} \frac{\partial \tilde{L}}{\partial \underline{\ddot{q}}} - \frac{d}{dt} \frac{\partial \tilde{L}}{\partial \underline{\dot{q}}} + \frac{\partial \tilde{L}}{\partial \underline{q}} = 0 \quad (6)$$

$$\frac{d}{dt} \frac{\partial \tilde{L}}{\partial \underline{\dot{u}}} - \frac{\partial \tilde{L}}{\partial \underline{u}} = 0 \quad (7)$$

ought to be supplemented by the equation

$$\frac{\partial L}{\partial \dot{u}} \Big|_{t=t_1} = 0 \quad (8)$$

since  $\underline{u}(t_1)$  remains unspecified (the free boundary condition), while  $\underline{u}(t_0) = \underline{0}$ . Elimination of  $\underline{\lambda}$  from Eqs. (6)-(8) then leads to Eq. (3).

$$\text{Since } \frac{\partial}{\partial \underline{q}} (\underline{\lambda}^T \underline{f}) = \frac{\partial}{\partial \underline{q}} \sum_k \lambda_k f_k = \sum_k \lambda_k \frac{\partial f_k}{\partial \underline{q}} = \frac{\partial f}{\partial \underline{q}} \underline{\lambda} \quad (9)$$

$$\text{where } \left( \frac{\partial f}{\partial \underline{q}} \right)_{ik} = \frac{\partial f_k}{\partial q_i} \quad (10)$$

$$\text{and similarly } \frac{\partial}{\partial \dot{\underline{q}}} (\underline{\lambda}^T \underline{f}) = \frac{\partial f}{\partial \dot{\underline{q}}} \underline{\lambda}, \quad \frac{\partial}{\partial \ddot{\underline{q}}} (\underline{\lambda}^T \underline{f}) = \frac{\partial f}{\partial \ddot{\underline{q}}} \underline{\lambda} \quad (11)$$

Eq. (6) reduces to

$$\frac{d^2}{dt^2} \left( - \frac{\partial f}{\partial \ddot{\underline{q}}} \underline{\lambda} \right) - \frac{d}{dt} \left( \frac{\partial f}{\partial \dot{\underline{q}}} - \frac{\partial f}{\partial \dot{\underline{q}}} \underline{\lambda} \right) + \frac{\partial L}{\partial \underline{q}} - \frac{\partial f}{\partial \underline{q}} \underline{\lambda} = 0 \quad (12)$$

$$\text{Eq. (7) to } \frac{d\underline{\lambda}}{dt} = \frac{\partial L}{\partial \underline{u}} \quad (13)$$

$$\text{and Eq. (8) to: } \underline{\lambda}(t_1) = 0 \quad (14)$$

$$\text{From (13) and (14): } \underline{\lambda}(t) = - \int_t^{t_1} \frac{\partial L}{\partial \underline{u}} d\tau \quad (15)$$

Now, substitution of (13) into (12) results into:

$$\begin{aligned} & - \frac{d}{dt} \frac{\partial L}{\partial \dot{\underline{q}}} + \frac{\partial L}{\partial \underline{q}} - \left( \frac{d^2}{dt^2} \frac{\partial f}{\partial \ddot{\underline{q}}} - \frac{d}{dt} \frac{\partial f}{\partial \dot{\underline{q}}} + \frac{\partial f}{\partial \underline{q}} \right) \underline{\lambda} - \\ & - \frac{d}{dt} \left( \frac{\partial f}{\partial \dot{\underline{q}}} \frac{\partial L}{\partial \underline{u}} \right) - \left( \frac{d}{dt} \frac{\partial f}{\partial \dot{\underline{q}}} - \frac{\partial f}{\partial \dot{\underline{q}}} \right) \frac{\partial L}{\partial \underline{u}} = 0 \end{aligned} \quad (16)$$

which obviously coincides with Eq. (3) by changing the signs of all terms, replacing  $\underline{\lambda}$  by Eq. (15), and returning to the original notation  $\underline{u} \rightarrow \underline{q}$ .

#### REFERENCES

1. Fatić, V. M., "Lagrangian Functionals for Nonlinear Resistive Networks, Part I: Mathematical Background," IEEE Intern. Symp. on Circuits and Systems, May 10-12, 1982, Rome, Italy, pp. 284-287.
2. Ibid, Part II: Applications, 26th Midwest Symp. on Circuits and Systems, Aug. 15-16, 1983, Puebla, Mexico, pp.511-514.

THE VARIATIONAL APPROACH TO ADIABATIC INVARIANCE:  
THEORY AND SOME APPLICATIONS TO LINEAR AND NONLINEAR OSCILLATORS \*

by

John G. Papastavridis \*\*  
Georgia Institute of Technology  
School of Engineering Science and Mechanics  
Atlanta, Georgia 30332  
U.S.A.

This paper contains a variational derivation of the adiabatic periodic motion theorems and related time-integral-of-energy results, including the virial theorem, and some of their applications to linear and nonlinear oscillators. Specifically: i) First, the Maupertuis-Euler-Lagrange (MEL) Action principle is formulated for the most general (scleronomous and holonomic) system; the derivation treats the time-dependent system parameters just like additional generalized coordinates and subjects them to similar variations. ii) Next, combination of MEL's principle with the first law of thermodynamics yields the adiabatic theorem; subsequent specializations of it lead to additional energetic equations. iii) The theory is then applied to the one d.o.f. linear and nonlinear oscillators; the effects of linear friction and a harmonic external force are also discussed; useful relations for the adiabatically varying system parameters are thus obtained.

REFERENCES

1. Polak, L. S., Variational Principles in Mechanics, Their Development and Application in Physics, (in Russian), Moscow, 1960, pp. 371-445.
2. Bogolioubov, N. N. and Mitropol'ski, J. A., Asymptotic Methods in the Theory of Nonlinear Vibrations, Fourth Edition (in Russian), Moscow, 1974, pp. 125-136, and 407-429.
3. Nayfeh, A. H., and Mook, D. T., Nonlinear Oscillations, New York: J. Wiley and Sons (Interscience), 1979, pp. 139-141.
4. Papastavridis, J. G. "Parametric Excitation Stability via Hamilton's Action Principle", J. of Sound and Vibration, Vol. 82, 1982, pp. 401-410.

---

\* Submitted for publication in Journal of Sound and Vibration.

\*\* Research supported by the U.S. National Science Foundation under Grant MEA-8303663.

ON THE APPLICATION OF THE BIOT THEORY  
TO SATURATED MARINE SEDIMENTS

by

A. Bedford, M. Stern and R. D. Costley  
Dept. of Aerospace Engineering & Engineering Mechanics  
The University of Texas  
Austin, TX 78712

Although the Biot theory appeared in 1956 [1,2], progress in correlating the theory with experimental measurements in saturated granular materials has come only recently, particularly through the work of Stoll and Bryan [3], Stoll [4], Berryman [5], Hovem and Ingram [6], and Johnson and Plona [7].

The reason for the extended period between the appearance of the theory and its successful application is the difficulty of evaluating the coefficients in the equations. Biot and Willis [8] showed how the elastic coefficients in the equations could be evaluated in terms of the porosity and elastic moduli of the constituents and of the drained granular medium. However, Stoll [4] pointed out that the granular medium should be treated as viscoelastic. Based upon experiments on dry granular media, he assumed that the granular medium could be characterized as having a logarithmic decrement that is independent of frequency. Subsequent evidence indicates that the actual behavior is more complicated as a result of the motion of the liquid in and out of the narrow gaps near grain contact points [9].

Biot [2] also evaluated the drag coefficient in his equations by considering the oscillatory motion of a liquid in a cylindrical pore and determining the resulting average velocity of the liquid and the shear stress at the pore wall. He considered only pores parallel to the motion. In this presentation, an extension of Biot's method is described which allows both the drag coefficient and the virtual mass coefficient to be determined for cylindrical pores of random orientation. The results indicate that both of these coefficients are functions of the material microstructure and of the frequency.

Using the determined values of the drag and virtual mass coefficient, and a viscoelastic model for the granular medium based upon the work of Murphy et al. [9], the Biot equations are compared with the data of Hovem and Ingram for water saturated glass beads [6].

References

1. M. A. Biot, "Theory of Elastic Waves in a Fluid Saturated Porous Solid. I. Low Frequency Range", *J. Acoust. Soc. Am.* 28, 168-178 (1956).
2. M. A. Biot, "Theory of Elastic Waves in a Fluid Saturated Porous Solid. II. Higher Frequency Range", *J. Acoust. Soc. Am.* 28, 179-191 (1956).
3. R. D. Stoll and G. M. Bryan, "Wave Attenuation in Saturated Sediments", *J. Acoust. Soc. Am.* 47, 1440-1447 (1969).

4. R. D. Stoll, "Theoretical Aspects of Sound Transmission in Sediments", *J. Acoust. Soc. Am.* 68, 1341-1350 (1981).
5. J. G. Berryman, "Elastic Wave Propagation in Fluid-Saturated Porous Media", *J. Acoust. Soc. Am.* 69, 416-424 (1981).
6. J. M. Hovem and G. D. Ingram, "Viscous Attenuation of Sound in Saturated Sand", *J. Acoust. Soc. Am.* 66, 1807-1812 (1979).
7. D. L. Johnson and T. J. Plona, "Acoustic Slow Waves and the Consolidation Transition", *J. Acoust. Soc. Am.* 72, 556-565 (1982).
8. M. A. Biot and D. G. Willis, "The Elastic Coefficients of the Theory of Consolidation", *J. Appl. Mech.* 24, 595-601 (1957).
9. W. F. Murphy, K. W. Winkler and R. L. Kleinberg, "Grain Contacts and Viscous Relaxation", *J. Acoust. Soc. Am.* 74 Suppl. 1, p. S58 (1983).

MECHANICAL MODELING OF THE SHRINKING AND SWELLING  
OF POROUS ELASTIC SOLIDS

by

Stephen C. Cowin  
Department of Biomedical Engineering  
Tulane University  
New Orleans, LA 70118

A method of mechanical modeling of the swelling and deswelling and of shrinking of porous elastic materials using the theory of elastic materials with voids [1,2] is described [3] and developed by example [4]. The example for shrinkage is the drying of wood; the example for swelling in a material with nonconnected voids is irradiated stainless steel; and the example for swelling and deswelling in a matrix with connected voids is the osmotic swelling and deswelling of articular cartilage. Although the concepts underlying this modeling process are general, theories of shrinking and swelling-deswelling must be material specific and mechanism (i.e., shrinking or swelling-deswelling) specific.

The method involves the introduction of fields of spherically self-equilibrated force systems called centers of compression or centers of dilation in the classical theory of elasticity. However, in the classical theory of elasticity centers of compression or dilation are singularities which usually only exist at isolated points [5]. In the theory of elastic materials with voids the centers of compression or dilation exist at every point in the medium and are not associated with singularities at any point. The kinematic variable conjugate to the center of compression or dilation is the change in solid volume fraction, or equivalently, the porosity of the material. These conjugate force and kinematic variables are combined along with those traditional in the theory of elasticity to form the theory of elastic materials with voids [1,2].

The general mechanism of swelling or shrinking is illustrated in the case of homogeneous deformations of a porous elastic solid subjected to surface tractions and no surface force. The overall size and shape of the body is changed due to change in the field of centers of compression (dilation) with no associated changes in the surface tractions or gravitational forces acting on the body. The changes in the field of centers of compression (dilation) are induced by changes in the liquid contained in the pores of the body. In the case of drying wood the evaporation of the structural or bound water contracts the wood cell in the same way drying a plum turns it into a prune, and thereby establishes a local field of compression centers. In the case of the osmotic swelling of articular cartilage the osmotic pressure difference between the perfusant fluid and the structural fluid induces a field of dilation centers. This mechanism is reversible by changing the salinity of the perfusant.

In order to illustrate these ideas, the solutions to specific problems associated with shrinking and swelling of materials are presented. The warping deformation induced in a piece of green lumber by the drying process is calculated. The stress-strain-osmo-

tic pressure experiments on articular cartilage recently reported in the literature [6] are modeled. The swelling induced in a piece of stainless steel by its irradiation is calculated.

#### REFERENCES

- [1] Cowin, S. C. and J. Nunziato, "Linear Elastic Materials with Voids", J. Elasticity. Vol. 13, 1983, pp 125-147.
- [2] Nunziato, J. W., and S. C. Cowin, "A Non Linear Theory of Elastic Materials with Voids", Arch. Rat. Mech. Anal., Vol. 44, 1979, pp 175-201.
- [3] Cowin, S. C., Mechanical Modeling of the Shrinkage and Swelling of Porous Elastic Solids, in preparation.
- [4] Cowin, S. C., Modeling of the Shrinkage Mechanism in Drying Wood and the Swelling Mechanisms in Irradiated Stainless Steel and Articular Cartilage, in preparation.
- [5] Love, A. E. H., A Treatise on the Mathematical Theory of Elasticity, Cambridge, 1927, p. 187.
- [6] Grodzinsky, A. J., V. Roth, E. Myers, W. D. Grossman, and V. C. Mow, "The Significance of Electromechanical and Osmotic Forces in the Non-equilibrium Swelling Behavior of Articular Cartilage in Tension", J. Biomechanical Engr., Vol. 103, 1981, pp 221-231.

**KINETIC THEORY FOR DENSE SYSTEMS OF INELASTIC DISKS**

by

J.T. Jenkins and M.W. Richman  
Cornell University  
Department of Theoretical and Applied Mechanics  
Ithaca, New York 14853

We review and expand upon kinetic theories for dense, two dimensional systems of identical, rough, inelastic, circular disks.

The derived balance laws and constitutive relations are used to predict the mean velocity of the disks, the mean energy of their velocity fluctuations, and the mean energy of their fluctuations in spin in several simple flows.

The predictions are compared with the values of these fields measured in numerical simulations and air table experiments.

QUASI-STATIC MOTION OF A HETEROGENEOUS MEDIUM VIA  
DYNAMIC RANDOM FIELD

by

Martin Ostoja-Starzewski  
Department of Electrical Engineering  
McGill University  
Montreal, Canada

In this paper we develop a formulation for the mechanics of a medium with a discrete random microstructure in the quasi-static approximation. Specifically, the formulation is developed for the water saturated soil. First, a graph  $G_s = (V_s, E_s)$  is introduced to represent the solid phase with  $V_s$  being the vertices at the centers of mass of the visco-elasto-plastic grains and  $E_s$  the edges connecting the nearest neighbors. In general, we have a Markov random field  $P_s$  on  $G_s$ , whose evolution is governed by a fundamental dynamical semi-group  $W$ . We give an application to the clay consolidation problem. Through a covering graph we generate  $G_f = (V_f, E_f)$  for the incompressible viscous fluid phase,  $V_f$  corresponding to a set of pores and  $E_f$  to the random channel network in the medium.  $W$  leads then to a dynamic Markov random field  $P_f$  on  $G_f$  with the local conditional probability  $p$  being governed by the pore pressure. The consolidation problem becomes reduced to the uniqueness problem\* for the measures  $p$  and  $P_f$  under prescribed boundary conditions. It is then established that for a critical  $p = p_c$  the channel network becomes disconnected, which corresponds to the transition in the consolidation curve for clay. The second part of this curve is then naturally given through  $P_f$  converging asymptotically to an equilibrium measure. We end by indicating how a similar formulation may be applied to model the microcrack formation and fracture processes in structured solids.

\* See e.g. "Markov Random Fields and their Applications", R. Kindermann and J. L. Snell, Am. Math. Soc., Contemporary Mathematics Series, Vol. 1, Providence, RI, 1980.

SURFACE-EXCESS INTERFACIAL CONSERVATION LAWS AND CONSTITUTIVE  
EQUATIONS: A RATIONAL DERIVATION VIA MATCHED ASYMPTOTIC  
EXPANSIONS

by

H. Brenner  
Department of Chemical Engineering  
Massachusetts Institute of Technology  
Cambridge, Massachusetts 02139

L. Ting  
D. T. Wasan  
Department of Chemical Engineering  
Illinois Institute of Technology  
Chicago, IL 60616

Three-dimensional continuum conservation laws displaying generally steep (but nevertheless continuous) changes in properties across a diffuse interfacial region are employed to derive their two-dimensional surface-excess conservation counterparts. In contrast with prior *ad hoc* analyses, the derivation is effected rationally via a singular perturbation expansion of the exact three-dimensional conservation equations using the method of matched asymptotic expansions. In this perturbation procedure the surface-excess interfacial conservation laws arise naturally as matching (boundary) conditions between the two distinct outer expansions characterizing the bulk conservation laws applicable on either side of the interface. In a rheological context, the *a priori* assumption of Newtonian constitutive behavior for the diffuse three-dimensional continuum is shown to yield the accepted Boussinesq-Scriven equations characterizing the two-dimensional Newtonian interface. Appearing therein are surface-excess phenomenological coefficients expressed as integrals (in a direction normal to the interface) of the comparable diffuse three-dimensional phenomenological coefficients.

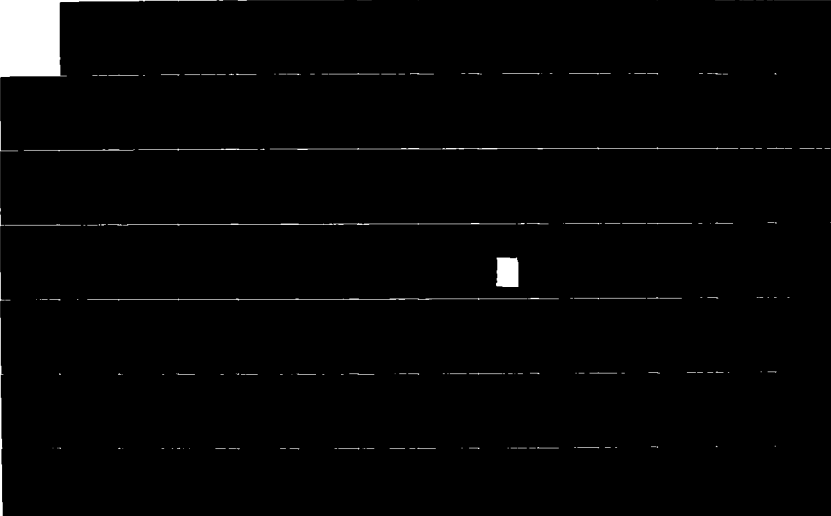
AD-A171 026

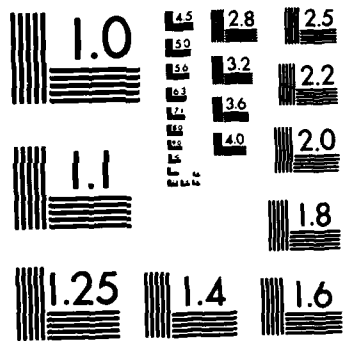
ABSTRACTS 21ST ANNUAL MEETING SOCIETY OF ENGINEERING  
SCIENCE INC OCTOBER 1-5 (U) VIRGINIA POLYTECHNIC INST  
BLACKSBURG D FREDERICK ET AL. 1984 ARO-21008. IC-CF  
DAAG29-84-M-0119 F/G 5/2

5/6

UNCLASSIFIED

NL





XERO COPY RESOLUTION TEST CHART  
NATIONAL BUREAU OF STANDARDS-1963-A

ON THE RHEOLOGICAL RESPONSE OF  
RANDOMLY STRUCTURED FIBROUS SYSTEMS

by

Y.M. Haddad  
University of Ottawa  
Department of Mechanical Engineering  
Ottawa, ONTARIO K1N 6N5

This paper is concerned with a new micromechanical approach to the rheological response of randomly structured, fibrous systems that could satisfy certain imposed macroscopic boundary conditions. This approach recognizes that the structure of the fibrous system consists of a randomly arranged, approximately two-dimensional array of viscoelastic fibres bonded together with inter-molecular bonds at regions where they cross. The theory, thus, takes into account the rheological response of the single fibres, the bonding effect between the fibres and other significant microstructural properties. Due to the inherent randomness of the physical and geometrical characteristics of the microstructure, probabilistic concepts are used. Furthermore, the elements forming the microstructure of a fibrous network in general have time-dependent characteristics [1,2]. Therefore, in dealing with such systems, it appears appropriate to consider the significant field quantities involved in the deformation process as stochastic variables and the deformation process itself is seen in this approach as a stochastic process [3].

In order to describe the mechanical response of a fibrous network having a distinct microstructure, it is necessary to consider the response of an actual structural element which on a local scale may differ considerably from an average response if the phenomenological approach were taken. In this regard, a new model of the structural element of the fibrous system is introduced. This model attempts to include the contribution of a single fibre segment between two neighbouring junctions, as well as the interfibre bonding effect within an associated junction area. Here, the nonlinear viscoelastic response of the fibre-segment is characterized by solving the time-dependent kernel equation [1] to incorporate available experimental data concerning the relaxation behaviour of such fibres. On the other hand, the response behaviour of the inter-fibre bonding is formulated by using a bonding potential form within the realm of unit cell theory [4]. Further, the inter-correlation between the bonding response to that of the associated fibre-segment is established in connection with the random orientation of the surrounding microstructure [5].

In order to extend the analysis for the practical case of a two-dimensional network, it is necessary to make use of "mesoscopic quantities" arising from considerations of the existence of a statistical ensemble of microelements within an intermediate domain of the material specimen [6]. Further, it is equally important to find a connection between the microscopic and the macroscopic res-

ponse formulations. In this context, it is useful to employ operational representation of the various relations. Hence, the notion of a "Material Operator" characteristic of the viscoelastic response of an intermediate domain of the material is introduced. It contains in its argument those stochastic variables or functions of such variables distinctive of the microstructure within the intermediate domain.

The research work is directed towards the following objectives:

1. Establishing a set of "Governing Response Equations for the fibrous system that are based on statistical and probabilistic theories. These response equations are presented in a generalized manner and, hence, are applicable to various types of fibrous systems.
2. Prediction of the probabilistic distributions of internal stresses in the microstructure of a fibrous system.
3. Establishing the evolution of the distributions of internal stresses as families of interacting stochastic processes [7] leading to the final relaxation or fracture of the macroscopic system.

A numerical evaluation of the proposed model is carried out by using available experimental data concerning the rheology of individual, natural fibres.

#### REFERENCES

1. Haddad, Y.M., "Numerical Analysis in Nonlinear Viscoelasticity", Int. J. Engg. Sci., Vol. 18, No. 2, 1980, pp. 325-331.
2. Haddad, Y.M., "A Theoretical Approach to Interfibre Bonding of Cellulose", J. of Colloid and Interface Sci., Vol. 76, No. 2, 1980, pp. 490-501.
3. Haddad, Y.M., "Response Behaviour of a Two-dimensional Fibrous Network", Ph.D. Thesis, McGill University, Montreal, 1975.
4. Bollmann, W., "Crystal Defects and Crystalline Interfaces", Springer-Verlag, New York, 1970.
5. Haddad, Y.M., "A Microstructural Approach to the Rheology of Fibrous Systems", J. of Colloid and Interface Sci. (to be published).
6. Axelrad, D.R., "Foundations of the Probabilistic Mechanics of Discrete Media", Pergamon Press, New York, 1984.
7. Doob, J.L., "Stochastic Processes", John Wiley and Sons Inc., New York, 1953.

## FIRST AND SECOND SOUND IN BINARY MIXTURES OF GASES

by

Angelo Morro

University of Genova

Department of Biophysical and Electronic Engineering  
16145 Genova, Italy

Owing to the extensive literature on the subject, we are now accustomed to considering second sound in liquid helium. Also we are aware of many thermodynamic theories leading to second sound (rate-temperature waves) in heat conductors thus ruling out the paradox of instantaneous speed of propagation. Nevertheless the lack of appropriate experimental evidence seems to cast the subject of second sound into the framework of speculative topics. Such is not the case; it is the purpose of this paper to show why there are experimental difficulties in revealing second sound in gases and, meanwhile, to point out favourable circumstances for efficient experiments.

Look at a binary mixture of nonreacting gases. Starting with the usual balance equations for mass, momentum, and energy and disregarding the inessential body force we arrive at the system of equations

$$\begin{aligned} \rho \dot{c} + \operatorname{div} \mathbf{J} &= 0, \\ \dot{\rho} + \rho \operatorname{div} \mathbf{v} &= 0, \\ (\partial \mathbf{J} / \partial t) + \operatorname{div}(\mathbf{J} \otimes \mathbf{v}_2) + (\mathbf{J} \cdot \operatorname{grad}) \mathbf{v} - \operatorname{div} \mathbf{T}_2 + c \operatorname{div} \mathbf{T} &= \mathbf{p}_2, \\ \rho \dot{v} - \operatorname{div} \mathbf{T} &= \mathbf{0}, \\ \rho \dot{\epsilon} + \operatorname{div} \mathbf{q} - \mathbf{T} \cdot (\operatorname{grad} \mathbf{v}) &= 0, \end{aligned} \quad (1)$$

where  $c$  is the concentration (of the component 2),  $\mathbf{J}$  the diffusion flux,  $\mathbf{v}$  the velocity (of the mixture),  $\mathbf{T}$  the stress,  $\epsilon$  the energy, and  $\mathbf{q}$  the heat flux. The components of the mixture are assumed to be inviscid and non-heat-conducting and then

$$\mathbf{T}_\alpha = -p_\alpha \mathbf{1}, \quad \alpha = 1, 2, \quad \mathbf{q} = q \mathbf{J}, \quad q = \epsilon_2 - \epsilon_1 + p_2 / \rho_2 - p_1 / \rho_1.$$

Moreover, the growth of linear momentum  $\mathbf{p}$  is taken to be linear in  $\mathbf{u}_2 = \mathbf{v}_2 - \mathbf{v}$ , namely  $\mathbf{p}_2 = -m \mathbf{u}_2$ ,  $m \geq 0$ . For the sake of definiteness in calculations we regard the components as perfect gases and then we write

$$\epsilon_\alpha = z_\alpha R \theta / M_\alpha + \epsilon_\alpha^0, \quad p_\alpha = \rho_\alpha R \theta / M_\alpha, \quad \alpha = 1, 2,$$

$2z_\alpha$  being the number of degrees of freedom,  $M_\alpha$  the atomic weight,  $\theta$  the temperature. Accordingly, the system (1) consists in fact of nine equations in the nine unknowns  $c$ ,  $\rho$ ,  $\theta$ ,  $\mathbf{J}$ ,  $\mathbf{v}$ .

In order to investigate the consequences of the system (1) on linear waves we observe first that a solution to (1) may be given the form

$$\begin{aligned} c &= c_0 + \bar{c}(\mathbf{x}, t), & \rho &= \rho_0 + \bar{\rho}(\mathbf{x}, t), & \theta &= \theta_0 + \bar{\theta}(\mathbf{x}, t), \\ \mathbf{J} &= \bar{\mathbf{J}}(\mathbf{x}, t) & \mathbf{v} &= \bar{\mathbf{v}}(\mathbf{x}, t), \end{aligned}$$

$c_0$ ,  $\rho_0$ ,  $\theta_0$  being constant, provided  $\bar{c}$ ,  $\bar{\rho}$ ,  $\bar{\theta}$ ,  $\bar{\mathbf{J}}$ ,  $\bar{\mathbf{v}}$  satisfy a proper counterpart of (1). Assume now that the barred fields are described

by plane waves as

$$\bar{\phi} = \hat{\phi} \exp[i(\omega t - \mathbf{k} \cdot \mathbf{x})].$$

For the sake of definiteness let the wave number vector  $\mathbf{k}$  be given the form  $\mathbf{k} = (k, 0, 0)$ . Then it follows at once that  $\hat{\mathbf{J}} = (\hat{J}, 0, 0)$ ,  $\hat{\mathbf{v}} = (\hat{v}, 0, 0)$ . So the unknowns are in fact five only, namely  $\hat{c}$ ,  $\hat{\rho}$ ,  $\hat{\theta}$ ,  $\hat{J}$ ,  $\hat{v}$ . Upon letting  $\lambda = \omega/k$  and observing that

$$\hat{J} = \lambda \rho \hat{c}, \quad \hat{v} = \lambda \rho^2 \hat{\rho}, \quad \theta = [(q - \epsilon_c)/\epsilon_\theta] \hat{c} + [p/\epsilon_\theta \rho^2] \hat{\rho}$$

we arrive at the system

$$\begin{aligned} (\lambda^2 - V_1^2) \hat{\rho} + [p_\theta(\epsilon_c - q)/\epsilon_\theta - p_c] \hat{c} &= 0, \\ -[P_\theta p/\epsilon_\theta \rho^3 + P_\rho/\rho] \hat{\rho} + [(1 + im/\omega c \rho)\lambda^2 - V_2^2] \hat{c} &= 0. \end{aligned} \quad (2)$$

Here

$$V_1^2 = p_\rho + p p_\theta / \epsilon_\theta \rho^2, \quad V_2^2 = p_c / \rho + P_\theta (q - \epsilon_c) / \rho \epsilon_\theta$$

while  $p_c$ ,  $p_\rho$ ,  $p_\theta$ ,  $\epsilon_c$ ,  $\epsilon_\theta$  denote partial derivatives and  $P_c = (p_2)_c - c p_c$ ,  $P_\rho = (p_2)_\rho - c p_\rho$ ,  $P_\theta = (p_2)_\theta - c p_\theta$ . In the decoupled case the system (2) accounts for density waves with speed  $V_1$  and concentration waves with speed  $V_2$ . Indeed, since  $\epsilon_\rho = 0$ ,  $V_1$  is just the usual adiabatic sound speed. Accordingly, at least theoretically, first sound and second sound may occur in a binary mixture of gases. Moreover, independently of the value of the coupling parameter

$$C = [P_\theta p / \epsilon_\theta \rho^3 + P_\rho / \rho] [p_\theta (\epsilon_c - q) / \epsilon_\theta - p_c],$$

the system (2) always admits two real values for the wave speed.

Some insights into the experimental setting may be gained by looking at some quantitative aspects. Second sound is better revealed if the coupling parameter  $C$  is negligible against  $V_1^2 V_2^2$ . It is easily seen that this happens if  $c \ll 1$  and/or  $(M_2 - M_1)^2 \ll M_1 M_2$ . Thus better experimental results may be obtained by adjusting the concentration or by choosing appropriate gases with nearly the same atomic weights. Unfortunately, second sound turns out to be severely damped because of the exchange of momentum, between components, described by the coefficient  $m$ .

#### References

- Bampi, F., Morro, A, "Exchange of energy and momentum between gases at different temperatures", *Phys. Fluids*, Vol. 25, 1982, pp. 2207-2210.  
 Dreyer, W., "Zur Thermodynamik von Helium II - Superfluides Helium, mit und ohne Wirbellinien als binäre Mischung", Ph. D. Dissertation, Berlin, 1983.

## MECHANICAL BEHAVIOR OF PAPER

by

Richard W. Perkins  
Syracuse University  
Department of Mechanical and Aerospace Engineering  
Syracuse N.Y. 13210

Paper is a nonwoven material composed of pulped wood fibers. The mechanical behavior of the system depends on the properties of the wood fibers, the nature of the bonds between fibers and the internal geometry of the fibrous network. For short duration, low stress situations at normal environmental conditions the material behaves elastically while for high stress situations the material exhibits essentially plastic behavior.

The macroscopic behavior can be investigated by a micro-mechanical approach where the characteristic element is selected as the individual fiber plus the portions of fibers that are bonded to the fiber in its immediate vicinity. Fibers may be treated as straight elements with statistical distributions of length and orientation, or, more realistically, as kinked or gradually curved elements. The fiber element must be modelled as having different properties in compression than those in tension when the fiber strains exceed the elastic limit. The interfiber bonds may be treated as ideal elastic-plastic elements.

The paper deals with the development of a micromechanics model for use in simulating the macroscopic elastic and post-elastic response of the material. The results of experiments are presented that provide information concerning the nature of the internal structure of the fibrous network, and correlation between experimental observation of mechanical behavior and the results of simulated behavior using the micromechanics model.

## STRUCTURAL OPTIMIZATION : TOWARD A RELIABLE C.A.D. TOOL

by

C. FLEURY  
Research Associate,  
NFSR

V. BRAIBANT  
Research Assistant,  
NFSR

Aerospace Laboratory  
University of Liège  
21, Rue E. Solvay  
B-4000 Liège  
BELGIUM

In this paper it is shown how modern structural optimization concepts have now evolved into a powerful Computer Aided Design tool that can really be used for dealing with practical problems.

As a basis a new and rather general mathematical programming method is first described, that is capable of solving efficiently a broad class of optimization problems. This method uses mixed direct/reciprocal design variables in order to get conservative, first order approximations to the objective function and to the constraints. By this approach the primary optimization problem is thus replaced with a sequence of explicit subproblems. Each subproblem being convex and separable, it can be efficiently solved by a dual formulation. An attractive feature of the new method is that it has an inherent tendency to generate a sequence of steadily improving feasible designs.

Applied to optimal sizing problems, the method generalizes previous approaches, such as the well known mathematical programming and optimality criteria approaches. Because the algorithm requires only the current values and gradients of the functions describing the non linear programming problem, it can be applied to any objective function and to any type of constraint. This constitutes of course a major step in the ongoing developments of structural sizing codes based on finite elements.

New results in shape optimal design are next presented, that yield convergence properties as good as those obtained in the pure sizing case : the overall optimization process usually requires less than ten finite element analyses. The idea is to resort to the CAD concept of patch to represent the structure by a set of "design elements". The geometry of each design element is controlled by a limited number of master nodes through the use of Bezier or B-Splines blending functions. In such an optimization problem the design variables are the locations of some conveniently selected master nodes.

Examples of application to various structural optimization problems will be offered, that demonstrate the generality and the efficiency of the approach presented. In particular real life aerospace structures will be considered : optimal sizing of an engine mount structure for a strap-on booster and shape optimal design of an axi-

symmetric flange joint for the same structure. These two practical applications are concerned with the European launcher ARIANE L4 and they involve thousands of finite elements and degrees of freedom. In these examples it will be seen that a reliable optimization method should also include the capability of generating a feasible design in the frequently encountered case where two or more constraints are in conflict. It can even happen that some of the constraints are really incompatible - i.e. the feasible domain in the design space is empty - in which case, through relaxation techniques, the optimization algorithm must provide the designer with the best infeasible solution.

In the presentation emphasis will be placed on the use of optimization methods in the framework of a CAD system : interactivity, colour computer graphics, pre- and post-processors of the finite element and optimization modules, etc ... The benefits that the designer can gain from optimization will be shown on practical applications.

GENERIC MODELING AND DESIGN SENSITIVITY  
-ADVANCED TOOLS FOR CAD PROCESS

by

B. Prasad

Research Staff

Ford Motor Company  
Scientific Research Laboratories  
P. O. Box 2053  
Dearborn, Michigan 48121

The generation and modification of detailed finite element models necessary to examine the effects of component shape on stresses and/or deflections is expensive and time consuming. Alternatively, Generic modeling techniques offer the potential advantage of substantially reducing the model modification time by controlling the geometry through a finite set of design parameters. This paper describes a generic modeling procedure, which has been developed using Engineering Analysis Language (EAL), for creating such models that can be linked with an analysis run stream. In addition, because finite element analysis programs do not normally have a capability of evaluating the effects of changing the design (henceforth called sensitivity) on the structural behavior, and because such a capability is desirable for effective utilization of materials and resources, and for timely decisions on design modifications, a computerized procedure for design sensitivity has been developed using a general purpose finite element program EISI/EAL. The procedure is capable of predicting sensitivity of design to changes in the design parameters. The term "design sensitivity" is used to indicate not only the computation of required derivatives but also evaluations of appropriate direction of moves for different design situations and determination of relative importance of design parameters for improving design performance. The procedure is based on efficient derivative computation and post processing schemes that reduce the total time and user's involvement.

## SENSITIVITY DERIVATIVES OF ITERATIVELY CALCULATED SOLUTIONS

by

Raphael T. Haftka  
Department of Aerospace and Ocean Engineering  
Virginia Polytechnic Institute & State University  
Blacksburg, Virginia 24061

A new technique for calculating finite difference derivatives of the solution of iteratively solved systems of equations is proposed. The new approach permits derivative calculations with small difference perturbations without having excessive accuracy problems. The technique is applied to a simple algebraic problem as well as to linear structural problems solved by an element-by-element implementation of a preconditioned conjugate gradient procedure. Two truss examples are used to demonstrate the improved accuracy of the proposed approach.

The new technique also permits more independent control of the accuracy of a quantity and its derivatives. The new technique should be useful, therefore, in applications where accuracy requirements are dissimilar. Structural optimization is a typical such application. The usefulness of the flexibility of the new technique is demonstrated by applying it to the minimum weight design of one of the truss examples. Significant computational savings are demonstrated by applying different accuracy requirements to stresses and their derivatives.

## STRUCTURAL SYNTHESIS USING A GENERAL-PURPOSE OPTIMIZATION PROGRAM

by

Garret N. Vanderplaats  
Naval Postgraduate School  
Monterey, California 93943

Structural synthesis may conveniently be separated into analysis and optimization. The use of Finite Element techniques for analysis is well established and widely used. On the other hand, formal optimization techniques are unfamiliar to many practicing structural engineers. However, this part of the structural synthesis process has matured considerably in recent years so that general-purpose numerical optimization software can be used as a design tool with little theoretical knowledge of the underlying mathematics.

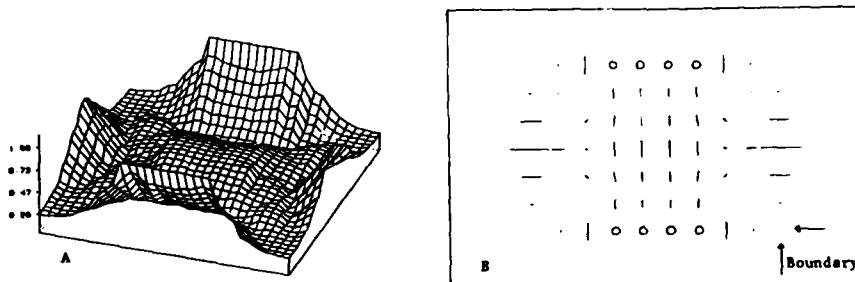
The use of a general-purpose optimization program in structural synthesis is described. The advantages of this approach are shown to be rapid program development, generality in the choice of design variables, objective functions and constraints, clear modularity of the software, and extendability to multi-disciplinary design. The penalty for this generality is a reduction in the computational efficiency as compared to the use of special purpose techniques. Numerous example applications are given using the general-purpose optimization program, CONMIN. These include design of stiffened composite panels, turbine rotors and blades, aircraft structures, automotive components and machine parts. It is concluded that, while much research and development remains, the general technology for structural synthesis is well in hand, and that major effort is now needed to transfer this technology to the engineering community.

## OPTIMAL DESIGN OF RIB-REINFORCED PLATES

by

Martin P. Bendsoe  
 The Technical University of Denmark  
 Mathematical Institute  
 DK-2800 Lyngby, Denmark

We consider the optimal design of linearly elastic, solid plates equipped with two fields of mutually orthogonal fields of infinitely many, infinitely thin integral stiffeners. As distributed design parameters we use the thickness of the solid part of the plate as well as the densities and directions of the stiffeners. This problem is connected with the question of existence of solutions to problems of optimal design of plates using just the plate thickness as the variable, and a numerical study of optimization within the extended class of plate configurations has been carried out. The stiffened plates are described by a homogenized plate equation and the results indicate that the inclusion of ribstiffened plates as admissible designs regularizes plate optimization problems, as well as giving very efficient designs. For comparison, optimization of plates stiffened with beams and optimization of plates with slope-constrained thickness function has also been carried out.



Configuration of an optimally designed ribstiffened, clamped plate of given volume and with upper and lower constraints on the thickness.. A.: Distribution of material.  
 B.: Directions and densities of stiffeners; in points  $\odot$  the plate is solid caused by a density equal to 1.

A GENERALIZED VARIATIONAL FORMULATION  
FOR STRUCTURAL OPTIMIZATION PROBLEMS

J. E. Taylor  
Aerospace Engineering Department  
Univ. of Michigan, Ann Arbor, MI 48109-2140

The accounting for *separate load configurations* and/or the possibility of having *different response modes* in structural optimization problems are factors that enter into the problem formulation directly through the constraints for the equations of mechanics. Problems with features such as these are termed multipurpose design problems. Multicriteria (or vector) optimization problems are distinguished by the property that the solution design is to be optimum at once with respect to two or more independent criteria. The generalized formulation discussed in this paper covers the multicriteria design of multipurpose structures. At the same time it has incorporated in it the means to represent for the various 'purposes' two or more different but related structural forms. The latter capability is needed where possible damaged or degraded states of the structure are to be taken into account (e.g., as in fail-safe design) in the prediction of optimal design.

The purpose is to provide a variational formulation and demonstrate the associated necessary conditions for this broad form of problem statement. A min-max interpretation is used for the reduction of the multicriteria problem to scalar form (see, e.g., [1]). This step requires the assignment of relative weight factors to the separate criteria. The variational problem statement for min-max problems with the max on an argument with local measure makes use of the development reported in [2]. Either or both the context for the principal function (primary context) of the structure and the contexts for the damaged structures (secondary contexts) may reflect multicriteria or multipurpose requirements. The relationships among the structures associated with the primary and secondary contexts appear in explicit form as constraints. With the introduction of appropriate notation, the variational statement for the most general problem including all of the features cited above is given in relatively simple form.

- [1] Bendsøe, M. P., Niels Olhoff and J. E. Taylor, "A Variational Formulation for Multicriteria Structural Optimization," J. Struct. Mechs. (to appear).
- [2] Taylor, J. E. and M. P. Bendsøe, "An Interpretation for Min Max Structural Design Problems Including a Method for Relaxing Constraints," Intntl. J. Solids and Structs. (to appear), also see DCAMM Report 256, December 1982.

OPTIMIZATION OF A MULTIVARIABLE PROCESS BY THE  
STEEPEST DESCENT APPROACH

by

K. T. Ewida, BSc Eng., Ph.D. Eng., Mem IES, Mem SEE  
Asst. Professor, Environmental Sciences Department  
Faculty of Engineering  
Zagazig University  
Zagazig, Egypt

In a multivariable process such as the environmental pollution one where its response surface is represented by a multivariable function such as:

$$Y = f(x_1, x_2, \dots, x_n)$$

where

Y = objective variable of the process  
 $x_1$  ---  $x_n$  = variables controlling the process

The most common method for optimizing the response surface is the one using the regression analysis approach. In this paper an alternative approach is suggested where the steepest descent method (1) can be employed and the set of simultaneous differential equations it generates can be solved by the analogue computer. All optimal coefficients of the response surface equation can also be obtained at the steady state condition and an optimal model for the process can be developed.

Reference

1. Steinmetz, H. L., "Using the Method of Steepest Descent", I.&E.C., January 1966.

## UNSTABLE BEHAVIOR OF SOME DISSIPATIVE PHYSICAL SYSTEMS

by

M. Carme Calderer  
Oregon State University  
Department of Mathematics  
Corvallis, OR 97331

It is a well known fact that solutions to certain initial boundary value problems in three-dimensional nonlinear elasticity exists only on a finite time interval  $(0, t_{\max})$ ,  $t_{\max} > 0$ . When a continuation theorem is available one can actually prove that non-global existence in time occurs by finite time blow-up of some norm of the solution as  $t$  approaches  $t_{\max}$ . This behavior is exhibited by hyperelastic bodies for which the stored energy function is that of a weak material. Instabilities of certain equilibrium solutions also occur.

In this presentation, I shall examine whether the presence of dissipative mechanisms in the system, which cause the energy to decay, are able to prevent finite time blow-up and instabilities of solutions. First, supposing that the material is of fading memory type and ignoring thermal effects I shall present a class of initial boundary value problems for which finite time blow-up of some solutions still occur, under appropriate constitutive hypotheses. In particular, viscoelastic materials that exhibit such a behavior may be found among the class studied by Doi and Edwards for polymer melts and that studied by Coleman and Noll for viscoelastic fluids.

Finally, I shall consider similar problems for thermoelastic materials, taking thermal effects into account. One can find as well a class of constitutive equations for which finite time blow-up of solutions still occurs. A physical interpretation of such material family will be given.

## ON GRADIENT SENSITIVE MATERIALS OF KORTEWEG TYPE

by

J. E. Dunn  
Sandia National Laboratories  
Albuquerque, NM 87115

and

J. Serrin  
Department of Mathematics  
University of Minnesota  
Minneapolis, MN 55455

In 1901 the Dutch physicist Korteweg proposed, as a way to model capillarity effects in fluids, a constitutive equation for the stress that contained not only the usual dependence on the temperature  $\theta$  and current mass density  $\rho$  but also depended on  $\text{grad } \rho$  and  $\text{grad}^2 \rho$ , the first and second spatial gradients of the density. Specifically, Korteweg postulated a compressible fluid model in which the "elastic" or "equilibrium" part of the Cauchy stress  $\underline{T}$  was given by

$$\underline{T} = (-p + \alpha \Delta \rho + \beta |\text{grad } \rho|^2) \underline{1} + \delta \text{grad } \rho \otimes \text{grad } \rho + \gamma \text{grad}^2 \rho, \quad (K)$$

where  $\Delta \rho \equiv \text{tr}(\text{grad}^2 \rho)$  is the Laplacian of  $\rho$  and where  $\rho$ ,  $\alpha$ ,  $\beta$ ,  $\delta$ , and  $\gamma$  are material functions of  $\rho$  and  $\theta$ .

Korteweg's form (K) thus yields a symmetric stress tensor in a very special elastic material of grade 3. It thus differs from the higher grade theories of elasticity which were studied in the early 1960's and which generally led to couple stresses and non-symmetric forms for  $\underline{T}$ . In any case, as is well known, Korteweg's form (K) and, indeed, all higher grade theories of elasticity are incompatible with the usual forms of momentum and energy balance and entropy inbalance (i.e., the Clausius-Duhem inequality) when those laws are applied in the manner suggested by Coleman and Noll.

Here I will discuss a particularly simple resolution of the above incompatibility which rests upon merely permitting the longer range spatial interactions which one is tacitly modeling in higher grade theories to have an associated energy flux  $\underline{u}$ , which we call the interstitial work flux. It turns out that  $\underline{u}$  is intimately related to the free energy's dependence on higher gradients, and that this in turn leads to a special, nontrivial structuring of the dependence of the stress on higher gradients. Indeed, if  $\psi = \psi(\rho, \theta, \underline{d})$ ,  $\underline{d} \equiv \text{grad } \rho$ , is the constitutive equation for the Helmholtz free energy, then our theory yields that in an elastic, fluid-like material

$$\underline{T} = -p \{ \rho \psi_\rho + \underline{d} \cdot \psi_{\underline{d}} \} - \rho \underline{d} \otimes \psi_{\underline{d}} - \text{div} \{ \underline{K} + \underline{E} \}, \quad (I)$$

where  $\mathbb{K}$  is the third order tensor

$$\frac{1}{2} \rho^2 \{ \psi_d \otimes \underline{1} - \underline{1} \otimes \psi_d \},$$

and where  $\mathbb{E}$  is a third order tensor, skew in its first and third places, undetermined by  $\psi$ . In particular, our theory is compatible with forms like Korteweg's (K) provided that the nonclassical coefficients  $\alpha$ ,  $\beta$ ,  $\delta$ , and  $\gamma$  obey certain compatibility conditions.

Less specially, accounting for the interstitial work flux  $\underline{u}$  allows for a higher gradient theory much richer than that hidden in the form (K). Indeed, the form (I) allows us to prove a far reaching generalization of the equal area rule of Maxwell without appeal to the thermostatics of phase transitions.

DYNAMICS OF PHASE TRANSITIONS:  
MECHANICAL, ANALYTICAL, AND NUMERICAL ASPECTS

by

M. Slemrod  
Department of Mathematical Sciences  
Rensselaer Polytechnic Institute  
Troy, New York 12181

This talk discusses the role of higher gradient theories in the dynamics of phase transitions. Specifically, I will show how mathematical analysis gives qualitative information as to the nature of dynamic phase transitions in a van der Waals fluid. Furthermore, I will explain how the mechanics suggests numerical methods for solving the initial value problem for a van der Waals fluid. The results of numerical experiments will be given which tend to validate my approach.

## A THEORY OF ANISOTROPIC FLUIDS

by

Ernest H. MacMillan  
University of Minnesota  
Aero Engineering & Mechanics  
Minneapolis, MN 55455

A continuum theory of anisotropic fluids extending those of Ericksen and Leslie<sup>1</sup> will be presented.

Recent experiments<sup>2</sup> on liquid crystalline polymers suggest that the local ordering of these fluids, when under the influence of viscous forces, can assume a configuration other than the uniaxially symmetric one chosen in liquid crystal theory.

Thus, there is some hope that the increased generality of this new theory, which allows of a variety of local symmetries, is not specious; in particular, that this theory or some variant of it will be successful in describing liquid crystalline polymers - presently an area under intense technological development.

References

1. Leslie, F.M., Theory of Flow Phenomena in Liquid Crystals, Advances in Liquid Crystals (G.H. Brown, ed.), Vol. 4, 1-81, Academic Press, New York, 1979.
2. Wissbrun, K., Orientation Development in Liquid Crystal Polymers, Orienting Polymers Lect. Notes Math., Springer-Verlag, in press. (Proceedings of the I.M.A. workshop in oriented polymers, March, 1983).
3. Chandrasekhar, S., Liquid Crystals, Cambridge University Press, Cambridge, 1977. (General reference).

A VISCOPLASTIC THEORY WITH ANISOTROPIC HARDENING AND  
ITS APPLICATION TO PRESSURE-SHEAR PLATE IMPACT EXPERIMENTS

by

A. Gilat

The Ohio State University  
Department of Engineering Mechanics  
Columbus, OH 43210

An elastic/viscoplastic theory that includes anisotropic strain hardening is used in the analysis of experimental results from pressure-shear plate impact experiments on commercially pure alpha titanium. The theory is a combination of the elastic/viscoplastic formulation of Perzyna [1] and the anisotropic strain hardening model for time independent plasticity introduced by Mroz [2]. The plastic strain rate is taken in the form proposed by Perzyna [1]. The form consists of an assumed function which determines the magnitude of an effective plastic strain rate vector and a flow potential which gives the direction of the plastic strain rate vector. The flow potential is a surface obtained by isotropic expansion of a yield surface. Hardening can be introduced by changes in the shape, size and location of the yield surface. In the present study, the yield surface translates with a constant size and shape. The translation is taken to be in the form proposed by Mroz [2]. However, changes are introduced to the Mroz model in order to adopt it for use in a time dependent theory.

The theory is used in the analysis of pressure-shear plate impact experiments conducted by Gilat [3]. In these experiments plastic waves of combined pressure and shear are produced in a plate. Due to the difference in the speed of the pressure and shear waves, every section in the plate experiences a different non-proportional loading path. This aspect of the experiment provides an opportunity to examine the effect of the hardening law in the constitutive relations. Good agreement between theory and experiment is observed. The current results show that the model used here predicts the material response better than isotropic or kinematic strain hardening models, results for which are included in [4].

REFERENCES

- [1] Perzyna, P., "Fundamental Problems in Viscoplasticity," Advances in Applied Mechanics, Academic Press, New York, Vol. 9, 1966, pp. 321-332.
- [2] Mroz, Z., "On the Description of Anisotropic Workhardening," J. Mech. Phys. Solids, 1967, Vol. 15, pp. 163-175.
- [3] Gilat, A., "An Experimental and Numerical Investigation of Pressure-Shear Waves in 6061-T6 Aluminum and Alpha-Titanium," Ph.D. Thesis, Brown University, Providence, R.I., 1982.
- [4] Clifton, R.J., Gilat, A. and Li, C.H., "Dynamic Plastic Response of Metals Under Pressure-Shear Impact," Material Behavior Under High Stress and Ultrahigh Loading Rates, Mescall, J. and Weiss, V., eds., Syracuse University Press, Syracuse, N.Y., 1983.

SOME COUPLED ELASTICITY-GRAIN BOUNDARY  
DIFFUSION PROBLEMS

by

Asher A. Rubinstein  
State University of New York at Stony Brook  
Department of Mechanical Engineering  
Stony Brook, New York 11794

The diffusive grain boundary void growth is one of widely accepted mechanisms of high temperature creep failure. The diffusive material redistribution is driven by chemical potential gradient which is related to a normal stress acting on the grain boundary. Therefore, the nucleation of voids as well as their growth process strongly depend on the stress field along the grain boundary.

The aim of this work is the analysis of various types of possible sources of stress concentration and the history of stress relaxation.

The typical problem would be based on consideration of an elastic (linear in this case) half plane ( $y \geq 0$ ) with diffusion equation  $D\sigma''(x) + \delta = 0$ , governing the condition on the boundary  $y = 0$ , which represents the grain boundary. (Here  $D$  is the diffusivity coefficient,  $\sigma$  is a normal stress on  $y = 0$  ( $\sigma_{yy}$ ),  $\delta = 2u_y$  is a grain boundary "thickening"). Considering for simplicity plane strain case, the following problems are of interest: single dislocations on grain boundary and distant from the grain boundary, dislocation pile-ups, voids on grain boundary. The shape of voids considered is crack-like or equilibrium (cylindrical caps). The relaxation of stress concentrations for periodically distributed voids is considered as well.

The main attention in this presentation is given to a mathematical formulation of these problems and to methods of solution of obtained singular integral equations.

The formulations are based on application of analytic potentials used in plane elasticity problems and formulation of singular integral equations. Solutions for single dislocations are used as an influence function in these formulations.

Results give the practically important time parameters and extreme values of acting stresses, which enable one to predict possible void nucleation or most favorable loading regimes.

## THREE-DIMENSIONAL MODELING OF INERT METAL-LOADED EXPLOSIVES

by

James D. Kershner, Charles L. Mader, and George H. Pimbley  
Los Alamos National Laboratory  
Los Alamos, New Mexico 87545 (USA)

The reactive three-dimensional hydrodynamic code 3DE has been used to investigate the reactive hydrodynamics of a matrix of tungsten particles in HMX. A propagating detonation proceeding through the matrix of tungsten particles gives calculated detonation velocities and pressures that are much higher than observed. If the heterogeneous shock initiation Forest Fire rate for HMX is used to describe the reactive kinetics, some of the individual detonation wavelets between the tungsten particles fail. The shocked explosive continues to decompose and release energy after shock passage.

Equations of state are described for a tungsten and a lead-loaded explosive that reproduce the observed performance of these nonideal explosives. Evidence is presented that the explosives have a flat top Taylor wave characteristic of weak detonations.

## SIMULATION OF GRANULAR MATERIAL FLOW IN TWO-DIMENSIONS\*

by

Otis R. Walton  
Lawrence Livermore National Laboratory  
Livermore, CA 94550

Direct simulation of the motion of large numbers of inelastic frictional particles is providing details of the the flow behavior that would be difficult to obtain in the laboratory. Models that calculate the motion of circular and arbitrary shaped polygonal particles in two-dimensions are being used to study gravity flow on inclined surfaces. Simplified force models and careful bookkeeping allow large numbers of particles to be handled efficiently. The nature of gravity flow on inclined surfaces is of interest to various energy related programs including oil shale processing, coal gasification, inertial confinement fusion reactor design, and high-temperature solids-receivers for solar energy. Both the rheologic behavior of the flowing solid and the interactions between the flowing layers and the underlying surface are of interest. Calculations to date have primarily examined the interactions with the inclined boundary and flows from one incline to another. Circular particle calculations show a layer of rolling particles next to a smooth frictional incline over which the remainder of the flowing layer glides. Physical tests with circular plexiglas particles confirm the existence of such a layer. Percolation of small particles down through a shearing layer and inversion of the layer upon transfer to another incline sloping in the opposite direction are other qualitative observations from these "computer experiments." A small sample size, periodic boundary, version of the model for circular particles in a uniform shearing field is being used to examine how various parameters in the interparticulate force models affect the shear behavior of an assembly of particles.

\*Work performed under the auspices of the U.S. Department of Energy by the Lawrence Livermore National Laboratory under contract number W-7405-ENG-48.

## Finite Element Solution of Ballistic Penetration of Subseabed Sediments

Thomas R. Canfield  
Division 1531  
Sandia National Laboratories  
Albuquerque, New Mexico 87185

A current concept for disposing of high-level nuclear wastes is to use ballistic penetrometers to emplace these materials in subseabed sediments. A vehicle designed to carry a waste package would be taken by ship to a remote drop sight where it would be released and allowed to free fall to terminal velocity before impact with the seafloor. Following impact, it would penetrate the sediment and eventually come to rest at some depth below the seafloor. Successful burial requires that an adequate depth of penetration is achieved, and the hole created during penetration close completely and encapsulate the waste package. Numerical simulation appears to be a practical method for studying this type of problem.

A dynamic finite-element computer code, MARBLE, has been written to perform simulations of mechanical events of this type. It employs an arbitrary Lagrangian-Eulerian (ALE) formulation to treat fluid regimes and a purely Lagrangian formulation in solid regimes. The ALE formulation permits the use of an adaptive mesh to conform to the specific needs of the problem. In MARBLE, the velocity of the arbitrary mesh is controlled by the use of an inverse distance-weighting smoothing algorithm. In addition, the mesh can be controlled point by point through the use of prescribed velocity or displacement time histories. These same types of constraints may also be imposed on the materials. Interactions between materials are accomplished through the use of two types of interfaces. In one case, pairs of nodes are tied together and in the other, a master-slave type of slide line is used. Finally, an incremental form of Lysmer's absorbing boundary has been developed to model unbounded regimes. The Flanagan-Belytschko quadrilateral finite element is used and allows modeling of plane strain and axisymmetric continuum mechanics problems. There are several rate-type elastic-plastic material models in the code. In particular, an elastic-plastic soil-cap model was used to simulate the sediment material in the penetration calculation. The seawater was modeled as an inviscid hydrodynamic fluid.

A calculation has been performed demonstrating the code's capability. In it a hypothetical emplacement vehicle, 0.2 m in radius by 3.35 m in length, was allowed to fall at a constant velocity of 40.0 m/sec through a spherical region of space 5.0 m in radius. The upper half of the hemisphere, where the penetrator starts, consists of seawater and the lower hemisphere is sediment. Absorbing boundaries are applied to all external surfaces of the sphere. It

takes 84.0 msec for the vehicle to completely penetrate the sediment. Hole closure is observed to occur very quickly and be complete 41.0 msec after passage of the blunt tail into the sediment. This results in the formation of a cone-shaped cavity of fluid being trapped directly behind the tail. Since the hole never reopens, this fluid remains attached to the tail and follows the emplacement vehicle as it continues to penetrate into the sediment.

This work performed at Sandia National Laboratories supported by the U.S. Department of Energy under contract number DE-AC04-76DP00780.

by

Gerald L. Goudreau

University of California, Lawrence Livermore National Laboratory  
P. O. Box 808, Livermore, CA 94550

The weapons mission of the Department of Energy nuclear design laboratories has required the strongest possible scientific computing base of ever growing quantity and quality. The '80s is the decade of the Cray, as both Lawrence Livermore National Laboratory (LLNL) and Los Alamos National Laboratories (LANL) move from CDC to their current Cray/XMP mainframes. Four Cray-1s and an XMP are in place, with several XMP upgrades ahead before the Cray-2. Conventional weapons work for the Department of Defense, inertial confinement and isotope separation laser work, as well as reactor safety studies for the Nuclear Regulatory Commission (NRC) now also require high technology engineering computations to complement and bring to fruition the scientific innovation.

The Methods Development Group in Engineering has built a spectrum of codes tuned to the computers of this decade and responsive to the myriad problems generated by the diverse Laboratories challenges. This talk centers on the linear and nonlinear solid and structural mechanics codes and their performance in the Livermore Cray environment. Hallquist's DYNA2D/DYNA3D are explicit, while NIKE2D/NIKE3D are implicit large deformation inelastic Lagrangian continuum finite element codes. GEMINI is a new general purpose linear structures code.

The DYNA and NIKE codes are well documented in [1-4], and others therein referenced. These Lagrangian continuum finite element codes spatially discretize the equation of motion in the current geometry, where the element stress divergence is assembled from the current Cauchy stress and linear displacement gradient/nodal displacement matrix.

For an explicit code, the centered time integration rule defines a right hand side where all the effort is centered, especially where localization of the motion through a strain measure allows application of a point constitutive law to that locally homogeneous strain history for the determination of stress and then discrete forces.

The application of an implicit algorithm to a nonlinear dynamic or quasi static process requires an iterative solution of the end point or current geometry for a small or large increment depending

---

<sup>1</sup>Work performed under the auspices of the U.S. Department of Energy by the Lawrence Livermore National Laboratory under contract number W-7405-Eng-48.

on dynamics, path dependence of constitutive law, and significant features in the loading history. NIKE uses a secant Newton process involving BFGS updates requiring infrequent stiffness reformations in a time step.

Detailed operation counts for DYNA3D were published in [1,2], and for NIKE2D in [6]. Not only have operation counts been optimized, but advantage of the CRAY-1 FORTRAN vectorization in scalar product, scalar vector, and "element chunking" strategies are employed.

NIKE3D currently has the Hughes shell element formulation [5] as implemented by Slater/Hallquist [4]. This low order finite strain element is an ideal companion to our NIKE solid element.

GEMINI is our new general purpose linear structures code by Murray [7], which has replaced SAPIV. It has significant internal reorganization, the FISSLE solver, a new subspace package built around FISSLE, and a new plate/shell element. This code treats strictly linear statics and dynamics, with emphasis on large eigenvalue solving for modal dynamic response.

#### REFERENCES

1. Goudreau G. L. and J. O. Hallquist, "Recent Developments in Large Scale Finite Element Hydrocode Technology," J. Comp. Meths. Appl. Mechs. Eng., Vol. 30, 1982, pp. 725-757.
2. Hallquist, J. J., "Theoretical Manual for DYNA3D," UCID-19401, University of California, Lawrence Livermore National Laboratory, Livermore, Calif., 1983.
3. Hallquist, J. O., "DYNA3D User's Manual, (Nonlinear Dynamic Analysis of Solids in Three Dimensions)," UCID-19592, Rev. 1, University of California, Lawrence Livermore National Laboratory, Livermore, Calif., 1984.
4. Hallquist, J. O., "NIKE3D: An Implicit, Finite-Deformation, Finite Element Code for Analyzing the Static and Dynamic Response of Three-Dimensional Solids," UCID-18822, Rev. 1, University of California, Lawrence Livermore National Laboratory, Livermore, Calif., 1984.
5. Hughes, Thomas J.R. and W. K. Liu, "Nonlinear Finite Element Analysis of Shells: Part I. Three Dimensional Shells," Comp. Meths. in Appl. Mech., Vol. 26, 1981, pp. 331-362 .
6. G. L. Goudreau, et al., "Efficient Large-Scale Finite Element Computations in a Cray Environment," Proceedings: Impact of New Computing Systems on Computational Mechanics, ASME Winter Meeting, 1983.
7. Murray, R. C., "GEMINI - An Efficient Computer Program for Three Dimensional Linear Static and Seismic Structural Analysis," Dr. of Engineering Thesis, University of California, Davis, Calif., 1982. (User's Manual in preparation.)

STRUCTURAL ANALYSIS COMPUTATIONAL CAPABILITIES AND ORGANIZATION AT  
SANDIA NATIONAL LABORATORIES

by

R. D. Krieg  
Applied Mechanics - 1  
Sandia National Laboratories  
Albuquerque, New Mexico 87185

The structural analysis department of roughly forty people at Sandia National Laboratories, Albuquerque, serves as a service/consulting group to the Labs in the capacity of structural analysts. Its software and hardware have been configured into a reasonably efficient operation in the sense of minimizing the analyst's time in completing an analysis. The software is divided into three distinct categories: preprocessors, problem solvers, and postprocessors, and these are interfaced with neutral files. A file is written as output from all software in one category so that it can be read by all software in the succeeding category. This software is implemented on a network consisting of the department's VAX11/780 and VAX11/750 as well as the Lab's Cray-1S. The pre- and postprocessing is principally performed on the VAXes while number crunching is confined to the Cray-1S. The analyst can interact with the VAXes on short tasks, such as file preparation and manipulation, where interaction is most valuable, while the Cray-1S is available for the computationally intensive tasks. Files can be transferred between computers from terminals on the analysts' desks. With this arrangement the system is responsive and the analyst's time is productive.

Quality Assurance (QA) procedural requirements on structural analyses in general and the software in particular are becoming an important part of the structural analysis atmosphere at Sandia. These requirements tend to stifle progress and increase paperwork. We have attempted to take a positive approach and use these restraints to our advantage where possible. Our QA procedures center around a set of files which contain the official versions of software used by the department. Each piece of software has a sponsor who acts as a consultant and is responsible for maintenance on that particular piece of software. Proliferation of software and multiple versions of programs are tempered by this procedure. Levels of QA have been defined such that even new and undocumented codes are available in the system.

The structural analyses codes are almost exclusively finite element codes. They can be categorized as 2D and 3D static and dynamic codes, as 2D fracture mechanics codes, and as general purpose codes. Most analyses are static 2D analyses. Over the past several months, the group has averaged 74% static 2D runs, with 11% dynamic 2D runs. Fracture mechanics analyses in 2D account for another 10%. Three-dimensional runs account for only 5% of the runs. This is not indicative of the proportion of analysts' time spent. This is due to the long times required of the analyst for mesh generation and post-processing for each of the 3D runs compared to that required for 2D analyses. The department totals about 150 runs per day on the Cray-1S. In spite of this impressive number of analyses, the principal

bottleneck in production structural analysis is still the time required for documentation. Code development in the department has been concentrated in user friendly graphics and nonlinear analyses. This has resulted in a large number of complex nonlinear analyses being performed in the department. Roughly 20% of the computer runs made are on linear or almost linear analyses. The problem sizes range from small numbers of elements on linear elastic 2D configurations to several thousand elements on non-linear 3D configurations. Runs are occasionally hours long on the Cray-1S. This translates into roughly three million CP seconds of Cray-1S time per year for the department.

Sandia has a wide diversity of projects and the structural analysis department is involved in a majority of these. Weapons and weapon components; nuclear waste repository designs in hard rock, salt, and sub-seabed media; cask design for nuclear materials and analyses of postulated accidents in their transport; and reactor safety are some of the projects in which we are active. Problem descriptions and results from these areas will be presented.

## AN EXPERIMENTAL AND NUMERICAL ANALYSIS OF LARGE HOLES IN THIN SHELLS

by

V. Dayal, Graduate Student  
Department of Aerospace Engineering  
Texas A&M University  
College Station, TX

Prof. P. G. Hansen  
Chairman, Department of Engineering Mechanics  
University of Missouri-Rolla  
Rolla, MO

Large holes in thin shells have been analysed by Photoelastic and Finite Element methods and compared with results obtained theoretically (1) and experimentally (2) by strain gages. Photoelasticity has been used earlier (3) for curvature parameter  $\mu$  up to 2. This work extends to  $\mu = 4$ .

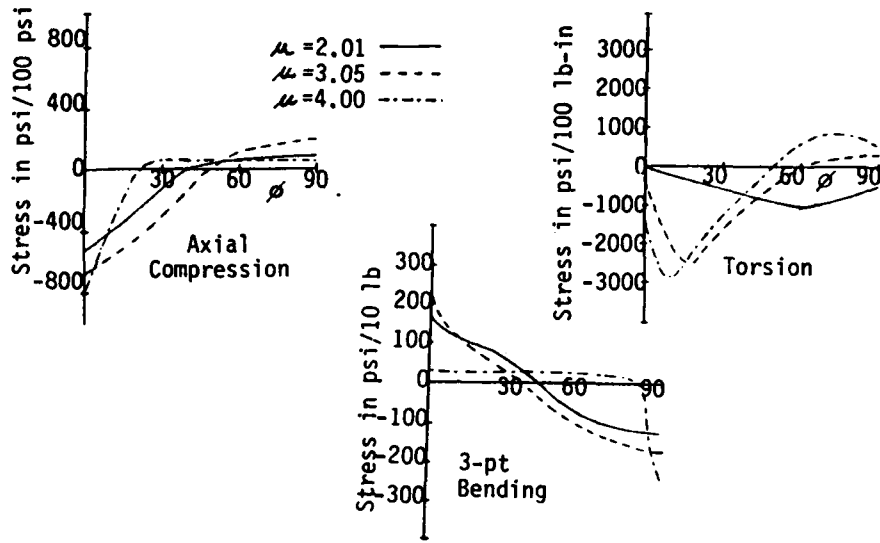
The Photoelastic model was prepared by moulding the semi-polymerized sheet. Holes were cut on high speed milling m/c. The transmission polariscope was set up to obtain stresses on one wall of the shell. Axial compression, torsion and 3-point bending loads were applied.

The Shell geometry and the FE mesh with an 8 node 40 DOF element was generated on SUPERTAB. A 4x4x2 Gauss integration scheme was used.

Membrane stresses for  $\mu = 2,3,4$  have been obtained by photoelasticity and plotted as a function of angle  $\phi$  around the hole. Stresses are evenly distributed around the hole for  $\mu = 2,3$ . When  $\mu = 4$ , i.e. the hole diameter is of the order of the shell diameter, stresses are confined to the area close to  $\phi = 0$ . Gauss point stresses have been extrapolated to the hole boundary at the stress conc. points and compared with the Stress Conc. obtained from theoretical, photoelastic and strain gage results.

## References

1. Lekerkerker, J. G., "Stress Concentration Around Circular Holes in Cylindrical Shells", Proc. Eleventh Intl. Cong. Appl. Mech., Munich, 1964, pp. 283-288.
2. Bull, J. W., "Stresses Around Large Circular Holes in Uniform Circular Shells", J. of Strain Analysis, Vol. 17, No. 1, 1982, pp. 9-12.
3. Rajaiah, K. and Durelli, A. J., "Optimization of Hole Shapes in Circular Cylindrical Shells Under Axial Tension", Exp. Mech., May 1981, pp. 201-204.



## SOME RECENT ADVANTAGES IN TURBULENT JETS

by

William K. George, Stewart J. Leib, Mark N. Glauser  
Department of Mechanical and Aerospace Engineering  
State University of New York at Buffalo

In 1971, Crow and Champagne published photographs of puff-like structures in a forced turbulent jet mixing layer. Since then there has been considerable interest in trying to objectively determine the nature of such structures, and whether in fact they exist in unforced flows (c.f. Hussain 1981).

In 1967 Lumley proposed two different, but complementary, approaches to the objective determination of coherent structures. The first uses an orthogonal decomposition to extract eigenvectors from two point velocity measurements, the lowest order eigenvector representing the largest structure. Where there are partial homogeneities, or when the flow is stationary, the eigenfunctions are the harmonic ones and the coherent features are impossible to identify. To organize these fluctuating Fourier modes into coherent features a second decomposition is used, the shot-noise decomposition.

An experimental program has been underway at the Turbulence Research Laboratory of the University at Buffalo to attempt to generate sufficient data to apply these decompositions to determine the structure of the turbulence in the jet mixing layer.

The experiment has generated cross-spectral data at seven positions across the mixing layer. The 49 cross-spectra have then been decomposed to show the time development of the streamwise velocity component of the large eddies in the mixing layer. Continuing experiments will yield information on the other components of velocity and on the streamwise and azimuthal variations of these structures.

The results to date show clearly the existence of a large scale structure in the mixing layer containing 20% of the turbulent energy. The second and third order structures contain together another 20% of the energy, the remainder being contained in structures impossible to resolve because of statistical and numerical errors.

The implications of these findings on the problem of turbulence modelling could be profound. If, in fact, the large scale features of turbulent flows can be resolved on such a coarse grid, a direct decomposition of the Navier-Stokes equation (Lumley 1980) might represent a fruitful approach. The largest eddies would be calculated directly and the remainder of the turbulence modelled in more traditional ways.

Acknowledgements

The work described above has been carried out by Mark Glauser, Stewart Leib and Muhammed S.S. Khwaja as a part of their thesis research. This research has been supported by the National Science Foundation under Contract No. ENG76-17466 and the Air Force Office of Scientific Research under Contracts No. F4962078C0047 and F4962080C0053.

References

- Crow, S.C. and Champagne, F.H, "Orderly Structure in Jet Turbulence", J. Fl. Mech., Vol. 48, Part 3, 1971, pp. 547-591.
- Hussain, A.K.M.F., "Coherent Structures and Studies of Perturbed and Unperturbed Jets", Proc. of Int. Conf. on Role of Coherent Structures in Modelling Turbulence and Mixing, Univ. Politechnic, Madrid, 1981.
- Lumley, J.L., "The Structure of Inhomogeneous Turbulent Flows", in Atmospheric Turbulence and Radio Wave Propagation (Yaglom and Tatarsky, ed.) Nauka, Moscow, 1967, pp. 166-178.
- Lumley, J.L., "Coherent Structures in Turbulence", Transition and Turbulence, Academic Press, New York, 1981, pp. 215-241.

## ENTRAINMENT IN FREE TURBULENT FLOWS

by

Rene Chevray

Dept. of Mechanical Engineering  
Columbia University

It is characteristic of turbulent flows that, unless being bounded by solid boundaries or being of infinite extent, they present zones in which nonturbulent flow becomes turbulent and perhaps also vice-versa. The manner in which entrainment occurs and where it takes place is a question which has been of much interest in recent years and one which we are addressing here.

Information on local entrainment can be obtained by studying simultaneously cine film pictures made synchronously with data collected by laser doppler velocimetry. Such experiments typically involve three distinct schemes: flow visualization, velocity measurements and synchronization. For our case, the reaction between gaseous ammonia and gaseous hydrogen chloride which produces dense white fumes of ammonium chloride was selected to study a two-dimensional shear layer. The details of this technique which has been proven useful has been described earlier<sup>1</sup>. While information on the velocity field was provided by a L.D.V., synchronization was provided by a counter the precise count of it was both displayed on the film and fed simultaneously with velocity information to the data acquisition system. The velocity of the interface was obtained by studying the history of the bounding surface from the cine film frames. In this initial region of the developing shear layer where the three dimensional disturbances do not yet play an important role, we have then obtained information about the entrainment in two dimensions. Reconstructed pictures showing at which location as well as giving the value of the entrainment are presented.

Another question of importance in the study of partially bounded or free turbulent flows is whether potential fluid can be engulfed within turbulent regions, and also if bulk disengagement of turbulent fluid into a potential region can take place. To this effect, an axisymmetric jet facility was built and a circuit developed to determine whether an electrode is electrically connected or disconnected from the surrounding fluid. By using electrically conductive salt water in one zone and de-ionized water in the other, it is possible to verify whether a genuine hole, or a truly disengaged turbulent blob, exists at the probe location. Intriguingly, bulk disengagement seems to exist while so far, no holes have been observed. This result about bulk disengagement might be surprising at first but considering that there are flows in which we have zero net entrainment (i.e. converging channel) in which the instantaneous entrainment cannot be null everywhere<sup>2</sup> it is reasonable to assume that there exist regions where turbulent fluid disengage from the main body of the turbulent fluid.

The mechanisms by which bulk disengagement occurs is described and some ideas about reentrainment of such structures are put forward. These observations and measurements will be incorporated into existing models predicting the development and further evolution of free turbulent flows.

References

1. Sherikar, S. V. and Chevray, R., "Aerosol Formation for Reacting Flow Visualization", Turbulent Shear Flows 3, Springer Verlag, 1982.
2. Townsend, A. A., Private Communication.

Acknowledgements: Support from the National Science Foundation under Grant CPE-82-19349 is gratefully acknowledged.

## TURBULENCE AMPLIFICATION IN STAGNATION FLOW

by

Willy Z. Sadeh<sup>1</sup>  
Colorado State University  
Fort Collins, Colorado 80523

Turbulent fluctuations present in flow about a body are susceptible to experiencing selective amplification as they are converged by the mean flow toward the body stagnation zone. A satisfactory explanation for the amplification of freestream turbulence and for the effect of the amplified turbulence upon the body boundary layer is offered by the vorticity-amplification theory. This theory advocates that the stretching of cross-vortex tubes in the mechanism responsible for the selective amplification at scales larger than a certain neutral scale, the emergency of a coherent substructure near the body stagnation zone, and the penetration of amplified turbulence into the body boundary layer. The basic ideas of the vorticity-amplification theory and the importance of amplification at scales larger than the neutral scale are briefly discussed.

Experimental results on the amplification of freestream turbulence in flow about (i) a circular cylinder and (ii) a symmetric airfoil at subcritical Reynolds numbers are presented. The results attest to the occurrence of amplification at scales larger than the neutral scale. Development of a coherent substructure near the stagnation zone of a circular cylinder was visualized. An aft shift up to 50 deg in the separation point and a reduction in the mean drag coefficient up to about 97 percent of its laminar counterpart were obtained for a circular cylinder as a result of the penetration of amplified turbulence into the boundary layer. A turbulent parameter and a turbulent separation parameter were advanced to identify the effect of amplified turbulence and of the background turbulence integral scale on the pressure distribution and the position of the turbulent separation angle for any given Reynolds number-background turbulence situation.

---

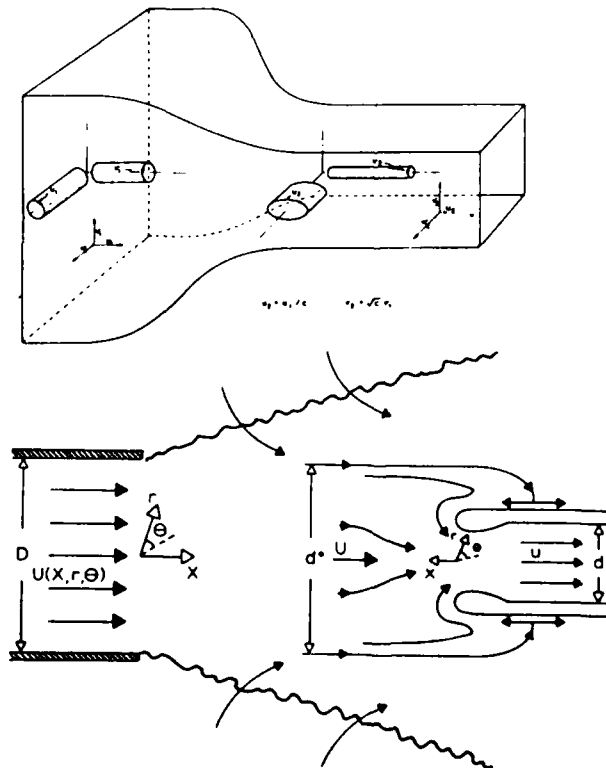
<sup>1</sup>Professor of Engineering and Fluid Mechanics, Department of Civil Engineering, Member SES.

EFFECTS OF LARGE STREAMLINE-CONTRACTION AND FINITE  
SCALE ON AMBIENT TURBULENCE

Mahinder S. Uberoi and Randall T. Nishiyama\*  
University of Colorado, Boulder, Colorado 80309

Effects of windtunnel contraction on ambient grid generated turbulence and the effect of intake flow on the ambient turbulence in the center of a large jet are experimentally compared. In the contraction the ratio of final to initial mean velocities is varied up to a value of 22 and the corresponding  $v/u=3.4$ , where  $v$  and  $u$  are the intensities of turbulence perpendicular and parallel to the mean flow respectively. In the case of the intake we have taken into account the effective size of the intake relative to the scale of the turbulence and  $v/u$  had a value of 8.5 for the final to the initial mean velocity ratio of 8.6, which is the most anisotropic turbulence measured in any reported experiment so far. The difference between the contraction and the intake can be explained in terms of the anisotropy caused by the distortion of turbulence, the equipartition of turbulent energy among the three components of the turbulent velocity, and the scale of turbulence relative to the scale of the streamline-contraction.

\*Present address: David Taylor Model Basin, Washington, D.C.



Schematics of the two experimental arrangements.

## PULSATING LAMINAR FLOW THROUGH A PIPE ORIFICE

by

E. H. Jones, Jr. and R. A. Bajura  
West Virginia University  
Mechanical and Aerospace Engineering Department  
Morgantown, WV 26506-6101

A study of laminar pulsating flow through a 45 degree bevel pipe orifice was performed using finite difference approximations to the governing stream function and vorticity transport equations. The computational scheme transformed the distance from  $(-\infty)$  to  $(+\infty)$  into the region from  $(-1)$  to  $(+1)$  for the streamwise coordinate. Solutions were obtained for orifice bore/pipe diameter ratios of 0.2 and 0.5 for bore Reynolds numbers in the range from 0.8 to 64 and Strouhal numbers from  $10^{-5}$  to  $10^2$ . Stream and vorticity function plots were generated for all cases and the time dependent discharge coefficient was computed and averaged over a cycle of pulsation. The numerical solutions agree closely with available experimental data for steady flow discharge coefficients. The results show that the effects of pulsation on the discharge coefficient can be correlated by using the product of the orifice bore Reynolds and Strouhal numbers.

EFFECT OF ALONG-STRIKE INHOMOGENEITY  
ON SURFACE STRAIN DISTRIBUTIONS

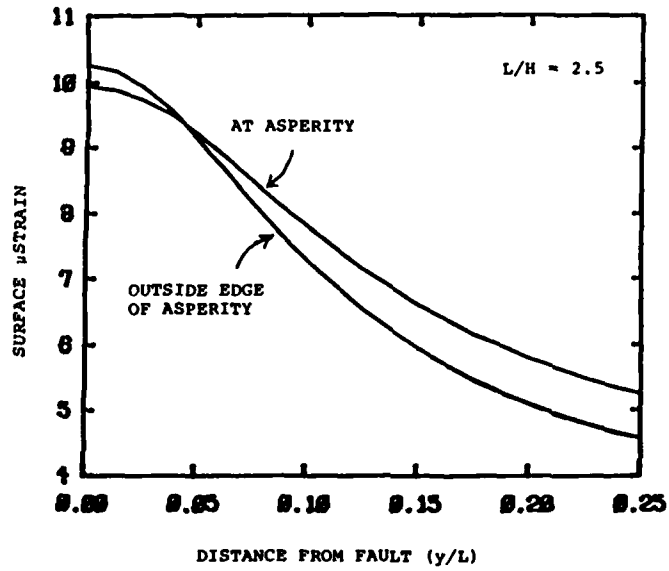
by

Victor C. Li  
Massachusetts Institute of Technology  
Department of Civil Engineering  
Cambridge, MA 02139

For a given tectonic load (such as due to relative tectonic plate movements), the surface strain near a plate boundary should be sensitive to the slip motions which depend on the material properties in the fault zone. In this paper we present a simple model of a strike slip plate boundary which emphasizes the influence of along-strike strength inhomogeneity on the surface-strain distributions. At the same time the locked upper crustal ligament (which eventually fails seismically) is also simulated by variable strength in the depthwise direction. The resulting three dimensional model is effectively treated by the line-spring technique introduced by Rice.

Along a given profile perpendicular to the fault line, we found that the surface shear strain decays away from the fault, as expected. The rate of decay, however, depends on the local fault strength (see figure below). At a zone on asperity, i.e. at higher local fault strength characterized by the magnitude of the maximum fracture energy, the shear strain close to the fault is less than that at a weaker part of the fault. This is consistent with the prediction of larger amount of slip penetration at a weaker part of the fault. The surface strain near the plate boundary is sensitive to the front of the slip zone. However at a larger distance away from the plate boundary, the surface strain is more sensitive to the overall load carrying capability. Thus at a zone of asperity, the surface strain is higher than that at a weaker part of the fault. In comparing the strain profiles for a weak and a strong part of the fault, it is seen that a reversal occurs at a distance roughly corresponding to the depth of the seismogenic zone.

The pattern of strain distribution will also depend on the strength contrast and geometry of the asperity zone. These results, together with the variation of progressive slip penetration along strike, are examined in the context of precursory seismicity patterns, and initiation of plate boundary ruptures.



Surface strain profiles at near rupture instability.

## EARTHQUAKE INSTABILITY MODEL FOR SOUTHERN CALIFORNIA

by

William D. Stuart  
U.S. Geological Survey  
Pasadena, CA 91106

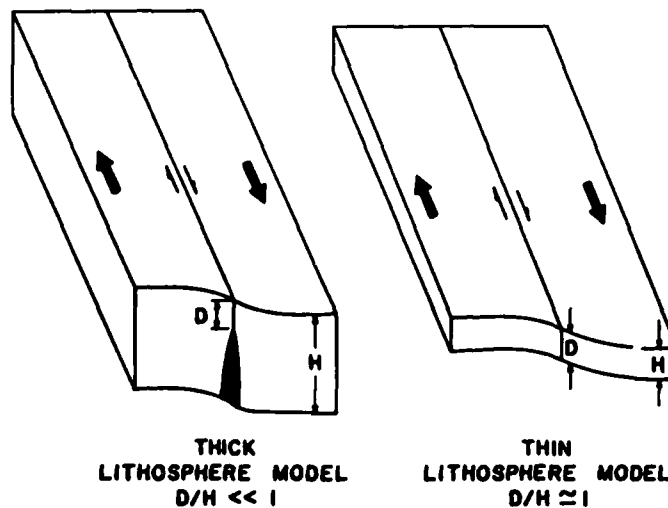
In an attempt to forecast great earthquakes in southern California, a mechanical model for unstable slippage of the San Andreas fault has been constructed. The halfspace model represents the fault zone by vertical rectangular dislocations of uniform slip, and the brittle fault properties by a slip softening law with spatially variable peak stress. Unstable slippages of one or more sections of the fault at various times correspond to historic and prehistoric earthquakes, as inferred by K. Sieh and his co-workers from stream offsets and the like, are used to constrain the variation of fault strength in the model, and thus also the parameters of future instabilities. The model is able to simulate the variation of seismic slip for the 1857 earthquake and similar earlier events, as well as the sequence of events that have ruptured the presently locked section of the San Andreas fault. As is usual for instability models, accelerated fault slip precedes instabilities.

CYCLIC DEFORMATION RELATED TO GREAT EARTHQUAKES AT  
PLATE BOUNDARIES

by

Wayne Thatcher  
U.S. Geological Survey  
Menlo Park, California 94025

Recent work in modeling the large-scale motions on major strike-slip and reverse faults is reviewed emphasizing the observational constraints supplied by geodetic survey measurements. Kinematic models of the earthquake deformation cycle (coseismic strain release due to fault slip to depth  $D$ , postseismic transient, interseismic strain accumulation) attribute interearthquake aseismic movements to episodic and steady fault slip at depth in a strong elastic plate (thick lithosphere model) or adjustments of shallow fault motions by flow in an underlying weak asthenosphere (thin lithosphere model).



At strike slip plate boundaries both models predict significant postearthquake temporal declines in shear strain rate near the fault accompanied by a progressive broadening of the zone of deformation adjacent to it. Data from the San Andreas fault demonstrate a temporal decrease in strain rate but provide only indirect support for the predicted diffusion of strain into the adjacent plate interiors. However,

postearthquake surveys are too infrequent to observe details of the postseismic transient and spatial coverage is too sparse to confirm the strain diffusion effects directly. Observational constraints at convergent (reverse faulting) plate boundaries are much better. The transient movements have two timescales. The first, of about a year or less, corresponds to deformation concentrated close to the coseismic fault. The second, longer timescale is associated with a diffusion-like spread of the deformation into the overthrust plate. The two models predict similar but not identical deformation patterns at convergent boundaries, and comparison with observations suggests the superiority of the thin lithosphere model.

AN EXPERIMENTAL CONSTITUTIVE RELATION FOR CLAYEY FAULT GOUGE,  
USEFUL FOR MODELLING EARTHQUAKE RUPTURE IN CENTRAL CALIFORNIA

by

Chi-yuen Wang and Chaw-long Chu  
University of California  
Dept. of Geology and Geophysics  
Berkeley, CA 94720

Since most shallow earthquakes occur on pre-existing fault zones, the mechanical properties of fault-zone materials are expected to be important in affecting the characteristics of earthquake-related phenomena. Recent experimental studies have shown that the characteristics of frictional sliding between rocks along a pre-cut "fault" is strongly modified by the presence of gouge materials on the sliding surface. Recent theoretical studies of faulting have also emphasized the importance of the rheological properties of fault zone materials. Since our knowledge of the constitutive relation of fault zone materials is still very incomplete, various assumptions on the constitutive relation were made in modeling fault mechanics. These assumptions include a power law between strain rate and stress, a linear viscoelastic relation, strain softening or displacement softening, strain rate softening, and velocity softening. The results of these analyses showed that the form and the spatial and temporal distributions of earthquake precursors and the onset of fault instability depend critically on the constitutive relation for the fault zone.

Inferences on the constitution of the San Andreas fault zone in central California is made based upon interpretation of existing geophysical data for the fault zone, in light of laboratory data for material properties at elevated pressures. Through this procedure we have arrived at a viable model that the San Andreas fault zone in central California throughout its seismogenic regime is composed of saturated fault gouge rich in clays. This model also appears to be compatible with our understanding of mineral stability under the probable P/T conditions and the geochemical environment along the fault zone. It implies that a model for the constitutive relation based on experimental data for clayey fault gouges is needed in order to provide better constraints on the theoretical models and to develop a strategy suitable for earthquake prediction in central California.

A constitutive relation of saturated clayey gouge samples is obtained from experimental results. These experiments were carried out at various strain rates and confining pressures, on saturated, clayey fault gouge from the San Andreas and Hayward fault zones in central California, as well as on API standard clays. This constitutive relation may be described by a spherical pore model for porous material, and may be presented in two different stress regimes:

- (1) Before yielding  $e + N \frac{\dot{e}}{e(e+1)} = A + B \log(-P_w) + C$
- (2) After yielding,  $e + N' \frac{\dot{e}}{e(e+1)} = A' \log t + B' \log(\sigma - P_w) + C'$

where  $N$ ,  $A$ ,  $\beta$ ,  $C$ , and  $N'$ ,  $A'$ ,  $B'$ ,  $C'$  are empirical constants,  $e$  the void ratio,  $\dot{e}$  the rate of change in  $e$ ,  $\tau$  the shear stress,  $\sigma$  the normal stress,  $P_w$  the pore pressure.

As a test for the above constitutive relation, samples of different thicknesses were examined under the same conditions; it was shown that this constitutive relation satisfactorily predicts the experimental results.

Microscopic examination of some sheared samples showed that the experimentally observed work-hardening may be associated with cataclastic reduction in grain size, with corresponding reduction in pore space and increase in the number of grain-to-grain contact. We suggest that these processes may also occur in natural faults and the empirical relations shown above may have potential application in modeling earthquake rupture of clay-rich fault zones.

FOUNDATION OF A LINEAR HIGH-ORDER THEORY OF ANISOTROPIC LAMINATED  
COMPOSITE SHELLS

by

Liviu Librescu  
Faculty of Engineering  
Tel-Aviv University  
Tel-Aviv, Israel

Demands for more efficient structures resisting severe and complex operational conditions as well as the advent of new exotic composite materials have created a great deal of interest for further analytical studies of anisotropic laminated composite shells. As it was conclusively shown, the classical methods of analysis based on the Love-Kirchhoff (L.K.) assumption are inapplicable in many important instances. This is especially true whenever the constituent layers of the shell structure exhibit high degrees of anisotropy in the physical and mechanical properties. Such features are typical of certain composite and refractory materials which are used with increased frequency in the various branches of the advanced technology. In such cases more refined theories are needed. They should include transverse shear and transverse normal deformations and should account for the high-order effects. The available results in this field concern principally the refined theories of flat plates. As far as the author of the paper is aware, no attempt to substantiate a general high-order theory of anisotropic multilayered shells has been given in the field literature. The present work is devoted to the substantiation of a general theory of shells of arbitrary shape which incorporates the effects of: transverse shear and transverse normal deformations; material anisotropy; structural lamination; high-order effects (including the dynamical ones); the presence of a steady temperature field. Towards this end use is made of a variational theorem of 3-D linear continuum-dynamics together with a high-order representation of the displacement field throughout the laminated thickness. This yields the appropriate dynamics field equations expressed in terms of the high-order *stress* and *strain* measures.

The problem of the necessary requirements that the theory should fulfill, as well as the one of continuity conditions at the surfaces between the contiguous layers are thoroughly investigated. Special attention is given to the formulation of some general theorems of the high-order theory of anisotropic laminated shells which have their counterparts in the 3-D theory of elastodynamics. They concern: the theorem of power and energy; the uniqueness theorem; Graffi reciprocal theorem; the principles of minimum potential energy and minimum complementary energy; the theorem of orthogonality of modes of free vibration. The problem of the applicability of the static-geometric analogy in the high-order shell theory is also envisaged in the paper.

Finally by using some of the previously mentioned results, the transient response problem of anisotropic multilayered subjected to an external forcing field of given time history is approached.

The paper represents a generalization and continuation of some previous works of the author, namely:

1. L. Librescu: Statics and Kinetic of Anisotropic and Heterogeneous Shell-type Structures, Noordhoff. Int. Publ. Chap. II., 1975.
2. M. Brull and L. Librescu, Strain measures and compatibility equations in the linear high-order shell theories, Quart. Appl. Math., April 1982, 15-25.
3. L. Librescu, Refined geometrically non-linear theories of anisotropic laminated shells, Quart. Appl. Math. (in press).

MODELING STIFFENED GRAPHITE-EPOXY COMPRESSION PANELS FOR BUCKLING  
AND POSTBUCKLING RESPONSE PREDICTION

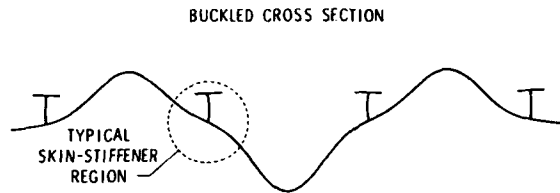
by

Norman F. Knight, Jr.  
NASA Langley Research Center  
Hampton, VA 23665

The design of stiffened panels with buckled skins is important in the aerospace industry because of the significant weight saving potential of buckled skin designs when compared with buckling resistant designs. In buckled skin designs, local skin buckling is allowed which results in additional load being transferred to the stiffeners. A study was made to identify the modeling detail required to analyze postbuckling response of stiffened panels using a nonlinear finite element structural analysis computer code called STAGS (Almroth and Brogan, 1978). The buckling load and corresponding mode shape obtained with PASCO (Anderson and Stroud, 1979), an efficient and accurate code for calculating initial buckling results, were used as standards for comparing buckling results in this study. The panel selected for this study is a flat graphite-epoxy panel with a 16-ply quasi-isotropic skin and four I-shaped stiffeners as shown in Figure 1.

The buckled cross section of the panel as determined by PASCO is shown in Figure 2a. The cross section indicates that the stiffener webs deform and that local bending occurs near the skin-stiffener interface. Several finite element models with varying levels of modeling complexity in the skin-stiffener region are shown in Figure 2b. In the analysis of stiffened panels, the traditional approach has been to model the stiffeners as discrete beams which lump stiffener properties at the stiffener attachment points. As such, the discrete beam model, denoted STAGS-1, has a larger effective stiffener spacing and neglects not only the cross sectional deformations of the stiffener but also any local bending near the skin-stiffener interface. To model the local bending near the skin-stiffener interface, a plate model, STAGS-2, of the attachment flanges is used; however, stiffener rolling is still not allowed. The next refinement, STAGS-3, treated the stiffener webs, in addition to the attachment flanges, as plate elements which then allows both local bending of the skin and cross sectional deformations of the web to be predicted accurately.

A comparison between test and nonlinear analysis results for the STAGS-3 model are shown in Figures 3 and 4. The out-of-plane deflection  $w$  normalized by skin thickness  $t$  near a buckle crest as a function of applied load  $P$  normalized by the analytical buckling load  $P_{cr}$  is shown in Figure 3. The membrane strain distribution across the skin centerbay at panel midlength for several values of the applied load is shown in Figure 4. The membrane strain  $e$  is normalized by the strain at buckling  $e_{cr}$ . The results indicate that high membrane strains and bending gradients exist at the stiffeners after skin buckling occurs which are sufficient to cause a local skin-stiffener separation and contribute to overall panel failure (Starnes, Knight and Rouse, 1982). These figures show that test and analysis results correlate very well up to failure.



(a) Buckled cross section.

Figure 2. Effect of analytical modeling detail on the buckling calculations for a specimen with a 16-ply skin and a 17.8-cm stiffener spacing.

ANALYTICAL MODEL	MODEL OF TYPICAL SKIN-STIFFENER REGION	BUCKLED CROSS SECTION OF TYPICAL SKIN-STIFFENER REGION	DEVIATION FROM PASCO BUCKLING RESULTS
PASCO			---
STAGS -1			-10.6%
STAGS -2			17.9%
STAGS -3			1.4%

□ PLATE ELEMENT    ■ BEAM ELEMENT

(b) Analytical models of the skin-stiffener region.

Figure 2. Concluded.

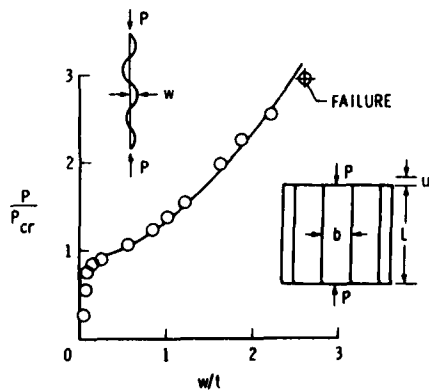


Figure 3. Out-of-plane deflection near a point of maximum buckling-mode amplitude.

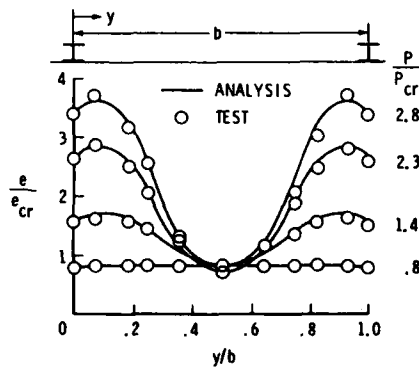


Figure 4. Longitudinal membrane strain distributions across the center bay of the specimen.

Careful attention to local modeling is required to achieve this level of accuracy in predicting panel response. An analytical effort to predict panel failure is being formulated which will include the effects of interlaminar stresses and transverse shear.

#### References

1. Almroth, B. O. and Brogan, F. A.: The STAGS Computer Code. NASA CR-2950, 1980.
2. Anderson, M. S. and Stroud, W. J.: A General Panel Sizing Computer Code and Its Application to Composite Structural Panels. AIAA Journal, Vol. 17, No. 8, August 1979, pp. 892-897.
3. Starnes, J. H., Jr., Knight, N. F., Jr. and Rouse, M.: Post-buckling Behavior of Selected Flat Stiffened Graphite-Epoxy Panels Loaded in Compression. AIAA Paper No. 82-0777, 1982.



Figure 1. Typical test specimen.

ANALYSIS OF IMPACT RESPONSE OF INITIALLY STRESSED  
AND BUCKLED COMPOSITE LAMINATES

by

J.K. Chen and C.T. Sun  
School of Aeronautics and Astronautics  
Purdue University  
West Lafayette, IN 47907

Due to the relatively poor properties of composite materials in resisting impact loads, the impact problem of composite laminated plates has received a lot of attention for the last decade. A survey of impact problems involving composite material was given by Tan and Sun [1]. Most of the impact problems were formulated for laminates which were free from stress and deformation in the initial state. In reality, static prestresses frequently arise in a manner due to manufacturing processes, assembly techniques, and operation environment such as aerodynamic loads, etc.

In the impact analysis, an accurate account of the contact behavior becomes a very important step. Recently, Yang and Sun [2] have established static contact laws which account for the permanent indentation using graphite/epoxy composite laminates and spherical steel indentors of various sizes. It was also shown that the strain responses calculated using the finite element method and these contact laws agreed with the experimental measurements quite well [1, 3]. In this study, the contact law obtained by [1] is incorporated into a finite element program for the impact analysis. The Newmark time integration scheme is used for numerical solutions.

In the numerical analysis, the effects of initial stress, impact velocity, size, and mass of the impactor on the contact force and the dynamic response of a laminate are investigated. For the initially buckled laminated plates, two static postbuckling responses of the laminates produced by uniaxial compression and shear forces, respectively, are considered. The impact response includes contact force histories, dynamic deflections, and dynamic strains in the plate for various buckling conditions. In addition, the free vibration problem of buckled laminated plates is also solved to determine the range of natural frequencies which are needed to choose a proper time interval for time integration in the impact analysis.

It is found that initial tensile stresses tend to intensify the contact force while reducing the contact time, and an opposite conclusion is obtained for initial compressive stresses. However, initial compressive stress may result in more severe dynamic response. It is also found that impact response is approximately linearly proportional to the impact velocity of the impactor. Heavier impactors not only intensify the contact force but also increase the contact time. A more severe dynamic response of the plate is also induced by a more massive impactor. It is found that the effect of geometry of the indenter on the overall impact response is not sensitive. For buckled plates, more severe postbuckling of a plate causes higher contact

force but reduces the total contact time as well as the deflection of the plate. However, since the initial stress and the stiffened bending rigidity over the plate are not uniform, no simple rules can be established for predicting the effect of preloads on the dynamic strain response in a buckled plate.

1. Tan, T.M. and Sun, C.T., "Wave Propagation in Graphite/Epoxy Laminates Due to Impact," NASA CR-168057, Dec. 1982.
2. Yang, S.H. and Sun, C.T., "Indentation Law for Composite Laminates," NASA CR-165460, July 1981.
3. Wang, T., "Dynamic Response and Damage of Hard Object Impact on a Graphite/Epoxy Laminate," Ph.D. Dissertation, Purdue University, 1982.

ON THE OPTIMIZATION OF FLUTTER  
CHARACTERISTICS OF LAMINATED ANISOTROPIC  
CYLINDRICAL SHELLS

by

Gheorghii V. Vasiliev  
Nat. Insti. of Sci. and Techn.  
Creation  
Bucharest, Roumania

The influence of different geometrical and mechanical parameters of finite length circular cylindrical multilayered and anisotropic shells on their flutter characteristics is investigated, in order to obtain the optimization of parameters taken into account.

The boundary value problem to determine the conditions of the appearance of flutter vibration concerns a four order differential equation of aeroelastic dynamic equilibrium of the shell with suitable boundary conditions on its edges. The governing equation is obtained on the base of Donnell-Vlasov technical theory and the aerodynamic load is established by the means of the piston theory.

An axial-symmetric shape of the flutter vibration is considered and its critical speed and the corresponding complex frequency are obtained by examination of the eigenvalues of the boundary problem.

A comparative analysis of the conditions for flutter type vibration appearance is made by variation of geometrical and mechanical characteristics of the shell, as :

- relative overall thickness and relative length of the shell ;
- relative layer thicknesses and ratios of their mechanical properties ;
- ratios of elastical properties of orthotropic layers ;
- specific weight of the shell.

The conclusions about the reciprocal influence and the interaction of the examined parameters as well as their influence on the overall shape of the examined multilayered anisotropic cylindrical shell and on the optimum size of its isotropic and/or orthotropic layers are given.

References

- Krumhaar H., "Supersonic flutter of a Cylindrical Shell of Finite Length in an Axisymmetrical Mode" AFOSR 1574, Cuggenheim Aeronaut. Laboratory - California Inst. of Technology Pasadena, California, 1961.
- Krumhaar H., "Supersonic flutter of Circular Cylindrical Shell of Finite Length in an Axisymmetrical Mode" Internat J. of Solids and Structures, No.1, 1965, pp. 23-57.
- Holt M., Strack S., "Supersonic Panel Flutter of a Cylindric Shell of finite Length" J. of Aero/Space Sci. No.3, 1961.
- Vasiliev G. V., "Studiul flutterului supersonic al invelitorilor cilindrice ortotrope și eterogene. Influența parametrilor constructivi și fizico-mecanici" Studii Cerc. Mec. Apl. vol.32, No.4, 1973, pp.813-849.

ON THE EFFECTS OF ENVIRONMENTAL CONDITIONING ON RESIDUAL STRESSES  
IN COMPOSITE LAMINATES

by

B. D. Harper, Assistant Professor  
Department of Engineering Mechanics  
The Ohio State University  
Columbus, OH 43210-1181

Y. Weitsman, Professor  
Mechanics and Materials Center  
Civil Engineering Department  
Texas A&M University  
College Station, TX 77843

This paper presents an experimental and theoretical investigation of moisture effects in graphite/epoxy composites. The experiments involved exposure of anti-symmetric, cross-ply laminates to various levels of fixed and fluctuating humidity and measurements of the resulting, time-dependent curvatures. Those data were compared with computed values based upon linear elasticity and linear, rheologically simple, viscoelasticity. Good agreement was noted between data and viscoelastic predictions during the moisture absorption stage from the initially dry condition. However, increasing disparity between theory and experiment developed during subsequent drying and humidity cycling conditions. This disparity is attributed to the growth of moisture-induced damage, indicating that drying and moisture cycling are more detrimental to the integrity of composites than moisture absorption, even though they may be associated with a smaller total moisture content.

## FREE EDGE STRESS REDUCTION IN A CAPPED LAMINATE

Paul R. Heyliger and J. N. Reddy  
Department of Engineering Science and Mechanics  
Virginia Polytechnic Institute and State University  
Blacksburg, VA 24061

Classical lamination theory (CLT) is typically used in the analysis of fiber reinforced composite laminates. In the plane stress state assumed in CLT, stresses that act through the thickness of the laminate are not accounted for. The occurrence of interlaminar stresses is dependent upon two conditions: the presence of a free edge and a mismatch of material properties between the layers of the laminate. Analytical and experimental studies indicate that very large interlaminar stresses exist at the free edge of symmetric laminates under uniform axial extension [1]. Such large stresses may result in delamination.

One proposed method of reducing the free edge stresses involves wrapping an additional lamina or collection of laminae around the edge of the laminate, forming a cap or shoe. The cap provides stiffness to the free edge, reducing the displacements and stresses and preventing delamination.

For a symmetric composite laminate under uniform axial extension, all stresses and strains are independent of the axial coordinate. Using the three dimensional elasticity equations, the displacements may be computed by solving a triplet of second-order, coupled partial differential equations over a two-dimensional domain. Applying symmetry considerations to the laminate facilitates the specification of the boundary conditions and reduces the problem domain to a quadrant of the laminate cross section (see Figure 1). As the three equations are not solvable by closed form methods, the finite element method can be used to obtain an approximate solution to the problem.

Analyses of symmetric composite laminates indicate that a cap greatly reduces the displacements and interlaminar stresses near the free edge of the laminate. The fiber orientation of the cap would depend upon the physical characteristics of the laminate. For instance, a laminate with large  $\tau_{xz}$  stresses near the free edge would require a cap with the fibers parallel to the axial coordinate to reduce the  $\partial u/\partial z$  component of strain. This paper discusses the parametric effects of the geometry and lamination scheme of the cap on the free edge stress distributions.

## REFERENCE

1. Pipes, R. Byron, and N. J. Pagano, "Interlaminar Stresses in Composite Laminates Under Uniform Axial Extension," J. Composite Materials, October, 1970, pp. 538-548.

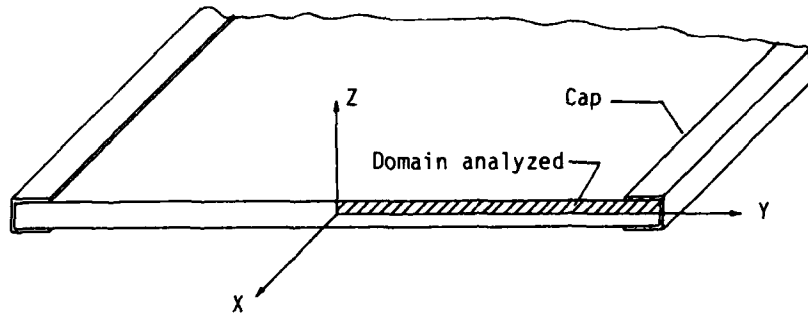


Fig. 1 Geometry and problem domain for a capped laminate

THE ROTATIONAL DYNAMICS OF  
FLEXIBLE STRUCTURES

by

John Baillieul  
Division of Applied Sciences  
Harvard University  
Cambridge, MA 02138

and

Scientific Systems, Inc.  
54 Rindge Avenue Extension  
Cambridge, MA 02140

Modeling the rotational dynamics of flexible structures involves a synthesis of ideas from the theory of elasticity and rotating rigid body dynamics. These dynamics are derived for a class of structures which we feel displays most of the important features to be encountered with any flexible structure. A qualitative theory is developed for this class of models, and the asymptotic behavior is studied in detail.

## ON DYNAMIC BIFURCATION PHENOMENA

by

K. Huseyin  
Department of Systems Design  
University of Waterloo  
Waterloo, Ontario, Canada, N2L 3G1

The method of intrinsic harmonic balancing, which was first introduced to analyze the phenomenon of Hopf bifurcation exhibited by discrete autonomous systems [1], is adopted for the analysis of other dynamic bifurcation phenomena which may arise in the study of autonomous systems. Indeed, if some of the conditions underlying Hopf bifurcation are violated, a number of distinct behaviour characteristics may be exhibited. Thus, symmetric bifurcation tangential bifurcation, cusp bifurcation, and a double-hopf bifurcation may take place depending on the way the pair of eigenvalues of the Jacobian crosses the imaginary axis and whether or not certain key coefficients vanish simultaneously at the crossing point. It is demonstrated that, unlike the phenomenon of Hopf bifurcation, in these so-called degenerate cases the existence of bifurcating family of limit cycles cannot be guaranteed. Indeed, existence conditions emerge as an integral part of the analyses, and will be outlined for each case. The asymptotic equations of the bifurcation paths, the family of limit cycles, and frequency-amplitude relationships are given in general terms which can be used in the analyses of specific problems directly.

Systems are often under the influence of more than one independent parameter, and the stability behaviour of the system as these parameters vary is of primary concern. Most of the work concerning instability of such multiple-parameter systems has been limited either to static bifurcations, characterized by a vanishing Jacobian, or linear systems. Here, the features of the post-critical oscillatory behaviour of an autonomous 2-parameter system in the vicinity of a critical point, where the real part of a pair of eigenvalues vanishes, are explored. Three distinct situations are identified, and the asymptotic equations of a behaviour-surface are derived. The analogy between this surface and the equilibrium surface associated with static bifurcations is demonstrated. In the terminology of catastrophe theory the surface obtained for a particular dynamic bifurcation phenomenon is akin to fold catastrophe. Associated limit cycles are also obtained. An illustrative example is discussed.

[1] Huseyin, K. and Atadan, A.S., "On the Analysis of Hopf Bifurcations", Int. J. Engng. Sci., 21, 1983, pp 247-262.

## MAPPINGS OF THE PLANE AND DYNAMICS

by

R. A. Broucke  
Department of Aerospace Engineering  
and Engineering Mechanics  
The University of Texas at Austin  
Austin, TX 78712

We study in detail several mappings of the plane with the purpose of comparing with the surfaces of section in Two-Degree-of-freedom Dynamical Systems. We compare the results especially from the point of view of numerical difficulties; mappings versus dynamics as well as applicability: To which extent can we apply the properties of mappings to real dynamical systems?

We mainly concentrate on the Area-preserving maps which are representative of the conservative dynamical systems. We compute the Kolmogorov Entropy and Lyapunov Characteristic Numbers both for the mappings and for the real Dynamical Systems.

We also study the phenomenon of Period Doubling and Universal Constants in the mappings, in dynamical systems (systems with a Cubic or a Quartic Potential) and in the Three-Body Problem in Celestial Mechanics.

Finally, we study some numerical methods for determining the Heteroclinic or Homoclinic points in the unstable manifold belonging to the hyperbolic field points of a mapping. A total of 10 different area-preserving mappings of the plane were investigated.

## HIERARCHIAL DYNAMIC SOLUTION STRATEGIES

by

Joseph Padovan  
Departments of Mechanical and Polymer Engineering  
University of Akron  
Akron, Ohio 44325

## ABSTRACT

In recent years, literally a multitude of transient solid, fluid and heat transfer analyses have involved some form of modelling nonlinearity. For studies employing the finite element (FE) analysis procedure, typically the governing nonlinear equations for time dependent problems are solved via either explicit or implicit type solution algorithms. Usually for problems involving only a small number of frequency spectra, implicit schemes are employed to obtain the time transient. For nonlinear situations, the equations resulting from the implicit formulation are solved via the incremental Newton Raphson scheme (INR). This follows from the fact that INR based schemes possess significant numerical capacities. For instance, the recently developed pseudo updated (BFGS) and elliptically/hyperbolically constrained INR procedures have enhanced computational efficiencies together with the ability to handle turning points as well as self-adaptively define global zones of convergence.

Regardless of such improved computational capacities, the implicit scheme solved via the INR procedure or its many variants possesses several important disadvantages, in particular: (i) The need for global level updating and assembly of the dynamic stiffness; (ii) Global level inversion or pseudo updating/inversion as in the BFGS; (iii) Awkward blocking and I/O for out of core problems; (iv) Control of individual degrees of freedom awkward; and, (v) Iterations occur on a global level hence contributing to difficulties in controlling individual degrees of freedom. For small problems, such difficulties are overcome by using the direct crunching power of main frame or mini computers with attached array processors. As simulations become large, the awkward blocking and I/O for out of core problems makes INR based implicit numerical algorithms less attractive. In this context, the development of a more efficient scheme becomes attractive.

With the foregoing in mind, the presentation will develop an alternative algorithmic formulation of the implicit scheme which possesses enhanced computational characteristics. In particular the approach taken is to generate a solution strategy which (i) Has hierarchial application levels (degree of freedom, nodal, elemental, material groups, substructural as well as global); (ii) Bypasses need for global level direct or pseudo BFGS inversion; (iii) Bypasses need for global level updating; (iv) Has an algorithmic structure enabling a simplified I/O flow for out of core problems; (v) Possesses self adaptive attributes enabling hierarchial control (locally and globally), and lastly; (vi) Provides for continuous/intermittant hierarchial updating. In the context of the foregoing comments, the presentation will give a detailed outline of the

field equations employed, the development of the hierarchical implicit algorithm as well as several dynamic benchmark examples.

## REFERENCES

Padovan, J. and Arechaga, T., "Formal Convergence Characteristics of Elliptically Constrained Incremental Newton Raphson Algorithm", International Journal of Engineering Science, Vol. 1, pp 1077, 1982.

Padovan, J. and Tovichakchaikul, S., "On the Solution of Elastic-Plastic Static and Dynamic Postbuckling Collapse of General Structures", Computers and Structures, Vol. 16, pp 199, 1983.

by

Charles W. Bert  
The University of Oklahoma  
School of Aerospace, Mechanical and Nuclear Engineering  
Norman, OK 73019

The falling-domino concept has received considerable political as well as recreational attention in the past decade or so. The problem was formally stated in 1971 by Daykin [1], and McLachlan et al. [2] presented experimental data in dimensionless form. However, to the best of the present investigator's knowledge, no analytical or numerical solution to the problem has been presented.

A row of identical dominoes standing on end on a plane is assumed to have equal spacing. The first domino in the row is given a small initial impulse, and the problem is to determine the speed at which the "falling wave" propagates along the row. Additional assumptions are that the dominoes are rigid, that there is no sliding or liftoff at the domino-table contact, and that the friction between dominoes is negligible.

The problem is solved by integrating by quadratures. The first integral is integrated exactly, and the second integral is solved numerically for the general case and in closed form for the case when certain terms are neglected. Both solutions exhibit the same trend as displayed by the aforementioned experimental results, with the numerical results being a quantitative agreement as well.

#### References

- [1] Daykin, D.E., "Falling Dominoes" (Problem), SIAM Review, Vol. 13, 1971, p. 569.
- [2] McLachlan, B.G., Beaupre, G., Cox, A.B., and Gore, L., "Falling Dominoes" (Solution), SIAM Review, Vol. 25, 1983, pp. 403-404.

A NUMERICAL ANALYTICAL APPROACH TO THE STUDY OF CHAOTIC BEHAVIOUR  
IN NONLINEAR SYSTEMS.

by

Raffaele Dragani, and Sergio Larosa  
Dipartimento di Automatica e Informatica  
Politecnico - Corso Duca degli Abruzzi, 24 - 10129 Torino - Italia

It has been discovered by Lorenz in [1] that a third order autonomous differential Eq. exhibit 'chaotic motions' associated with 'strange attractors'. An accurate analysis, with increasing attention, has been reported about the Lorenz problem by several authors (see, i.e., the papers by Ruelle [2] and Dragani-Sara [3]). Further theoretical studies have been performed and a general theory concerning the stability has been presented by Husseyn [4].

This paper has the following objectives: i) to reduce the deterministic Eqs. of the nonlinear multi-degree-of-freedom vibrating systems in the form proposed by Lorenz; ii) to present a method which allows a study of the chaotic motions; iii) to bridge some of the communication gaps that may exist between the studies in the nonlinear oscillations and in ergodic theory. Let [3]

$$M_i \ddot{q}_i + \sum_k K_{i,k} (q_i - q_k) + \phi_i(q_1, \dots, q_n) + \psi_i(\dot{q}_1, \dots, \dot{q}_n) = p_i \cos vt; \quad i, k=1, \dots, n(1)$$

be the mathematical model of a large number of nonlinear oscillators studied in the literature in recent years [5]. We reduce Eqs. (1) to

$$\dot{\underline{x}} = \underline{f}(\underline{x}; \lambda) + \underline{g}(t); \quad \underline{x}: I \rightarrow R^{2n}, \quad t \in I = (0, \infty) \quad (2)$$

where  $\lambda$  is a scalar real parameter influencing the behaviour of the system. We perform a local analysis of the system very near the critical points; the exact nonlinear system (1) can be approximated by a linear system near a critical point for identification of the nature of the critical points of the linear system. Finally we compare the results of theoretical analysis with the ones obtained by numerical analysis of Eqs. (2) using a procedure previously applied to study the periodic solutions of the nonlinear differential equation deduced in [5].

#### References

- [1] Lorenz, J. Ath. Sci., Vol. 20, 1963, p. 130.
- [2] Ruelle, Takens, Comm. Math. Phys., Vol. 20, 1977, p. 167.
- [3] Dragani, Sarra, Proc. IX Int. CANGAM, Saskatoon (Canada), 1983, p. 175.
- [4] Husseyn, Mandadi, Proc. XV IUTAM, Toronto, 1980, p. 281.
- [5] Dragani, Sarra, Mech. Res. Comm., Vol. 8, 1981, p. 23.

PERIOD DOUBLING BIFURCATIONS AND MODULATED MOTIONS  
IN FORCED MECHANICAL SYSTEMS<sup>1</sup>

by

S. Tousi, A. K. Bajaj  
School of Mechanical Engineering  
Purdue University  
West Lafayette, Indiana 47907

Weakly nonlinear and periodically forced two degrees-of-freedom mechanical systems, that exhibit internal resonance, are studied for their steady-state solutions. The two linear natural frequencies are in the ratio of 1:3 and the frequency of external excitation is close to the lower natural frequency. The nonlinearities arise only from the potential energy function and are odd in the generalized coordinates. Using the method of averaging [1], the system is transformed into a 4-dimensional autonomous system in amplitude and phase variables.

Constant solutions of the averaged system correspond, as is well known, to the steady-state periodic oscillations of the forced oscillators and these oscillations have been studied extensively [2]. For systems with internal as well as external resonance and with quadratic nonlinearities, Sethna and Bajaj [3] showed that over some interval of detuning, constant solutions of the averaged system may be unstable and this transition is by the Hopf bifurcation. Using perturbation methods they then proved that for detuning near the critical values the averaged system has a limit cycle and therefore the oscillators perform amplitude modulated motions. The frequency of amplitude modulation is much smaller than that of the main motion which occurs at the excitation frequency.

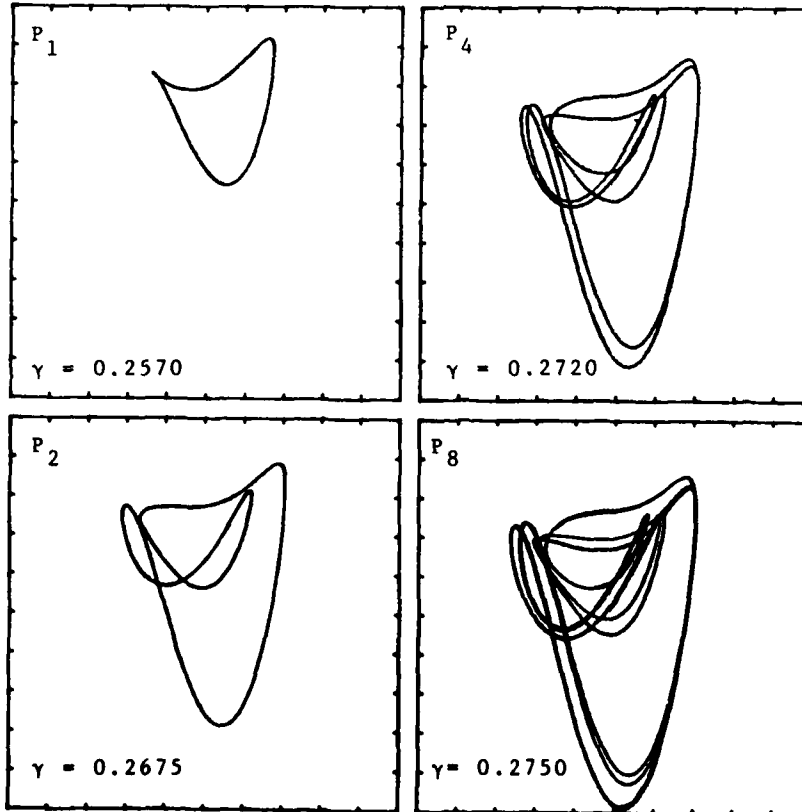
The oscillators in present work also exhibit similar behavior. It is shown that for low damping the constant solutions of the averaged system are unstable over some interval in detuning. The transition in stability is due to Hopf bifurcation. The bifurcated period solutions are constructed and their stability is analyzed via Floquet theory. This is accomplished numerically. It is seen that the periodic solutions connect the two Hopf bifurcation points in the steady state response curves. For large damping the complete upper branch of constant solutions is stable. As damping is reduced some portion of the upper branch destabilizes. Periodic solutions of the averaged system for this interval in detuning parameter are all stable. Reduction in damping results in the destabilization of these periodic solutions. This change in stability is due to one Floquet multiplier leaving the unit circle via -1 and it leads to period-doubling bifurcations [4]. Thus, there is an interval in detuning parameter over which the constant and the periodic solutions

<sup>1</sup> This work was supported by funds from the National Science Foundation under Grant MEA-8117086.

of the averaged system are unstable and the period-doubled solution is stable. Correspondingly the modulated motions of the oscillators undergo bifurcations into more complex modulations. For small enough damping there is a sequence of period-doubling bifurcations (see Figure) in the averaged system which may ultimately lead to chaotic motions [4].

References:

1. Hale, J. K., "Ordinary Differential Equations", Wiley-Interscience, New York, 1969.
2. Nayfeh, A. H., Mook, D. T., "Nonlinear Oscillations", Wiley-Interscience, New York, 1979.
3. Sethna, P. R., Bajaj, A. K., "Bifurcations in Dynamical Systems with Internal Resonance," J. Appl. Mech., Vol. 45, No. 4, 1978, pp. 895-902.
4. Guckenheimer, J., Holmes, P. J., "Nonlinear Oscillations, Dynamical Systems, and Bifurcations of Vector Fields," Springer-Verlag, New York, 1983.



AN EVALUATION OF THE GALERKIN METHOD FOR THE  
SOLUTION OF NONLINEAR WAVE PROPAGATION PROBLEMS

by

Asghar Googerdy, Dept. of Mathematics and Computer Science  
Barber-Scotia College, Concord, NC 28025

John Peddieson, Jr., Dept. of Mechanical Engineering  
Tennessee Technological U., Cookeville, TN 38505

The Galerkin method is frequently employed to solve nonlinear wave-propagation problems in finite regions. It is of interest to evaluate the accuracy of this method. In the present paper a contribution toward this goal is made by applying the Galerkin method to the problem:

$$\begin{aligned} \partial_t^2 u &= \partial_x^2 u + \epsilon \partial_x u \partial_x^2 u, \quad \epsilon \ll 1 \\ u(0,t) &= 0, \quad u(\pi,t) = 0, \quad u(x,0) = \sin(x), \quad \partial_t u(x,0) = 0 \end{aligned} \quad (1)$$

which arises, among other places, in the study of longitudinal wave propagation in an elastic bar. A trial solution of the form:

$$u(x,t) = \sum_{n=1}^N f_n(t) \sin(nx) \quad (2)$$

is employed.

This problem is a useful test case for three reasons. (a) The differential equations for the  $f_n$ 's can be obtained in a general closed form, thus facilitating the determination of the influence of  $N$ . (b) Several perturbation solutions of (1) are available for comparison. (c) Shocks in the strain  $e = \partial_x u$  and the velocity  $v = \partial_t u$  appear after a finite time, thus creating a severe test of the Galerkin method.

In order to facilitate comparison with existing perturbation solutions, the governing equations for the  $f_n$ 's are reduced to differential equations governing amplitudes and phase angles by the two-variable perturbation method. For  $N = 2$  these equations can be solved in closed form to yield the final result.

$$u(x,t) = \operatorname{sech}(ct/8) \cos(t) \sin(x) - (1/2) \tanh(ct/8) \sin(2t) \sin(2x) + \dots (3)$$

For  $N \gg 2$  the solutions are carried out numerically. Comparisons of solutions for different values of  $N$  with each other and with existing perturbation solutions reveal that a moderate value of  $N$  (8-10) is sufficient to represent the shock-formation process with reasonable accuracy.

NONLINEAR DYNAMICS OF TUBES CARRYING A PULSATILE FLOW<sup>1</sup>

by

A. K. Bajaj  
School of Mechanical Engineering  
Purdue University  
West Lafayette, Indiana 47907

The nonlinear dynamics of a cantilever tube conveying a pulsatile flow and undergoing planar motions is investigated. The system behavior depends on the flow rate, the mass ratio of the tube and the fluid, and the amplitude and the frequency of flow pulsations. The mean flow is near its critical value at which the downward vertical position of the tube gets unstable and undergoes Hopf bifurcation into a limit cycle. The pulsations in flow are assumed to be small and harmonic with frequency nearly twice that of the bifurcating limit cycle.

In a recent work [1] the author studied a similar problem of the two-segment articulated tubes system for its periodic solutions. Using the method of alternative problems he showed that, in addition to the usual pump response observed in parametrically excited systems, the articulated tubes system also has stable as well as unstable isolated solution branches. Furthermore, for some parameter combinations the stable solutions can get unstable and may then bifurcate into amplitude modulated motions.

In the present work, for mean flow near its critical value, the method of averaging is used to reduce the governing partial differential equation into a set of two first order equations. These equations govern the dynamics of the tube and depend on three parameters. They are studied for their constant and periodic solutions. Using local bifurcation theory [2] and some results from the codimension-two unfolding of singularities [2,3], a partial bifurcation set is constructed. It is shown that the averaged equations have constant as well as periodic solutions depending on the flow rate and the detuning. This implies the existence of "phase-locked" and "drift" oscillations (amplitude modulated motions) for the cantilever tube.

#### References

1. Bajaj, A. K., "Interactions Between Self and Parametrically Excited Motions in Articulated Tubes", J. Appl. Mech. (to appear) 1984.
2. Guckenheimer, J., Holmes, P. J., "Nonlinear Oscillations, Dynamical Systems, and Bifurcations of Vector Fields," Springer-Verlag, New York, 1983.
3. Carr, J., "Applications of Center Manifold Theory," Springer-Verlag, New York, 1981.

<sup>1</sup> This work was supported in part by funds from the National Science Foundation under Grant MEA-8117086.

ON THE VANISHING FIRST VARIATION  
OF A FUNCTIONAL

by

Cecil D. Bailey  
Dept. of Aero/Astro Engineering  
Ohio State University  
Columbus, OH 43210

The validity of the equation which Hamilton called the law of varying action is now recognized. As a result, it can now be shown that the "double property" as pointed out by Hamilton for his "Principle Function," was never realized because of the calculus of variations. In particular, the vanishing first variation of a functional as defined in the calculus of variations, although correct in the space domain, is shown to be in error in the time domain. Further, the validity of the requirement in the calculus of variations, that the "varied path" function,  $\eta$ , must vanish at the end points, is shown to be in error in both the space and time domains. Two separate equations, either of which represent the vanishing first variation of a functional as proposed by Euler, and thus the "double property" as predicted by Hamilton, are presented for both the space domain and the time domain.

by

Laurence I. Gould  
Department of Physics  
Temple University  
Philadelphia, PA 19122

Nonlocal (integro-differential) linear second-order equations of motion are related to their balance laws, continuity equations or conservation laws without explicitly introducing a Lagrangian. The results are relevant for physical systems whose equations of motion may be relativistic and either classical or quantum. They can facilitate obtaining global conservation laws for such quantities as energy and momentum. Applications of the formalism are given for both local and nonlocal equations of motion. They are chosen from elasticity theory and nonrelativistic quantum mechanics. The incorporation of boundary conditions is also indicated. Details will be published elsewhere<sup>2</sup>.

---

<sup>1</sup> Based on the author's Ph.D. thesis (Temple University, 1982).

<sup>2</sup> L. I. Gould, J. Math. Phys. (submitted for publication).

## THERMAL BUCKLING OF LAMINATED PLATES

by

T. R. Tauchert  
Department of Engineering Mechanics  
University of Kentucky  
Lexington, KY 40506

Buckling of homogeneous plates under in-plane thermal forces can be formulated in terms of two linear, uncoupled problems: an in-plane problem governing the membrane effects; and an eigenvalue problem for the transverse deflection, in which membrane forces are assumed fixed. In contrast, for heterogeneous plates it is generally not possible to treat the membrane and flexure problems separately, and resort to an approximate method of solution is usually necessary. A special case of interest where a closed-type solution for bifurcation buckling of an anisotropic heterogeneous plate can be established is investigated in this paper. The problem considered is that of a rectangular angle-ply laminate resting on simple supports, and subject to a uniform temperature rise. Thermoelastic buckling is analyzed using both the classical thin-plate theory, and the shear-deformation (Reissner-Mindlin) theory for moderately thick plates. Numerical examples are presented which illustrate the effects of ply-angle, number of layers, plate thickness and aspect ratio upon the thermal buckling load.

AN ACCURATE SINGULAR FINITE ELEMENT FOR  
STRESS INTENSITIES IN THERMAL PROBLEMS

by

Morris Stern  
The University of Texas at Austin  
Department of Aerospace Engineering and Engineering Mechanics  
Austin, TX 78712

In an earlier paper it was demonstrated that the use of special crack tip finite elements with a "square root of  $v$ " interpolation field could greatly reduce the requirement for a refined mesh to obtain accurate stress intensity factors due to thermal and/or mechanical loading in cracked structures. Nevertheless, it was found that the variation in the stress field as one circles the crack tip was not very well modelled by these elements. A possible reason for this behavior was conjectured to be that the dominant  $v^2$  singularity in the temperature field drives an important (for accurate modelling)  $v^{3/2}$  singularity in the displacement field which was not incorporated in the original element.

A new crack tip element with this refinement and with all the advantages of the original element family including consistency, conformability, compatibility with standard polynomial elements and availability of simple accurate quadrature formulas has been developed. There is a marked increase in the accuracy of the representation of the crack tip stress field at essentially no cost in computation time. These results are illustrated with several examples.

REFERENCE

Stern, M., "On Calculating Thermally Induced Stress Singularities". Thermal Stresses in Severe Environments, ed. D.P.H. Hasselman and R.A. Heller. Plenum Press, New York, 1980, pp. 123-134.

## THERMAL BUCKLING OF THIN CANTILEVERED PLATES

by

O. W. Dillon, Jr. and R. DeAngelis  
University of Kentucky  
Lexington, KY 40506

This is an elastic buckling analysis of a thin and wide plate subjected to temperature profiles which vary along the plate. These profiles approximate those used in the manufacturing of silicon ribbon for use as solar cells. Buckling occurs in all processes presently being investigated for their potential in mass producing silicon ribbon.

We assume the particular variation of the stress function in the width direction and thereafter the analysis is "exact". The analysis is similiar to the well known Reissner and Stein procedure for such plates.

Finite differences are used to evaluate those temperature profiles for which the assumed stress function variation is likely to be adequate.

It is found that wide plates buckle in torsion since the boundary stresses are self-equilibrated. The main result is a table of critical thickness versus plate width for the profiles considered. These agree rather well with experiments.

ANALYSIS OF THERMAL STRESSES IN A SOLID CIRCULAR CYLINDER  
SUBJECTED TO TRANSIENT CONDUCTIVE HEAT TRANSFER

J. R. Thomas, Jr., D. P. H. Hasselman,  
H. Hencke, and M. Gundappa

Departments of Mechanical and Materials Engineering  
Virginia Polytechnic Institute and State University  
Blacksburg, Virginia 24061

The literature of thermal stresses contains many studies of stresses induced by transient heating and cooling of solids in various geometries. The thermal environment in these studies is, to our knowledge, invariably described by convective or radiative heat flow boundary conditions. There are circumstances, however, in which heat flow to or from the specimen could be principally by conduction. Examples include thermal stress testing of samples in highly conductive fluids such as liquid metals, extrusion processes in which hot billets came in contact with the cooler walls of an extrusion die, and the very early stages of convective cooling before convective currents become significant.

To model this condition a study was conducted of thermal stresses in an infinitely long cylinder subjected to transient heating or cooling by sudden immersion in an infinite conductive medium, both with <sup>(1)</sup> and without <sup>(2)</sup> thermal contact resistance at the interface. The transient temperature and thermal stress distributions were derived analytically by Laplace transform solution of the relevant heat conduction equation in both media, and subsequent integration of the resulting temperature profile. The required inverse transforms were evaluated by numerical integration.

Survey calculations were performed for various conductivity ratios between the cylinder and the surroundings. The thermal stress was found to be a function principally of the volumetric heat capacity ratio and the thermal conductivity ratio. When the specimen has a high thermal conductivity relative to the surroundings, the temperatures in the cylinder were found to be quite uniform, with correspondingly small thermal stresses; conversely, low relative specimen conductivity led to steep thermal gradients and large stresses. The largest tensile stresses occur in the surface at the instant the cooling begins, and can be expressed very simply in the form

$$\sigma_{\max}^* = (N_k^{1/2} + 1)^{-1},$$

where  $N_k = \rho_1 c_1 k_1 / \rho_2 c_2 k_2$ . The maximum compressive stresses occur at the center of the cylinder some time after the initiation of the transient. Another important finding is that the maximum stress is independent of the specimen size. For convective cooling the maximum stress increases with specimen size.

If a thermal contact resistance between the cylinder and the surrounding medium is introduced in the analysis, a temperature discontinuity develops at the interface. For a given conductivity ratio, the thermal gradients in the cylinder are correspondingly smaller, leading to reduced thermal stresses.

#### References

1. Gundappa, M., J. R. Thomas, Jr., and D. P. H. Hasselman, "Analysis of Thermal Stresses in a Solid Circular Cylinder Subjected to Conductive Heat Transfer with Thermal Boundary Conductance," submitted for publication.
2. Hencke, H., J. R. Thomas, Jr., and D. P. H. Hasselman, "Role of Material Properties in the Thermal Stress Fracture of Brittle Ceramics Subjected to Conductive Heat Transfer," J. Am. Ceram. Soc. (in press).

## RESPONSE OF STRUCTURES TO LASER HEATING

by

Richard B. Hetnarski  
Rochester Institute of Technology  
Department of Mechanical Engineering  
Rochester, NY 14623

A discussion of problems related to the effects caused in structures by heating with a laser beam is presented. A survey of the literature for problems that have been solved is also given.

When the surface of an opaque material is exposed to laser radiation a number of effects occur of which only few have been analyzed in some depth. In view of the fact that only simple cases have been described analytically, some answers to most pressing questions have been received by numerical and experimental methods. But the effort should be directed to proper understanding of the nature of the effects caused by laser radiation. The problems may be approached either by the discrete, atomistic methods of analysis or by the methods of continuum mechanics. It is the latter approach that is the topic of this presentation.

Even relatively low level of laser radiation may cause high gradients of temperature in the structure. As a consequence, thermal stresses may be of such intensity that the material fails. For proper description of the effects the true spatial and temporal distribution of the power of a laser pulse should be considered; coupled theory of thermoelasticity must be employed; the variation of material and thermal parameters should be included. The problems should be considered as at least two-dimensional. If the material is not homogeneous or not isotropic additional important complications arise. Other effects include propagation of dilatational and Rayleigh waves.

The survey presents also problems related to higher level of power, when laser radiation causes chemical degradation and melting, followed by charring or by ablation; these problems are of special importance in composite materials.

## STATISTICAL FRACTURE OF BRITTLE MATERIALS UNDER THERMAL STRESS

by

A. F. Emery, C. Wallace, N. Juhlin  
Department of Mechanical Engineering  
University of Washington  
Seattle, Washington 98195

A series of tests was conducted on thin disks of alumina, 99.5% pure, 98% dense, to determine the sensitivity to thermal shock. The disks were thermally shocked, to varying degrees of shock intensity, and segregated into two classes: those that failed thermally; those that survived without apparent damage. Those that survived were subsequently tested mechanically and their fracture strength determined.

The statistical parameters of fracture, using both the Weibull and the Batdorf models, were then determined by fitting the POF data. For the mechanically tested specimens this was simple since the state of stress is easily related to the applied load. On the other hand, the stresses induced by the thermal tests must be computed by an iterative procedure using temperature dependent properties. The statistical parameters were obtained for both volume and surface flaws in virgin specimens, 4 point bend specimens, and thermally shocked specimens. The thermally shocked data indicated that two separate classes of fracture existed: a) early time failure in which the probability of failure was greater than that of the overall distribution, b) late time failure in which the POF agreed well with the statistical models. A comparison of the data suggest that at early times, the failure is primarily due to surface flaws which are subjected to high stresses. As time continues, the surface stresses diminish and the stresses in the interior increase. As a consequence, the late time failure thus appears to be more related to volume flaws.

This paper discusses the development of finite element programs to compute the thermal stresses and the associated probability of failure using the several different statistical models. These techniques are then applied to the data to gain some understanding of the failure mechanism. Speculation about the origin of failure is reinforced by SEM examination of the specimens. It appears that thermal failure can be regarded as a transient phenomena in which different flaw populations act at different times, leading to surface failure at early times, and if the material succeeds in surviving these, to volume failure at later times.

## SHAPE OPTIMIZATION OF ELASTIC STRUCTURES

by

K. K. Choi  
E. J. Haug  
Department of Mechanical Engineering  
The University of Iowa  
Iowa City, IA 52240

Recent developments in structural shape design sensitivity analysis [1,2], using the material derivative concept and variational formulation of the equations of elasticity, are employed to obtain derivatives of structural response with respect to change of the shape of an elastic structure. A derivation of the formulation is presented and demonstrated to provide accurate design sensitivity calculation for displacement response, eigenvalue response, and stress. Numerical implementation of design sensitivity analysis result is discussed using smooth boundary parameterization that are consistent with finite element numerical solution of the boundary-value problem. Design sensitivity analysis results are used with an optimization algorithm to solve example problems.

REFERENCES

1. Choi, K. K. and Haug, E. J., "Shape Design Sensitivity Analysis of Elastic Structures," J. of Struct. Mech., Vol. 11, No. 2, 1983, pp. 231-269.
2. Haug, E. J., Choi, K. K., and Komkov, V., Design Sensitivity Analysis of Structural Systems, Academic Press, to appear, 1984.

A GENERAL AUTOMATED AEROSPACE  
STRUCTURAL DESIGN TOOL

by

Erwin H. Johnson  
Northrop Corporation, Aircraft Division  
Dynamics and Loads Research Department  
Hawthorne, California 90250

D. H. Herenden  
Universal Analytics, Inc.  
7740 West Manchester Boulevard  
Playa Del Rey, California 90291

and

Vipperla B. Venkayya  
Air Force Wright Aeronautical Laboratories  
Wright-Patterson Air Force Base, Ohio 45433

An ongoing program, "Automated Strength-Aeroelastic Design of Aerospace Structures," is described whose goal is to develop an automated procedure that can assist in the preliminary design of aircraft and space structures. The program is sponsored by the Air Force Wright Aeronautical Laboratories, with Northrop Corporation as the principal contractor and Universal Analytics, Inc. as a subcontractor.

The program is motivated by considerable advances that have been made in recent years across a broad spectrum of relevant disciplines, the most notable being improved computer hardware and an improved understanding of the techniques of automated design. The project is divided into six phases: (1) system design, (2) system development, (3) engineering software development, (4) pilot code development, (5) structural design studies and (6) modeling guidelines. In the system design task, a higher order language entitled MAPOL (Matrix Programming Oriented Language) has been defined to drive the engineering software, which is written in FORTRAN 77. A unique data base combines the flexibility of a relational organization for engineering data with the efficiency of a sequential packed organization for the numerous matrices.

For the procedure to be truly useful in the preliminary design of aerospace structures, it must include all the technical disciplines which could significantly impact the design. The engineering analyses include those related to structural analysis (static, dynamic and thermal), aeroelastic analysis (static and dynamic), sensitivity analysis, optimization and control system analysis.

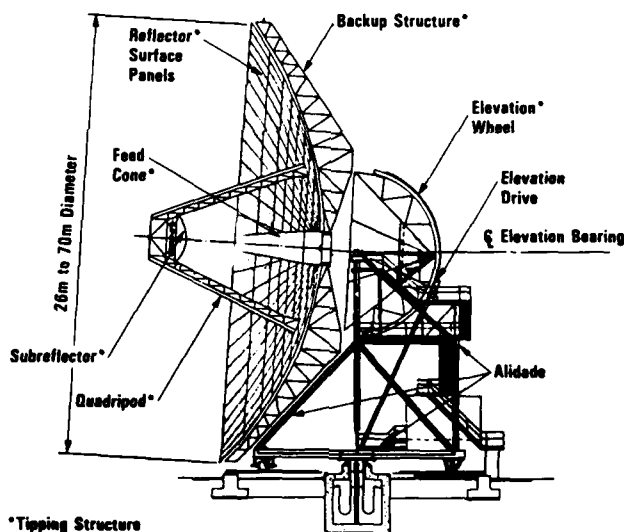
The presentation will focus on the philosophy of the system design with emphasis on the innovative features that have been developed. Limited results that have been obtained to date will also be presented to allow an assessment of the eventual utility of the final procedure.

DESIGN OPTIMIZATION OF 70M ANTENNA STRUCTURE  
WITH REFLECTIVE SYMMETRY

by

Roy Levy and Douglas Strain  
Jet Propulsion Laboratory  
Pasadena, California

Large diameter microwave antennas are complex and costly structures that are required to meet precise performance constraints under a variety of environmental loadings. The constraints relate to either the accuracy of their surfaces compared to a theoretically perfect surface or to the boresight pointing error of the microwave beam. Typical specifications for precision antenna structures with diameters of 26 to 70 meters restrict the allowable root mean square error of the surface to less than one millimeter and the error of the beam to a few seconds of arc. The figure below illustrates the principle components of a typical microwave antenna structure system in this diameter class.



The gravity and wind loading tend to be critical with respect to the performance constraints. The gravity loading depends upon the relative change in orientation of the gravity vector over the elevation angle range from horizon to zenith, and strong winds can impinge on the structure from many directions. Structural design of the tipping structure, which consists of elevation gear wheel, reflective surface panel-supporting backup structure, and subreflector-supporting quadripod, is the key to meeting the constraints. Beyond this, optimization of the tipping structure design can satisfy the constraints economically.

The objective of the tipping structure design is to optimize (minimize) the structure weight while meeting the surface accuracy and boresight pointing error constraints with the structure subject

to wind and gravity loadings. This problem is efficiently treated by optimality criteria methods that derive the design variables (areas of rod or thickness of plate finite elements of the structure model) directly from a set of Lagrange multipliers determined for the governing constraints. A separate nonlinear mathematical programming problem is solved to determine the multipliers. The solution of the optimization problem, which is nonlinear, is obtained iteratively; a trial design is analyzed to determine its performance and then redesigned to meet the constraints while optimizing the weight. The analysis-design cycles are repeated until convergence.

Processing the design optimization model imposes a significant demand upon computer resources. This demand can be reduced for large structures by modelling only one side of the tipping structure, since it is symmetrical about a vertical plane. Well known methods of reflective symmetry can be used to decompose any arbitrary loading into one symmetrical and one anti-symmetrical loading. These two loadings are applied separately to the half-structure model and the response of both sides of the structure can be synthesized from the responses to these two loads. The method for design requires that all the information for both halves of the structure be available in core simultaneously. To invoke design optimization with reflective symmetry requires a major reorganization of the software to accommodate the requirements of the design phase and to incorporate the functions of assembling the response.

A current project that consists of extending three Jet Propulsion Laboratory antennas from 64 meter to 70 meter diameters made it necessary to undertake the coding for reflective symmetry design. In this case, the 12,000 degree of freedom analysis coefficient matrix was estimated to require about 1-1/2 hours for matrix reduction at each cycle. A 5 cycle design investigation could have required about 12 hours of exclusive use of a UNIVAC 1100/80 computer. Whether or not there was enough core to handle the problem is also questionable. Processing of the half structure model required only about ten minutes for each of two matrix reductions per cycle and about 3 hours for a five cycle design.

The relative economies of reflective symmetry design increase with problem size. Conversely, since extra matrix and computer overhead operations are entailed, it may not be economical for small problems.

AN INTERACTIVE CUTTING PLANE ALGORITHM FOR  
MULTIOBJECTIVE OPTIMIZATION: APPLICATION TO URBAN RUNOFF CONTROL

by

G. V. Loganathan and Hanif D. Sherali  
Virginia Polytechnic Institute and State University  
Civil Engineering/Industrial Engineering and Operations Research  
Blacksburg, Virginia 24061

An interactive cutting plane algorithm is presented for solving multiobjective optimization problems. The multiobjective optimization problem is formulated as the constrained maximization of an implicit utility function defined over the objective functions. The principal contribution of the algorithm is that it requires only the Decision Maker's local preferences over the criterion functions (marginal rates of substitution) for the purposes of implementation. Based on this information available at a given number of points in the objective function space at any stage, a piecewise linear concave objective function is generated. A subproblem, which maximizes this function over the feasible region is then solved to obtain a new point. If a suitable termination criterion is satisfied, then this point is declared as the most preferred (or optimal) solution to the multiobjective program. Otherwise, a cutting plane is generated at this point, which essentially modifies the piecewise linear concave objective function, and the process is repeated by solving the new resulting subproblem. The optimal solutions of the subproblems are shown to be efficient solutions for the multiobjective programming problem. Furthermore, it is proven that either the algorithm terminates finitely with a best compromise solution, or else every convergent subsequence of the sequence of the subproblem solution points converges to a best compromise solution.

The algorithm is applied to the multi-faceted urban drainage management problem. The conflicting and incommensurable goals of planning land use/stormwater interface are analyzed. Each parcel of land is characterized by physical elements such as soil type and slope. In addition to the physical characteristics, man made changes like provision of transportation facilities and water supply also affect the value of land. Thus, there is a supply side characterized by the availability of service facilities in vacant land. There is also a demand side characterized by the service requirements of different land use activities. Urbanization leads to increased runoff and water pollution. A proper comprehensive land use plan must involve the interrelationships between the environment and the cost and benefits of urban development. The cutting plane algorithm is used to find the most preferred solution among the objectives: best land use plan, minimization of pollution and cost.

## SOME RECENT DEVELOPMENTS IN STRUCTURAL OPTIMIZATION

by

Niels Olhoff  
Department of Solid Mechanics  
The Technical University of Denmark, DK-2800 Lyngby  
Denmark

Abstract - This paper gives an account of recent developments within the field of optimal structural design, with the main emphasis laid on fundamental aspects. We first present a generalized variational formulation for a large class of single-criterion optimization problems with local or global design objectives. An assessment of the rapidly developing area of multicriterion optimization will then be given, and a new variational approach to this type of problem will be presented. Finally, we discuss two classes of problems for which it has recently been recognized that particularly careful formulation is required for correct optimal solution. These classes comprise, respectively, certain optimization problems involving eigenvalues, and problems concerning design of, e.g. plates, shells, and composite materials.

OPTIMIZATION OF CYLINDRICAL SHELLS  
SUBJECTED TO DESTABILIZING LOADS

by

George J. Simitzes  
Georgia Institute of Technology  
School of Engineering Science and Mechanics  
Atlanta, GA. 30332

Cylindrical shells are widely used as structural configurations in air, space surface and marine vehicles, as well as in other structures. In most such cases, they are acted upon by destabilizing loads. Instability (buckling) then, could be, and in numerous cases is, the primary consideration for design.

In several uses, especially in the aircraft and spacecraft industry, the demand for lightweight efficient structures has led the design engineer to structural optimization and/or to the use of new manmade materials with improved property characteristics and features. In all cases, the effort has been to achieve lightweight, economical, durable, easily maintained and damage tolerant structural components and configurations.

The emphasis of the present paper is to concentrate in the area of cylindrical shell configurations, which are subjected to destabilizing loads, and to touch upon the factors that affect their optimization. Moreover, a design procedure for achieving minimum weight design of eccentrically and orthogonally stiffened, metallic, imperfect, thin, cylindrical shells, which are subjected to destabilizing loads (applied either individually or in combination) is outlined. In trying to accomplish this goal, it is important to be aware of and knowledgeable in certain body of knowledge that affects the outcome. This involves certain elements which are, in many instances, interrelated, and they include: optimization procedure, failure mode interaction, imperfection sensitivity, material selection and dynamic instability. All of these elements are separately discussed and expanded. Wherever appropriate, demonstrative examples are employed.

Finally, the suggested design procedure is demonstrated through several examples of metallic structural configurations. The load conditions are uniform axial compression and uniform torque applied individually. The configurations and load conditions are typical of aircraft fuselages.

## OPTIMAL DESIGN OF STRUCTURES IN NONLINEAR RESPONSE

by

Z. Mroz

Institute of Fundamental Technological Research  
Polish Academy of Sciences  
Warsaw, Poland

M. P. Kamat

Department of Engineering Science & Mechanics  
Virginia Polytechnic Institute & State University  
Blacksburg, Virginia 24061

R. H. Plaut

Department of Civil Engineering  
Virginia Polytechnic Institute & State University  
Blacksburg, Virginia 24061

A uniform formulation of sensitivity analysis for beams and plates is presented in terms of generalized stresses and strains. Both physical and geometric nonlinearities can be treated within this formulation. Next, optimal design problems for stress and deflection constraints are formulated and the relevant optimality conditions are derived using the concept of a linear adjoint structure. Following this, several numerical solutions of optimal design problems are presented.

In the first example, a beam with clamped, immovable ends is subjected to a uniformly distributed transverse load. The material is linearly elastic, but geometric nonlinearities occur due to the stretching of the beam. For a given total volume of material, the distribution of material along the beam is determined so as to minimize a measure of the deflection. The second example also involves a clamped beam, but stretching does not occur. Instead, the nonlinearity comes from a nonlinear moment-curvature relation. The loading, design variable, and objective are the same as in the first example.

The calculus of variations is used to derive the equations governing the adjoint problem and the optimality criterion. The adjoint problem depends on the solution of the original problem, and the optimality criterion involves both original and adjoint variables in a nonlinear differential equation. An iterative procedure is applied to obtain optimal solutions. Finally, the resulting designs for the cases of geometric and physical nonlinearities are compared.

SENSITIVITY ANALYSIS OF PROBLEMS OF ELASTICITY  
WITH UNILATERAL CONSTRAINTS

by

Martin P. Bendsøe\*, Niels Olhoff\*\* and Jan Sokolowski\*\*\*

- \*) Mathematical Institute, Building 303,  
The Technical University of Denmark, DK-2800 Lyngby,  
Denmark
- \*\*\*) Dept. of Solid Mechanics, Building 404,  
The Technical University of Denmark, DK-2800 Lyngby,  
Denmark
- \*\*\*) Systems Research Institute of the Polish Academy of  
Sciences,  
ul. Newelska 6, 01-447 Warszawa, Poland

Abstract

We develop a unified approach for sensitivity analyses of unilateral problems for discrete and continuous elastic structures. Sensitivity analyses are crucial in problems of redesign or optimization of structures, and the label covers, in this paper, the problem of determining the variation of structural response subject to variations of the design, material and loading. This type of problem is inherently non-linear and non-differentiable for structures with unilateral constraints and, in general, only directional sensitivities can be obtained.

Employing modern methods of functional analysis and the principle of minimum potential energy, we establish a general result for determination of sensitivities, and the implications for discrete or discretized structures are discussed in some detail. Four example problems are covered for illustration of different aspects of the sensitivity analysis and in order to show how to handle variations of unilateral constraints.

NECESSARY CONDITIONS FOR GENERALIZED BOLZA PROBLEMS  
HAVING MULTIPOINT BOUNDARY CONDITIONS

Dean A. Carlson  
Department of Mathematics and Statistics  
University of Missouri-Rolla  
Rolla, Missouri 65401

Given real numbers  $t_0 < t_1 \dots < t_k$ , we consider the generalized Bolza problem of minimizing the functional

$$\ell(x(t_0), x(t_1), \dots, x(t_k)) + \int_{t_0}^{t_k} L(t, x(t), \dot{x}(t)) dt$$

over all absolutely continuous functions  $x: [t_0, t_k] \rightarrow E^n$  where  $\ell$  and  $L$  are given proper extended real valued functions which are locally Lipschitzian. The above formulation includes problems of optimal control having multipoint boundary conditions. Using the methods of nonsmooth analysis, initiated by Rockafellar [2] and Clarke [1], we obtain necessary conditions for optimality in the form of an Euler-Lagrange inclusion and jump conditions at the intermediate times  $t_j$ . Specifically we obtain the following theorem.

**Theorem.** Let  $t_0 < t_1 \dots < t_k$  be given, let  $\ell: E^{nk} \rightarrow E^1 \cup \{+\infty\}$  be locally Lipschitz, and let  $L: [t_0, t_1] \times E^n \times E^n \rightarrow E^1 \cup \{+\infty\}$  be measurable in  $t$  and locally Lipschitz in  $(x, \dot{x})$ . Then a necessary condition for  $x^*: [t_0, t_k] \rightarrow E^n$  to be a local optimal solution for the generalized Bolza problem is that there exists a function  $p: [t_0, t_k] \rightarrow E^n$  which is absolutely continuous on each subinterval  $[t_{j-1}, t_j]$ ;  $j = 1, 2, \dots, k$ ; such that the Euler-Lagrange inclusion

$$(\dot{p}(t), p(t)) \in \partial L(t, x(t), \dot{x}(t)) \text{ , a.e. on } [t_0, t_k]$$

and such that the jump conditions,

$$(p(t_0^+), p(t_1^+) - p(t_1^-), \dots, p(t_{k-1}^+) - p(t_{k-1}^-), -p(t_k^-)) \\ \in \partial \ell(x(t_0), x(t_1), \dots, x(t_k))$$

where  $p(t^-) = \lim_{s \rightarrow 0^-} p(t+s)$  and where  $\partial F$  denotes the generalized gradient in the sense of F. Clarke.

References.

1. F. H. Clarke, The Euler-Lagrange Differential Inclusion, J. of Differential Equations Vol. 19, (1975), pp. 80-87.
2. R. T. Rockafellar, Conjugate Duality and Optimization, Regional Conference Series in Applied Mathematics Vol. 16, SIAM Publications, Philadelphia, Pa., (1974).

A BICRITERIA APPROACH FOR SOLVING  
LINEAR BENEFIT-COST PROBLEMS

by

G. V. Loganathan  
Department of Civil Engineering  
Virginia Polytechnic Institute and State University  
Blacksburg, VA 24061

In water resources planning, benefit-cost ratio and net benefit maximization are widely used as project evaluation criteria. The linear benefit and cost functions defined over a linear constraint set of a benefit-cost ratio problem lead to a linear fractional program; the net benefit maximization problem is a linear program. In general the optimal solutions for these problems are different. Usually two different problems need be solved to find the optima. An algorithm is presented wherein both the optima can be found by solving a single parametric linear program. It is shown that one of the efficient corner points of the following bicriteria problem: (i) maximization of benefit, (ii) minimization of cost will always qualify as an optimal solution to the linear fractional program. In general a different efficient corner point will become an optimal solution for the net benefit maximization problem. The efficient extreme points of the bicriteria problem are generated by solving a parametric linear program. Since there are only a finite number of efficient extreme points, the algorithm will converge. The algorithm is applied to farm planning for optimizing benefits per man day of labor.

## ON AN ADAPTIVE MESH FINITE ELEMENT CFD ALGORITHM

by

A. J. Baker  
 University of Tennessee  
 Department of Engineering Science and Mechanics  
 Knoxville, TN 37996-2030

A penalty-Galerkin finite element algorithm for constructing semi-discrete approximate solutions to the unsteady multi-dimensional Navier-Stokes/Euler equations in generalized coordinates has been derived and evaluated [1]. Denoting the vector dependent variable set as  $q(x,t) \equiv \{\rho, \rho u, \rho e, p, \sigma\}$ , for the usual fluid mechanics definitions, the penalty-Galerkin algorithm constrains the error in the associated semi-discrete approximation  $q^h(x,t)$  in the form

$$\int_{R^n} N_k L(q^h) dx + \beta \int_{R^n} \nabla N_k L^C(q^h) dx \equiv 0 \quad (1)$$

In equation 1,  $L(\cdot)$  is the Navier-Stokes equation set,  $L^C(\cdot)$  is the substantial derivative  $\partial/\partial t + u \cdot \nabla$ , and  $N_k(\cdot)$  is the finite dimensional subspace, complete to degree  $k$  and written in the cardinal coordinate system  $\eta$ , upon which  $q^h(x,t)$  is projected.

The interpretation of the subspace  $N_k$  becomes modified in the extension to an adaptive mesh framework. In this instance, the cardinal basis elements become time-dependent, such that,

$$q^h(x,t) \equiv \int_e N_k(\eta,t)^T Q(t)_e \quad (2)$$

where the elemental column matrix  $Q(t)_e$  contains the time-dependent evaluation (solution) of  $q^h(\cdot)$  at the nodes of the discretization  $\Omega^h = \int_e \Omega_e = \int_e R_e^n \times t$ . The lead term in both  $L(\cdot)$  and  $L^C(\cdot)$  is  $\partial/\partial t$ ; hence, for an adaptive mesh

$$\frac{\partial}{\partial t} q^h(x,t) = \int_e \left[ N_k^T \frac{dQ_e}{dt} + \frac{\partial}{\partial t} N_k^T Q_e \right] \quad (3)$$

The remaining terms in both  $L(\cdot)$  and  $L^C(\cdot)$  are not formulationally affected by an adaptive mesh procedure. Considering equation 3, the first term yields the conventional mass matrix definition when inserted into the first term in equation 1, ie.,

$$\int_e \int_{R_e^n} N_k N_k^T \frac{dQ_e}{dt} dx \Rightarrow [\text{Mass}] Q' \quad (4)$$

For the second term in equation 3, the corresponding contribution to equation 1 becomes

$$\int_e \int_{R_e^n} N_k \frac{\partial}{\partial t} N_k^T Q_e dx \Rightarrow [\text{Mesh Velocity}] Q \quad (5)$$

For comparison, the second terms in both  $L(\cdot)$  and  $L^C(\cdot)$  are the non-linear fluid convection terms. Restricting attention to the first term, substitution of  $q^h$  yields

$$\int_{R_e^n} N_k u^h \cdot \nabla N^T Q_e dx \Rightarrow [\text{Fluid Velocity}] Q \quad (6)$$

Combining equations 4-6, and inferring the remaining terms in  $L(\cdot)$  and  $L^C(\cdot)$ , the penalty Galerkin adaptive mesh algorithm statement, equation 1, takes the functional form

$$[\text{Mass}] Q' + [\text{Mesh} + \text{Fluid Velocity}] Q + \dots = 0 \quad (7)$$

Therefore, the implementation of an adaptive mesh algorithm within the finite element algorithm amounts to adjustment of the matrix equivalent of the fluid convection velocity by the (Lagrangian) mesh velocity.

A one-dimensional example, for the  $k=1$  basis, serves to illustrate the formulation. The mass matrix is familiar as the assembly (S),

$$[\text{Mass}] \equiv \int_e \left( \frac{h_e}{6} \begin{bmatrix} 2 & 1 \\ 1 & 2 \end{bmatrix} \right) \quad (8)$$

where  $h_e$  is the measure (length) of the finite element domain  $R_e^1$ . The fluid convection velocity matrix is, correspondingly,

$$[\text{Fluid Velocity}] \equiv \int_e \left( \frac{1}{6} U_e^T \begin{bmatrix} -\binom{2}{1} & -\binom{1}{2} \\ \binom{2}{1} & \binom{1}{2} \end{bmatrix} \right) \quad (9)$$

where the elements of  $U_e$  contain the fluid velocity at the nodes of  $R_e^1$ . The mesh velocity matrix, equation 5, is [2],

$$[\text{Mesh Velocity}] \equiv \int_e \left( \frac{1}{6} \dot{X}_e^T \begin{bmatrix} \binom{-1}{1} & \binom{1}{-1} \\ \binom{-2}{2} & \binom{2}{-2} \end{bmatrix} \right) \quad (10)$$

where the elements of  $\dot{X}_e$  are the (Lagrangian) speed of the (x) nodal coordinates of  $R_e^1$ . Note in particular, that each element of the hypermatrix inner product in equation 10 yields the form,

$$\pm (\dot{X}_2 - \dot{X}_1)_e = \pm \frac{d}{dt} (h_e) \quad (11)$$

which is the time rate of change of the measure of  $R_e^1$ .

Numerical results will be presented documenting application of the adaptive mesh penalty Galerkin finite element algorithm to the CFD problem class.

- [1] Baker, A. J., *Finite Element Computational Fluid Mechanics*, McGraw-Hill/Hemisphere, New York, 1983.
- [2] Baker, A. J., "On Optimization Aspects of a CFD Finite Element Penalty Algorithm," in J. Whiteman (ed), *Proc. MAFELAP 1984*, Academic Press, London, in press.

ADAPTIVE REGRIDDING IN A FINITE ELEMENT METHOD  
FOR TRANSIENT REACTION-DIFFUSION PROBLEMS

by

Michael Bieterman

Division of Computer Research and Technology  
National Institute of Health, Bethesda, Maryland

Numerical methods which automatically adjust space grids to solve time-dependent partial differential equations are being developed at an ever increasing rate. We will examine several aspects of one such method, which has been analyzed, implemented in an easy to use FORTRAN package, and applied primarily to models arising in biology and physical chemistry. This method employs piecewise linear finite elements in one space dimension, implicit integration formulas in time, and various kinds of computed intermediate feedback in attempting to control the total accuracy at moderate cost. The principles highlighted here are somewhat tailored to the present problem setting and method, but they play roles in all similar methods in one and more dimensions.

APPLICATION OF THE EULERIAN-LAGRANGIAN KINEMATIC  
DESCRIPTION TO ADAPTIVE FINITE ELEMENT ANALYSIS

by

Robert B. Haber  
University of Illinois at Urbana-Champaign  
Department of Civil Engineering  
Urbana, IL 61801

The Eulerian-Lagrangian description (E.L.D.) [1] is a general, large-deformation kinematic model for solid mechanics problems. Its distinguishing feature is that both the undeformed and deformed configurations associated with a given reference volume are treated as solution variables. In the context of stiffness analysis using isoparametric finite elements, the undeformed and deformed geometries associated with each parent element are variable. Undeformed node coordinates and displacements appear in the solution vector. The material particle associated with a node and the set of material particles within an element can change during analysis.

The ability to vary continuously the undeformed geometry with the E.L.D. provides the basis for adaptive analysis methods that do not require remeshing. The E.L.D. is useful for two classes of problems requiring adaptive mesh adjustment. The first class involves conventional mixed boundary value problems in which the motivation for mesh adjustment arises from the need for improved solution accuracy. In the second class of problems, complete boundary information is not available prior to analysis. Solution of these problems requires the mesh to adjust to changing boundary information generated during analysis.

An example of the first type of problem is the determination of node positions that yield the minimum potential energy solution for a given structure and mesh topology. The problem can be solved by treating changes in node positions as a form of geometric non-linearity. Nonlinear stiffness equations derived from the principle of stationary potential energy and the E.L.D. are presented in [1]. Solution of these equations satisfies the conditions of equilibrium and mesh optimality simultaneously.

Frictional contact problems fall into the second class of adaptive analysis problems. A key part of the solution of these problems involves the identification of zones of stick, slip and separation. Since there are different boundary conditions on stress and displacement in each type of zone, it is desirable to adjust finite element meshes so that element boundaries coincide with the transitions between zones. This requires an adaptive analysis procedure since the transition locations are not known prior to analysis and can change during progressive loading. The requirement of maintaining geometric compatibility between two bodies in contact can be addressed without the use of unilateral displacement constraints by forcing the deformed coordinates of contact node pairs to coincide, while allowing the undeformed coordinates to adjust independently to satisfy the contact conditions in each zone. Application of the E.L.D. to frictional contact problems is discussed

in [2].

Crack propagation studies also constitute a form of the second class of problem, since the boundary geometry along the crack path must be determined during analysis and changes continuously. Conventional Lagrangian finite element approaches can model discrete increments of crack growth by remeshing the structure or allowing the crack to grow along existing grid lines. Continuous variations of crack length are possible with the E.L.D. by changing the undeformed coordinates of nodes along the crack without changing the mesh topology. This capability can be used to obtain explicit expressions for energy release rates corresponding to true variations of crack length [3, 4]. Continuing research involves the application of the E.L.D. to crack growth studies under static and dynamic conditions.

1. Haber, R. B., "A Mixed Eulerian-Lagrangian Displacement Model for Large-Deformation Analysis in Solid Mechanics", Comp. Methods Appl. Mech. Engng., to appear.
2. Haber, R. B. and Hariandja, B. H., "An Eulerian-Lagrangian Finite Element Approach to Large-Deformation Frictional Contact", in Advances and Trends in Structural and Solid Mechanics, A. K. Noor and J. M. Housner (eds.), Pergamon Press, (1984).
3. Haber, R. B. and Koh, H. M., "Explicit Expressions for Energy Release Rates Using Eulerian-Lagrangian Virtual Crack Extensions", Int. J. Num. Methods Engng., to appear.
4. Haber, R. B. and Koh, H. M., "An Eulerian-Lagrangian Virtual Crack Extension Method for Mixed-Mode Fracture Problems", Proc. 25th Structures, Structural Dynamics and Materials Conference, AIAA/ASME/ASCE/AHS, (May 1984).

ADAPTIVE COMPUTATION OF STRESSES  
IN PLANE ELASTICITY

by

Barna A. Szabo  
Center for Computational Mechanics  
Washington University  
St. Louis, Missouri 63130

The finite element solution minimizes the error in energy norm, however the purpose of computations is rarely, if at all, the computation of strain energy. In stress analysis for example the displacements, stresses, bending moments, stress intensity factors, stress concentration factors, natural frequencies etc. are usually of interest.

In this paper the characteristics of finite element solutions of problems in plane elasticity are examined. For this class of problems the computation of stresses, stress concentration factors and stress intensity factors is of primary importance.

It is known that in the case of the p-version the stress field exhibits strong oscillatory behavior when one or more stress singularities occur. This oscillatory behavior is closely related to the smoothness of the exact solution: The smoother the exact solution, the less pronounced are the oscillations. These oscillations are beneficial in the sense that the faster rate of convergence of the p-version in energy (as compared with the h-version based on quasiuniform meshes) is owed to the property of polynomials that they are able to oscillate with increased frequency as the polynomial degree is increased and the wavelength of oscillations decreases with distance measured from element boundaries. On the other hand, stress oscillations are confusing when stresses are of primary interest. Computational experiments have shown that the boundaries of finite elements attenuate stress oscillations. The attenuation is so substantial that with proper mesh design the error in stress maxima, outside of the immediate neighborhood of stress singularities, can be reduced to under five percent for all stress analysis problems of practical importance.

The following are the main conclusions:

1. When only stress intensity factors are of interest then the coarsest possible mesh and polynomial degree not greater than 8 are generally sufficient for the computation of stress intensity factors to within 5 percent relative error. If greater precision is desired then greater care must be exercised in mesh design: The mesh should be strongly graded toward the singularity. The quality of the approximation can be estimated by the usual extrapolation technique which provides a basis for estimating the strain energy of the exact solution. The relative errors in stress intensity factors and strain energy are approximately the same.

2. When stresses are of interest, corner singularities and notches with small corner radii should be 'isolated' by a layer of small elements and the neighborhood of corner singularities must be treated differently from the rest of the domain:

In the neighborhood of singular points (i.e. within the small elements that isolate the singularity) the stresses should be computed from the eigenfunctions of the Navier-Lame equations. This requires the computation of the stress intensity factors. The advantage is that the stress field can be visualized in the entire neighborhood. Alternatively, if stresses at a few selected points are of interest then the Babuska-Miller extraction procedure can be used.

In the neighborhood of notches with small corner radii the elements should be of about the same size as the notch radius. Elsewhere the elements can be large, provided that the aspect ratios are not excessive. The p-version is not sensitive to large aspect ratios: 20:1 is generally acceptable.

Outside of the neighborhood of singular points (and outside of the small elements that isolate them) the choice of procedure depends on the degree of precision required and whether the analysis is performed for purposes of design or design certification.

When local stress maxima are of interest and the desired degree of precision is such that 5 percent relative error is acceptable then it is possible to compute the stresses directly from the finite element solution even when the mesh is coarse, provided of course that the singularities have been isolated by small elements. Greater precision can be achieved by improved mesh design coupled with p-extension.

When stresses at specific points are of interest then local mesh refinement coupled with p-extension is generally sufficient for computing stress values to within 3 percent relative error. Alternatively, the Babuska-Miller extraction technique can be used.

3. Nearly optimal mesh design is possible on the basis of information concerning convergence in strain energy.

SELF ADAPTIVE MESH REFINEMENT FOR BOUNDARY  
ELEMENT SOLUTIONS OF LAPLACE EQUATION

Joseph J. Rencis  
Robert L. Mullen  
Department of Civil Engineering  
Case Western Reserve University  
Cleveland, Ohio 44106

A self adaptive mesh refinement technique is developed for boundary element solutions of the two dimensional Laplace equation. The method is energy based and applied on the element level to estimate the residual error associated with a mesh. The energy differential of each element provides a criteria for determining where a given mesh should be refined. This technique is used to analyze problems with and without singularities.

Furthermore, the use of adaptive refinement in conjunction with various iterative solution methods is explored. By utilizing the energy based mesh refinement strategy, the results of the previous mesh can be used to provide an excellent initial estimate for the iterative solution of the upcoming mesh. As the system is not changing dramatically from one iteration to the next, various iterative schemes appear attractive by eliminating the cost of directly solving the complete system of equations. Results for both constant and linear two dimensional isotropic elements are compared.

## NUCLEATION AND TRIGGERING OF EARTHQUAKE FAULTING

James H. Dieterich  
U.S. Geological Survey  
Menlo Park, California 94025

Laboratory study of slip on simulated faults has demonstrated the existence of time-, velocity-, and history-dependent processes that perturb sliding strength. Constitutive laws with time- and velocity dependence that employ a state-variable to represent displacement history effects reproduce the details of the experimental data and provide a framework for unifying other friction parameters including fracture energy. Such constitutive laws have been used in time- marching computations for a slider-spring approximation to earthquake slip on a fault patch. For patches much larger than a critical radius any initial stress,  $\tau_i$ , above a critical stress,  $\tau_c$ , results in accelerating slip leading to instability. Following a step in stress,  $\Delta\tau = \tau_i - \tau_c$  the logarithm of the time to instability decreases as  $\Delta\tau$  is increased. The time to unstable slip shows a direct linear scaling with the magnitude of the velocity-dependent coefficient in the constitutive law. As the velocity coefficient goes to zero there is no delay between the time the critical stress is reached and the onset of instability. If the velocity parameter for natural faults is significantly less than the laboratory derived values, then tidal triggering of earthquakes should be apparent. Using representative constitutive parameters extrapolated to conditions of natural earthquake faulting, the time delay varies from 1 to  $10^7$  seconds depending on the magnitude of  $\Delta\tau$ . Displacements during accelerating slip are proportional to the displacement weakening parameter  $d_c$ , but the duration of stable accelerating slip is independent of  $d_c$ . Unless  $d_c$  for earthquake faults in nature is significantly larger than that observed on simulated faults in the laboratory, premonitory displacements may be too small to detect directly using current strain observation methods. Estimates of fracture energy and observations of after-slip yield some evidence that  $d_c$  for earthquake faulting may be significantly larger than laboratory measurements.

AD-A171 026

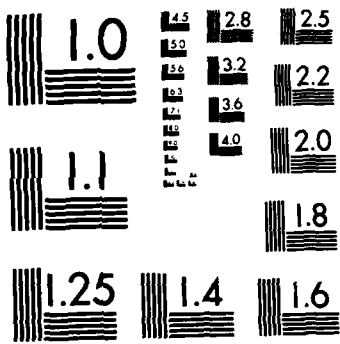
ABSTRACTS 21ST ANNUAL MEETING SOCIETY OF ENGINEERING  
SCIENCE INC OCTOBER 1-7 (1) VIRGINIA POLYTECHNIC INST  
BLACKSBURG & FREDERICK ET AL. 1984 A80-21000 EC-CF  
DAG29-84-M-0119 P/G 5/2

6/6

UNCLASSIFIED

NL

END  
DATE  
FILMED  
10-86



MICROCOPY RESOLUTION TEST CHART  
NATIONAL BUREAU OF STANDARDS-1963-A

THE EFFECT OF PRE-SLIP  
ON APPARENT SHEAR FRACTURE ENERGY

ANDY RUINA  
Theoretical and Applied Mechanics  
Cornell University  
Ithaca, NY 14853

Consideration of pre-stress, originating from pre-slip, may account for the difference between laboratory and field estimates of shear fracture energy on slipping faults.

A non-uniform distribution of pre-slip can, as does a plastic endzone, reduce the strength of the stress singularity in the elastic field near the tip of a slip zone. The effect of this reduction is best illustrated by an extreme example. A material that has finite shear strength and instantaneous slip weakening at failure has zero fracture energy. However, an appropriate non-uniform pre-slip reduces the stresses at the tip of a slip zone to a finite value, even when the macroscopic energy available for fracture appears non-zero. Thus, a material with zero fracture energy can resist the spread of an slipping zone and will, in large-scale estimates, have non-zero fracture energy.

Pre-stress can, even when the material fracture energy is zero, lead to field estimates of fracture energy as large as the product of a characteristic length and the shear strength squared divided by an elastic modulus. In the case of a slip between elastic slabs constrained by rigid boundaries the characteristic length is the thickness of the slab. In the case of a macroscopically homogeneous full space with a semi-infinite slip zone, the characteristic length is the characteristic wavelength of the previous inhomogeneous slip.

CRUSTAL EARTHQUAKE INSTABILITY IN RELATION TO THE  
DEPTH VARIATION OF FRICTIONAL SLIP PROPERTIES

by

Simon T. Tse and James R. Rice  
Division of Applied Sciences  
Harvard University  
Cambridge, MA 02138

Recent stability studies using constitutive relations of the type found by Dieterich, Ruina and others to describe frictional slip of rocks in the laboratory have provided a new explanation of the depth cut-off of shallow crustal earthquakes. The class of friction laws that we employ has the property that the sliding stress depends on normal stress, temperature, slip rate and sliding history. For sliding at a fixed slip rate  $V$  and fixed environment (e.g. normal stress, temperature, etc.), the shear strength  $\tau$  evolves towards a steady state value  $\tau^{ss}(V)$ . Stability analyses show that in a system of low enough elastic stiffness and  $d\tau^{ss}(V)/dV < 0$  (i.e. velocity weakening), steady state sliding is unstable to any perturbation. Conversely,  $d\tau^{ss}(V)/dV > 0$  (velocity strengthening) implies stable steady state sliding to small perturbation independent of the elastic stiffness. Experiments by Dieterich and by Tullis and Weeks on Westerly granite with mature sliding surfaces indicate that  $d\tau^{ss}(V)/dV$  is negative at room temperature, whereas higher temperature experiments by Stesky show that  $d\tau^{ss}(V)/dV$  turns positive above approximately  $300^{\circ}\text{C}$ . Therefore, in the case of the Earth, where temperature increases with depth, the above observations seem to suggest that the depth cut-off of crustal earthquake activity can be understood in terms of the variation of the frictional response with depth, from a regime with  $d\tau^{ss}(V)/dV < 0$  to one with  $d\tau^{ss}(V)/dV > 0$ .

Following Mavko, a two dimensional quasi-static strike-slip fault model is analysed, but using different numerical procedures and depth variation of frictional properties. The frictional properties used here are based on the laboratory data mentioned above and the Lachenbruch-Sass depth variation of temperature for the San Andreas fault. The model is able to simulate many seismological features such as the confinement of crustal earthquakes to shallow depths, the development of locked patches, the recurrence time for the seismic cycle, the seismic stress drop and displacement, etc. In dealing numerically with coseismic motion, a limiting slip speed is imposed. The validity of this assumption is examined for simpler single degree of freedom slip systems.

SURFACE DEFORMATION AND THE EARTHQUAKE CYCLE  
IN THE IMPERIAL VALLEY, CALIFORNIA AND THE ANDEAN  
BACK-ARC, WESTERN ARGENTINA

by

Robert Reilinger  
Air Force Geophysics Lab  
Hanscom Air Force Base, MA 01731

and

Department of Earth, Atmospheric and Planetary Sciences  
Massachusetts Institute of Technology  
Cambridge, MA 02139

The spatial and temporal patterns of surface deformation as delineated by repeated geodetic measurements provide information on the processes of strain build up and release along earthquake faults. Particularly detailed observations are available for a system of en echelon, strike-slip faults in the Imperial Valley, California and for a high angle thrust fault in the Sierras Pampeanas of western Argentina. In the Imperial Valley, the geodetic observations include co-seismic deformation for the 1940,  $M \sim 7.1$  earthquake and span the full interseismic period between the 1940 and 1979 Imperial Valley earthquakes. Vertical and horizontal deformations in the Imperial Valley suggest a simple scenario consisting of large co-seismic, right-lateral, strike-slip on the southern part of the Imperial fault which transferred stress to the northern part of the Imperial fault and the Brawley fault (en echelon fault north-east of the Imperial fault). While some of this stress was released during the post-seismic period by aseismic creep, the overall shallow slip (co-seismic plus post-seismic) was apparently larger on the southern part of the Imperial fault than on the northern part of this fault or on the Brawley fault. The 1979,  $M \sim 6.6$  earthquake may have eliminated some of this difference in shallow slip.

Repeated leveling measurements in western Argentina are used to constrain models of pre-, co-, and post-seismic faulting associated with the 1977,  $M \sim 7.4$  San Juan earthquake. The co-seismic pattern of uplift ( $\sim 1$  m) in conjunction with seismic observations suggest 4 m of slip on a N-S trending, west dipping ( $35^\circ$ ) fault at a depth of 17 km. There is some evidence that slip occurred on the deeper part of this fault prior to the earthquake (possibly induced by an earthquake in 1944) and that slip propagated up-dip during the post-seismic period. The observed deformation, together with simple geological observations, suggest a recurrence time for earthquakes of this magnitude on this fault of about 1000 years and average shortening rates over the past 5 MY of about 1 cm/yr across this portion of the Andean back-arc region.

by

G. B. McFadden and S. R. Coriell  
National Bureau of Standards  
Washington, D.C. 20234

During directional solidification of a binary alloy, a planar crystal-melt interface may become unstable and develop into a cellular non-planar interface, exhibiting periodic structure transverse to the growth direction.

We report here steady state two-dimensional cellular shapes calculated by finite difference techniques. We assume that the thermal properties of the melt and crystal are identical and that the cells are periodic and two dimensional. For a specified interface shape, we solve the partial differential equations for temperature in the crystal and melt and for solute concentration in the melt. The solutions are constructed such that all boundary conditions except the Gibbs-Thomson equation are satisfied. The Gibbs-Thomson equation is then used in an iterative fashion to find the correct interface shape. An artificial time dependence is introduced which accelerates the convergence of the iterative scheme.

Numerical results have been obtained for an aluminum alloy containing silver for solidification velocities of 0.01 and 1.0 cm/s, which correspond to the constitutional supercooling and absolute stability regimes, respectively.

---

\*This work was supported by the Defense Advanced Research Projects Agency.

THE STEFAN PROBLEM WITH IMPURITIES:  
AN ENTHALPY FORMULATION

by

R. E. White  
Department of Mathematics  
North Carolina State University  
Raleigh, North Carolina 27645-8205

A generalization of L. I. Rubinstein's model for dilute binary alloys is presented. The present model also generalizes the enthalpy formulation of the pure Stefan problem. It has several capabilities: it can (1) implicitly track, in 1, 2 or 3 space dimensions, the solid-liquid interface, (2) be given a careful mathematical analysis, and (3) account for certain types of "mushy" regions. However, the present version does not attempt to model supercooling, surface tension effects, or dendrite growth. The numerical method of semi-implicit time discretization and the Galerkin finite element method for the space variables will be described. An algorithm for approximating the solution of the resulting non-linear algebraic system will be given.

PATTERN FORMATION IN CONVECTION LAYERS AND  
ON SOLIDIFICATION INTERFACES

by

David J. Wollkind  
Department of Applied Mathematics  
Washington State University  
Pullman, WA 99164-2930

A comparison is made between the rolls and convection cells characteristic of free-surface flow in thin viscous layers (of gases and liquids) and the bands and hexagonal structures (nodes and cells) observed during the plane front solidification of dilute binary alloys with an emphasis on the geometry of these patterns. In particular, the long-time behavior of the relevant critical points of the appropriate six-disturbance amplitude equations characteristic of the nonlinear stability analyses of the respective governing systems are interpreted with the aid of group representation and bifurcation theory in regard to rotational symmetry, translational invariance, and orbital stability of patterns. Further, the differences between the results of these two analyses are exploited to help explain why the alloy problem gives rise to dendritic growth which has no analog for convection while the convective one can exhibit a transition to turbulence which does not occur during solidification.

## HETEROGENEOUS FREEZING AND THAWING OF AQUEOUS SOLUTIONS

by

Ronald L. Levin  
Biomedical Engineering & Instrumentation Branch  
Division of Research Services  
National Institutes of Health  
Bethesda, Maryland 20205

Most analyses of solidification and melting phenomena deal with either pure substances or multicomponent solutions in which the liquid-solid interface is assumed to be planar. Unfortunately, due to the ability of the ice phase to virtually exclude all solutes above the eutectic temperature and the relatively low mass diffusivity of aqueous solution systems, the liquid regions adjacent to the interface of such systems become "constitutionally supercooled". Under these conditions, planar liquid-solid interfaces are less stable than higher order dendritic structures. The purpose of the present study is therefore to present a model for the "heterogeneous" freezing and thawing of simple aqueous solutions which is not limited by the questionable assumption of a single, planar liquid-solid interface not encumbered by the mathematical complexities associated with geometrically more complicated dendritic structures. Consequently, by assuming that the solid and liquid regions of the system are in local thermodynamic equilibrium at all times during cooling and warming and that the total mass, but not volume, of the system is fixed, a single nonlinear parabolic partial differential equation is derived to describe the simultaneous transport of heat and mass. Our analysis indicates that the main temperature "wave" is accompanied by a subsidiary, weak solute diffusion "wave" even under conditions where there is no flow of solute or solvent into or out of the system. Furthermore, as expected, numerical solution of our transport expressions for the case of a finite domain, symmetric system which is being cooled or warmed at a constant rate shows that the extent of the transient nonuniformity in the temperature, ice volume fraction and osmolality (moles solute per unit volume water) fields increases with the magnitude of the cooling/warming rate and that the response of a partially frozen system to warming is not the "mirror image" of the response of an unfrozen system to cooling.

by

V. Alexiades, D. G. Wilson and A. Solomon  
Oak Ridge National Laboratory  
Oak Ridge, Tennessee 37830

A macroscopic mathematical model describing the idealized solidification of a mixture or binary alloy is presented. The formulation is global in the form of a pair of conservation laws for mass and energy which are valid over the entire region occupied by the solidifying material. This approach generalizes the idea of coupling the separate equations for the diffusion of temperature and material. The problem is formulated in a weak or distributional sense. It is not required to explicitly track the interfacial region which may develop into a "mushy zone". Both problem formulation and numerical results are discussed.

by

A. Solomon, V. Alexiades and D. G. Wilson  
Oak Ridge National Laboratory  
Oak Ridge, Tennessee 37830

The heat equation formulation of heat transfer in a solidifying material suffers from the problem that it predicts an infinite speed of propagation of heat. In recent years this problem has assumed increasing importance with the greater appearance of "intense" processes involving large temperature gradients and heat input rates. An alternative formulation of heat transfer via the use of the telegraphers equation has been suggested in recent years. In this paper we discuss its use when coupled with a phase change process, indicating a variety of numerical and theoretical problems that are at present unresolved. We also discuss some aspects of solidification of a supercooled melt and binary alloy which are related to this formulation.

NUMERICAL AND EXPERIMENTAL STUDY OF INWARD  
SOLIDIFICATION OF SPHERES

BY

Luiz F. Milanez and Kamal A.R. Ismail  
UNICAMP  
13100 Campinas - S. Paulo, Brazil

The main objective of this study is to analyse theoretically and experimentally the solidification process in spherical geometry. This analysis is carried out in terms of interface position with respect to time, velocity of solidification front and temperature profile. A numerical method of moving mesh is applied to obtain solution to the problem. Calculations are done for Biot number ranging from 1 to  $\infty$  and stefan number ranging from 0.1 to 3.0.

In order to verify the numerical calculations and evaluate the numerical method an experimental rig is designed, constructed and instrumented. Movements of the solidification front are measured using dipstick and thermocouple technique. Lead and tin are used as phase change material. The experiments carried out used both water and air as cooling fluids. The experimental procedure covered a range of Biot number varying from 0.36 to 4.2. Comparison between numerical and experimental results showed good agreement.

REFERENCES

Murray, W.D. & Landis, F., "Numerical and Machine Solutions of Transient Heat Conduction Problems Involving Melting or Freezing," Journal of Heat Transfer, Trans. ASME, pp. 106-112, 1959.

A STUDY OF THE COMBUSTION OF SINGLE FIRES  
AIMING AT A BETTER KNOWLEDGE OF ACCIDENTAL FIRES

M. Lebey

Departement of Energetics, E.N.S. Arts et Métiers  
151 Bd de l'Hopital, 75 640 Paris CEDEX 13, FRANCE

Ph. Arquès

University of Valenciennes and Hainaut Cambresis  
59 326 Valenciennes CECEX, FRANCE

Fire is one of the natural or accidental calamities that men can only control through constant research of better safety standards. The continuous evolution of these standards connected with the development of industrial civilization allows to set more and more precise security rules for individuals and collectivities. The three principal aims of these rules are as follows: 1) reduce fire hazards, 2) increase the means of detection and of analysis of fires, 3) limit the spread of combustion once a fire has started.

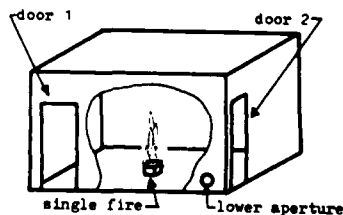


Fig.1 : experimental disposition

Considering the scarcity of physical and thermal data which would allow the determination of combustion rates, we chose to try to improve the methods of analysis applied to fires by studying the evolution of the combustion of single fires. We showed through experimentation that the semi-empirical relation established by Vibe which describes the evolution of the combustion in closed enclosures, also permits to describe the

evolution of single fires under constant pressure conditions (fig. 1). This relation which gives the evolution of burnt mass of fuel  $M_b(t)$  as a function of time  $t$  (fig. 2) is written as :

$$M_b(t) = M_{ic} \left( 1 - \exp\left(-\frac{k}{m+1} \cdot t^{m+1}\right) \right) \quad (1)$$

where  $M_{ic}$  is the initial mass of fuel,  $m$  is an exponent of the characteristics of combustion,  $k$  is a proportionality coefficient. The relation (1) describes the evolution of various single fires with given values of exponent  $m$  and of the proportionality coefficient  $k$ .

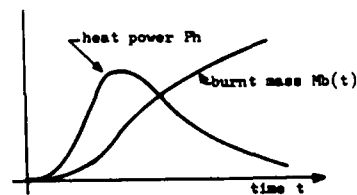


Fig.2 : evolution of the burnt mass  $M_b(t)$  and of the heat power  $Ph$

In the first part of our analysis we made evident the main parameters which govern the values of exponent  $m$  and of the coefficient  $k$  in wood crib fires developing in semi-confined enclosures (situation shown in fig.1, with only the lower aperture open). Each wood crib was assembled from oak sticks of  $40 \times 27 \text{ mm}^2$  cross section, the length of sticks depending on the wood crib sizes. The total initial mass of the wood crib varied from 1.6kg to 18kg. Each crib was ignited locally with  $40 \text{ cm}^3$  of alcohol in 15 mm deep steel pan located under the crib. We pointed out in the adopted experimental disposition the existence of a critical initial mass of fuel  $M_c$ , such that if the initial mass  $M_{if}$  of fuel is less than  $M_c$ , the combustion is always a complete one. If, on the contrary, the initial mass  $M_{if}$  is greater than the initial mass  $M_c$ , the combustion becomes incomplete at the point where the burnt mass value  $M_b(t)$  becomes greater than  $M_c$  (in all our experiments

the critical mass  $M_c$  had a value of 6.9kg). For all experiments, the first part of our analysis concerns solely the periods of time during which the combustion is complete ( $M_b(t) \leq M_c$ ). This analysis showed that the value of the exponent  $m$  and of the coefficient  $k$  are functions of the initial richness  $R_i$  which we defined for each experiment as the ratio of the initial mass of fuel  $M_{if}$  to the critical mass  $M_c$  ( $R_i = M_{if}/M_c$ ). The corresponding functions (fig.3) are as follows:

$$m = 0.11 R_i + 0.8 \quad k = 1.75 (R_i - 0.2)^{-0.72}$$

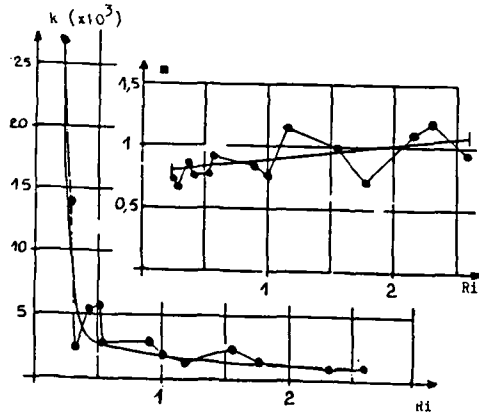


Fig.3: values of the exponent  $m$  and of the coefficient  $k$  as functions of the initial richness  $R_i$

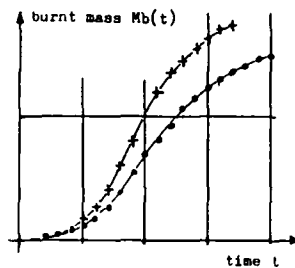


Fig.4: comparison between the evolution of two same wood crib fires : one (+) located in an open space and the other (\*) located in an enclosure.

In the second part of our analysis we showed that in the relation (1) the parameters  $m$  and  $k$  are characteristics of the evolution of combustion of single wood crib fires located in given situations. Thus, (fig.4) for two identical wood crib fires, it was observed : 1) that the maximum of the heat power is attained sooner and 2) the total duration of the combustion is shorter for the fire located in an open space than for the fire placed in an enclosure with one aperture kept open. This type of comparison shows: 1) that the sooner the maximum of heat power is attained, the higher is the value of the exponent  $m$ , 2) that the shorter the duration of the total combustion, the higher is the value of the coefficient  $k$ . Due to the multiplicity of conditions, no analytical relation could be established as yet between the values of  $m$  and  $k$  and the forms of the enclosures where the wood crib fires were studied.

The derived function of the relation (1) and the physical and thermal characteristics of the fuel concerned give the expression of the evolution of the heat power  $Ph$  as a function of time:  $Ph = H \cdot dM_b(t)/dt$ , where  $H$  stands for the heat of combustion of the fuel. The velocity of the spreading of combustion in fires depends on the magnitude of the heat power  $Ph$ .

AN ORIGINAL APPLICATION OF ELECTROMAGNETIC SHAPING:  
AMORPHOUS METAL ELABORATION

by

R. De Framond, M. Garnier, Gis Madylam, I.M.G.  
Domaine Universitaire BP 68  
38402 Saint Martin D'Herès, France

The famous properties of the metallic glasses give them lots of metallurgical applications. To have in the solid state the same structure as in the liquid state, these metals must undergo a very quick tempering ( $10^6$  K/s), which is the difficulty of such an elaboration. This operation is made by pouring the liquid metal on a moving water-cooled surface, ejecting immediately the tempered alloy with high speed. The quality of such a process depends on the puddle nature on the water-cooled surface, and on the stability of a liquid metal jet flowing through a characteristic alternating magnetic field.

The pulsation  $\omega$  being very high, the irrotational forces are very important compared with the rotational forces and are able to contain or shape a molten alloy. Concerning this shaping, we study three theoretical problems: a free-boundary problem for the liquid metal surface: the latter depends on the magnetic field which depends itself on the surface geometry; an electromagnetic problem for the inductors; a stability problem for the liquid metal.

One calculates the equilibrium shape of the metallic jet from two hypothesis: bi-dimensional geometry and negligible magnetic skin depth. The equilibrium of the free surface results from the competition between the electromagnetic and the superficial tension forces. The method consists in minimizing the E total energy of the system. The problem being bi-dimensional, the variational method of minimization of the energy function is defined in relation to  $\Omega$  geometric areas which are introduced from a series of conformal transformations.

In the linear analysis, one shows that the magnetic field is of the same effect as the surface tension in the case of a plane geometry, that is to say, a stabilizing effect. The stabilization is more important for a high  $\omega$ , pulsation of the inducting currents and when the angle between the U velocity vector of the fluid and the B magnetic field vector is close to zero.

At least one studies the internal fluid motion of the metallic fluid inside the melt crucible to perform the latter in view to minimize the perturbations created by the electromagnetic melting process.

An experimental apparatus has been fitted up with a mercury circuit converging to a measure center. In the latter, the metallic fluid flows by gravity from a nozzle as one of several stable circular jets. It falls through an alternating magnetic field created by inductor which, in conjunction with a capacitor battery in parallel, are crossed by high frequency (250 kHz) alternating currents leading to an electromagnetic skin depth inside the metal of about 1 mm. A

water cooled circuit is used to eliminate heat dissipation. With this apparatus are studied the shaping of the liquid metal ribbon, the stability, and the evolution of forced-perturbations for different frequencies (stroboscope, high-speed camera). Similar studies are made - for the stability experiments - with an apparatus for amorphisation of flow temperature alloys. The stabilizing effect of the magnetic field is experimentally observed: the length where the metal strip is stable is increased before breaking into small unstable jets.

#### REFERENCES

- [1] Brancher, J. P., Etay, J., Sero Guillaume, O., "Formage d'une lame metallique liquide: calculs et experiences", J. Mec. Th. et Appl., 1984.
- [2] Sneyd, A. D., Moffatt, M. K., "Fluid Dynamical Aspects of the Levitation Melting Process", J. of Fluid Mech., Vol. 117, 1982.
- [3] Casanova, P., Joud, J. C., Senillou, C., Yavari, A. R., "Elaboration de Rubans Larges de Verres Metalliques", Les Memoires Scientificques de la Revue de Metallurgie, 1984.

ANALYSIS OF REFRIGERANT MIXTURES CYCLES  
FOR SHIPBOARD APPLICATIONS

by

B.C. Hwang  
Naval Ship Research and Development Center

R.W. Murphy and W.L. Jackson  
Oakridge National Laboratory

C. Wu  
United States Naval Academy

A consistent thermodynamic methodology was developed for mixed-refrigerant cycle analysis. When applied to a simple refrigeration problem, the methodology indicated that cycle coefficient of performance could be increased by up to 9% by changing the working fluid from pure R-114 to the optimum R-12/R-114 mixture. When applied, along with a trial heat transfer algorithm, to an existing Navy shipboard heat pump model, the same method showed a 17% increase in equipment capacity for space cooling when the working fluid changed from pure R-114 to a mixture of 20% R-12 and 80% R-114. These examples indicate that refrigerant mixtures offer the potential for (1) reduced energy use and/or (2) increased capacity for equipment in situations of interest to the Navy. However, appropriate experimental data, especially in the heat transfer area, are required to reduce analysis uncertainty so as to more accurately quantify potential benefits.

THE APPLICATION OF QUICK-RETURN MECHANISMS  
TO RECIPROCATING COMPRESSORS

by

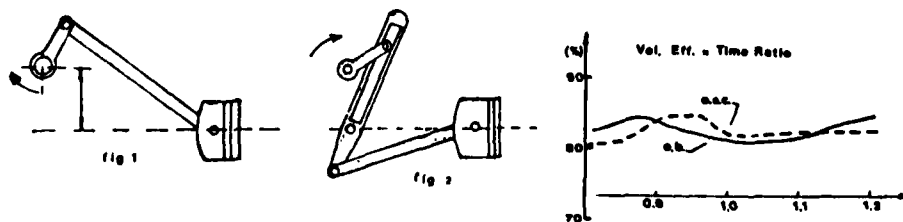
R. B. dos Santos & J. A. R. Parise  
Pontificia Universidade Catolice do Rio de Janeiro  
Department of Mechanical Engineering  
22453 Rio de Janeiro, Brazil

Volumetric efficiency is one of the most important aspects of reciprocating compressor performance. It is basically affected by the clearance volume and the pressure drop across valve passages.

The present paper studies how volumetric efficiency is affected when the traditional slider-crank mechanism is substituted by quick-return mechanisms. These are characterized by unsymmetrical ascending and descending piston velocities. This implies in lower gas velocities through either the suction or discharge valve, with consequent reduction of pressure drop. A computer program [1] was employed to simulate the performance of a reciprocating compressor driven through: an off-set slider-crank (Fig. 1) and an oscillating beam mechanism (Fig. 2).

Predicted values for the volumetric efficiency were obtained for a number of suction to discharge time ratios (Fig. 3). For moderate time ratios best results were obtained for longer discharge periods ( $t_s/t_d < 1$ ). However, the oscillating beam mechanism presented a sensible improvement in volumetric efficiency for very long suction periods. It is shown that the practical feasibility of this mechanism increases with the time ratio. In practice, at high speeds, inertia forces and vibration may become a problem.

- [1] Cartwright, W. G. and Parise, J. A. R., "Simulation of a Refrigeration Multi-Cylinder Single Stage Reciprocating Compressor", Proc. Sixth Brazilian Congress Mech. Eng., Rio de Janeiro, 1981, pp. 363-372.



CHOICE OF WORKING FLUIDS FOR MIXED-REFRIGERANTS  
LOW TEMPERATURE ENERGY CONVERSION APPLICATIONS

by

Professor C. Wu  
United States Naval Academy  
Department of Mechanical Engineering  
Annapolis, MD 21402

Mixed-refrigerants air conditioning, refrigerator and heat pump are potential energy conversion devices of removing heat from a cold space or supplying heat to a relative low temperature space. Desirable mixed-refrigerants should possess physical, thermodynamic, and chemical properties which permit their efficient operation in air conditioning systems. In addition to economical considerations, there should be no danger to health in case of their escape due to leaks or other causes in an air conditioning system. These physical, thermodynamic, chemical, economical, safety and specific properties are listed and discussed in this paper.

## FLAME RESPONSE TO A SOUND WAVE

by

Luiz F. Milanez

UNICAMP

Department of Mechanical Engineering

13100 Campinas - S. Paulo, Brazil

Combustion oscillations are generally produced by interactions between flame fronts and sound waves set up in the combustion chamber and in the supply line. In this research a simple premixed methane-air flame is used and the oscillations are produced by means of a loud speaker in the mixture supply tube, and the flame oscillations are studied by various means including photography, stroboscopic techniques and sound pressure level measurements. The objective is to study the magnitude and phase of the flame oscillations as the frequency and amplitude of the supply oscillations are varied. From these results the time between discharge of the fuel and its burning can be evaluated.

Frequencies ranging from 25 to 100 Hz were studied for different methane-air ratios with emphasis on stoichiometric mixture. It was found that the position of greatest flame front area does not correspond to the maximum outward mass flow. That is, there is a phase difference between the velocity maximum and the maximum flame front area, and this difference tends to increase with frequency. The time lag determined experimentally was found equal to  $2.5 \times 10^{-3}$  s for all frequencies. According to a theoretical formula obtained by Merk the time lag should be  $4.0 \times 10^{-3}$  for this situation. One of the reasons for this discrepancy is that in deriving the theoretical time lag equation it has been assumed that the flame retains its conical shape during the vibrations which is not strictly true.

## REFERENCES

- Blackshear Jr., P.L., "Driving Standing Waves by Heat Addition", 4th Symposium Int. on Combustion, 1953.
- Merk, H.J., "An Analysis of Unstable Combustion of Premixed Gases", 6th Symposium Int. on Combustion, 1975.

## FLAME STRUCTURE OF A DISTILLATE-OIL/WATER EMULSION SPRAY

by

S.R. Gollahalli and N. Siddiqui  
 The University of Oklahoma  
 School of Aerospace, Mechanical and Nuclear Engineering  
 Norman, Oklahoma 73019

Emulsification of fuel oils with water has received a great deal of attention in recent years because of its potential to reduce the emissions of pollutants from spray combustors. Several full-scale combustor studies and elemental-scale droplet combustion studies of emulsified fuels have been reported [1,2]. However, the number of diagnostic studies on the effects of emulsification on the flame structure of burning sprays under controlled conditions is limited [3,4]. Hence, the investigation reported in this paper was directed to study the differences between the radial profiles of temperature and composition ( $O_2$ ,  $CO$ ,  $NO$ ,  $SO_2$ ) at the axial locations of the burning sprays of ASMT No. 2 oil and its emulsion with 5% water (by volume). An airblast atomizer was used and the primary and secondary air flow rates were controlled to maintain the fluid-dynamic effects invariant so that the observed effects could be attributed to only emulsification of the oil. The temperature was measured with a silica-coated Pt-Pt/Rh thermocouple and the readings were corrected to account for radiation losses. The gas samples were drawn through a quartz probe and analyzed with several analytical instruments.

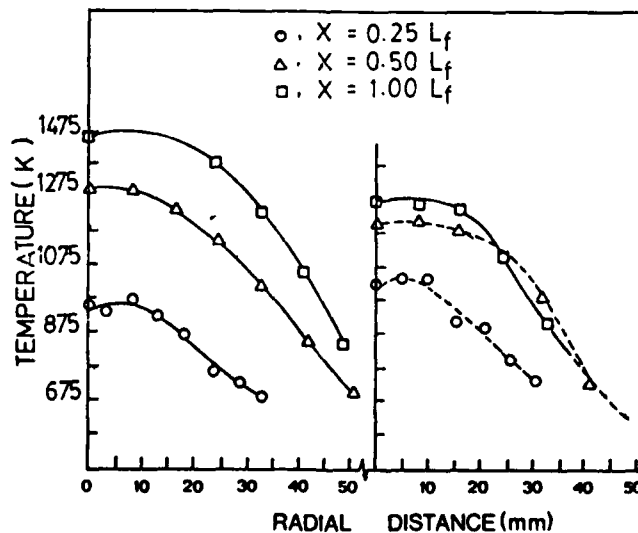


Fig. 1: Effects of Emulsification on the Radial Temperature Profiles at Three Axial Locations. (Left) No. 2 Oil, (Right) No. 2 Oil-5% (Vol) Water Emulsion

Figures 1 and 2 show the effect of emulsification on the temperature and NO concentration profiles. The results show that emulsification delays the evaporation of drops in the near-nozzle region, decreases CO emission and increases NO and SO<sub>2</sub> emission from the flame. The results can be explained by the changes in the basic physico-chemical processes caused by emulsification.

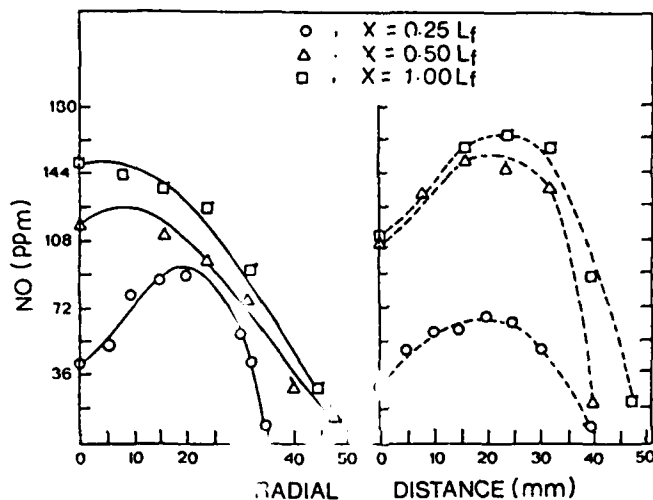


Fig. 2: Effects of Emulsification on the Radial Concentration Profiles of NO at Three Axial Locations. (Left) No. 2 Oil, (Right) No. 2 Oil-5% (Vol) Water Emulsion

#### REFERENCES

1. Gollahalli, S.R., "An Experimental Study of the Unsupported Drops of Residual Oils and Emulsions", *Comb. Sci. and Techn.*, Vol. 19, 1979, pp. 245-250.
2. Marshall, W., "Experiments With Novel Fuels for Diesel Engines", Report BERC/TPR-77-8, Dept. of Energy, 1978.
3. Jahani, H. and Gollahalli, S.R., "Characteristics of Burning Jet A Fuel and Jet A Fuel Water Emulsion Sprays", *Comb. and Flame*, Vol. 37, 1980, pp. 145-154.
4. Gollahalli, S.R., Nasrulla, M., and Bhashi, J.A., "Combustion and Emission Characteristics of Burning Sprays of Steady Residual Oil Sprays", *Comb. and Flame*, Vol. 55, 1984, pp. 93-102.

## WORKPIECE ACCURACY IN SHEET METAL OPERATIONS

T. R. Chandrupatla

GMI Engineering & Management Institute  
1700 West Third Ave.  
Flint, Michigan

Every manufacturing process leaves its own characteristic marks on the workpiece. The geometry of tooling, the deformation caused by the work forces and the material properties influence the final shape achieved. In this article, the accuracy aspects of stamping and drawing operations are considered.

## A PUBLIC TRANSIT SYSTEM DESIGN FOR A METROPOLITAN CITY

by

Subhash C. Sarin  
Virginia Polytechnic Institute and State University  
Department of Industrial Engineering and Operations Research  
Blacksburg, Virginia 24061

Soumen Ghosh  
Department of Management Science  
The Ohio State University  
Columbus, Ohio 43210

This paper describes a study done to design a public transit system for metropolitan Columbus, Ohio. Within the last few years the increment in the number of buses to serve the growing demand in the metropolitan area has been at the average rate of 50 vehicles per year. Moreover, the fleet size of the Central Ohio Transit Authority (COTA) which provides transit service in this region, is expected to nearly double by 1985. This growing trend of the transit needs of the public in this region demands designing the transit system of Columbus, so that the fleet can be used most effectively, both in providing better service to the public and at the same time proving to be most cost effective to operate. We present here such a design for this region. The decision variables to be determined are: (i) the structure of routes, (ii) the trip density for each route, (iii) the bus schedule for each route, (iv) the number of buses on each route, and (v) the transit market share of each route along with the determination of total operating cost for each route and the total revenue to be generated by each route. In addition, various productivity measures are found for each route in order to judge their characteristics accurately. The optimal values of these decision variables while meeting the physical constraints is the principle focus of the design process.

## ROADWAY LIGHTING DESIGN

by

L. Ellis King  
The University of North Carolina at Charlotte  
Department of Civil Engineering  
Charlotte, NC 28223

During the hours of darkness, the motorist on an unlighted highway encounters a driving environment far different from that encountered during daylight hours. The already complex daytime driving task is further complicated by a loss of visibility due to darkness which reduces the amount and quality of visual information available to the motorist. The driver may be considered as a limited capacity information processor whose performance is adversely affected by any reduction in information which contributes to performing the driving task in a safe and efficient manner. This is reflected in the nighttime accident rate which is approximately three times greater than the daytime rate. The ability to see contributes to safe and orderly movement of traffic on our highways. However, in many instances, limitations of the human eye prevent vehicle headlighting alone from completely satisfying visual night driving requirements. In these cases, fixed lighting aids the driver by improving his efficiency and giving early warning of hazards ahead in or near the roadway. The driver can then use this early information in a timely fashion to formulate his response to any unsafe condition.

Recommended highway lighting practices for North America are set forth in the American National Standard Practice for Roadway Lighting. The latest revision of the Standard Practice includes, in addition to the previous illuminance method for design, a luminance method which incorporates veiling luminance. In the past, roadway lighting designs have generally been based upon levels of surface illuminance. This approach, however, fails to take into account a very significant factor, namely, the light reflecting properties of the surface being illuminated. Although the importance of this factor has been known to illuminating engineers for some time, practically speaking, it could not be taken into account because of the many difficulties involved in doing so. These included measuring the directional reflectance properties of the roadway surface in question and computing the roadway luminance, the latter process involved many long and tedious calculations. These voluminous and repetitious calculations readily lend themselves to processing by microcomputers, which are now widely available. A computer program has been developed which uses formulas and procedures set forth in the Standard Practice for calculating values of illuminance, luminance and veiling luminance for user-defined roadway lighting systems. With the aid of the computer, many system designs can be investigated and compromises through approximations, shortcut procedures and rules of thumb are not necessary. Repeated re-designs, reiterations, and modifications are practical with regard to both time and cost.

ELECTRIFICATION OF A TRANSMISSION BELT RUNNING AGAINST  
GROUNDED METAL PULLEYS

by

J. L. Jarvis

Department of Mechanical Engineering and  
Engineering Production, University of Wales Institute  
of Science and Technology, Cardiff, UK

R. S. J. Palmer

School of Mechanical & Production Engineering  
Nanyang Technological Institute  
Singapore 2263

If any two surfaces are brought together so that they are in intimate contact then charge transfer occurs, and subsequent separation of the surfaces may result in each acquiring a net surface charge. If one of the contacting surfaces is an insulator then its likelihood of electrification on separation is greatly increased. In the case of an insulating transmission belt running against grounded metal pulleys, continuous contact and separation of the belt and pulley occurs. Thus conditions are ideal for electrification, and insulating drive belts present a common electrostatic hazard.

A study was made of the electrification of a two-pulley drive in which an endless chrome leather belt ran against mild steel pulleys. The work was carried out in a relative humidity controlled chamber. The effect on the electrification of belt speed, belt resistivity, the number of belt-pulley contacts, belt-pulley contact pressure, and the velocity of the belt relative to the pulley was studied.

No charge was carried away by the belt if the product of belt surface resistivity times belt speed was less than  $0.64 \times 10^{10} \Omega \cdot \text{m} \cdot \text{s}^{-1}$ . This was very near the theoretical prediction of Horvath and Berta.

## OPTIMAL DESIGN OF A SOLID OF REVOLUTION THERMAL DIFFUSER

by

Young W. Chun  
Department of Mechanical Engineering  
Villanova University  
Villanova, PA 19085

During the past decades much work has been done on the study of structural optimization. However shape optimization is a relatively new class of structural optimization problems that are expected to be important in future applications. Instead of selecting explicit design parameters or functions defining dimensions of a structure, as is normally done in structural optimization, the shape of the elastic solid under consideration plays the role of the design variable. Such problems cannot be easily reduced to a formulation that characterizes shape with a design function that appears explicitly in the formulation.

In an earlier investigation [1], the shape optimization of a structural component with constraints on heat flux was considered assuming the structural component as a plate. This paper presents recent developments in the shape optimal design of structural components (specifically thermal diffusers) treating them as more realistic solids of revolution. A priori specification on the input heat flux is given, and a constraint is placed on the output heat flux. Minimum weight is taken as the design objective. Finite element method is used to obtain the temperature distribution at each stage of optimization process. The material derivative concept of continuum mechanics and the adjoint variable method are used to obtain design sensitivity of cost and constraints with respect to boundary movement. The boundary is parametrized and sensitivity results are used to obtain derivatives of constraints with respect to parameters defining the boundary. A nonlinear programming technique is then used to numerically construct optimal designs.

Reference

1. Chun, Y.W., "Optimal Design of Heat Conducting Structural Elements," Mathematical Modelling in Science and Technology, Proceedings of the Fourth ICMM, August 1983, Zurich, Switzerland.

DISTRIBUTION OF GAS AND LIQUID PHASES  
IN THE CORE OF A TURBULENT TWO-PHASE ANNULAR FLOW

by

Flavio Dobran  
Stevens Institute of Technology  
Hoboken, N.J. 07030

The distribution of gas and liquid phases in the core of a turbulent two-phase annular flow was studied by means of a mixing length turbulence model. The core flow was assumed to be isothermal, fully-developed, axisymmetric, and of a high quality. Turbulence modeling of the two-phase flow field was carried out by assuming a relationship between the liquid phase and gas phase turbulence, and by assuming that the gas phase turbulence can be modeled by the mixing length turbulence model. The gas volumetric fraction distribution predicted by the model showed that in an upflowing situation the liquid phase tends to concentrate near the center of the pipe, while, in down-flowing situation, it tends to concentrate near the liquid film interface. An increase in the interfacial shear stress at the liquid film-core interface is shown to decrease the liquid phase concentration close to the liquid film interface in upflow and to increase it in downflow. Larger interfacial shear stresses also tend to produce smaller void fraction gradients in both upflow and downflow. Comparison of the upflow and downflow data of bubbly flows and flows without the liquid film, (where a denser dispersed phase is distributed in a lighter continuous phase), with analytical results is shown to be good.

LIMITATIONS OF THE NEAR-WALL  $k$ - $\epsilon$  TURBULENCE MODEL

Peter S. Bernard

Dept. of Mechanical Engineering, The University of Maryland  
College Park, Maryland 20742

Considerable uncertainty has surrounded the development of low Reynolds number variants of the  $k$ - $\epsilon$  closure equations for use next to solid boundaries. In this talk it will be shown that closure to the  $\epsilon$  equation can be derived systematically by taking advantage of its close similarity to the exact equation for the vorticity covariance field. The latter relation has been closed previously [1] using a formal Lagrangian analysis that avoids the use of modeling per se. For high turbulent Reynolds numbers the derived  $\epsilon$ -equation is identical to its commonly accepted form. In the low Reynolds number case it agrees with that suggested by Hanjalic and Launder [2] with the addition of two new terms. Tests of the revised  $\epsilon$ -equation as part of the  $k$ - $\epsilon$  closure have been carried out for channel flow. Some improvement in the prediction of  $k$  over previous models is found to occur, though serious errors remain.

A recent determination [3] using experimental channel flow data of the turbulent energy budget adjacent to a solid surface is compared to that predicted by the closed  $k$ - $\epsilon$  equations. This reveals a significant defect in the accepted model for the pressure diffusion term in the  $k$  equation which may be responsible for the inaccuracies found in the  $k$  predictions.

## REFERENCES

- [1] Bernard, P.S. and Berger, B.S., SIAM J. Appl. Math., 42, 453 (1982).
- [2] Hanjalic, K. and Launder, B.E., J. Fluid Mech., 74, 593 (1976).
- [3] Bernard, P.S. and Berger, B.S. AIAA J., 22, 306 (1984).

A THREE-STAGE TURBULENCE STRATEGY:  
EXTRACT AND PREDICT BIG EDDIES; MODEL LITTLE ONES

by

Fred R. Payne, The University of Texas at Arlington  
Arlington, Texas 76019

Turbulence may be the most demanding discipline of inorganic nature. Reasons for this are evident: essential nonlinearities, major dissipative processes, stochasticism, full four-dimensionality in space and time, continuum rather than discrete phenomena, dispersiveness, and vorticity (Lumley, 1959); closure is unavoidable for the infinite hierarchy of equations under the linear Reynolds (1874) decomposition. The first closure effort was Boussinesq's (1877) definition of austach or exchange coefficient; the eddy viscosity/conductivity is an intrinsically exact expression. However, Boussinesq merely trades the unknown Reynolds stress for an unknown "eddy" viscosity. Little progress was made until Prandtl (1921), via physical arguments, defined his "mixing length" analogously to the mean-free-path in kinetic theory of gases. Prandtl-Boussinesq ideas dominated turbulent calculations for four decades until the advent of large digital computers; elaborations upon these primitive concepts still, generally, attempt to model turbulence locally rather than globally in frequency or wave-number space by use of up to fifteen(15) constants which must be modified for minor flow geometry changes.

Townsend (1956,1976) was first to study seriously a "two-component" model wherein the "big eddies" drained energy from the mean flow and, in turn, gave up energy down the spectral cascade to the heat sink due to viscous action by the small eddies. He was handicapped by a lack of theory and, essentially, played a guessing game for the large-scale-structure. Lumley (1966a) provided the first mathematically rational definition of big eddies by his Proper Orthogonal Decomposition Theorem (PODT) as a response to Townsend's efforts. Payne (1966) implemented PODT for the 2-D wake of a circular cylinder; see also Payne and Lumley (1967). Lemmerman and Payne (1977) reported on Lemmerman's (1976) PODT calculations for the 2-D boundary-layer; Lieb, Glauser and George (1983) applied PODT to the axisymmetric jet and Moin (1983) likewise to two-point velocity correlations numerically generated in a channel flow.

Lumley (1966b) extended the "Orr-energy" method of nonlinear flow stability analysis to turbulence via a second extremum principle. Orr (1907) postulated a global extremum of the disturbance kinetic energy; Lumley maximized the eddy viscosity and obtained a linear eigen-val-

ue PDE problem. Payne(1968) implemented Lumley's concept and predicted the neutral modes in the 2-D wake. Comparisons with PODT-extracted eddies gave good qualitative agreement. [See Payne, 1978 for a public report on the 1968 work.] Other predictions are: Hong(1978) and Wadia (1979) in the 2-D boundary-layer, and Hong(1983) for a curved mixing layer. The predicted neutral modes again agreed fairly well with PODT extractions. This work, excepting Hong's, was critiqued by Payne(1982).

Payne(1979) and Chuang and Payne(1979) applied a third concept of Lumley(1967), namely that of "small eddy viscosity," to Lemmerman's PODT results in the boundary-layer. Chuang (1978) removed Lemmerman's eddies from the totality of correlation data and calculated several small eddy viscosities; most were either constant or slowly and linearly varying across the full layer.

Finally, Payne (1983) unified all three approaches into a proposed strategy for turbulence studies, namely, 1) extract PODT eddies from experiment or numeric correlations; 2) predict the neutral Lumley-modes and compare to PODT; and 3) remove PODT eddies from the total correlation and calculate "small-eddy" coefficients for modeling in dynamical equations. Further details of the tripartite approach will be forthcoming at SES.

- Boussinesq, J.(1877), Mem. Pres. Acad. Sci. Paris, v23  
 Chuang,, S-C and Payne, F. R. (1978), Appl. Nonlinear Analysis, Acad. Press, p507-518  
 Hong, S-K (1978), MSAE Thesis, UTA  
 Hong, S-K (1983), Ph.D. Dissertation, Purdue  
 Lemmerman, L. A. (1976), Ph.D. Dissertation, UTA  
 ----- and Payne, F.R.(1977), AIAAJ Paper No. 77-717  
 Lumley, J. L. (1959), "Turbulence" in Encl. Physics, Perg  
 Lumley, J. L. (1966a), Doklady Akad. Nauk SSSR, Moscow  
 Lumley, J. L. (1966b), Int. Memo, Ord Res Lab, Penn State  
 Lumley, J. L. (1967), Private Communication  
 Moin, P. (1983), XXXVIth Annual APS-FDD, Houston  
 Leib, S, Glauser, M, George, W(1983), XXXVIth APS-FDD  
 Orr, W. (1907), Proc. Roy Irish Acad, vol XXVII, page 69  
 Payne, F. R. (1966), Ph.D. Dist., Penn State; report to USN/ONR under Contract Nonr 656(33)  
 -----, & Lumley, J(1967), Phys Fluids, SII, page S194-5  
 Payne, F. R. (1968), Rep.to USN/ONR under Nonr 656(33)  
 Payne, F. R. (1978), Nonlinear Eq. in Abstract Spaces, Acad Pr, page 417-438  
 Payne, F. R. (1979), Applied Nonlinear Analysis, Acad Press, page 675-688  
 Payne, F. R. (1982), Nonlinear Phenom. in Math. Sci., Acad. Pr, page 781-791  
 Payne, F. R. (1983), XXXVIth APS-FDD, Houston  
 Prandtl, L. (1921), Zeit. Angew. Math. Mech., vi, p431  
 Reynolds, O. (1874), Proc. Manch. Phil. Soc., v14, p7-12  
 Townsend, A. A.(1956,76), The Structure of Turbulent Shear Flows, Cambridge U. Press; 1st, 2nd Edit.  
 Wadia, A. R. (1979), Ph.D Dissertation, UTA

A FINITE ELEMENT ANALYSIS OF INCOMPRESSIBLE TURBULENT BOUNDARY  
LAYER FLOWS USING TRANSIENT ADAPTIVE GRIDS

D. G. Howlett, S. W. Kim, and F. R. Payne  
Department of Aerospace Engineering  
University of Texas at Arlington  
Arlington, Texas 76019

The boundary layer equations are parabolic partial differential equations. It has been shown that the numerical solution of these equations using the semi-discrete Galerkin finite element method yields an accurate solution for laminar boundary flows, even when coarse grids are used (1). However in turbulent boundary layer flows, the tangential velocity grows to more than thirty per cent of the external inviscid velocity within the inner one per cent of the boundary layer thickness. Consequently, it is necessary to use refined meshes near the wall, which degrades the computational efficiency. Moving finite elements proposed by Mueller and Carey (2) is generalized and further developed to solve turbulent boundary layer flows using partial differential equation turbulence models. A review of literature on turbulent boundary layer flows reveals that partial differential equation turbulence models had been quite successful for free shear layer flows; whereas they are not so satisfactory for wall flows. For example, Soliman and Baker (3) reported a dissipation function profile which contain a sharp peak very near the wall; and Ng and Spalding (4) divided the space-like domain into two regions for their numerical analysis, one being very close to the wall and the other consisting of the outer boundary layer region. In the present study, emphasis is upon the use of adaptive grids, which evolve along the time-like coordinate, and upon the performance of different turbulence models. Computational results are compared with both experiments and solution by other numerical methods.

References

1. S. W. Kim and F. R. Payne, "Finite Element Analysis of Incompressible Laminar Boundary Layer Flows," Proceedings of the 5th Int. Symposium on Finite Elements and Flow Problems, U.T. Austin, 1984, Also will appear in the Int. J. Num. Meth. Fluids.
2. A. Mueller and G. F. Carey, "Stefan Problems Using Moving Elements," Proceedings of the 5th Int. Symposium on Finite Elements and Flow Problems, U.T. Austin, 1984.
3. M. O. Soliman and A. J. Baker, "Accuracy and Convergence of a Finite Element Algorithm for Turbulent Boundary Layer Flow," Computer Meth. Applied Mech. Engr., Vol 28, pp. 81-102, 1981.
4. K. H. Ng and D. B. Spalding, "Predictions of Two-Dimensional Boundary Layers on Smooth Walls with a Two-Equation Model of Turbulence," Int. J. Heat Mass Transfer, Vol. 19, pp. 1161-1172, 1976.

SWIRL DEVELOPMENT IN CYLINDRICAL COMBUSTION CHAMBER  
OF RECIPROCATING ENGINE

by

Ph.M. Arquès

The University of Valenciennes and Hainaut Cambrèsis  
59326 Valenciennes Cedex  
France

A good understanding of the mechanisms of mixture development in an injection engine and flame propagation in homogeneous or biphasic mixtures necessitates the development of investigation means to define the swirl flows which exist with or without flame in the combustion chamber  $\sqrt{1/}$

This combustion chamber may be at a constant volume but, then the results obtained are difficult to transpose, or with a variable volume. In this latter case, the movement of a mobile part of the chamber may result from the relative displacement of different components of the crank connecting rod system or again from the ballistic movement of a piston which is immobilised when the chamber volume is minimal.

After a presentation of the different ways of controlling the piston displacement in a rapid compression machine, we present the work executed in such a machine to determine the swirl flow pattern created in a cylindrical chamber for which the gas intake is tangential. This volume disposition is representative of the combustion chamber "COMET", "KOUCHOUL", etc.

Rapid compression machine

/2,3,4(Fig:1)

The use of a rapid compression machine is justified by these considerations :

- . facility of bringing piston movement into play ,
- . reduction of the apparatus volume,
- . possibility of quick mechanical modifications of the machine and , in particular , of the chamber ,
- . good accessibility of the chamber faces for a schlieren observation.

The design of the machine is developed with these objectives :

- . obtainment , during the compression , of a piston velocity defined with the time ,
- . immobilisation of the piston when the chamber volume is minimal or return of the piston to the lower dead center,
- . airtightness of the combustion chamber without lubrication of the components in relative linear displacement,
- . understanding of heat transfer between gas and wall of the cylindrical chamber .

Experiments

In this particular case , we have chosen to mix air coming from the variable volume with carbonic gas in the cylindrical chamber in order to increase the density difference and thus to make the mixture phenomenon more perceptible .When air is introduced into the chamber filled with carbonic gas , we

distinguish 3 periods :

1st period : a swirl created by the canal edge opening (fig.2) into the cylindrical chamber takes form and increases, fed by air coming from the variable volume . (Fig : 3). The swirl center goes to the middle of the cylindrical chamber with a displacement velocity of 1.3 m/s .

2nd period : air finishes filling up the cylindrical chamber while swirling . The swirl center curves round the chamber middle with a velocity which decreases from 1400 to 350 revolutions a minute.

3rd period : the piston is stopped , there is a swirl of mixture in the cylindrical chamber . The angular velocity of this swirl center round the chamber center is 350 revolutions a minute.

#### References

1. Arquès Ph.M. "Flow and flame propagation in the Kouchoul engine". I Mech E .C393-80 p17 .1980.
2. Fayette Taylor C. "The internal combustion engine in theory and practice". The MIT press. Vol 2. 1966.p112
3. Hartley.J "Stratified charge engine without the complexity" The Engineer n° 6270.1976. p38.
4. Haslett, R.A., Monaghan, M.L. and McFadden, J.J. "Stratified charges engines ". SAE 76 07 55 . 1976.

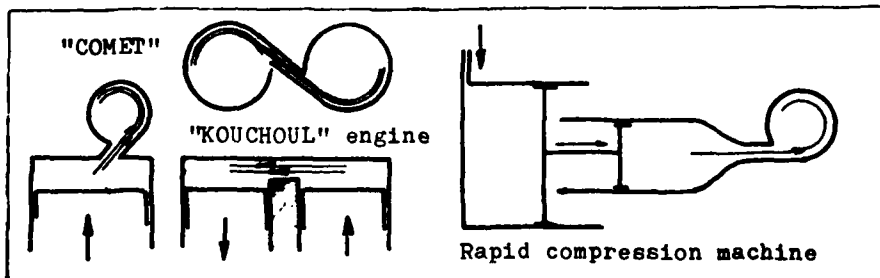


Fig:1

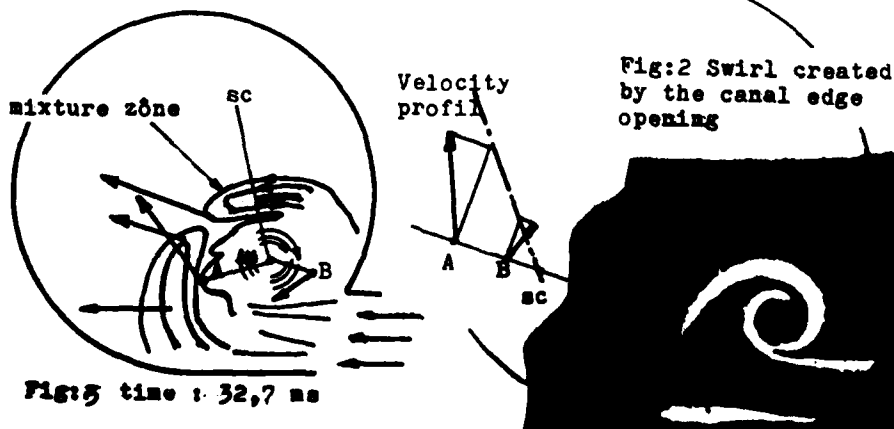


Fig:5 time : 32,7 ns

Fig:2 Swirl created by the canal edge opening

THERMODYNAMIC CYCLES OF PNEUMATIC STORAGE WITH  
TURBINE AND RECIPROCATING ENGINES

by

Philippe M. Arquès

The University of Valenciennes and of Hainaut Cambrésis  
59326 Valenciennes Cedex FRANCE

In order to resolve the conflicting and erratic situations between production and instantaneous consumption of electricity which occur just a few hours a day, the electric power /1/ companies have been led to adopt different solutions, from the financial incitement to switch off on application for some consumers, to the design of electric power stations with daily or weekly compressed air energy storage. In this case, air is compressed in a reservoir during off-peak hours; this air is reheated and expanded in a engine which drives an electric generator. The engine choice is not indifferent to the way in which the fuel energy goes through the different thermodynamic transformations. /2/

The energetic parameters of such a cycle are :/1,3/

- The mass expansion work in the engine ( $W_m$ ) characterizes the isothermal air compressor and the expansion machine sizes.
- The expansion work per cubic meter of reservoir ( $W_v$ ) characterizes the size of the air storage reservoir.
- The specific consumption ( $C_s$ ) of the expansion engine during the peak hours.
- The pumping energy ( $W_s$ ), ratio between the energy necessary for pumping and the expansion work.
- The efficiency of this cycle ( $E_f$ )
- The ratio between energy of nuclear or fossil origin ( $E_n$ ).

The expansion engines which can be used in this instance are either rotative (gas turbine) or volumetric (reciprocating) engines. (Fig : 1 A). In the first case, the extreme pressure and temperature ratios of the cycle do not exceed 50 and 3 respectively. Whereas for the reciprocating engine cylinders these ratios reach 200 and 6 respectively.

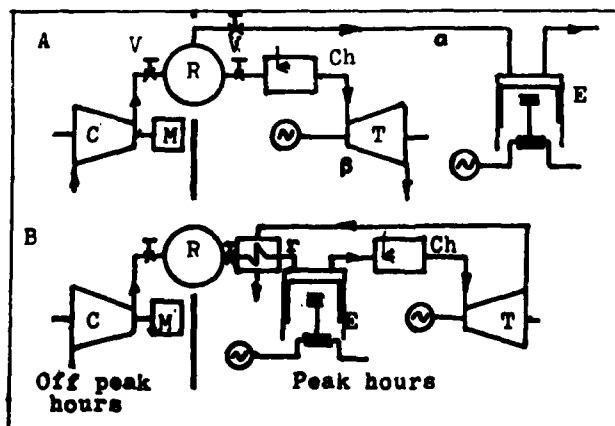
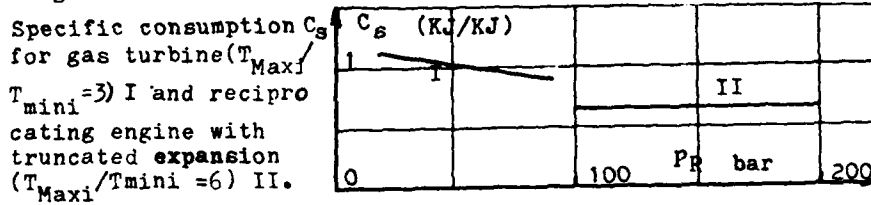


Fig 1

C : compressor  
Ch : Combustion chamber  
E : Reciprocating engine  
M : Motor  
T : Turbine  
R : Reservoir  
r : reheat  
~ : Generator  
T : Shut-off valve

Specific consumption of theoretical cycle are a little lower in the case of reciprocating engine because for these engines the expansion is truncated .(Fig 2 ).This effect can be offset by recovering the exhaust gas energy with a low pressure gas turbine . (Fig : 1 B).

Fig : 2



This paper presents the computed characteristics for different theoretical -LENOIR cycle $4/4$ -and actual cycles including and combining reciprocating and gas turbine engines, reheater or combustion chamber. In the case of actual cycles, the energetic characteristics are compared with those of the "Huntorf" plant.(Table :1).

	Power (1)		$W_m$	$W_v$	$C_s$	$W_s$	$E_f$	$E_n$	
	Plant	Turb.							
	Mw	Mw	MJ/Kg	MJ/m <sup>3</sup>	KJ/Kg				
Recip.Eng.	294		1031	206	1.42	.56	.50	.39	Fig:IA
Preheat+R.E. +C.Ch.+Turb.	386	82	1556	201	1.22	.37	.62	.30	Fig:IB
Gas Turbine ("Huntorf")	290	290	695	47	1.63	.80	.41	.49	Fig:IA

- (1) 4 engines of 18 cylinders (bore x stroke = .57 x .60 m)
- (2) Reservoir volume at constant pressure with buffer -20 % for engines running 2 hours per day.

	Reservoir (2)		Mass air flow	Capital cost	Operating cost
	volume	press.			
	m <sup>3</sup>	bar	Kg/s	\$/Kw	\$/Kwh
Recip.Eng.	11 400	200	280	210.3	.0792
Preheat+R.E. +C.Ch.+Turb.	20 200	200	352	214.45	.0747
Gas Turbine ("Huntorf")	60 000	46	410	283.73	.0986

1. ZAUG, P., STYS, Z.S. "Centrales avec réservoir d'air, spécialement pour les conditions US" Rev. BROWN BOVERI 12-80.1980.p723-733.  
 2. KARTSOUNES, GT. DALEY, J.G. "The use of reciprocating engine in compressed air energy storage power plants" Proceed. Symposium "Compressed air energy storage" Pacific Grove (CA) 1978. p.77-509  
 3. ARQUES, Ph. M. "Thermodynamic cycle of reciprocating internal combustion engines with compressed air energy storage" 19th meeting Society of Engineering Science, abstract, 1982 .p207.  
 4. FAYETTE TAYLOR, C. "The Internal Combustion Engine in Theory and Practice". The MIT press. Vol:1 .1966.p38.

INDEX OF AUTHORS  
(Page number followed by session designation)

Abdel-Aziz, A.F.	299 (16PM5)	Best, W.A.	72 (15AM8)
AbdelMohsen, M.H.	359 (17AM2)	Bhaduri, S.	307,308 (16PM6)
Abeyaratne, R.	117 (15PM4)	Bieterman, M.	464 (17PM5)
Adusumilli, R.S.S.	305 (16PM6)	Blair, S.A.	171 (15PM9)
Agarwal, R. K.	137 (15PM5)	Boerio, F.J.	1 (15AM1)
Ahmadian, M.	206 (16AM3)	Boler, F.	248 (16AM7)
	270 (16PM2)	Braibant, V.	380 (17AM5)
Aifantis, E.C.	167 (15PM8)	Brandeis, J.	257 (16AM8)
	195 (16AM2)	Breazeale, M.A.	339 (16PM9)
Alexiades, V.	478,479 (17PM7)	Brenner, H.	374 (17AM4)
Allael, D.	101 (15PM3)	Broucke, R.	433 (17PM2)
Allen, D.H.	181 (16AM1)	Brown, S.D.	196 (16AM2)
Al-Shayea, N.	265 (16PM1)	Brunn, P.O.	232 (16AM5)
Altshuller, D.	168 (15PM9)	Bruno, D.	349 (17AM1)
Amiri, A.F.	307 (16PM6)	Buczek, M.B.	79 (15PM1)
Anand, L.	156 (15PM7)	Bunch, W.H.	68 (15AM8)
Arafa, E.A.	61 (15AM7)	Burger, C.	356 (17AM2)
Agarwal, R.K.	137 (15PM5)	Burns, S.J.	198 (16AM2)
Arques, P.M.	481 (17PM8)	Burton, T.D.	150 (15PM6)
	501,503 (17PM9)		
Arulanandan, K.	256 (16AM8)	Calderer, M.C.	388 (17AM5)
Ascione, L.	349 (17AM1)	Canfield, T.R.	397 (17AM7)
Ashour, H.A.	200 (16AM2)	Cardenas-Garcia, J.F.	98 (15PM2)
Azad, A.K.	265 (16PM1)	Carlson, D.A.	460 (17PM4)
		Carlson, D.E.	275 (16PM3)
Bae, K.S.	11 (15AM2)	Chakrapani, N.	37 (15AM4)
Bahar, L.Y.	363 (17AM3)	Chamis, C.C.	76 (15PM1)
Bailey, C.D.	442 (17PM2)	Chandra, A.	297 (16PM5)
Baillieul, J.	431 (17PM2)	Chandrashekhara, K.	86 (15PM1)
Baird, D.G.	301 (16PM6)	Chandrupatia, T.R.	491 (17PM8)
	354 (17AM2)	Chang, H.-Y.	99 (15PM2)
Bajaj, A.K.	438,441 (17PM2)	Chang, O.	204 (16AM3)
Bajura, R.A.	411 (17AM8)	Chang, S.H.	35 (15AM4)
Baker, A.J.	462 (17PM5)	Chapman, R.N.	228 (16AM5)
Balas, M.J.	267 (16PM2)	Chavez, P.F.	342,343 (16PM9)
Balci, H.	82 (15PM1)	Chen, P.C.T.	103 (15PM3)
Baluch, M.H.	265 (16PM1)	Chen, P.J.	342,343 (16PM9)
Bammann, D.J.	165 (15PM8)	Chen, J.K.	424 (17PM1)
Banthia, V.	293 (16PM5)	Cheney, J.A.	311 (16PM7)
Bassanini, P.	47 (15AM5)	Cherny, S.G.	138 (15PM5)
Batzle, M.L.	249 (16AM7)	Chevray, R.	407 (17AM8)
Bazer, J.	340 (16PM9)	Chiriatti, G.	17 (15AM3)
Beatty, M.F.	266 (16PM2)	Choi, K.K.	451 (17PM4)
Bedford, A.	368 (17AM4)	Chona, R.	92 (15PM2)
Bendsøe, M.P.	385 (17AM5)	Chou, T.W.	280,283 (16PM4)
	459 (17PM4)	Chu, C.C.	12 (15AM2)
Bergman, L.A.	268 (16PM2)	Chu, C.L.	417 (17AM9)
Berkcan, E.	104 (15PM3)	Chu, S.	335 (16PM9)
Bernard, P.S.	497 (17PM9)	Chugh, Y.P.	160 (15PM7)
Bert, C.W.	23 (15AM3)	Chun, Y.W.	495 (17PM8)
	436 (17PM2)	Chung, T.J.	46 (15AM5)

Clifton, R.J.	147 (15PM6)	Fatic, V.M.	365 (17AM3)
Cohen, G.H.	104 (15PM3)	Fei, Z.	190 (16AM1)
Comrie, P.R.	231 (16AM5)	Ferber, M.K.	196 (16AM2)
Conrad, H.	11 (15AM2)	Ferlano, F.	17 (15AM3)
Cooper, J.M.	257 (16AM8)	Flaherty, J.E.	103 (15PM3)
Cooper, T.	163 (15PM8)	Fleury, C.	380 (17AM5)
Coriell, S.R.	474 (17PM7)	Floryan, J.M.	233 (16AM6)
Corradini, G.	83 (15PM1)	Fosdick, R.L.	118 (15PM4)
	174 (15PM9)	Fourney, W.L.	92 (15PM2)
Costin, L.S.	252 (16AM7)	Framond, de, R.	483 (17PM8)
Costley, R.D.	368 (17AM4)	Fredriksson, B.	29 (15AM4)
Cowin, S.C.	151 (15PM7)	Furtsch, T.A.	3 (15AM1)
	370 (17AM4)		
Craig, K.G.	57 (15AM7)	Garnier, M.	483 (17PM8)
Crawford, A.M.	254 (16AM7)	George, W.K.	405 (17AM8)
Creus, G.J.	143 (15PM6)	Getting, I.C.	248 (16AM7)
Curtis, J.	231 (16AM5)	Ghalambor, A.	330 (16PM8)
		Ghosh, S.	492 (17PM8)
Dafalias, Y.F.	256 (16AM8)	Gilat, A.	393 (17AM6)
Dahan, M.	6 (15AM1)	Gladstone, D.H.	130 (15PM5)
Daniel, I.M.	185 (16AM1)	Glauser, M.N.	405 (17AM8)
Das Gupta, A.	279 (16PM3)	Glockner, P.G.	219 (16AM4)
	327 (16PM8)	Gollahalli, S.R.	489 (17PM8)
Dayal, V.	403 (17AM7)	Goodings, D.J.	322 (16PM7)
DeAngelis, R.	446 (17PM3)	Googerdy, A.	440 (17PM2)
Denda, M.	264 (16PM1)	Goree, J.G.	346 (17AM1)
Desch, P.	304 (16PM6)	Gorji, M.	120 (15PM4)
Devilbiss, T.A.	3 (15AM1)	Gorla, R.S.R.	241 (16AM6)
Dieterich, J.H.	470 (17PM6)	Gorman, D.J.	107 (15PM3)
Diller, K.R.	66 (15AM8)	Goudreau, G.L.	399 (17AM7)
Dillon, O. W.	446 (17PM3)	Gould, L.I.	443 (17PM2)
Dixon, J.M.	318 (16PM7)	Grant, W.	72,73 (15AM8)
Dobran, F.	496 (17PM9)	Gregory, M.A.	79 (15PM1)
Dost, S.	82 (15PM1)	Griffin, J.M.	330 (16PM8)
	341 (16PM9)	Grimaldi, A.	349 (17AM1)
Dragani, R.	437 (17PM2)	Griskey, R.G.	224 (16AM5)
Duffy, J.	87 (15PM2)	Groehs, A.G.	143 (15PM6)
Dullum, O.	163 (15PM8)	Groves, S.E.	181 (16AM1)
Dunn, J.E.	389 (17AM6)	Gundappa, M.	447 (17PM3)
Dvorak, G.J.	77 (15PM1)	Gupta, A.	217 (16AM4)
Ejezie, S.U.	159 (15PM7)	Haber, R.B.	465 (17PM5)
Ekmann, J.M.	225 (16AM5)	Haddad, Y.M.	375 (17AM4)
Elber, W.	260 (16PM1)	Hadhri, T.	28 (15AM3)
Emery, A.F.	450 (17PM3)	Haftka, R. T.	383 (17AM5)
Epstein, J.S.	89 (15PM2)	Hahn, H.T.	182 (16AM1)
Epstein, M.	341 (16PM9)	Hansen, P.G.	403 (17AM7)
Eringen, A.C.	337 (16PM9)	Harper, B.D.	428 (17PM1)
Ersoy, Y.	338 (16PM9)	Harris, C.E.	187 (16AM1)
Ewida, K.T.	387 (17AM5)	Harrop-Williams, K.	159 (15PM7)
		Hartnett, J.P.	223 (16AM5)
Falade, A.	235 (16AM6)	Hartnett, M.J.	31 (15AM4)
Farr, W.A.	64 (15AM7)	Hasselman, D.P.H.	286 (16PM4)
Fathi, A.	106 (15PM3)		447 (17PM3)

Hassibi, M.A.	13 (15AM2)	Kenner, V.H.	14 (15AM2)
Haug, E.J.	451 (17PM4)	Kershner, J.D.	395 (17AM7)
Hayatadavoudi, A.	330 (16PM8)	Khalil, M.B.	130 (15PM5)
Heller, J.L.	60 (15AM7)	Kikuchi, N.	188 (16AM1)
Hencke, H.	447 (17PM3)	Kim, J.	287 (16PM4)
Henriksen, M.	303 (16PM6)	Kim, S.W.	132,136 (15PM5)
Herakovich, C.T.	79 (15PM1)		500 (17PM9)
Herendeen, D.H.	452 (17PM4)	Kinderlehrer, D.	123 (15PM4)
Hetnarski, R.B.	449 (17PM3)	King, L.E.	493 (17PM8)
Heyliger, P.R.	429 (17PM1)	Kishore, N.N.	347 (17AM1)
Hill, G.A.	305 (16PM6)	Kiusa'aas, J.	217 (16AM4)
Hogan, H.A.	303 (16PM6)	Knight, G.	68 (15AM9)
Hoger, A.	278 (16PM3)	Knight, N.F.	421 (17PM1)
Holcomb, D.J.	252 (16AM7)	Ko, H.Y.	320 (16PM7)
Holloway, D.C.	98 (15PM2)	Koelsch, T.A.	246 (16AM7)
Holsapple, K.A.	312 (16PM7)	Koh, S.L.	309 (16PM6)
Hopkins, M.A.	323 (16PM8)	Kovenya, V.M.	138 (15PM5)
Horan, J.V.	98 (15PM2)	Krause, J.R.	357 (17AM2)
Howlett, D.G.	500 (17PM9)	Krausz, A.S.	162 (15PM8)
Hsu, C.T.	177 (15PM9)		194 (16AM2)
Hui, D.	16 (15AM3)	Krausz, K.	162 (15PM8)
	215 (16AM4)		194 (16AM2)
Huseyin, K.	432 (17PM2)	Krieg, R.D.	401 (17AM7)
Hwang, B.C.	485 (17PM8)	Krousgrill, C.M.	101 (15PM3)
		Kruszewski, E.T.	116 (15PM3)
Ibrahim, N.A.	262 (16PM1)	Kulacki, F.A.	43 (15AM5)
Inman, D.J.	206 (16AM3)		281,283 (16PM4)
	270 (16PM2)		328 (16PM8)
	361 (17AM3)	Kulbe, K.D.	66 (15AM8)
Irwin, G.R.	92 (15PM2)	Kumar, R.	45 (15AM5)
Ismail, K.A.R.	480 (17PM7)	Kumar, S.K.	236 (16AM5)
		Kwack, E.Y.	223 (16AM5)
Jackson, W.L.	485 (17PM8)	Kwatny, H.G.	363 (17AM3)
James, R.D.	119 (15PM4)		
Jarvis, J.L.	494 (17PM9)	Laohakul, C.	231 (16AM5)
Jen, D.H.	309 (16PM6)	Larosa, S.	437 (17PM2)
Jenkins, J.T.	332 (16PM8)	Lau, K.C.	254 (16AM7)
	372 (17AM4)	Laws, N.	77 (15PM1)
Johnson, C.P.	271 (16PM2)	Lebey, M.	481 (17PM8)
Johnson, E.H.	452 (17PM4)	Leckie, F.A.	261 (16PM1)
Johnson, G.C.	49 (15AM6)	Lee, C.Y.C.	14 (15AM2)
Johnson, W.C.	50 (15AM6)	Leib, S.J.	405 (17AM8)
Jolles, M.I.	91 (15PM2)	Levin, R.L.	477 (17PM7)
Jones, E.H.	411 (17AM8)	Levy, A.J.	199 (16AM2)
Ju, Y.B.	301 (16PM6)	Levy, R.	453 (17PM4)
Juhlin, N.	450 (17PM3)	Lewis, G.	24 (15AM3)
Junkins, J.L.	269 (16PM2)	Li, C.A.	347 (17AM1)
		Li, V.C.	412 (17AM9)
Kabilan, A.P.	170 (15PM9)	Libal, A.	210 (16AM4)
Kallakin, V.	256 (16AM8)	Librescu, L.	419 (17PM1)
Kamat, M.P.	458 (17PM4)	Liebowitz, H.	9 (15AM2)
Karamanlidis, D.	207,209 (16AM3)	Liu, C. F.	222 (16AM4)
Kassir, M.	350 (17AM1)	Loganathan, G.V.	455,461 (17PM4)
Katsube, N.	157 (15PM7)	Lun, C.K.K.	324 (16PM8)

Lustig, R.	3 (15AM1)	Nader, T.	177 (15PM9)
Ma, C.L.	84 (15PM1)	Nakazawa, M.	33 (15AM4)
Maceri, F.	349 (17AM1)	Napolitano, M.	133 (15PM5)
MacMillan, E.H.	392 (17AM6)	Naylor, D.	288 (16PM4)
MacSithigh, G.P.	118 (15PM4)	Nelson, D.A.	240 (16AM6)
Mader, C. L.	395 (17AM7)	Nicholson, J.W.	268 (16PM2)
Maderspach, V.	26 (15AM3)	Nicoletto, G.	93 (15PM2)
Madylam, G.	483 (17PM8)	Niemiec, W.	242 (16AM6)
Maguire, D.M.	281 (16PM4)	Nishiyama, R.T.	410 (17AM8)
Mahadevan, S.	356 (17AM2)	Nomura, S.	280 (16PM4)
Mahmoud, F.F.	292,299 (16PM5)	Nweke, E.	188 (16AM1)
Majda, G.	147 (15PM6)	Oden, J.T.	35 (15AM4)
Maker, B.N.	52 (15AM6)	Okamoto, N.	33 (15AM4)
Malkus, D.S.	301 (16PM6)	Olaosebikan, L.	89,95 (15PM2)
Mallik, D.	356 (17AM2)	Olhoff, N.	456,459 (17PM4)
Malone, J.B.	128 (15PM5)	Ostojca-Starzewski, M.	373 (17AM4)
Mann, U.	239 (16AM6)	Ovunc, B.A.	109 (15PM3)
Mansfield, L.	211 (16AM4)	Oz, H.	205 (16AM3)
Margolin, L.G.	259 (16AM8)	Ozisk, M.N.	284 (16PM4)
Martins, J.	35 (15AM4)	Padhye, A.	158 (15PM7)
Masih, R.	19 (15AM3)	Padovan, J.	434 (17PM2)
Matic, P.	7 (15AM2)	Pagano, N.J.	81 (15PM1)
Matus, R.J.	132 (15PM5)	Pajewski, L.A.	83 (15PM1)
Maugin, G.A.	333 (16PM9)	Pal, D.	60 (15AM7)
Mazumdar, P.K.	11 (15AM2)	Palmer, R.S.J.	494 (17PM8)
Mbaeyi, P.N.O.	178 (15PM9)	Papastavridis, J.G.	367 (17AM3)
McCleary, S.L.	205 (16AM3)	Papple, M.L.C.	41 (15AM5)
McFadden, G.B.	474 (17PM7)	Parise, J.A.	486 (17PM8)
Meade, K.P.	68 (15AM8)	Passman, S.L.	273 (16PM3)
Mehta, D.C.	229,230 (16AM5)	Patel, B.R.	229,230 (16AM5)
Mei, C.C.	313 (16PM7)	Patwardhan, A.	68 (15AM8)
Meirovitch, L.	202 (16AM3)	Pawlak, T.P.	292 (16PM5)
Messick, D.L.	3 (15AM1)	Payne, F.R.	498,500 (17PM9)
Mikulecky, D.C.	74 (15AM8)	Peddleson, J.	440 (17PM2)
Milanez, L.F.	480 (17PM7)	Perkins, R.W.	379 (17AM4)
	488 (17PM8)	Peters, D.A.	55 (15AM7)
Monasa, F.	24 (15AM3)	Peters, J.F.	146 (15PM6)
Montagnana, M.	17 (15AM3)	Petroski, H.J.	99 (15PM2)
Montgomery, R.C.	201 (16AM3)	Pimbley, G.H.	395 (17AM7)
Montgomery, S.T.	342,343 (16PM9)	Pimprakar, M.S.	21 (15AM3)
Morris, D.H.	187 (16AM1)	Pindera, M.J.	145 (15PM6)
Morro, A.	377 (17AM4)	Plaut, R.H.	458 (17PM4)
Mostovoy, S.	2 (15AM1)	Plescia, G.	17 (15AM3)
Moyer, E.T.	9 (15AM2)	Plesha, M.E.	258 (16AM8)
Mroz, Z.	458 (17PM4)	Plett, E.G.	130 (15PM5)
Mukherjee, S.	293 (16PM5)	Popplewell, N.	106 (15PM3)
Mullen, R.L.	469 (17PM5)	Porcu, A.	17 (15AM3)
Muncaster, R.G.	274 (16PM3)	Post, D.	352 (17AM2)
Muralidhar, K.	43 (15AM5)	Prasad, B.	382 (17AM5)
Murphy, R.W.	485 (17PM8)	Prasad, V.	328 (16PM8)
Murty, V.D.	295 (16PM5)		
	310 (16PM6)		

Prevost, J.H.	153 (15PM7)	Savage, S.B.	324 (16PM8)
	255 (16AM8)	Sawyers, K.	124 (15PM4)
	317 (16PM7)	Sayar, B.A.	13 (15AM2)
Progar, D.J.	3 (15AM1)		111 (15PM3)
		Scanlan, R.H.	317 (16PM7)
Quinn, R.D.	202 (16AM3)	Schapery, R.A.	181 (16AM1)
		Scheidler, M.	277 (16PM3)
Ragab, S.A.	126 (15PM4)	Schlein, E.H.	243 (16AM6)
Rajagopal, K.R.	226 (16AM5)	Schmidt, R.	218 (16AM4)
	276 (16PM3)	Schmidt, R.M.	314 (16PM7)
	300 (16PM6)	Schroedl, M.A.	91 (15PM2)
Rajatabhothi, R.	271 (16PM2)	Schwartz, C.W.	92 (15PM2)
Rath, H.J.	304 (16PM6)	Scobelev, B.Y.	139 (15PM5)
Rathy, R.K.	306 (16PM6)	Scoccia, G.	83 (15PM1)
Ravi-Chandar, K.	97 (15PM2)		174 (15PM9)
Read, H.E.	141 (15PM6)	Scott, R.A.	188 (16AM1)
Read, M.R.	354 (17AM2)	Seaman, L.	163 (15PM8)
Reddy, B.D.	290 (16PM5)	Seine, H.	287 (16PM4)
Reddy, J.N.	86 (15PM1)	Serrin, J.	389 (17AM6)
	222 (16AM4)	Sethna, P.R.	360 (17AM3)
	429 (17PM1)	Shahinpoor, M.	154 (15PM7)
			325 (16PM8)
Reed, H.L.	38 (15PM5)	Shaker, M.A.	200 (16AM2)
Rehfield, L.W.	15 (15AM2)	Shapiro, B.	231 (16AM5)
Reid, J.W.	62 (15AM7)	Shaughnessy, E.J.	240 (16AM6)
Reilinger, R.	473 (17PM6)	Shawki, T.G.	147 (15PM6)
Reissner, E.	121 (15PM4)	Shen, H.H.	323, 332 (16PM8)
Rencis, J.J.	469 (17PM5)	Sherali, H.D.	455 (17PM4)
Rezayat, M.	100 (15PM3)	Shidlovskaja, I.I.	244 (16AM6)
Rice, J.R.	472 (17PM6)	Shidlovsky, V.P.	244 (16AM6)
Richman, M.W.	372 (17AM4)	Shippy, D.J.	100 (15PM3)
Rionero, S.	173 (15PM9)	Siddiqui, N.	489 (17PM8)
Rizzo, A.R.	231 (16AM5)	Siginer, A.	112 (15PM3)
Rizzo, F.J.	100 (15PM3)		237 (16AM6)
Rogers, W.	158 (15PM7)		7 (15AM2)
Romack, G. M.	262 (16PM1)	Sih, G.C.	457 (17PM4)
Rosakis, A.J.	97 (15PM2)	Simitses, G.J.	125 (15PM4)
Rowlands, R.E.	344 (17AM1)	Simpson, H.C.	172 (15PM9)
	359 (17AM2)	Singh, H.N.	306 (16PM6)
Rubayi, N.A.	353 (17AM2)	Singh, R.P.	70 (15AM8)
Rubinovitch, M.	239 (16AM6)	Singh, S.	351 (17AM2)
Rubinstein, A.A.	394 (17AM6)	Sirkis, J.S.	171 (15PM9)
Ruina, A.	471 (17PM6)	Sisson, R.D., Jr.	179, 180 (15PM9)
		Sivanandan, K.S.	391 (17AM6)
Sadegh, A.M.	350 (17AM1)	Slemerod, M.	89 (15PM2)
Sadeh, W.Z.	409 (17AM8)	Smith, C.W.	46 (15AM5)
Salamon, V.J.	36 (15AM4)	Sohn, J.L.	459 (17PM4)
	292, 296 (16PM5)	Sokolowski, J.	478, 479 (17PM7)
Sam, R.G.	229, 230 (16AM5)	Solomon, A.	185 (16AM1)
Sanderson, K.A.	3 (15AM1)	Soo, H.C.	125 (15PM4)
Sandhu, R.S.	161 (15PM8)	Spector, S.	248 (16AM7)
Sankar, N.L.	128 (15PM5)	Spetzler, H.	40 (15AM5)
Santos, dos, R.B.	486 (17PM3)	Speziale, C.G.	309 (16PM5)
Sarin, S.C.	492 (17PM8)	Squire, W.	
Sarma, L.V.K.V.	236 (16AM6)		

Stern, M.	368 (17AM4)	Walton, O.R.	257 (16AM8)
	445 (17PM3)		396 (17AM7)
Stinchcomb, W.W.	183 (16AM1)	Wan, F.Y.M.	213 (16AM4)
Strain, D.	453 (17PM4)	Wang, A.S.D.	347 (17AM1)
Stuart, W.D.	414 (17AM9)	Wang, C.-Y.	417 (17AM9)
Sturges, L.D.	135 (15PM5)	Wang, H.-S.	283 (16PM4)
Sun, C.T.	424 (17PM1)	Wasan, D.T.	374 (17AM4)
Swaminadham, M.	114 (15PM3)	Watson, T. J.	91 (15PM2)
Swift, A.H.P.	55 (15AM7)	Weiner, J.H.	192 (16AM2)
Szabo, B.A.	467 (17PM5)	Weitsman, Y.	4 (15AM1)
Szeri, A.Z.	226 (16AM5)		428 (17PM1)
Szyszkowski, W.	219 (16AM4)	Wempner, G.	212 (16AM4)
		Weng, G.J.	51 (15AM6)
Tarasuk, J.D.	41 (15AM5)	Whitcomb, J.D.	291 (16PM5)
	62,64 (15AM7)	White, R.E.	475 (17PM7)
	288 (16PM4)	Wicks, T.	129 (15PM5)
	357 (17AM2)	Wiederhorn, S.M.	193 (16AM2)
Tauchert, T.R.	444 (17PM3)	Wightman, J.P.	3 (15AM1)
Taya, M.	287 (16PM4)	Williams, S.	73 (15AM8)
Taylor, C.E.	351 (17AM2)	Wilson, D.G.	478,479 (17PM7)
Taylor, J.E.	386 (17AM5)	Wilson, D.R.	136 (15PM5)
Thatcher, W.	415 (17AM9)	Wineman, A.S.	276 (16PM3)
Thomas, J.R.	447 (17PM3)	Wisniewski, H.L.	279 (16PM3)
Ting, C.S.	149 (15PM6)	Wolla, J.M.	346 (17AM1)
Ting, L.	374 (17AM4)	Wollkind, D.J.	476 (17PM7)
Tousi, S.	438 (17PM2)	Wong, T.	251 (16AM7)
Trevino, P.A.L.	175 (15PM9)	Wu, H.C.	142 (15PM6)
Triantafyllidis, N.	52 (15AM6)	Wu, C.	485,487 (17PM8)
Troitsky, M.S.	21 (15AM3)		
Tsai, Y.M.	263 (16PM1)	Xu, T.X.	296 (16PM5)
Tse, S.T.	472 (17PM6)		
		Yackovlev, V.N.	243 (16AM6)
Uberoi, M.S.	410 (17AM8)	Yae, K.H.	361 (17AM3)
Udwadia, F.E.	203 (16AM3)	Yamamoto, T.	315 (16PM7)
Unger, D.J.	54 (15AM6)	Yanagidani, T.	247 (16AM7)
		Yin, W.L.	190 (16AM1)
Valanis, K.C.	140 (15PM6)	Young, M.I.	115 (15PM3)
Van Reet, J.	308 (16PM6)		208 (16AM3)
Van Wormer, K.A.	175 (15PM9)	Young, P.R.	3 (15AM1)
Vanderby, R.	68 (15AM8)		
Vanderplaats, G.N.	384 (17AM5)	Zachary, L.W.	345 (17AM1)
Varahamurti, R.	150 (15PM6)	Zheltovodov, A.A.	243 (16AM6)
Vasilev, G.V.	426 (17PM1)	Zielinski, Z.A.	21 (15AM3)
Venkayya, V.B.	452 (17PM4)		
Veragan, P.M.	58 (15AM7)		
Vera, P.D.S.	221 (16AM4)		
Voloshin, A.	356 (17AM2)		
Volpe, R.	83 (15PM1)		
	174 (15PM9)		
Wallace, C.	450 (17PM3)		
Wallis, G.B.	229 (16AM5)		
Walters, R.W.	133 (15PM5)		

DATE  
FILMED  
0-8